Novel models of stretch-induced injury in mouse oligodendrocytes and organotypic culture of cerebellar slices : study of pathophysiological mechanisms

Elena Chierto

UNIVERSITÉ PARIS DESCARTES

THÈSE DE DOCTORAT

Spécialité : **Neurosciences**

École Doctorale Médicament, Toxicologie, Chimie, Imageries (MTCI)

Pour l'obtention du grade de

Docteur de l'Université Paris Descartes

Présentée par

Elena CHIERTO

Novel models of stretch-induced injury in mouse oligodendrocytes and organotypic culture of cerebellar slices: study of pathophysiological mechanisms

Soutenue publiquement le 20 Janvier 2017

Devant le jury composé de :

Dr Catherine COIRAULT	Rapporteur
Dr Abdel GHOUMARI	Rapporteur
Dr Assaad EID	Examinateur
Dr Delphine MEFFRE	Examinatrice
Dr Fatiha NOTHIAS	Examinatrice
Pr François RANNOU	Examinateur
Pr Mehrnaz JAFARIAN-TEHRANI	Directrice de thèse

ACKNOWLEDGEMENTS

Au moment d'écrire ces remerciements, beaucoup d'émotions me submergent ; j'arrive maintenant à la fin de ce long parcours de thèse, souvent difficile mais aussi terriblement enrichissant. Je suis arrivée à Paris il y a quatre ans désorientée et sans avoir d'idée claire sur mon avenir, maintenant, je quitte cette magnifique ville en ayant grandi, avec plus de confiance en moi. Ce manuscrit est le résultat d'un grand travail qui a été possible grâce à tous les gens qui ont m'ont aidée au cours de ces années et que je souhaite remercier du plus profond de mon cœur.

Ma première pensée va à ma directrice de thèse, le Pr Mehrnaz Jafarian-Tehrani, qui m'a accueillie sous son aile quand je suis arrivée en tant qu'étudiante du projet Unipharma Graduates. Dès les premiers mois, elle a cru en moi et elle m'a poussée à me jeter dans cette aventure et je ne pourrai jamais la remercier assez pour cela. Grâce à son optimisme inépuisable, sa ténacité et sa passion pour son travail elle a su me transmettre la force pour dépasser les périodes d'incertitude en faisant ressortir le meilleur de moi. Son soutien et sa confiance en moi m'ont beaucoup touchée. Je considère qu'elle n'est pas seulement ma directrice de thèse, mais aussi un point de référence dans ma vie professionnelle et humaine.

Je tiens aussi à remercier le Dr Delphine Meffre, qui m'a vu avancer dans ce parcours et qui a été toujours capable de me donner des conseils précieux à la paillasse comme dans la vie quotidienne. Elle m'a beaucoup appris et son soutien était essentiel pour arriver jusqu'ici. Pendant ces années avec elle, j'ai découvert une personne avec un grand cœur, toujours disponible et ouverte quand j'en avais besoin.

J'exprime également mon respect et ma profonde reconnaissance au Pr Charbel Massaad, pour m'avoir accueilli dans son équipe et pour ses précieux conseils et discussions scientifiques.

J'adresse ma profonde gratitude à l'ensemble des membres du jury qui me font l'honneur de juger mon travail :

Madame le Docteur Catherine Coirault, pour s'être rendue disponible à exercer la fonction de rapporteur de ce travail de thèse. Je lui exprime toute ma gratitude et mes remerciements pour le temps consacré à la lecture de cette thèse et pour les points de réflexion soulevés.

Monsieur le Docteur Abdel Ghoumari, pour avoir accepté de juger mon travail de thèse en qualité de rapporteur et pour toutes les remarques et suggestions qui m'ont permis d'améliorer la qualité de ce manuscrit, et je lui suis très reconnaissante.

Monsieur le Professeur François Rannou, pour avoir accepté de juger mon travail en tant qu'examinateur, ainsi que pour l'intérêt porté à ce projet de recherche et pour ses précieux conseils scientifiques.

Madame le Docteur Fatiha Nothias, pour sa disponibilité et pour avoir accepté d'être membre de mon jury de thèse en tant examinatrice. Je lui exprime ma chaleureuse gratitude et considération.

Monsieur le Docteur Assaad Eid, pour me faire l'honneur d'évaluer mon travail de thèse en qualité d'examinateur ainsi que pour ses conseils scientifiques, je lui exprime toute ma gratitude et ma reconnaissance.

Je souhaite aussi exprimer ma profonde gratitude au Ministère français de la Recherche pour m'avoir offert un financement pour conduire cette thèse et également je tiens à remercier l'Institut de Formation Doctoral de l'Université Paris Descartes et la Fondation des Gueules Cassées pour leur soutien financier permettant la réalisation de ce projet de recherche.

J'exprime ensuite mon respect et ma profonde reconnaissance au Monsieur le Professeur Robert Barouki pour m'avoir accueillie au sein de l'unité INSERM 1124, et je remercie également tous les gens adorables qui en font partie.

Je souhaite remercier profondément le Pr Barclay Morrison, et toute son équipe, de m'avoir accueillie au sein de son laboratoire (Neurotrauma and Repair Laboratory at Biomedical Engineering, Columbia University, New York) pendant trois mois. Grace à cette expérience et aux discussions scientifiques partagées j'ai pu réaliser une partie de mon projet qui sinon aurait difficilement abouti.

Pendant ma thèse j'ai eu la chance de travailler dans une équipe magnifique qui m'a beaucoup soutenue et je tiens à remercier tous mes collègues de l'équipe «Nouvelles thérapies de la myélinisation» :

Merci à Alex Carreté pour son aide précieuse et le temps dédié à mon projet. Je tiens à le remercier aussi pour m'avoir appris la différence entre « bulle » et « boule », il avait comme objectif de m'apprendre parfaitement le français avant que je parte et, malgré la défaite, j'apprécie beaucoup son effort. Je tiens à remercier aussi le Dr Gemma Llufriu-Dabén, on a commencé ce parcours presque ensemble en partageant le bureau aussi que des bons moments et des échanges scientifiques. Je lui exprime mon admiration pour son profond engagement et ténacité tout le long de ce parcours qu'est la thèse. Ma reconnaissance va aussi au Dr Emeline Camand, qui a vu naitre ce projet et qui m'a formée tout au debut de ma thèse. Elle s'est montrée toujours disponible et son aide a été indispensable.

Un énorme merci va à mes trois stagiaires italiennes, Francesca Castoldi, Francesca Sapone et Giulia Cristinziano, avec lesquelles je ne partage pas seulement la nationalité mais aussi la passion pour ce travail, *grazie ragazze*. Leur aide a été indispensable, je ne serais jamais arrivée jusqu'ici sans leur participation à ce projet. J'adresse un grand merci aussi à Anara Alshanbayeva, pour sa précieuse contribution à ce travail. Je garde des souvenirs précieux de mon expérience avec elles toutes.

Je tiens également à remercier le Dr Julien Grenier pour être un peu « fou » mais en même temps capable de donner de précieux conseils scientifiques quand il y a besoin. Merci au Dr Françoise Courtin pour sa sympathie et son rire unique et inimitable ainsi que pour partager son expertise avec nous, les « petits ». Mes remerciements s'adressent également au Pr Sophie Bernard, avec son caractère fort et déterminé, pour les échanges scientifiques et sa disponibilité. Merci aux autres thésards de l'équipe, avec lesquels j'ai partagé cette expérience: Stéphanie Eid pour son empathie et disponibilité même à distance, Nirmal Kumar Sampathkumar (our Nimu) pour sa profonde gentillesse et enfin Venkat Sundaram, je n'oublierai jamais leur débridée danse indienne.
Je tiens aussi à remercier le Dr Anne Simon pour sa générosité, pour les discussions scientifiques ainsi que ses gâteaux toujours hyper bien réussis et enfin le Dr Céline Becker et Hoël Pinchon qui nous ont récemment rejoints. Une mention particulière pour les « anciens » de l'équipe : le Dr Ghjuvan'Ghjacumu Shackleford, notre corse, pour son caractère très franc et direct et aussi capable de grande générosité et le Dr Mehdi Hichor pour ses encouragements constants et son soutien qui m'ont beaucoup touchée. Un énorme

merci aussi à Julia Montanaro (et sa famille) qui m'a toujours aidée depuis mon arrivée ici et qui m'a ouvert la porte de sa maison quand je n'en avais pas encore.

Mes remerciements s'adressent aussi à tous les collaborateurs qui ont contribué à la réalisation de ce travail, le Dr François Etienne pour son solide support technique et ses précieux conseils en physique, le Pr Didier Borderie pour avoir participé avec enthousiasme à ce projet et aussi le Dr Stéphanie Dupuy, Jean-Maurice Petit et Claire Mader pour leur aide indispensable.

Merci à tous les membres de l'équipe 9 du Pr Frédéric Charbonnier avec lesquels on partage le labo (et aussi important, la cafet) pour contribuer à une ambiance de travail très agréable, difficile à trouver ailleurs, et pour tous les échanges scientifiques.

Je n'oublie pas tous mes amis auxquels j'exprime ma plus profonde gratitude pour m'avoir toujours supportée. Tous mes amis en Italie, avec une mention particulière pour Stefano et Federica, que malgré la distance j'ai toujours sentis si proches de moi. Et aussi les amis que j'ai eu la chance de rencontrer à Paris et avec lesquels j'ai créé des liens indissolubles et qui m'ont permis de me changer les idées quand j'en avait besoin, en particulier : Aurora, Davide, Saverio, Ilaria, Raffaella. Merci à vous tous pour être là.

Mes derniers remerciements (que j'ai traduit en italien plus en bas) iront évidemment à tous ceux qui m'ont plus particulièrement assuré un soutien affectif pendant ce travail doctoral : ma famille et mon copain.

Je souhaite remercier de tout mon cœur Pierluigi, Pigi, qui depuis désormais 7 ans m'accompagne dans ce parcours qu'est la vie. La distance ne nous a jamais fait peur et nous a rendus plus forts. Sa présence a été pour moi un soutien fondamental dans les moments plus difficiles en m'aidant à voir le côté positif. Je le remercie parce que ses sentiments n'ont jamais vacillé et pour voir en moi un personne meilleure que celle que je suis.

Je remercie mes deux grands-mères, *nonna* Mariuccia et *nonna* Paola, les piliers de ma famille, pour m'avoir toujours gâtée et pour avoir rempli ma vie de sérénité depuis l'enfance.
Et forcement pour finir, un grand merci à mes parents, à qui je dois tout, et sans qui je ne serai jamais arrivée à la fin de ce long parcours. Merci à ma mère toujours si forte, même dans les moments les plus sombres. Merci à mon père qui avant de partir m'a offert un bracelet portant un papillon pour voler loin et un gouvernail pour ne pas perdre la direction.

Les mots ne suffisent pas à leur exprimer ma reconnaissance, je vis pour les rendre fiers de moi et j'espère être digne de leur amour inconditionnel.

Un grazie di cuore a Pierluigi, Pigi, che mi è accanto nella vita ormai da 7 anni. La distanza non ci ha mai fatto paura e ci ha anzi resi più forti. La sua presenza è stata per me un sostegno fondamentale nei momenti più difficili, aiutandomi a vedere il lato potitivo. Lo ringrazio perchè il suo affetto non ha mai vacillato e per vedere in me una persona migliore di quella che sono.

Ringrazio le mie due nonne, nonna Mariuccia e nonna Paola, pilastri della mia famiglia, per non avermi mai fatto mancare nulla, avermi viziata e aver riempito la mai vita di serenità fin dall'infanzia.
Infine un grazie infinito ai miei genitori, a cui devo tutto e senza i quali non sarei mai arrivata alla fine di questo percorso. Grazie a mia mamma cosi forte anche nei momenti più bui. Grazie a mio papà che prima di partire mi ha regalato un braccialetto con una farfalla per poter volare via e un timone per non perdere la rotta. Le parole non bastano per esprimere loro la mia gratitudine, vivo per renderli orgogliosi di me e spero di essere all'altezza del loro amore così incondizionato.

TABLE OF CONTENTS

Article 1:

Chierto E, Castoldi F, Meffre D, Cristinziano G, Sapone F, Carreté A, Borderie D, Etienne F, Rannou F, Massaad C, Jafarian-Tehrani M . “Significant oligodendroglial alterations in response to stretch-induced injury” (*submitted to Scientific Reports*)

LIST OF PUBLICATIONS AND COMMUNICATIONS

INTERNATIONAL PUBLICATIONS:

Chierto E, Castoldi F, Meffre D, Cristinziano G, Sapone F, Carreté A, Borderie D, Etienne F, Rannou F, Massaad C, Jafarian-Tehrani M . "Significant oligodendroglial alterations in response to stretch-induced injury" *(submitted to Scientific Reports)*

Llufriu-Dabén G, Meffre D, **Chierto E,** Carreté A, Massaad C, Jafarian-Tehrani M. "Etazolate promotes oligodendrocyte differentiation and remyelination after demyelination in organotypic cerebellar slice cultures" *(under revision)*

Chierto E, Cristinziano G, Meffre D, Sapone F, Massaad C, Jafarian-Tehrani M. "Effect of etazolate on cell death and ROS production after tBHP-induced oxidative stress in mouse oligodendrocytes 158N cell line" *(in prep.)*

INTERNATIONAL PUBLICATIONS AND COMMUNICATIONS (not related to this work):

Borrione P, Grasso L, **Chierto E**, Geuna S, Racca S, Faiola F, Di Gianfrancesco A, Pigozzi F. Experimental model for the study of platelet-derived growth factors effects on early phases of the muscle healing process. *Blood Transfusion* 2014;12 Suppl 1:s221-8.

Borrione P, Spaccamiglio A, Rizzo M, Termine A, **Chierto E**, Campostrini N, Quaranta F, Di Gianfrancesco A, Pigozzi F. Urinary hepcidin identifies a serum ferritin cut-off for iron supplementation in young atlete: a pilot study. *J Biol Regul Homeost Agents* 2011; 25(3):427-434.

Poster:
Di Gianfrancesco A, Grasso L, **Chierto E**, Geuna S, Racca S, Ciminelli E, Pigozzi F, Borrione P. Experimental model for the study of the effects of platelet derived growth factors on muscles. XXXII World congress of sports medicine, Rome. 27-30 September 2012.

ORAL COMMUNICATIONS:

***Chierto E,** Castoldi F, Meffre D, Cristinziano G, Borderie D, Sapone F, Etienne F, Rannou F, Massaad C, Jafarian-Tehrani M "Development of novel in vitro models of stretch-induced injury in mouse oligodendrocytes and cerebellar slices" Les journées scientifiques de l'Ecole Doctorale MTCI, Paris, 27-28 June 2016.

***Chierto E,** Castoldi F, Meffre D, Cristinziano G, Borderie D, Sapone F, Etienne F, Rannou F, Massaad C, Jafarian-Tehrani M "Mechanostimulation of oligodendrocytes promotes oxidative stress and changes in myelin proteins" Data Club de l'Unité INSERM 1124, Paris, 7 April 2016.

***Chierto E,** Castoldi F, Meffre D, Cristinziano G, Borderie D, Sapone F, Etienne F, Rannou F, Massaad C, Jafarian-Tehrani M "Development of an innovative model of traumatic brain injury" Lab Meeting, Columbia University, New York City, 8 June 2015.

Llufriu-Dabén G, Meffre D, **Chierto E**, Camand E, Massaad C, Jafarian-Tehrani M. ADAM10 activation: a new pharmacological strategy to promote remyelination? Club de Neuroprotection, 9ème rencontre annuelle, Maison de l'Amérique Latine. Paris, France, 5 Décembre 2014.

presented by myself

POSTER COMMUNICATIONS:

Chierto E, Castoldi F, Cristinziano G, Meffre D, Sapone F, Borderie D, Etienne F, Rannou F, Massaad C, Jafarian-Tehrani M "Mechanostimulation of oligodendrocytes promotes oxidative stress and changes in myelin proteins" Young Researcher in Life Science, Institut Pasteur, Paris, 8-10 March 2016.

Chierto E, Castoldi F, Meffre D, Sapone F, Llufriu-Dabén G, Etienne F, Petit XP, Rannou F, Massaad C, Jafarian-Tehrani M "Stretch-induced injury in oligodendrocytes: alteration in cellular redox status and myelin gene expression" 2eme Journée Scientifique du CICB-Paris, Paris, 11 September 2015. **Winner of the best poster prize.**

Chierto E, Castoldi F, Meffre D, Sapone F, Llufriu-Dabén G, Etienne F, Petit XP, Rannou F, Massaad C, Jafarian-Tehrani M "Stretch-induced injury in oligodendrocytes: alteration in cellular redox status and myelin gene expression" Les journées scientifiques de l'Ecole Doctorale MTCI. Villetaneuse, France 23-24 Juin 2015.

Chierto E, Castoldi F, Meffre D, Sapone F, Llufriu-Dabén G, Etienne F, Petit XP, Rannou F, Massaad C, Jafarian-Tehrani M "Stretch-induced injury in oligodendrocytes: alteration in cellular redox status and myelin gene expression" The Brain Beyond Neurons, Paris, France, 11-12 May 2015.

Chierto E, Castoldi F, Meffre D, Llufriu-Dabén G, Etienne F, Petit XP, Rannou F, Massaad C, Jafarian-Tehrani M "Oligodendrocyte response to stretch-induced injury". 10ème édition du Congrès des Jeunes Chercheurs en Biologie-Prix René Descartes. Institut Imagine, Paris, 8 October 2014.

Llufriu-Dabén G, **Chierto E**, Meffre D, Camand E, Alex Carreté, Massaad C, Jafarian-Tehrani M. Etazolate, an α-secretase activator, enchances remyelination in an *ex vivo* model of demyelination in organotypic cerebellar slices. Les journées scientifiques de l'Ecole Doctorale MTCI. Villetaneuse, France 23-24 Juin 2015.

Llufriu-Dabén G, **Chierto E**, Meffre D, Camand E, Alex Carreté, Massaad C, Jafarian-Tehrani M. Etazolate, an alpha-secretase activator, enchances remyelination in an *ex vivo* model of demyelination in organotypic cerebellar slices. «The Brain Beyond Neurons ». Paris, France, 11-12 Mai 2015.

Llufriu-Dabén G, **Chierto E**, Meffre D, Camand E, Massaad C, Jafarian-Tehrani M. ADAM10 activation as a therapeutic target for the protection of myelin sheaths in an *ex vivo* model of lysolecithin-induced demyelination. 10ème édition du Congrès des Jeunes Chercheurs en Biologie-Prix René Descartes. Institut Imagine, Paris, France, 8 Octobre 2014.

Llufriu-Dabén G, **Chierto E**, Meffre D, Camand E, Massaad C, Jafarian-Tehrani M. ADAM10 activation as a therapeutic target for the protection of myelin sheaths in an ex vivo model of lysolecithin-induced demyelination. Les journées scientifiques de l'Ecole Doctorale MTCI. Université Paris Descartes, Site des Cordeliers, Paris, France, 29-30 Avril 2014.

LIST OF ILLUSTRATIONS

TABLES

FIGURES

LIST OF ABBREVIATIONS

^{14}C	Carbon -14
158N	158N oligodendrocyte cell line
2D	Bi-dimensional space
3D	Three-dimensional space
4-HNE	4-hydroxy- 2-nonenol
8-OHdG	8-hydroxy-2- deoxyguanosine
Aβ	β-amyloid peptide
AD	Alzheimer's disease
ADAM	A Disintegrin And Metalloproteinase peptidases
AhR	Aryl Hydrocarbon Receptor
AIF	Apoptosis- Inducing Factor
AMPA	α-amino-3-hydroxy-5-methyl-4-isoxazolepropionic acid
ANOVA	Analysis of variance
AOPP	Advanced Oxidation Protein Products
Apaf-1	Apoptotic protease activating factor-1
AP-1	Activator Protein 1
APP	Amyloid Precursor Protein
ARE	Antioxidant Response Element
ATG-1	Autophagy-related 1
ATP	Adenosin triphosphate
BBB	Blood-Brain Barrier
BCL	B-Cell Lymphoma 2
BDNF	Brain-Derived Neurotrophic Factor
BMPC	Bone Marrow derived Progenitor Cell
BrdU	Bromodeoxyuridine
BSA	Bovine Serum Albumin
BSMC	Bladder Smooth Muscle Cell
Ca^{2+}	Calcium
CaBP	Calbindin protein

cAMP	Cyclic adenosine monophosphate
Caspr	Contactin associated protein
CAT	Catalase enzyme
CBF	Cerebral Blood Flow
CCI	Controlled Cortical Impact
CDC	Centers for Disease Control and prevention
CDPs	Cysteine-dependent phosphatases
cGMP	Cyclic guanosine monophosphate
Cl^-	Chloride
CM-H2DCFDA	Carboxy-dichloro-dihydro-fluorescein diacetate
CNP or CNPase	2',3'-Cyclic-nucleotide 3'-phosphodiesterase
CNS	Central Nervous System
COX	Cyclooxygenases
CREB	cAMP Response Element-Binding protein
Ct	Cycle threshold
DAI	Diffuse Axonal Injury
DCF	2',7' fluorescent dichlorofluorescein
DCFH-DA	Dichlorofluorescin diacetate
DHE	Dihydroethidium
$DiOC_6(3)$	3,3'-dihexyloxacarbocyanine iodide
DIV	Days *In Vitro*
DMEM	Dulbecco's Minimal Essential Medium
DMSO	Dimethyl sulfoxide
DNA	Deoxyribonucleic acid
DNPH	2,4-dinitrophenylhydrazine
DRG	Dorsal Root Ganglion
DTNB	5,5′-dithiobis(2-nitrobenzoic acid)
DUOX	Dual oxidase
ECM	Extracellular matrix
EDTA	Ethylenediaminetetraacetic acid
EGF	Epidermal Growth Factor
eGFP	enhanced Green Fluorescent Protein
ELISA	Enzyme linked immunosorbert assay
eNOS	endothelial Nitric Oxide Synthase

EPR	Electron Paramagnetic Resonance
ERK	Extracellular signal–Regulated Kinases
ESR	Electron Spin Resonance
ET-1	Endothelin-1
Etaz	Etazolate
FACS	Fluorescence-Activated Cell Sorting
FAK	Focal Adhesion Kinases
Fe^{2+}	Iron
FSC	Forward scatter
GABA	Gamma-aminobutyric acid
$GABA_A$	$GABA_A$ receptor
$GABA_B$	$GABA_B$ receptor
GalC	galactocerebroside
GCS	Glasgow Coma Scale
GDNF	Glia cell-Derived Neurotrophic Factor
GFAP	Glial Fibrillary Acidic Protein
GFP	Green Fluorescent Protein
GPx	Glutathione peroxidase
GR	Glutathione reductase
GSH	Glutathione
GSSG	Glutathione disulphide
GST	Glutathione S-transferase
H_2O_2	Hydrogen peroxide
HDAC	Histone deacetylase
HO-1	Heme oxygenase-1
ICC	Immunocytochemistry
ICP	Intracranial pressure
IGF1	Insuline-like growth factor
IH	Intracranial hypertension
IHC	Immunohistochemistry
IL	Interleukin
iNOS	inducible Nitric Oxide Synthase
IP3	Inositol trisphosphate

JAK	Janus kinase
JNK	c-Jun N-terminal Kinase
K^+	Potassium
KARs	Kainate receptors
Keap1	Kelch-like ECH-associated protein 1
KO	Knock-Out
LDH	Lactate dehydrogenase
LMWA	Low-Molecular-Weight Antioxidants
LN	Laminin
LPS	Lipopolysaccharide
Lyso	Lysolecithin
MAG	Myelin Associated Glycoprotein
MAO	Monoamine oxydases
MAPKs	Mitogen-Activated Protein Kinases
MBP	Myelin Basic Protein
MCT1	Monocarboxylate transporters 1
MDA	Malondialdehyde
Mg^{2+}	Magnesium
mGluRs	Metabotropic glutamate receptors
MOG	Myelin Oligodendrocyte Glycoprotein
MPT	Mitochondrial Permeability Transition
mRNA	Messenger ribonucleic acid
MSC	Mechanosensitive ion channels
mtDNA	Mitochondrial DNA
mTOR	mammalian Target Of Rapamycin
Na^+	Sodium
NAC	N-acetylcysteine
NaCh	Sodium channel
NAD(P)H	Nicotinamide Adenine (Phosphate) Dinucleotide
NF-κB	Nuclear Factor κB
NMDA	N-Methyl-D-Aspartate aspartic acid
nNOS	neuronal Nitric Oxide Synthase

·NO	Nitric Oxide radical
NO	Nitric Oxide
NQO1	NADPH Quinone Oxidoreductase 1
Nrf2	NF-erythroid 2 (E2)-Related Factor 2
NOS	Nitric Oxide Synthase
NOX	NADPH oxidase
NSPC	Neural Stem Progenitor Cells
$^1O_2$	Singlet oxygen
O_2	Oxygen
$O_2\cdot^-$	Superoxide ion radical
·OH	Hydroxyl radical
$ONOO^-$	Peroxynitrite anion
OPCs	Oligodendrocyte Precursor Cells
p38	p 38 mitogen-activated protein kinases
PAC	Pressure Activated Channels
PARP	Poly ADP Ribose Polymerase
PBS	Phosphate-Buffered Saline
PBS-GTA	PBS (0.2% Gelatin, 0.25% Triton-X, 0.1% sodium Azide)
PCR	Polymerase Chain Reaction
PDE4	Phosphodiesterase 4
PDGFR-α	Platelet-Derived Growth Factor receptor α
PFA	Paraformaldehyde
PI	Propidium Iodide
PKB	Protein Kinase B
PLL	Poly-L-Lysine
PLP	Proteolipid protein
PNS	Peripheral Nervous System
PTA	Post-Traumatic Amnesia
PVDF	Polyvinylidene difluoride
RNA	Ribonucleic acid
RNS	Reactive Nitrogen Species
RO·	Alkoxyl radical
ROO·	Peroxyl radical
ROS	Reactive Oxygen Species

RT	Room Temperature
RT-qPCR	Reverse Transcription-quantitative Polymerase Chain Reaction
RTK	Receptor Tyrosine Kinase
S100B	S100 calcium-binding protein B
SAC	Stretch-Activated Channel
SAKC	Stretch-Activated K^+-channel
SAPKs	Stress-Activated Protein Kinase
sAPPα	soluble Amyloid Precursor Protein α
SC	Schwann Cell
SDS	Sodium Dodecyl Sulfate
SEM	Standard Error of the Mean
SGZ	Subgranular zone
SIC	Stretch-Inactivated Channel
SMI-312	Pan-Axonal Neurofilament Marker
SOD-1	Cytoplasmic superoxide dismutase - 1
SOD-2	Mitochondrial superoxide dismutase - 2
SOD-3	Extracellular superoxide dismutase - 3
SRF	Serum Response Factor
SSC	Side scatter
STAT	Signal Transducer and Activator of Transcription
SVZ	Subventricular zone
SV-40	Simian Virus 40
*t*BHP	*tert*-butyl hydroperoxide
TAI	Traumatic Axonal Injury
TBI	Traumatic Brain Injury
TBST	Tris Buffer Saline with 0.1% Tween20
TNF	Tumor Necrosis Factor
TRP	Transient Receptor Potential channels
TUNEL	Terminal deoxynucleotidyl transferase dUTP nick-end labeling assay
WB	Western Blot
Veh	Vehicle
VGCC	Voltage-dependent Ca^{2+} channels

WHO	World Health Organization
WT	Wild Type
YAP	Yes-Associated Protein
ΔΨm	Mitochondrial membrane potential

PREFACE

Traumatic brain injury (TBI) is an insult to the brain, resulting from the application of external mechanical forces. TBI can lead to a heterogeneous pathology, starting from a primary insult that triggers a secondary injury characterized by a complex cascade of metabolic, cellular and molecular alterations. The post-TBI pathophysiological cascades include glutamate excitotoxicity, perturbation of calcium homeostasis, increase in free radical generation or oxidative stress, mitochondrial dysfunction, inflammation, apoptosis and diffuse axonal injury. Among the secondary events triggered, the oxidative stress has a relevant role in the aetiology of progressive neuropathology in TBI and oligodendrocytes and myelin sheaths appear to be particularly sensitive to oxidative stress.

TBI compromises the survival of oligodendrocytes and myelin integrity. The increasing clinical and experimental evidences suggest that demyelination may play an important role in the pathophysiology of TBI showing degeneration of white matter, with loss of myelin and oligodendrocytes. All these studies demonstrated that myelin is early affected after TBI, however, the pathophysiological mechanisms underlying this loss of myelin are not yet well known.

The aim of my PhD project was to characterize the response of oligodendrocytes and myelin sheaths following a traumatic event. To achieve this goal, the development of *in vitro* and *ex vivo* models of traumatic injury was necessary for the analysis and comprehension of this response. Since strain is known to be an important component of TBI leading to tissue damage, we focused our attention in the development of a stretch-induced injury. Numerous studies in the literature were performed on different CNS cell types, but oligodendrocytes have received less attention. Oligodendrocytes are known to be mechanosensitive, there are in fact some studies exploring the effect of a mechanical stimulation on these cells; nevertheless no study has addressed so far the effects of stretch-induced injury in oligodendrocytes.

This PhD dissertation starts with an introduction in order to elucidate and recall some notions that were necessary to present the ideas and the choices we made behind this work. I will start with a presentation of myelin and TBI, followed by a chapter on mechanostimulation with particular attention to the stretch force, followed by an overview on oxidative stress and its importance in TBI, and finally a brief chapter on etazolate, a promising compound for the treatment of TBI. After this introduction I will present my results obtained during three years

of PhD, starting from the development of *in vitro* models of stretch-induced injury, the observed cell response to stretch in three different cell models (158N cell line, the mixed glial primary culture and the oligodendrocyte-enriched primary culture), the development of the *ex vivo* model (cerebellar organotypic culture) of stretch-induced injury and the preliminary results obtained. The last section of results is dedicated to the study of the antioxidant potential of etazolate *in vitro* on the 158N cell line and its protective role in an *ex vivo* model of lysolecithin-induced demyelination on cerebellar organotypic slices.

Finally I will conclude this dissertation with a discussion about the interpretation of results, the conclusions that can be drawn from this work and the future perspectives of this project that will be continued by other students.

This work has been performed at INSERM Unit 1124 at the Faculty of Basic and Biomedical Sciences (Paris Descartes University) and part of the data obtained will be submitted to a peer review for publication (*Scientific Reports*).

INTRODUCTION

CHAPTER 1

Myelin in the central nervous system

The central nervous system (CNS) is the part of the nervous system that includes brain and spinal cord. The brain is contained and protected by the skull, while the spinal cord in continuity with the brain, is protected by the vertebra.

The CNS is composed by grey and white matter. The grey matter consists mainly of neuronal bodies and dendrites, while the white matter consists mainly of axons that are mostly myelinated. White matter owes its name to the light appearance resulting from the lipid content of myelin that gives a white colour. The human brain presents a cortical grey matter on the outer part of cortex, while the inner part is more composed by white matter. There is also a subcortical grey matter composed by different nuclei.

Both tissues, but markedly more the white matter, contain the glial cells as astrocytes, ependymal cells, microglial cells and oligodendrocytes usually referred as supporting cells of the CNS. Their main functions are to surround and insulate one neuron from another and hold them in place, to supply nutrients and oxygen to neurons, to remove and clean up dead cells or debris and in general to maintain an appropriate chemical environment for neuronal signalling.

The relative quantity of white and grey matter varies in different species of mammals, given that white matter constitutes around 15% and 50% of the brain weight in rodents and humans, respectively (Zhang and Sejnowski, 2000).

1.1 Oligodendrocytes

Oligodendrocytes are first discovered in the early 20th century by Pio del Rio Hortega who gave them the name “oligodendroglia” (Del Rio Hortega, 1922). He foresaw a relation between this cells and myelination that was then confirmed in 1924 (Penfield, 1924). Nowadays it is well recognised that myelin, a concentrically laminated membrane structure

that wraps around axons, is formed by oligodendrocytes in CNS and by Schwann cells in the peripheral nervous system (PNS). Each Schwann cells can generate a single myelin sheath around a single axon. By contrast each oligodendrocyte can generate multiple sheaths around multiple axons and the same axon can have sequential myelin sheaths derived from different oligodendrocytes.

Oligodendrocytes undergo different developmental stages before becoming mature myelinating cells. During this differentiation they undergo a morphological transformation, increasing their ramifications or branching, and also sequentially expressing different cellular markers and transcription factors. The different developmental stages of the oligodendrocyte lineage have been well characterized based on the sequential expression of lipid and protein antigens (Baumann and Pham-Dinh, 2001). Oligodendrocytes are classified in i) oligodendrocyte precursor cells (OPCs) that are bipolar, migratory and proliferative cells, expressing Olig1/2, NG2, A2B5, PDGFRα that are subsequently downregulated during differentiation, ii) Pre-oligodendrocytes that develop more branches and express Nkx2.2, NG2, PDGFRα, A2B5, iii) Non-myelinating oligodendrocytes expressing O4, O1, GalC and A2B5 and finally iv) Myelinating mature oligodendrocytes that express MBP, PLP, MAG, CNP, CC1 (APC), GalC, MOG, GSTpi, NogoA. Mature oligodendrocytes form “myelin-like” membranes *in vitro* and myelin sheaths that enwrap axons *in vivo* (Baumann and Pham-Dinh, 2001; Jackman et al., 2009; Simons and Nave, 2016) (**Fig. 1**).

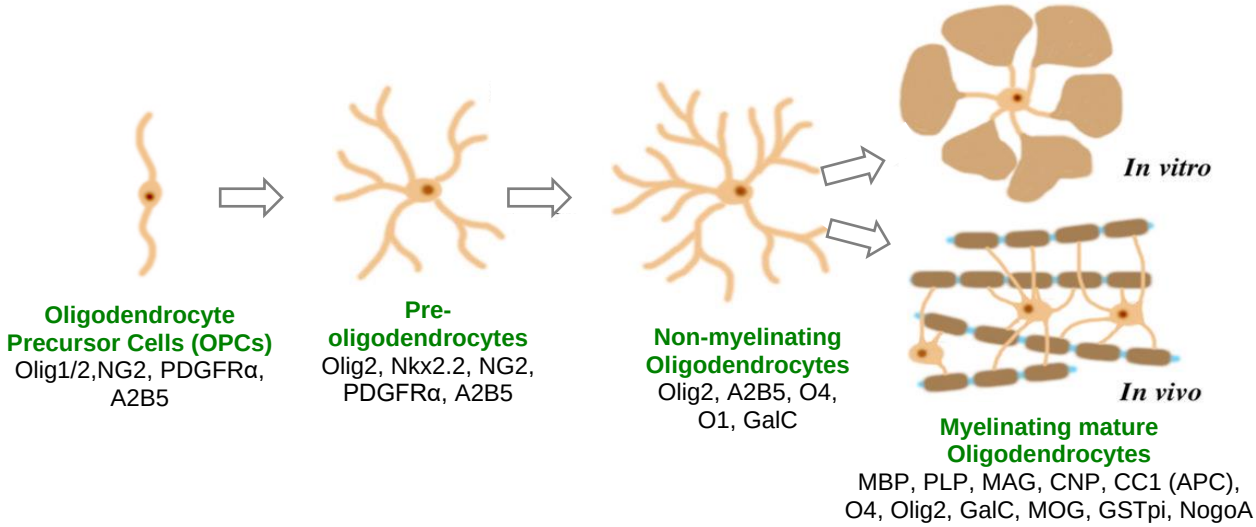

Figure 1: Representation of different developmental stages of the oligodendrocyte lineage. Schematic drawing of morphological and antigenic progression from precursor cells to myelinating mature oligodendrocytes, through pre-oligodendrocytes and non-myelinating oligodendrocytes. The most common markers are shown (adapted from Baumann and Pham-Dinh, 2001; Jackman et al., 2009).

1.2 Myelin sheaths

1.2.1 Myelination

Myelination is a complex sequence of events that comprises different steps starting from proliferation and migration of OPCs, recognition of target axons and axon-glia signalling, differentiation of OPCs into myelinating oligodendrocytes, membrane outgrowth and axonal wrapping, trafficking of membrane components, myelin compaction, and finally node formation (Simons and Nave, 2016).

Some OPCs remain in a precursor state and other OPCs differentiate into mature myelinating oligodendrocytes. During development, myelinating oligodendrocytes derive from OPCs following different waves of proliferation. In rodents, the first oligodendrocytes originate in the ventral forebrain at 12.5 days embryonal days (E12.5) and then from the cortex after birth. The earliest-formed oligodendrocytes, are later eliminated during postnatal development (Kessaris et al., 2006). Myelination in humans also begins prenatally in telencephalic ventricular zone at 5 gestational weeks (Jakovcevski et al., 2009). Once the myelination begins, OPCs must be properly positioned because mature oligodendrocytes appear to have very little capacity to migrate into new positions or to delay myelin synthesis. To ensure that all axons will be property myelinated, an excess of oligodendrocytes is produced and then the excess will be later eliminated by apoptosis (Barres and Raff, 1994; Raff et al., 1993; Trapp et al., 1997).

Nowadays little is known about the selection of axons for myelination (Simons and Lyons, 2013). One hypothesis is that in the absence of any molecular signals, myelin sheaths are preferentially made on the axons of largest and intermediate caliber, and not on the smallest caliber targets (corresponding to <200 nm axons *in vivo*, or <400 nm nanofibers *in vitro).* However it seems that if small-caliber axons express specific signals, oligodendrocytes can recognize them and initiate the myelination, they appear to be controlled more tightly by local axon-oligodendrocyte signals (Simons and Nave, 2016). At the same time, there are evidence showing that the target size alone can determine the initiation of myelination (Lee et al., 2012b). It has been shown that OPCs can initiate myelination on inert polystyrene fibers that mimic axons, suggesting that oligodendrocytes (unlike Schwann cells) do not require axonal adhesion molecules and growth factors to initiate the formation of myelin (Bechler et al., 2015). The authors also showed that oligodendrocytes from different regions generate myelin sheaths of different lengths meaning that precursor cell populations have intrinsic properties that affect myelin sheath lengths in function of their anatomic origin (Bechler et al., 2015).

The formation of myelin sheaths is considered one of the most complex transformations of a plasma membrane. In fact, it includes timely coordinated cell-cell interaction, the extension

and wrapping of the plasma membrane around the axon, and the extrusion of cytoplasm from newly generated multilamellar membrane stacks.

The inner turn, or leading edge, advances underneath of earlier-formed layers and at the same time each layer extends laterally, resulting in different myelin thickness along the length of the growing myelin segment (Hughes and Appel, 2016; Salzer and Zalc, 2016). This implies that the material necessary for the myelin synthesis has to be transported through the developing myelin to the inner layer facing the axon. There is an elaborated system of cytoplasmic channels within compacted myelin that allows to the myelin components to be synthesized at several subcellular localizations and to be transported to the growing myelin sheath at the leading edge.

Its thickness is tightly regulated and correlates with diameter of the axon surrounded. It is usually expressed by the “g ratio” (axon diameter / total fiber diameter). In general, oligodendrocytes generate between 20 and 60 myelinating processes and the final myelin sheath can be composed of 100 or more lamellae or membrane turns (Hildebrand et al., 1993; Matthews and Duncan, 1971; Simons and Nave, 2016).

A myelin sheath cross section observed by electron microscopy shows major dense lines, resulting from the apposition of cytoplasmic leaflets, and light lines called intraperiod lines formed by the apposition of the outer leaflets of the plasma membranes of adjacent oligodendrocytic processes. Myelin in the internodal region is separated from the axon by a gap called periaxonal space (**Fig. 2**).

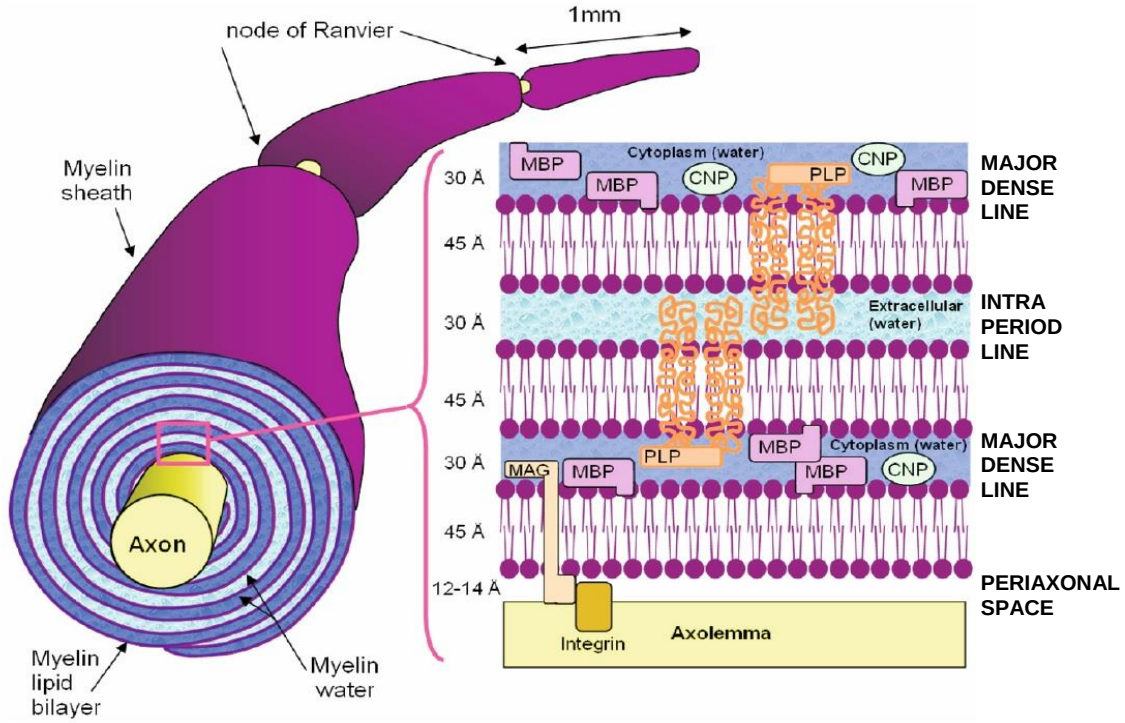

Figure 2: Multilamellar myelin sheath surrounding an axon in CNS. Enlargement shows the major dense line, the intraperiod line and the periaxonal space. The principal myelin proteins are also shown (MBP, PLP, CNP, MAG) (adapted from Laule et al., 2007).

Regarding the timeline of myelination, it is a process that begins prenatally and then persists after birth. It is known that OPCs maintain the capacity of proliferation, migration and differentiation even in the adult CNS. The density and distribution of OPCs is important in adulthood, even if their role is not well elucidated. They can generate new oligodendrocytes under normal condition, in order to replace dying oligodendrocytes and maintain the integrity of myelin sheath (Yeung et al., 2014; Young et al., 2013), to modulate angiogenesis (Yuen et al., 2014). Besides, it seems that OPCs are also required for acquiring new motor skills (Fields, 2015; McKenzie et al., 2014; Xiao et al., 2016). In pathological condition, they can also respond to demyelinating injuries (Hughes et al., 2013; Tripathi et al., 2010) (see § 1.3 for demyelination). There are increasing evidences showing that myelination process continues much later during adulthood than previously thought, up to 8 or 9 months in rodents (Mengler et al., 2014; Rivers et al., 2008; Young et al., 2013), and ≥30 years in humans (Miller et al., 2012; Yeung et al., 2014). The number of mature oligodendrocytes generated in adulthood is unexpectedly large. In fact, around 30% of the total oligodendrocytes in the corpus callosum of 8-month-old mice are generated after 7 weeks of age (Rivers et al., 2008; Zhu et al., 2011).

In the adult, myelin proteins exhibit very little turnover, indicating that the mature myelin sheath is normally quite stable. In humans, myelin is exchanged at high rate but the number of oligodendrocytes in white matter is quite stable. Yeung and collaborators showed, thanks to an analysis of the integration of nuclear bomb test-derived ^{14}C, that the oligodendrocyte generation rate in humans is 0.32% per year, meaning an exchange of 1/300 oligodendrocytes per year, constant from 5 years of age. In mice, it is 100-fold higher from 36.5% to 182% per year, during adolescent and adult stages. These results suggest that in humans, oligodendrocyte turnover contributes only in minimal part to myelin modulation and probably the mature oligodendrocytes are able to carry out and facilitate the neural plasticity (Yeung et al., 2014). In adults, OPCs differentiate and generate a myelin sheath that is slightly different compared to early-born myelin. In fact, the newly generated internodal segment presents a shorter length. This characteristic is also an indicator of post-injury remyelination (Young et al., 2013) (see § 1.3 for remyelination).

The process of myelination has similarities in all species and it occurs in an orderly and region-dependent pattern. Generally for the CNS, it begins in the spinal cord and proceeds rostrally. Within the cerebral lobes, it involves first primary motor and sensory area of the cerebral cortex and corpus callosum (Downes and Mullins, 2013). In humans, the myelin synthesis begins in the peripheral nervous system, brain stem and spinal cord (Inder and Huppi, 2000). Myelination advances at differing rates in different regions of the brain and generally it proceeds from inferior to superior and posterior to anterior, commencing in the occipital lobe followed by the temporal and frontal lobes (Semple et al., 2013; Volpe, 2000).

In the case of cerebellum, a highly myelinated tissue, it has been shown in rat that at 10 days post-natal, the cerebellum is myelinated in all area at some extent, with the 8th cerebellar lobule that is myelinated first (Downes and Mullins, 2013).

Myelinated axons present periodic interruptions in the myelin sheaths. The myelinated regions called internodes are separated by short portions of the axon that are left uncovered, called nodes of Ranvier (**Fig. 3**). Usually internodes present a length of 20 µm –200 µm, while nodes of Ranvier present a length of ~1 µm, corresponding to <1% of the territory of the myelinated axon. Node of Ranvier are critical for neuronal conduction. They are flanked by paranodal junctions, sites of closest apposition between axons and myelinating glia, that in turn are flanked by juxtaparanodal regions. Once the myelin sheaths are synthetized, they go through a process of compaction except at the end of the internodes, at the paranodal loops. The myelin membrane forms septate junctions with the axonal surface due to different adhesion proteins, in particular Caspr and contactin on the axonal side and Neurofascin-155 on the glial surface (Salzer et al., 2008) (**Fig. 3**).

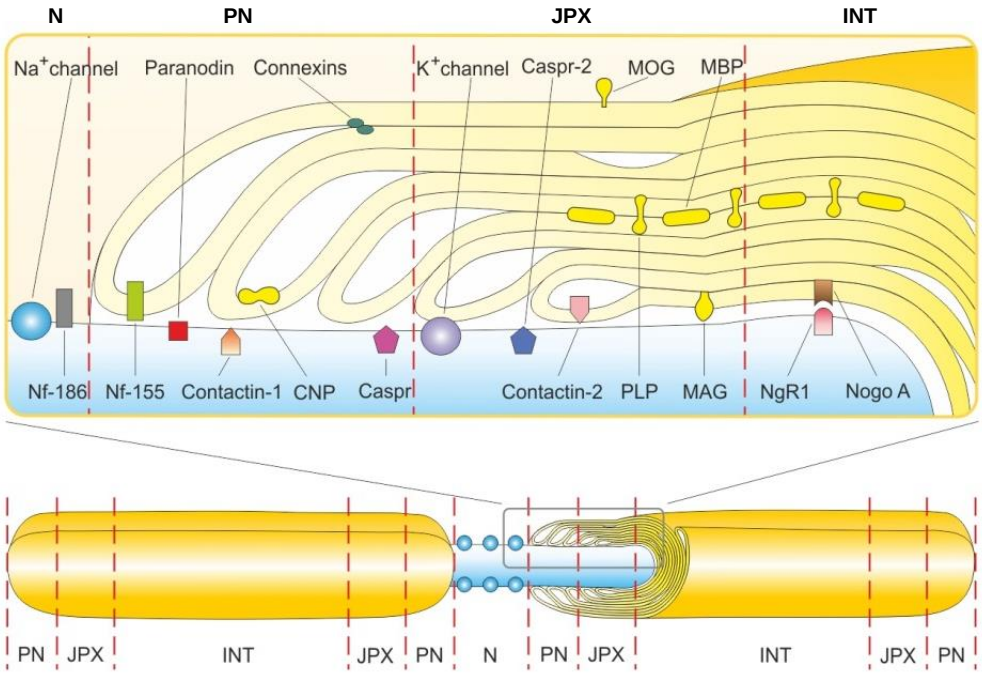

Figure 3: Longitudinal section of a myelinated axon through the node of Ranvier. The nodal (N), paranodal (PN), juxtaparanodal (JPX) and internodal (INT) axon regions are shown. Na^+ channels are located in the nodal region while K^+ channels are in the juxtaparanodal region. Paranodal (Caspr, Contactin-1) and juxtaparanodal (Caspr-2, Contactin-2) proteins are shown tighter with the principal myelin proteins (MBP, PLP, CNP, MAG, MOG). Additional abbreviations: Nogo A: Neurite outgrowth inhibitor A; NgR1: Nogo-receptor 1; Nf-186: Neurofascin 186 (adapted from Podbielska et al., 2013).

The paranodal junctions promote accumulation of voltage-gated sodium channels at the node and separates them from potassium channels in the juxtaparanodes (Salzer and Zalc, 2016). Voltage-gated sodium channels are in fact concentrated at nodes of Ranvier and they

are downregulated along the axon plasma membrane between the nodes; in this way the current flow is spatially restricted to the nodal region assuring a saltatory conduction down the axon. Paranodal junctions function as an electrical seal that limits current leakage underneath the sheath. All these characteristic result in dramatic increases in conduction velocity in myelinated fibers compared to unmyelinated ones. Nevertheless in the CNS, some fiber tracts remain unmyelinated as the dopaminergic axons in the medial forebrain bundle and part of the parallel fibers in the cerebellum.

1.2.2 Structure

Myelin is unique among plasma membrane equivalents because of its high lipid content. In fact, it is composed of ~70% lipids and 30% proteins (Norton and Cammer, 1984; Quarles et al., 2006), while other membranes have typically 30-50% lipids. The different myelin components are synthetized and then transported through the developing myelin to the inner layer facing the axon.

A peculiar characteristic of myelin is the stability; the myelin components have a half-life on the order of several weeks to months. In fact, a study using the pulse chase technique and mass spectrometry to analyse protein synthesis, showed that myelin proteins are among the most long-lived proteins in mouse together with histones, nucleoporins, and lamins (Toyama et al., 2013).

1.2.2.1 Lipids

Various classes of lipids are present in oligodendrocytes and myelin sheaths. They include glycosphingolipids, galactosphingolipids, phospholipids (predominantly sphingomyelin but also phosphatidylcholine, phosphatidylethanolamine, phosphatidylserine and phosphatidylinositol), saturated long-chain fatty acids and cholesterol. The latter is required for myelin sheath assembly. Among glycolipids, the most represented is the galactocerebroside (GalC). Myelin also comprises a high proportion of plasmalogens, an ether phospholipids, with saturated long-chain fatty acids (Chrast et al., 2011). Cholesterol and glycosphingolipids are the principal lipid components of myelin representing the ~27% and 31% of total myelin lipids, respectively (Jackman et al., 2009). Myelin presents ~20% of the fatty acids with hydrocarbon chains longer than 18 carbon atoms (compared with 1% in grey matter) and only 6% polyunsaturated fatty acids (compared with 20% in grey matter) (Simons and Nave, 2016).

Lipids are disposed asymmetrically on the two sides of the plasma membrane with glycolipids, GalC and sulphatide, clustering on the external side and phospholipids clustering on the internal side (Greer, 2013)

1.2.2.2 Proteins

Proteins found in myelin sheaths and oligodendrocytes are typical of this structure and cell type. There are two main proteins that constitute ~80% of myelin proteins: PLP and MBP (Greer, 2013; Nave and Werner, 2014) (**Fig. 4**).

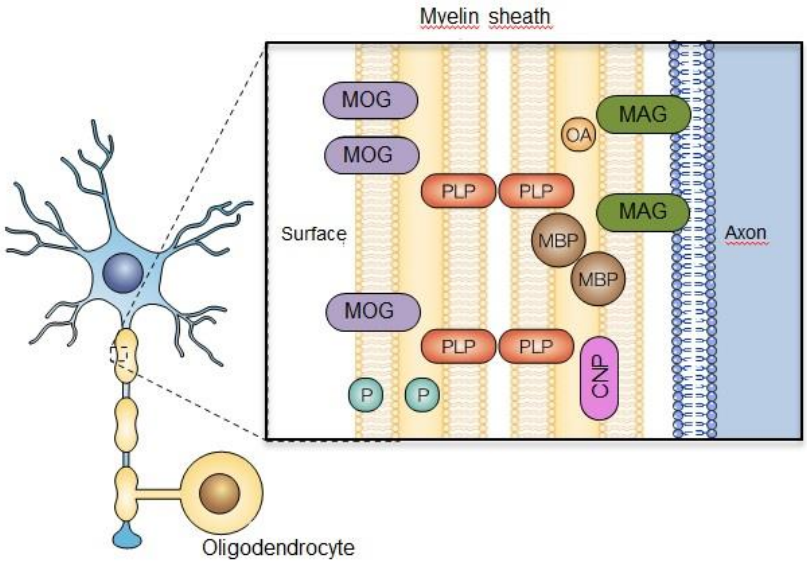

Figure 4: Schematic representation of the distribution of myelin proteins synthesized by oligodendrocytes. The main proteins MBP, PLP, MAG, MOG and CNP are represented in the plasma membrane of a myelin sheath (adapted from Hemmer et al., 2002).

- PLP (Proteolipid Protein) – 26 kDa: PLP and its alternatively spliced isoform DM20, identical to PLP apart from deletion of a 35 amino acids, constitute over 50% of the total protein of CNS myelin. PLP is an integral membrane protein, and it is highly conserved during evolution as human and rodent PLP being identical (Greer, 2013). PLP is a highly hydrophobic protein and it has an affinity for phospholipids and cholesterol. For this reason it is thought to have an important role in myelin compaction and stabilisation, by promoting membrane cohesion at the extracellular side, the intraperiod line (Greer, 2013; Hobson et al., 2002; Simons et al., 2000).

- MBP (Myelin Basic Protein) – from 14 to 21.5 kDa: MBP is the second most abundant proteins in CNS myelin, representing about 30% of the total myelin protein content. There are several MBP isoforms ranging in molecular weight from 14 to 21.5 kDa. The full-length, early-developmental 21.5 kDa splice isoform has a role to promote oligodendrocyte proliferation and differentiation. In fact, its transcript is increased in early myelination in human and mouse and it is present in OPCs in culture. The 18.5-kDa isoform is the most predominant in the adult CNS and it has a role on membrane adhesion (Harauz and Boggs, 2013). MBP is localized at the

cytoplasmic surface in the major dense line and it adheres the cytosolic surfaces of oligodendrocyte membranes together, it is believed to act as a “glue” between the cytoplasmic faces of the myelin membrane leaflets (Aggarwal et al., 2013; Greer, 2013; Quarles et al., 2006). MBP is positively charged, so it can interact with negatively charged phospholipids and also with cytoskeletal components, as actin filaments and microtubules. MBP is thought to have a role in the stabilization of actin fibres in compact myelin (Harauz et al., 2009). Myelin compaction is mediated by MBP progresses from the outside to the inside of the myelin sheath, in fact compaction begins first in the outermost layers of myelin, suggesting that the addition of new layers by the growth of the inner tongue occurs faster than the MBP-mediated compaction (Snaidero et al., 2014).

- CNP or CNPase (2', 3'-Cyclic-Nucleotide 3'-Phosphodiesterase) – 46 and 48 kDa: CNP is a membrane-associated enzyme located at the cytoplasmic side of the myelin sheath. Its amount varies in an age-dependant (immature myelin has more) and species-dependant manner. However, CNP remains a minor protein with ~ 4% of total myelin protein content. CNP at 46/48 kDa is present in the CNS myelin (Greer, 2013; Quarles et al., 2006), and it is commonly used as biochemical myelin marker. However very low levels of CNP are also present in other cell types. CNP is localized in specific regions of myelin sheaths, i.e. oligodendroglial processes, inner and outer tongue processes and lateral loops, and in general in non compact cytoplasm-containing regions of the myelin sheath (Braun et al., 1988; Lee et al., 2005).The precise role of CNP is not clear. It seems to regulate cytoskeletal dynamics. In fact, it can bind cytoskeletal elements such as F-actin and tubulin (Lee et al., 2005; Myllykoski et al., 2012). It seems also to play a role in branching and process formation of oligodendrocytes (Lee et al., 2005). An enzymatic activity has also been reported, the enzyme is active on 2′, 3′-byclic nucleotides (as 2′, 3′-cAMP, cGMP and analogues) which are all hydrolysed to the corresponding 2′-isomer (Lee et al., 2001; Myllykoski et al., 2012; Quarles et al., 2006). CNP appears to be a factor that delays myelin compaction, in fact mouse lacking CNP1 present a faster and extended compaction, while overexpression of CNP1 results in areas of myelin that lack compaction. The equilibrium between CNP and MBP levels seems to regulate the speed of compaction in early development (Gravel et al., 1996; Snaidero et al., 2014).

- MAG (myelin associated glycoprotein) – 100 kDa: MAG is a glycoprotein located at the innermost layer of myelin sheets and it remains in contact with the axonal

membrane. It is a minor protein representing less than 1% of the total myelin protein content (Quarles, 2002). MAG has a single transmembrane domain with glycosylated extracellular part of the molecule, composed of five Ig-like domains and eight or nine sites for N-linked glycosylation, and an intracellular carboxy-terminal domain. In rodents MAG presents two isoforms generated by alternative splicing, which differ in their cytoplasmic domains. The longer isoform (L-MAG) predominates early in development, while the shorter isoform (S-MAG) increases during development to become prominent in adult rodents. MAG is located in the periaxonal membrane of myelin sheath and not in the multilamellar compact myelin. This suggests a role in adhesion and signalling between oligodendrocytes and axon in both directions. MAG is not essential for myelination, since MAG null mice is able to myelinate. Nevertheless, these mice present delayed myelination, abnormalities of myelin sheath as well as degeneration of periaxonal oligodendroglial processes (Lopez, 2014; Quarles et al., 2006).

- MOG (myelin-oligodendrocyte glycoprotein) – 26kDa: MOG is another minor transmembrane glycoprotein (<1% of total proteins), containing a single Ig-like domain and one site for N-linked glycosylation. It is located on the outermost turn of the myelin membrane (Quarles et al., 2006). Its function remains unclear, the surface location suggests a role in signal transduction from the extracellular matrix to oligodendrocytes. MOG null mice develop an apparently normal phenotype. MOG has been extensively studied as a target antigen in autoimmune aspects of demyelinating diseases of the CNS as multiple sclerosis (Correale and Tenembaum, 2006; Greer, 2013)

1.2.2.3 Enzymes associated with myelin

A large number of enzymes have been discovered in myelin (Leeden, 1992), suggesting that myelin is metabolically active in synthesis, processing and metabolic turnover of some of its own components. They have a role in maintaining the structure of myelin sheaths and also in exchanging molecules with the adjacent axon (Morell and Quarles, 1999).

Few enzymes, as the mentioned CNP, are specific to myelin and oligodendrocytes. The other enzymes are not myelin-specific, but they are intrinsic to myelin as different kinases (cAMP-stimulated kinase, calcium/calmodulin-dependent kinase, protein kinase C), proteases and phosphoprotein phosphatases. Myelin enzymes are also involved in the synthesis and transformation of lipids, as steroid-modifying enzymes and cholesterol-esterifying enzymes, and in the phosphoinositide metabolism (Quarles et al., 2006).

Moreover some of these enzymes present in the myelin sheaths are thought to play a role in ion transport as carbonic anhydrase and Na^+/ K^+-ATPase (Quarles et al., 2006).

1.2.3 Function

Myelination of axons is a key vertebrate acquisition to increase conduction velocity, within reasonable space constraints. In fact, the velocity conduction of an unmyelinated axon range from 0.5 to 10 m/s, while in a myelinated axons is up to 150 m/s. This marked increase is due to the fact that the generation of axonal potential is time consuming and in myelinated axons it occurs only at specific points, the node of Ranvier, where the myelin is absent. When an axon potential is generated at one node of Ranvier, the current elicited flows passively thought the myelinated segment, the internode, until the next node is reached. This process is repeated all along the length of the axon and because the current flows across the neuronal membrane only at the nodes this propagation is called saltatory, the action potential "jumps" from node to node (Purves et al., 2001). Then variation in conduction velocity can be found within myelinated axons depending on individual parameters, as the axon diameter, myelin thickness, internodes length (increasing the length increases the speed until a maximum is achieved) and node length (increasing the length results in delayed action potential propagation) (Fields, 2014; Salzer and Zalc, 2016).

Myelin acts as a biological insulator, but it is now clear that it also has other roles, providing trophic support to axon as well as maintaining axonal integrity. It is also required for the maintenance of normal axon transport and long-term survival (Nave, 2010a). Moreover it facilitates the communication between neurons, the myelinating cells and the environment (Nave, 2010a; Nave and Trapp, 2008). Myelination also reduces the energy consumption due to action potential propagation, because action potentials and ion currents are restricted to less than 0.5% of the axon's surface (Nave, 2010b). Because the myelin sheaths cover almost the entirely surface of axons, their access to nutrients in the extracellular milieu is limited to short gaps, the nodes of Ranvier. Astrocytes contact the axons at nodes and they can provide glucose to neurons, but the surface of contact with axon is much greater for oligodendrocytes (Butt et al., 1994a, 1994b).

The myelinating oligodendrocytes can compensate this physical insulation providing themselves a metabolic support for the axon, in fact oligodendrocytes and axons are metabolically coupled (Nave, 2010a). For the maintenance of axon function, the condition of no myelin instead of defective myelin seems to be better, if associated with loss of axon-glia metabolic coupling. Myelin and its wrapped axon can be regarded as a one functional unit not only morphological, but also metabolically coupled. Mature oligodendrocytes use aerobic glycolysis which generates lactate and pyruvate. This glycolysis is sufficient to maintain

oligodendrocytes themselves and the myelinated axons (Bercury and Macklin, 2015; Funfschilling et al., 2012). It has been proved that they can transfer energy metabolites, as indeed lactate and pyruvate, to axons thought monocarboxylate transporters 1 (MCT1) present on the inner membrane of the glial sheath and on the axon. Lactate can in fact replace glucose as source of energy in neurons. MTC1 disruption leads to impaired supply of the local energy and consequent axonal dysfunction and ultimately to neuron degeneration (Lee et al., 2012c; Morrison et al., 2013).

Furthermore, different myelin proteins such as PLP, MBP, MAG or CNP, also perform a trophic function for axons (Griffiths et al., 1998; Lappe-Siefke et al., 2003; Nave, 2010a; Nguyen et al., 2009). In fact, disruption of these oligodendroglial proteins with different functions, leads to a disruption of axonal transport and axonal integrity without affecting myelination (Morrison et al., 2013). Oligodendrocytes may also influence neuronal survival *via* the production of neurotrophic factors, such as the BDNF, neurotrophin-3, GDNF and IGF1.

To mention Simons and Nave “whereas the myelin sheath has been regarded for a long time as an inert insulating structure, it has now become clear that myelin is “alive” and metabolically active with cytoplasmic-rich pathways, myelinic channels, for movement of macromolecules into the periaxonal space” (Simons and Nave, 2016).

1.3 Demyelination and Remyelination

Demyelination is defined as damage and loss of the myelin sheath that surrounds axons. It is a pathological process that can be caused by traumatic events or diseases which induce damage in myelin and oligodendrocytes. Demyelination can be distinguished in primary, if consequence of a direct insult to oligodendrocytes, or secondary, if myelin degenerates as consequence of primary axonal loss (Franklin and Ffrench-Constant, 2008).

In normal conditions, the voltage-gated Na^+ channels are concentrated at the node of Ranvier while voltage-gated K^+ channels are located in the juxtaparanodes allowing a saltatory conduction, as reported above. As a consequence, demyelination leads to a blockade of conduction due to the disruption of the nodes and internodes organisation (**Fig. 5**). The disruption of the node structure leads to a reorganisation of Na^+ channels together with paranodal (Caspr / paranodine) and juxtaparanodal proteins (Caspr2 protein / K^+ channels) that are diffusely distributed on denuded axons (Coman et al., 2006).

Over time, this blockade can be resolved due to an adaptive response that increases and redistributes sodium channels along the axolemma allowing a continuous conduction along the demyelinated segment (Felts et al., 1997) (**Fig. 5,** “late demyelination”).

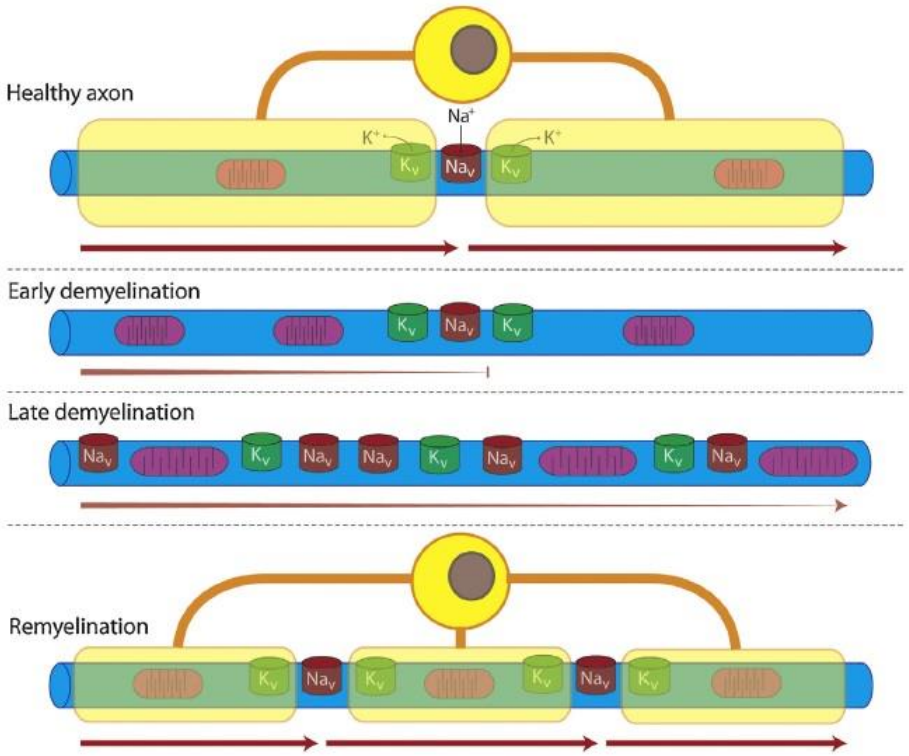

Figure 5: Schematic representation of demyelination and myelination processes in a myelinated axon. Demyelination is a myelin loss that provokes a disruption of the nodal structure with a dispersion of sodium and potassium channels all along the uncovered axon. Remyelination, on the other side, is a regenerative process that restores the nodal structure and the saltatory conduction relocating the sodium and potassium channels in the nodal and paranodal region, respectively. The new myelin presents thinner myelin and shorter internodes compared to the original myelin sheath (Plemel et al., 2014)

However this increase in sodium channels induces a greater sodium influx into the axon with increased metabolic cost for conduction. The elimination of Na^+ excess requires in fact the activity of the Na^+/K^+ ATPase at the expense of ATP. Mitochondria increased in size in demyelinated axons probably to compensate this increased energy demand. If ATP falls below a certain threshold, together with the increase of Na^+, there is a reversal of Na^+/Ca^{2+} exchanger and release of glutamate and other transmitters. This results in Ca^{2+} overload that in turn leads to protease activation, mitochondrial dysfunction, free radical formation and finally axonal loss (Plemel et al., 2014). Demyelination leaves the axon in a vulnerable state, they are in fact more susceptible to damage and prone to axonal degeneration (Irvine and Blakemore, 2008).

Remyelination is a spontaneous regenerative process in which the myelin sheath is restored together with its functions. It is a process naturally regulated in the body and it is very efficient in a healthy CNS, while it can be defective or absent in particular pathological conditions, as multiple sclerosis. Remyelination re-establishes the nodal structure, sodium and potassium channels are relocated in nodes and internodes respectively, restoring the

axonal salutatory transmission (Franklin and Ffrench-Constant, 2008). This process requires the generation of new mature oligodendrocytes derived from adult OPCs. The main sources are the subventricular zone (SVZ) and the subgranular zone (SGZ) in the CNS (Maki et al., 2013; Ortega et al., 2013). Progenitor cells receive and respond to numerous extrinsic and epigenetic factors and they switch from a quiescent state to a regenerative phenotype (Franklin and Ffrench-Constant, 2008). The tissue reconstruction is complete but remyelinated axons present some differences compared to original myelin sheath. In fact, remyelination results in thinner myelin and in shorter internodes with a higher density of mitochondria than normal (Blakemore and Murray, 1981; Gledhill and McDonald, 1977; Zambonin et al., 2011). This can be due to the fact that the new myelin sheaths derived from adult OPCs that, as reported above, elaborate shorter but many more internodes than oligodendrocytes generated during early postnatal life (Young et al., 2013). However a study reported that at late time points of recovery, newly remyelinated axons have comparable internode thickness and length to developmentally myelinated axons (Powers et al., 2013).

CHAPTER 2

Traumatic brain injury

Traumatic brain injury (TBI) is defined as “alteration of brain function, or other evidence of brain pathology, caused by external forces” (Menon et al., 2010). This external assault leads to a complex cascade of events that can results in "visible” disabilities as motor dysfunction or “invisible” disabilities as cognitive problems. In particular, TBI can lead to neurocognitive deficits, as inability to form visuospatial association, poor executive function, impaired attention, and also psychological issues, as depression that is diagnosed in more than 30% of TBI survivors. TBI can also have consequences on the personality, as impulsivity, aggressive behaviour, and on the decision-making capacity (Roozenbeek et al., 2013). The causes of TBI are diverse, given the age of the patients and the geographic zone, including vehicle-related accidents, falls, firearms, sport-related injuries in civilians and explosive blasts and other combat injuries among military population.

2.1 Epidemiology

TBI constitutes a serious public health and socioeconomic problem worldwide given the fact that TBI is a major cause of death and lifelong disability in young population. TBI is considered as a heterogeneous pathology in term of aetiology and gravity. In fact different factors, including diverse comorbidities, age, sex and the genetic predisposition (as for example polymorphisms for the genes coding for apolipoprotein E, different cytokines and the microtubule-associated protein tau) play a role in the TBI outcome (Bennett et al., 2016; Kabadi and Faden, 2014; Maas et al., 2015; Roozenbeek et al., 2013). It is estimated that around 5.3 million people in USA (Langlois and Sattin, 2005) and 7.7 million people in Europe (Tagliaferri et al., 2006) are living with a TBI-related disability. TBI, with an average incidence of 243 per 100 000 people, is among the most frequent neurological disorder worldwide (Rutland-Brown et al., 2006; Tagliaferri et al., 2006). Moreover this raise in the incidence of TBI, principally due to the increasing use of motor vehicles in middle- and low-income countries, shows substantial variation between countries (see review Roozenbeek et al., 2013 for TBI epidemiology). The CDC (Centers for Disease Control and Prevention) reported that in USA 1.7 million people sustain a TBI each year (Faul et al. 2010), while in Europe this number raises up to 2.5 million people (Maas et al., 2015). In high-income

countries, the population affected by TBI shifted towards elderly, given an increase in both the median age and the number of patients over 50 years (Roozenbeek et al., 2013). This can be explained by an improved traffic safety and consequent reduction of traffic accidents which primarily occur in younger individuals, and also by the increased life expectancy and greater mobility in the elderly (Faul et al. 2010).

2.2. Classification

In head-injured patients, TBI is classified as mild, moderate, or severe based on the Glasgow Coma Scale (GCS). The GCS was published in 1974 and measures level of consciousness at the trauma scene or at the emergency department admission considering eye, verbal and motor responses. Patients receive a score between 3, indicating deep unconsciousness, and either 14 (original scale) or 15 (modified or revised scale) indicating a fully awake person (Teasdale and Jennett, 1974). In addition, the duration of loss of consciousness and post-traumatic amnesia (PTA), which comprises the period of time between the incident and the moment when the patient retrieves the memory, represent important parameters that, with the GCS, can help for a better understanding of TBI severity (Key et al., 1993; Saatman et al., 2008).

- Mild TBI: GCS ≥ 13, PTA < 24h, loss of consciousness < 30 min.
- Moderate TBI: 9< GCS <12, 24h < PTA < one week, 30 min < loss of consciousness < 24h
- Severe TBI: GCS ≤ 8, PTA > one week, loss of consciousness > 24h.

In terms of patient survival, the GCS score, especially the GCS motor score, remains one of the strongest predictors of TBI outcome (Steyerberg et al., 2008).
There is also another parameter for TBI classification and it is based on the severity of axonal injury. The external forces in TBI result in damage of white matter tracts that is characterized by the presence of diffuse axonal injury (DAI). The severity of DAI is classified based on the areas of white matter with traumatic axonal injury (TAI), determined from neuropathological evidence of axon damage (Adams et al., 1989) or neuroimaging (Kim and Gean, 2011) (see § 2.4.1 for DAI and TAI). The location and extent of axonal damage can diffuse, increasing the injury severity, which has led to clinical classification as grades of DAI. Grade I DAI involves lesions in areas of grey matter-white matter junctions in the corona radiata. Grade II DAI includes the Grade I area as well as the corpus callosum, with extension from the splenium toward the genu with increasing severity. Grade III DAI involves all the precedent lesion sites with the addition of brainstem tracts (Armstrong et al., 2016a).

2.3 Post-traumatic injuries

Once TBI occurs, a number of short- and long-term detrimental processes begin to affect the brain. The initial insult first leads to a primary injury caused by the mechanical damage from shearing, tearing and/or stretching of neurons, axons, glia and blood vessels. The primary injury includes skull fractures, brain contusions, damage to blood vessels (haemorrhage) and axonal injuries. The primary injury can roughly be defined as focal or diffused. Focal injury occurs in a specific location, while diffuse injury occurs over a more widespread area. It should be noticed that focal and diffuse injuries may both arise following a single TBI and often their diverse combination makes the damage heterogeneous (Andriessen et al., 2010) (**Fig. 6**). Focal brain damage, produced by mechanical forces directly acting on the skulls, can be due to a penetrating head injury in which the skull is perforated, or due to contusion that results in compression of the tissue underneath the cranium at the site of impact (coup) or on the opposite site (contre coup) (Pudenz and Shelden, 1946). The location and severity of impact determine the consequent cerebral pathology and deficits. Focal injury includes cortical or subcortical contusion or laceration as well as intracranial bleeding that lead to the formation of different haematomas as subdural, epidural and intraventricular haematomas (Blennow et al., 2012). Diffuse injuries are caused by stretching and tearing of the brain tissue even without skull fracture or direct impact to the brain surface. They can result from acceleration/deceleration forces common in concussion, high speed motor vehicle accidents and shaken baby syndrome (Andriessen et al., 2010; Gennarelli, 1983; Gennarelli et al., 1982). Diffuse injury includes distributed damage to axons, diffuse vascular injury, ischemic and hypoxic brain injury, and brain swelling. The main form of diffuse injury is called diffuse axonal injury (DAI) (Blennow et al., 2012).

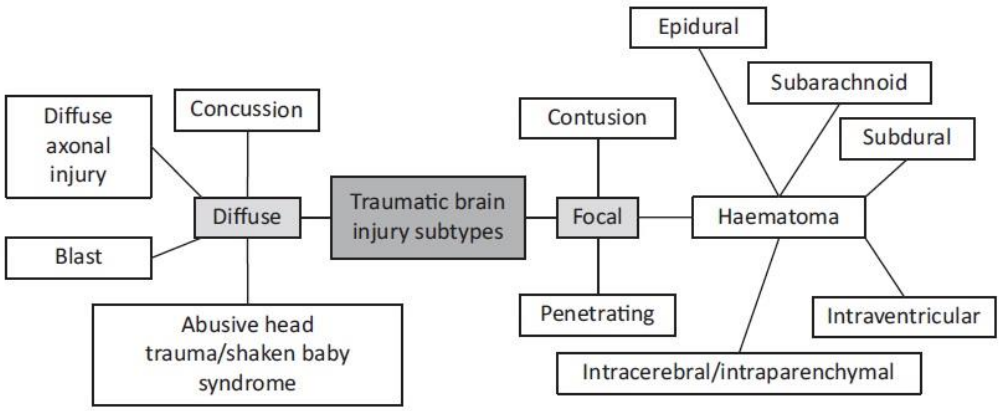

Figure 6: Traumatic brain injury subtypes. There are several different variants of TBI that can be broadly divided into focal and diffuse injuries (Hill et al., 2016).

Brain tissue is heterogeneous in terms of tissue consistency. As a consequence, certain segments of the brain move at a higher rate than others causing shear, tensile and

compressive forces within the brain tissue (Gentry et al., 1988). Studies in biomechanics showed that three principal characteristics are critical for the post-traumatic sequelae: the direction of acceleration, its duration and finally the type of acceleration, as rotational and/or translational. In general, brief acceleration of the brain affects cortical region while sustained acceleration causes the damage at the deeper brain structure (Meaney and Smith, 2015).

2.3.1 Primary injury

Primary injury is the initial injury that occurs at the moment of impact. It involves the physical destruction of intracranial structure and direct damage to brain parenchyma. At the macroscopic level, it includes contusions, hematomas and lacerations, and at the cellular level, depending on the injury severity, it may cause cell death and primary axotomy.

Laceration

Laceration is the most severe form of primary brain injury. It is usually associated with skull fractures in penetrating and perforating head trauma but it may also occur in the absence of skull fracture (Sande and West, 2010). It takes place when the brain tissue is mechanically cut or torn.

Contusion

Contusion is the result of a vascular and tissue injury. It is localised at the surface of the brain involving the superficial grey matter and generally appears as a haemorrhagic lesion. It is distinguished from a laceration since the pia mater remains intact, and from an hematoma, since the blood is intermixed with brain tissue in the case of contusion (Kurland et al., 2012).
It is possible that in addition to blood extravasation from the primary contusion, an additional extravasated blood derives from explicit or latent coagulopathy that provokes delayed bleeding of microvessels ruptured following the primary injury. These lead to a progression of contusion and blood accumulation, producing a mass effect, compressing the adjacent tissues and eventually leading to further ischemia (Kurland et al., 2012).

Haemorrhage

Haemorrhage is by definition a spilling of blood out of the circulatory system. It can be associated with contusion and hematoma, defined as a localised collection of blood. Intracranial bleeding can be intra-axial, inside of the brain, or extra-axial, outside of the brain. There are three types of extra-axial haemorrhages: epidural haematoma, subdural haematoma, and subarachnoid haemorrhage (Sande and West, 2010). In mammals, the

meninges are diverse membranes enveloping the brain, from the skull to brain tissue, as the dura mater, the arachnoid mater, and the pia mater. Epidural haematomas occur between the inner table of the skull and the outer layer of the dura, while subdural haematomas occur between the inner layer of dura and the arachnoid. Finally, subarachnoid haemorrhages are bleeding into the subarachnoid space, located between the arachnoid membrane and the pia mater.

The collection of blood in the subarachnoid, subdural, and epidural spaces may result in brain compression and severe neurologic dysfunction. In particular subarachnoid and intraventricular haemorrhages are typical of severe TBI and they are predictive of bad outcome (Dawodu, 2016; Wardlaw et al., 2002).

Primary axotomy

High-velocity translational and rotational forces act at cellular level provoking a shear and stretch of axons to braking point. Primary axotomy is a mechanical transaction of the axon that occurs immediately after the impact. It can directly induce cell death or partially damage the axon triggering molecular pathways that result in secondary axotomy / axon degeneration (Hill et al., 2016).

2.3.2 Secondary injury

The primary injury triggers a secondary wave characterized by a complex cascade of metabolic, cellular and molecular alterations such as glutamate excitotoxicity, perturbation of cellular calcium homeostasis, increased free radical generation and lipid peroxidation, mitochondrial dysfunction, inflammation, apoptosis and diffuse axonal injury (Xiong et al., 2013). The secondary injury occurs within seconds to minutes after the traumatic insult and can last for days, months, or even years. It can lead to elevated intracranial pressure, blood-brain barrier (BBB) disruption, brain edema, cerebral hypoxia, myelin lesions, ischemia and delayed neurodegeneration (Abdul-Muneer et al., 2015; Lozano et al., 2015; Xiong et al., 2013) (**Fig. 7**).

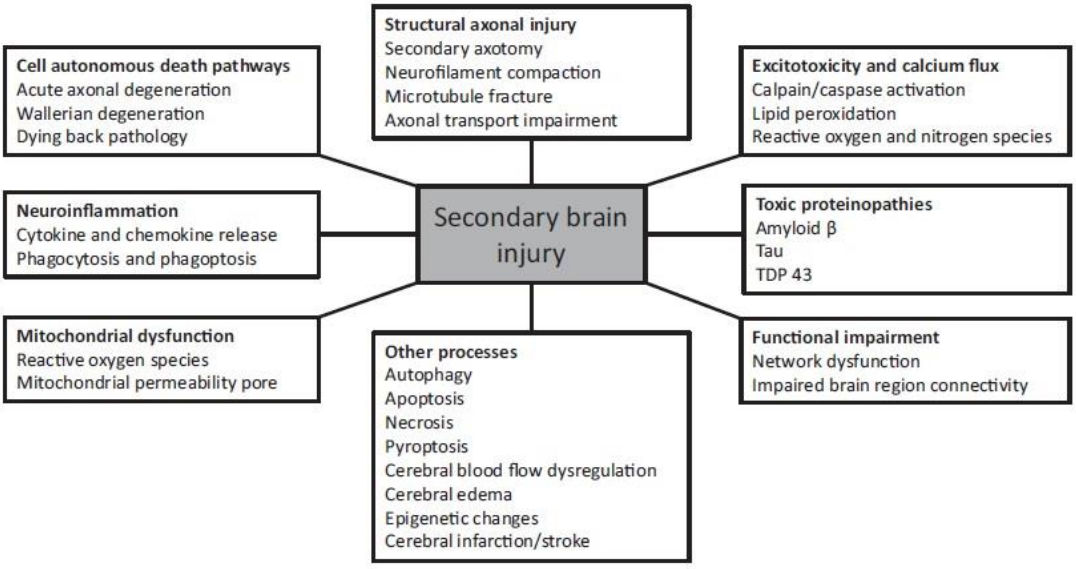

Figure 7: Cellular and molecular changes resulting in secondary brain injury. Following a traumatic brain injury different cellular processes are initiated leading to further cellular dysfunction and death (Hill et al., 2016).

Brain edema

Brain edema is defined as an increase in liquid content in the brain tissue (Pappius, 1974). Two types of edema have been identified as vasogenic or cytotoxic. The vasogenic edema is due to the breakdown of the endothelial tight junctions in the blood-brain barrier (BBB), as a consequence of the primary injury. This provokes BBB dysfunction, allowing an influx of peripheral immune cells and circulating factors within brain parenchyma (Chodobski et al., 2011). The increased BBB permeability leads to an increase in water content and consequent brain edema and higher intracranial pressure, which are directly related to ischemia and further cell death (ElAli et al., 2011; Yang et al., 2013). In the case of cytotoxic edema, an alteration of cellular metabolism occurs that impairs the functioning of the sodium and potassium pumps in the glial cell membrane. This leads to an intracellular accumulation of sodium and by consequence an increase in water content resulting in cell swelling (Unterberg et al., 2004). Edema appears within hours after injury and usually it is located close to the point of impact.

Intracranial hypertension

Intracranial hypertension (IH) is due to the limited space of the intracranial cavity. The constituents of the skull, blood, cerebrospinal fluid and brain tissue, are incompressible and this implies that the total volume must remain constant. Changes in volume of one compartment is accompanied by reciprocal changes of the others, following a relationship known as the Monro-Kellie hypothesis (Mokri, 2001). Modest changes in the brain tissue do not produce a compromising rise in intracranial pressure because the volumes of blood and

cerebrospinal fluid are decreased. However it is not the case when a large extra-cerebral mass appears, as in case of edema or hematoma (Dóczi, 1993). Normal values of intracranial pressure (ICP) are comprised between 5 and 15 mmHg and can vary with age. Values of ICP superior to 20 mmHg are considered pathological and results in IH (Rangel-Castilla et al., 2008). TBI-induced hematomas, haemorrhagic contusions and edema provoke a mass effect, compressing the adjacent tissues and leading to an increase of ICP (Kurland et al., 2012; Marmarou et al., 2000; Rangel-Castilla et al., 2008). In some cases, a surgical decompression is required in order to decrease ICP and prevent death (Kurland et al., 2012).

Cerebral Ischemia

Cerebral ischemia is an insufficient supply of blood to the brain causing a shortage of oxygen and glucose needed for cellular metabolism. This results in cerebral hypoxia and eventually death of brain tissue. It occurs within hours after the primary impact and is one of the major consequences of TBI, present in 91% of cases (Graham et al., 1989). Ischemia usually is considered a focal lesion but it can also involve the whole brain. Under physiological condition, the cerebral blood flow (CBF) is around 52-55 mL/100g/min and in case of ischemia it can decrease to 22 mL/100g/min after 6 hours post-TBI. CBF below the threshold for infarction (CBF < 18 ml/100g/min) is found in one-third of the subject studies (Bouma et al., 1991).

2.4 White matter injury

Previous studies were heavily focused on the effects of TBI on grey matter due to neuronal impairment. However, more recent research shows an equivalent importance of white matter in brain damage following a TBI. White matter atrophy demonstrates significant involvement of white matter in moderate-severe forms of TBI in the acute phase (72h) post-TBI (Herrera et al., 2016) and in patients who survive to a chronic post-injury stage (Bendlin et al., 2008; Green et al., 2014; Herweh et al., 2016; Kim et al., 2008; Sidaros et al., 2009; Tomaiuolo et al., 2012). White matter injury after TBI includes both traumatic axonal injury and myelin pathology that are described below (**Fig. 8**).

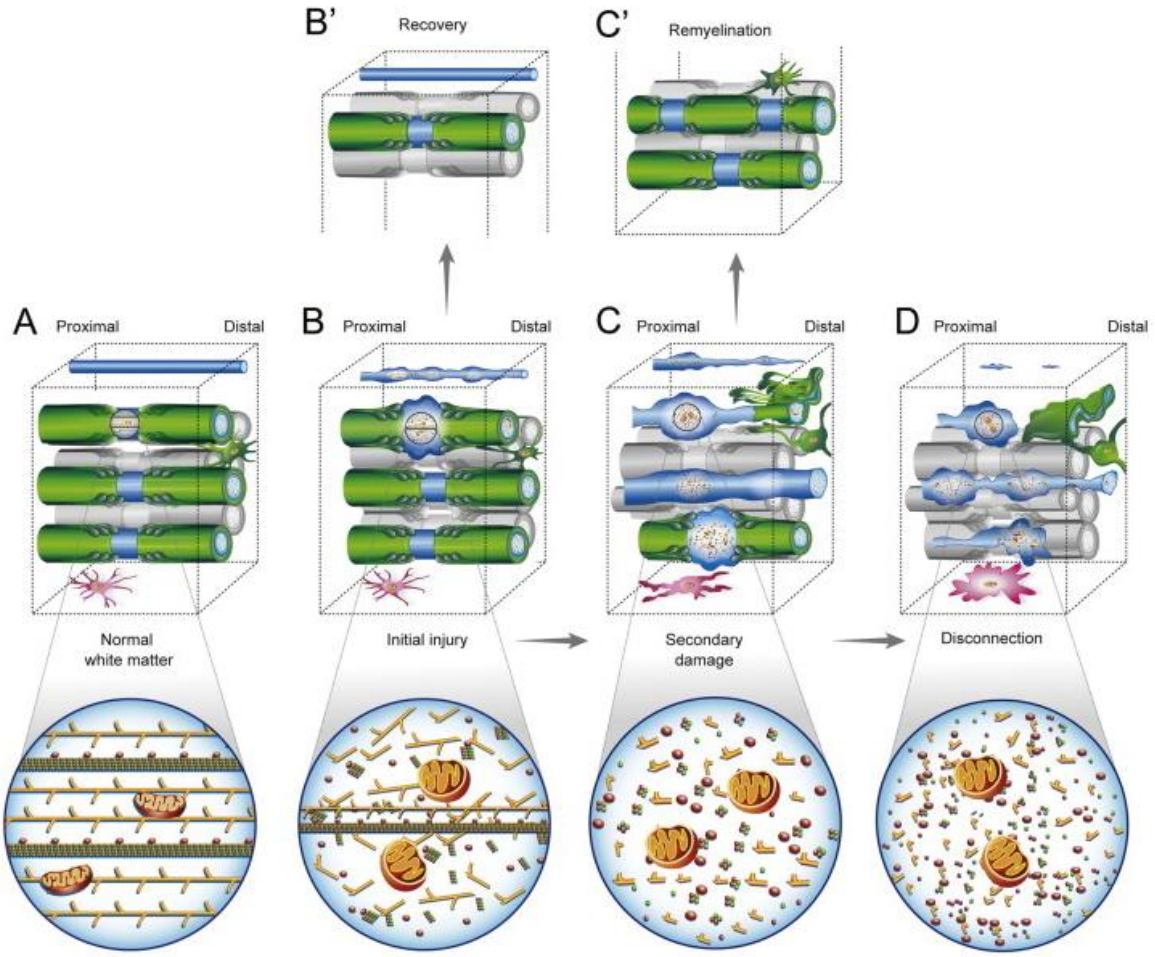

Figure 8: Progression of axon and myelin injury after TBI. A: Normal myelinated and unmyelinated fibers are presented (axons in blue and myelin sheaths in green). Oligodendrocytes and microglial cells are presented in green and rose, respectively. Enlargement shows normal cytoskeletal elements (microtubules transporting vesicles and neurofilaments) and mitochondria. B-D: Progression of axon and myelin pathology after TBI with axon degeneration and disruption of associated myelin accompanied by neuroinflammation (microglial activation). Axon damage can lead to irreversible fragmentation and disconnection. Enlargement shows breakdown of cytoskeletal elements and mitochondrial swelling. Myelinated axons can recover from the initial reversible phase of axon damage (showed in B') or also undergo remyelination after myelin loss (showed in C') with shorter myelin internodes typical of this process (Armstrong et al., 2016b).

2.4.1 Traumatic or diffuse axonal injury

One of the most common and severe consequences of TBI is the traumatic or diffuse axonal injury (TAI or DAI, respectively). Axons can grow up to ten thousand times the volume of their cellular body. They have an elongated structure that makes them vulnerable to mechanical injury. The term “diffuse axonal injury” was first introduced by Adams and colleagues to describe a clinical and pathological syndrome (Adams et al., 1989). But this term is itself a misnomer because technically the distribution of this injury is not “diffuse” but “multifocal” (Johnson et al., 2013), so it is more appropriate to refer this pathology as TAI (**Fig. 9**).

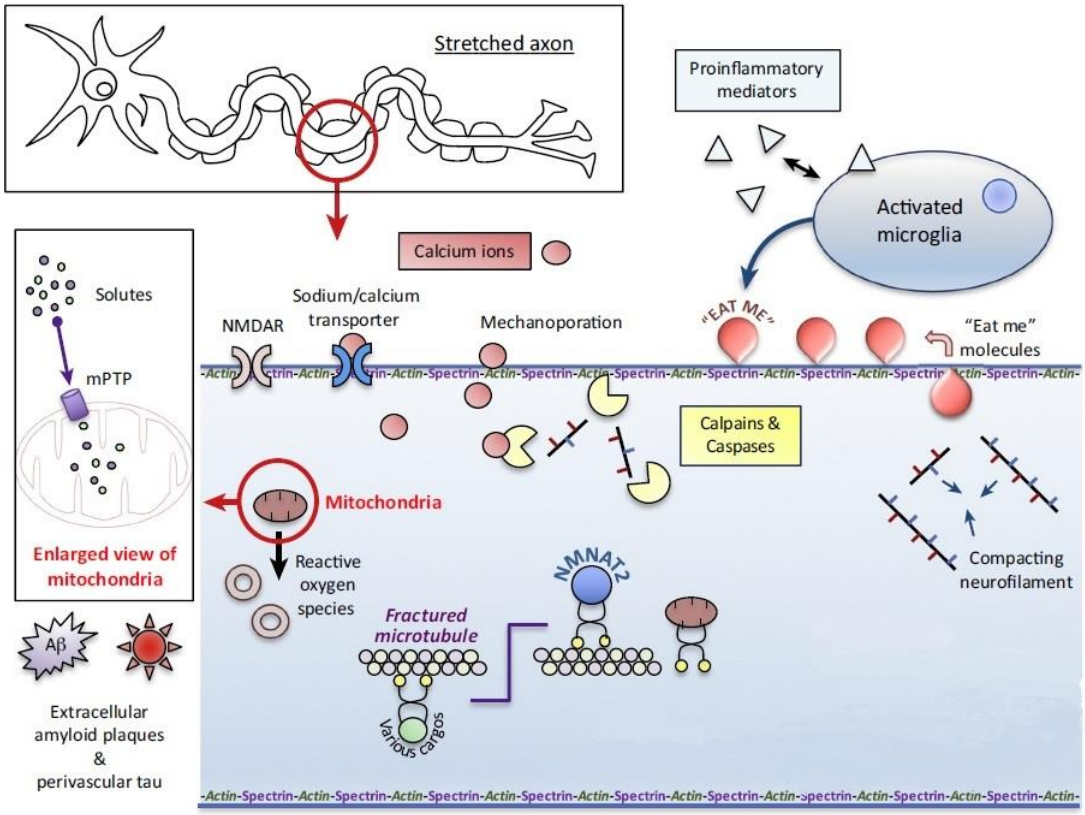

Figure 9: Molecular mechanisms in traumatic axonal injury (TAI). Mechanical stretch gives an ondulated aspect to stretched axons and different injury pathways are activated. Membrane mechanoporation and opening of exchange channels lead to an increase of intracellular calcium that activates calpains that, in turn, degrades structural proteins. Microglial cells are also activated producing pro-inflammatory cytokines. Calcium increase also induces generation of mitochondrial permeability pore (mPTP), with consequent solute influx and mitochondrial swelling and dysfunction. Reactive oxygen species are also generated resulting in oxidative damage. Neurofilaments tend to compact and microtubules are fractured leading to impairment of axonal transport with failure to deliver nicotinamide mononucleotide adenylyl transferase 2 (NMNAT2) and subsequent Wallerian degeneration. “Eat-me” signals as phosphatidyl serine are externalized and may initiate phagoptosis of damaged neurons by microglia. Abbreviations: NMDA receptor, a glutamate ionotropic receptor (adapted from Hill et al., 2016).

This injury reflects the selective vulnerability of white matter axons to damage induced by mechanical forces at the moment of the impact, it preferentially involves the corpus callosum, internal capsules, brainstem and cerebellar peduncles (Adams et al., 1982, 1989). White matter axons are vulnerable to injury under certain circumstances. During normal head movement, strain deformation is not detrimental for the brain tissue. In fact, axons are compliant and ductile under stretch, they come back to their original length and shape when stretch is removed (Dennerll et al., 1989). However during a trauma, they behave differently becoming vulnerable (Di Pietro et al., 2013; Smith and Meaney, 2000; Smith et al., 1999). The threshold of maximum elasticity is in fact exceeded resulting in damage. The degree of the force applied and the duration influence the magnitude of axonal damage. It has been estimated that brain injury occurs at strain between 10% and 65% at strain rates of

approximately 10-50 s^{-1} (LaPlaca and Thibault, 1997; Morrison et al., 1998; Morrison III et al., 1998). Nonetheless the primary axotomy remains relatively rare, in the majority of cases it is observed as a “secondary axotomy” (Christman et al., 1994).

After TBI, axonal degeneration is due to different subsequently events starting from alteration of axonal transport, axonal swelling followed by secondary disconnection and finally Wallerian degeneration. Wallerian degeneration is a process consequent to a nervous fiber cut or crushed, in which the distal part of the axon separated from the neuron's cell body degenerates (Kanamori et al., 2012). Interruption of axonal transport results in accumulation of transported materials and axonal swellings within hours following the trauma. These zones of axonal swelling, called “axonal viscosity” appear isolated or periodically along the length of an intact axon (Tang-Schomer et al., 2012). Instead, a large single swelling is an “axonal bulb” or “retraction bulb”, which represents a complete axonal disconnection. It is widely recognised as hallmark of TAI (Johnson et al., 2013; Oppenheimer, 1968). Several immunohistological analyses were performed to identify the material accumulated in these regions and the amyloid precursor protein (APP) has been identified in damaged axons within 2h following injury (Grady et al., 1993; Gultekin and Smith, 1994; Sherriff et al., 1994). APP accumulation is recognised as the gold-standard for the identification of axonal pathology (Gentleman et al., 1993; Sherriff et al., 1994).

The regions of axonal swelling give to the axons an ‘undulated’ morphology that is typical of a stretch injury (Hånell et al., 2015; Tang-Schomer et al., 2012). These undulations have been linked to microtubule dysfunction. In fact, microtubules have a micro elasticity nature and they are susceptible to breakage because, if rapidly stretched, they become the stiffest portion of the axon. These fractured microtubules lead to the axonal swelling and axonal transport impairment (Tang-Schomer et al., 2010, 2012). Moreover, calcium homeostasis disruption triggers microtubule disassembly and calpain-mediated proteolytic degradation of cytoskeletal proteins as neurofilament proteins (Barkhoudarian et al., 2011; Giza and Hovda, 2001; Tang-Schomer et al., 2010). TAI is also reported in the case of mild TBI (Bazarian et al., 2007; Mayer et al., 2010; Miles et al., 2008; Oppenheimer, 1968) and the severity of TAI is proportional to the deceleration forces (Elson and Ward, 1994).

2.4.2 Myelin injury

Myelin is a major component of white matter. However the implication of myelin and its integrity after TBI remain poorly understood. Depending on the injury severity, TBI exhibits heterogeneous damage with different implications for the survival of oligodendrocytes and for myelin repair (Armstrong et al., 2016a). It is proved that myelin plays an important role in axon vulnerability following white matter injury. Unmyelinated fibers are more susceptible to

damage than myelinated ones (Reeves et al., 2005, 2012; Staal and Vickers, 2011). This is confirmed by the fact that along myelinated fibers, the axon initial segment, which is not myelinated, is the primary site of axotomy. Moreover mechanical stretch appears to initially damage axons at the nodes of Ranvier between myelin sheaths and in the adjacent paranodal regions (Maxwell, 1996; Maxwell et al., 1991; Reeves et al., 2012; Sun et al., 2012a).

Myelinated axons that are subjected to primary or secondary axotomy undergo Wallerian degeneration as described above. The myelin sheaths of the distal part collapse but this process of myelin degradation is relatively slow because the BBB limits myelin opsonisation and the oligodendrocytes contribute in a very small part to myelin clearance (Vargas and Barres, 2007). This slow clearance can impair the repair, since myelin debris contain myelin associated molecules that inhibit axonal regeneration (Geoffroy and Zheng, 2014) and also can inhibit the differentiation of precursor cells that are necessary for myelin repair and remyelination (Baer et al., 2009; Kotter et al., 2006). Moreover, myelin debris can stimulate the microglia activation in the white matter promoting neuroinflammation (Clarner et al., 2012).

Demyelinating insults contribute to axonal degeneration and functional impairments. However, demyelination may be followed by a spontaneous regenerative remyelination that is critical to restore electrical impulse conduction and protect axons from degeneration or further injury (Miron et al., 2010; Redford et al., 1997) (**Fig. 8**). Experimental animal models of CNS demyelination indicate that remyelination is mediated by newly generated oligodendrocytes derived from OPCs (Gensert and Goldman, 1997). Astrocytes and microglia are critical for this process: microglia contribute to the clearance of debris and both cell types participate in creating a permissive environment for remyelination (Alizadeh et al., 2015; Kotter et al., 2001; Loughlin et al., 1997; Zhang et al., 2006). Following a TBI, the biosynthesis of new myelin sheaths can also result in abnormal structures designed as excessive myelin figures. This excess of myelin can be the consequence of a dysregulation of myelin-axon signalling leading to an aberrant production of new myelin sheaths necessary for the remyelination (Armstrong et al., 2016a; Mierzwa et al., 2015; Sullivan et al., 2013). Mierzwa and collaborators found that excessive myelin figures are increased from 3 days to 2 weeks post-TBI and that they are positively correlated with axon degeneration (Mierzwa et al., 2015).

Controversies are described in the literature in the context of demyelination following TBI. A study reported that a moderate axonal strain does not induce an immediate or progressive demyelination. In fact, axons are still myelinated at 48 h post-injury, in spite of significant increase in the proportion of degenerated MBP over time (Staal and Vickers, 2011). This is in accordance with another study reporting only minimal alteration of myelin, with no loss of it,

after mild fluid percussion injury in mice, despite the presence of injured axons, which were subsequently progressing to secondary degeneration (Spain et al., 2010). However, there are increasing clinical and experimental evidences suggesting that demyelination may play an important role in the pathophysiology of TBI. A degeneration of white matter with a persistence of neuroinflammation has been observed years after a single TBI in humans, in particular a reduction in the corpus callosum thickness with survival >1 year post-injury was reported (Johnson et al., 2013). This is in agreement with another study where a clear reduction in the volume of the corpus callosum is observed after ~1 year after TBI and this reduction becomes more pronounced after ~8 years indicating that the neural degeneration after TBI continues long after the head trauma (Tomaiuolo et al., 2012). Histochemical analysis of rat brains following fluid percussion injury showed a loss of myelin staining in association with white matter atrophy up to 1 year post-injury (Bramlett and Dietrich, 2002). Furthermore, apoptotic oligodendrocytes have been observed acutely and chronically following TBI in humans. Such loss of oligodendrocytes is known to be a significant factor underlying demyelination after injury (Caprariello et al., 2012). Studies in human and rats demonstrated also that TBI induces widespread myelin loss and oligodendrocyte apoptosis that are accompanied by an increase in the number of OPCs (Flygt et al., 2013, 2016). A study revealed that degenerating axons are distributed among intact fibers in the corpus callosum from 3 days to 6 weeks post-TBI in mice. The intact axons exhibit significant demyelination at 3 days post-injury and evidence of remyelination at 1 week. Persistent neuroinflammation and astrogliosis are also reported in the area of axon and myelin pathology (Mierzwa et al., 2015).

Works in demyelinating diseases as multiple sclerosis have shown that demyelination leaves intact axons more vulnerable to subsequent damage whereas remyelination protects axons and leads to recovery of function (Bruce et al., 2010; Irvine and Blakemore, 2008).

All these data demonstrated that myelin is early affected after TBI, however, the pathophysiological mechanisms underlying this loss of myelin are not yet well known. Some clinical magnetic resonance imaging studies have shown a direct relationship between white matter injury and reduced functional connectivity within important brain networks and impaired cognitive function following TBI (Kinnunen et al., 2011; Sharp and Ham, 2011). A recent study based on multimodal neuroimaging, revealed that patients within 7 days following moderate TBI and presenting higher levels of complaints show a concomitant reduction of structural connectivity and cortical surface area. Alterations of white and grey matter are localised in similar brain regions and they are correlated to each other (Dall'Acqua et al., 2016). Overall, the preservation of the myelin sheaths, either reducing demyelination or accelerating remyelination is considered a new therapeutic approach in the context of TBI (Shi et al., 2015). Imaging studies demonstrate that the cerebellum, rich in myelinated fibers,

is often affected after TBI, although this region has received little attention in evaluating the mechanisms of TBI (Park et al., 2007). Parallel clinical and experimental studies have confirmed that the mechanisms of injury extend to cerebellum (Biran et al., 2012; Mouzon et al., 2012; Staffa et al., 2012). A recent study analysed the cerebellar white matter in the acute-phase in moderate TBI patients and they found that the white matter integrity is altered in the middle cerebellar peduncle and the pontine crossing (Wang et al., 2016).

2.5 Pathophysiological mechanisms following TBI

As discussed above, the primary injury triggers a secondary wave of biochemical cascades and metabolic changes that can leads to progressive neurodegeneration and delayed cell death, exacerbating the damage from the primary injury (Kabadi and Faden, 2014; Sullivan et al., 1999). The secondary injury is characterized by pathophysiological mechanisms as excitotoxicity, mitochondrial dysfunction, oxidative stress and inflammation (**Fig. 10**).

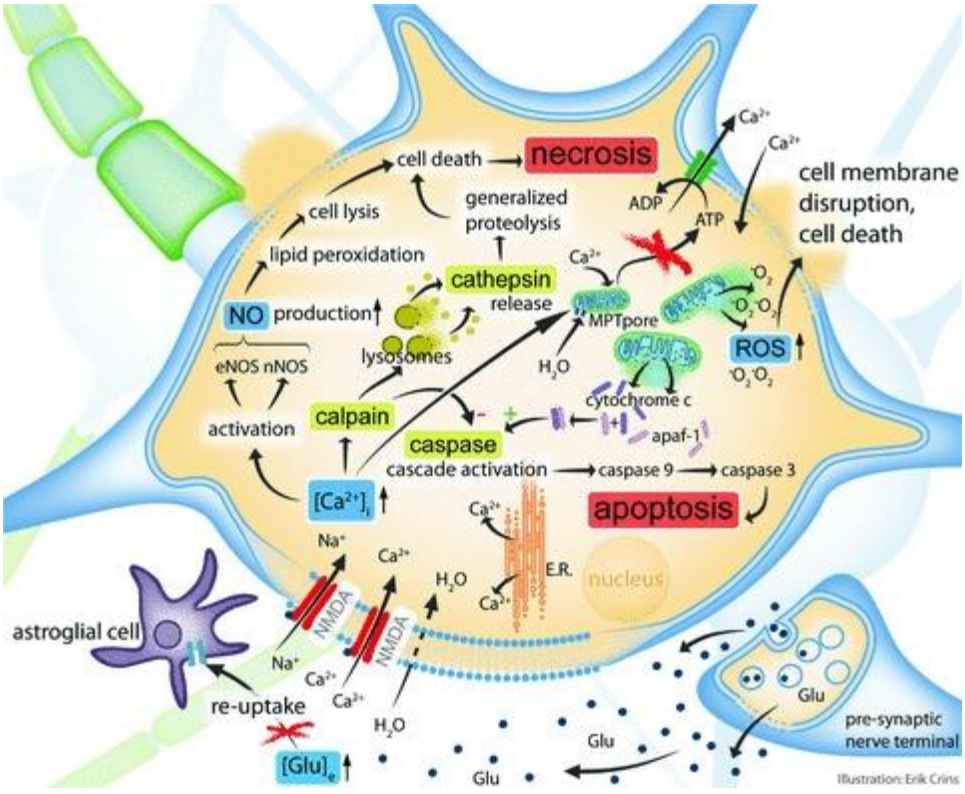

Figure 10: Simplified pathophysiological molecular and cellular processes after focal TBI. A traumatic brain injury results in increased extracellular glutamate with subsequent Ca^{2+} influx that, in turn, initiates several intracellular cascades (four are shown here). Left upper corner: The activity of NOS enzymes (eNOS and nNOS) is increased resulting in nitric oxide production, consequent lipid peroxidation and eventually cellular necrosis. Left middle part: following calcium increase calpain activity is augmented resulting in lysosomal membrane rupture, cathepsin release and cellular necrosis. Right upper corner: Intracellular calcium increase causes mitochondrial calcium overload and alteration of mitochondrial membrane permeability. Mitochondrial dysfunctions lead to ROS production, release of cytochrome-c into the cytoplasm thus provoking cellular damage and death. Glu: Glutamate; [Glu]e: extracellular glutamate concentration; NMDA: N-methyl-D-aspartate aspartic acid; E.R.: endoplasmatic reticulum; $[Ca^{2+}]i$: intracellular Ca^{2+} concentration; nNOS: neuronal NOS; eNOS: endothelial NOS; MPT: membrane permeability transition; ATP: adenosine triphosphate; ADP: adenosine diphosphate; ROS: reactive oxygen species; apaf-1: apoptosis activating protein-1; $^{\cdot}O_2$: oxygen radical (Andriessen et al., 2010).

All these processes contribute to neurological deficits separately but, at the same time, they are simultaneous worsening the progressive outcome of TBI (Lozano et al., 2015; Schmidt et al., 2005).

2.5.1 Excitotoxicity

As a consequence of TBI, a depolarization of nerve cells takes place resulting in uncontrolled and excessive release of excitatory neurotransmitter glutamate. This cascade of pathological events is called excitotoxicity. It has been shown that extracellular levels of glutamate are elevated in both experimental and human TBI. In particular, glutamate can raise up to 50-fold following focal parenchymal contusion in patients (Bullock et al., 1995, 1998). It has been shown that raised levels of glutamate are toxic and are associated with worse outcome in head injured patients (Bullock et al., 1998; Chamoun et al., 2010; Koura et al., 1998). Glutamate is released by pre-synaptic vesicles after depolarisation, but it can also leak through damaged cell membrane. The normal system of glutamate re-uptake by astrocytes can be compromised or even abolished aggravating the situation.

Excitotoxic cell death is deeply linked to the downstream calcium ion influx modulation and dysregulation. In fact, excessive extracellular glutamate initiates a massive influx of Ca^{2+} and Na^{+} into neurons and glial cells (Choi, 1987). Glutamate is able to bind different ionotropic receptors as the N-methyl-D-aspartate aspartic acid (NMDA) receptors, the α-amino-3-hydroxy-5-methyl-4-isoxazolepropionic acid (AMPA) receptors and the kainate receptors (KARs) and the metabotropic glutamate receptors (mGluRs) over activating the ion channels responsible for Na^{+} and Ca^{2+} influxes (Faden et al., 1989; Park et al., 2008).

Moreover, it has been shown that there is an acute increase of intracellular calcium primary derived from internal stores, as endoplasmatic reticulum. This results in depolarization of the neuronal membrane activating voltage-dependent Ca^{2+} channels (VGCC) which also results in an additional increase of Ca^{2+} influx (Choi, 1987). As a consequence, a passive movement of water across the membrane produces axonal swelling, a typical hallmark of axonal injury.

High cytosolic Ca^{2+} alters different cellular processes as protein phosphorylation, microtubule construction and protease activation resulting in loss of neuronal function. Calcium-dependent enzymes are activated, especially calpain-1 and -2 that are non-lysosomal cysteine proteases (Pike et al., 2000). In normal condition, their basal activity is low, and they are involved in cell signalling and plasticity (Saatman et al., 2010). In response to calcium influx, consequent to axonal injury, calpains move from the cytosol to the plasma membrane where they cause widespread proteolysis of different molecules, as those located in the membrane, adhesion and structural proteins including cytoskeletal proteins (Yang et al., 2013). Calpains (Kampfl et al., 1996; Saatman et al., 1996), and to a lesser extent caspase-3 (Pike et al., 2000), irreversibly cleave αII spectrin, a neuronal membrane-associated

scaffolding protein, into fragments of various molecular weights which are used as biomolecular markers of this process. It has been suggested that calpain activation is also associated with lysosomal membrane disruption leading to leakage of hydrolytic lysosomal enzymes, like cathepsin, that will cause severe damage to the cytoplasm and eventually cell death by necrosis (De Duve and Wattiaux, 1966; Yamashima, 2004; Yamashima et al., 2003). Calpains can cause long-term deficiencies in axonal transport and plasticity resulting in persistent dysfunctions.

Calcium alterations can also induce the generation of nitric oxide, a free radical with detrimental effects, by nitric oxide synthase (NOS), the isoforms that are calcium-dependent enzymes (Cherian et al., 2004; Griffith and Stuehr, 1995).

In addition, the alteration in calcium and other ions increases the activity of membrane pumps in order to restore ionic balance, but this leads to increased glucose consumption, depletion of energy stores, impaired oxidative metabolism with consequent anaerobic glycolysis and lactate production which provoke acidosis and edema (Barkhoudarian et al., 2011; Giza and Hovda, 2001).

2.5.2 Mitochondrial dysfunction

To counteract the increase of intracellular Ca^{2+} concentration, mitochondria work as calcium buffer, they absorb the ions to maintain homeostasis (Nicholls, 1985; Sullivan et al., 1999). However after TBI the calcium load becomes too large from excitotoxicity and the function of mitochondria, as oxidative phosphorylation processes, becomes impaired (Xiong et al., 1997). The mitochondrial membrane permeability transition (MPT) pores, associated with the inner membrane, are calcium-dependent and are activated with an excess in calcium ions resulting in membrane depolarization (Bernardi, 1992; Kristal and Dubinsky, 1997; Mbye et al., 2008; Scorrano et al., 1997). Without a membrane potential the mitochondria are not able to produce ATP and the energy production of the cell is compromised (Lifshitz et al., 2003), as it has been demonstrated in human mitochondria after focal TBI (Verweij et al., 2000). The decrease of ATP production is even more dangerous if considering that energy demand becomes higher shortly after TBI (Marklund et al., 2006). Moreover, the increased calcium concentration in mitochondria leads to passive water entry resulting in osmotic swelling (Lifshitz et al., 2003; Singh et al., 2006), that exacerbate the already compromised mitochondrial functions (Singh et al., 2006; Xiong et al., 1997).

It has been reported that, in patients with severe TBI, the severity of mitochondrial impairment assessed by high-resolution proton magnetic resonance spectroscopy, correlates with TBI outcome (Signoretti et al., 2008).

Compromised mitochondria become one of the principal sources of ROS, leading to oxidative stress and lipid and protein damage (Maciel et al., 2001; Singh et al., 2006). Moreover, the pro-apoptotic protein cytochrome-c, located between the inner and outer membranes of the mitochondria, is released into the cytoplasm resulting in cell apoptosis (Büki et al., 2000; Krajewski et al., 1999; Robertson et al., 2007).

With mitochondrial breakdown, toxins and apoptotic factors are released into the cell, activating the caspase-dependent apoptosis (Cheng et al., 2012). Mitochondrial dysfunctions are involved in both necrosis and apoptosis (Kruman and Mattson, 1999) (see below § 2.5.5 for details on cell death).

2.5.3 Inflammation

A complex cascade of inflammatory response is initiated following TBI, with release of cytokines, chemokines and growth factors by different cell types (Wang et al., 2013). In particular, a rapid activation of microglia/macrophages, cells responsible of the immune defence in CNS, is reported (Loane and Byrnes, 2010; Venkatesan et al., 2010). Resident microglia are rapidly activated and peripheral macrophages are mobilized to the site of injury initiating the release of effector molecules and recruitment of other immune cells (Amor et al., 2010; Jin et al., 2012; Lozano et al., 2015). Microglia present two different phenotypes, M1 and M2, depending on the microenvironment in which they are activated. The M1 phenotype is promoted in presence of lipopolysaccharide and interferon γ and it is characterized by the synthesis of pro-inflammatory cytokines and low levels of anti-inflammatory cytokines (Hernandez-Ontiveros et al., 2013; Kumar and Loane, 2012). In contrast, some cytokines as IL-4 or IL-13 are able to induce the M2 phenotype (Chhor et al., 2013) that reduces the inflammatory response decreasing the synthesis of pro-inflammatory cytokines and increasing the production of anti-inflammatory cytokines as IL-10 and the transforming growth factor 1β (Hernandez-Ontiveros et al., 2013; Kumar and Loane, 2012).

Wang and collaborators found that microglia appears as M2 phenotype early after a TBI (peak at 5 days after injury), but it decreases rapidly thereafter in favour of a shift to M1 phenotype. The number of M1 microglia increases in cortex, striatum and corpus callosum during the first week and remains elevated until at least 14 days after TBI. They also reported that the severity of white matter injury is correlated with activation of M1 phenotype (Wang et al., 2013). Another study in humans reported persistent inflammation, assessed by the presence of reactive microglia, and white matter degeneration for many years after a single TBI (Johnson et al., 2013).

The inflammatory response is also accompanied by the infiltration of neutrophils, monocytes, and lymphocytes across the BBB (Fluiter et al., 2014). These inflammatory cells secrete

prostaglandins, free radicals, pro-inflammatory cytokines, and other inflammatory mediators that, in turn, up-regulate the expression of other pro-inflammatory chemokines and cell adhesion molecules in the endothelial cells of the BBB (Bellander et al., 2001; Fluiter et al., 2014). This leads to an increase of the permeability of the BBB resulting in an amplification of the inflammatory response (Chodobski et al., 2011). Sustained microglial activation and inflammation also produce neurotoxic molecules and free radicals, promoting other mechanisms of secondary cell death (Hernandez-Ontiveros et al., 2013; Kabadi and Faden, 2014).

2.5.4 Oxidative stress

There are abundant evidences showing a considerable increase in the production of ROS following TBI, resulting in oxidative stress that has a significant role in the aetiology of secondary injury after TBI (Abdul-Muneer et al., 2015; Cornelius et al., 2013; Mendes Arent et al., 2014). Free radicals, collectively called as reactive oxygen species (ROS) and reactive nitrogen species (RNS), are generated during normal physiological processes. Under physiological conditions, the endogenous defence system is able to prevent the formation or to scavenge free radicals, protecting tissues from oxidative damage (Mendes Arent et al., 2014). Under pathological conditions, as trauma, the excessive production of free radicals can oxidize macromolecules, such as DNA, proteins, carbohydrates, and lipids (Valko et al., 2006). Mitochondrial dysfunction, excitotoxicity mediated by glutamate, alteration of blood flow, ischemia are only some reasons contributing to this oxidative stress (Rodríguez-Rodríguez et al., 2014) (see § 4.7 for details on oxidative stress and TBI).

2.5.5 Cell death

TBI can induce a “primary” or “secondary” cell death, where the former refers to immediate cell death due to physical trauma and disruption of cellular membrane and the latter refers to a delayed cell death in surrounding and/or distant region from the point of impact (Stoica and Faden, 2010). There are numerous pathways and pathophysiological processes involved in cell degeneration and death. These processes can differ depending on the injury type and the time course of the injury and they may also converge. To give some examples, cell death mechanisms include caspases and pro-apoptotic members of Bcl-2 family (apoptosis), JNK and ATG orthologs (autophagy), ERK2 (paraptosis, a type of programmed cell death), PARP/AIF (PARP/AIF-dependent death), calpains/cathepsis (calcium-dependent death) and JNK (oncosis, a type of accidentally cell death caused by failure of ionic pumps) among others (Stoica and Faden, 2010). Most of these mechanisms take place simultaneously, they are redundantly activated. Cell death can occur *via* different mechanisms. Below the

principals are described as necrosis, apoptosis and autophagy. Necrosis is considered as a passive process, energy independent, associated with loss of membrane integrity and organelle and cell swelling. Apoptosis is, on the contrary, an energy dependent process characterized by cytoplasmic and nuclear condensation and fragmentation. It only occurs in presence of ATP, and it requires functional mitochondria (Ankarcrona et al., 1995; Liu et al., 1996). In tissue with extensive mitochondrial dysfunction and disruption more necrosis will be found. During apoptosis there is no membrane rupture and no inflammatory response as compared to necrosis. Autophagy literally means "self-devouring", it is a process that involves lysosomal degradation of proteins and organelles that are unnecessary or dysfunctional. Under physiological conditions, autophagy increases during nutrient deprivation, playing a protective role *via* generation of amino acids and energy (Bredesen, 2008).

Calpains are the key enzymes as regulators in the process of calcium-dependent cell death. They can be involved in both necrosis and apoptosis (Ashkenazi and Dixit, 1998; Wang, 2000). It has been suggested that the type of cell death is associated with intracellular calcium levels. In fact, low Ca^{2+} levels seem to favour apoptosis, while high Ca^{2+} would promote necrosis (Choi, 1995; Zipfel et al., 2000).

Caspases are cysteine aspartic acid-proteases activated by proteolytic cleavage and they play a central role in the apoptotic cell death. The morphological changes typical of apoptosis (membrane budding, chromatin condensation and fragmentation) requires caspase-dependent cleavage of specific substrate. Caspase can be activated through two different pathways, intrinsic and extrinsic. The intrinsic pathway involves the mitochondrial outer membrane permeabilization and consequent release of cytochrome c in the cytosol. There the cytochrome c forms a complex with the apoptosis-inducing factor (Apaf-1) to activate in turn caspase-9 and caspase-3 (Yakovlev and Faden, 2001). The extrinsic pathway is mediated by cell surface death receptors, involving TNF and FAS receptors (Ashkenazi and Dixit, 1998; Wang, 2000). All necrosis, apoptosis and autophagy have been described following TBI (Andriessen et al., 2010; Ankarcrona et al., 1995; Clark et al., 2008; Rink et al., 1995; Stoica and Faden, 2010). Necrosis is found in the early post-traumatic period, while apoptosis is observed in a later period, within hours and days after injury (Wong et al., 2005). Autophagy is observed between 2 and 48 h after TBI with a peak at 24 h post-TBI (Clark et al., 2008; Lai et al., 2008).

All the pathophysiological mechanisms described above are interconnected and create a vicious circle. In fact, excitotoxicity results in activation of necrotic and apoptotic processes, that lead to an increase of inflammation and of oxidative stress that, in turn, elicit additional cell death and so forth worsening the situation. Damage associated with primary brain injury

can only be prevented. Therefore clinical efforts are focusing on the prevention, recognition and treatment of secondary brain injury. The slow progression of secondary cascades can be in fact targeted for therapeutic interventions (Xiong et al., 2013).

2.6 *In vitro* and *ex vivo* experimental models of TBI

Many *in vivo, ex vivo* and *in vitro* models of brain injury have been previously reported. The *in vivo* TBI models imitate the natural process of injury and the most well known are the controlled cortical impact (CCI), the weight drop/impact acceleration and the fluid percussion models (Cernak, 2005). The *in vivo* models have the advantage of mimicking the actual event of head injury but, due to the complexity of the *in vivo* situation, accessibility to the tissue of interest becomes limited (Morrison et al., 1998). In order to understand the response of individual cells as a result of the injury inflicted, it is important that the cells are isolated from the systemic effects which may inhibit or alter their individual response (Cargill and Thibault, 1996).

As we already saw the brain is encapsulated into a rigid skull and the mechanical response to an injury would be a combination of stretch, compression and shear, with no presence of change of volume (Morrison et al., 2006). All the *in vivo* models combine and consider the holistic effect of TBI to the brain, but not specific effects of stretch, compression and strain. Thus, not all observations are possibly done on *in vivo* models, more focused and repeatable models are necessary. *In vitro / ex vivo* models can be used in order to evaluate the response of specific cell types in well-controlled and environmentally isolated experiments (Geddes-Klein et al., 2006). Moreover these models are considered an alternative to animal testing, so they raise less ethical issues.

The *in vivo*, ex vivo and *in vitro* models have to be considered complementary, since they provide different information and they allow the analysis of different aspects of TBI.

The principal *in vitro* / *ex vivo* models are described as follows:

Transection

The transection models re-create *in vitro* the primary axotomy that can be found for example following penetrating injuries. The axotomy can be reproduced at the level of a single-cell (Chuckowree and Vickers, 2003) or on a cell monolayer using a plastic stylet or blades (Mukhin et al., 1997, 1998; Tecoma et al., 1989). The model of cell monolayer exposes the surrounding cells to secondary effects such as excitotoxicity and glial activation. These models of transection can be useful to perform high-throughput therapeutic discovery and

testing. However it has to be considered that primary axotomy is relevant only for a small percentage of brain injuries.

Compression

This model reproduces a focal injury using weight-drop and impactor methods (Sieg et al., 1999). The severity of the injury can be controlled modifying different parameters as the shape of the impactor and force, depth, duration of the impact. In slices of tissue the impact generate a region of primary injury directly below the impactor and a secondary injury in the surrounding tissue (Church and Andrew, 2005).

Hydrostatic pressure

These models are based on a cell injury chamber where a static or transient pressure is applied in order to induce an injury (Murphy and Horrocks, 1993; Shepard et al., 1991). Brain tissue is nearly incompressible so, under hydrostatic conditions, the brain deformation is very small. Therefore concerning the static models, extreme values of pressure are needed to achieve a cellular response. Dropping a weight onto a sealed chamber produces instead transient pressure waves that reproduce the time curse of pressure changes during a closed head TBI. The waves pass through the tissue, inducing a deformation which results in cellular injury (Panickar et al., 2002).

Fluid shear stress

The application of fluid shear forces provokes a cellular deformation that reproduces the fluid shear stress of brain during impact. Any fluids, liquids or gases, moving along solid boundary will produce a shear stress on that boundary. These models can reproduce a fluid shear on a monolayer, using a rotating disk positioned above cells (LaPlaca and Thibault, 1997) or also on single cell discharging air or media on individual axons (Chung et al., 2005) (**Fig. 11a**).

Shear strain

Shear deformation is one of the major initiator of closed-head TBI. Shear strain can be applied on brain slices (Bottlang et al., 2007) and on hydrogel construct containing brain cells in 3D cultures (LaPlaca et al., 2005). The magnitude and deformation rate are controlled and can be adjusted to obtain different grade of injury severity (**Fig.11b**).

Stretch injury models

Stretch is known to be an important component of TBI. In fact a major force causing injury of nervous tissue is rapid tissue deformation and strain, or, more simply stretch (Ellis et al., 1995). Different stretch devices have been developed for both cells and organotypic slices cultured on stretchable substrates. The idea is to deform the substrate to indirectly deform the adherent sample (**Fig.11c**). As for shear strain, the magnitude and deformation rate can be adjusted to obtain different grade of injury severity (see chapter 3 on mechanostimulation, § 3.1).

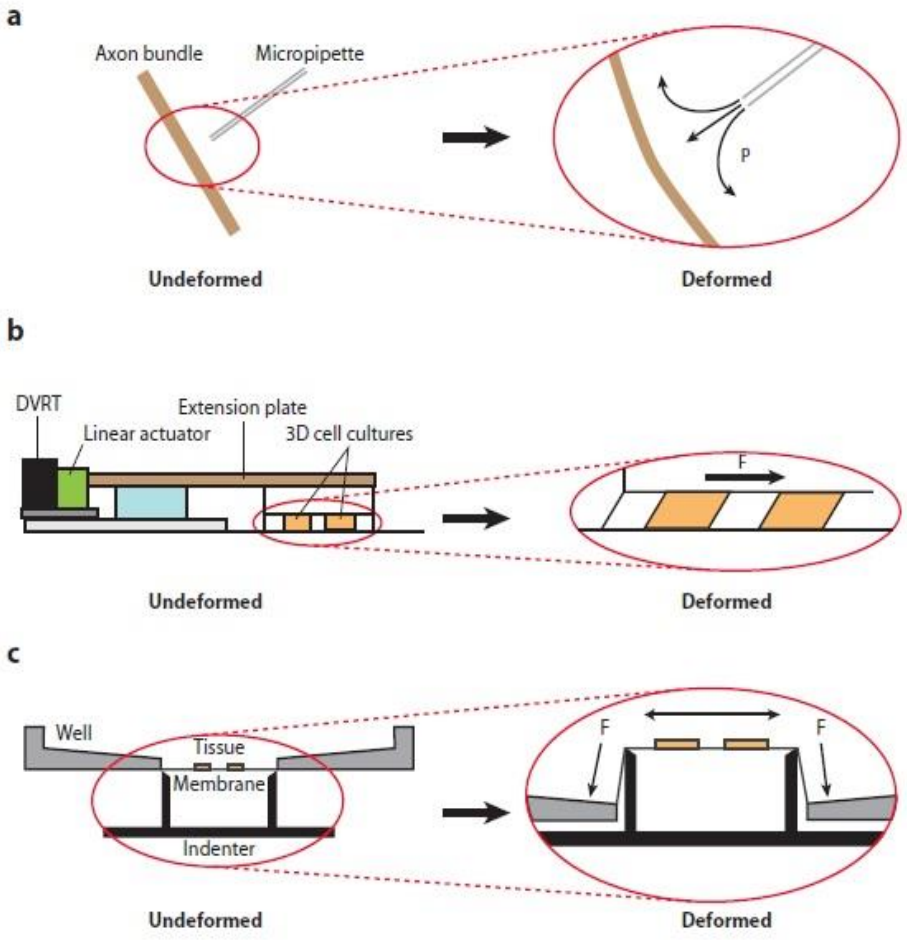

Figure 11: Schematic illustrations of *in vitro* / *ex vivo* models of TBI. (a) Axonal bundles are deformed by a pulse of fluid directed by a micropipette. (b) A simple shear is applied to a hydrogel construct containing brain cells in 3D culture. The magnitude and rate of deformation are under feedback control. (c) Equibiaxial stretch of cultures is achieved through deformation of the culture substrate by pulling the clamped membrane over a hollow cylinder. The magnitude and rate of the applied strain are under feedback control. F: force; P: pressure (Morrison et al., 2011)**.**

The *in vitro* models can be performed on immortalized cell lines or dissociated primary cultures (Morrison et al., 1998, 2011). The immortalized cell lines are easy to procure and manipulate, well characterized and generally not expensive. However the disadvantage is

that the process of immortalization can modify some intracellular cascades thus altering the normal cellular response to injury. Primary cultures are derived from mechanical or enzymatic dissociation from brain tissue. It is possible to analyse the effect of injury on single cell type or even the interaction between different cell types in case of mixed culture. One disadvantage is that cells are harvested from embryonic or postnatal tissue and the age at the harvest can significantly affect the cellular response. Moreover, cells are cultivated on monolayer which is different from the *in vivo* construct.

The *ex vivo* models are realized on brain slices in acute preparations or organotypic culture (Morrison et al., 1998, 2011). These models have the advantage of maintaining the three-dimensional architecture of the *in vivo* structure with heterogeneous cell populations as well as the local connectivity between them. Acute preparations are fresh explant of brain tissue. Injury models have been performed on acute preparation for rat cortex and hippocampus and guinea pig cerebellum. There are no restrictions on the age of the harvested tissue but the slices cannot be conserved more than 8 h. The organotypic culture instead can be maintained in culture for extended period, more than 7 days, allowing a recovery from the trauma of excision but the slices usually derived from animals younger than 11 days postnatal.

The utility of an *in vitro* / *ex vivo* model is evaluated on the ability to reproduce the *in vivo* process following a TBI. The main goal in TBI research is to identify new therapeutic strategies. In general, if a compound provides benefit both *in vitro* / *ex vivo* and *in vivo*, there is a high chance that the same cascades are activated and the model can be considered relevant (Morrison et al., 2011).

CHAPTER 3

Mechanostimulation in the central nervous system

Mechanostimulation can be defined as a stimulation induced by a mechanical force and mechanosensitivity is the capacity of responding to a mechanical stimulation which is common to a wide variety of cells in many different organisms, ranging from bacteria to mammals. Mechanical stress can modulate physiological or pathological processes at the molecular, cellular, and systemic level (Kamkin and Kiseleva, 2005).

Various form of force application transmitted either directly to the cell membrane or *via* the surface receptors elicit a biological response. Some responses can be observed in a matter of second, for example mechanically gated channels could be activated within milliseconds latencies (Hamill and Martinac, 2001). Other responses need more time to be observed but can last for hours after the initial event such as gene expression, protein synthesis or morphological changes (Goldmann, 2014).

Movement can be defined by the basic physical components (mass × acceleration) of a segment or body. The mass × acceleration of a body segment is defined as force (force=mass × acceleration, Newton's second law of motion). The application of force over a given area of tissue during movement results in stress to the tissue “stress=force/area”, where force may be applied in any direction such as tension, shear, and compression (Tipler, 1982). Although movement is a major source of physical stress on tissues, other forces generated inside (e.g., isometric muscle contractions) and outside (e.g., gravity) of the body may also contribute to tissue stress. The range of stresses to which different tissues are physiologically exposed varies a lot. Cytoskeletal structures are involved in the sensing and transmitting of external forces. How cells respond to mechanical stress depends not only on specific molecular sensors and signalling pathways but also on their internal mechanical properties that determine how the cell deforms when subjected to forces (Goldmann, 2014).

In order to use force as a signal and coordinate cell behaviour in tissues, cells must sense different types of stress or strain (Davidson et al., 2009). The transduction of a mechanical signal, or mechanotransduction, resembles classical biochemical signal transduction. A specific mechanical force, which can be distinguished by its magnitude, orientation, and/or

frequency, must be recognized by specific mechanosensing machinery (Chanet and Martin, 2014). Several molecules or molecular complexes can directly respond to physical stress or strain by changing conformation or macromolecular assemblies. Classic examples are the unfolding or stretching of molecules or the opening of ion channels under mechanical forces that would transduce a signal to downstream-signalling pathways (Hoffman et al., 2011) (**Fig 12**).

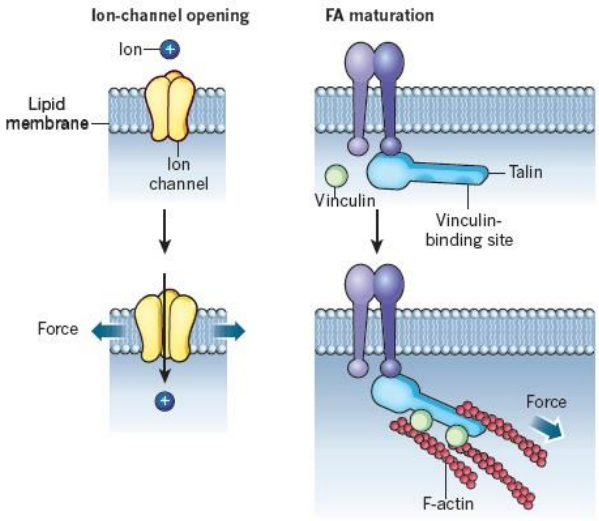

Figure 12: Switch-like models of mechanotransduction. Cells are mechanically integrated structures, in which the extra cellular matrix (ECM) and actin cytoskeleton are connected by integrins and focal adhesion (FA) proteins. Forces can be applied directly through the ECM and transmitted through the cytoskeleton to mechanosensitive components, such as FAs, to mediate cellular response to a given force. Many ion channels are integrated within this network. An applied force induces conformational change of an ion channel, a common mechanism of mechanotransduction, and membrane tension can cause ion-channel opening. Talin connects the integrin cytoplasmic tail to F-actin; tension on talin exposes vinculin-binding sites, and the subsequent binding of vinculin (green) reinforces the linkage (Hoffman et al., 2011).

The primary target for mechanical stimulation is the plasma membrane of the cell, which can respond to different physical stress changing the open state probability of mechanosensitive ion channels. These mechanosensitive channels include stretch-activated channels (SAC) (Bass et al., 2003; Franco-Obregón and Lansman, 2002; Martinac and Hamill, 2002; Yamaguchi, 2004), stretch-inactivated channels (SIC) (Chakfe and Bourque, 2001; Franco-Obregón and Lansman, 2002; Martinac and Hamill, 2002; Schumacher et al., 2000) and pressure-activated channels (PAC) (Kohler et al., 2001a, 2001b; Martinac et al., 1987). Besides the channels described above there are stretch-activated K^+-channels (SAKC), that can be Ca^{2+} sensitive (Filipovic and Sackin, 1992; Kawahara, 1990; Sackin, 1987) or Ca^{2+} insensitive (Kirber et al., 1992; Pacha et al., 1991). Thus, by acting on ion channels in the plasma membrane, mechanical stress can elicit a multitude of biochemical processes, both

transient and long-lasting, inside a cell (Kamkin and Kiseleva, 2005). In addition, mechanical constraints that alter cell geometry can lead to rearrangements of the cytoskeleton, as stress fiber formation and orientation (Vignaud et al., 2012) (see § 3.2).

3.1 Factors that influence the cellular response to applied strains

Nearly all cells in the human body are subjected to mechanical forces due to tensile stress and strain imposed at the tissue level. The stretch of cell cultures is usually expressed in terms of strain, named the Lagrangian strain, and the calculation is defined as "Strain = (l-L)/L", where l= final length and L= initial length. In another word, the strain is defined as the ratio of the total deformation of a given body to its original form or configuration (i.e. membrane strain of 20% denotes that membrane has been deformed 20% relative to its original conformation). Cells respond to applied strain in a way that is dependent to different parameters as the contractile state of the cell, the spatial and temporal pattern of applied strain and the dimensionality and mechanical properties of the substrate (**Fig. 13**). The responses range from morphological changes, and signal transduction to further affect cell functions such as cell proliferation, apoptosis, migration and differentiation (Sears and Kaunas, 2016).

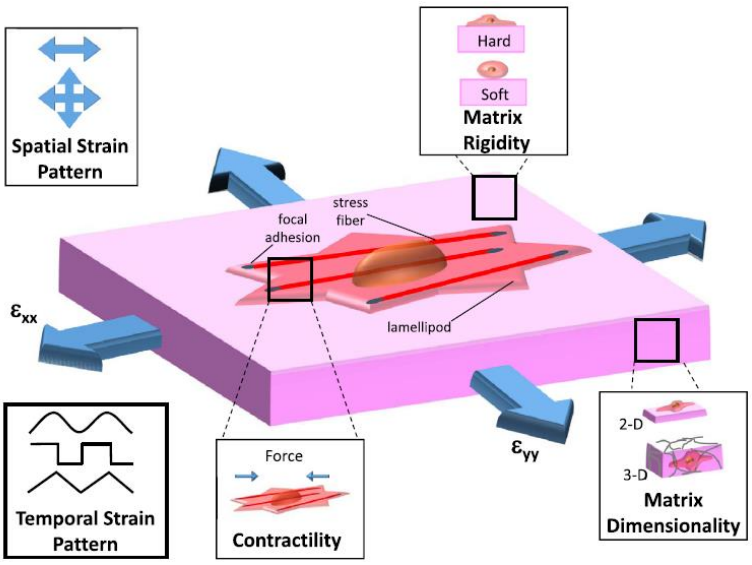

Figure 13: Parameters that influence the cellular response to applied strains. Cell response to an applied strain is dependent on the spatial and temporal pattern of applied strain (ε) and on the dimensionality and rigidity of the substrate (Sears and Kaunas, 2016)**.**

An overview of parameters that influence cell response to an applied stretch is given below:

Spatial strain patterns

The most studied deformations are the “uniaxial”, “biaxial” and ”equiaxial” stretching (**Fig. 14**). For the “uniaxial” strain the substrate is stretched along one axis, for the “biaxial” strain the substrate is stretched in two perpendicular directions within the same plane, and for the “equiaxial” strain (also called “equibiaxial” or “radial”), stretch is applied in all directions. Each cell type *in vivo* is submitted to different kind of stretch. To be more relevant, the spatial strain pattern, more adapted to the cell type and the biological process studied, has to be chosen. For example, the uniaxial stretch is physiologically relevant in vascular cells. In fact, inflation of the vessel due to the blood pressure will produce an uniaxial circumferential strain (Gerstmair et al., 2009; Kurpinski et al., 2006). In the case of equibiaxial stretch, it provides a more realistic environment for tissues that experience stretch in more than one direction *in vivo*, such as connective tissues (Bell et al., 2012). The spatial strain pattern influences the cellular response. In fact, early studies on fibroblasts, arterial smooth muscle cells and endothelial cells showed that cyclic uniaxial strain resulted in either perpendicular or oblique alignment of the cells and stress fibers relative to the strain axis (Buck, 1980; Dartsch and Betz, 1989; Dartsch et al., 1986), while cyclic equibiaxial stretch results in no cell or stress fiber alignment in endothelial cells (Kaunas et al., 2006; Wang et al., 2001). Stress fibers are the major tensor-bearing structure in non-muscle cells, they are composed of actin bundles and non-muscle myosin II plus various crosslinking proteins (see § 3.2).

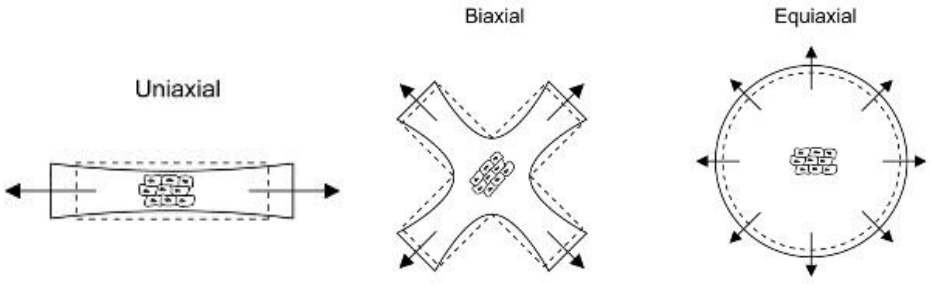

Figure 14: Illustration of three types of strain which can be applied to cells cultured on a flexible membrane. “Uniaxial” strain (on the left): the substrate is deformed along one axis; “biaxial” strain: the force is applied in two perpendicular axes (in the middle); “equiaxial” strain: stretch is applied equally in all directions (on the right) (adapted from Davis et al., 2015).

Temporal Strain Patterns

Stretch can be “static” or “cyclic / dynamic”. For the static stretch, the substrate is elongated and then held in the lengthened position over a period of time. The cyclic stretch consists in multiple repetitions, cycles, of stretch when the stretch force is repeatedly applied and

released over a period of time. The duration of stretch as well as the strain rate can vary. The strain rate is the change in strain of a material with respect to time, it is a specified strain which is delivered to something, for example cells, over time (i.e. 20% strain at $1s^{-1}$ strain rate means that 20% change in substrate length is reached in 1 second).

It is known that cell alignment depends not only on strain magnitude but also on strain frequency. In particular the alignment increases with increasing strain frequency up to ~1 Hz, a saturation value above which there is no increase in alignment (Jungbauer et al., 2008). Different cell types (as fibroblast, endothelial cells, osteoblasts and myocytes) respond differently when the substrate is subjected to a static or cyclic strain. In fact, following a static strain cells tend to align themselves parallel to the direction of stretch (Collinsworth et al., 2000; Eastwood et al., 1998), while following a cyclic stretch they tend to reorient themselves perpendicular to the direction of stretch (Dartsch et al., 1986; Moretti et al., 2004; Neidlinger-Wilke et al., 1994, 2002; Wang et al., 2001; Zahn et al., 2011). Moreover, if cells are subjected to stretch at very low frequencies, (0.0001 s^{-1} and 0.001 s^{-1}), they do not reorient at all, they remain randomly oriented (Hsu et al., 2009; Jungbauer et al., 2008). Cyclic uniaxial stretch in endothelial cells induces stress fiber alignment in a strain rate-dependent manner, while cyclic equibiaxial stretch does not, and instead it decreases cell spreading in a strain rate-dependent manner (Hsu et al., 2010). A rapidly applied static strain transiently activates JNK, ERK and p38 pathways, while no activation is observed when the rate of strain is decreased by 100-fold (Hsu et al., 2010). Similarly, in endothelial cells and vascular smooth muscle cells, the activation of these kinases is present in response to cyclic stretching at 1Hz, reduced at lower frequencies and absent upon stretching at 0.01Hz (Hosokawa et al., 2002; Hsu et al., 2010).

Matrix Rigidity /Substrate stiffness

It is now largely demonstrated that cells respond to the local extra-cellular matrix stiffness to regulate cellular processes ranging from cell-cell and cell-substrate adhesions (Reinhart-King et al., 2008; Reinhart-King, 2008; Wang et al., 2002), motility (Engler et al., 2004; Lo et al., 2000; Palecek et al., 1997; Pelham and Wang, 1997), cell spreading (Giannone et al., 2004) and differentiation (Engler et al., 2006). By pulling on the surrounding matrix through cell-matrix adhesions and sensing the mechanical resistance of the matrix, cells respond through modulation of cytoskeletal dynamics and organization (Engler et al., 2004; Pelham and Wang, 1997; Saez et al., 2005). Cells are only sensitive to differences in rigidity within a narrow range comparable to the rigidity of the cell (Zemel et al., 2010). In different cell types (as fibroblasts, endothelial cells, mesenchymal cells), the extent of cell spreading and stress fiber formation are proportional to matrix rigidity (Fu et al., 2010; Mih et al., 2012; Yeung et

al., 2005). In U2OS osteosarcoma cells, the reorientation can be different on rigid and soft substrates. In fact, cells and their actin stress fibers are oriented perpendicular to the direction of cyclic stretch on stiff substrate and parallel to the stretch direction on soft substrate (Tondon and Kaunas, 2014).

It's noteworthy that much of what is known about the biology of myelination has been discovered from cell culture studies performed on *in vitro* substrata that are orders of magnitude stiffer than the CNS tissue *in vivo*. Stiffness is expressed by Young's elastic moduli (E) and the elasticity range of the human brain tissue is E ~ 0.1–1 kPa (Christ et al., 2010; Levental et al., 2007; Lu et al., 2006; Miller et al., 2000). Some properties of cells cultured on polystyrene or glass surfaces, which are orders of magnitude stiffer than brain tissue, may differ from those occurring *in vivo*. In fact, the stiffness of the formers are ~ 3 and 70 GPa, respectively, while brain tissue is markedly softer (**Fig. 15**). Regarding oligodendrocytes, they are mechanosensitives and respond to substrate / matrix stiffness; in general survival, proliferation and maturation were found to be optimal on intermediate range of physiological brain tissue stiffness (Jagielska et al., 2012; Urbanski et al., 2016) (see § 3.7.4 for details on oligodendrocytes and mechanostimulation).

The Bioflex® Plates, containing silicone membrane and used for this work, presented a stiffness of 930 kPa that is far from the *in vivo* condition, but still closer to the physiological conditions than the substrata that are ordinarily used for cell culture (**Fig. 15**).

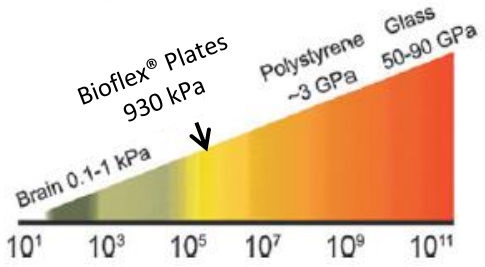

Figure 15: Comparison of stiffness range (Young's modulus, Pa) between brain tissue, Bioflex® Plates containing silicone membrane used in this work, polystyrene and glass (adapted from Jagielska et al., 2012).

Recently Cui and co-workers reported that in fibroblasts, the lack of substrate stiffness-induced cell stress can be compensated by simultaneous cyclic stretching at low magnitude (1-5%) and low frequency (optimum 0.1 Hz) applied on soft substrates. Strain at the higher magnitude of 15% reduces the cell spreading, reflected by the total cell area, even at low frequency (Cui et al., 2015). These findings are in agreement with the previous study that cyclic strain can compensate for experimentally induced loss of intracellular tension in aortic endothelial cells (Kaunas et al., 2005) and with another study where two mechanical cues, the stiffness of culture substrate and dynamic stretch, were combined. In fact, valvular

interstitial cells grown on soft substrate exhibit a rounded morphology but, upon application of 10% cyclic equibiaxial stretch, they spread to the same extent as those cultured on stiff substrate. Besides, cells grown on stiffer substrate are bigger but they reduce their cell area when the same 10% equibiaxial stretch is applied (Throm Quinlan et al., 2011).

Matrix Dimensionality

Our knowledge of many biological processes is largely based on studies using cell cultures performed on flat, two-dimensional (2D) substrates, as plastic or glass coverslips. However cells grow physiologically in a complex three-dimensional (3D) environment. This awareness and the development of new technologies over the past years have encouraged scientists to develop 3D culture. Micro environmental cues are known to impact cell function. Lots of efforts were made in order to understand how these cues act in a 3D matrix and what are the differences compared to a 2D culture. Cells grown on a 2D monolayer are flat, they can spread and adhere in the horizontal plane but they have no support for growing in the vertical dimension, so it means that they have a forced apical-basal polarity (Baker and Chen, 2012). The 3D culture elicits a more physiological state, with changes in cell geometry and organization that directly impact cell functions. It's also important to underline that the dimensionality is strictly linked to the matrix stiffness. In fact, traditional 2D cultures are performed on glass or plastic which are supraphysiological in terms of stiffness. The matrix used for 3D culture is not necessarily at the physiological range of stiffness, but to date most of the 3D systems offer a matrix with low stiffness (**Fig. 16**).

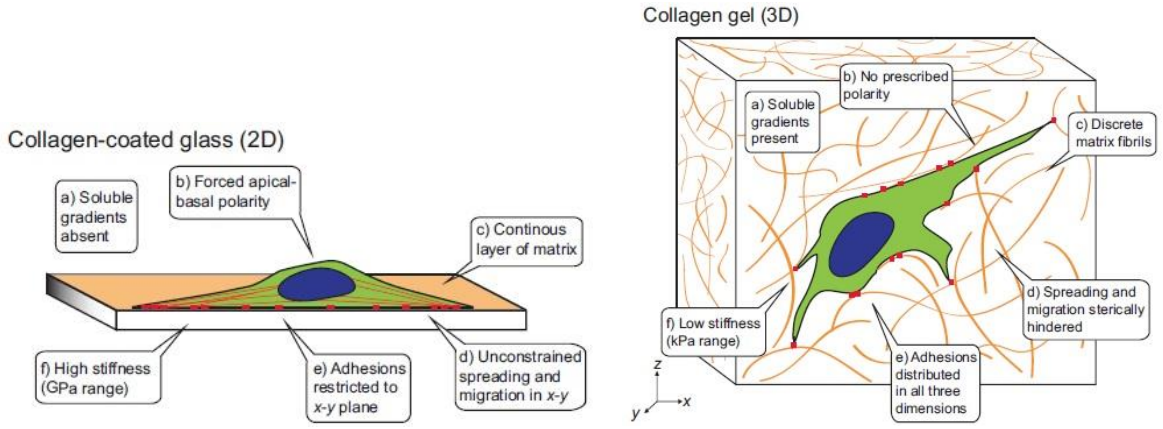

Figure 16: Adhesive, topographical, mechanical, and soluble cues in 2D and 3D cultures. The cues encountered by a cell are strikingly different between an extra cellular matrix (ECM) coated glass or plastic surface (2D) and a typical 3D ECM, such as collagen (Baker and Chen, 2012).

There are growing evidences showing that cell behaviour is different when cultivated on 2D or 3D environment. Cukierman and colleagues studied the adhesions between fibroblastic

cells and extracellular matrix in 3D cultures and they found that 3D-adhesions differ from focal adhesions characterized on 2D substrates, in terms of cytoskeletal components, content of integrins and paxillin, and phosphorylation of focal adhesion kinase (FAK) (Cukierman, 2001) (see paragraph 3.2). Chiron et al. characterized the interaction between muscle cells and a 3D matrix. They reported that adhesion sites in 3D culture are smaller in size than in rigid 2D culture whereas expression of adhesion site proteins is higher in 3D *versus* 2D culture. Moreover the cell differentiation was shown to be faster in 3D culture (Chiron et al., 2012). Another study has been performed on normal and LMNA-mutated myoblasts (LMNA gene encodes for A-type lamins, mutations of this gene cause laminopathies). The authors reported that the use of 2D hard substrates (GPa value) minimizes the differences between control and mutated myoblasts. By contrast when cells are grown in soft 3D matrix (4-12 kPa), the differences in cytoskeletal rearrangement and transcriptional changes are undeniable between normal and mutant myoblasts (Bertrand et al., 2014).

In addition, 3D culture impacts cell response to a stretch stimulus. Cells subjected to a static-stress or cyclic uniaxial strain in a 3D matrix underwent morphological changes and their differentiation is improved. These responses appeared to be increased under cyclic stretch *versus* static-stress (Nieponice et al., 2007). The same group found that bone marrow derived progenitor cell (BMPC) aligns perpendicular to the direction of applied stretch in 2D culture (Hamilton et al., 2004), while in 3D culture the long axis of the BMPCs aligns parallel to the direction of applied stress (Nieponice et al., 2007). It has to be considered that in 2D experiments, the effect of mechanical strain is studied on cells that are adherent to a flat silicone membrane. Therefore the resulting strain is uniform and homogeneous as a consequence of 2D cell deformation compared to 3D cultures. Since the most of 3D tissues are fibrous and heterogeneous, the force is not necessarily transmitted in the same way in all directions. It depends on cell orientation and how the cell is bound to the matrix fibers (Baker and Chen, 2012).

3.2 Effect of stretch on cell cytoskeleton

Cell cytoskeleton is a complex network consisting in actin microfilaments, microtubules, and intermediate filaments (**Fig. 17**). It forms the dynamic architecture of the cell. Cytoskeletal structures are involved in the sensing of external forces and transmitting those forces.

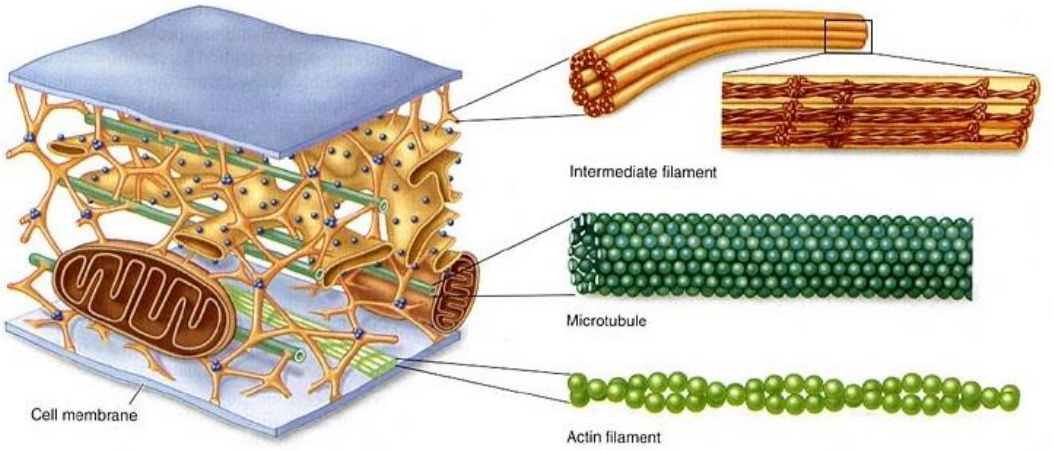

Figure 17: The components of the cytoskeleton. The cytoskeleton is composed of three types of protein fibers: intermediate filaments, microtubules and actin filaments (Johnson, 2006)**.**

Several methods have been developed to investigate the influence of tensile strain on cells cultured on elastomeric sheets. In many different cell types, cells tend to align themselves perpendicular to the direction of stretch, such as endothelial cells (Dartsch and Betz, 1989; Moretti et al., 2004), smooth muscle cells (Kanda et al., 1992), fibroblasts (Jungbauer et al., 2008; Neidlinger-Wilke et al., 2002; Wang et al., 2001), tumor cells and mesenchymal stem cells (Tondon and Kaunas, 2014). Sears and Kaunas recently reviewed the remodelling of cytoskeletal structure during alignment and in general how adherent cells respond to applied stretch (Sears and Kaunas, 2016).

Microtubules

Uniaxial tensile stress is known to induce microtubule growth in the direction of force application (Kaverina et al., 2002), while equibiaxial strain promotes an increase in the total polymerized microtubule mass (Putnam et al., 2001). A study demonstrated that a functional microtubule network is not required for cell alignment following cyclic stretch. In fact, focal adhesions and the actin cytoskeleton undergo dramatic reorganization perpendicular to the direction of stretching forces even without microtubules (Goldyn et al., 2009). However, the same group showed that microtubule stability, with acto-myosin, regulates the kinetics of cell reorientation, even if microtubules do not play significant role in reorientation itself (Goldyn et al., 2010).

Intermediate filaments

It is proved that intermediate filaments contribute to the mechanical integrity and organization of cells (Kim and Coulombe, 2007), but their role in stretch-induced morphological changes

seems to be minor. For example, myoblasts expressing mutated desmin (p.D399Y desmin mutation disorganizes the desmin intermediate filaments network in muscle cells) show altered dynamics of perpendicular alignment in response to cyclic stretching, yet still aligned to a comparable extent as myoblasts expressing wild-type desmin (Leccia et al., 2013).

Actin microfilaments

It is well demonstrated that actin microfilaments are the cytoskeleton component the most involved in alignment process. In fact, disruption of the actin cytoskeleton completely blocks stretch-induced cell alignment (Goldyn et al., 2009; Kaunas et al., 2005). Actin filaments are organized *via* actin-associated proteins into higher order structures, including lamellipodia and filopodia. In particular cofilin, profilin, and the Arp2/3 proteins act together to promote the rapid turnover of actin filaments. Cofilin binds to actin filaments and enhances the rate of dissociation of actin monomers, while profilin, can reverse the effect of cofilin and stimulates the incorporation of actin monomers into filament. Finally, Arp2/3 proteins serve as nucleation sites to initiate the assembly of new filaments. Actin microfilaments can also form contractile bundles of parallel microfilaments, termed stress fibers, through interactions with non-muscle myosin II (Blanchoin et al., 2000).

Stress fibers are the major tension-bearing structures in adherent, non-muscle cells (Burridge, 1981) and are critical to cell functions involving cell alignment (Goldyn et al., 2009; Hsu et al., 2009), cell adhesion (Tojkander et al., 2012) and contractility (Chrzanowska-Wodnicka and Burridge, 1996). Stress fibers are anchored to focal adhesions, which consist of integrins and many other so-called focal adhesion proteins, as vinculin, that serve to physically connect the extracellular matrix to the actin cytoskeleton and sense mechanical forces (Cramer et al., 1997; Naumanen et al., 2008) (**Fig. 18**). It is known that stretch-induced cell alignment is generally preceded by alignment of stress fibers (Faust et al., 2011; Goldyn et al., 2010). Moreover, high level of biaxial strain increases actin depolymerization in tendon cells (Lavagnino et al., 2015) and chondrocytes (Campbell et al., 2007).

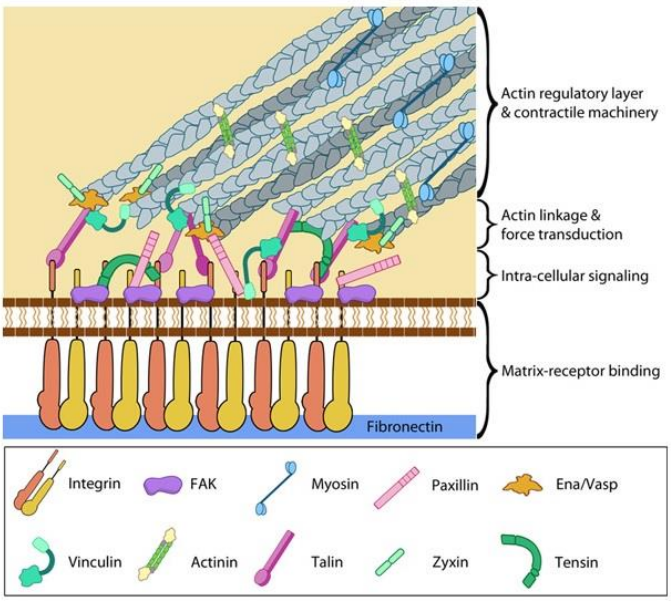

Figure 18: Stress fibers and focal adhesion organization. A mature focal adhesion contains hundreds of proteins that are grouped based on their contribution to four basic processes: receptor/matrix binding, linkage to actin cytoskeleton, intracellular signal transduction, and actin polymerization. The combined activity of the mechanosensitive components forms the mechanoresponsive network. (https://www.mechanobio.info/topics/mechanosignaling/cell-matrix-adhesion/focal-adhesion/focal-adhesion-assembly/)

3.3 Signalling pathways activated by stretch

Mechanotransduction is viewed as a force-induced process initiating biochemical responses (e.g., changing binding affinity, altering phosphorylation state, and/or conformation change) and initiating the activation of signalling pathways leading to gene expression, protein synthesis, and cellular phenotype change (Goldmann, 2014). A mechanical stretch can induce different responses according to different spatial and temporal pattern of strain. However, some pathways can be altered in all conditions of stretch, regardless of strain magnitude, strain rate and duration of stretch. A particularly stretch-responsive pathway involves the mitogen-activated protein kinases (MAPKs). The MAP kinases comprise a family of ubiquitous proline-directed, protein-serine/threonine kinases, which take part to different signal transduction pathways. They are known to regulate different cellular processes as cell survival, proliferation, differentiation, migration, mitosis and apoptosis (Pearson et al., 2001) and they are also known to be involved in mechanically-induced signalling in various cell types, being implicated in the signal transduction from the cell membrane to the nucleus. MAP kinases are regulated by phosphorylation cascades, with two upstream protein kinases activated in series (called MAPKKK and MAPKK/MEK) leading to activation of a MAPK (**Fig. 19**). A characteristic of this cascade is the amplification of the signal, and it can occur if each successive protein in the cascade is more abundant than its regulator.

The family of MAPK consists of three principal subgroups, extracellular signal-regulated kinase (ERK), c-Jun NH2- terminal kinase (JNK), and p38. Cell division, migration, and survival generally involve ERK signalling, while cellular and environmental stresses activate the p38 MAPK and JNK pathways, and for this reason JNKs are also known as SAPKs, stress-activated protein kinases (Hoefen and Berk, 2002; Kyriakis and Avruch, 2012; Owens and Keyse, 2007; Vezza et al., 2016).

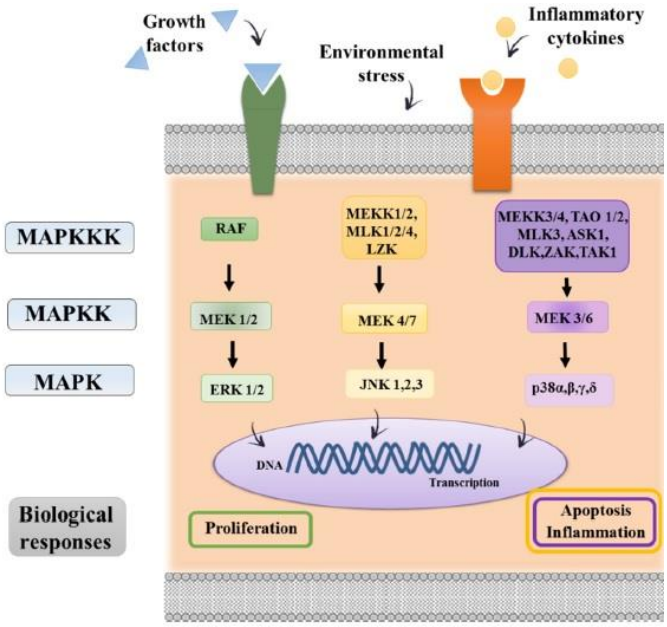

Figure 19: MAP Kinase pathways. The mitogen-activated protein kinase (MAPK) cascades are signal transduction pathways that involve a chain of three kinases activating each other in a series (MAPKKK, MAPKK, and MAPK). The result of phosphorylation of various MAP kinase isoforms is the activation of the three main MAP kinases pathways: ERK (extracellular signal-related kinase), JNK (c-Jun NH2-terminal kinase) and p38 MAPK (Vezza et al., 2016).

As MAPK activation is controlled through phosphorylation, its assessment should adequately reflect the kinase activity. MAPK phosphorylation was analysed by immunoblotting in bovine pulmonary arterial endothelial cells submitted to a 10% cyclic stretch showing an activation of ERK1/2, JNK1/2, and p38 following stretch. Their activation plays a role in transcriptional activation of AP-1/TRE, showing an increase of the binding activity of the transcriptional factor AP-1 (Kito et al., 2000). It has been demonstrated that isoforms of JNK and ERK MAPKs were phosphorylated in a tension-dependent manner in rat skeletal muscle preparations, in particular a strong relationship between peak tension and p54 JNK MAPK was observed (Martineau and Gardiner, 2001).

Some differences in pathway activation have been also reported due to different spatial and temporal patterns of strain. For example, when myotubes are subjected to uniaxial and multiaxial stretch, both resulted in an increase in ERK (ERK1/2) and protein kinase B (PKB/Akt) phosphorylation, but only multiaxial stretch induced ribosomal S6 kinase

phosphorylation (Hornberger et al., 2005). Another study in vascular endothelial cells showed that a cyclic equibiaxial stretch, with no stress fiber orientation, results in JNK (JNK1) activation for up to 6 h, while an uniaxial stretch results in transient JNK activation. In fact, in the latter case it is followed by a return to basal level as the actin stress fibers become oriented perpendicular to the direction of stretch. Moreover, if the direction of stretch is changed by 90°, JNK is reactivated as stress fibers become re-oriented perpendicular to the new direction of stretch (Kaunas et al., 2006). In bovine aortic endothelial cells, cyclic stretch transiently activates JNK (T183/Y185 JNK), ERK (T202/Y204 ERK) and p38 (T180/Y182 p38) in a strain rate-dependent manner, accompanied by stress fibers alignment for uniaxial strain and cell retraction for equibiaxial strain. No sign of activation has been observed when the rate of strain is decreased by 100-fold (Hsu et al., 2010). Similarly, the activation of these kinases observed in response to cyclic stretching at 1Hz is reduced at lower frequencies and absent upon stretching at 0.01Hz (Hosokawa et al., 2002; Hsu et al., 2010).

Some evidences highlight other pathways activated by stretch. A study showed that a mechanical stretch is able to induce the activation of JAK/STAT pathway in rat cardiomyocytes (Pan et al., 1999). Mechanical activation of the mTOR/p70S6K signalling pathway has also been reported in muscle cells *in vitro* (Hornberger, 2004; Hornberger and Chien, 2006; Nakai et al., 2015; Sasai et al., 2010).

Moreover physical stimuli in general are known to modulate the activity of transcription factors as, for example, armadillo/β-catenin, serum response factor (SRF), yes-associated protein (YAP) and nuclear factor kB (NF-kB) (Mendez and Janmey, 2012).

YAP signalling has emerged as a particularly important regulator of the mechano-response (Dupont et al., 2011). YAP is a crucial member of the Hippo pathway, and is expressed in almost all cell types (Mendez and Janmey, 2012). YAP is inactivated by phosphorylation that provokes its exclusion from the nucleus. When YAP is nuclear, it interacts with a number of coactivators, including its paralog TAZ (transcriptional coactivator with PDZ-binding motif) (Lei et al., 2008). YAP's involvement in mechanotransduction was studied in different human cell types plated on soft *versus* stiff substrates, cells grown on stiff substrates show an increase in the YAP transcription and the nuclear localization of YAP protein (Dupont et al., 2011).

Other studies showed that shear stress causes nuclear NF-kB translocation inducing gene expression in both endothelial cells (Khachigian et al., 1995) and preosteoblastic cell line (Chen et al., 2003). NF-kB is also activated in chondrocytes in response to dynamic compressive strain (Nam et al., 2009) and in osteoblasts following oscillatory, but not continuous, fluid flow (Young et al., 2010).

Focus on pathways activated by stretch-induced injury

As reported above, a mechanical stretch-induced injury has been used to study the effects of traumatic injury *in vitro* that replicates many of the post-traumatic responses observed *in vivo*, including mitochondrial abnormalities, increase in cell permeability (Ellis et al., 1995), and in calcium concentration (Rzigalinski et al., 1998), and depletion and release of intracellular ATP (Ahmed et al., 2000). Mechanical injury also activates ERK (Neary et al., 2003), and p38 (Zhou et al., 2011) in astrocytes. Astrocytes cultured on deformable membranes and subjected to a rapid, reversible stretch-induced injury show an activation of ERK within a min after injury up to 3h, and a peak between 10 to 30 min. Activation of ERK is dependent on the rate and magnitude of injury. ATP released by mechanical injury is one of the signals that trigger ERK activation (Neary et al., 2003). NF-κB is also activated in a context of injury and repair and it is central to innate immunity. Pulmonary epithelial high cyclic stretch (22 % equibiaxial strain) activated NF-κB, enhanced interleukin-8 (IL-8) production, caused cell injury, and reduced cell survival. In contrast, physiologic stretch (10 % strain) did not activate inflammation or cause cell injury (Horie et al., 2016).

Another consequence of a traumatic event is an increase in calcium level that has been reported within seconds of trauma induced by fluid shear stress (LaPlaca and Thibault, 1997), biaxial stretch (Geddes and Cargill, 2001; Weber et al., 1999), and uniaxial stretch (Lusardi et al., 2004a). Long-lasting calcium increase has been observed in various animal models of trauma (Fineman et al., 1993; Nilsson et al., 1996; Xiong et al., 1997). The magnitude of calcium increase is directly related to the applied strain magnitude and rate (Geddes and Cargill, 2001; LaPlaca and Thibault, 1997; Lusardi et al., 2004a; Weber et al., 1999). Therefore, it is generally considered as one of the initiating factors in transducing a mechanical insult into a cellular response.

Probably the best known mechanism leading to calcium influx in mechanically injured neurons is the activation of NMDA receptor, that has been demonstrated after fluid shear stress (LaPlaca and Thibault, 1997), mild to moderate biaxial stretch (Ahmed et al., 2002) and uniaxial stretch (Lusardi et al., 2004b). Post-injury changes in intracellular calcium signalling can lead to altered neuronal function under agonist stimulation (Weber et al., 1999, 2001). There are also several studies reporting a link between the activation of purinergic receptors after mechanical stimuli and the subsequent activation of intracellular signalling cascades (Neary and Kang, 2006; Neary et al., 2003, 2005). Activation of cysteine proteases, calpain, and caspase-3 also occurs hours following injury. Calpain activation (1-6 h) is associated with nuclear morphological alterations, typical of necrotic (hyperchromatism) or apoptotic death (condensed, shrunken nuclei), while caspase-3 activation is associated mainly with apoptotic bodies, suggesting in general that the injury

includes both apoptotic and necrotic forms of cell death (Pike et al., 2000). It has been observed *in vitro* that there is a damage progression in injured neurons over the days following the initial trauma that should be taken into account for the evaluation of short and long-term treatment options.

It is important to point out that different mechanical insults, in particular different strain fields (uniaxial or biaxial) induce the activation of different cascades and so different responses to potential secondary excitotoxic injury mechanisms (Geddes-Klein et al., 2006). Moving from *in vitro* findings to *in vivo* models, with their associated complex strain fields, is delicate and emphasizes the need to further study how all these mechanical conditions can separately affect cell fate following mechanical injury.

3.4 Mechanostimulation in physiological condition

Nearly all cells in the body are subjected physiologically to mechanostimulation at a different degree according to their function and the belonging tissue. For example cells from cardiovascular system are permanently subjected to mechanical forces due to pulsatile nature of blood flow and shear stress. In particular, endothelial cells and smooth muscle cells are the major cells that face mechanical forces (Jufri et al., 2015; Shyu, 2009). Besides, skeletal muscle cells (Morita et al., 2013), chondrocytes (Lee et al., 2000) and osteoblasts (Xu et al., 2012) are also physiologically subjected to mechanical stresses. Another example of physiological mechanical stimuli is during development, when mechanical tension may impact cell fate decisions during embryogenesis and control morphogenetic movements during convergent extension. During development and homeostasis, tissue growth is tightly regulated to generate, repair, or renew organs with precise size, structure, and function (Lecuit and Le Goff, 2007; Schwank and Basler, 2010). Thus, individual cells in a tissue must somehow sense the overall size or growth state of a tissue to prevent over proliferation that would lead to inappropriate tissue size or tumor formation. Much effort has focused on secreted signals that regulate tissue growth, but tissues also experience mechanical stress during growth that could, in principle, serve to globally coordinate cell growth across a tissue. Tissues can grow either by increasing their cell volume or by increasing cell number through cell division/proliferation. In both cases, cell growth might engender local stress in the context of a tissue where cells exhibit intercellular adhesion and are thus not free to immediately rearrange in a manner that would relieve stress (Chanet and Martin, 2014). Therefore the development of organisms and organ systems would not proceed without applied forces and mechanics.

3.5 Mechanostimulation in pathological condition

Physical forces regulate a large number of physiological processes. However mechanical stimuli can also lead to pathological conditions, since a dysregulation of mechanical responses contributes to major human diseases (Orr et al., 2006). For example stretch can promote hypertrophy of cardiomyocytes (MacKenna, 2000; Sadoshima et al., 1992; Yamazaki et al., 1995) and hyperplasia in cardiac fibroblasts (Sadoshima et al., 1992). Fibroblasts are numerically the most abundant cells in the myocardium and they are responsible for the deposition of the extracellular matrix (ECM). These cells modulate the ECM synthesis according to the type and extent of mechanical stimuli applied, switching from a normal to a pathological deposition (Villarreal and Kim, 1998).

The ECM of tendons and ligaments is also modified in response to mechanical loading. In fact, fibrocartilage appears in sites where tendons and ligaments are subjected to compression. Fibrocartilage is a dynamic tissue and degenerative changes can lead to some common pathologies known as enthesopathies, e.g. tennis elbow, golfer's elbow and jumper's knee (Benjamin and Ralphs, 1998). The development and pathobiology of bone is also strictly dependent on mechanical forces, and gravity. The locomotion stimulates local bone remodelling to maintain optimal performance. Reduced mechanical stimulation due for example to a sedentary life or limb paralysis results in bone loss (reduced bone formation and increased bone reabsorption). Osteoporosis is known to be affected by diet and endocrine status, but mechanical stimulation remains the major cause (Burger and Klein-Nulend, 1999; Raisz, 1999).

Mechanical forces, in particular shear stresses, playing on the endothelium of the vascular wall, are associated with blood flow and they play important roles in the control of vascular tone, the regulation of arterial structure and remodelling. The response to these mechanical stimuli is part of normal vascular physiology, but hemodynamic forces can also play a role in vascular pathologies, particularly in relation to the localization of atherosclerotic lesions. Atherosclerosis in fact occurs preferentially in region when the flow is disturbed as branch points and areas of high curvature (Davies, 1995; Nerem, 1992).

Then last but not least, changes in mechanical environment are also shown to be responsible for tumor progression. For example in breast cancer, tumorigenesis is accompanied by collagen crosslinking and ECM stiffening. This lead to a promotion of focal adhesions and invasion of oncogenically initiated mammary tissue, so the increase of tissue stiffness promotes tumor progression *in vivo* (Levental et al., 2009).

3.6 Mechanostimulation in the nervous system

Contrary to general thoughts, the nervous system is subjected to motor forces, in fact body movements stress the nerves in multiple ways. Considerable mechanical forces (movements, deformation) act upon the spinal cord, and the peripheral nerves, despite the changing condition, continue to conduct stimulation and impulses (Barral and Croibier, 2007). Considering the brain, the situation is different because usually cells are not subjected to mechanical forces. The brain is in fact considered a “mechanically protected” organ and do not have a clear constant level of mechanical stimulation. An excess of mechanostimulation can lead to a trauma.

Thanks to biomechanics, it is possible to study and understand how a dynamic loading in the CNS can result in an injury. The transition from physiology to pathophysiology is very important and should be considered. Early pathophysiological changes can influence important cellular processes as cell survival, proliferation, reintegration and repair of the injured tissue in long-term. This long-term response, initiated when forces are transferred to the cellular/molecular scale at the time of injury, is a key contributor to the outcome of head-injured and spinal cord-injured patients (Meaney and Smith, 2015).

Mechanosensivity was studied by various methods in different components of the nervous system, with a particular attention to the mechanosensitive ion channels (Calabrese et al., 1999; Cho et al., 2002; McCarter et al., 1999; Menconi et al., 2001; Mutai and Heller, 2003; Schumacher et al., 2000; Su et al., 2000; Takahashi and Gotoh, 2000). The main question to be answered is how the mechanical forces affecting the membrane are transformed into biochemical responses at cellular level, which regulate the growth and differentiation of cells. Meaney and Smith recently reviewed the possible mechanosensors present in the CNS, using the term mechanosensors to describe receptors and channels in the CNS that respond directly to the mechanical stimulation (Meaney and Smith, 2015). They conceive these receptors to express a dose-response to an applied mechanical force that is similar to a dose-response curve that describe the property of a ligand-receptor binding interaction. So, in the same way, this dose-response curve should change when the rate of applied force is modified. In addition, it has to be considered that mechanosensors may respond differently to different mechanical input, for example, some receptors may be sensitive only to the pressure applied, while other receptors may respond to other types of deformation, as tension and compression (Meaney and Smith, 2015). At present, despite their potential importance, the knowledge of the mechanoactivation profiles for most receptors, expressed in the brain, is very limited.

There are in particular two mechanosensors that are known to respond to mechanical forces in the brain:

- NMDA receptor, a glutamate receptor and ion channel protein. Some studies show that this receptor can “sense” the forces that are applied during a traumatic injury (Kloda et al., 2007; Paoletti and Ascher, 1994; Zhang et al., 1996). In condition of normal resting membrane potentials, magnesium can bind to specific sites on the receptor, limiting the passage of other cations across the receptor. As a consequence of mechanical loading, the magnesium block is removed and the channel becomes activated. It is known that the NMDA receptor mediates stretch-induced calcium influx leading to neuronal excitotoxicity and it is considered one of the common mediators for the acute and progressive events that occur following TBI (DeRidder et al., 2006; Faden et al., 1989; Geddes-Klein et al., 2006; Singh et al., 2012).
  Important for the mechanosensing property is the molecular tethering of the receptor to the cytoskeleton and in particular a single serine residue of the NR2B subunit of the receptor seems to control this mechanosensitivity (Singh et al., 2012).

- α-subunit of the voltage-gated sodium channel (NaCh). The α subunit forms the core of the channel and it is functional on its own (Marban et al., 1998). The initial response to mechanical forces induces changes in calcium homeostasis, and calcium elevation leads to calpain (a calcium-dependent protease)-dependent proteolysis of NaCh channel. A prolonged activation of calpains results in proteolysis of numerous cellular substrates including cytoskeletal components and membrane receptors contributing to the evolution of different neurodegenerative diseases (Camins et al., 2006; Schoch et al., 2013). It is reported that proteolysis of NaCh α-subunits appears after ischemic injury to the isolated spinal cord, after elevation of intracellular Na^+ in cultured neurons, and also after mechanical injury to cultured axons (Iwata et al., 2004; Jette et al., 2006; Paillart et al., 1996; von Reyn et al., 2009; Wolf et al., 2001). Stretch provokes Ca^{2+} entry into cells and some studies demonstrated that two prominent candidates for channel-mediated influx are NMDA receptors and NaChs, since stretch activates both of them (Geddes-Klein et al., 2006; Wolf et al., 2001). Von Reyn and collaborators studied the effect of calpain-mediated proteolysis following a stretch induced injury *in vitro* and they found that direct activation of either NMDA receptors or NaChs results in NaCh proteolysis. There is an initial phase with rapid changes (<15 minutes) in channel integrity followed by a degradation phase (4-6 hours) that precedes any evidence of neuronal death (von Reyn et al., 2012). It is not clear if the later degradation phase can be blocked to rescue neurons in the

network or if it is irreversible leading to the removal of the neuron from the injured network.

There are other receptors that are known to activate and/or change their properties after mechanical injury but it is not clear whether if they directly respond to the mechanical force:

- AMPA receptors, a class of non-NMDA-type ionotropic transmembrane receptors for glutamate. It is demonstrated that there is loss of desensitization property of this receptor (Goforth et al., 1999). It can be due to the upstream activation of NMDA receptor and not to the molecular structure of the receptor itself (Goforth et al., 2004). To date, there are no evidences that AMPA receptors are direct mechanosensors.
- GABA receptors, a class of receptors that respond to the neurotransmitter gamma-aminobutyric acid (GABA). It is proved that a mild stretch-induced injury altered the $GABA_A$ currents in rat cortical neurons. In particular there is a potentiation of $GABA_A$ current but this is directly dependent on NMDA receptor activation following neural injury (Kao et al., 2004).

In glial cells, it is known that a focal mechanical stimulation can induce intracellular Ca^{2+} waves that are mediated by release of ATP and glutamate (Charles et al., 1991) but, so far, no mechanoactivated receptors are described for this phenomenon.
Despite their importance, the knowledge of sensors, both in neurons and glial cells, is limited. All the mechanosensors described so far, once activated, can have broad implications in the function of neuroglial circuitry and it is important to elucidate their function in order to protect the networks in ensuing hours to days after the initial injury.

3.7 Stretch-induced injury on different brain-derived cell types

We are particularly interested in cell strain because it is known to be an important component of TBI. In fact, a major force causing injury of nervous tissue is rapid tissue deformation and strain, or, more simply stretch (Ellis et al., 1995).
Mechanical loading of tissues can occur by static or dynamic processes. Most biologically significant injury is produced by impulsive (acceleration, deceleration) forces or by impact of the brain with moving or stationary objects, causing tissue strain. The tissue strain can be compressive, shear, or tensile, and all three may occur after TBI. Linear tensile strain occurs when forces act to increase the length of an object. As already reported in the paragraph 3.1, if the initial length is “L” and the final length is “l”, then the fractional increase in length (l -L)/L is known as the linear tensile strain. More simply the linear tensile strain may be called stretch (Ellis et al., 1995).

Since the 90's, investigators have developed, or tried to develop, models to reproduce a traumatic injury on different cell types derived from brain. The most widely used approach to reproduce an injury is to deform cell monolayers or organotypic tissue slices cultured onto flexible substrates. As substrate, flat elastomeric sheets are used, with polydimethylsiloxane (PDMS) as the elastomer of choice, which are coated with extracellular matrix molecules before the cell or tissue culture. The strain applied to the sheet is then transmitted to the cells via matrix-integrin bonds. The idea is to deform the substrate to indirectly deform the culture/slice sample (Cargill and Thibault, 1996; Lusardi et al., 2004b; McKinney et al., 1996; Morrison III et al., 1998; Smith et al., 1999). Below is reported an overview of the studies on the different types of brain-derived cells (**Fig. 20**), neurons and glial cells, alone or combined in mixed culture and organotypic cultures (see **Table 1, 2 and 3).**

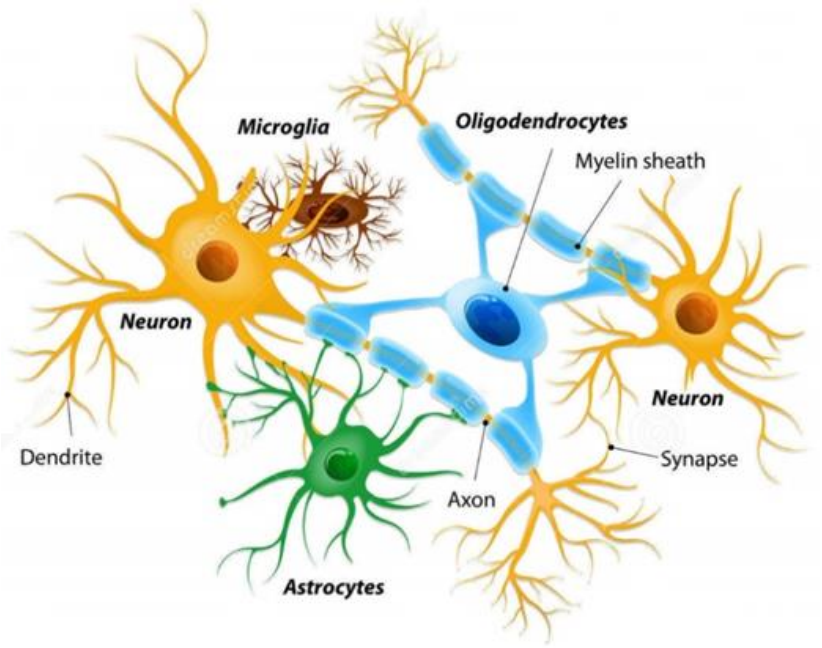

Figure 20: Representation of neurons and neuroglial cells. Glial cells are non-neuronal cells in the brain, including oligodendrocyte, microglia, and astrocytes (http://www.shutterstock.com/pic-235015666/stock-vector-neurons-and-neuroglial-cells-glial-cells-are-non-neuronal-cells-in-brain-there-are different.html).

Table 1: Principal studies reproducing a stretch-induced injury in different cell types of the CNS (1/5)

References	Cell type	Device	Strain parameters	Biological output and techniques	Observation/measurement
Ellis et al., 1995	Primary rat astrocytes	Model 94A cell injury controller	Equibiaxial stretch: 31, 38, 54, and 72% stretch for 1 to 100ms	Cell injury (PI & fluorescein diacetate uptake, LDH release, electron microscopy)	Cell injury proportional to cell deformation. Max dye uptake at 50ms within 2h after injury
McKinney et al., 1996	Primary rat astrocytes, neuronal plus glial cells and rabbit aortic endothelial cells	Model 94A cell injury controller (Ellis et al. 1995)	Equibiaxial stretch: 31, 38, 54, 72, 89, 130, or 170% for 50ms	Cell injury, response to ROS scavenger (PI uptake)	↑cell injury with ↑ % of strain in all cell types. Endothelial cells are more resistant. ROS scavenger has no effect on neurons and glia but it ↓PI uptake in endothelial cells
Cargill and Thibault, 1996	NG108-15 cell line (neuroblastoma cross glioma hybrid cells)	Custom made cell deformation system	Equibiaxial stretch: 0.12 (12%) s^{-1} or 9.6 (960%) s^{-1}	Cell injury (intracellular Ca^{2+} alterations with real time epifluorescent microscopy)	High rates (~10 sec-1): ↑ of Ca^{2+} influx exponentially related to magnitude. Low rates: ↑ of Ca^{2+} influx independent of magnitude
LaPlaca and Thibault, 1997	NT2 cell line (differentiated in neurons)	Cell shearing injury device (CSID)	Shear stress 0.01 to 0.53 at high rate (800 dyne cm^{-2} s^{-1})	Cell surface strain (fluorescent video analysis), cell injury (free Ca^{2+} entry and LDH release)	Ca^{2+} changes depend on strain rate. Cell death depend on a combination of high strain and strain rate
Rzigalinski et al., 1997, 1998	Primary rat astrocytes	Model 94A cell injury controller (Ellis et al. 1995)	Equibiaxial stretch: 38% for 50ms	Cell injury (PI uptake, LDH release), Extracellular and total Ca^{2+} assessment	Rapid entry of Ca^{2+} in astrocytes. ↓Extracellular Ca^{2+} lead to ↑injury and vice versa Rapid ↑ Ca^{2+} but not sustained (basal level in 15min). Ca^{2+} released from intracellular stores. IP3 linked pathway altered after injury
Ostrow et al., 2000, 2011	**Primary rat astrocytes (adult astrocyte cultures derived from stereotactic striatal gelatin implants)**	**Flexcell FX-3000® Strain Unit**	**Cyclic biaxial stretch: 0–20% for 15, 60 and 120s at 0.1-1 Hz**	**Cell injury (intracellular Ca^{2+} alterations with real time microscopy), IP3 and endothelin-1 (ET-1) production, proliferation (BrdU)**	**Stretch ↑ cytoplasmatic Ca^{2+}, ↑IP3, ↑ ET-1 (Ostrow et al., 2000) ↑ET-1 driven by Ca^{2+} influx through stretch-activated ion channels. ET-1 production correlates with cell proliferation (Ostrow et al., 2011)**
Geddes and Cargill, 2001	NG108-15 cell line	Cell straining apparatus (CSA)	Equibiaxial strain: magnitude from 0.1 to 0.75 , strain rate from 1 s^{-1} to 25 s^{-1}	Cell injury (intracellular Ca^{2+} alterations with real time epifluorescent microscopy)	Peak change in Ca^{2+} influx. Percent of responding cells depend on strain rate (1 s^{-1} to 10 s^{-1}) and magnitude (0.1 to 0.3)

* Studies using Flexcell device are highlighted in bold.

Table 1: Principal studies reproducing a stretch-induced injury in different cell types of the CNS (2/5)

References	Cell type	Device	Strain parameters	Biological output and techniques	Observation/measurement
Slemmer et al., 2002	Primary mice hippocampal cells (neurons and glia)	Model 94A cell injury controller (Ellis et al. 1995)	Equibiaxial stretch: 31, 38, 54% for 50ms (single & repeated TBI)	Cell injury (PI & fluorescein diacetate uptake, NSE & S-100β release)	↑cell death with ↑ % stretch. Repeated injury ↑cell death and ↑ NSE & S-100β release compared to single injury
Arundine et al., 2003	**Primary mouse cortical and hippocampal neuronal culture**	**Flexcell FX-3000® Strain Unit**	**Static stretch: 30% for 1sec**	**Cell injury (PI uptake and Ca^{2+} loading) , cell morphology (membrane tracer DiI & ICC), electrophysiology**	**Stretch alone: no effect on membrane integrity, viability, electrophysiological function. Stretch ↑ vulnerability to subsequent challenges with L-glutamate or NMDA**
Pfister et al., 2003	NG108-15 cell line (differentiated in neurons)	Custom made injury device	Uniaxial strain: 20%–70%, strain rates from 20 to 90 s^{-1}	Cell injury (morphologically approach neurite: swelling and presence of necrotic-like cell bodies)	Cells exhibited swellings within 8 h after injury
Arundine, 2004	**Primary mouse cortical neuronal culture**	**Flexcell FX-3000® Strain Unit**	**Static stretch: 30% for 1sec**	**Cell injury (PI uptake, WB, ICC), mitochondrial membrane potential (TMRM), ROS production (DHR), DNA fragmentation (TUNEL)**	**Stretch alone: no cell death but irregular nuclear morphology, ↑ROS. Stretch and NMDA: DNA fragmentation, mitochondrial dysfunction and ↑ROS, apoptosis**
Lusardi et al., 2004a	Primary rat hippocampal neuronal cells	Custom made injury device	Uniaxial strain: 5 to 50% stretch at strain rates from 20 to 100 ms	Cell injury (intracellular Ca^{2+} alterations with real time epifluorescent microscopy)	Immediate ↑ Ca^{2+} influx after stretch. Response depends on strain rate and magnitude
Lusardi et al., 2004b	Primary rat hippocampal neuronal cells	Custom made injury device	Uniaxial strain: 1-2, 3-6, 12-17, >50% at strain rate 20.5ms, 205ms or 1354 ms	Cell injury (intracellular Ca^{2+} alterations & PI uptake)	Low strain 1–2% elicited ↑ Ca^{2+} influx, strains 3–6% exceeded the ratio triggered by the toxic dose of NMDA at 100 mM. Only strain >50% caused neuronal death at 24 h following stretch

Table 1: Principal studies reproducing a stretch-induced injury in different cell types of the CNS (3/5)

References	Cell type	Device	Strain parameters	Biological output and techniques	Observation/measurement
Slemmer et al., 2004	Primary mouse cerebellar cell culture (neurons and glia)	Model 94A cell injury controller (Ellis et al. 1995)	Equibiaxial stretch: 31, 38, 54% for 50ms	Cell injury (PI & fluorescein diacetate uptake, NSE & S-100β release, IHC)	↑cell death with ↑ % stretch. ↑ NSE & S-100β release. S-100β levels are higher than in hippocampal cells (Slemmer et al., 2002)
Engel et al., 2005	Primary mouse cortical culture	Model 94A Cell Injury Controller	Equibiaxial stretch: 31 or 38% for 50ms	Cell injury, response to SOD and NOS inhibitors (PI uptake)	Stretch: ↑cell death Stretch+ischemia: ↑↑ cell death SOD and NOS inhibitors reduced neuronal death against stretch alone but not against combined injury
LaPlaca et al., 2005	Primary rat astrocytes and neurons (3D culture)	3D cell shearing device (3-D CSD)	Shear strains 0.25 or 0.50 (shear angle up to 45°) at rates from 1 to 30 s^{-1}	Cell viability (fluorescent probes LIVE/DEAD) and neurite orientation (confocal microscopy)	Cell death in astrocytes and neurons depend on a combination of high strain and strain rate (no differences between 0.25 and 0.5 at high strain rate)
Geddes-Klein et al., 2006	Primary rat cortical neurons	Custom made injury device (Lusardi et al. 2004b)	Uniaxial or Biaxial: 10%, 30 or 50% at 15ms	Cell injury (intracellular Ca^{2+} alterations & carboxyfluorescein uptake)	Immediate ↑ Ca^{2+} influx after stretch, magnitude of Ca^{2+} entry higher in biaxial than uniaxial strain. No cell death within 24 h of injury
Lau et al., 2006	**Primary mouse cortical culture**	**Flexcell FX-3000® Strain Unit**	**Static stretch: 30% for 1sec**	**Cell injury (PI uptake, WB, ICC), DNA fragmentation (TUNNEL), ROS production (ICC, protein tyrosine nitration)**	**Stretch ↑tyrosine nitration of procaspase-3, but not caspase-9 or Apaf-1. Caspase-mediated apoptosis is inhibited in stretched neurons *in vitro* and in TBI *in vivo***
Ellis et al., 2007	Primary rat neurons, astrocytes and microglia	Model 94A cell injury controller (Ellis et al. 1995)	Equibiaxial stretch: 31, 38, 54% for 50ms	Cell injury (PI uptake, S-100β release)	Trauma released S100B from all cell types (immediate post-injury release from astrocytes and microglia)
Bhattacharya et al., 2008	**Primary rat somatosensory neurons**	**Flexcell FX-3000® Strain Unit**	**Static equibiaxial stretch: 2-20% for a 2 $^{-S}$period**	**Overview of mechanosensitive neuronal subpopulations (live-cell Ca^{2+} imaging)**	**Different intensities activate distinct subsets of sensory neurons, ↑ Ca^{2+} influx**

Table 1: Principal studies reproducing a stretch-induced injury in different cell types of the CNS (4/5)

References	Cell type	Device	Strain parameters	Biological output and techniques	Observation/measurement
Uchida et al., 2008	**Primary rat spinal cord cells**	**Flexercell FX-3000® Strain Unit**	**Cyclic stretch: max 12% for 48h, cycles of 1 second**	**Cell injury (LDH release) Expression of neurotrophic factors and receptors (ICC, PCR)**	**6h after stretch: ↓n° cells, ↑LDH until plateau at 12h, loss neurites 24h after stretch: swollen irregular shaped soma, bleb formation, and fragmented neurites**
Gladman et al., 2010	**Primary rat spinal nerves and associated DRG cells (nociceptive and non-nociceptive neurons, non-neuronal cells)**	**Flexcell Tension Plus, FX-4000T™ system**	**Static equibiaxial stretch: 20% for 5 min, 1 h, 6 h or 18 h. Strain rate of 2%/s.**	**Cell injury (EthD-1 and caspase assay), neurite length measure (ICC)**	**Cell death proportional to strain duration and higher when stretch is combined with hypoxia in neurons. No cell death in non-neuronal cells after stretch and hypoxia.**
Gladman et al., 2012; Lim et al., 2013	**Primary DRG neurons from wild-type or fat-1 mice (↑ω-3 PUFAs and ↓ω-6 PUFAs)**	**Flexcell Tension Plus, FX-4000T™ system**	**Static equibiaxial stretch: 20% for 1 h. Strain rate of 2%/s.**	**Cell injury (EthD-1), neurite length measure (ICC)**	**Cell death higher after stretch in WT neurons, ↑levels of ω-3 PUFAs ↑ the resistance to mechanical injury (Gladman et al., 2012) ↑levels of ω-3 PUFAs and ↓ ω-6/ω-3 ratio confer neuroprotection against a combined stretch and hypoxic injury (Lim et al., 2013)**
Karumbaiah et al., 2012	Primary rat astrocytes, microglia and neurons	Custom made Cell Stretch Device (CSD)	Cyclic biaxial stretch: 3% strain, frequency 0.2 Hz for 2h (neurons) 4h (microglia), 18h (astrocytes)	Cell viability (fluorescent probes LIVE/DEAD), cytokine expression (PCR) , gliosis marker (zymograms and WB)	Astroctes and microglia: ↑Interleukin receptor antagonist IL-36Ra, ↑markers of reactive gliosis (GFAP, Neurocan) Neurons: ↑pro-apoptotic genes
Rogers et al., 2012b	**Human optic nerve head astrocytes**	**Flexercell® Tension Plus FX-4000T system**	**Equibiaxial dynamic stretch: cycle of 0% to 3%, or 0% to 12%, for either 2 h or 24 h at 1Hz**	**Glial cell activation and protein regulation after stretch (proteomics, WB)**	**Experiment yielded 573 proteins. Principal pathways implicated in the activation of astrocytes (maybe role in glaucomatous optic neuropathy)**

Table 1: Principal studies reproducing a stretch-induced injury in different cell types of the CNS (5/5)

References	Cell type	Device	Strain parameters	Biological output and techniques	Observation/measurement
Rogers et al., 2012a	**Human lamina cribrosa cells (glial cell found within the optic nerve head)**	**Flexercell® Tension Plus FX-4000T system**	**Equibiaxial dynamic stretch: cycle of 0% to 3%, or 0% to 12%, for either 2 h or 24 h at 1Hz**	**Protein regulation after stretch (proteomics, WB)**	**Experiment yielded 526 proteins. Principal pathways involved in protein synthesis, cellular movement, cell-to-cell signalling, and inflammation**
Higgins et al., 2013	**Human SH-SY5Y neuroblastoma cell line**	**Flexcell FX-5000**	**Equibiaxial dynamic stretch: 10% for 120 min/d for 7 days at 0.25 Hz**	**Neurite length and number (ICC), cytoskeleton status (ICC, PCR)**	**Stretch: more and longer neurites (even without a soluble neurogenic stimulatory factor)**
Andrews et al., 2016	**Primary human adult brain microvascular endothelial cells**	**Flexcell Tension System FX-5000**	**Biaxial stretch: 12 or 22% for 1s**	**Vascular remodelling following trauma (ICC, WB, flow cytometry)**	**↑ tight junction proteins occludin, PECAM-1 and ICAM-1. Activation of ARF6 (extracellular vesicle production). Following TBI *in vivo* : remodelling cerebral endothelium, production extracellular microvesicles**
Berretta et al., 2016	**Primary mouse cortical neurons plated on top of reactive astrocytes (astrocytes are stretched)**	**Flexcell FX-4000 Strain Unit**	**Triangular stretch: 23% for 130 ms**	**Investigate the effects of Sonic hedgehog (Shh) on neuronal sprouting (ICC, ELISA, PCR, WB)**	**Mechanical trauma impaired neurite outgrowth, Shh ↑neurites length. Shh-mediated neurite outgrowth is Smo-dependent**

* Studies using Flexcell device are highlighted in bold.

Apaf-1: Apoptotic peptidase activating factor 1; Arf6: ADP-ribosylation factor 6; BrdU: bromodeoxyuridine; CSA: cell straining apparatus; CSID: cell shearing injury device; DHR: dihydrorhodamine; DiI: fluorescent lipophilic cationic indocarbocyanine dye; ELISA: enzyme-linked immunosorbent assay; ET-1: endothelin-1; EthD-1: ethidium homodimer-1; GFAP: glial fibrillary acidic protein; ICAM-1: intercellular adhesion molecule 1; ICC: immunocytochemistry; IP3: inositol trisphosphate; LDH: lactate dehydrogenase; NG108-15 cell line: neuroblastoma cross glioma hybrid cells; NMDA : N-methyl-D-aspartate; NOS: nitric oxide synthases; NSE: neuron-specific enolase; NT2 cell line: pluripotent human embryonal carcinoma cell line; PCR: polymerase chain reaction; PECAM-1: platelet endothelial cell adhesion molecule; PI: propidium iodide; PUFAs: polyunsaturated fatty acids; ROS: reactive oxygen species; S-100β: calcium-binding protein B; Shh: sonic hedgehog; Smo: smoothened protein; SOD: superoxide dismutase; TMRM: tetramethylrhodamine, methyl ester; TUNEL: terminal deoxynucleotidyl transferase dUTP nick end labelling; WB: western blot

Table 2: Studies on mechanostimulation and oligodendrocytes

References	Cell type	Device	Mechanical stimulus	Biological outcomes and techniques	Observation/measurement
Rosenberg et al., 2008	Primary rat OPCs/DRG neurons co-culture	Beads	Cell density Beads	OPCs response to spatial and geometric constraints (ICC, WB)	Critical OPCs density is required for differentiation. Beads density and dimension affect OPCs differentiation in OPC/DRG co-culture
Jagielska et al., 2012	Primary rat OPCs	NA	Different substrate stiffness (from 0.1 to 70 kPa & glass 70GPa)	OPCs response to different stiffness (ICC, AFM-based measurement, time-lapse imaging)	Survival, proliferation and migration optimal on 0.1-1 kPA. Differentiation ↑ with increasing stiffness
Arulmoli et al., 2015	Primary mice neural stem and progenitor cell (NSPC)	J-Flex device	Static equibiaxial strain: 10% for 3 (neurons), 7(astrocytes) or 5-7 days (oligodendrocytes)	NSPC differentiation (ICC)	Stretch ↓ differentiation of NSPC into oligodendrocytes (it doesn't affect neurons & astrocytes)
Hernandez et al., 2016	Primary rat OPCs/DRG neurons co-culture	Portable "cell-compression" device or microspheres	Uniaxial compression for 1 or 30 min Cell density Microspheres	Epigenetic changes following three stimuli :high cell density, microspheres, compression (ICC, PCR, Co-IP, WB)	All stimuli resulted in formation of heterochromatin, meaning ↑ differentiation and myelination
Lourenço et al., 2016	Primary rat OPCs CG-4 cell line	NA	Different substrate stiffness (2.5, 6.5 and 10 kPa)	OPCs response to substrate stiffness and ECM protein (ICC, WB)	The optimal stiffness for differentiation and maturation is 6.5 kPa. Laminin-2 ↑ differentiation
Urbanski et al., 2016	Primary rat OPCs and Schwann cells (SC)	NA	Different substrate stiffness (1.5 and 30 kPa)	OPCs and SC response to different stiffness (ICC, WB)	For OPCs rigid substrate ↓ OPCs branching and myelination, ↑nuclear localization of Olig1, Yap and lamins For SC effect on morphology but not on differentiation

AFM: atomic-force microscopy; CG-4 cells: a rat glial precursor cell line; Co-IP: Co-Immunoprecipitation; DRG: dorsal root ganglion; ECM: extracellular matrix; ICC: immunocytochemistry; NA: not applicable; NSPC: neural stem and progenitor cell; OPC: oligodendrocyte precursor cell; PCR: polymerase chain reaction; SC: schwann cells; WB: western blot.

Table 3: Principal studies reproducing a stretch-induced injury in organotypic brain slices (1/2)

References	Cell type	Device	Strain parameters	Biological outcomes and techniques	Observation/measurement
Morrison III et al., 1998	NA	Custom made injury device	Biaxial strains between 0.10 and 0.65, strain rates as high as 15 s^{-1}	NA	Mechanical characterization of an *in vitro* device designed to reproduce injury in living brain tissue
Morrison et al., 2000a	Rat organotypic brain slice culture	Custom made injury device	Biaxial strain: strain mean 0.18, strain rate mean 10 s^{-1}	Expression of 18 genes related to cell death and survival (DNA array hybridization)	48h after stretch: ↑NGF, ↓Bcl-2, CKIIα, CREB, PKC1β, GAD65
Morrison et al., 2000b	Rat organotypic brain slice culture	Custom made injury device	Biaxial strain: 0.0<strain<0.47, mean 0.16; 0<strain rate<22 s^{-1}, mean 6 s^{-1}	Expression of 22 genes related to cell death and survival (DNA array hybridization), membrane permeability (LDH release)	24h after stretch: ↑BDNF, NGF, and TrkA ↓ Bcl-2, CREB, and GAD65
Morrison III et al., 2003	Rat organotypic hippocampal slice culture	Custom made injury device	Equibiaxial strain: strain 0.10,0.20 or 0.50 at strain rate 10, 20, 50 s^{-1}	Cell damage (PI), traumatic axonal injury (APP)	Cell death depends on both strain magnitude and rate and occurs after several days. Presence of traumatic axonal injury
Morrison et al., 2006	Rat organotypic hippocampal slice culture	Custom made injury device	Equibiaxial strain: strain 0.10 at 20 s^{-1} (mild) or 0.35 at 10 s^{-1} (severe)	Cell damage (PI)	Reproducible equi-biaxial deformation, cell damage positively correlates with strain magnitude
Cater et al., 2006	Rat organotypic hippocampal slice culture	Custom made injury device	Equibiaxial strain: 30 combinations of strain (0.05–0.50) and strain rate (0.1–50 s^{-1})	Cell damage (PI)	Cell death dependent on time post-injury (max 4 days) , on strain magnitude but not on strain rate
Cater et al., 2007	Rat organotypic hippocampal slice culture	Custom made injury device	Equibiaxial strain: strain 0.35 at 50 s^{-1}	Cell damage (PI), morphology (IHC for MAP-2 & βIII-tubulin), electrophysiological function (microelectrode arrays)	↓MAP2 & βIII-tubulin fluorescence, loss of synaptic function (more pronounced in severe injury *versus* mild). Blocking NMDA receptors ↓ neuronal injury, blocking NMDA & VDCCs, ↓ cell damage and attenuate reduction of synaptic function

Table 3: Principal studies reproducing a stretch-induced injury in organotypic brain slices (2/2)

References	Cell type	Device	Strain parameters	Biological outcomes and techniques	Observation/measurement
Elkin and Morrison III, 2007	Rat organotypic cortex slice culture	Custom made injury device	Equibiaxial strain: strain 0.10, 0.20 or 0.50 at strain rate 0.1, 1, 10, 20, 50 s^{-1}	Cell damage (PI)	Cell death depends on strain magnitude, strain rate, and time post-injury. Cortex less vulnerable compared to hippocampus (cell death less pronounced but appears earlier)
Kang and Morrison, 2015	Rat organotypic cortex slice culture	Custom made injury device	Equibiaxial strain: strains (up to 0.59) and strain rates (up to 26 s^{-1})	Cell damage (PI), electrophysiological function (microelectrode arrays)	Neural event magnitude depends on strain and strain rate. Compared to hippocampus, cortex is less spontaneously active, less excitable, and less prone to significant changes in electrophysiological function in response to strain or strain rate
Effgen and Morrison, 2016a	Rat organotypic hippocampal slice culture	Custom made injury device	Equibiaxial strain: strain mean 12.9, strain rate mean 5.3 s^{-1} Repeated mTBI: 1, or 2 mild stretch injuries 24, 72, or 144 h apart	Cell damage (PI), electrophysiological function (microelectrode arrays), morphology (IHC for MAP-2, pNF-H, GFAP, IBA1, SMI31)	Initial stretch: ↑vulnerability to a subsequent. Two mild stretch injuries at 24h apart: ↑ tissue injury, cell death, damage to dendrites, nitrite production, astrogliosis, and loss of long-term potentiation
Effgen and Morrison, 2016b	Rat organotypic hippocampal slice culture	Custom made injury device	Equibiaxial strain: strain mean 12.9, strain rate mean 5.3 s^{-1} Repeated mTBI: 2 mild stretch injuries 24h apart	Cell damage (PI), electrophysiological function (microelectrode arrays), morphology (IHC for MAP-2, pNF-H, GFAP, IBA1, SMI31)	Two mild stretch injuries at 24h apart: ↑ cell death, astrogliosis, and loss of long-term potentiation. Memantine ↓ the effect of injury for all outcome measured

APP: amyloid precursor protein; Bcl-2: B-cell lymphoma 2 (anti-apoptotic gene); BDNF: brain-derived neurotrophic factor; CREB: cAMP response element binding protein; CKIIα : α-subunit of calcium/calmodulin-dependent protein kinase II; GAD65: 65,000 mol. wt isoform of glutamate decarboxylase; GFAP: glial fibrillary acidic protein; IBA1: ionized calcium-binding adapter molecule 1; IHC: immunohistochemistry; LDH: lactate dehydrogenase; MAP-2: microtubule-associated protein 2; NA: not applicable; NGF: nerve growth factor; NMDA : N-methyl-D-aspartate; PI: propidium Iodide; PKC1β: 1β isoform of protein kinase C; pNF-H: phosphorylated neurofilament heavy; SMI31 :neurofilament protein; TrkA: Tropomyosin receptor kinase A; VDCC: voltage-dependent calcium channels.

3.7.1 Neurons

As expected, neurons are by far the most studied cells in the area. Several *in vitro* models of neuronal injury were developed to directly assess the effects of biomechanical parameters (as strain, strain rate, pressure) on the immediate and long-term cellular responses. All these models use primary cell culture of neurons isolated from rodent or immortal cell lines, to study biomolecular and electrophysiological effects of mechanical loading on neurons (Geddes and Cargill, 2001; Geddes-Klein et al., 2006; LaPlaca and Thibault, 1997; LaPlaca et al., 2005; Lusardi et al., 2004a). Lots of devices are available for studying the neuronal response to both biaxial stretch (Ellis et al., 1995; Geddes and Cargill, 2001; Morrison III et al., 1998) and uniaxial stretch (Lusardi et al., 2004b; Pfister et al., 2003). Slemmer and collaborators used an *in vitro* model of stretch injury on primary cerebellar neurons and they found an increase in cell damage and neuronal loss following equibiaxial stretch (Slemmer et al., 2004).

Some studies associate the mechanical stretch with a secondary insult, as L-glutamate, NMDA or hypoxia. Arundine and colleagues exposed cultured cortical neurons to sublethal mechanical stretch and cells maintained cell membrane integrity, viability, and electrophysiological function. However, neurons that survive primary insults remain vulnerable to secondary injuries. In fact, stretch as an initial insult induces in the cells a heightened vulnerability to subsequent challenges with L-glutamate or NMDA (Arundine et al., 2003). The increased vulnerability of stretched neurons to secondary insults seems to be associated with mitochondrial dysfunction, and an unexpectedly high production of reactive oxygen species (ROS). ROS scavengers and NO synthase (NOS) inhibitors prevented cell death and DNA degradation (Arundine, 2004). Another *in vitro* model combining mechanical stress with a secondary insult showed that stretch injury alone causes significant neuronal loss and membrane damage, and a combination of stretch and ischemia is able to provoke greater neuronal loss compared to stretch injury alone (Engel et al., 2005).

Several studies used the Flexcell® Tension System to reproduce a stretch-induced injury, notably on cortical neurons (Arundine, 2004; Arundine et al., 2003; Lau et al., 2006) and dorsal root ganglion neurons (Gladman et al., 2010, 2012; Lim et al., 2013) (**Table 1).**

3.7.2 Astrocytes

One of the earliest cell stretching systems was developed on astrocytes in order to study both single-cell response alone or in a cellular monolayer. To reproduce an injury in single cell, an astrocyte was mechanically poked with the blunt end of a glass pipette tip (Charles et al., 1991). Ellis and collaborators developed in 1995 a model of stretch-induced injury on astrocyte monolayer cultured on elastomeric sheets for examining cell morphology,

electrophysiology and also biochemical consequences of stretch. They found a correlation between the level of mechanical deformation and cellular injury. In fact, injured cells have shown cytoskeletal alterations, organelle disruption and also changes in intracellular calcium ion influx proportional to the level of mechanical deformation (Ellis et al., 1995). They found a significant cellular death within 24h from the initial mechanical insult. However, it did not propagate from the initial site of mechanical failure meaning that cells did not lyse inducing secondary death in neighbouring cells at the studied time point. Cell death was therefore driven by the mechanically-initiated intracellular events. The same group in following studies showed that, injury induces a rapid influx of extracellular Ca^{2+} into the astrocyte (Rzigalinski et al., 1997) and this is released from IP3-sensitive intracellular calcium stores (Chen et al., 2004; Rzigalinski et al., 1998). Injured astrocytes were also used as a cellular model of choice to study the role of membrane repair (Lamb et al., 1997), mitochondria and ATP regulation (Ahmed et al., 2000) and also the cascades regulating free radical generation and IP3 signalling (Floyd et al., 2001; Hoffman et al., 2011). Other studies showed that mechanical injury leads to alterations in volume-activated ion channels, in particular stretched astrocytes express a dysfunctional cation current instead of an osmoregulatory anion current and this can exacerbate cell swelling in injured astrocytes (Di et al., 2000). Stretch induced-injury also leads to an increase in intracellular sodium with reversing of Na^{+}/Ca^{2+} exchange (Floyd et al., 2005) and production of endothelin-1 to influence vascular tone (Ostrow et al., 2000) (**Table 1**).

3.7.3 Microglia

The CNS is composed of 5–20 % microglial cells (Lawson et al., 1990), which are responsible for the brain's innate immune response (Amor and Woodroofe, 2014; Colton, 2009; Delpech et al., 2015).

Few studies are available on mechanostimulation induced by stretching on microglia alone. Eder and colleagues induced a stretch on cell membrane by a movement of few micrometers of the recording patch pipette in order to study the effect of stretch-activated Cl^{-} channels on microglia ramification (Eder et al., 1998). Ellis and collaborators performed a stretch-induced injury on three different cell types each alone, neurons, astrocytes and microglia, and they showed that all three released S100B, a biomarker of TBI. Astrocytes and microglia were examined at 15 min and 1 h post-injury showing an immediate post-injury release, while neurons were examined at 24h and 48h after injury and S100B has been found to be increased at both time, with a concentration inferior to that in astrocytes and microglia (Ellis et al., 2007). A biaxial stretch device was also used to simulate electrode-induced strain and brain micromotion on astrocytes, microglia and neurons separately. In this study, glial cells

were submitted to a cyclic low magnitude strain as ~3% strain with a frequency of ~0.2 Hz, for a duration of 18 h for astrocytes, 4 h for microglia and 2 h for dissociated cortical neurons. In stretched astrocytes and microglia, the authors fond an upregulation of pro-inflammatory factors, reactive gliosis markers but also IL-36Ra that is believed to possess anti-inflammatory properties. The cyclic stretch of cortical neurons in presence of IL-36Ra significantly upregulate a number of pro-apoptotic factors resulting in neurons more vulnerable to apoptosis (Karumbaiah et al., 2012).

Microglial cells are highly active and mobile cells. They are exposed to different chemical and mechanical signals during their way to the site of damage. While the chemical signalling on microglia has been studied in detail, the understanding of mechanical signalling is still very limited. Nowadays, there are increasing studies exploring these mechanical signals, by measuring traction forces exerted by microglia as a function of substrate stiffness. Morphology of microglial cells becomes more complex on stiffer substrates, with lamellipodia-like structures at the tips of long processes (Bollmann et al., 2015; Moshayedi et al., 2014), their spread area increases on stiffer substrate and it is also shown that microglia preferentially migrate toward stiffer regions (Bollmann et al., 2015) (**Table 1**).

3.7.4 Oligodendrocytes

Despite all studies performed on different CNS cell types, oligodendrocytes have received less attention. None of the studies has addressed so far the effects of stretch-induced injury in oligodendrocytes. There are few studies exploring the effect of a mechanical stimulation, not necessarily stretching, on OPCs and oligodendrocytes.

Jagielska and collaborators showed that OPCs are mechanosensitive. While OPCs adhesion is independent of substrate stiffness, their survival and proliferation are optimal within the intermediate range of physiological brain tissue stiffness (E ~ 0.1–1 kPa). The assessment of the cell migration, in terms of velocity and distance, has shown that cells grown on polystyrene exhibited larger velocity of migration compared to those grown on soft substrates. The OPC differentiation, assessed by cell morphology, spread area and percentage of cell expressing MBP, has increased with increasing substrate stiffness (Jagielska et al., 2012). Lourenço and collaborators also evaluated the influence of substrate's stiffness on the differentiation and maturation of OPCs *in vitro*, showing that 6.5 kPa is the most appropriate stiffness (Lourenço et al., 2016). Moreover, OPCs respond to mechanical signals. In particular, cell density affects the differentiation of oligodendrocytes. It seems that OPCs must reach a critical density in order to start the differentiation. In fact, in OPC-DRG co-cultures, OPCs differentiate faster at high density (around 2 millions) as confirmed by immunostaining and Western blot analysis for MBP and PDGFR-α (Rosenberg

et al., 2008). According to the above study, another group reported that high-density plating results in increased myelination assessed by the staining of three myelin markers: MBP, CNP and MAG. They also studied the effect of compression generated by microsphere cultured with OPCs or by a mechanical device. They found that this mechanical stimulus induces a reorganization of nuclear structures, in particular formation of heterochromatin, as the presence of H3K9me3 positive heterochromatin and higher number of chromocenters, as hallmark of differentiation and increased myelination (Hernandez et al., 2016). A very recent study by Urbanski and collaborators has addressed the effect of different matrix stiffness on oligodendrocytes and Schwann cells by testing a soft matrix that reproduces a native environment (~ 1.3 kPa) and a rigid matrix that reproduces an injured tissue (~ 30 kPa). OPCs grown on rigid lesion-like matrix present less complex branching morphology and express lower levels of maturation markers suggesting that rigidity impairs branching and differentiation of oligodendrocytes. In contrast, Schwann cells develop normally in both soft and stiffer matrices (Urbanski et al., 2016). Mechanical forces, as stretching, also play a role during development. One study addressed the effect of equibiaxial static strain on the differentiation of neural stem progenitor cells (NSPC). Stretch is able to induce NSPC differentiation into oligodendrocytes but not neurons or astrocytes (Arulmoli et al., 2015)

Overall, the above studies analysed only the effect of mechanical forces on oligodendrocytes (see **Table 2)** but not in a context of mechanical injury. Therefore, the interest in developing a cellular model for studying stretch-induced injury in oligodendrocytes became more and more evident. It is noteworthy that treatment strategies in the context of TBI should consider the injury severity and aim to protect all CNS cell type populations, including astrocytes and oligodendrocytes, that are also affected along neurons during injury (DeRidder et al., 2006).

3.7.5 Mixed cell culture and organotypic slice cultures

All the information about mechanotransduction within CNS came from the studies performed on astrocytes and neurons, as well as studies on microglia, endothelial cells and also investigations on cross-talk among cell types (Ellis et al., 2007; McKinney et al., 1996). The model of stretch-induced mechanical injury developed by Ellis et al. in 1995 on astrocytes achieved a widespread use. It was adapted to design further studies using other cell types as rat cortical neurons and glia (Ellis et al., 1995; McKinney et al., 1996; Weber et al., 1999, 2001), as well as rat septo-hippocampal cultures (Pike et al., 2000), and mouse hippocampal (Slemmer et al., 2002) and cerebellar cultures (Slemmer et al., 2004) (**Table 1**).

Mc Kinney et al. examined the response of mixed neuronal plus glial cells, astrocytes, and aortic endothelial cells to stretch-induced injury. Stretch was able to cause damage with an increase of cell permeability, proportional to the degree of strain. Astrocytes and neuronal

plus glial cultures are similarly responsive to injury, whereas endothelial cells are more resistant. All the cell types analysed are capable of repair, however in endothelial cells the process of repair is more rapid (McKinney et al., 1996). Another study showed that cells from hippocampus may be susceptible to cumulative damage following repeated mild traumatic insults, since both glial cells and neurons appear to exhibit increased signs of damage after repetitive injury (Slemmer et al., 2002).The same group showed that the relative amount of S-100β*,* a marker of cell damage, released by cerebellar cells was several-fold higher than what reported for injured hippocampal cells, showing that cerebellar cultures were more sensitive to injury. This suggests that different brain regions respond differently to mechanical stress (Slemmer et al., 2004).

Quite recently, models of stretch-induced mechanical injury were developed on organotypic brain slice culture, literally a living slice of brain cultured over time, which maintains many aspects of *in vivo* biology preserving the 3D architecture with heterogeneous cell populations as well as the local connectivity between them. These models complete and integrate information obtained from studies using mixed neuronal glial cultures that are not designed to mimic the *in situ* architecture of the brain (Chen et al., 2009). Over years, slice culture systems have been successfully established from a variety of brain regions including hippocampus (Newell et al., 1995), striatum (Ostergaard et al., 1995), cortex (Plenz et al., 2011), spinal cord (Krassioukov et al., 2002) and cerebellum (Birgbauer et al., 2004). The difficult part in order to perform a stretch-induced mechanical injury is to cultivate these slices on elastomeric sheets. In fact, for a classical organotypic culture, slices are cultivated on particular supports, a semipermeable membrane, and the tissue is not covered by culture medium allowing a gas exchange with air (Stoppini et al., 1991), an important condition for the survival of slices. Morrison and collaborators first developed in 2000 an hippocampal organotypic culture on silicone membrane where slices, upon several days of culture, were submitted to a mechanical stretch (Morrison et al., 2000a, 2000b). Injured slices showed the presence of traumatic axonal injury assessed by accumulation of amyloid precursor protein (APP) and cell death was dependent on both cell magnitude and rate (Morrison III et al., 2003). The same team tested 30 combinations of strain (0.05–0.50) and strain rate (0.1-50 s^{-1}) and they found that cell death depend on time post-injury (max 4 days) and on strain magnitude (Cater et al., 2006). The expression of some genes related to cell death and survival was analysed concluding that injured organotypic tissue has some level of correspondence with activated genes reported for TBI *in vivo* (Morrison et al., 2000a, 2000b). The same group found that stretch leads to morphological changes in neuronal cell bodies and processes, and loss of synaptic function accompanied by dendritic damage identified by both fragmented pattern of βIII-tubulin immunoreactivity and a loss of MAP-2 immunostaining

(Cater et al., 2007). They also showed that hippocampus and cortex don't respond in the same way to a stretch-induced injury, in particular cortex is less vulnerable with a threshold for injury above 10% and below 20% Lagrangian strain. Cell death begins earlier in cortex (1 day post-injury *versus* 3 days) and is less sustained than in hippocampus (Elkin and Morrison III, 2007) (**Table 3**).

CHAPTER 4

Oxidative stress

In chemistry, every compound that can accept electrons is called oxidant or oxidizing agent, while a compound that donates electrons is called reductant or reducing agent (Cao and Prior, 1998; Prior and Cao, 1999). Reduction is a chemical reaction in which a substance gains electrons, while an oxidation is when a substance loose electrons. When a reductant donates its electrons, it causes another substance to be reduced, and, when an oxidant accepts electrons, it causes another substance to be oxidized (Hrbac and Kohen, 2000; Schafer and Buettner, 2001).
In biology, in an oxidation process there is usually a gain of oxygen, whereas a reduction leads to an oxygen removal. An oxidation process is always accompanied by a reduction process and the full reaction is known as redox reaction. These are the basis for numerous biochemical pathways and cellular chemistry, biosynthesis, and regulation (Shapiro, 1972). In biology, the terms reductant and oxidant can be better replaced by antioxidant and pro-oxidant, respectively (Cao and Prior, 1998; Prior and Cao, 1999). The organism must face both pro-oxidants and antioxidants continuously, the balance between these two species is tightly regulated and the maintenance of the homeostasis is crucial for different vital cellular functions (Kohen and Nyska, 2002).

Reactive oxygen species (ROS) and reactive nitrogen species (RNS) are pro-oxidants compounds often referred as ROS/RNS together. The harmful effect of free ROS and RNS radicals causing potential biological damage is termed oxidative stress and nitrosative stress, respectively. Here, I focus my dissertation on oxidative stress.

The term “ROS” includes all unstable metabolites of molecular oxygen that are classified into two groups, radicals and non-radicals (**Table 4**).
The radical group counts nitric oxide radical (·NO), superoxide ion radical ($O_2{\cdot}^-$), hydroxyl radical (·OH), peroxyl (ROO·) and alkoxyl radicals (RO·) (Kohen et al., 2004). These radical species, also called free radicals, contain at least one unpaired electron in the shells around the atomic nucleus and are capable of independent existence (Halliwell and Gutteridge,

1985; Rice-Evans and Burdon, 1994). This unpaired electron results in high reactivity of these species because they have affinity to donate or obtain another electron to attain stability. The oxygen molecule itself, O_2, is also a radical because it contains two unpaired electrons on two different orbits (Halliwell and Gutteridge, 1985), but it is not reactive due to the so-called spin restriction, which does not allow the donation or acceptance of another electron before rearrangement of the spin directions around the atom. The primary free radicals that are generated in cells are superoxide and nitric oxide. Superoxide is generated through either incomplete reduction of oxygen in electron transport systems or as a specific product of enzymatic systems, while ·NO is generated by nitric oxide synthases. Both are reactive and can readily react to form a series of other ROS and RNS (Rahal et al., 2014).

The non-radical group contains a lot of compounds, such as hypochlorous acid ($HOCl^-$), hydrogen peroxide (H_2O_2), organic peroxides, aldehydes, ozone (O_3), and singlet oxygen ($^1O_2$). Some of these substances are extremely reactive although not radical by definition. H_2O_2 in particular is able to cross the cellular membranes, through specific aquaporin channel, and it can reach sites distant from its source to modify DNA and protein. Moreover, in presence of transition metals, H_2O_2 can generate the hydroxyl radical (·OH) that is highly reactive.

Reactive Oxygen Species (ROS)

Radicals:	
$O_2^{\cdot-}$	Superoxide
$OH^{\cdot}$	Hydroxyl
$RO_2^{\cdot}$	Peroxyl
$RO^{\cdot}$	Alkoxyl
$HO_2^{\cdot}$	Hydroperoxyl

Non-Radicals:	
H_2O_2	Hydrogen peroxide
$HOCl^-$	Hypochlorous acid
O_3	Ozone
$^1O_2$	Singlet oxygen
$ONOO^-$	Peroxynitrite

Reactive Nitrogen Species (RNS)

Radicals:	
$NO^{\cdot}$	Nitric Oxide
$NO_2^{\cdot}$	Nitrogen dioxide

Non-Radicals:	
$ONOO^-$	Peroxynitrite
ROONO	Alkyl peroxynitrites
N_2O_3	Dinitrogen trioxide
N_2O_4	Dinitrogen tetroxide
HNO_2	Nitrous acid
NO_2^+	Nitronium anion
NO^-	Nitroxyl anion
NO^+	Nitrosyl cation
NO_2Cl	Nitryl chloride

Table 4: Different types of ROS and RNS produced in the cell. Common reactive oxygen and nitrogen species are reported divided into radicals and non-radicals species (Dhawan, 2014).

ROS are produced as a normal product of aerobic metabolism, and they are maintained within physiological, non-toxic levels, thanks to multiple enzymatic and non-enzymatic systems that have been developed in living cells during evolution (Poli et al., 2004). Oxidative stress occurs when the homeostatic processes fail and free radical generation is much beyond the capacity of the body's defences. In biological systems, oxidative stress can

be due to an excessive production of ROS/RNS and/or a deficiency of enzymatic and non-enzymatic antioxidants.

4.1 Origin of reactive oxygen species

Although the exposure of the organism to exogenous ROS is extremely high, the exposure to endogenous sources is much more important and extensive, since it is a continuous process during the life span of every cell in the organism (Kohen, 1999).

Mitochondria

Generally the most important source of cellular ROS are mitochondria (Dayem et al., 2010; Inoue et al., 2003; Liu et al., 2002). They are responsible of a continuous production of ROS due to the electron transport chain located in the mitochondrial inner membrane, which is essential for the energy production inside the cell (Inoue et al., 2003; Valko et al., 2006). Mitochondria generate ATP through a series of oxidative phosphorylation reactions. The reduction of oxygen to water in the mitochondria for ATP production occurs through the donation of 4 electrons to oxygen to produce water (Fleury et al., 2002). During this process, one- or two-electron reductions instead of four electron reductions of O_2 can occur, leading to the formation of $O_2{\cdot}^-$ or H_2O_2, and these species can be converted to other ROS (**Fig. 21**).

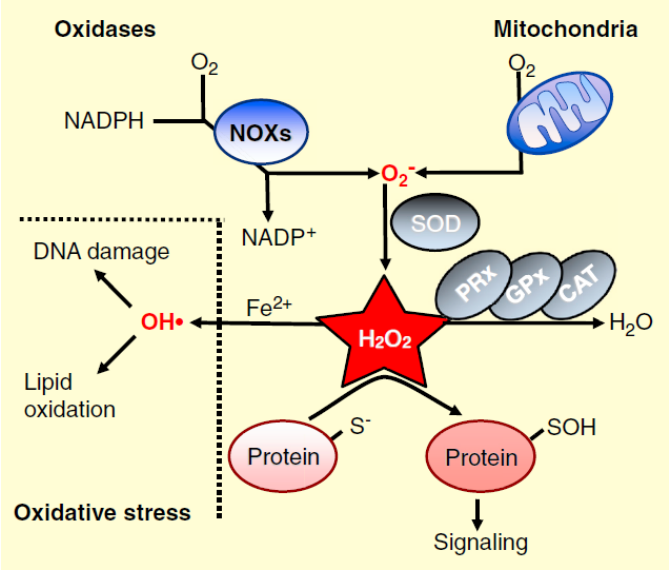

Figure 21: Diagram illustrating the basics of ROS. Intracellular superoxide ($O_2{\cdot}^-$) can be produced by electron leak from aerobic respiration in mitochondria or by the oxidation of NADPH by NAPH oxidase enzymes (NOXs). Superoxide is rapidly converted into hydrogen peroxide (H_2O_2) by compartment-specific superoxide dismutases (SODs). H_2O_2 is capable of oxidizing cysteine residues on proteins to initiate redox biology. Alternatively, H_2O_2 may be converted to H_2O by cellular antioxidant proteins, such as peroxiredoxins (PRx), glutathione peroxidase (GPx), and catalase (CAT). When H_2O_2 levels increase uncontrollably, hydroxyl radicals ($\cdot OH$) form *via* reactions with metal cations (Fe^{2+}) and irreversibly damage cellular macromolecules (Schieber and Chandel, 2014).

In many cases, there is a leakage of ROS from the mitochondria into the intracellular environment (Ames et al., 1995). The massive production of mitochondrial ROS is increased further in the aging cell, where the function of the mitochondrion is impaired and its membrane integrity damaged (Brunk and Terman, 2002).

Peroxisomes

Peroxisomes are ubiquitous subcellular organelles which play an important role in the metabolism of plasmalogens, long chain fatty acids, cholesterol, bile acids, docosahexaenoic acid, eicosanoids and hydrogen peroxide (van den Bosch et al., 1992; Kovacs et al., 2002; Lazo et al., 1990; Verhoeven and Jakobs, 2001). Peroxisomes contain at least 50 different enzymes, which are involved in a variety of biochemical pathways as fatty acid oxidation. The oxidation of a fatty acid is accompanied by the production of hydrogen peroxide (H_2O_2) from oxygen, which is then decomposed by the enzymatic activity of catalase. A number of myelin lipids are metabolized in peroxisomes and many peroxisomal diseases are associated with white matter abnormalities, highlighting the role of peroxisomal metabolism in the nervous system and in particular in white matter (Kassmann, 2014; Powers and Moser, 1998; Singh et al., 2004).

NADPH oxidases

Enzymes are another source of endogenous ROS. Some enzymes produce ROS as by-product of their activity but there are also some enzymes designed to produce ROS. In particular, in the last years, NADPH oxidase family members have emerged as the major contributors to $O_2^{\cdot -}$ generation (Angeloni et al., 2015; Brennan et al., 2009). Superoxide anion can, in fact, be generated both enzymatically, e.g. during the NADPH oxidase reaction, and non-enzymatically in the mitochondrial respiratory chain (**Fig. 21**). The NADPH oxidases (NOXs) and dual oxidases (DUOXs) are multi-subunit enzymes localized in the plasma membrane, and in the membranes of phagosomes (in neutrophils). This family of enzymes generates ROS in a regulated manner, in response to growth factors, cytokines and calcium signals. They use NADPH as a source of electrons to reduce molecular oxygen.

The first enzyme to be discovered to “intentionally” produce ROS in mammalian cell is the NOX expressed in phagocytes, now known as NOX2. This enzyme generates a large amount of ROS, in particular superoxide and hydrogen peroxide, during the “respiratory burst” in order to kill phagocytised microbes. Then, other isoforms have been identified and in total the human NOX family consists of seven isoforms (NOX1, NOX2, NOX3, NOX4, NOX5, DUOX1, and DUOX2) (Lambeth and Neish, 2014). These isoforms are distributed in

various tissues and cells with high expression of certain isoform only in specific organs and cells (**Table 5**).

In the first step, one electron is added to the molecular oxygen in a univalent reduction to generate superoxide anion ($O_2 \cdot^-$) using NADPH or NADH as the electron donor:

$2O_2 + NAD(P)H \rightarrow 2\ O_2 \cdot^- + NAD(P)^+ + H^+$

Enzyme	Highest level of expression
gp91phox (NOX2)	Phagocytes
NOX1	Inducible: colon and vascular smooth muscle
NOX3	Fetal kidney
NOX4	Kidney, osteoclasts, ovary and eye; widespread
NOX5	Spleen, sperm, mammary glands and cerebrum
DUOX1	Thyroid, cerebellum and lungs
DUOX2	Thyroid, colon, pancreatic islets and prostate

Table 5: Human NOX/DUOX enzymes and principal sites of expression (Lambeth, 2004).

The NOX1, NOX2, NOX3, NOX4, NOX5 isoforms have found to be expressed in the brain (Lambeth, 2004; Sorce and Krause, 2009). It seems that NOX isoforms are often co-expressed in various regions of the CNS and that NOX expression, in certain regions, appears to be inducible and not constitutive. The expression of NOX has also been investigated in different CNS cell type using *in vitro* primary cultures. Studies investigating the role of NADPH oxidase within the nervous system have focused primarily on microglia, neurons, astrocytes, endothelial cells, and infiltrating leukocytes (Brennan et al., 2009; Lipton and Rosenberg, 1994; Trotti et al., 1998). It is known that NOX1, NOX2 and NOX4 are present in neurons, astrocytes and microglia, but the peculiar function in these different cells is not fully understood (Cooney et al., 2013; Sorce and Krause, 2009). Regarding NOX3, it is found to be expressed in the inner ear (Bánfi et al., 2004). In oligodendrocytes, the NADPH oxidase expression has been investigated and confirmed only in the past few years (Cavaliere et al., 2012; Johnstone et al., 2013). Recently, Accetta and collaborators measured the expression of NOX enzymes by semi-quantitative and real-time PCR in MO3-13 cells (human oligodendrocyte cell line) and demonstrated that NOX3 and NOX5 isoforms are expressed (Accetta et al., 2016). Another study reported for the first time that DUOX-1 and 2 are expressed in the rat brain as well as in human neuroblastoma cells and in MO3-13 cells (Damiano et al., 2012).

Other enzymes

Other enzymes designed to produce reactive species are the nitric oxide synthases (NOS), a family of enzymes that produce ·NO from L-arginine (Cañas, 1999). There are three isoforms of NO synthases: neuronal NOS (nNOS), endothelial NOS (eNOS) and the inducible NOS (iNOS). The latter is activated in stress condition and it produces ·NO at high concentration that can induce damage to different cellular components as lipids, proteins and DNA directly or lead to the formation of the very reactive peroxynitrite anion (nitroperoxide) $ONOO^-$ (Akyol et al., 2004; Halliwell and Whiteman, 2004).

All the three isoforms utilize L-arginine and molecular oxygen as substrates and require the cofactor NADPH. NOS isoforms produce ·NO but they can also catalyse other leak and side reactions, such as superoxide production at the expense of NADPH (Förstermann and Sessa, 2012).

Other sources of ROS may involve peroxisomal oxidases, cytochrome P-450 enzymes, cyclooxygenases (COX), monoamine oxydases (MAO), xanthine oxidases, lipoxygenases, myeloperoxidases, aldehyde oxidases, dehydrogenases, tryptophan dioxygenases, and flavoprotein dehydrogenases. In these cases, the production of ROS is a side reaction of normal enzymatic function (Angeloni et al., 2015; Dhawan, 2014).

The compartmentalization of ROS production within the cell is very important to determine whether if damage process or redox signalling is occurring (Schieber and Chandel, 2014). For an effective redox signalling, H_2O_2-dependent oxidation of target proteins occurs close to the source of H_2O_2. For example a protein target of H_2O_2 that has been generated by NADPH oxidases, that are membrane proteins, are also located at the plasma membrane. Mitochondria are known to move dynamically towards their targets, allowing H_2O_2 generated by these organelles to activate signalling pathways (Al-Mehdi et al., 2012). In the same way, superoxide accumulation in mitochondria has different outcomes from superoxide accumulation in the cytosol, in part due to a high content of iron-sulfur cluster proteins in the mitochondrial matrix. In fact, SOD2 (mitochondrial superoxide dismutase) knockout mice have a more severe pathological phenotype compared with SOD1 (cytoplasmic superoxide dismutase) knockout mice (Schieber and Chandel, 2014) (see paragraph 4.4.1 for details on SOD).

Therefore, the type of ROS produced and their localization determine whether, and at which extent, the signalling or oxidative damage occurs. To summarize, ROS have two faces: a small increase in ROS levels activates signalling pathways to initiate biological processes, while high levels of ROS result in damage to DNA, protein or lipids (Schieber and Chandel, 2014).

4.2 Physiological context: ROS signalling

ROS are appreciated as signalling molecules, since they regulate different physiological processes as cell differentiation, tissue regeneration, and prevention of aging. An example of beneficial role of free radical is the molecule of nitric oxide (·NO). ·NO is formed from arginine by the action of the enzyme NO-synthase (NOS) (Pryor, 2006). ·NO physiologically is produced by two constitutive isoforms of NOS, in particular during vasodilating processes by the endothelial NOS (eNOS) or during transmission of nerve impulses by the neuronal NOS (nNOS). In a condition of stress, ·NO is instead produced at high concentration by a third NOS isoform that is inducible (iNOS) (Miyamoto et al., 2002; Olszanecki et al., 2002; Pavanato et al., 2003) and, in this context, ·NO can cause damage to different cellular constituents (Akyol et al., 2004; Halliwell and Whiteman, 2004).
In general ROS act as signalling molecules when present in low concentration, they can for example promote cell proliferation and cell survival. Redox system regulates ROS-mediated signalling *via* direct oxidative modification of redox-sensitive signalling proteins. Their actions are mediated through oxidative / nitrosative reactions. These molecules may attack cysteine residues on proteins *via* oxidative / nitrosative modifications and alter many proteins, e.g. transcription factors, kinases, and phosphatases, which in turn may affect downstream signalling cascades and alter cell fate (Dhawan, 2014).

Nrf-2/Keap1/ARE pathway

The transcription factor NF-erythroid 2 (E2)-related factor 2 (Nrf2) is known as a member of the NF-E2 basic leucine zipper family of proteins. Under physiological condition, Nrf2 is constitutively bound to cytoplasmic regulatory protein Kelch-like ECH-associated protein 1(Keap1) which serves to prevent its nuclear translocation, and targets Nrf2 for ubiquitin-proteasome degradation. Under condition of oxidative or xenobiotic stress, Nrf2 is translocated from the cytoplasm to the nucleus, where it binds antioxidant response element (ARE) in the regulatory region of many genes.
When drugs or xenobiotics enter in a cell, they are metabolized by a group of enzymes, known as drug metabolizing enzymes, divided into three groups: the phase I, II, and III enzymes. Each group has distinct role, phase I enzymes oxidize drugs or xenobiotics, while phase II enzymes conjugate products of phase I reactions making them more hydrophilic. Finally, phase III enzymes transport or extrude the final metabolites out of cells (Zhang et al., 2013). The major regulator of phase II genes is Nrf2, and these genes are not only implicated in the detoxification of xenobiotics but also in the antioxidant defence. Over two hundred Nrf2/ARE driven genes are exploited for detoxification and antioxidant defence, among these some of the major phase-II antioxidant enzymes such as NAD(P)H: quinone oxidoreductase-

1 (NQO1), heme oxygenase-1 (HO-1), and glutathione S-transferase (GST) (Jain, 2005; Owuor and Kong, 2002) (**Fig. 22**).

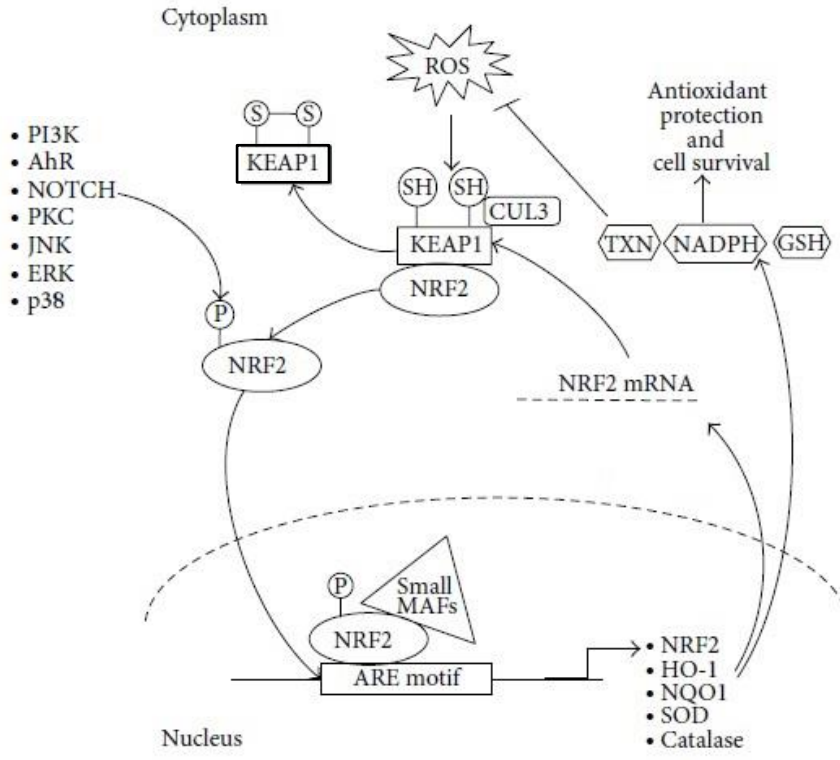

Figure 22: Overview of ROS-mediated NRF2 activities. Fine balance between free circulating cytoplasmic NRF2 bound to the regulatory protein KEAP-1 and the phosphorylated nuclear NRF2. AhR: aryl hydrocarbon receptor; Cul3: Cullin 3; ERK: extracellular signal-regulated kinase; GSH: glutathione; HO-1: Heme oxygenase 1; JNK: c-Jun NH2- terminal kinase; KEAP1: Kelch-like ECH-associated protein 1; NADPH: Nicotinamide adenine dinucleotide phosphate; NOTCH: Notch receptor; NQO1: NAD(P)H: quinone oxidoreductase 1; NRF2: transcription factor NF-erythroid 2 (E2)-related factor 2; PI3K: Phosphoinositide 3-kinase; PKC: Protein kinase C; p38: p38 kinase; SOD: Superoxide dismutase; TXN: Thioredoxin (adapted from Ayers et al., 2015).

NQO1 is one of the major phase-II antioxidant enzymes. It is localized in the cytoplasm and uses either NADPH or NADH as the hydride donor. It catalyses the two electron reduction of quinone to the redox-stable hydroquinone, preventing free radical formation from quinone derivatives (Talalay et al., 1995; Zhu and Li, 2012).

Heme oxygenases catalyse the first and rate-limiting step of heme catabolism, the breakdown of heme to carbon monoxide, biliverdin and iron. Biliverdin, is then degraded to bilirubin, both biliverdin and bilirubin have antioxidant properties (Yoshida and Kikuchi, 1974). There are two isoforms of active HO, HO-1 and HO-2. Whereas HO-2 is expressed constitutively, HO-1 is only expressed in an inducible manner and belongs to the phase II enzymes (Ferrándiz and Devesa, 2008).

Thus, Nrf2–ARE signalling has been shown to play an important neuroprotective role against oxidative damage and maintain the homeostasis of oxidative/anti-oxidative status.

The Nrf2 transcription factor is also known for being involved in a cross talk with other cellular signalling pathways (**Fig. 22**), as the aryl hydrocarbon receptor (AhR, involved in

minimizing xenobiotic toxic activities), the p53 pathway (involved in over 50% of human cancers), the NF-κB pathway and the NOTCH signalling pathway.

MAPK and SAPKs pathways

Mitogen-activated protein kinases (MAPKs) include ERK1/2, JNKs and p38. The JNK kinases are also known as SAPKs, stress-activated protein kinases. Both experimental and human studies have provided sufficient evidence to show that oxidative stress can activate MAP kinase *via* Ras pathway. MAPKs are shown to regulate AP-1, a transcription factor involved in control of cell growth and apoptosis (Knebel et al., 1996). AP-1 redox-mediated regulation has been demonstrated both at transcription and translation levels. Oxidative stress is shown to promote AP-1 activity by inhibition of histone deacetylases (HDAC), by activating MAPK pathways (Yu et al., 2007). ·NO is also shown to modulate AP-1 through S-glutathionylation.

NF-κB signalling

The nuclear factor κ-light-chain-enhancer of activated B cells (NF-κB) is part of a family of transcription factors of central importance in inflammation and immunity. Several studies demonstrate that NF-κB proteins are redox-sensitive transcriptional factors, since they can be activated or inhibited in response to oxidative stress and they are regulated *via* redox-mediated mechanism at multiple levels of activation pathways (Kabe et al., 2005; Morgan and Liu, 2011; Pantano et al., 2006). NF-κB activity influences ROS levels *via* increasing expression of antioxidant proteins (for example SOD, CAT, thioredoxin, NQO1 and HO1) and also pro-oxidant proteins (for example NOX2, xanthine oxidase and inducible NOS). Moreover, in turn, ROS have an effect on NF-κB pathway, in general they stimulate it in the cytoplasm, but inhibit NF-κB activity in the nucleus (see review Morgan and Liu, 2011).

Phosphatidylinositol - 3 - kinase (PI3K / Akt pathway)

Signal transduction *via* PI3 kinase plays an important role in the regulation of cell growth, proliferation, survival, and motility. Depending on the type and duration of ROS, PI3K signalling is activated or inhibited, thus modulating cell survival pathways. Activation of PI3K/ Akt pathways is tightly kept in check by phosphatases. ROS are shown to modulate this pathway mainly through oxidative modification of cysteine-dependent phosphatases (CDPs), which results in sustained activation of PI3K/Akt signalling, whereas redox modification of kinases results in down-regulation of PI3K/Akt signalling (Pelicano et al., 2006; Salmeen and Barford, 2005).

4.3 Pathological context: oxidative stress

Oxidative stress can be viewed as an imbalance between the pro-oxidant and antioxidant systems in the body in favour of the pro-oxidants (**Fig. 23**). Pro-oxidant is any endobiotic or xenobiotic that induces oxidative stress either by generation of ROS or by inhibiting antioxidant systems. It can include all reactive molecules present in cells or tissues that can cause damage to biological targets such as lipids, DNA, and proteins, and on the defending systems of the cell (Rahal et al., 2014). The ROS-induced damage of different cellular components is detailed in the paragraph 4.5. During pathophysiological conditions ROS are produced at an elevated rate, thus promoting oxidative damage with cellular and tissue injury. At extremely high levels or persistent cellular ROS, these are shown to promote cell death (Filomeni et al., 2015; Kamata et al., 2005; Valencia and Morán, 2004).

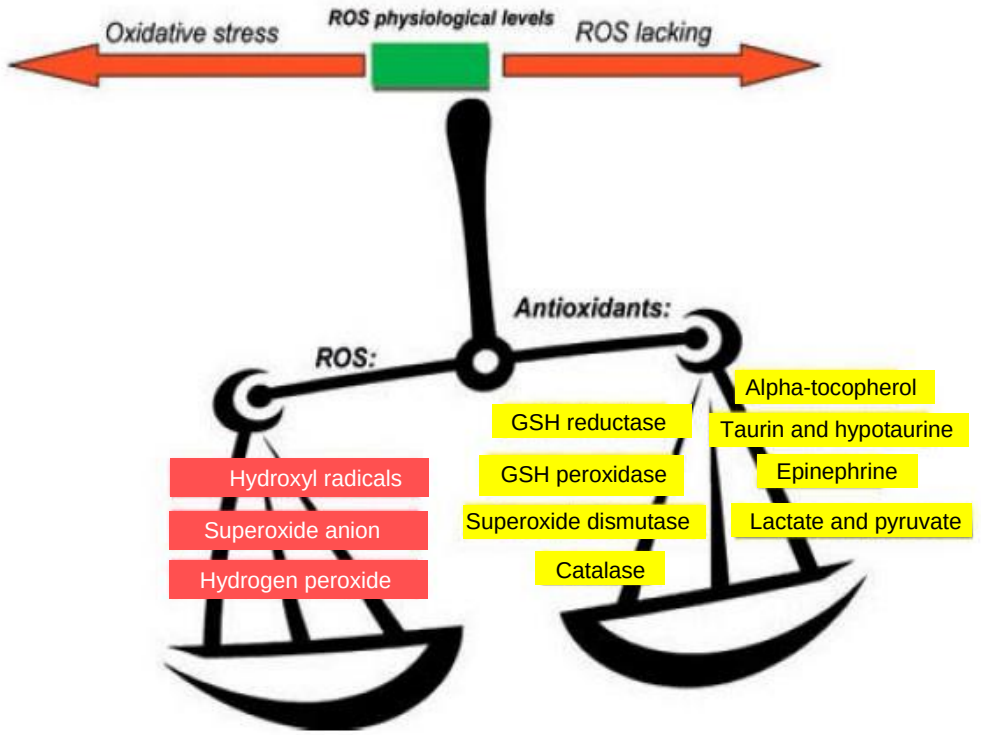

Figure 23: Imbalance between oxidant and antioxidant systems. The shift in the balance between oxidants and antioxidants systems in favour of oxidants is termed “oxidative stress” (adapted from Adly, 2010).

4.4 Antioxidant defence

All organisms possess inherent cellular defences to overcome oxidative stress that are collectively termed as antioxidants. An antioxidant (reductant or reducing agent) can be classified as a compound capable of preventing the pro-oxidation process, or biological oxidative damage (Cao and Prior, 1998; Prior and Cao, 1999).

To counteract the oxidative stress taking place, the cell has different strategies available including repair mechanism, physical mechanisms of protection against damage, and finally, the most important, the different antioxidant defence mechanisms. Endogenous antioxidant can be classified in two groups, the antioxidant enzymes and the low-molecular-weight antioxidants (LMWA) (Kohen and Nyska, 2002). These molecules are usually distributed within the cytoplasm and various cell organelles. The primary antioxidant enzymes, such as superoxide dismutase, catalase, and several peroxidases catalyse a complex cascade of reactions to convert ROS to more stable molecules, such as water and O_2. Besides the primary antioxidant enzymes, a large number of secondary enzymes act in close association with small molecular-weight antioxidants to form redox cycles that provide necessary cofactors for primary antioxidant enzyme functions. These enzymatic and non-enzymatic antioxidant systems are necessary for sustaining life by maintaining a delicate intracellular redox balance and minimizing undesirable cellular damage caused by ROS (Durackova, 2010).

4.4.1 Antioxidant enzymes

Superoxide dismutase

Superoxide dismutases (SOD) are enzymes that, as discovered by McCord and Fridovich in 1969, catalyse the dismutation of superoxide ($O_2 \cdot^-$) into oxygen and hydrogen peroxide (**Fig. 24**) (McCord and Fridovich, 1969). In humans, there are three SOD isoenzymes: the dimeric copper or zinc coordinated SOD1 (Cu/ZnSOD) located in the cytoplasm, the tetrameric manganese-coordinated SOD2 (MnSOD) located in mitochondria and the tetrameric extracellular copper or zinc co-ordinated SOD3 (Fridovich, 1997).

SODs prevent the accumulation of superoxide, which can damage and inactivate proteins containing iron-sulfur clusters. Accumulation of superoxide is therefore more associated with oxidative stress than redox signalling.

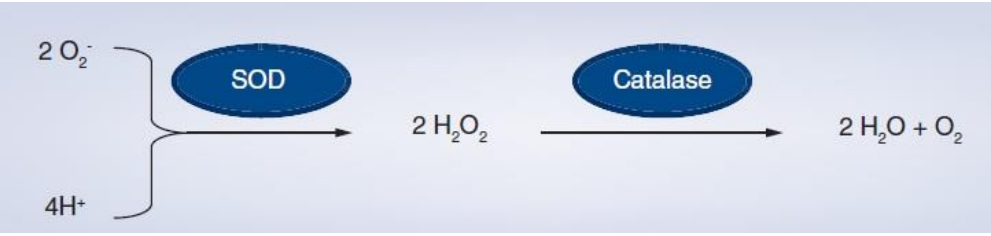

Figure 24: Enzymatic reaction catalysed by superoxide dismutase (SOD) and catalase (CAT). SOD catalyses the detoxification of superoxide to hydrogen peroxide which decomposes to water and oxygen, by peroxidases, in particular, by catalase (Ibitoye et al., 2016).

Catalase

The final product on the dismutation reaction (H_2O_2) can be removed by the catalase (CAT) enzyme or by members of the peroxidase family including glutathione peroxidase (Chance et al., 1979).The catalase neutralizes hydrogen peroxide in water and oxygen (**Fig. 24**).

The catalase is a tetramer, each subunit contains ferric ions (Fe^{3+}) of the heme group that undergo oxidation following interaction with the first molecule of H_2O_2 to produce Fe^{4+} in a structure called compound 1 (Lardinois, 1995). A second molecule of H_2O_2 serves as an electron donor and results in the destruction of the two H_2O_2 molecules involved to produce an oxygen molecule.

Peroxidases

Peroxidases are a large family of enzymes that typically converts hydrogen peroxide to water. Peroxidase has a high affinity for H_2O_2 and can remove H_2O_2 even at low concentration (Chance et al., 1979; Halliwell and Gutteridge, 1985). For this reaction they need two hydrogen atoms that they take from a “donor” molecule. The electron donors in these reactions are small molecules, such as glutathione. The removal of H_2O_2 is expensive since it consumes valuable molecules in the cellular environment. In fact, two molecules of glutathione are consumed for a removal of one molecule of H_2O_2 (Kohen and Nyska, 2002). This reaction is catalysed by glutathione peroxidase (GPx) (**Fig. 25**).

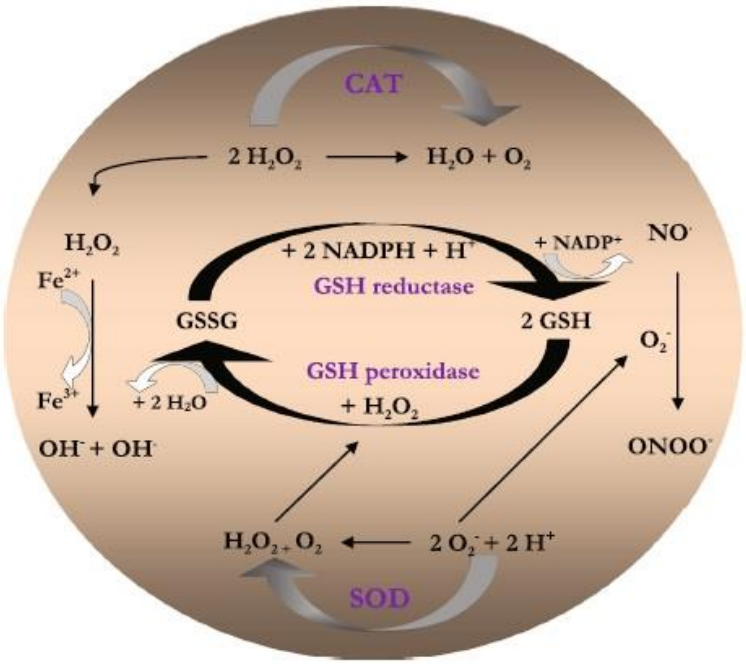

Figure 25: The enzymatic antioxidative mechanisms. The principal antioxidant enzymes and their mechanism of actions are reported. SOD: superoxide dismutase, CAT: catalase, GSH: gluthathione, GSSG: glutathione disulphide (Ljubisavljevic, 2016).

Other enzymes

There are other enzymes that support the activity of primary antioxidant enzymes. For example glucose-6-phosphate dehydrogenase supplies reducing equivalents (NADPH) that are necessary for cellular function and important for the regeneration of oxidized antioxidants (Chance et al., 1979). The reduction of glutathione disulphide (GSSG) to glutathione (GSH) is catalysed by glutathione reductase (GR), that is crucial for the regulation of intracellular oxidative stress (**Fig. 25**).

4.4.2 Low-molecular-weight antioxidants (LMWA) or scavengers

Low-molecular-weight antioxidants or scavengers have many advantages compared to enzymatic antioxidants, since they are small molecules that can penetrate the cell membrane and reach their biological target. They can be regenerated within the cell and they possess a wide spectrum of activities toward a large variety of ROS. These molecules share all a common mechanism. They react directly with a radical to neutralize it by donating an electron(s). In this way the scavenger itself is converted to a radical but not in a reactive form. This mechanism works well if the concentration of scavengers is high enough to compete with the biological target on the deleterious species (Kohen and Gati, 2000).

Glutathione is a classic example of a scavenging antioxidant. It forms the first line of defence and efficiently scavenges reactive species (Haenen and Bast, 2014). It is a low-molecular mass, thiol-containing tripeptide. Glutamic acid-cysteine-glycine (GSH) in its reduced form and GSSG in its oxidized form, in which 2 GSH molecules join *via* the oxidation of the SH groups of the cysteine residue to form a disulphide bridge (Halliwell and Gutteridge, 1985). GSH is present in high concentrations (mM range) in humans, animals, plants and aerobic bacteria. It is a cofactor for the enzyme glutathione peroxidase, acting as antioxidant donating the electrons necessary for the decomposition of H_2O_2. This compound is not only a scavenger, it is also involved in many biochemical pathways and cellular functions such as metabolism, maintenance of communication between cells (Barhoumi et al., 1993), prevention of oxidation in SH protein groups, and copper transport (Chance et al., 1979; Gul et al., 2000). Glutathione can also act as a chelating agent for copper ions and prevent them from participating in the Haber-Weiss reaction (reaction that generates ·OH from H_2O_2 and $O_2{\cdot}^-$, it is catalysed by iron). It serves as a cofactor for several enzymes and plays a role in protein folding, degradation, and cross-linking. In addition to these biochemical functions, it can scavenge ROS directly since GSH can interact with ·OH, ROO·, and RO· radicals as well as with $HOCl^-$ and $O_2{\cdot}^-$. After the reaction with ROS, it becomes a glutathione radical, which can be regenerated to its reduced form (Gul et al., 2000; Halliwell and Gutteridge, 1985).

The low-molecular-weight antioxidants category also includes uric acid, vitamin A (retinoids) and carotenoids, in particular beta carotene that has a high-antioxidant activity as it quenches free radicals. The α-tocopherol (vitamin E) is an effective hydrogen donor and so antioxidant. It is a fat-soluble and free radical chain breaking antioxidant due to the presence of hydroxyl (-OH) group in its structure. Ascorbic acid (vitamin C) acts as a hydrogen donor and reverses oxidation, and can act both as an antioxidant and as a pro-oxidant. Fruits and vegetables in the diet are main source of vitamin C and other non-enzymatic antioxidants, e.g., flavonoids and related polyphenols. The concentration of these antioxidants is low and varies depending on their location. Bilirubin, melatonin, ubiquinol, lipoic acid, albumin, ferritin, ceruloplasmin, and transferrin also show antioxidant properties and can indirectly reduce or inhibit generation of reactive species (Dhawan, 2014; Kohen and Nyska, 2002). A summary of enzymatic and non-enzymatic antioxidants is given below (**Table 6**).

Enzymatic antioxidants	Nonenzymatic antioxidants
Thioredoxin (Trx)	Vitamins C, E, A
Peroxiredoxins (Prx)	Thiols
Glutaredoxin (Grx)	β-Carotene
Glutathione peroxidase (Gpx)	Polyphenols
Reduced glutathione (GSH)	NAC
Oxidized glutathione (GSSG)	Zinc, selenium
Glutathione reductase (GR)	Glutathione
Extracellular glutathione peroxidase (eGPx)	Uric acid
Catalase	Lycopene
Peroxidase	Allyl sulfide
Superoxide dismutase	Indoles
	Gallic acid
	Hesperitin
	Catechin
	Chrysin

Table 6: Enzymatic and non-enzymatic antioxidants that protect against ROS/ RNS generation (Dhawan, 2014).

It has to be considered that as the free radicals share a physiological as well as pathological role in the body, the same antioxidant molecule can have a double effect. Due to its free radical scavenging activity, it may act as disease promoter, by neutralizing the physiologically desired ROS molecules, or as disease alleviator by removing the excessive levels of ROS species (Rahal et al., 2014). This can explain why pharmacological strategies to overcome the deleterious effects of the ROS and RNS have not been always successful in clinical trials for different diseases (Dhawan, 2014; Steinhubl, 2008). Redox-based therapeutic/preventive

strategies should be evolved maintaining redox homeostasis to modulate redox-sensitive factors which govern cell fate (Dhawan, 2014).

4.5 Biological targets of ROS

ROS produced in tissues, under a condition of oxidative stress, can damage cellular components and macromolecules, as lipid, nucleic acids, and proteins (Kohen and Nyska, 2002; Rahal et al., 2014; Schieber and Chandel, 2014) (**Fig. 26**). ROS can affect different cellular processes inducing an alteration in calcium influx, mitochondrial swelling and lysis (Bhatti et al., 2005).

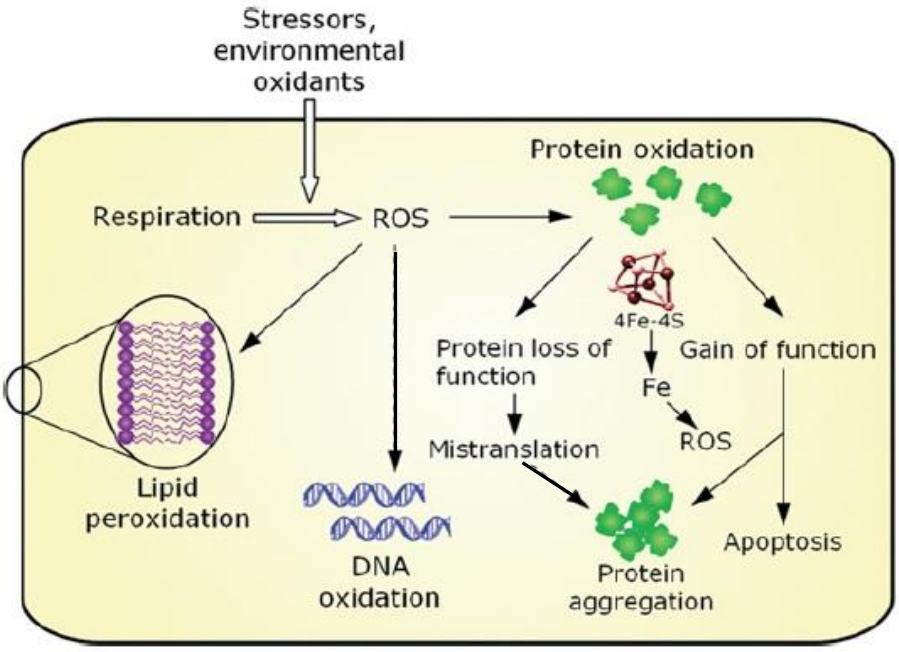

Figure 26: Major routes of ROS actions in cells. ROS can damage cellular components and macromolecules inducing lipid peroxidation, nucleic acids oxidation and proteins oxidation. This last process can leads to an alteration of protein functionality, with loss or gain of function and possibly resulting in protein aggregation and apoptosis (adapted from Avery, 2011)

Lipids

The polyunsaturated fatty acids are one of the favoured oxidation targets for ROS and all cellular membranes are vulnerable to oxidation due to their high concentrations of unsaturated fatty acid. The damage to lipids, usually called lipid peroxidation, occurs in 3 stages: initiation, propagation and termination. Oxygen-free radicals, particularly superoxide anion radical ($O_2\cdot^-$), hydroxyl radical (·OH), and alkylperoxyl radical (·OOCR), are potent initiators of lipid peroxidation. During the first stage, the radical abstract a hydrogen atom from a methylene group in the lipid. This process affects polyunsaturated fatty acids, because of their multiple double bonds in between which lie methylene bridges ($-CH_2-$). The

presence of a double bond adjacent the methylene group weakens the bond between the hydrogen and carbon atoms so that it can easily be removed from the molecule.

As a consequence of hydrogen abstraction, the remaining fatty acid radical retains one electron and it is not very stable. It reacts with molecular oxygen to form a peroxyl-fatty acid radical ROO· during the propagation stage. These radicals are capable of abstracting another hydrogen atom from a neighbouring fatty acid molecule, which leads again to the production of fatty acid radicals that undergo the same reactions and interaction with oxygen, allowing a propagation of the reaction. The last stage, chain termination, occurs when one ROO· interacts with another radical or antioxidants (Kohen and Nyska, 2002). A single initiation can lead to a chain reaction resulting in peroxidation of all the unsaturated lipids in the membrane.

The end products of lipid peroxidation, such as malondialdehyde (MDA), 4-hydroxy- 2-nonenol (4-HNE), and F2-isoprostanes, are accumulated in biological systems and can be used as marker of oxidative stress (Rahal et al., 2014).

It is noteworthy that the brain is highly susceptible to lipid peroxidation because of its elevated oxygen consumption and richness in polyunsaturated fatty acids (Hall and Braughler, 1993) and iron (Zaleska and Floyd, 1985). Lipid peroxidation causes alterations in cell membrane fluidity, increases permeability of membranes, and decreases membrane activity, leading to cell injury.

DNA

Even though DNA is a stable, well protected molecule, ROS can interact with it and cause several damages as modifications of bases, single- and double-DNA breaks, loss of purines, DNA-protein cross linkage, damage to deoxyribose sugar and also damage to the DNA repair system (Poulsen et al., 2000). Not all ROS cause damage to DNA, the principal responsible is hydroxyl radical. The predominant detectable oxidation product of DNA bases *in vivo* is 8-hydroxy-2- deoxyguanosine (8-OHdG) due to ·OH radical attack to guanine at its C-8 position. The interaction with other less reactive ROS, as $O_2\cdot^-$ and H_2O_2, does not lead directly to damage but these species serve as sources for other reactive intermediates as ·OH *via* the Haber-Weiss reaction. NO and $O_2\cdot^-$ might lead to the formation of $ONOO^-$ that can easily cause DNA damage similar to that obtained when hydroxyl radicals are involved (Ames, 2001; Halliwell, 1999; Kohen and Nyska, 2002). Oxidation of DNA bases can occur in both nuclear and mitochondrial DNA. Mitochondrial DNA is particularly sensible to oxidative damage because of his proximity to a primary source of ROS and its deficient repair capacity compared with nuclear DNA. Moreover the redox modulation of transcription factors can

produce an increase or decrease in their specific DNA binding activities, thus modifying the gene expression (Rahal et al., 2014).

Proteins

Proteins are also a target for ROS attack. In particular, ·OH, RO·, and nitrogen-reactive radicals predominantly cause protein damage. Hydrogen peroxide and superoxide in physiological concentration exert a weak effect on proteins but those containing -SH group can undergo oxidation following interaction with H_2O_2. A first-degree oxidation of cysteine residues within proteins is not pathological, since it serves as a reversible signal transduction mechanism. It is estimated that thiolate oxidation in living cells occurs in the nanomolar range of H_2O_2, whereas higher levels of H_2O_2 further oxidize thiolate anions to sulfinic (SO2H) or sulfonic (SO3H) species. These sulfinic and sulfonic modifications can be irreversible and result in permanent protein damage (Schieber and Chandel, 2014).
Proteins can be subjected to different ROS modification as peroxidation, damage to specific amino-acid residues, degradation, and fragmentation having as consequences loss of enzymatic activity, changes in the type and level of cellular proteins and altered cellular functions (Davies, 1987; Grune et al., 1997; Stadtman et al., 1988).
The products of protein oxidation are usually aldehydes, keto compounds, and carbonyls.

4.6 Assessment of oxidative stress

Reactive oxygen species

Most radicals are short-lived species (seconds). They quickly react with other molecules, making it difficult to directly assess the presence of ROS. Electron spin resonance (ESR) spectroscopy, or electron paramagnetic resonance (EPR) spectroscopy, is the only analytical approach that enables direct detection of free radicals, such as ·NO, superoxide, and hydroxyl radical (Jiang et al., 1996; Rice-Evans and Burdon, 1994).
·NO, produced by NO-synthases, is used for example as marker of multiple sclerosis. ·NO, nitrate (NO^{3-}) and nitrite (NO^{2-}), often as a total value (tNOx) are measured in plasma or serum (Ibragic et al., 2012; Tavazzi et al., 2011).
Different probes were also developed in order to detect different ROS as reviewed by Gomes and collaborators (Gomes et al., 2005). One of the probes is carboxy-dichloro-dihydro-fluorescein diacetate (CM-H2DCFDA), a general oxidative stress indicator. Since 1965, a method employing dichlorofluorescin diacetate (DCFH-DA) is used to measure hydrogen peroxide in aqueous solution (Brandt and Keston, 1965; Paul and Sbarra, 1968). DCFH-DA is a stable non-fluorescent compound that can be “activated” by alkaline hydrolysis to non-

fluorescent 2‘7”dichlorofluorescin (DCFH). DCFH is then rapidly oxidized to highly fluorescent 2’,7’dichlorofluorescein (DCF) in the presence of hydrogen peroxide (Bass et al., 1983).

Transcriptional regulators of ROS

Nrf-2 is an important transcriptional factor that regulates the expression of multiple anti-oxidant genes (see paragraph 4.2). Nrf-2 protein expression is thus used to evaluate the redox status of cells. Elevated ROS results in Nrf-2 translocation to the nucleus and activation of the antioxidant defence (Mota et al., 2015; Tasset et al., 2013). Usually the expression of HO-1 and NQO1 is also evaluated, two antioxidant genes regulated by Nrf2 (Cheng et al., 2013; Hong et al., 2010).

Enzyme involved in the antioxidant deference

The activity of several anti-oxidant enzymes is often used as marker of oxidative stress, such as superoxide dismutase, catalase, NO-synthase, glutathione peroxidase and glutathione reductase (Mota et al., 2015; Tasset et al., 2013; Tunez et al., 2011).

End products of oxidation

Ongoing oxidative damage is also analysed by measurement of secondary products including derivatives of amino acids, nucleic acids, and lipid peroxidation.

Determination of lipid damage is assessed by the measurement of the end products of lipid peroxidation, such as malondialdehyde (MDA), 4-hydroxy- 2-nonenol (4-HNE) (Chen et al., 2007; Dexter et al., 1994; Yoritaka et al., 1996), 2-propenal (acrolein) (Carini et al., 2004; Uchida, 2003a) and isoprostanes (Cracowski et al., 2002; Montuschi et al., 2004). Compared with free radicals, the aldehydes are relatively stable and can diffuse within or even escape from the cell and attack targets far from the site of the original event (Uchida, 2003b). Some of these aldehydes have been shown to exhibit an easy reactivity with various biomolecules, including proteins, DNA, and phospholipids, generating stable products at the end of a series of reactions that are thought to contribute to the pathogenesis of many diseases.

Cellular DNA damage can be caused by ROS generated under different conditions, and several techniques have been developed to measure the oxidatively modified nucleobases in DNA (Dizdaroglu et al., 2002; Halliwell, 2002; Halliwell and Gutteridge, 1985). DNA subjected to hydroxyl radical attack generates a wide range of base and sugar modification products (Dizdaroglu et al., 2002) but the predominant detectable oxidation product of DNA bases is 8-hydroxy-2-deoxyguanosine (8-OHdG), the most utilized marker of DNA damage (Tasset et al., 2013; Tunez et al., 2011).

Proteins are major targets for ROS/RNS because of their high overall abundance in biological systems. Proteins are also primarily responsible for most functional processes within cells. It has been estimated that proteins can scavenge the majority (50%–75%) of generated ROS/RNS (Davies et al., 1999). Protein damage is evaluated by products of protein oxidation as aldehydes, keto compounds, and carbonyls. Advanced oxidation protein products (AOPP) are final cross-linking products of protein oxidation that can be used as marker of oxidative stress (Santulli et al., 2015; Tunez et al., 2011; Witko-Sarsat et al., 1996, 1998). Carbonyl (CO) groups, aldehydes and ketones, are produced on protein side chains (especially on Proline, Arginine, Lysine, and Threonine) when they are oxidized. Carbonyls are chemically stable, which is useful for both their detection and storage (Dalle-Donne et al., 2003). Carbonyl derivatives are also generated during the oxidative cleavage of proteins by the α-amidation or by oxidation of glutamyl side chains, leading to formation of a peptide in which the N-terminal amino acid is blocked by an a-ketoacyl derivative (Berlett and Stadtman, 1997). CO group can also be introduced into proteins by secondary reaction of the nucleophilic side chains of Cysteine, Histidine, and Lysine residues, with aldehydes (4-HNE, MDA) produced during lipid peroxidation. Moreover reactive carbonyl derivatives (ketoamines, ketoaldehydes, deoxyosones) can be generated as a consequence of the reaction of reducing sugars, or their oxidation products with lysine residues of proteins (glycation and glycoxidation reactions). Hence, the presence of carbonyls is not necessarily indicative of oxidation of amino acid residues in proteins, and it is advisable to establish whether the CO groups come from direct or indirect modification of the amino acid side chain with additional assay, for example the detection of lipid peroxidation adducts. In any case, protein carbonyl content is the most commonly used marker of protein oxidation (Chevion et al., 2000; Dalle-Donne et al., 2006; Hensley et al., 1995; Pamplona et al., 2005; Sorolla et al., 2008, 2010).

Thiols are organosulfur compound that contain a carbon-bonded sulfhydryl or sulphydryl (–C-SH or R-SH) group. It is known that electrophiles, organic free radicals, and ROS act to damage proteins through mechanisms that involve the direct oxidation of cysteine thiol groups or the formation of mixed thiol disulfides. Under conditions of moderate oxidative stress, oxidation of Cysteine residues can lead to the reversible formation of mixed disulfides between protein thiol groups and low-molecular-mass thiols (S-thiolation), particularly with GSH (S-glutathionylation) (Dalle-Donne et al., 2006). Sulfur switches are shown as sensors in redox signalling pathways, the detection of thiols is commonly used as marker of oxidative stress (Harris and Hansen, 2012; Himmelfarb et al., 2000; Santulli et al., 2015).

Ratio of GSH/GSSG

Glutathione is the first line of defence and efficiently scavenges reactive species, the measurement of both reduced glutathione (GSH) and glutathione disulfide (GSSG) is often used as an indicator of oxidative stress. A decrease of the ratio GSH/GSSG indicates a shift to an oxidized form of GSH, suggesting the presence of oxidative stress at the cellular or tissue level (Dalle-Donne et al., 2006; Durackova, 2010; Tunez et al., 2011).

Ratio NADPH/NADP$^+$

The three major antioxidant components in cells are the glutathione system, catalase, and superoxide dismutase. The reduced glutathione is regenerated by glutathione reductase depending on NADPH. Catalase does not need NADPH to convert hydrogen peroxide to water but has an allosteric binding site for NADPH that maintains catalase in its active conformation. Superoxide dismutase does not use NADPH to convert superoxide to hydrogen peroxide. However, if this is not adequately reduced chemically by catalase or glutathione, the increased hydrogen peroxide levels will quantitatively increase and inhibit the superoxide dismutase. Hence, the entire antioxidant system depends on NADPH. A decrease of the ratio NADPH/NADP$^+$ indicates a shift to oxidized form, NADP$^+$, suggesting the presence of oxidative stress (de Arruda Grossklaus et al., 2013; Galea et al., 2012).

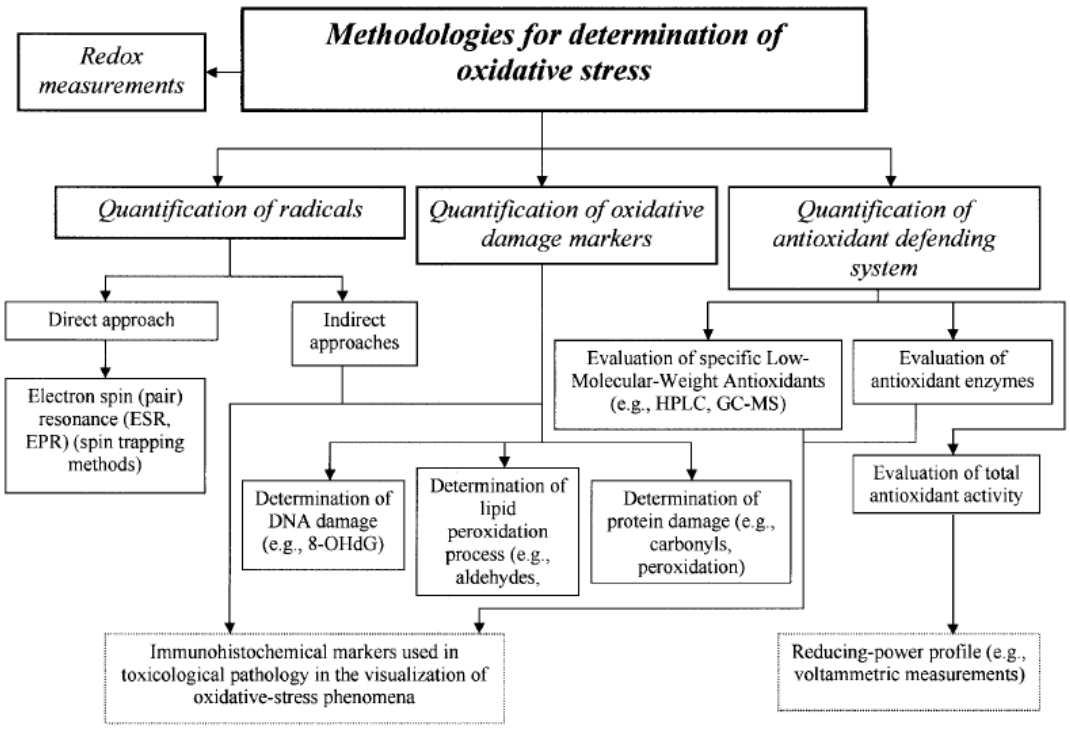

Figure 27: Classification of methods used to determine and quantify oxidative stress. The principal methods are indicated divided in three group, based on quantification of i) radicals, ii) oxidative damage markers, iii) antioxidant defence system (Kohen and Nyska, 2002).

4.7 Oxidative stress and TBI

The CNS is extremely sensitive to free radical damage because of a relatively small total antioxidant capacity. The brain is unusually rich in ascorbate, which has a relatively high antioxidant potential (Halliwell, 1992; Harrison and May, 2009), however this is not enough to protect this organ against oxidative stress. On the contrary, the brain is highly sensitive to oxidative stress because it consumes about 20-30% of inspired oxygen and contains high levels of both polyunsaturated fatty acids and redox transition metals, making it an ideal target for a free radical attack (Sultana et al., 2013). Oxidative modifications affect the physiological functions of cell components and oxidative stress has been reported in different neurodegenerative diseases as Parkinson's disease, Alzheimer's disease, amyotrophic lateral sclerosis, and Huntington disease (for review see Gan and Johnson, 2014; Zhang et al., 2013). There are also abundant evidences showing a considerable increase in the production of ROS following TBI and this increase has a significant role in the aetiology of progressive neuropathology of TBI (Abdul-Muneer et al., 2015; Cornelius et al., 2013; Mendes Arent et al., 2014). Abundant evidences show that after a traumatic, hypertensive, or ischemic injury, oxygen radicals contribute to observed changes in cerebrovascular reactivity (DeWitt and Prough, 2009; Rubattu et al., 2014; Truelove et al., 1994), blood-brain barrier permeability (Obermeier et al., 2013; Schleien et al., 1994), infarct size (He et al., 1993), and brain edema (Himadri et al., 2010).

Following TBI, the blood flow is compromised triggering a cerebral hypoxia or ischemia with the consequent reduction of oxygen and glucose supply to the brain. Some studies reported that the most common free radical generated almost immediately following TBI is superoxide (Kontos and Povlishock, 1986; Kontos and Wei, 1986). Within the injured nervous system, different possible sources contribute to the production of superoxide radical.

There is a transition from an aerobic to an anaerobic metabolism that generates a state of acidosis responsible of the activation of pH-dependent calcium channels (Xiong et al., 2004). In aqueous environments, as in the cytoplasm, $O_2{\cdot}^-$ exists in equilibrium with the hydroperoxyl radical ($HO_2{\cdot}$) which is more lipid soluble and a more powerful oxidizing agent (Gutteridge, 1995). Under the acidic condition, characteristic of TBI, there is a shift of the equilibrium in favour of $HO_2{\cdot}$ increasing lipid peroxidation that can induce brain tissue damage by different mechanism. The increased Ca^{2+} influx, often secondary to glutamatergic excitotoxicity and/or the activation of the calcium dependent proteases and phospholipases, lead to structural alteration of the inner mitochondrial membrane with consequent impairment of the mitochondrial electron transport chain and increase in ROS/RNS production (Kowaltowski et al., 1995; Xiong et al., 2004). A severe increase of Ca^{2+} can lead to the opening of the mitochondrial permeability transition pore resulting in extrusion of

mitochondrial Ca^{2+} and other components. This event discharges and uncouples the electron transport chain, preventing ATP production, and it can result in necrotic or apoptotic cell death (Sullivan et al., 2005). Moreover during blood flow restoration or reperfusion, enzyme involved in ROS production can find enough oxygen to generate large quantity of ROS/RNS, strongly contributing to oxidative stress in TBI (Ikonomidou and Turski, 2002).

In addition to mitochondrial dysfunction and excitotoxicity mediated by glutamate, there are also other sources of ROS in TBI as the formation of bradykinin. Bradykinin is an inflammatory mediator able to activate the phospholipase A2 with consequent release of arachidonic acid that can serve as source of free radicals (Abbott, 2000; Moochhala et al., 2005). Arachidonic acid may also facilitate NADPH oxidase activity, further increasing ROS production (Rubinek and Levy, 1993). NADPH oxidases merit to be mentioned, because it has been widely demonstrated that these enzymes play a crucial role in the development of secondary injury after TBI (Choi et al., 2012; Cooney et al., 2013; Dohi et al., 2010; Ferreira et al., 2013; Loane et al., 2013; Zhang et al., 2012). NOX upregulation occurs immediately after TBI and lasts for several days significantly contributing to oxidative stress damage and neuronal cell death. Moreover, some evidences suggest that NOX family may be a causative factor in the onset of neurodegenerative disease related to TBI. Considering the involvement of the different isoforms, NOX2 is the most responsive to injury. The expression of NOX isoforms depends on injury status and cell type, NOX2 is especially expressed by neurons and microglia, NOX3 by neurons and NOX4 by all three cell types (Angeloni et al., 2015).

At later time, TBI triggers a series of inflammatory processes that contribute to neuronal damage and failure of functional recovery. These processes are mediated by infiltrating inflammatory cells, as activated microglia, neutrophils, and macrophages that produce multiple pro-inflammatory mediators and can be additional sources of ROS (Lewén et al., 2000; Pun et al., 2009). Red blood cell lysis, due to mechanical trauma, is another important source of oxidative stress in TBI. The main consequence of red blood cells lysis is the release of free hemoglobin (Ascenzi et al., 2005) whose oxidation to oxyhemoglobin and methemoglobin contributes to ROS generation (Asano, 1999; Marzatico et al., 1993). In conclusion, many different ROS sources synergistically contribute to the onset of an extensive and profound condition of oxidative stress in TBI (**Fig. 28**).

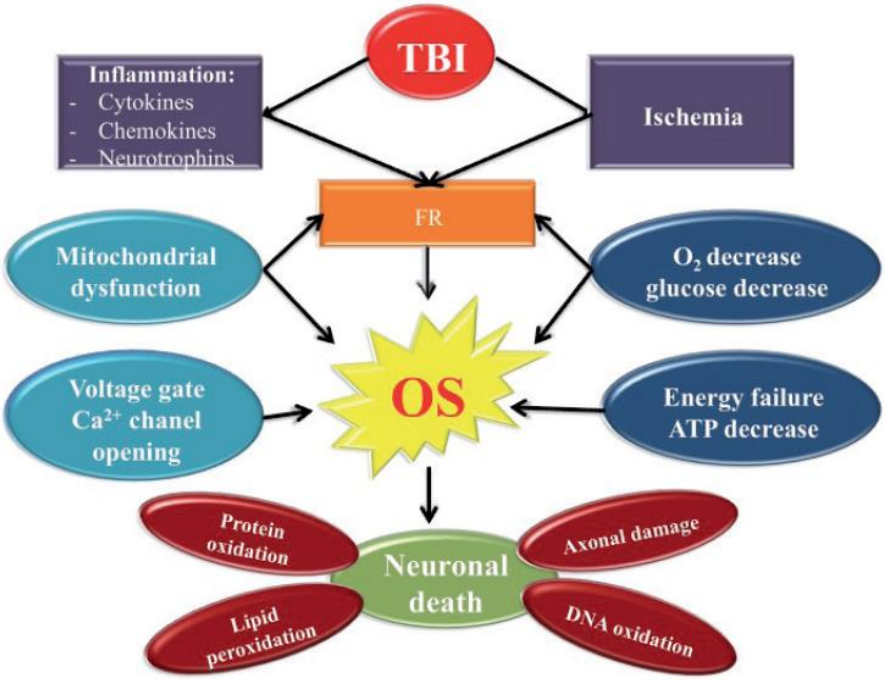

Figure 28: Oxidative stress and related mechanisms during brain ischemia and traumatic brain injury. Free radicals produced following TBI generate an oxidative stress that can result in neuronal death due to different mechanisms, as macromolecules oxidation. TBI: traumatic brain injury; FR: free radicals; OS: oxidative stress (Luca et al., 2015).

There are increasing evidences showing that Nrf2/ARE pathway plays an important neuroprotective role through inhibiting inflammatory cytokines, inducing the expression of detoxifying enzyme and maintaining the homeostasis of calcium ion in the secondary brain injury after TBI (Cheng et al., 2013; Hatic et al., 2012; Hong et al., 2010; Jin et al., 2009; Lu et al., 2015; Zhao et al., 2007).

It is known that after TBI, an assembly of oxidative stress markers (carbonylated proteins, lipid peroxides, ROS, RNS) are produced in the brain, while the activity of the most studied antioxidant defence enzymes varies (Rodríguez-Rodríguez et al., 2014). Oxidative stress occurs simultaneously in various conditions during and after TBI, but its correlation with the severity and outcome is not very well understood. The activity of some antioxidant enzymes (GPx, GR, SOD, CAT) change randomly in animal models of TBI sometimes increasing (DeKosky et al., 2004; Schwarzbold et al., 2010), sometimes decreasing (Dehghan et al., 2013; Silva et al., 2013) or even presenting no changes (Oztürk et al., 2008; Potts et al., 2009). Glutathione has been shown to decrease in rats (Dehghan et al., 2013; Kochanek et al., 2013), but not in mice (Blasiole et al., 2013; Dehghan et al., 2013; Homsi et al., 2009; Kochanek et al., 2013; Lomnitski et al., 1999), demonstrating a species-specific characteristic. High levels of lipid peroxidation markers, MDA, 4-HNE and acrolein, were found to be increased after TBI, indicating that lipid peroxidation is an important contributor to

this disorder (Ansari et al., 2008; Hall et al., 2004; Inci et al., 1998). Lipid peroxidation was evaluated in injured brain tissue subjected to mild and severe trauma in guinea pig. For the mild injury, a significant increase of lipid peroxidation is observed immediately after trauma with a gradually decrease, to attain by 36 hours the normal levels, showing a clearance of peroxides from the tissues. After severe trauma, the lipid peroxidation levels are increased rapidly and maintain elevated over 36 hours (Inci et al., 1998). In addition, 4-HNE and acrolein are evaluated in the ipsilateral and contralateral hippocampus following cortical contusion. 4-HNE is found to be increased at 3h post-trauma with peak values at 24-48h and is sustained up to 96 h (Ansari et al., 2008).

Oxidative damage to DNA also occurs early in TBI as demonstrated by 8-OHdG, that is increased within the first 15 minutes after trauma (Mendez et al., 2004). Proteins are also affected. Increased level of protein carbonyls are assessed after mild TBI and these alterations were reversed by administration of the antioxidant vitamin E, showing that oxidative damage to proteins may have an important role in neuronal death (Aiguo Wu et al., 2010). Protein carbonyl and lipid peroxidation are also increased after a mild injury while no changes, or even a decrease, are observed in severe TBI (Schwarzbold et al., 2010). It's undeniable that there is an induction of oxidative stress following a TBI. However, no correlation has been found between the level of oxidative stress and the severity of trauma (Petronilho et al., 2010; Schwarzbold et al., 2010).

4.8 Oxidative stress, oligodendrocytes and demyelination

Myelination requires that oligodendrocytes first construct and then maintain an extensive plasma membrane, and for this a vast supply of both precursor molecules and oxidative substrates is required (Roth and Núñez, 2016). Oligodendrocytes are one of the cells with the highest metabolism in the brain, since proper myelination requires large amounts of oxygen and ATP. A high metabolism, with high-energy consumption, means also large amounts of toxic by-products, such as hydrogen peroxide and ROS. Oligodendrocytes are also highly sensitive to oxidative stress because of their lipid-rich membranes where unsaturated long-chain fatty acids are unusually concentrated (French et al., 2009). In other cell types, the production of ROS is contrasted by GSH and other antioxidant mechanisms, while in oligodendrocytes the antioxidant defence is less robust. For example, astrocytes are relatively resistant to oxidative stress, astrocytes from primary culture have an intracellular concentration of approximately 5 mM glutathione and they are rich in cytochrome-P450 (Juurlink et al., 1996; Wilson, 1997). Oligodendrocytes only have less than 1 mM glutathione (Juurlink, 1997), making them 5 times more vulnerable to oxidative stress than astrocytes. This is a consequence of the lower activity of glutathione synthetase. GSH reductase activity

and GSH peroxidase activity in oligodendrocytes are at 50% and 15% of enzyme activity compared to astrocytes, respectively (Ljubisavljevic, 2016; Thorburne and Juurlink, 1996). Lower activity of SOD has also been shown in oligodendrocyte culture compared to microglial cells and astrocytes (Arend et al., 2013; Fernandez-Fernandez et al., 2012; Ljubisavljevic and Stojanovic, 2015). In oligodendrocytes, peroxisomes are also an important ROS source since they are present in large numbers in the process of active myelination (Ljubisavljevic and Stojanovic, 2015). In addition to their relatively poor antioxidant production, oligodendrocytes are even more susceptible to oxidative stress due to the need of iron as a cofactor for myelin production (Cheepsunthorn et al., 1998; Thorburne and Juurlink, 1996). They are the most iron-loaded cells of the CNS and intracellular accumulation of iron can stimulate the conversion of hydrogen peroxide to a hydroxyl radical, resulting in production of free radicals (Braughler et al., 1986; Juurlink, 1997). Therefore, oligodendrocytes can be easily damaged and they are particularly sensitive to both hypoxia and oxidative stress, especially during their terminal differentiation phase and while generating myelin sheaths. Oligodendrocyte precursor cells (OPCs) are more sensitive to oxidative stress than mature oligodendrocytes (Ljubisavljevic, 2016; Roth and Núñez, 2016). OPCs are poor in antioxidant defences and it is proved that their maturation is inhibited by reactive species (French et al., 2009; Volpe et al., 2011). Mature forms are better protected from oxidative stress by higher level of glutathione (Back et al., 1998) and by the switch from an oxidative to a glycolytic metabolism (Funfschilling et al., 2012). Nonetheless, mature oligodendrocytes are still vulnerable to oxidative stress. If anti-oxidant systems are not properly regulated, oligodendrocytes are left vulnerable to oxidative and free radical damage (Li et al., 2005). Since oligodendrocytes lack the appropriate antioxidant defence, their fate in the presence of free radical insult is largely dependent upon antioxidant support from other cells (Johnstone et al., 2013).

CNS in general has a relatively limited potential for anaerobic metabolism which makes it especially sensitive to hypoxia and oxidative stress (Yokoyama et al., 2008). In particular, it has been shown that the brain tissue is more sensitive to oxidative stress, in comparison to the spinal cord or the peripheral nervous system (Macco et al., 2013; Schnell et al., 1999). This could be due to the lower content of thiol redox system in the spinal cord and peripheral nerves in comparison to the brain tissue (Schnell et al., 1999). The most important effect of ROS damage is reported to be in oligodendrocytes, which are the key cells in the process of myelin creation in the CNS. Some studies have shown that oligodendrocytes are sensitive to ROS at the concentrations much lower than toxic concentrations for other glial cells, astrocytes, and microglia. ROS have in general short half-life (seconds) so they realize their effects in their immediate environment in relation to the place of their production. During the

process of myelin production and remyelination, the peroxisomal fraction of oligodendrocytes increases the volume and density, in accordance with metabolic requirements, thus representing an important independent ROS source (Singh et al., 2004; Sullivan et al., 2013; Zeis et al., 2008). Therefore, oligodendrocytes are particularly predisposed to damage by means of oxidative stress during the process of remyelination which is parallel to the process of active demyelination (Fancy et al., 2010). Moreover proteins are oxidized in condition of oxidative stress, including the myelin proteins MBP and PLP that are altered and, as a consequence, more susceptible to trypsin degradation. Under *in vitro* conditions, myelin, being altered by oxidative stress, is easily subjected to degradation by the effects of extracellular proteases (Chaitanya et al., 2013). Moreover, delamination of myelin sheath makes new amounts of myelin components prone to being damaged by ROS.

Overall, oxidative stress seems to be a critical player in the pathophysiology of demyelination as reported in different studies (Haider, 2015; Hamilton et al., 2013; Lee et al., 2012a; Ljubisavljevic, 2016; Ljubisavljevic and Stojanovic, 2015; di Penta et al., 2013; Shi et al., 2015; Vladimirova et al., 1998) (**Fig. 29**).

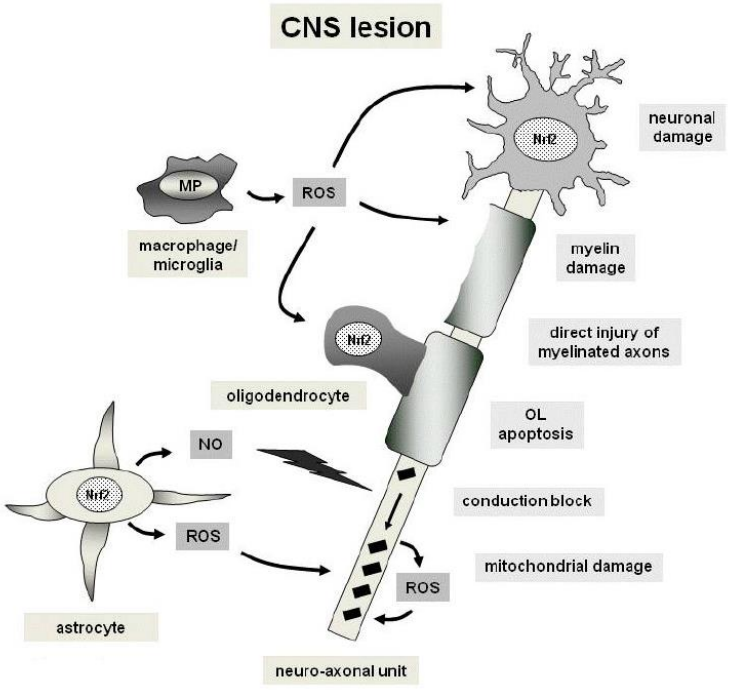

Figure 29: Mechanisms of oxidative injury and cytoprotection in a demyelinating CNS lesion. ROS and RNS lead to damage of neurons, axons, myelin and oliogdendrocytes (indicated by arrows). This process may also involve mitochondrial damage. Black squares indicate mitochondria accumulating in injured axons. The cytoptrotective transcription factor Nrf2 is present in neurons, oligodendrocytes and astrocytes as part of the cellular anti-oxidative response. Abbreviations: OL, oligodendrocyte; MP, myeloperoxidase (Lee et al., 2012a).

There are different *in vitro* models for reproducing an oxidative stress, a fundamental condition is that the redox balance has to be pushed in favour of the pro-oxidant systems. The ROS production can be stimulated by different methods, for example exposing cells to

γ-irradiation, to elevated oxygen tension (hyperoxia), to extracellular $O_2\cdot^-$ and H_2O_2, or by using free radical-generating drugs, such as paraquat, menadione and *tert*-butyl hydroperoxide (*t*BHP).

4.9 An *in vitro* model of oxidative stress induced by *tert*-butyl hydroperoxide (*t*BHP) in oligodendrocytes

We are particularly interested in *tert*-butyl hydroperoxide (*t*BHP), a membrane-permeant oxidant compound that generates *tert*-butoxyl radicals resulting in lipid peroxidation and depletion of intracellular glutathione (Adams et al., 1993, 1996). For this reason, *t*BHP has been extensively used as oxidative stress-inducing agent to study the effect of free radicals in different cell types and regions of the brain (He et al., 2015; Hughes et al., 2014; Pan et al., 2011; Peterson et al., 2008). Low doses of *t*BHP cause mostly apoptosis, while higher concentrations lead to both necrosis and apoptosis in the brain (Mukherjee and Adams, 1997; Mukherjee et al., 1995).

French and collaborators used an *in vitro* model of oxidative stress induced by *t*BHP in oligodendrocytes. They used a concentration of 5μM with an incubation time from 24h to 72h and they showed that oxidative stress arrested maturation of oligodendrocytes without an increase in cell death (French et al., 2009). These results suggested that oxidative stress may directly interfere with the program of oligodendrocyte differentiation leading to the demyelination associated with brain injury.

CHAPTER 5

Therapeutical strategies

Despite the progress made for the care of TBI patients, the current treatment is still symptomatic. The vast majority of clinical trials testing neuroprotective strategies validated in pre-clinical experiments are revealed ineffective. A Neurotrauma Pharmacology Workgroup was established in 2014 by the U.S. Army Medical Research and Materiel Command in order to establish a strategic research plan for developing pharmacological treatments that improve clinical outcomes after TBI. The pharmacological compounds of most interest for the treatment of TBI, nowadays in clinical trial of phase II and III, are acetylcholinesterase inhibitors, amantadine, cyclosporine A, erythropoietin, glyburide, growth hormone, lithium, methylphenidate and atomoxetine, minocycline, N-acetylcysteine (NAC), progesterone, simvastatin/other statins (see for review Diaz-Arrastia et al., 2014).

As reported in the paragraph 4.7 oxidative stress is responsible of different aspects of the secondary injury following TBI, raising a considerable interest in the development of antioxidant therapies for neuroprotection. Despite the promising results in preclinical studies, evidence of successful antioxidant therapy in clinical practice is limited (Rigg et al., 2005). There are in fact several drawbacks to the use of exogenous antioxidants, as the limited penetrability through the BBB, the rapid metabolism and instability of these compounds, short therapeutic windows, and a very narrow therapeutic dosage range, resulting in toxicity at higher doses (Gilgun-Sherki et al., 2002; Rigg et al., 2005). Nevertheless, natural antioxidants and modified antioxidants are promising candidates for future drugs to treat TBI (Mendes Arent et al., 2014).

Below a description of a promising pharmacological compound for TBI, the etazolate, is given. This compound already used by our group, shows a neuroprotective effect in *in vivo* and *ex vivo* models of TBI (Siopi et al., 2013; Llufriu-Dabén et al. 2016a,b under revision). Etazolate has also shown an antioxidant effect *in vivo* (see below) but this has never been confirmed as a direct effect *in vitro*. In the present work etazolate has been compared with a known powerful antioxidant, the N-acetylcysteine (NAC) (see § 5.2 below), in order to study its potential anti-oxidant effect in an *in vitro* model of *t*BHP-induced oxidative stress in the

oligodendrocyte 158N cell line. The success of the antioxidant therapy in TBI is limited probably because reducing the oxidative stress alone is not enough to have a positive outcome. Our interest in etazolate is based on its pleiotropic effect since etazolate is also known to have other properties as anti-inflammatory, and pro-cognitive.

5.1 Etazolate

Etazolate (SQ20009, EHT0202) is a pyrazolopyridine derivative compound (**Fig. 30**). It is known for different pharmacological properties and different mechanism of action. It is a i) positive allosteric modulator of the $GABA_A$ receptor, ii) antagonist of the adenosine receptor iii) phosphodiesterase inhibitor selective for the type 4 phosphodiesterase (PDE4) isoform iv) α-secretase activator (Barnes et al., 1983; Chasin et al., 1972; Daly et al., 1988; Marcade et al., 2008).

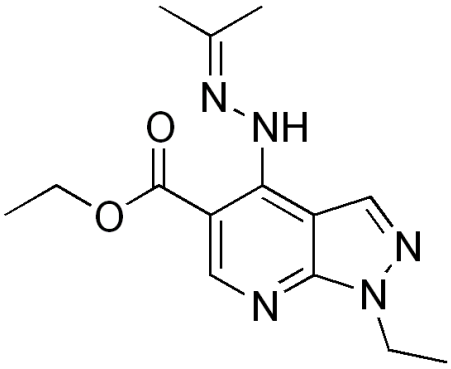

Figure 30: Chemical structure of etazolate or 1-Ethyl-4-[(1-methylethylidene)hydrazino]-1H-pyrazolo-[3,4-b]-pyridine-5-carboxylic acid, ethyl ester hydrochloride.

i) positive allosteric modulator of the $GABA_A$ receptor

Different studies have demonstrated the effect of etazolate as a modulator of $GABA_A$ receptor (Thompson et al., 2002). It has been shown that etazolate in low concentration reinforce the benzodiazepines binding to their specific site on $GABA_A$ receptors (Leeb-Lundberg et al., 1981; Supavilai and Karobath, 1979; Williams and Risley, 1979). The synergy between etazolate and benzodiazepines suggests that their action is due to different binding sites. It seems that the etazolate acts *via* the binding sites of picrotoxin and / or barbiturates on the $GABA_A$ receptor (Barnes et al., 1983; Ticku and Davis, 1982). The γ-aminobutyric acid (GABA) is the principal inhibitory neurotransmitter in the CNS and it can bind two different receptors, the ionotropic $GABA_A$ and the metabotropic $GABA_B$.

The $GABA_A$ -R is a ligand-gated ion channel expressed in neurons, astrocytes, microglia and oligodendrocytes in the CNS. Different studies showed that GABA has a role in the

development of oligodendrocytes, interstitial neurons and white matter in the developing CNS (Wu and Sun, 2015). Developing oligodendrocytes express $GABA_A$ receptor and GABA is able to induce a cell depolarization by acting on this receptor and increasing the intracellular Cl^- levels (Lin and Bergles, 2004). $GABA_A$ receptor activity also exhibits a protective effect on oligodendrocyte survival and Na-K-2Cl cotransporter isoform1 (NKCC1) is required for GABAergic trophic effects (Wang et al. 2003). In addition, a study demonstrated that a progesterone metabolite (3α,5α-tetrahydroprogesterone) is able to stimulate the MBP expression *ex vivo* and this effect could be inhibited by a selective $GABA_A$ receptor antagonist (bicuculline) suggesting a role of $GABA_A$ receptors in myelination (Ghoumari et al., 2003).

The $GABA_A$-R can also bind other endogen ligands, like neurosteroids, as well as pharmacological compounds as benzodiazepines, barbiturates, alcohols and the pyrazolopyridines as etazolate modulating the receptor activity. An important number of neurodegenerative pathologies are associated with a dysregulation of the GABAergic pathway, e.g. Parkinson disease, Huntington disease, schizophrenia, autism and epilepsy. There are evidences showing that after TBI there is dysregulation of GABA homeostasis and signalling (Guerriero et al., 2015; Imbrosci and Mittmann, 2011). The pharmacological activation of the GABAergic signalling has been proposed as therapeutic strategy. Nevertheless the use of benzodiazepines in TBI patients is discouraged, in fact the use of these compounds for the treatment of sleep disorders in traumatized patients seems to limit the functional recovery (Talsky et al., 2010).

ii) antagonist of the adenosine receptor

Etazolate is an antagonist of adenosine receptors with a particular selectivity for the types A_1 and A_2 (Daly et al., 1988). The type A_1 is the most abundant, widely express in the SNC and other tissues as adipose tissue, cardiac muscle ad neutrophils. It induces the adenylate cyclase inhibition with consequent reduction of cyclic adenosine monophosphate (cAMP) levels. The type A_2, on the other side, induces the adenylate cyclase activation increasing cAMP levels. The subtype A_{2A} is expressed in neurons and can modulate the transmission of GABA, acetylcholine as well as glutamate (Sachdeva and Gupta, 2013). Antagonist of A_{2A} receptor has been proposed as anti-parkinsonian treatment (Sachdeva and Gupta, 2013). The activation of this A_{2A} receptor has a role in the inhibition of pro-inflammatory cytokines in multiple sclerosis (Vincenzi et al., 2013). Moreover activation of A_{2A} receptor results in the inhibition of oligodendrocytes maturation *in vitro* (Coppi et al., 2013, 2015), while the activation of A_1 receptor induces OPCs differentiation, and promotes myelination (Stevens et al., 2002). In the CNS, adenosine dysregulation has been demonstrated following TBI but,

due to heterogeneity of post-traumatic consequences and the multiple role of adenosine, the adenosine receptors are not considered as a target for TBI treatment (Lusardi, 2009).

iii) phosphodiesterase inhibitor selective for the PDE4 isoform

Etazolate is a selective inhibitor of type 4 phosphodiesterase (PDE4) enzyme, in particular the variants PDE4C and PDE4D (Wang et al., 1997). PDE4 is the primary enzyme for metabolizing cAMP and it is expressed in different cell type including oligodendrocytes (Maurice et al., 2014; Whitaker et al., 2008). The second messenger, cAMP plays a key role in biochemical processes that regulate the cognitive process of memory consolidation. The activation of the cAMP/CREB is associated with consolidation and retention of long-term memory but not short-term (Menniti et al., 2006; Rose et al., 2005). PDE4 inhibitors may represent a way to regulate neuronal protection and plasticity by increasing cAMP levels and influencing cAMP/CREB/ BDNF signalling (Manji and Duman, 2001).

Another PDE4 inhibitor, the rolipram, showed beneficial effect blocking the detrimental Aβ's effect on dendritic spine (Shrestha et al., 2006), reversing Aβ-induced cognitive impairment and improving synaptic and cognitive functions by increasing cAMP levels *via* the PDE-CREB pathway (Gong et al., 2004; Wang et al., 2012). A recent study also demonstrated that raising cAMP with rolipram is accompanied by reduced levels of Tau protein aggregates and improved cognitive performance in a mouse model of tauopathy (Myeku et al., 2016). Other studies also showed that rolipram is able to reduce acute oligodendrocyte death after spinal cord injury in rat (Whitaker et al., 2008), to promote remyelination after cuprizone- or lysolecithin-induced demyelination in rat and mice (Sun et al., 2012b) and also to promote myelination and neurite outgrowth in a rat *in vitro* spinal cord injury model (Boomkamp et al., 2014). Moreover the administration of different PDE4 inhibitors (rolipram, milrinone, irsogladine, zaprinast and rottlerin) was also shown to enhance OPC differentiation increasing intracellular cAMP and MAPK kinases activity in primary OPC cultures. Rolipram also results in enhanced differentiation of OPCs *in vivo* within focal areas of toxin-induced demyelination and promotes remyelination (Syed et al., 2013). In the context of TBI, the cAMP levels are reduced and the pre-treatment with rolipram is able to restore cAMP levels, contrasting inflammation and traumatic axonal injury (TAI) (Atkins et al., 2007). Nevertheless, when the treatment is realised immediately after the trauma, the rolipram results in worsening the pathology (Atkins et al., 2012, 2013). Rolipram was developed as antidepressant and was used for this purpose in clinical trials phase I/II but this trial was stopped because of its side effects of nausea and emesis seen in some patients, it was poorly tolerated (Bielekova et al., 2009).

Considering etazolate, different studies have shown an antidepressant effect in different depression models. The inhibition of the activity of the hypothalamic-pituitary-adrenal axis,

responsible of the antidepressant effect, is associated with the restauration of the PDE-CREB pathway (Guo et al., 2014; Jindal et al., 2013a, 2015; Wang et al., 2014).

iv) α-secretase activator

The effects of etazolate as an α-secretase stimulator have been described for the first time by Marcade et al. (Marcade et al., 2008). They observed an increase in production of sAPPα after the treatment with etazolate in cortical neurons. These observations were also confirmed *in vivo*, in fact the oral administration of etazolate (10 mg / kg / day for 15 days) increases the release of sAPPα in guinea pig brains (Marcade et al., 2008).

Amyloid precursor protein (APP) is the precursor of β-amyloid peptide (Aβ) that is involved in Alzheimer disease. APP can be processed *via* two alternative, the non-amyloidogenic and the amyloidogenic, pathways. The non-amyloidogenic secretory pathway includes cleavage of APP to soluble APP (sAPPα) by α-secretases, member of a disintegrin and metaloprotease (ADAM) family, within the Aβ peptide sequence precluding the formation of Aβ. In contrast, the amyloidogenic pathway includes cleavage of APP by β- and γ-secretases resulting in the production of the toxic Aβ peptide (Checler, 1995; Nunan and Small, 2000).

The presence of Aβ plaques is typical of the Alzheimer disease but it is also reported after acute severe brain trauma (Ikonomovic et al., 2004; Roberts et al., 1994). Moreover, in addition to the Aβ peptides accumulated, the enzymes responsible for its production, β- and γ-secretases, are also accumulated in the acute phases of TBI in rodents and in humans (Blasko et al., 2004; Loane et al., 2009; Uryu et al., 2007).

Regarding sAPPα, obtained *via* the non-amyloidogenic pathway, it has been shown to have a neuroprotective effect. Brain administrations of sAPPα increase the synaptic density, and improve memory and learning in mice (Meziane et al., 1998). In addition, sAPPα is also able to protect neurons *in vitro* from excitotoxicity and ROS produced by glutamate and Aβ peptide (Goodman and Mattson, 1994; Mattson et al., 1993). Moreover, studies showed that sAPPα levels are significantly reduced after experimental TBI *in vivo* (Lesné et al., 2005; Siopi et al., 2011) and intracerebral administration of sAPPα can restore cognitive and motor functions post-TBI, and is able to reduce diffuse axonal injury (DAI) and apoptotic cells in the cortex and hippocampus (Corrigan et al., 2012; Thornton et al., 2006).

Marcade and collaborators showed that etazolate neuroprotective mechanism is associated with sAPPα release, because first, etazolate is able to release sAPPα in a dose dependent way, second, sAPPα mimics the neuroprotective effect of etazolate and third, sAPPα neutralization or the prevention of its production using ADAM inhibitors prevents etazolate effects on Aβ-induced neuronal death. This study also showed that the neuroprotective effects of etazolate are in the same way blocked by $GABA_A$ receptor antagonists suggesting

a link between $GABA_A$ signalling, the α-secretase pathway and neuroprotection (Marcade et al., 2008).

Etazolate belongs to a family of molecules with anxiolytic properties (Patel et al., 1985), it was first employed in different pre-clinical studies as antidepressant and anxiolytic (Ankur et al., 2013; Guo et al., 2014; Jindal et al., 2012, 2013a, 2013b, 2015; Wang et al., 2014) and then it was discovered to implement other beneficial effects as anti-inflammatory, neuroprotective, antioxidant and pro-cognitive effect. Etazolate exerts an anti-inflammatory effect by reducing the production of pro-inflammatory cytokines in a model LPS-induced depression. The antidepressant and anti-inflammatory effects seem to depend on the inhibition of PDE4 and the activation of the cAMP/pCREB/BDNF signalling (Guo et al., 2014). Our group confirmed that etazolate reduces neuroinflammation and showed for the first time that a single post-traumatic administration of etazolate offers persistent neuroprotection following TBI in mice. Etazolate attenuates microglial/macrophage activation, and IL-1β production and is able to restore sAPPα levels after TBI (Siopi et al., 2013). Moreover, this study investigated the acute and long-term effects of the etazolate on TBI-induced cerebral oedema, histological alteration and neurological deficits showing that the therapeutic efficacy of etazolate on all three parameters examined are sustained when the compound was delivered up to at least 2h post-TBI (Siopi et al., 2013). The neuroprotective effect of etazolate was first affirmed by Marcade and collaborators in an *in vitro* model of Aβ-induced toxicity (Marcade et al., 2008) and then confirmed in a model of olfactory bulbectomy-induced depression where it contrasted the behavioural alterations, morphological changes and neuronal loss in the hippocampus (Jindal et al., 2015).

Etazolate was also shown to have antioxidant effect in an *in vivo* model of chronic unpredictable stress depression in mice attenuating the increase of oxidative markers in the brain. In particular it is able to counteract the lipid peroxidation and the nitrosative level and it normalizes the reduced GSH level in brain and the activity of the anti-oxidant enzymes SOD and CAT that are found to be reduced in depressed animals (Jindal et al., 2013b). The same group confirmed this antioxidant effect in a model of olfactory bulbectomy-induced depression in mice where the etazolate contrasted the oxidative and nitrosative stress (Jindal et al., 2015).

Etazolate has also pro-cognitive effects, reducing foraging and memory deficits in normally aged rats (Drott et al., 2010), and improving recognition memory as well as reducing locomotor hyperactivity in a mouse model of TBI by mechanical percussion (Siopi et al., 2013). Recently our team also showed that etazolate is able to reduce myelin loss in an *ex vivo* weight-drop model of trauma (Llufriu-Dabén et al., 2016a under revision) and also to

induce oligodendrocytes differentiation and remyelination in an *ex vivo* model of lysolecithin-induced demyelination (Llufriu-Dabén et al., 2016b under revision).

Etazolate also entered a phase I and II clinical trial for the treatment of Alzheimer disease (AD), with the appellation EHT-0202. The phase I trial was performed on 156 healthy volunteers (60-75 years old) and showed that etazolate is well tolerated even if some CNS-related adverse events of mild intensity are observed as headache, hypersomnia, disturbance in attention and balance disorder in a total of 6 volunteers (Vellas et al., 2011). The phase II trial was performed in France between 2008 and 2009 on 159 patients affected by AD (60-75 years old). The principal objective of this study was to assess the clinical safety and tolerability of EHT0202 that was administered in combination with one acetycholinesterase inhibitor over a 3-month period at 40 mg or 80 mg, twice a day. In general EHT0202 is shown to be safe and well tolerated despite some psychiatric and neurologic adverse events reported mostly for the highest dose, suggesting a potential dose-related effect. Due to the limited number of patients and limited duration, this trial was not powered to show efficacy, even if some signs of amelioration were observed in some patients (Vellas et al., 2011).

5.2 N-acetylcysteine (NAC)

NAC is the N-acetyl derivative of the amino acid L-cysteine, it is a synthetic precursor of glutathione, one of principal molecule in the anti-oxidant defence (Zafarullah et al., 2003). The thiol (sulfhydryl) group confers in addition antioxidant properties to this molecule that acts as a potent ROS scavenger (**Fig. 31**). Moreover, NAC possess reducing properties, thanks to its thiol-disulfide exchange activity. For example, it can induce the cell cycle arrest in hepatic stellate cells modulating the MAPK pathway, through direct interaction with target proteins containing cysteine residue or thiol group such as Raf-1, MEK and ERK (Kim et al., 2001; Sun, 2010). For all these reasons, NAC is known to be a potent antioxidant (Aruoma et al., 1989; Samuni et al., 2013).

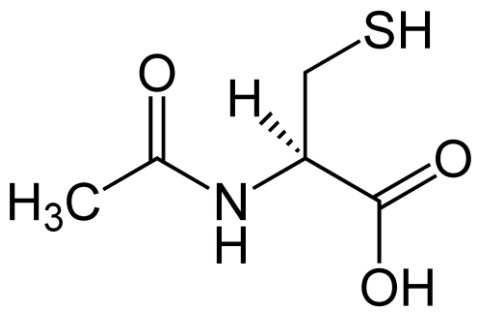

Figure 31: Chemical structure of N-acetylcysteine (NAC).

NAC is on the World Health Organization's List of Essential Medicines (WHO Model List 2015) and actually used as an antidote for paracetamol (acetaminophen) poisoning as well as mucolytic.

Neurological and psychiatric disorders have a multifactorial ethology involving inflammatory pathways, glutamatergic transmission, oxidative stress, mitochondrial function, apoptosis, and intracellular calcium modulation (Dean et al., 2011). NAC plays a role in most of these pathways, and for this reason it has been employed in more than 20 clinical trials in various psychiatric disorders and circa 10 clinical trials in neurological disorders as spinocerebellar disease, myoclonus epilepsy, Alzheimer's disease, Parkinson's disease and Down's syndrome (see for review Arakawa and Ito, 2007; Bavarsad Shahripour et al., 2014). In most of these studies, NAC had positive effects on clinical outcomes, it is generally safe and well tolerated even at high doses, and the most frequently reported side effects are of mild entity as nausea, vomiting, and diarrhoea (Bavarsad Shahripour et al., 2014). NAC has well-documented neuroprotective effects in the CNS but despite the many promising prospects, some clinical trials in several diseases have failed (Aitio, 2006). This can be due to its low (6-10%) bioavailability (Günther et al., 2015; Sunitha et al., 2013).

Below we will focus our attention on NAC treatment for cerebral trauma. Several pre-clinical studies reported beneficial effects against TBI-mediated oxidative stress. NAC reduces oxidative stress following lateral fluid-percussion injury in rat by counteracting the induction of HO-1, and it also results in decreased volume of injury (Yi and Hazell, 2005). If administered 1h after TBI, it can restore mitochondrial respiratory functions and calcium transport and it is able to restore brain GSH levels from 1h to 14 days and mitochondrial GSH levels from 12 h to 14 days post-TBI. This effect disappears if given 2h post injury (Xiong et al., 1999). A study reported an anti-inflammatory effect in a rat model of cortical contusion trauma. In fact, NAC decreases several inflammatory cytokines and the activation of NF-kB resulting in reduced brain oedema, BBB permeability, and apoptotic index in the injured brain (Chen et al., 2008). Other studies reported that NAC inhibits the activation of NF-kB and TNF-α production by LPS suggesting that post-TBI NAC administration may decrease inflammatory response in the injured brain moreover oxidative stress (Hoffer et al. 2002; Akca et al. 2005; Hsu et al. 2006). NAC exerts neuroprotective effects reducing oxidative stress, apoptosis, and calcium entry in models of open and closed head trauma in rat (Hicdonmez et al., 2006; Nazıroğlu et al., 2014). Studies also reported a pro-cognitive effect of NAC. In fact, NAC is shown to significantly reduce behavioural deficits in two models of experimental TBI in two different species (weight drop in mice and fluid percussion injury in rats) when administered within 30-60 minutes after injury (Eakin et al., 2014). NAC and monocline co-administration improves cognition and memory after a controlled cortical impact in rat. In particular, the

histological analysis performed 2 weeks after TBI revealed that the white matter, but not the grey matter, is preserved since the lesion volume is unaffected and the myelin loss is attenuated (Abdel Baki et al., 2010). Another study reported a protective effect of NAC *in vitro* on human OPCs treated with potassium cyanide suppressing apoptosis, and *in vivo* in rat, with hypoxic-ischemic encephalopathy, NAC induces a recovery of motor functions and an attenuation of demyelination in the corpus callosum (Park et al., 2015). NAC efficacy was also tested in a model of traumatic stretch-induced injury (50% membrane deformation, $10s^{-1}$ strain rate) on rat primary cortical neurons, alone and combined with probenecid. NAC is able to reduce GSH depletion, oxidative stress and cell death and the combined effect is found to be superior to NAC alone (Du et al., 2016).

Finally NAC was also employed in a clinical study in war veterans and beneficial effects were reported in the NAC group compared to placebo on the severity and resolution of sequelae due to a blast-induced mild TBI, as dizziness, memory loss and sleep disorders (Hoffer et al., 2013).

AIM OF THE WORK

TBI initiates a cascade of secondary pathophysiological events, as excitotoxicity, inflammation and oxidative stress. There are increasing experimental evidences suggesting that demyelination may play an important role in the pathophysiology of TBI. To date, the knowledge in the field of TBI highlights that a major force causing the injury of nervous tissue is due to a rapid tissue deformation, called strain, or, more simply, stretch. Thus, our hypothesis was to test whether the stretch-induced traumatic injury is able to initiate demyelination.

When I started my PhD, there were no models available to reproduce this kind of injury in oligodendrocytes. Therefore, in order to test our hypothesis, I had first to develop an *in vitro* model of stretch-induced injury in oligodendrocytes. I used three different cell models: i) the mouse oligodendrocyte 158N cell line, ii) the mixed glial primary culture and, iii) the oligodendrocyte-enriched primary culture. Cells were subjected to an equibiaxial static stretch using Flexcell® Tension system device in order to reproduce two models of stretch-induced injury: “mild” (20% strain for 20h) *versus* “moderate” (30% strain for 30 min) injury.

I developed both models based on the cell response to a stretch-induced injury i) at the cellular level by assessing cell morphology, myelin protein components, cell death, ROS production and cellular oxidative stress status and ii) at the molecular level by looking at the expression of different pro-/antioxidant genes and myelin genes together with the expression of the corresponding proteins when possible as well as the signaling pathways activated following stretch as MAPKs (ERK, JNK).

Later, to be more closer to the *in vivo* situation, we decided to move to an *ex vivo* model of stretch-induced injury using the organotypic culture of cerebellar slices, based on the cerebellum being a structure very rich in myelinated fibers. The organotypic culture provides a well-preserved architecture of brain tissue including all implicated cell populations. Here again, there were no models available for studying a stretch induced-injury in cerebellar slices, thus the first step was to perform a successful culture of cerebellar slices on the silicone membrane, since this type of culture has never been reported for the cerebellum. Once I have reached this important step, cerebellar slices were subjected to a “moderate” stretch, and the axonal and myelin injury was assessed. First the accumulation of amyloid precursor protein (APP), a marker of axonal injury, was measured at different time points after stretch. The expression of pro- /antioxidant genes and oxidative stress markers were

also assessed. The MAPKs pathway was also examined, as a particularly stretch-responsive pathway already shown in other cell types. Finally myelin genes and proteins were evaluated together with the morphology of the paranodal junctions in order to analyse the effect of stretch on myelin sheaths.

The second part of my PhD project was focused on the evaluation of the antioxidant potential of etazolate, a pyrazolopyridine derivative compound,that has been already shown, in part by our group, to be neuroprotective, anti-inflammatory and antioxidant *in vivo.* Our hypothesis was that etazolate has an antioxidant potential and it may be able to protect oligodendrocytes against oxidative stress. Thus, we first developed a *tert*-butyl hydroperoxide (*t*BHP)-induced oxidative stress *in vitro*. Then a study on cell viability and ROS production was conducted following NAC treatment, a known powerful antioxidant, in order to validate our model. Afterward, we tested the hypothesis of an antioxidant potential of etazolate and its protective effect on oligodendrocytes.

Finally the third part of my project was focused on the evaluation of the protective effect of etazolate on myelin sheaths in a model of lysolecithin-induced demyelination *ex vivo* on cerebellar organotypic slices and the data from this work were at the origin of PhD thesis of Gemma Llufriu-Dabén (defended on January 2016), where she showed the remyelinating activity of etazolate.

Overall, this work initiates for the first time the study of a stretch-induced injury in oligodendrocytes and organotypic cerebellar slices.

MATERIALS AND METHODS

1. Animals

Mixed glial primary cultures were performed on 1-3 day postnatal (P1-P3)-old mice obtained from wild-type C57Bl/6 mice (Janvier, Le Genest St Isle, France) or transgenic PLP-eGFP mice (generated by Dr. W.B. Macklin, Cleveland Clinic Foundation, Ohio, USA). In PLP-eGFP mice, the enhanced green fluorescent protein (eGFP) is expressed in the oligodendrocyte lineage under the control of the proteolipid protein (PLP) promoter. Organotypic cerebellar slice cultures were performed on 9-10 day postnatal (P9-P10)-old mice obtained from wild-type C57Bl/6 mice (Janvier, Le Genest St Isle, France). The animals were housed in a controlled temperature environment (22 ± 2 °C), under a 12h light/dark cycle, with access to food and water *ad libitum*. Animal care and experiments were approved by the Paris Descartes University (CEEA34.MJT.075.12) respecting the French regulations and the European Communities Council Directive of September 2010/63/UE, on the protection of animals used for scientific purposes.

2. Oligodendrocyte cell line culture

The oligodendrocyte 158N cell line, which preserves oligodendrocyte characteristics and expresses myelin proteins (Feutz et al., 1995; Ghandour et al., 2002), was kindly provided by Dr. S.M. Ghandour (Strasbourg, France). It was obtained by immortalization of oligodendrocytes from mice with the Simian Virus 40 (SV-40) large T antigen. Cells were seeded at the $6x10^5$ density in uncoated Petri dishes (100 mm of diameter), in Dulbecco's minimal essential medium (DMEM) supplemented with 5% heat inactivated fetal bovine serum (HI-FCS, Gibco, NYC, NY, USA), L-glutamine 2 mM, sodium pyruvate 1 mM, penicillin (0.1 U/mL)/streptomycin (0.1 µg/mL) and 0.5 µg/mL fungizone. Cells were grown at 37°C in a humidified atmosphere of 5% CO_2 and split, with cell dissociation buffer (Sigma C5914), twice a week.

For the preparation of the cells subjected to mechanical stretch, cells were trypsinized, with a solution of 0.05% trypsin in 50mL of EDTA 0.1M – pH 8, from the cell stock in Petri dishes and plated at the density of $3x10^5$ cells/1.5 mL per well on laminin-coated Bioflex® Plates (Dunn Labortechnik GmbH, BF-3001L). Cells were maintained in 5% CO_2, in a humidified atmosphere (90%) at 37°C for 72h before being submitted to a mechanical stretch

(**Fig. 33a and 34a**). After 48h of culture (the day before stretching), the medium was changed with 3 mL of fresh medium with 1% fetal bovine serum (HI-FCS, Gibco, NY, USA). Control (non-stretched) plates were prepared and underwent the same conditions, except that they did not receive the mechanical stretch.

3. Mixed glial primary culture

Mixed glial primary culture was prepared as previously described (Feutz et al., 2001; Meffre et al., 2015a) from brain hemispheres of newborn WT or PLP-eGFP mice (P0-P3). Briefly pups were decapitated and the hemispheres were collected in cold-PBS containing 5 mg/mL glucose. After removing meninges, the hemispheres were mechanically dissociated into DMEM (Invitrogen, France) and the solution obtained was filtered (100 µm, BD Biosciences). The cell suspension was plated on Petri dishes (100 mm of diameter) or on Bioflex® Plates (Dunn Labortechnik GmbH, BF-3001U) coated beforehand with 25 µg/mL poly-L-lysine (Sigma, St Louis, Missouris, USA), in DMEM supplemented with 10% heat inactivated fetal bovine serum (HI-FCS, Gibco, NY, USA), L-glutamine 2 mM, sodium pyruvate 1 mM, penicillin (0.1 U/mL)/streptomycin (0.1 µg/mL) and 0.5 µg/mL fungizone (Gibco, NY, USA). Cells were maintained in 5% CO_2, in a humidified atmosphere (90%) at 37°C for 14 days *in vitro* (DIV) before being submitted to a mechanical stretch (**Fig. 33b**) or before preparing the oligodendrocyte-enriched primary culture. The medium was replaced 5 days after the culture and then every 3-4 days. The day before stretching the medium was replaced with 3 mL of fresh medium with 2% fetal bovine serum. Uninjured (non-stretched) control plates were prepared and underwent the same conditions, except that they did not receive the mechanical stretch.

4. Oligodendrocyte-enriched primary culture

To prepare the oligodendrocyte-enriched primary culture, oligodendrocytes were collected from primary mixed glial cell culture (protocol mentioned above) plated in Petri dishes. We prepared these cultures as previously described (Feutz et al., 2001), with slight modifications. Oligodendrocytes growing on the astrocytes layer were detached by syringing the medium over the cells using an 18G syringe needle. The cell suspension was pre-plated in Greiner dishes for 7 min in the incubator in order to eliminate microglia and then centrifuged at 900 rpm for 8 min. The pellet containing oligodendrocytes was resuspended in DMEM supplemented with Insulin (5 µg/mL)–Transferrin (5 µg/L)–Selenium (5 pg/ml) cocktail (BD biosciences), 2% heat inactivated fetal bovine serum, penicillin (0.1 U/mL)/streptomycin (0.1 µg/mL) and 0.5 µg/mL fungizone. Cells were seeded at the 4-5x10^5 density on untreated Bioflex® Plates (Dunn Labortechnik GmbH, BF-3001U) coated beforehand with 25 µg/mL

poly-L-lysine. Cells were maintained in 5% CO_2, in a humidified atmosphere (90%) at 37°C for 2 DIV before being submitted to a mechanical stretch (**Fig. 33c and 34b**). Uninjured (non-stretched) control plates were prepared and underwent the same conditions, except that they did not receive the mechanical stretch.

5. Organotypic cerebellar slice culture

5.1 On Millipore culture inserts

The cerebellar slice culture protocol was used as described previously (Birgbauer et al., 2004). After decapitation of P10-old mice, the cerebellum was dissected out in phosphate-buffered saline (PBS) containing 5 mg/ml glucose and meninges were removed. Parasagittal slices (350 µm) were cut using a Macllwain Tissue Chopper. Isolated slices were transferred onto membranes of 30 mm diameter with 0.4 µm pore size (Millipore, Bedford, MA). The inserts were placed in 6-well tissue culture plates with 1 mL of medium containing 50% basal medium with Earle's salts (Life Technologies, 41010-026), 2.5% Hanks' balanced salt solution (Life Technologies, 14060-040), 25% horse serum (Life Technologies, 16050-122), glutaMAX® 1% (Thermo Fisher scientific, 35050061), 5 mg/mL D-glucose (Sigma, G8769), penicillin (0.1 U/mL)/streptomycin (0.1 µg/mL) and 0.5 µg/mL fungizone (Life Technologies). Slices were maintained at 35°C in an atmosphere of humidified 5% CO_2 and the medium was changed every 3-4 days. Cultures were maintained 7 DIV before being submitted to a lysolecithin-induced demyelination and the analysis were performed 72h after the treatment.

5.2 On Bioflex® Plates

Cerebellar slices were obtained as mentioned in the protocol above and four slices taken in the vermis of cerebellum were transferred on Bioflex® Plates (Dunn Labortechnik GmbH, BF-3001U) coated beforehand with a 320 µg/ml poly-L-lysine (Sigma, P9404) and laminine 80 µg/ml (Thermo Fisher scientific, 23017-015). The Bioflex® Plates were previously treated with an Ozone Cleaner (15 min) or Plasma Cleaner (2 min) in order to render the silicone surface hydrophilic and allow a better adhesion of the proteins contained in the coating solution. Cultures were initially fed with 800 µl of Neurobasal medium (Thermo Fisher scientific, 10888-022) supplemented with 1% B-27® (Thermo Fisher scientific, 17504-044), 1% GlutaMAX™ (Thermo Fisher scientific, 35050061) and 5 ml/mL glucose. The day after the culture, 50% of the medium was changed with fresh medium containing 50% basal medium with Earle's salts (Life Technologies, 41010-026), 2.5% Hanks' balanced salt solution (Life Technologies, 14060-040), 25% horse serum (Life Technologies, 16050-122), glutaMAX® 1% (Thermo Fisher scientific, 35050061), 5 mg/mL D-glucose (Sigma, G8769),

penicillin (0.1 U/mL)/streptomycin (0.1 µg/mL) and 0.5 µg/mL fungizone (Life Technologies). Then every 2-3 days, 50% of culture medium was changed. Cerebellar slices were cultured at 35 °C in a humidified atmosphere of 5 % CO_2 and maintained on a rocker (2D movement, inclination angle 14°, rocking rate 1cycle/min) to aid gas exchange and diffusion. To avoid an excessive evaporation of medium a humidifier was inserted in the incubator and turned on during 3 cycles of 10 minutes per day, equally distributed within 24h. Cultures were maintained 7 DIV before being submitted to a mechanical stretch (**Fig. 34c**) and the analysis were performed immediately (t 0h), 24h (t 24h) or 72h (t 72h) after the stretch.

6. *In vitro* models of mechanical stretch

Cells and cerebellar slices grown on BioFlex® six-well plates were submitted to a mechanical stretch using a Flexcell® FX 5000™ Tension System (Flexcell International corporation, NC, USA), a computer-regulated bioreactor that uses vacuum pressure to apply a strain to cells cultured on elastic silicone membranes. In brief, the vacuum pressure deforms the silastic membranes of the Bioflex® Plates and adherent cells to varying degrees controlled by the pulse pressure (Vande Geest et al., 2004). The extent of cell response, produced by deforming the silicone membrane on which the cells are grown, is dependent on the degree of stretch that depends on the percentage of substrate elongation and on the duration of stretch. These two parameters can be modified in accordance to the limits of this instrument, the substrate elongation (%) can vary from 0.8% to 33%.

Figure 32: Illustration of Flexcell® FX 5000TM Tension System

Two models of equibiaxial static stretch were developed, in order to reproduce two different injuries, here called mild and moderate.

6.1 Model of stretch-induced mild injury

Cells were exposed to an equibiaxial static stretch of 20% strain for 20h. The oligodendrocyte response was evaluated at time 0h or 24h post-stretch through different tests in order to study cellular, biochemical and molecular changes.

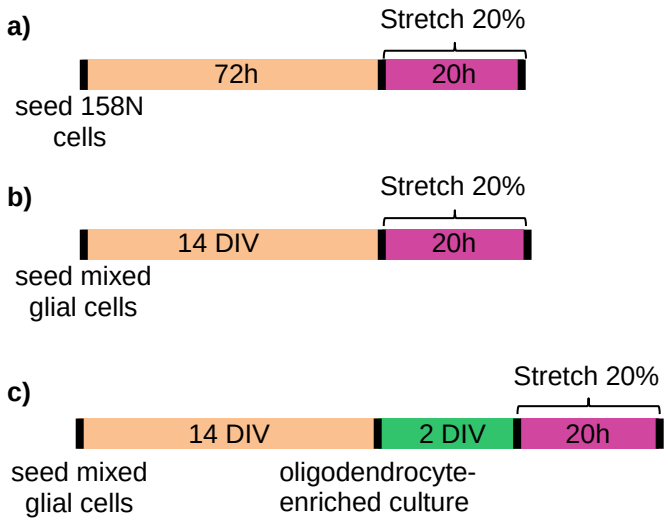

Figure 33: Schematic illustration of the protocols used to perform stretch-induced <u>mild injury</u>. (a) 158N cells were plated on laminin-coated Bioflex®Plates and maintained for 72h in culture before being subjected to a 20% static stretch for 20h. (b) Mixed glial primary culture was prepared from P0-P3 C57Bl/6 or PLP-eGFP mice, plated on Bioflex® Plates (coated with 25 µg/mL poly-L-lysine) and maintained for 14DIV before being subjected to a 20% static stretch for 20h. (c) Pure oligodendrocytes were collected from the astrocyte layer of mixed glial primary culture and plated on Bioflex® Plates (coated with 25 µg/mL poly-L-lysine). The oligodendrocyte-enriched primary culture was maintained in culture for 2 DIV before being submitted to a 20% static stretch for 20h. The response of oligodendrocytes was evaluated at time 0h or 24h post-stretch. DIV: days *in vitro*.

6.2 Model of stretch-induced moderate injury

Cells and cerebellar slices were exposed to an equibiaxial static stretch of 30% strain for 30 minutes. The response was evaluated through different tests in order to study cellular, biochemical and molecular changes at time 0h and 24h post-stretch for cells and 0h, 24h and 72h post-stretch for slices.

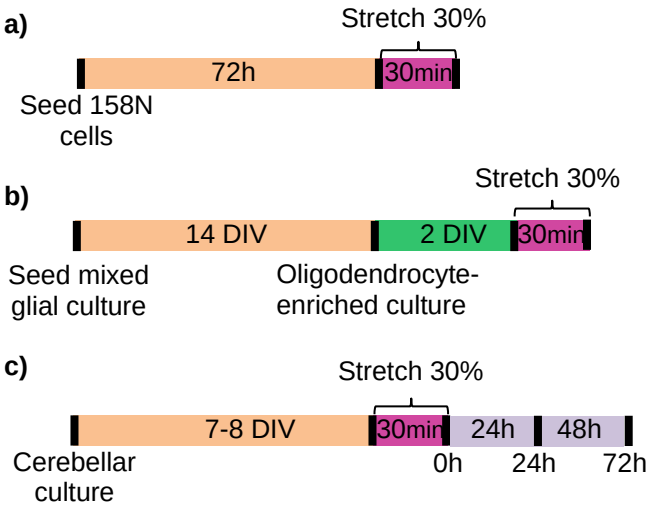

Figure 34: Schematic illustration of the protocols used to perform stretch-induced moderate injury. (a) 158N cells were plated on laminin-coated Bioflex® Plates and maintained for 72h before being subjected to a 30% static stretch for 30min. (b) Pure oligodendrocytes were collected from the astrocyte layer of mixed glial primary culture and plated on Bioflex® Plates (coated with 25 µg/mL poly-L-lysine). The oligodendrocyte-enriched primary culture was maintained in culture for 2 DIV before being submitted to a 30% static stretch for 30min. (c) Cerebellar slices were plated on Bioflex® Plates (coated with 320 µg/ml poly-L-lysine and 80 µg/ml laminin) and maintained for 7DIV before being subjected to a 30% static stretch for 30min. The response was evaluated at time 0h and 24h post stretch (a, b) and 0h, 24h and 72h post-stretch (c). DIV: days *in vitro*.

Models of injury using gel-filled human skulls have indicated that this range of stretch is relevant to the kind that occurs in humans after rotational acceleration-deceleration injury (Margulies et al., 1990; Meaney et al., 1995).

7. *In vitro* model of lysolecithin-induced demyelination in organotypic cerebellar slice culture

At 7 DIV (days *in vitro*), slices grown on Millipore culture inserts were treated with lysolecithin (0.5 mg/mL) (PubChem CID: 24798682; Sigma-Aldrich) or its vehicle (0.5% methanol:chloroform, 1:1) for 16h, as previously described (Birgbauer et al., 2004; Meffre et al., 2015a, 2015b). The slices were then treated either by vehicle (PBS 0.1M and DMSO 0.025% mixture) or etazolate (Tocris 0438) at the neuroprotective concentrations of 0.2 or 2 µM (Marcade et al., 2008). After 72h of treatment, cerebellar slices were fixed with 4% paraformaldehyde solution (PFA) for subsequent immunolabelling.

8. *In vitro* model of *t*BHP-induced oxidative stress

An *in vitro* model of *tert*-butyl hydroperoxide (*t*BHP)-induced oxidative stress was developed, using the oligodendrocyte 158N cell line. *t*BHP (Sigma 458139), an organic hydroperoxide, is extensively used as oxidative stress-inducing agent to study the effect of free radicals in different cell types (Adams et al., 1993, 1996). In order to validate the model, the cell viability

and ROS production were evaluated following N-acetylcysteine (NAC) treatment (Sigma A7250), a known powerful antioxidant. Once the model was validated we tested the potential antioxidant effect of etazolate (Tocris 0438). Cell viability and ROS production were assessed by two different techniques, flow cytometry and WST-1.

For FACS analysis:

Oligodendrocytes from 158N cell line were seeded in Petri dishes at the density of $8x10^5$ cells/well in a final volume of 10 ml medium with 5% fetal bovine serum, in a humidified atmosphere (37°C, 5% CO_2). The medium was changed after 48h of culture with fresh medium containing 1% fetal bovine serum. After 24h from the medium change (72h of culture in total), cells were trypsinized and they underwent the FACS protocol described below (see M&M, § 9). Once in suspension, cells were treated with 100 µM *t*BHP and incubated for 30 minutes at 35°C in an atmosphere of humidified 5% CO_2.

For Cell viability (WST-1) analysis:

Oligodendrocytes from 158N cell line were seeded in 96-well microplates at the density of $5x10^3$ cells/well in a final volume of 100 µL /well in medium with 5% fetal bovine serum, in a humidified atmosphere (37°C, 5% CO_2). After 72h of culture, *t*BHP was added to the cells in a final volume of 100 µL/well in medium with 1% fetal bovine serum, and the plate was incubated for 2h in a humidified atmosphere (37°C, 5% CO_2). To evaluate *t*BHP cytotoxicity, a dose-effect study (10, 20, 50 and 100 µM) has been performed. Cell viability was measured by WST-1 colorimetric assay as described below (see M&M, § 11).

9. Flow cytometric analysis

Cells from oligodendrocyte 158N cell line were trypsinized and collected in order to be analysed with the fluorescence-activated cell sorting (FACS) technique. Cells were centrifuged at 1 500 rpm for 3 min and, after being washed twice with PBS, 1×10^6 cells were suspended in 1 ml of PBS 0.1 M (Ca^{2+} and Mg^{2+} free). We used the BD FACSCanto™ II flow cytometer and for each analysis, 10.000 cells were counted on the gate R1 drawn on the FSC (Forward scatter)/SSC (Side scatter) biparametric histogram. We considered only the population of cells devoid of aggregates and debris. In order to evaluate the cell viability and ROS production, a double staining with propidium iodide (PI) and the carboxy-dichloro-dihydro-fluorescein diacetate (CM-H2DCFDA) was performed (Bass et al., 1983; Rothe and Valet, 1990). Cells were incubated with 1.25 µM of CM-H2DCFDA probe (Molecular Probes C6827) for 30 min at 37°C in the dark. The excess of probe was washed out with PBS and

cells were suspended in 1 ml of PBS (Ca^{2+} and Mg^{2+} free) and incubated 10 min with 1 µg/mL of PI (Sigma P4170) at room temperature. The cell-permeant CM-H2DCFDA probe passively diffuses into cells and is retained at intracellular level after cleavage by intracellular esterases. Upon oxidation by ROS, the nonfluorescent H2DCFDA is converted to the highly fluorescent 2',7'-dichlorofluorescein (DCF). The DCF fluorescence was recorded in FL-1 (530/30 nm) channel together with the PI fluorescence in FL-2 (585/42 nm). For stretching experiments we used the antioxidant compound N-acetylcysteine (NAC) at 5 mM, to serve as a ROS scavenger, and the oxidant *tert*-butyl hydroperoxide (*t*BHP) 100 µM, to serve as a positive control for ROS production.

10. Biochemical assays

All biochemical assays described below have been performed in collaboration with Pr. Didier Borderie (INSERM U1124) at Cochin Hospital. Cells from oligodendrocyte 158N cell line were washed with PBS, trypsinized and centrifuged at 600g for 10 min. After surfactant elimination, cells were suspended in 1 ml of Cell Lysis Reagent (Sigma C2978) complemented with protease inhibitor (cOmplete, Mini, EDTA-free, Roche). Cell lysates were then frozen at -80° until utilisation.

10.1 Determination of carbonyl level

Protein carbonyl groups were detected and quantified using 2,4-dinitrophenylhydrazine (DNPH) (Reznick and Packer, 1994). Briefly, 0.5 ml of cell lysates, (1 mg protein/ml) were treated with 0.5 ml of 10 mM DNPH in 2 M HCl, or with 0.5 ml of 2 M HCl alone for the blank. Samples were incubated for 1h at room temperature in the dark, and then treated with 10% trichloroacetic acid and centrifuged. The pellet was washed three times in ethanol/ethyl acetate and solubilized in 1 ml 6 M guanidine in 20 mM potassium phosphate, adjusted to pH 2.3 with trifluoroacetic acid (W/V); the resulting solution was incubated at 37°C for 15 min. Carbonyl concentrations were determined from the difference in absorbance at 370 nm between DNPH-treated and HCl treated samples, with ε_{370}=22,000 M^{-1} cm^{-1}. Carbonyl levels were expressed as nmoles of carbonyl/mg of proteins.

10.2 Thiol determinations

Thiol determinations were based on the thiol/disulphide reaction of thiol and Ellman's reagent, 5,5′-dithiobis(2-nitrobenzoic acid) DTNB (Hu, 1994). Fifty microliters of cell lysates, mixed with 1 ml 0.1 M Tris, 10 mM EDTA pH 8.2, constituting the blank reaction, was assessed at 412 nm (UVIKON spectrophotometer). The addition of 40 µl of 10 mM DTNB in methanol triggered the reaction and absorption at 412 nm was measured after stable colour

formation (20 min). The concentrations of thiol groups were calculated using a molar extinction coefficient of 13,600 M^{-1} cm^{-1}. Thiols were expressed as µmol/L.

10.3 Determination of advanced oxidation protein products (AOPP)

Advanced oxidation protein products (AOPP) were quantified as described previously (Witko-Sarsat et al., 1996). We placed 200 µl of cell lysates diluted 1:5 in phosphate-buffered saline into each well of a 96-well microtitre plate and added 20 µl of acetic acid to each well. For the standards, we added 10 µl of 1.16 M potassium iodide (Sigma, St Louis, MO, USA) to 200 µl of chloramine-T solution (0–100 mmol/l) (Sigma) in a well and then added 20 µl of acetic acid. The absorbance of the reaction mixture was immediately read at 340 nm against a blank consisting of 200 µl of phosphate-buffered saline, 10 µl of 1.16 M potassium iodide and 20 µl of acetic acid. AOPP concentrations are expressed as µmoles/L of chloramine-T equivalents.

10.4 Determination of superoxide dismutase (SOD) activity

The superoxide dismutase activity was evaluated using the nitroblue tetrazolium reduction technique previously described by Beauchamp and Fridovich (Beauchamp and Fridovich, 1971). Superoxide anion can be the substrate for the enzyme or act as oxidant for the tetrazolium salt. The diminution of oxidant properties of O_2^- is proportional to SOD activity. The measures are done on cell lysates. The generation of superoxide anion is realized by the addiction of 7 mg KO_2 in 10 ml of dicyclohexyl-18-crown-16. This preparation is placed 1h in the dark. Put into a microplate 50 µl of sample diluted ½ in bicarbonate buffer, 100 µl of anion superoxide preparation and 50 µl of tetrazolium salt diluted 1/50 in bicarbonate buffer. The lecture at 550nm is done after 2 minutes of incubation. In parallel a SOD standard curve is prepared (6.25 to 100 unit/ml). The results obtained are normalized to the protein content and expressed as units per mg of protein.

10.5 Determination of glutathione peroxidase (GPx) activity

The glutathione reductase activity was quantified using the Cayman's Glutathione Peroxidase Assay on cell lysates. GPx catalyzes the reduction of hydroperoxides, including H_2O_2, using reduced glutathione and thereby functions to protect the cell from oxidative damage. Cayman's Glutathione Peroxidase Assay measures GPx activity indirectly by a coupled reaction with GR. Oxidized GSSG, produced upon reduction of an organic hydroperoxide by GPx, is recycled to its reduced state by GR and NADPH. The oxidation of NADPH to NADP+ is accompanied by a decrease in absorbance at 340 nm. The rate of decrease in the absorbance at 340 nm is directly proportional to the GPx activity in the

sample. The results obtained are normalized to the protein content and expressed as units per mg of protein.

10.6 Determination of glutathione reductase (GR) activity

The glutathione reductase activity was quantified using the Cayman Chemical Glutathione Reductase Assay Kit on cell lysates. Glutathione reductase is a flavoprotein that catalyses the NADPH-dependent reduction of oxidized glutathione (GSSG) to glutathione (GSH). The Cayman Chemical Glutathione Reductase Assay Kit measures GR activity by measuring the rate of NADPH oxidation. The oxidation of NADPH to NADP+ is accompanied by a decrease in absorbance at 340 nm. Since GR is present at rate limiting concentrations, the rate of decrease in the A340 is directly proportional to the GR activity in the sample. The results obtained are normalized to the protein content and expressed as units per mg of protein.

10.7 Determination of reduced glutathione (GSH)

Levels of intracellular GSH were assessed spectrofluorimetrically by monochlorobimane staining (Bellomo et al., 1997). Cell lysates were incubated with 50 µM monochlorobimane diluted in PBS. The fluorescence intensities were measured after 15 min at 37°C using excitation and emission wavelengths of 380 and 485 nm, respectively. The intracellular GSH level was expressed as arbitrary units of fluorescence intensity.

10.8 Determination of lactate dehydrogenase (LDH) level

The lactate dehydrogenase is an intracellular enzyme, its increase indicates cellular damage with its consequent release into the medium. The LDH level was evaluated on supernatant, the medium culture of cells or slices. They were tested on a Roche Cobas 8000 analyser, with an ultraviolet spectrophotometric method. Lactate dehydrogenase catalyses the conversion of L-lactate to pyruvate; NAD^+ is reduced to NADH in the process. The initial rate of the NADH formation is directly proportional to the catalytic LDH activity. It is determined by measuring the increase in absorbance at 340 nm.

11. Cell viability assay: WST-1

WST-1 assay (Roche 11644807001) is based on the enzymatic cleavage of the tetrazolium salt WST-1 to formazan by cellular dehydrogenases present in viable cells. The generation of the dark yellow coloured formazan is directly correlated to viable cell number. After incubation, medium including *t*BHP was removed and cell viability evaluation was performed by adding 10 µL/well of Cell Proliferation Reagent WST-1 in a volume of 100 µL/well of medium with 1% fetal bovine serum. After 2h of incubation, the plate was shaken for 1 min

on a shaker and the absorbance of the reaction mixture was read at 440 nm against a blank consisting of medium with 1% fetal bovine serum, using a microplate reader (PowerWavex, Bio-Tek Instruments, INC.). The reference absorbance of 690 nm was used to correct for nonspecific background values.

12. Quantitative RT-PCR

Total RNA from cultured cells was obtained using Trizol reagent (Invitrogen, France) and 1 µg was reverse transcribed with random primers from Biolabs (Beverly MA, USA) and Reverse Transcriptase MLV-RT from Fisher Scientific (Hampton, New Hampshire, USA), according to the manufacturers' instructions. Quantitative PCR was performed with standard protocols using SYBRGreen (ABgene, France) as fluorescent detection dye in ABI PRISM 7000 in a final volume of 7 µl, which also contained 300 nM of primers (except for PLP and MAG with 100nM of primers) (Eurofins Genomics Operon, Orsay, France) and 50 ng of reverse transcribed RNA in 384-well plates. Melting curve analysis was applied to characterize the generated amplicons and to control the contamination by unspecific by-products. Each reaction was performed in triplicate and the mean of at least three independent experiments was calculated. Results were normalized to 26S mRNA level and calculated using the DDCt method. The results are expressed as $2^{-\Delta\Delta Ct}$ [$\Delta\Delta Ct = \Delta Ct$ gene of interest– ΔCt reference gene]. The primer sequences used in real-time PCR are listed below in the ***Table 7.***

REFERENCE GENE	***26S***	Forward Reverse	5'- AGG AGA AAC AAC GGT CGT GCC AAA A -3' 5'- GCG CAA GCA GGT CTG AAT CGT G-3'
PRO-OXIDANT GENE	***Duox-1***	Forward Reverse	5'-GGT GGT TGA GTC TAT GTT CC -3' 5'-CTT CTC CTG GCT GAT GTA G -3'
ANTIOXIDANT GENES	***Sod-1***	Forward Reverse	5'-GCC AAT GTG TCC ATT GAA GA-3' 5'-GTT TAC TGC GCA ATC CCA AT-3'
	Sod-2	Forward Reverse	5'-GAG CTG CCT TAC GAC TAT GG-3' 5'-TGA AGA GCG ACC TGA GTT G-3'
	Ho-1	Forward Reverse	5'-CAC GCA TAT ACC CGC TAC CT-3' 5'-CCA GAG TGT TCA TTC GAG CA-3'
	Nqo-1	Forward Reverse	5'-GCG AGA AGA GCC CTG ATT GTA CTG-3' 5'-TCT CAA ACC AGC CTT TCA GAA TGG-3'
TRANSCRIPTION FACTOR	***Nrf-2***	Forward Reverse	5'-TCT CCT CGC TGG AAA AAG AA-3' 5'-AAT GTG CTG GCT GTG CTT TA-3'
MYELIN GENES	***Plp***	Forward Reverse	5'-AGC AAA GTC AGC CGC AAA AC-3' 5'-CCA GGG AAG CAA AGG GGG-3'
	Mag	Forward Reverse	5'-ACT GGT GTG TGG CTG AGA AC-3' 5'-GGA TTA TGG GGG CAA ACT C-3'
	Cnp	Forward Reverse	5'- GAC AGC GTG GCG ACT AGA CT -3' 5'- CAC CTG GAG GTC TCT TTC CA -3'
	Mbp	Forward Reverse	5'-GGG AAG GGA GGA CAA CAC-3' 5'-CCG ATG GAG TCA AGG ATG-3'

Table 7: Primers used

13. Western blot

Proteins were extracted in cold RIPA buffer containing 50 mM Tris HCl, pH 7.5; 150 mM NaCl; 0.1% SDS; 0.5% sodium deoxycholate; 1% NP-40; 10 mM sodium pyrophosphatase; 0.1 mM sodium fluorate; ETDA 5 mM; protease inhibitor (cOmplete, Mini, EDTA-free, Roche) and phosphatase inhibitor (Protease Inhibitor Cocktail 2, P5726, Sigma). Protein content was determined using the reducing agent and detergent compatible protein assay kit (‘‘RC DC’’ protein assay, BioRad, Hercules, California, USA) with Bovine Serum Albumin (BSA) as standard. Aliquots of 30 µg of total extracts were used for each sample. Proteins (30 µg) were separated on 10% SDS-polyacrylamide gels by electrophoresis and blotted onto PVDF (polyvinylidene difluoride) membranes. Non-specific binding sites in the transblots were blocked at room temperature during 1h with 5% BSA diluted in Tris Buffered Saline with 0.1% Tween20 (TBST). Membranes were washed with TBST and then incubated overnight with the following primary antibodies diluted in 5% BSA-TBST: rabbit polyclonal PLP antibody (1:1000, Novus Biologicals NB10074503), mouse monoclonal MBP antibody (1:500, Millipore MAB381), rabbit polyclonal Nrf-2 (1:100, Abcam ab31163), rabbit monoclonal P-Nrf2 (1:100, Abcam ab76026), rabbit polyclonal ERK1/2 (1:500, Millipore 06-182), rabbit monoclonal P-ERK1/2 (1:500, Millipore 05-797R), rabbit polyclonal JNK (1:500, Cell Signaling 9252), rabbit polyclonal P-JNK (1:500, Cell Signaling 9251S), and rabbit polyclonal β-actin antibody (1:10000, Abcam ab8227). After three washes with TBST, membranes were then incubated at room temperature for 1h30 with the appropriate horseradish peroxidase coupled secondary antibody diluted in 5% BSA-TBST (anti-rabbit or anti-mouse: 1:20,000). Following three washes with TBST the specific bands were detected with the kit Pierce®ECL 2 Western Blotting substrate (Thermo Scientific, PI80196), using ImageQuant LAS4000 (GE Healthcare Life Sciences). Relative protein amounts were quantified with ImageJ 1.48v software, and normalized to β-actin.

14. Immunocytochemistry

At time 0h or 24h after stretching, cells were fixed with 4% paraformaldehyde at room temperature (25 min) for subsequent immunocytochemistry (ICC). The membranes with adherent cells were gently cut from the Bioflex® Plates. Samples were washed with PBS and permeabilized with 0.1% TritonX-100-PBS for 15 min. Then they were washed again with PBS and incubated with primary antibodies overnight at 4°C in BSA 5%-PBS. Primary antibodies, as anti-MAG (1:250; Millipore, Chemicon, MAB1567), anti-PDGFR-α (1:500; Santa Cruz sc-338), anti-vinculin (1:500; Sigma V91131), anti α-tubulin (1:4000; Sigma T6074) were used. Then the samples were washed with PBS and incubated with the secondary antibody in BSA 5%-PBS for 1h at RT. Secondary antibodies as Alexa

488 goat anti-mouse IgG (1:200; Invitrogen A21121), and Cy3 goat anti-rabbit (1:100; Jackson ImmunoResearch 111-165-003) were used. TRITC-phalloidin (1:2000; Sigma P1951) and Hoechst (1:50000; Sigma H2261) were used to label F-actin and cell nuclei, respectively. The samples were mounted with Permafluor (Thermo Scientific FM 150202) or Fluoromount (Southern Biotech, Birmingham, USA).

15. Immunohistochemistry

At time 0h, 24h or 72h after stretching, slices were fixed with 4% paraformaldehyde at room temperature for 40 min for subsequent immunohistochemistry (IHC). The IHC is done directly into the Bioflex® Plate, the membrane is cut only at the end for the mounting on the microscope slide.

Samples were washed with PBS and incubated with a blocking solution with 0.1M L-lysine for 1h. Then they were washed again with PBS and incubated with primary antibodies overnight on a rocker at room temperature in PBS-GTA (PBS containing 0.2% gelatin, 0.25% Triton-X, 0.1% sodium azide). Primary antibodies anti-MAG (1:1000; Millipore, Chemicon, MAB1567), anti-Calbindin (1:10000; Swant CB38a), anti-APP (1:700; Invitrogen 51-2700), anti-SMI312 (1:1000, Biolegend 837904), anti-Caspr (1:1000, Abcam ab34151) were used. Then the samples were washed with PBS and incubated with the secondary antibody in PBS-GTA for 2h on a rocker at room temperature. Secondary antibodies Alexa 488 goat anti-mouse IgG (1:1000; Invitrogen A21121), and Cy3 goat anti-rabbit (1:500; Jackson ImmunoResearch 111-165-003) were used. Finally the membranes were cut from the Bioflex® Plate and the samples were mounted with Permafluor (Thermo Scientific FM 150202) or Fluoromount (Southern Biotech, Birmingham, USA).

16. Immunofluorescence analysis

For the mixed glial primary culture, the GFP-fluorescence from PLP-eGFP cells was captured with a fluorescence microscope Olympus BX51 equipped with a QImaging Retiga camera (2000R). Images were obtained using a 20x lens (20x/NA 0.3; Zeiss EC-Plan-NEOFLUO) and processed with ImageJ 1.48v software. The number of $eGFP^+$ cells per field (0.26 nm^2), representing oligodendrocytes in the mixed culture, was counted in control and stretch conditions. Each field was randomly selected avoiding the edge of membrane, 10 fields per condition were analysed from three independent experiments.

For the oligodendrocyte-enriched primary culture, images were acquired using a fluorescence microscope Olympus BX51 equipped with a QImaging Retiga camera (2000R) using a 20x lens (20x/NA 0.3; Zeiss EC-Plan-NEOFLUO) or a confocal microscope LSM 710 (Carl Zeiss Inc., Germany) with a 20x objective (Plan-Neofluar 20x/0.5) or a 63x objective

(Plan-Neofluar 63x/1.3 OilDic). Confocal configurations were adapted for 346, 488 and 543 nm excitations corresponding to Hoechst, Alexa-488 and Cy3 fluorochromes, respectively. Images were then processed with LSM Image Browser (version 4.2). The number of Hoechst$^+$ cells per field (0.26 nm^2), the percentage of MAG$^+$ and PDGFR-α$^+$ cells, the area of MAG$^+$ and PDGFR-α$^+$ cells and the counting of ramifications of PDGFR-α$^+$ cells were determined on images acquired with the fluorescence microscope in control and stretch conditions using ImageJ 1.48v software. For the ramifications counting of PDGFR-α + cells, cells were divided into three group on the basis of the number of ramifications: less than 5 (<5), from 5 to 10 (5-10) and more than 10 (>10) ramifications using ImageJ 1.48v software. All the analyses were performed in 10-30 different fields (randomly selected avoiding the edge of the membrane) per condition, from at least three independent experiments. The analysis of cytoskeleton was performed on cells co-immunostained with actin and vinculin or actin and α-tubulin on images acquired with the confocal microscope with 63x objective.

For the organotypic cerebellar slice culture, images were acquired using a confocal microscope LSM 510 (Carl Zeiss Inc., Germany) with a 20x objective (Plan-Neofluar 20x/0.5) or 40x objective (Plan-Neofluar 40x/1.3 OilDic). Confocal configurations were adapted for 488 and 543 nm excitations corresponding to Alexa-488 and Cy3 fluorochromes, respectively. Images were then processed with LSM Image Browser (version 4.2).

For the slices subjected to a mechanical stretch, the intensities were determined on slices co-immunostained with MAG and CaBP using ImageJ 1.48v software in control and stretch conditions on images acquired with the 20x objective. The analysis was performed in 3 different fields per slice, localized in a region of interest around the apical ends of each lobule, for a total of 4-8 slices per condition. The analysis of APP accumulation was performed on slices co-immunostained with APP and SMI-312. The number of APP spheroids was quantified per slice, for a total of 4-8 slices per condition, with the 20x objective. The analysis of paranodal junctions was performed on slices co-immunostained with Caspr and MAG on images acquired with the 40x objective for a total of 4-6 slices per condition.

For the slices subjected to lysolecithin-induced demyelination, MAG and CaBP staining were quantified in a field of 500 µm^2 area in order to evaluate the percentage of myelinated axons. Quantification of intact myelin segments (MAG$^+$ fibers) per field was performed by counting the myelin segments crossing a line of 500 µm length traced randomly over the area field. The same procedure was used to quantify the axon segments (CaBP$^+$ fibers) crossing the same line used to count the myelin fibers. The ratio between MAG$^+$ fibers and CaBP$^+$ fibers was calculated in order to obtain the percentage of myelinated axons ((MAG$^+$/CaBP$^+$) x 100).

The quantification was performed on 3 different zones (0.2 mm^2 per zone) for each slice, localized at the apical extremities of cerebellar lobules, for a total of 4-6 slices per condition.

17. Pharmacological treatments

17.1 N-acetylcysteine (NAC) treatment against *t*BHP-induced oxidative stress in 158N cell line

Evaluation of cell viability by WST-1 analysis:

Oligodendrocytes 158N were seeded in 96-well microplates at the density of $5x10^3$ cells/well in a final volume of 100 µL /well in medium with 5% fetal bovine serum, in a humidified atmosphere (37°C, 5% CO_2). After 72h of culture, NAC 5 mM and *t*BHP 50 µM were added at the same time in a final volume of 100 µL/well in medium with 1% fetal bovine serum, and the plate was incubated for 2h in a humidified atmosphere (**Fig. 35**).

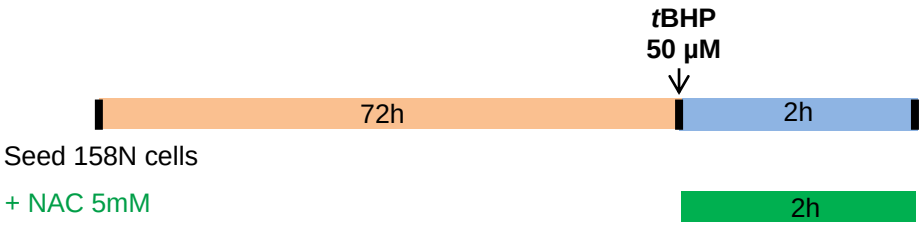

Figure 35: Time line for N-acetylcysteine (NAC) treatment against *t*BHP-induced oxidative stress in 158N cell line for WST-1 analysis: NAC and *t*BHP were incubated at the same time for 2h and cell viability was evaluated by WST-1 addition.

Evaluation of ROS production by FACS analysis:

Oligodendrocytes 158N were trypsinized and NAC 5 mM was added on cells in suspension in PBS 0.1 M (Ca^{2+} and Mg^{2+} free) and incubated for 1h in total in the incubator. After 30 min following cell suspension, *t*BHP at 100 µM was added in the same tube for further incubation of 30 min at 37°C, 5% CO_2 (**Fig. 36**). Then the probe CM-H2DCFDA (1.25 µM) was added and the FACS analysis was performed as previously described (see M&M, § 9).

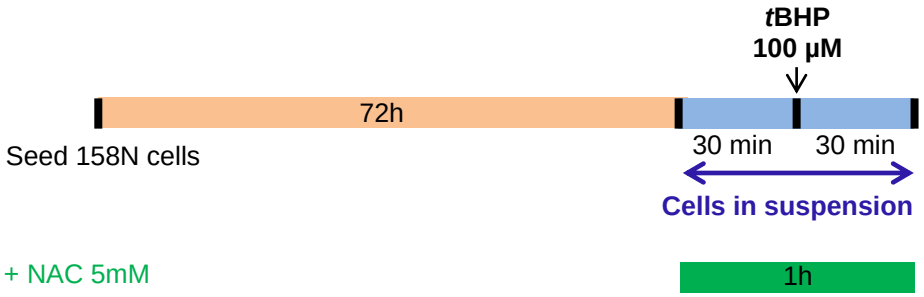

Figure 36: Time line for N-acetylcysteine (NAC) treatment against *t*BHP-induced oxidative stress in 158N cell line for FACS analysis: NAC 5 mM was added on cells and incubated for 1h in the incubator. After 30 min *t*BHP was added in the same tube and this was incubated for further 30 min in the incubator.

17.2 Etazolate treatment against *t*BHP-induced oxidative stress in 158N cell line

Evaluation of cell viability by WST-1 analysis:

Oligodendrocytes 158N were seeded in 96-well microplates at the density of $5x10^3$ cells/well in a final volume of 100 µL /well in medium with 5% fetal bovine serum, in a humidified atmosphere (37°C, 5% CO_2). After 72h of culture, *t*BHP 50 µM was added to the cells in a final volume of 100 µL/well in medium with 1% fetal bovine serum, and the plate was incubated for 2h in a humidified atmosphere. To evaluate the etazolate ability against *t*BHP-induced cytotoxicity a dose-effect study of etazolate was performed including the range of concentration of 0.02, 0.2, 2, 20 and 200 µM. Etazolate treatment started 24 hours before the 2h incubation of *t*BHP 50 µM, allowing the pre-treatment of cells with the compound (**Fig. 37**).

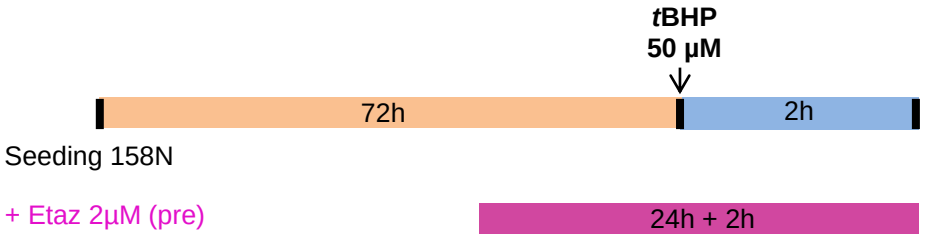

Figure 37: Time line for etazolate treatment against *t*BHP-induced oxidative stress in 158N cell line for WST-1 analysis: Etazolate 0.02, 0.2, 2, 20 and 200 µM was added 24h before the 2h incubation of *t*BHP and cell viability was evaluated by WST-1 addition. Etaz: etazolate.

Evaluation of ROS production by FACS analysis:

In order to evaluate the etazolate ability against *t*BHP-induced oxidative stress, etazolate 2 µM was tested using three different protocols.

a. Protocol with 1h etazolate incubation:

Oligodendrocytes 158N were trypsinized and etazolate 2 µM was added on cells in suspension in PBS 0.1 M (Ca^{2+} and Mg^{2+} free) and incubated for 1h in the incubator. After 30 min *t*BHP 100 µM was added in the same tube and this was incubated for further 30 min in the incubator. Then the probe CM-H2DCFDA (1.25 µM) was added and the FACS analysis was performed as previously described (see M&M, § 9) (**Fig. 38a**).

b. Protocol with 24h of etazolate pre-treatment:

Etazolate pre-treatment started on adherent cells, 24 hours before the trypsinization of cells. Then, cells were trypsinized and *t*BHP 100 µM was added on cells in suspension in PBS

0.1 M (Ca^{2+} and Mg^{2+} free) and incubated for 30 min in the incubator. Then the FACS analysis was performed as previously described (see M&M, § 9) (**Fig. 38b**).

c. Protocol with 24h of pre-treatment and 1h of etazolate incubation:

Etazolate pre-treatment started on adherent cells, 24 hours before the trypsinization of cells. Then, cells were trypsinized and fresh etazolate was added on cells in suspension in PBS 0.1 M (Ca^{2+} and Mg^{2+} free) and incubated for 1h in the incubator. After 30 min *t*BHP 100 µM was added in the same tube and this was incubated for further 30 min in the incubator. Then the FACS analysis was performed as previously described (see M&M, § 9) (**Fig. 38c**).

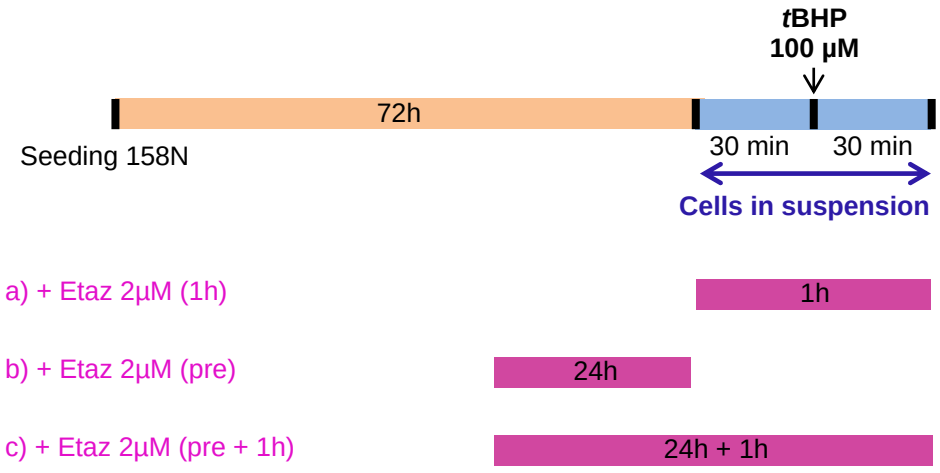

Figure 38: Time line for etazolate treatment against *t*BHP-induced oxidative stress in 158N cell line for FACS analysis: Etazolate 2 µM was tested on 158N cell line using three different protocols: (**a**) Protocol with 1h etazolate incubation, (**b**) Protocol with 24h of etazolate pre-treatment, (**c**) Protocol with 24h of etazolate pre-treatment and 1h of etazolate incubation. Etaz: etazolate.

17.3 Etazolate treatment against lysolecithin-induced demyelination in organotypic cerebellar slice culture

Slices were treated with lysolecithin (0.5 mg/mL) or its vehicle (0.5% methanol:chloroform, 1:1) for 16h, as described above and then they were treated either by vehicle (PBS 0.1M and DMSO 0.025% mixture) or etazolate at the neuroprotective concentrations of 0.2 or 2 µM for 72h (**Fig. 39**).

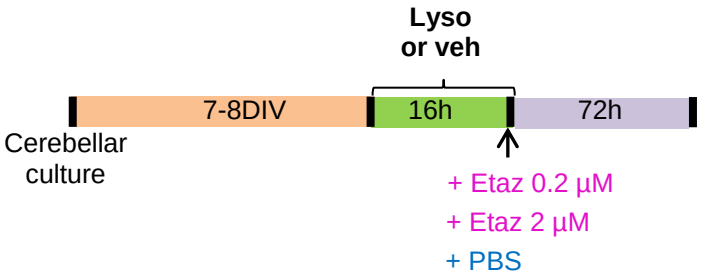

Figure 39: Schematic illustration of etazolate treatment against lysolecithin-induced demyelination in organotypic cerebellar slice cultures. Slices were treated with vehicle, methanol:chloroforme (1:1) or lysolecithin for 16h and then were subjected to PBS or etazolate treatment, at 0.2 or 2 µM, for 72h. Slices were fixed with PFA and processed for immunohistochemical studies. DIV: days *in vitro*; Lyso : lysolecithin; Veh: vehicle (methanol:chloroforme); Etaz: etazolate.

18. Statistical analysis

Unpaired student *t*-test was performed for two sets of data points, and one-way analysis of variance (ANOVA) with Bonferroni post-hoc test was used for comparison among multiple groups. The criterion for statistical significance was $p<0.05$ (*:$p<0.05$; **: $p<0.01$; ***: $p<0.001$). Data are expressed as mean values of *n* experiments ± SEM. All statistical analyses were performed with the software GraphPad Prism5.

RESULTS

FIRST PART

1. Development of a model of stretch-induced injury in oligodendrocyte 158N cell line

The first part of this work consisted in the development of an innovative model of stretch-induced injury in oligodendrocytes. As described in the introduction (see introduction, § 3.7.4), despite of numerous studies of stretch-induced injury performed on different CNS cell types, oligodendrocytes have received less attention. In fact, no study has assessed so far the effects of stretch-induced injury in oligodendrocytes. To set up the model, we decided to use first an oligodendroglial cell line, i.e. the 158N. Being a new model with no data reported in the literature, we had to test different parameters, summarized in the ***Table 8***. This first part of the work has been performed with the participation of Francesca Castoldi, Erasmus student in our team.

Tested parameters	Conditions
Cell density (nb of cell/well)	200 000 **300 000**
Days in culture before stretch	48h **72h**
Coating Bioflex® Plates	**Laminin** Collagen I
Percentage of strain	5% 10% **20%** **30 %**
Stretch duration	**30min** 1h 2h **20h**
Percentage of serum from 24h before stretch till the end of the experiment	**1%** 5%

Table 8: Table summarizing the different conditions tested during the development of the stretch-induced injury model in 158N cell line. The parameters that have been chosen for the following experiments are highlighted in bold pink.

Cell density and days in culture before stretch

First, the optimal cell density had to be assessed and the better results (in term of cell adherence, and cell confluence) were obtained with seeding of 300 000 cells per well in a 6-well Bioflex® Plate. Different assays were also performed in order to choose the proper timing of culture before stretch and, in our condition, it was found to be 72h. In this experimental design, cells were found to be well distributed in a homogeneous monolayer at 80% confluence before stretch, that was optimal for our experiment.

Coating Bioflex® Plates

Different coating were tested and the best results, considering cell adherence and cell viability, were obtained with laminin pre-coated Bioflex® Plates.

Percentage of serum during the experiment

Another important parameter to define was the percentage of serum in the culture medium during the time of stretching till the end of the experiment. In the literature some studies have reduced, or completely removed, the serum because it can mask the effect of the injury. Our cells are normally grown in medium containing 5% of fetal bovine serum and we tried to maintain the same percentage of 5% during the stretch time (more precisely from 24h before stretch till the end of the experiment) or to reduce it to 1%. The better results were obtained with the reduced percentage of serum, in fact the effects of stretch observed were more pronounced (in term of ROS production).

Stretching parameters (percentage of strain and duration)

For this work, I used the Flexcell® FX 5000TM Tension System in order to reproduce our model of mechanical stretch. The vacuum pressure deforms the silicone membrane of the Bioflex® Plate, and by consequence the adherent cells, to varying degrees controlled by the pulse pressure. The substrate elongation and the duration of stretch can be modified in accordance to the limits of this instrument, the substrate elongation (%) can vary from 0.8% to 33%.

We first tested a static equibaxial strain at 20% for 30min, 1h, 2h and 20h. For all these conditions cells were found to be adherent to the silicone membrane (assessed by Hoechst^{+} nuclei count of cells adherent to the membrane, data not shown) with no induction of cell death (assessed by PI staining, data not shown). Oligodendrocytes are particularly vulnerable to oxidative stress, as described above (see introduction). We decided therefore to look at the redox status of our cells to see if it was altered even without sign of cell death.

To verify our hypothesis we decided to check the expression of different pro-/antioxidant genes to see if they were modified following stretch. The superoxide dismutase (SOD) is an important enzyme in the antioxidant defence with a cytoplasmatic (SOD-1) and a mitochondrial (SOD-2) isoform. Nrf2 is a transcription factor that regulates the expression of many phase II detoxifying and antioxidant enzymes, such as heme oxygenase 1 (HO-1) and NAD(P)H:quinone oxidoreductase 1 (NQO1), which protect cells against oxidative stress. So as antioxidant genes, *Sod-1, Sod-2, Nrf-2, Ho-1* and *Nqo-1* were analyzed. As pro-oxidant gene the dual oxidase 1 (*Duox-1*), member of the NOX/DUOX family of NADPH oxidases, was analyzed. These enzymes transfer electrons across the biological membrane and they generate ROS. The expression of other members of NADPH oxidases family was also tested (*Nox-1, Nox-2, Nox-3, Nox-4)* but they were not detectable in our system. Finally, myelin genes were also analyzed, in particular *Plp, Mag,* and *Cnp* coding for the corresponding myelin proteins. In the ***Table 9*** the effect of stretch on the expression of these different genes is summarized for stretch duration of 30 min, 1h, 2h and 20h (see also **Fig. 40**). The major modifications were found for 20h, the time point chosen for the following experiments.

Stretch-induced mild injury (20%) *versus* control				
Genes	**30 min**	**1h**	**2h**	**20h**
Sod-1	↑90% (*)	↓30% (**)	=	↑20% (*)
Sod-2	=	=	=	↑30%(*)
Nrf-2	=	↓30%(***)	↑60%(*)	=
Ho-1	=	=	=	↑100%(***)
Nqo-1	↓55%(***)	=	=	↑50% (*)
Duox-1	↓40% (**)	=	=	↑70% (**)
Plp	=	↓ 25% (**)	=	=
Mag	=	=	=	↑400%(*)
Cnp	↑75%(**)	=	=	↑95%(**)

Table 9: Table summarizing the stretch effect on pro-oxidant, antioxidant and myelin gene expression in 158N cell line subjected to stretch (20% strain) for 30 min, 1h, 2h and 20h. RNA was extracted and RT-qPCR was performed in control and stretched conditions for the antioxidant genes *Sod-1, Sod-2, Nrf-2, Ho-1, Nqo-1,* the pro-oxidant gene *Duox-1* and the myelin genes *Plp, Mag* and *Cnp.* The percentage indicated is the percentage of induction (↑) or inhibition (↓) compared to the control condition. Sign of "=" is reported when no significant differences were observed compared to the control condition. Student's unpaired *t*-test was performed and significant differences are reported in brackets. *: $p<0.05$; **: $p<0.01$; ***$p < 0.001$. See Figure 40 for histograms corresponding to time 30 min, 1h and 2h and Figures 2 and 3 from Article1, for histograms corresponding to 20h.

A strain of 20% deformation is in the range of stretch relevant to the kind that occurs in humans after rotational acceleration-deceleration injury. It has been estimated that brain injury occurs at strain between 10% and 65% at strain rates of approximately 10-50 s^{-1} (LaPlaca and Thibault, 1997; Morrison et al., 1998; Morrison III et al., 1998). In our case we did not want to study the consequences of a rapid initial impact of TBI but instead to study the impact of the events that intervene secondary in the hours following TBI. That is why we chose a prolonged stretch, for 20h, at 20%. Our objective was also to reproduce another model of injury with a shorter period of stretch to see the initial response after a TBI in a range of minutes and not hours. We chose a stretch duration of 30 minutes, and the effects of stretch with strain rate of 20% and 30% were compared, considering the same genes described above (**Table 10 and Fig. 40**). The major alteration was assessed at 30% strain for 30 minutes, where the expression of three antioxidant genes (*Sod-1, Sod-2, Nrf-2*) were decreased together with the myelin gene *Plp.* This stretch was more "aggressive", since within 30 minutes it was able to affect the anti-oxidant system and myelin genes. Therefore, we chose the more severe strain at 30% for 30 minutes.

Stretch-induced injury for 30 min *versus* control		
Genes	**Mild (20%)**	**Moderate (30%)**
Sod-1	↑90% (*)	↓55% (*)
Sod-2	=	↓40% (*)
Nrf-2	=	↓30%(*)
Ho-1	=	=
Nqo-1	↓55%(***)	=
Duox-1	↓40% (**)	=
Plp	=	↓ 50% (**)
Mag	=	=
Cnp	↑75%(**)	=

Table 10: Table summarizing the stretch effect on pro-oxidant, antioxidant and myelin gene expression in 158N subjected to stretch (20% or 30% strain) during 30 minutes. RNA was extracted and RT-qPCR was performed in control and stretched conditions for the antioxidant genes *Sod-1, Sod-2, Nrf-2, Ho-1, Nqo-1,* the pro-oxidant gene *Duox-1* and the myelin genes *Plp, Mag* and *Cnp.* The percentage indicated is the percentage of induction (↑) or inhibition (↓) compared to the control condition. Sign of "=" is reported when no significant differences were observed compared to the control condition. Student's unpaired *t*-test was performed and significant differences are reported in brackets. *: $p<0.05$; **: $p<0.01$; ***$p < 0.001$. See Figure 40 for the histograms corresponding to 20% strain and see the Figure 2 and 3 from Article 1, for the histograms corresponding to 30% strain.

Based on our findings and other results presented in the article 1, two different stretch conditions reproducing stretch-induced mild or moderate injury were defined:

- Mild injury: equibiaxial static stretch of 20% strain for 20h
- Moderate injury: equibiaxial static stretch of 30% strain for 30 minutes

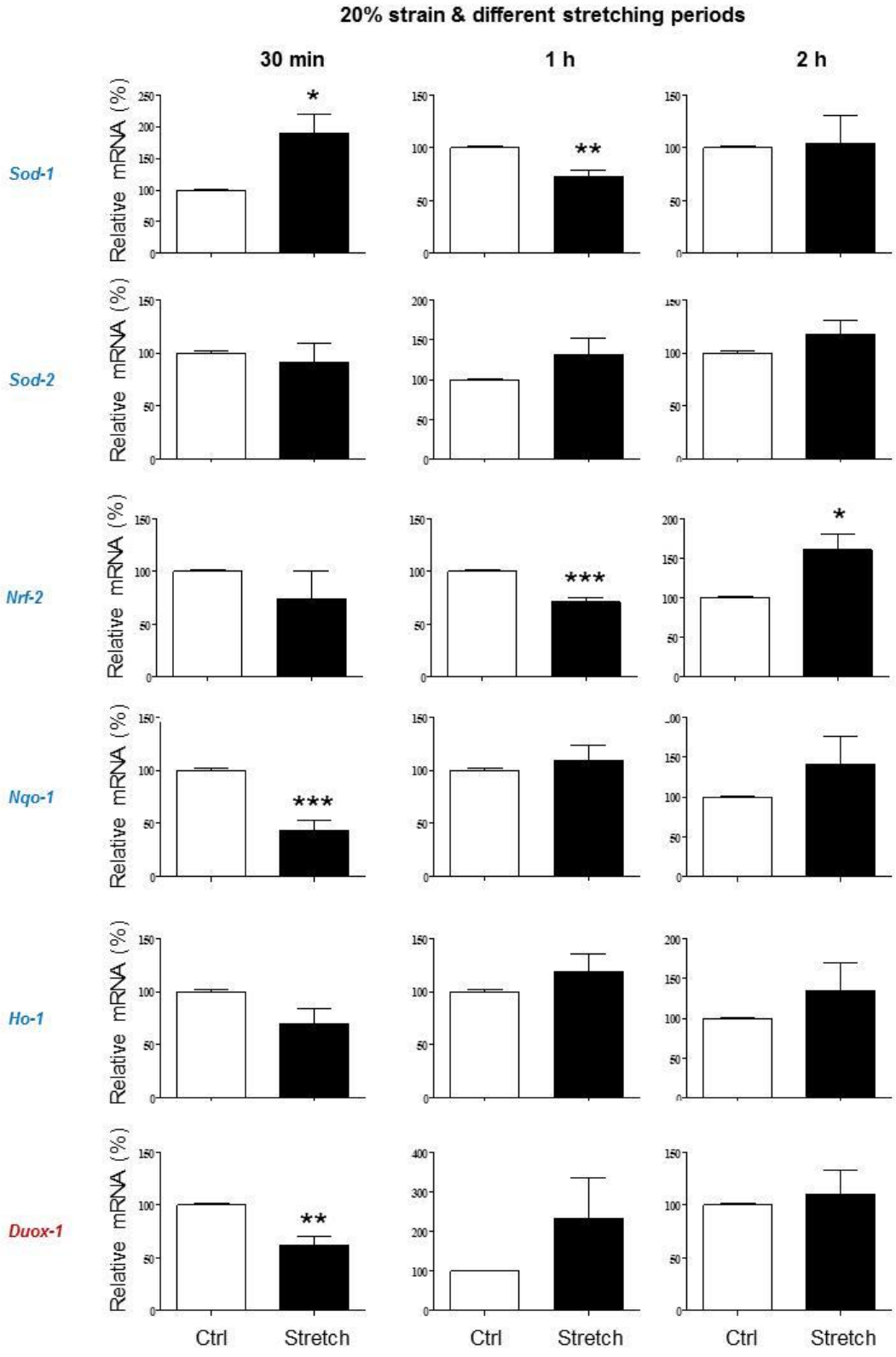

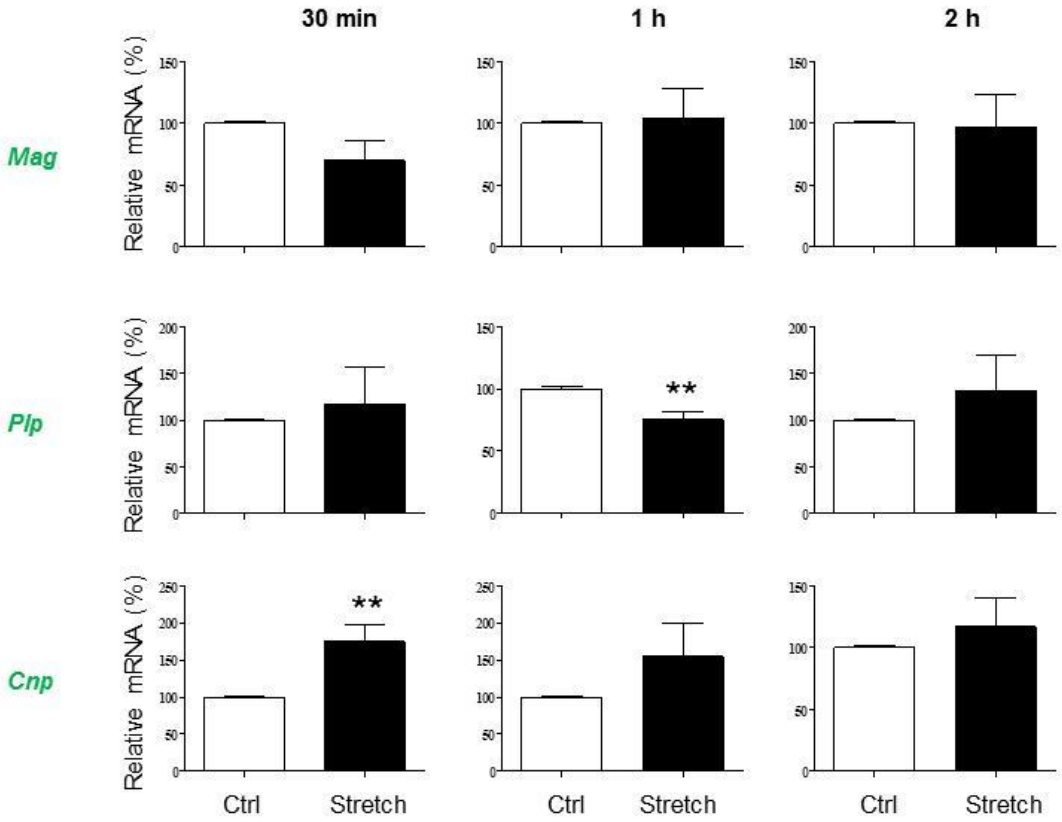

Figure 40: Evaluation of the stretch effect on pro-oxidant, antioxidant and myelin gene expression in 158N cell line subjected to stretch (20% strain) for 30 min, 1h and 2h. RNA was extracted and RT-qPCR was performed in control (Ctrl) and stretched (Stretch) conditions for the antioxidant genes *Sod-1, Sod-2, Nrf-2, Ho-1, Nqo-1,* the pro-oxidant gene *Duox-1* and the myelin genes *Plp, Mag* and *Cnp*. Results represent the mean±SEM of three independent experiments performed in triplicate. Student's unpaired *t*-test. *: $p<0.05$; **: $p<0.01$; ***$p < 0.001$.

2. Cellular and molecular responses of oligodendrocytes to stretch-induced mild and moderate injury **(see article 1)**

Once developed our two models of stretch-induced injury, the aim of our study was to decipher the cellular and molecular responses of oligodendrocytes to mild and moderate injury. Two *in vitro* cellular models were used: the mouse 158N cell line and the oligodendrocyte-enriched primary culture. Cells were subjected to an equibiaxial static stretch in order to reproduce two models of stretch-induced injury: mild (20% strain for 20h) *versus* moderate (30% strain for 30 min) injury. Our results showed that the mild stretch decreased the cell adherence and affected the cell morphology with a decrease of surface area in both mature and immature oligodendrocytes in the oligodendrocyte-enriched primary culture. The mild stretch in 158N cell line i) induced an increase in ROS production accompanied by protein oxidation (AOPP), alteration of GSH redox cycle and alteration of the anti-oxidant systems (*Sod-1, Sod-2, Ho-1, Nqo-1, Nrf-2*), and ii) induced an inhibition of ERK and an activation of JNK, two proteins belonging to the family of MAPKs kinases. However, mild stretch did not modify the expression and the amount of the myelin protein PLP whereas moderate stretch did markedly reduce the level of PLP, accompanied by an inhibition of ERK. The moderate stretch in oligodendrocyte-enriched culture induced i) a more pronounced alteration in cell morphology with cell ramification damage, and ii) a marked increase in ROS production accompanied by an increase of AOPP and carbonyls.

In conclusion, two *in vitro* models of stretch-induced injury were developed for the first time in oligodendrocytes and our data suggest that mechanical stretch causes loss of oligodendrocytes and demyelination after injury.

Article 1:

Chierto E, Castoldi F, Meffre D, Cristinziano G, Sapone F, Carreté A, Borderie D, Etienne F, Rannou F, Massaad C, Jafarian-Tehrani M "Significant oligodendroglial alterations in response to stretch-induced injury" (submitted to Scientific Reports)

Significant oligodendroglial alterations in response to stretch-induced injury

Elena Chierto, Francesca Castoldi, Delphine Meffre, Giulia Cristinziano, Francesca Sapone, Alex Carreté, Didier Borderie, François Etienne, François Rannou, Charbel Massaad, Mehrnaz Jafarian-Tehrani*

INSERM UMR 1124, Paris Descartes University, Sorbonne Paris Cité, Faculté des Sciences Fondamentales et Biomédicales, 45 rue des Saints-Pères, 75006 Paris, FRANCE. *Corresponding author

Abstract

Traumatic brain injury (TBI) is caused by rapid deformation, stretching and tearing of the brain tissue. After the initial mechanical trauma, a cascade of pathophysiological events is initiated. Understanding how the mechanical forces lead to tissue damage and particularly to myelin breakdown remains a considerable challenge. Clinical and experimental evidences suggest that demyelination may play an important role in the pathophysiology of TBI. The aim of our study was to develop an innovative model of brain injury induced by mechanical stretch in order to decipher the cellular and molecular responses of oligodendrocytes to stretch-induced injury. Two *in vitro* models were developed using the mouse 158N cell line and the oligodendrocyte-enriched primary culture. Cells were subjected to an equibiaxial static stretch using Flexcell® Tension system device in order to reproduce mild (20% strain) and moderate (30% strain) injury. Our results showed that the mild injury decreased the cell adherence and affected the cell morphology with a decrease of surface area in both mature and immature oligodendrocytes in the oligodendrocyte-enriched primary culture. In 158N cell line it i) induced an increase in reactive oxygen species (ROS) production accompanied by protein oxidation (AOPP), alteration of glutathione redox cycle and alteration of the anti-oxidant systems (*Sod-1, Sod-2, Ho-1, Nqo-1, Nrf-2*), and ii) induced an inhibition of ERK and an activation of JNK, two proteins belonging to the family of MAP kinases. The mild injury did not modify the expression and the amount of the myelin protein PLP, whereas the moderate injury did markedly reduce the level of PLP. The moderate injury also resulted in ERK inhibition. The moderate injury, in oligodendrocyte-enriched culture, induced a more pronounced alteration in cell morphology with cell ramification damage, and, in 158N cell line, a marked increase in ROS production accompanied by an increase of AOPP and carbonyls. In conclusion, two *in vitro* models of stretch-induced injury were developed for the first time in oligodendrocytes and our data suggest that mechanical stretch can induce loss of oligodendrocytes after injury.

Keywords: *oligodendrocytes; traumatic brain injury; mechanostimulation; stretch-induced injury; demyelination; oxidative stress, oligodendrocyte-enriched primary culture; 158N cell line*

INTRODUCTION

Traumatic brain injury (TBI) constitutes a serious public health and socioeconomic problem worldwide and is a major cause of death and disability, in particular among young population. Once TBI occurs, a number of short- and long-term detrimental processes begin to affect the brain. The initial insult first leads to a primary injury caused by the mechanical damage from shearing, stretching and/or tearing of neurons, axons, glia and blood vessels (Lozano et al., 2015). The primary impact triggers a secondary injury characterized by a complex cascade of metabolic, cellular and molecular alterations such as glutamate excitotoxicity, perturbation of cellular calcium homeostasis, increased free

radical generation, mitochondrial dysfunction, inflammation, apoptosis and diffuse axonal injury (Xiong et al., 2013). Previous studies have focused more on the effects of injuries on grey matter due to neuronal impairment. However, more recent findings show an equivalent importance of white matter in the brain damage following traumatic insult (Kim et al., 2008; Sidaros et al., 2009; Tomaiuolo et al., 2012).

Myelin, the concentrically laminated membrane structure that wraps around axons and works as biological insulator, is a major component of white matter. It is made up by oligodendrocytes in the central nervous system (CNS). Oligodendrocytes express several myelin-associated proteins sequentially expressed along the development, with progressive morphological maturation of cells. Oligodendrocyte precursor cells (OPCs) and pre-oligodendrocytes express different proteins such as platelet-derived growth factor receptor alpha (PDGFR-α), while mature oligodendrocytes express myelin basic protein (MBP), proteolipid protein (PLP), 2', 3'-cyclic-nucleotide 3'-phosphodiesterase (CNP), and myelin associated glycoprotein (MAG) (Baumann and Pham-Dinh, 2001; Greer, 2013; Simons and Nave, 2016). Mature oligodendrocytes form "myelin-like" membranes *in vitro* and myelin sheaths that enwrap axons *in vivo* (Jackman et al., 2009).

There are increasing clinical and experimental evidences suggesting that demyelination may play an important role in the pathophysiology of TBI (Armstrong et al., 2016a, 2016b). A marked white matter atrophy and degeneration has been observed in patients who survived from moderate to severe forms of TBI to a chronic post-injury stage (Herrera et al., 2016; Kim et al., 2008; Sidaros et al., 2009; Tomaiuolo et al., 2012; Wang et al., 2016). The white matter degeneration can be accompanied by a persistent neuroinflammation, even years after a single TBI in humans (Johnson et al., 2013). Studies in humans and in rats demonstrated also that TBI induces oligodendrocyte apoptosis and widespread myelin loss, followed by a concomitant increase in the number of OPCs (Caprariello et al., 2012; Flygt et al., 2013, 2016).

There are abundant evidences showing a considerable increase in the production of reactive oxygen species (ROS) following TBI, resulting in oxidative stress which has a significant role in the aetiology of progressive neuropathology in TBI (Abdul-Muneer et al., 2015). Free radicals are generated during normal physiological processes and, under these conditions, the endogenous defence system is able to prevent the formation or to scavenge these molecules, protecting tissues from oxidative damage (Mendes Arent et al., 2014). However, under pathological conditions, as TBI, ROS can damage and oxidize macromolecules, such as DNA, proteins, carbohydrates, and lipids (Rodríguez-Rodríguez et al., 2014; Valko et al., 2006). It is noteworthy that the CNS is extremely sensitive to free radical damage, because of its relatively small total antioxidant capacity (Cornelius et al., 2013; Sultana et al., 2013). In particular oligodendrocytes are highly sensitive to oxidative stress, because of their lipid-rich membranes, low glutathione reductase enzyme activity and low glutathione (GSH) amount (French et al., 2009; Thorburne and Juurlink, 1996).

Taken together, all these data suggest that myelin is early affected after TBI. However, the pathophysiological mechanisms underlying this loss of myelin are not yet well known. The development of an *in vitro* model of traumatic injury is a step forward in the comprehension of the response of oligodendrocytes to the injury and the myelination process post-injury.

Since brain is composed of incompressible tissue and it is encapsulated into a rigid skull, the mechanical forces applied to the brain tissue are a combination of stretch, compression and shear (Darvish and Crandall, 2001; Morrison et al., 2006). The major force causing injury of nervous tissue is not merely compression but rapid tissue deformation and strain, or more simply stretch (Ellis et al., 1995). The development of stretch-induced injury models is therefore motivated by a rigorous understanding of TBI

biomechanics to reproduce *in vivo* brain deformation. Many *in vivo* models of TBI have been developed (reviewed by Xiong et al., 2013), and they mimic different events following head injury but, due to the complexity of the *in vivo* situation, accessibility to the tissue of interest becomes limited. Thus, in order to understand the physiological response of individual cells as a result of the injury inflicted, it is important to isolate cells from the systemic effects, which may inhibit or alter their individual response (Cargill and Thibault, 1996). Considering the *in vitro* models of trauma, they allow the evaluation of the response of specific cell types in well-controlled and environmentally isolated experiments (Geddes-Klein et al., 2006) and they are, for this reason, complementary to *in vivo* models (Morrison et al., 2011; Salvador et al., 2013).

Among *in vitro* models of TBI, several reports adressed the effect of stretch-induced injury on different CNS cell types. They have cultured neurons, astrocytes and microglia, on deformable elastomeric substrates, where the mechanical stimuli is transmitted to the substrate and indirectly transferred to the adherent cells. Stretch injury results in structural changes to both glia and neurons (Arundine, 2004; Arundine et al., 2003; Ellis et al., 1995; Gladman et al., 2010, 2012) and generally the damage is proportional to the degree of strain in astrocytes, neuronal plus glial cultures, microglia and endothelial cells (Ellis et al., 2007; McKinney et al., 1996).

Despite all these studies on different CNS cell types, no models of stretch-induced injury in oligodendrocytes have been described so far. Therefore, in this study we developed two innovative models of stretch-induced injury in oligodendrocytes, comparing mild *versus* moderate injury, using two different cellular models, oligodendrocyte 158N cell line and oligodendrocyte-enriched primary culture. The effect of a static stretch has been evaluated on different cellular and molecular aspects, i.e. cell death, cellular oxidative status, expression of myelin genes and corresponding proteins, as well as aspect of cytoskeleton, cell morphology, cell adherence and degree of maturation/differentiation of oligodendrocytes.

MATERIALS AND METHODS

Animals

Experiments were performed on 1-3 day postnatal (P1-P3)-old mice obtained from wild-type C57Bl/6 mice (Janvier, Le Genest St Isle, France). The animals were housed in a controlled temperature environment (22 ± 2 °C), under a 12h light/dark cycle, with access to food and water *ad libitum*. Animal care and experiments were approved by the Paris Descartes University (CEEA34.MJT.075.12) respecting the French regulations and the European Communities Council Directive of September 2010/63/UE, on the protection of animals used for scientific purposes.

Oligodendrocyte cell line culture

The oligodendrocyte 158N cell line, which preserves oligodendrocyte characteristics and expresses myelin proteins (Feutz et al., 1995; Ghandour et al., 2002), was kindly provided by Dr. S.M. Ghandour (Strasbourg, France). Cells were maintained in Dulbecco's minimal essential medium (DMEM) supplemented with 5% heat inactivated fetal bovine serum (HI-FBS, Gibco, NYC, NY, USA), L-glutamine 2 mM, sodium pyruvate 1 mM, penicillin (0.1 U/mL)/streptomycin (0.1 µg/mL) and 0.5 µg/mL fungizone. Cells were grown at 37°C in a humidified atmosphere of 5% CO_2.

For the preparation of the cells subjected to mechanical stretch, cells were trypsinized and plated at the density of $3x10^5$ cells/1.5 mL per well on laminin-coated Bioflex® Plates (Dunn Labortechnik GmbH, BF-3001L). Cells were maintained in 5% CO2, in a humidified atmosphere (90%) at 37°C for 72h before being submitted to a mechanical stretch. After 48h of culture (the day before stretching), the medium was changed with 3 mL of fresh medium with 1% HI-FBS (Gibco, NY, USA). Control (non-stretched) plates were prepared and underwent the same conditions, except that they did not receive the mechanical stretch.

Oligodendrocyte-enriched primary culture

Mixed glial primary culture was prepared as previously described (Feutz et al., 2001; Meffre et al., 2015) from brain hemispheres of new-born mice (P0-P3). Cells were maintained in culture for 14 days *in vitro* (DIV) before preparing the oligodendrocyte-enriched primary culture. To prepare the oligodendrocyte-enriched primary culture, oligodendrocytes were collected from primary mixed glial cell culture as previously described (Feutz et al., 2001), with slight modifications.

Oligodendrocytes growing on the astrocyte layer were detached mechanically and the microglia were eliminated with a pre-plating step. The pellet containing oligodendrocytes was suspended in DMEM supplemented with Insulin (5 μg/mL)–Transferrin (5 μg/L)–Selenium (5 pg/ml) cocktail (BD biosciences), 2% HI-FBS, penicillin (0.1 U/mL)/streptomycin (0.1 μg/mL) and 0.5 μg/mL fungizone. Cells were seeded at the 4-5x10^5 density in untreated Bioflex® Plates (Dunn Labortechnik GmbH, BF-3001U) coated beforehand with 25 μg/mL poly-L-lysine. Cells were maintained in 5% CO_2, in a humidified atmosphere (90%) at 37°C for 2 DIV before being submitted to a mechanical stretch. Uninjured (non-stretched) control plates were prepared and underwent the same conditions, except that they did not receive the mechanical stretch.

***In vitro* model of mechanical stretch**

Cells grown on BioFlex® six-well plates were submitted to a mechanical stretch using a Flexcell® FX 5000™ Tension System (Flexcell International corporation, NC, USA), a computer-regulated bioreactor that uses vacuum pressure to apply a strain to cells cultured on elastic silicone membranes. In brief, the vacuum pressure deforms the silastic membranes of the Bioflex® Plates and the adherent cells to varying degrees controlled by the pulse pressure (Vande Geest et al., 2004).

Two models of stretch were developed, in order to reproduce two different injuries, here called mild and moderate injury. In the model of stretch-induced mild injury, cells were exposed to an equibiaxial static stretch of 20% strain for 20h and the output analyses were performed at time 0h post-stretch. In the model of stretch-induced moderate injury, cells were exposed to an equibiaxial static stretch of 30% strain for 30 minutes and the output analyses were performed at time 0h post-stretch. Models of injury using gel-filled human skulls have indicated that this range of stretch is relevant to the kind that occurs in humans after rotational acceleration-deceleration injury (Margulies et al., 1990; Meaney et al., 1995).

Flow cytometric analysis

Cells from oligodendrocyte 158N cell line were trypsinized and collected in order to be analysed with the Fluorescence-activated cell sorting (FACS) technique. Cells were centrifuged at 1.500 rpm for 3 min and, after being washed twice with PBS, 1 × 10^6 cells were suspended in 1 ml of PBS 0.1 M (Ca^{2+} and Mg^{2+} free). We used the BD FACSCanto™ II flow cytometer and for each analysis, 10.000 cells were counted on the gate R1 drawn on the FSC (Forward scatter)/SSC (Side scatter) biparametric histogram. We considered only the population of cells devoid of aggregates and debris.

In order to evaluate the cell viability and ROS production, a double staining with propidium iodide (PI) and the carboxy-dichloro-dihydro-fluorescein diacetate (CM-H2DCFDA) was performed (Bass et al., 1983; Rothe and Valet, 1990). Cells were incubated with 1.25 μM of CM-H2DCFDA probe (Molecular Probes C6827) for 30 min at 37°C in the dark. The excess of probe was washed out and cells were suspended in PBS (Ca^{2+} and Mg^{2+} free) and incubated 10 min with 1μg/mL of PI (Sigma P4170) at room temperature.

The cell-permeant CM-H2DCFDA probe passively diffuses into cells and is retained at intracellular level after cleavage by intracellular esterases. Upon oxidation by ROS, the nonfluorescent H2DCFDA is converted to the highly fluorescent 2',7'-dichlorofluorescein (DCF). The DCF fluorescence was recorded in FL-1 (530/30 nm) channel together with the PI fluorescence in FL-2 (585/42 nm). We used N-acetylcysteine (NAC) at 5mM, to serve as a positive control for the antioxidant activity, and *tert*-butyl hydroperoxide (*t*BHP) 100uM, to serve as a positive control for ROS production.

Biochemical analysis

Cells from oligodendrocyte 158N cell line were washed with PBS, trypsinized and centrifuged at 600g for 10 min. After surfactant elimination, cells were suspended in 1 ml of Cell Lysis Reagent (Sigma C2978) complemented with protease inhibitor (cOmplete, Mini, EDTA-free, Roche). Cell lysates were then analysed for all the following biochemical assays.

Determination of carbonyl levels - Protein carbonyl groups were detected and quantified using 2,4-dinitrophenylhydrazine (DNPH) as previously described (Reznick and Packer, 1994). Carbonyl levels were expressed as nmoles of carbonyl/mg of proteins.

Determination of advanced oxidation protein products (AOPP) - Advanced oxidation protein products (AOPP) were also assessed as described previously (Witko-Sarsat et al., 1996). AOPP concentrations are expressed as μmoles/L of chloramine-T equivalents.

Thiols determinations - Thiols determinations were based on the thiol/disulphide reaction of thiol and Ellman's reagent, 5,5′-dithiobis(2-nitrobenzoic acid) DTNB (Hu, 1994). Thiols were expressed as μmol/L.

Determination of Glutathione peroxidase (GPx) and Glutathione reductase (GR) activity - The GPx and GRx activities were quantified using the Cayman's Glutathione Peroxidase Assay Kit and

Reductase Assay Kit , respectively. The results obtained are normalized to the protein content and expressed as units per mg of protein.

Determination of reduced Glutathione (GSH) - Levels of intracellular GSH were assessed spectrofluorimetrically by monochlorobimane staining (Bellomo et al., 1997). The intracellular GSH level was expressed as arbitrary units (AU) of fluorescence intensity.

Determination of superoxide dismutase (SOD) activity - The superoxide dismutase activity was evaluated using the nitroblue tetrazolium reduction technique previously described by Beauchamp and Fridovich (Beauchamp and Fridovich, 1971). The results obtained are normalized to the protein content and expressed as units per mg of protein.

Quantitative RT-PCR

Total RNA from cultured cells was obtained using Trizol reagent (Invitrogen, France) and 1 µg was reverse transcribed with random primers from Biolabs (Beverly MA, USA) and Reverse Transcriptase MLV-RT from Fisher Scientific (Hampton, New Hampshire, USA), according to the manufacturers' instructions. Quantitative PCR was performed with standard protocols using SYBRGreen (ABgene, France) as fluorescent detection dye in ABI PRISM 7000 in a final volume of 7 µl, which also contained 300 nM of primers (except for PLP and MAG with 100nM of primers) (Eurofins Genomics Operon, Orsay, France) and 50 ng of reverse transcribed RNA in 384-well plates. Melting curve analysis was applied to characterize the generated amplicons and to control the contamination by unspecific by-products. Each reaction was performed in triplicate and the mean of at least three independent experiments was calculated. Results were normalized to 26S mRNA level and calculated using the DDCt method. The results are expressed as $2^{-\Delta\Delta Ct}$ [$\Delta\Delta Ct = \Delta Ct$ gene of interest– ΔCt reference gene]. The primer sequences used in real-time PCR are listed as following:

Sod1 forward: GCCAATGTGTCCATTGAAGA
Sod1 reverse: GTTTACTGCGCAATCCCAAT
Sod2 forward: GAGCTGCCTTACGACTATGG
Sod2 reverse: TGAAGAGCGACCTGAGTTG
Ho-1 forward: CACGCATATACCCGCTACCT
Ho-1 reverse: CCAGAGTGTTCATTCGAGCA
Nqo1 forward: GCGAGAAGAGCCCTGATTGTACTG
Nqo1 reverse: TCTCAAACCAGCCTTTCAGAATGG
Nrf-2 forward: TCTCCTCGCTGGAAAAAGAA
Nrf-2 reverse: AATGTGCTGGCTGTGCTTTA
Plp forward: AGCAAAGTCAGCCGCAAAAC
Plp reverse: CCAGGGAAGCAAAGGGGG
Mag forward: ACTGGTGTGTGGCTGAGAAC
Mag reverse: GGATTATGGGGGCAAACTC
Cnp forward: GACAGCGTGGCGACTAGACT
Cnp reverse: CACCTGGAGGTCTCTTTCCA
26S forward: AGGAGAAACAACGGTCGTGCCAAAA
26S reverse: GCGCAAGCAGGTCTGAATCGTG

Western blot assay

Proteins were extracted in cold RIPA buffer containing 50 mM Tris HCl, pH 7.5; 150 mM NaCl; 0.1% SDS; 0.5% sodium deoxycholate; 1% NP-40; 10 mM sodium pyrophosphatase; 0.1 mM sodium fluorate; 5 mM ETDA; protease inhibitor (cOmplete, Mini, EDTA-free, Roche) and phosphatase inhibitor (Protease Inhibitor Cocktail 2, P5726, Sigma). Protein content was determined using the reducing agent and detergent compatible protein assay kit (''RC DC'' protein assay, BioRad, Hercules, California, USA) with Bovine Serum Albumin (BSA) as standard. Aliquots of 30 µg of total extracts were used for each sample. Proteins (30µg) were separated on 10% SDS–polyacrylamide gels by electrophoresis and blotted onto PVDF (polyvinylidene difluoride) membranes. Non-specific binding sites were blocked at room temperature during 1h with 5% BSA diluted in Tris Buffered Saline with 0.1% Tween20 (TBST). Membranes were then incubated overnight with the following primary antibodies diluted in 5% BSA-TBST: rabbit polyclonal PLP (1:1000, Novus Biologicals NB10074503), rabbit polyclonal Nrf-2 (1:100, Abcam ab31163), rabbit monoclonal P-Nrf2 (1:100, Abcam ab76026), rabbit polyclonal ERK1/2 (1:500, Millipore 06-182), rabbit monoclonal P-ERK (1:500, Millipore 05-797R), rabbit polyclonal JNK (1:500, Cell Signaling 9252), rabbit polyclonal P-JNK (1:500, Cell Signaling 9251S), and rabbit polyclonal β-actin (1:10000, Abcam ab8227). Membranes were then incubated at room temperature for 1h30 with the appropriate horseradish peroxidase coupled secondary antibody diluted in 5%BSA-TBST (anti-rabbit: 1:20,000) and the specific bands were detected with the kit Pierce®ECL 2 Western Blotting substrate (Thermo Scientific, PI80196), using ImageQuant LAS4000 (GE Healthcare Life Sciences). Relative protein amounts were quantified with ImageJ 1.48v software, and normalized to β-actin.

Immunocytochemistry

At time 0h after stretching, cells were fixed with 4% paraformaldehyde at room temperature (25 min) for subsequent immunocytochemistry. The membranes with adherent cells were gently cut from the Bioflex® Plates. Samples were permeabilized with 0.1% TritonX-100-

PBS for 15 min and then incubated with primary antibodies overnight at 4°C in BSA 5%-PBS. Primary antibodies anti-MAG (1:250; Millipore, Chemicon, MAB1567), anti-PDGFR-α (1:500; Santa Cruz sc-338), anti α-tubulin (1:4000; Sigma T6074) were used. Then the samples were incubated with the secondary antibody, Alexa 488 goat anti-mouse IgG (1:200; Invitrogen A21121) and Cy3 goat anti-rabbit (1:100; Jackson ImmunoResearch 111-165-003) in BSA 5%-PBS for 1h at RT. TRITC-phalloidin (1:2000; Sigma P1951) and Hoechst (1:50000; Sigma H2261) were used to label F-actin and cell nuclei, respectively. The samples were mounted with Permafluor (Thermo Scientific FM 150202) or Fluoromount (Southern Biotech, Birmingham, USA).

Immunofluorescence analysis

Images were acquired using a confocal microscope LSM 710 (Carl Zeiss Inc., Germany) with a 20x objective (Plan-Neofluar 20x/0.5) or a 63x objective (Plan-Neofluar 40x/1.3 OilDic). Confocal configurations were adapted for 346, 488 and 543 nm excitations corresponding to Hoechst, Alexa-488 and Cy3 fluorochromes, respectively. Images were then processed with LSM Image Browser (version 4.2).

The number of $Hoechst^+$ cells, the percentage of MAG^+ and PDGFR-α^+ cells and also the area of MAG^+ and PDGFR-α^+ cells were determined using ImageJ 1.48v software. All the analyses were performed in 10-30 different fields (0.26 nm^2), randomly selected avoiding the edge of the membrane, per condition, from at least three independent experiments.

Statistical analysis

Unpaired student *t*-test was performed for two sets of data points, and one-way analysis of variance (ANOVA) with Bonferroni post-hoc test was used for comparison among multiple groups. The criterion for statistical significance was $p<0.05$ (*:$p<0.05$; **: $p<0.01$; ***: $p<0.001$). Data are expressed as mean values of *n* experiments ± SEM. All statistical analyses were performed with the software GraphPad Prism5.

RESULTS

Cellular and molecular response of oligodendrocyte 158N cell line to stretch-induced mild and moderate injury

Cells from the oligodendrocyte 158N cell line were exposed to mild injury (static stretch of 20% strain) or moderate injury (static stretch of 30% strain) and all output analyses were performed immediately after the end of stretching period (**Fig. 1-4**).

Stretch increased the level of intracellular ROS in 158N cell line in both mild and moderate injury

We used FACS to assess cell death and ROS production. In control and stretched cells, the number of PI^+ cells was less than 7% regardless of group condition and of stretch severity (**Fig. 1a, 1f**). Instead, the ROS production, evaluated by assessing redox sensitive intracellular conversion of H2DCFDA to DCF, was significantly increased in stretched cells compared to control. Stretch induced an increase in the number of DCF^+ / PI^- cells after mild (+15%, $p<0.05$) and moderate injury (+20%, $p<0.05$) (**Fig. 1b-c, 1g-h**). We next investigated whether if the amount of ROS produced during the stretch period was able to induce an alteration of cellular constituents, such as oxidation of proteins, evaluated by the amount of advanced oxidation protein products (AOPP) and carbonyls. The amount of AOPP in stretched cells was significantly increased compared to control group after mild (326 ± 19.05 *versus* 239 ± 18.62 µmol/mg; $p<0.05$) and moderate (338 ± 6.57 *versus* 287 ± 5.04 µmol/mg; $p<0.01$) injury (**Fig. 1d, 1i**). The amount of carbonyls groups was not different after mild injury (**Fig. 1e**), while it increased after moderate injury (20.40 ± 1.06 *versus* 15.63 ± 0.90 mmol/mg; $p<0.05$) (**Fig. 1j**).

Stretch altered glutathione levels and the enzymes involved in glutathione redox cycle in both mild and moderate injury

Stretch-induced mild injury provoked a decrease in the level of reduced GSH ($p<0.05$), one of the major antioxidant molecules, accompanied by a decrease of glutathione peroxidase (GPx) ($p<0.01$), the enzyme that detoxify H_2O_2 in water using 2GSH (**Tab. 1**). Regarding the moderate injury, the levels of GSH and GPx were also decreased after stretch and they were very close to significance ($p= 0.055$ and $p=0.058$, respectively). The oxidized glutathione (GSSG) was also assessed but it was not detectable in our system analysis. Glutathione reductase (GRx) and

thiols were not affected regardless of group condition and stretch severity (**Tab. 1**).

Stretch altered the antioxidant systems in both mild and moderate injury

Stretch applied to 158N cell line was able to induce ROS production leading to protein oxidation and alteration of glutathione redox cycle. Hence, we decided to analyse the status of the antioxidant systems in our cells (**Fig. 2**). The activity of superoxide dismutase (SOD), a major antioxidant enzyme, did not change in stretched cells after mild injury (**Fig. 2a**), while it did decrease after moderate injury (8.43 ± 0.35 *versus* 9.78 ± 0.17 U/mg, $p<0.05$) (**Fig. 2h**). The effect of stretch was also investigated at the mRNA level of the cytoplasmic form of this enzyme, *Sod-1*, and the mitochondrial form, *Sod-2*. Stretch induced an increase of both *Sod-1* (+20%, $p<0.05$) and *Sod-2* (+30%, $p<0.05$) expression after mild injury (**Fig. 2b, 2c**), while an opposite response was observed after moderate injury with a decrease in the expression of both *Sod-1* (-55%, $p<0.05$) and *Sod-2* (-40%, $p<0.05$), (**Fig. 2i, 2j**).

Next the expression of Nrf2 was evaluated, a transcription factor that regulates the expression of many phase II detoxifying and antioxidant enzymes, such as heme oxygenase 1 (HO-1) and NAD(P)H:quinone oxidoreductase 1 (NQO-1). The expression of *Ho-1* (+100%, $p<0.01$) and *Nqo-1* (+50%, $p<0.05$) were increased after mild injury in stretched cells compared to control (**Fig. 2d, 2e**), while Nrf-2 was not affected by stretch at both mRNA and protein level (**Fig. 2f, 2g**). However, moderate injury induced a tendency to decrease at the mRNA level of *Ho-1* and *Nqo-1* (**Fig. 2k, 2l**), and a significant decrease of Nrf-2 expression (-30%-fold, $p<0.05$) in stretched cells (**Fig. 2m**). At the protein level, moderate injury induced a tendency to decrease of activated Nrf-2 following stretch (**Fig. 2n**).

Stretch altered MAPKs activity in both mild and moderate injury

The mitogen-activated protein kinases (MAPKs), a family of kinases as the extracellular signal-regulated kinase (ERK), and c-Jun NH2-terminal kinase (JNK), constitute a particularly stretch-responsive pathway involved in cell response to stretch (Hoefen and Berk, 2002; Kyriakis and Avruch, 2012; Owens and Keyse, 2007). Thus, we decided to analyze the effect of stretch on ERK1/2 (44 and 42 kDa) and on JNK (54 and 46 kDa) in our two models of injury. Stretch reduced the ratio of P-ERK/ERK by 50% ($p<0.001$) in the mild injury and by 35% ($p<0.01$) in the moderate injury (**Fig. 3a, 3c**). Mild injury also affected JNK by increasing the ratio of P-JNK/JNK for the isoform of 54 kDa (+70%, $p<0.05$) and a tendency to increase for the isoform of 46 kDa (**Fig. 3b**). The moderate injury did not affect JNKs proteins (**Fig. 3d**).

Stretch altered PLP expression in both mild and moderate injury

The following step in this study was to evaluate the effect of stretch on PLP, one of the major myelin proteins, at mRNA and protein levels. Stretch-induced mild injury does not affect PLP (**Fig. 4a, 4b**), while the moderate injury significantly decreased PLP by 50% ($p<0.01$) at mRNA level and by 30% at protein level ($p<0.05$) (**Fig. 4c, 4d**).

Cellular and molecular response of oligodendrocyte-enriched primary cell culture to stretch-induced mild and moderate injury

Cells from oligodendrocyte-enriched primary culture were exposed to mild injury (static stretch of 20% strain) or moderate injury (static stretch of 30% strain) and all output analyses were performed immediately after the end of stretching period (**Fig 5-6; Fig. S1**).

Stretch affected the oligodendrocyte morphology in both mild and moderate injury

In order to understand if these models of injury are able to cause oligodendrocyte loss and demyelination we moved from 158N cell line, where significant alterations in the levels of antioxidant enzymes and of myelin protein were observed, to the oligodendrocyte-enriched primary culture, a model more suitable for the analysis of oligodendrocyte morphology.

In order to evaluate the effect of stretch on cell morphology, a double immunostaining was performed for actin and α-tubulin as components of cytoskeleton, microfilaments and microtubules, respectively. The morphology of oligodendrocytes was affected by stretch following mild injury, given that the cells are retracted with reduced total cell area (**Fig. S1a and Fig.5**). After moderate injury, the oligodendrocytes appeared deeply damaged, with less or, in the many cases, even no cell branches following stretch (**Fig. S1b**).

Stretch decreased the number of adherent cells, reduced the cell surface of both mature and immature oligodendrocytes and decreased the expression of myelin genes following mild injury

In order to analyse the effect of stretch on oligodendrocyte morphology and its differentiation, we labelled both mature and immature oligodendrocytes for MAG and PDGFR-α, respectively (**Fig. 5**). The number of Hoechst$^+$ nuclei was also quantified showing a decrease in the number of adherent cells by 50% following stretch ($p<0.0001$) (**Fig. 5a, 5b**). Besides, the effect of stretch on the area of MAG$^+$ and PDGFR-α$^+$ cells was evaluated highlighting the presence of smaller cells for both mature MAG$^+$ (14 223 ± 122 *versus* 20 351 ± 163 μm^2, $p<0.05$) and immature PDGFR-α$^+$ (3 649 ± 190 *versus* 4 331 ± 138 μm^2, $p<0.05$) oligodendrocytes (**Fig. 5c, 5d**). However, the percentage of MAG$^+$ (11.50 ± 0.29 *versus* 13.50 ± 0.87) and PDGFR-α$^+$ (86.33 ± 0.88 *versus* 80.33 ± 3.28) cells were not affected following stretch (**Fig. 5e**) meaning that there were less adherent cells but in the same proportion of mature and immature cells.

The effect of stretch was also assessed at the mRNA level of three myelin genes PLP, MAG and CNP, showing a decrease by 30% for MAG ($p<0.05$) (**Fig. 5f**), and no significant changes for PLP (**Fig. 5g**) and CNP (**Fig. 5h**).

Stretch decreased the number of adherent cells, deeply affected both mature and immature oligodendrocytes and decreased the expression of myelin genes following moderate injury

The effect of moderate stretch on the number of adherent cells showed a reduction by 50% of Hoechst$^+$ nuclei number in the stretch condition ($p<0.05$) (**Fig. 6a, 6b**). Some of these nuclei presented an elongated shape. Due to a severe cell damage following moderate injury, cellular branches were disrupted and the real shape of cells became impossible to identify as mature MAG$^+$ or immature PDGFR-α$^+$ oligodendrocytes.

Regarding the effect of stretch on myelin genes, PLP expression was decreased by 55% ($p<0.05$) (**Fig. 6d**), with no significant changes for MAG and CNP (**Fig. 6c, 6e**) after stretch.

DISCUSSION

The aim of this work was to understand the response of oligodendrocytes and the fate of myelin proteins following stretch-induced traumatic injury. Since strain is known to be an important component of TBI leading to tissue damage (Ellis et al., 1995), we focused our attention on the development of a model of stretch-induced injury. Numerous studies were performed on different CNS cell types, but oligodendrocytes have received less attention. Oligodendrocytes are known to be mechanosensitive. To date, some studies attempted to explore the effect of a mechanical stimulation on OPCs and oligodendrocytes (Arulmoli et al., 2015; Hernandez et al., 2016; Jagielska et al., 2012; Lourenço et al., 2016; Rosenberg et al., 2008; Urbanski et al., 2016). Nevertheless, only one study utilizes stretching as mechanical stimulus (static equibiaxial strain at 10% for 3 to 7 days) in order to differentiate primary neural stem and progenitor cells into neurons, astrocytes or oligodendrocytes (Arulmoli et al., 2015). It is a different context, since they studied the effect of stretch with a low strain on cell differentiation and not the effect of trauma, as stretch with high

strain, on oligodendrocytes. Therefore, no study has addressed so far the effects of stretch-induced injury in oligodendrocytes.
We first developed two *in vitro* models of stretch-induced injury i) to decipher the cellular and molecular responses of oligodendrocytes to stretch-induced mild and moderate injuries and ii) to understand whether if these models of injury cause oligodendrocyte loss and demyelination.

Among the secondary events triggered following TBI, the oxidative stress has a relevant role in the aetiology of progressive neuropathology in TBI (Abdul-Muneer et al., 2015) and oligodendrocytes are particularly vulnerable to oxidative stress (French et al., 2009; Thorburne and Juurlink, 1996).

Therefore, we assessed the ROS production in oligodendrocytes submitted to stretch-induced injury and we chose as a cellular model, the oligodendrocyte 158N cell line. Stretch did not induce cell death but caused significant cellular and molecular alterations as a significant increase in the production of ROS, resulting in protein oxidation (AOPP), after mild and moderate injuries, and in protein carbonylation after moderate injury. ROS are normally produced under physiological condition, without inducing cell damage because the antioxidant defence system protects cells against oxidative stress. However, under pathological conditions, ROS can damage and oxidize macromolecules, such as DNA, proteins, carbohydrates, and lipids (Rodríguez-Rodríguez et al., 2014; Valko et al., 2006). In our models, the free radicals produced after stretch attack proteins, even if it doesn't result in cell death. Moreover, the mild injury results in a decrease of reduced glutathione (GSH), accompanied by a decrease of glutathione peroxidase (GPx), the enzyme that detoxifies H_2O_2 in water by consuming 2GSH. Following the moderate injury, the levels of GSH and GPx are also decreased close to significance. Glutathione is the first line of defence and it is able to efficiently scavenge reactive species. The measurement of both reduced glutathione (GSH) and glutathione disulfide (GSSG) is often used as an indicator of the oxidative stress status. A decrease of the ratio GSH/GSSG indicates a shift to an oxidized form of GSH, suggesting the presence of oxidative stress at the cellular or tissue level (Dalle-Donne et al., 2006; Durackova, 2010; Tunez et al., 2011). In our system, it was not possible to detect GSSG but the dosage of GSH revealed a significant decrease of GSH, indicating an alteration in the glutathione equilibrium.

Considering the increased ROS production and the alteration in oxidative stress markers after stretch, we decided to investigate more deeply the cellular oxidative redox status analysing the anti-oxidant systems in 158N cells. As one of the major anti-oxidant enzymes, SOD was analysed at the mRNA level and for its enzymatic activity. The mild injury results in an increase in both *Sod-1* (cytoplasmic isoform) and *Sod-2* (mitochondrial isoform) at mRNA level but it did not result in an alteration of SOD activity. The moderate injury results in an opposite response reducing both *Sod-1* and *Sod-2* mRNA and also resulting in a decrease of SOD activity. We also analysed the expression of a transcription factor, Nrf-2, since Nrf2/ARE pathway is a major determinant of detoxifying phase II gene induction (Zhang et al., 2013). Upon exposure to ROS, Nrf2 is released from the Keap1-Nrf2 complex and it translocates from the cytoplasm to the nucleus, where it sequentially binds to the antioxidant response element (ARE), a regulatory enhancer region within gene promoters. This binding induces the expression of many phase II detoxifying and antioxidant enzyme genes such as *Ho-1* and *Nqo-1*, which protect cells against oxidative stress (Jain, 2005; Owuor and Kong, 2002). In 158N cell line, the mild injury did not affect Nrf-2 expression (neither at mRNA nor at protein level), in spite of an increase in the expression of the anti-oxidant genes as *Ho-1* and *Nqo-1*. Once again the response following the moderate injury goes to the opposite direction showing a decrease in the mRNA expression of Nrf-2, even if it was not confirmed at protein level. However, the expression of *Ho-1* and *Nqo-1* was not affected probably due to the short period of moderate injury.

Overall, the mild injury increases the anti-oxidant systems, showing that cells are able to activate their defence system, in order to strengthen their cellular response to oxidative stress. In contrast, the moderate injury induces an opposite response at the molecular level with a significant alteration of the antioxidant system rendering cells more vulnerable.

As we wanted also to study the effect of stretch on signalling pathways, our interest was focused on a particularly stretch-responsive pathway involving the mitogen-activated protein kinases (MAPKs). These kinases include extracellular signal-regulated kinase (ERK), c-Jun NH2-terminal kinase (JNK), and p38. MAPKs are known to regulate different cellular processes as cell survival, proliferation, differentiation, and migration (Pearson et al., 2001). They are also known to be involved in mechanically-induced signalling in various cell types being implicated in the signal transduction from the cell membrane to the nucleus. It has been demonstrated that isoforms of JNK and ERK are phosphorylated in a tension-dependent manner in rat skeletal muscle preparations (Martineau and Gardiner, 2001). In bovine aortic endothelial cells, cyclic stretch transiently activates JNK, ERK and p38 in a strain rate-dependent manner, accompanied by an alignment of stress fibres for uniaxial strain and by cell retraction for equibiaxial strain (Hsu et al., 2010). Moreover, mechanical injury activates in CNS glial cells, as astrocytes, ERK (Neary et al., 2003), and p38 (Zhou et al., 2011).

However, signalling pathways activated in oligodendrocytes in response to a mechanical stimulus has not been reported so far. In our model ERK pathway was found to be inhibited in both mild and moderate injuries, while JNK was activated after mild injury only. A recent study showed that the Ras/Raf/MEK/ERK pathway signalling is inhibited through the activation of the stress-activated JNK cascade. This effect is engaged by cancer therapeutics, that activates JNK through mitotic and oxidative stress (Ritt et al., 2016). We cannot exclude a similar pathway regulation in our system, even though ERK is downregulated also after moderate injury, when JNK is not activated. MAPKs isoforms are preferentially activated by distinct stimuli, ERK is more involved in cell division, migration, and survival, while p38 and JNK are more responsive to cellular and environmental stresses (Hoefen and Berk, 2002; Kyriakis and Avruch, 2012; Owens and Keyse, 2007; Vezza et al., 2016). In our system, given the activation of JNK following stretch, it confirms that mechanical stretch activates the JNK pathway known to respond to environmental stresses. However, the activation of JNK in our model seems to be strain-dependent since it is not activated following stretch-induced moderate injury.

Another objective of our study was to understand if stretch-induced injury initiates oligodendrocyte loss. To answer this question we analysed in the 158N cell line the expression of PLP, one of the major myelin proteins. While mild injury did not alter this protein, moderate injury provoked a significant decrease of PLP at both mRNA and protein levels. Overall, our findings suggest that stretch induces myelin protein alteration depending on the severity of stretch.

In order to analyse the effect of stretch on oligodendrocytes morphology, we used the oligodendrocyte-enriched primary culture, a primary culture with more than 95% of oligodendrocytes. Cells subjected to the mild injury showed a significant decrease in cell adherence after stretch and, regarding the morphology, cells appeared retracted in the stretched condition as confirmed by a significant decrease of surface area of immature ($PDGFR\text{-}\alpha^+$) and mature (MAG^+) oligodendrocytes following stretch. Nevertheless the proportion of mature and immature oligodendrocytes did not change after stretch meaning that they were equally affected by stretch. The analysis on the expression of myelin genes resulted in a decrease of *Mag* mRNA in line with the immunolabelling studies. Cells can respond to a mechanical stretch by increasing or by decreasing their spread area, generally as a function of stretch magnitude and strain frequency, if a dynamic stretch is applied. For example,

a cyclic equibiaxial stretch of 10% in aortic endothelial cells decreases cell spreading at 1Hz, but not at 0.01Hz. Cells retract to ~80% of their original area after 5 min and maintained this retracted area throughout the 60 min of experiment (Hsu et al., 2010). Cui and coworkers showed in fibroblasts that strain at higher magnitude, 15%, reduced the cell spreading, reflected by the total cell area, even at low frequency (Cui et al., 2015). Our results are in line with these findings, since 20% of strain magnitude is able to affect cell area in our study. When primary oligodendrocytes were subjected to moderate stretch, the effect was more drastic. There were less adherent cells and those who were attached to the silicone membrane presented a severe cell damage.. Primary oligodendrocytes appeared more sensitive to stretch-induced injury compared to the cell line. Taken together, the strain at 20% results in a reduced cell area or cell retraction, while the strain at 30% of strain results in a more severe damage that compromises the analysis of cell morphology.

In conclusion, we developed for the first time two *in vitro* models of stretch-induced injury, mild and moderate, to decipher the cellular and molecular response of oligodendrocytes to stretch. Our data suggest that oligodendrocytes constitute a cellular target to counteract demyelination following stretch-induced injury.

Acknowledgments
This work was supported by the non-profit organization "*Fondation des Gueules Cassées*" (grants to MJT), Paris Descartes University and by INSERM (*Institut National de la Santé Et de la Recherche Médicale*). E.C. is a recipient of PhD fellowship from French Ministry of Research. The authors acknowledge Jean-Maurice Petit, responsible of Imaging facility, for confocal microscopy assistance and Dr Stéphanie Dupuy, responsible for FACS facility, for flow cytometry assistance.

REFERENCES

Abdul-Muneer, P.M., Chandra, N., and Haorah, J. (2015). Interactions of Oxidative Stress and Neurovascular Inflammation in the Pathogenesis of Traumatic Brain Injury. Mol. Neurobiol. *51*, 966–979.

Armstrong, R.C., Mierzwa, A.J., Sullivan, G.M., and Sanchez, M.A. (2016a). Myelin and oligodendrocyte lineage cells in white matter pathology and plasticity after traumatic brain injury. Neuropharmacology *110*, 654–659.

Armstrong, R.C., Mierzwa, A.J., Marion, C.M., and Sullivan, G.M. (2016b). White matter involvement after TBI: Clues to axon and myelin repair capacity. Exp. Neurol. *275*, 328–333.

Arulmoli, J., Pathak, M.M., McDonnell, L.P., Nourse, J.L., Tombola, F., Earthman, J.C., and Flanagan, L.A. (2015). Static stretch affects neural stem cell differentiation in an extracellular matrix-dependent manner. Sci. Rep. *5*, 8499.

Arundine, M. (2004). Vulnerability of Central Neurons to Secondary Insults after In Vitro Mechanical Stretch. J. Neurosci. *24*, 8106–8123.

Arundine, M., Chopra, G.K., Wrong, A., Lei, S., Aarts, M.M., MacDonald, J.F., and Tymianski, M. (2003). Enhanced vulnerability to NMDA toxicity in sublethal traumatic neuronal injury in vitro. J. Neurotrauma *20*, 1377–1395.

Bass, D.A., Parce, J.W., Dechatelet, L.R., Szejda, P., Seeds, M.C., and Thomas, M. (1983). Flow cytometric studies of oxidative product formation by neutrophils: a graded response to membrane stimulation. J. Immunol. Baltim. Md 1950 *130*, 1910–1917.

Baumann, N., and Pham-Dinh, D. (2001). Biology of oligodendrocyte and myelin in the mammalian central nervous system. Physiol. Rev. *81*, 871–927.

Beauchamp, C., and Fridovich, I. (1971). Superoxide dismutase: improved assays and an assay applicable to acrylamide gels. Anal. Biochem. *44*, 276–287.

Bellomo, G., Palladini, G., and Vairetti, M. (1997). Intranuclear distribution, function and fate of glutathione and glutathione-S-conjugate in living rat hepatocytes studied by fluorescence microscopy. Microsc. Res. Tech. *36*, 243–252.

Caprariello, A.V., Mangla, S., Miller, R.H., and Selkirk, S.M. (2012). Apoptosis of oligodendrocytes in the central nervous system results in rapid focal demyelination. Ann. Neurol. *72*, 395–405.

Cargill, R.S., and Thibault, L.E. (1996). Acute alterations in [Ca2+] i in NG108-15 cells subjected to high strain rate deformation and chemical hypoxia: an in vitro model for neural trauma. J. Neurotrauma *13*, 395–407.

Cornelius, C., Crupi, R., Calabrese, V., Graziano, A., Milone, P., Pennisi, G., Radak, Z., Calabrese, E.J., and Cuzzocrea, S. (2013).

Traumatic Brain Injury: Oxidative Stress and Neuroprotection. Antioxid. Redox Signal. *19*, 836–853.

Cui, Y., Hameed, F.M., Yang, B., Lee, K., Pan, C.Q., Park, S., and Sheetz, M. (2015). Cyclic stretching of soft substrates induces spreading and growth. Nat. Commun. *6*, 6333.

Dalle-Donne, I., Rossi, R., Colombo, R., Giustarini, D., and Milzani, A. (2006). Biomarkers of oxidative damage in human disease. Clin. Chem. *52*, 601–623.

Darvish, K.K., and Crandall, J.R. (2001). Nonlinear viscoelastic effects in oscillatory shear deformation of brain tissue. Med. Eng. Phys. *23*, 633–645.

Durackova, Z. (2010). Some current insights into oxidative stress. Physiol. Res. *59*, 459.

Ellis, E.F., McKinney, J.S., Willoughby, K.A., Liang, S., and Povlishock, J.T. (1995). A new model for rapid stretch-induced injury of cells in culture: characterization of the model using astrocytes. J. Neurotrauma *12*, 325–339.

Ellis, E.F., Willoughby, K.A., Sparks, S.A., and Chen, T. (2007). S100B protein is released from rat neonatal neurons, astrocytes, and microglia by *in vitro* trauma and anti-S100 increases trauma-induced delayed neuronal injury and negates the protective effect of exogenous S100B on neurons: Endogenous S100B and brain cell injury. J. Neurochem. *101*, 1463–1470.

Feutz, A.C., Bellomi, I., Allinquant, B., Schladenhaufen, Y., and Ghandour, M.S. (1995). Isolation and characterization of defective jimpy oligodendrocytes in culture. J. Neurocytol. *24*, 865–877.

Feutz, A.C., Pham-Dinh, D., Allinquant, B., Miehe, M., and Ghandour, M.S. (2001). An immortalized jimpy oligodendrocyte cell line: defects in cell cycle and cAMP pathway. Glia *34*, 241–252.

Flygt, J., Djupsjö, A., Lenne, F., and Marklund, N. (2013). Myelin loss and oligodendrocyte pathology in white matter tracts following traumatic brain injury in the rat. Eur. J. Neurosci. *38*, 2153–2165.

Flygt, J., Gumucio, A., Ingelsson, M., Skoglund, K., Holm, J., Alafuzoff, I., and Marklund, N. (2016). Human Traumatic Brain Injury Results in Oligodendrocyte Death and Increases the Number of Oligodendrocyte Progenitor Cells. J. Neuropathol. Exp. Neurol. *75*, 503–515.

French, H.M., Reid, M., Mamontov, P., Simmons, R.A., and Grinspan, J.B. (2009). Oxidative stress disrupts oligodendrocyte maturation. J. Neurosci. Res. *87*, 3076–3087.

Geddes-Klein, D.M., Schiffman, K.B., and Meaney, D.F. (2006). Mechanisms and consequences of neuronal stretch injury in vitro differ with the model of trauma. J. Neurotrauma *23*, 193–204.

Ghandour, M.S., Feutz, A.-C., Jalabi, W., Taleb, O., Bessert, D., Cypher, M., Carlock, L., and Skoff, R.P. (2002). Trafficking of PLP/DM20 and cAMP signaling in immortalized jimpy oligodendrocytes. Glia *40*, 300–311.

Gladman, S.J., Ward, R.E., Michael-Titus, A.T., Knight, M.M., and Priestley, J.V. (2010). The effect of mechanical strain or hypoxia on cell death in subpopulations of rat dorsal root ganglion neurons in vitro. Neuroscience *171*, 577–587.

Gladman, S.J., Huang, W., Lim, S.-N., Dyall, S.C., Boddy, S., Kang, J.X., Knight, M.M., Priestley, J.V., and Michael-Titus, A.T. (2012). Improved Outcome after Peripheral Nerve Injury in Mice with Increased Levels of Endogenous Omega-3 Polyunsaturated Fatty Acids. J. Neurosci. *32*, 563–571.

Greer, J.M. (2013). Autoimmune T-cell reactivity to myelin proteolipids and glycolipids in multiple sclerosis. Mult. Scler. Int. *2013*, 151427.

Hernandez, M., Patzig, J., Mayoral, S.R., Costa, K.D., Chan, J.R., and Casaccia, P. (2016). Mechanostimulation Promotes Nuclear and Epigenetic Changes in Oligodendrocytes. J. Neurosci. *36*, 806–813.

Herrera, J.J., Bockhorst, K.H., Kondraganti, S., Stertz, L., DeQuevedo, J.L., and Narayana, P.A. (2016). Acute white matter tract damage following frontal mild traumatic brain injury. J. Neurotrauma.

Hoefen, R.J., and Berk, B.C. (2002). The role of MAP kinases in endothelial activation. Vascul. Pharmacol. *38*, 271–273.

Hsu, H.-J., Lee, C.-F., Locke, A., Vanderzyl, S.Q., and Kaunas, R. (2010). Stretch-Induced Stress Fiber Remodeling and the Activations of JNK and ERK Depend on Mechanical Strain Rate, but Not FAK. PLoS ONE *5*, e12470.

Hu, M.L. (1994). Measurement of protein thiol groups and glutathione in plasma. Methods Enzymol. *233*, 380–385.

Jackman, N., Ishii, A., and Bansal, R. (2009). Oligodendrocyte development and myelin biogenesis: parsing out the roles of glycosphingolipids. Physiol. Bethesda Md *24*, 290–297.

Jagielska, A., Norman, A.L., Whyte, G., Vliet, K.J.V., Guck, J., and Franklin, R.J.M. (2012). Mechanical Environment Modulates Biological Properties of Oligodendrocyte Progenitor Cells. Stem Cells Dev. *21*, 2905–2914.

Jain, A.K. (2005). Nuclear Import and Export Signals in Control of Nrf2. J. Biol. Chem. *280*, 29158–29168.

Johnson, V.E., Stewart, J.E., Begbie, F.D., Trojanowski, J.Q., Smith, D.H., and Stewart, W. (2013). Inflammation and white matter degeneration persist for years after a single traumatic brain injury. Brain *136*, 28–42.

Kim, J., Avants, B., Patel, S., Whyte, J., Coslett, B.H., Pluta, J., Detre, J.A., and Gee, J.C. (2008). Structural consequences of diffuse traumatic brain injury: a large deformation tensor-based morphometry study. NeuroImage *39*, 1014–1026.

Kyriakis, J.M., and Avruch, J. (2012). Mammalian MAPK Signal Transduction Pathways Activated by Stress and Inflammation: A 10-Year Update. Physiol. Rev. *92*, 689–737.

Lourenço, T., Paes de Faria, J., Bippes, C.A., Maia, J., Lopes-da-Silva, J.A., Relvas, J.B., and Grãos, M. (2016). Modulation of oligodendrocyte differentiation and maturation by combined biochemical and mechanical cues. Sci. Rep. *6*, 21563.

Lozano, D., Gonzales-Portillo, G.S., Acosta, S., de la Pena, I., Tajiri, N., Kaneko, Y., and Borlongan, C.V. (2015). Neuroinflammatory responses to traumatic brain injury: etiology, clinical consequences, and therapeutic opportunities. Neuropsychiatr. Dis. Treat. *11*, 97–106.

Margulies, S.S., Thibault, L.E., and Gennarelli, T.A. (1990). Physical model simulations of brain injury in the primate. J. Biomech. *23*, 823–836.

Martineau, L.C., and Gardiner, P.F. (2001). Insight into skeletal muscle mechanotransduction: MAPK activation is quantitatively related to tension. J. Appl. Physiol. *91*, 693–702.

McKinney, J.S., Willoughby, K.A., Liang, S., and Ellis, E.F. (1996). Stretch-induced injury of cultured neuronal, glial, and endothelial cells. Effect of polyethylene glycol-conjugated superoxide dismutase. Stroke J. Cereb. Circ. *27*, 934–940.

Meaney, D.F., Smith, D.H., Shreiber, D.I., Bain, A.C., Miller, R.T., Ross, D.T., and Gennarelli, T.A. (1995). Biomechanical analysis of experimental diffuse axonal injury. J. Neurotrauma *12*, 689–694.

Meffre, D., Massaad, C., and Grenier, J. (2015). Lithium chloride stimulates PLP and MBP expression in oligodendrocytes via Wnt/β-catenin and Akt/CREB pathways. Neuroscience *284*, 962–971.

Mendes Arent, A., Souza, L.F. de, Walz, R., and Dafre, A.L. (2014). Perspectives on Molecular Biomarkers of Oxidative Stress and Antioxidant Strategies in Traumatic Brain Injury. BioMed Res. Int. *2014*, 1–18.

Morrison, B., Cater, H.L., Benham, C.D., and Sundstrom, L.E. (2006). An in vitro model of traumatic brain injury utilising two-dimensional stretch of organotypic hippocampal slice cultures. J. Neurosci. Methods *150*, 192–201.

Morrison, B., Elkin, B.S., Dollé, J.-P., and Yarmush, M.L. (2011). In vitro models of traumatic brain injury. Annu. Rev. Biomed. Eng. *13*, 91–126.

Neary, J.T., Kang, Y., Willoughby, K.A., and Ellis, E.F. (2003). Activation of extracellular signal-regulated kinase by stretch-induced injury in astrocytes involves extracellular ATP and P2 purinergic receptors. J. Neurosci. *23*, 2348–2356.

Owens, D.M., and Keyse, S.M. (2007). Differential regulation of MAP kinase signalling by dual-specificity protein phosphatases. Oncogene *26*, 3203–3213.

Owuor, E.D., and Kong, A.-N.T. (2002). Antioxidants and oxidants regulated signal transduction pathways. Biochem. Pharmacol. *64*, 765–770.

Pearson, G., Robinson, F., Beers Gibson, T., Xu, B.E., Karandikar, M., Berman, K., and Cobb, M.H. (2001). Mitogen-activated protein (MAP) kinase pathways: regulation and physiological functions. Endocr. Rev. *22*, 153–183.

Reznick, A.Z., and Packer, L. (1994). Oxidative damage to proteins: spectrophotometric method for carbonyl assay. Methods Enzymol. *233*, 357–363.

Ritt, D.A., Abreu-Blanco, M.T., Bindu, L., Durrant, D.E., Zhou, M., Specht, S.I., Stephen, A.G., Holderfield, M., and Morrison, D.K. (2016). Inhibition of Ras/Raf/MEK/ERK Pathway Signaling by a Stress-Induced Phospho-Regulatory Circuit. Mol. Cell *64*, 875–887.

Rodríguez-Rodríguez, A., Egea-Guerrero, J.J., Murillo-Cabezas, F., and Carrillo-Vico, A. (2014). Oxidative stress in traumatic brain injury. Curr. Med. Chem. *21*, 1201–1211.

Rosenberg, S.S., Kelland, E.E., Tokar, E., Asia, R., and Chan, J.R. (2008). The geometric and spatial constraints of the microenvironment induce oligodendrocyte differentiation. Proc. Natl. Acad. Sci. *105*, 14662–14667.

Rothe, G., and Valet, G. (1990). Flow cytometric analysis of respiratory burst activity in phagocytes with hydroethidine and 2',7'-dichlorofluorescin. J. Leukoc. Biol. *47*, 440–448.

Salvador, E., Neuhaus, W., and Foerster, C. (2013). Stretch in brain microvascular endothelial cells (cEND) as an in vitro traumatic brain injury model of the blood brain barrier. J. Vis. Exp. JoVE e50928.

Sidaros, A., Skimminge, A., Liptrot, M.G., Sidaros, K., Engberg, A.W., Herning, M., Paulson, O.B., Jernigan, T.L., and Rostrup, E. (2009). Long-term global and regional brain volume changes following severe traumatic brain injury: a longitudinal study with clinical correlates. NeuroImage *44*, 1–8.

Simons, M., and Nave, K.-A. (2016). Oligodendrocytes: Myelination and Axonal Support. Cold Spring Harb. Perspect. Biol. *8*, a020479.

Sultana, R., Perluigi, M., and Allan Butterfield, D. (2013). Lipid peroxidation triggers neurodegeneration: a redox proteomics view into the Alzheimer disease brain. Free Radic. Biol. Med. *62*, 157–169.

Thorburne, S.K., and Juurlink, B.H. (1996). Low glutathione and high iron govern the susceptibility of oligodendroglial precursors to oxidative stress. J. Neurochem. *67*, 1014–1022.

Tomaiuolo, F., Bivona, U., Lerch, J.P., Di Paola, M., Carlesimo, G.A., Ciurli, P., Matteis, M., Cecchetti, L., Forcina, A., Silvestro, D., et al. (2012). Memory and anatomical change in severe non missile traumatic brain injury: ~1 vs. ~8 years follow-up. Brain Res. Bull. *87*, 373–382.

Tunez, I., Sánchez-López, F., Agüera, E., Fernández-Bolaños, R., Sánchez, F.M., and Tasset-Cuevas, I. (2011). Important role of oxidative stress biomarkers in Huntington's disease. J. Med. Chem. *54*, 5602–5606.

Urbanski, M.M., Kingsbury, L., Moussouros, D., Kassim, I., Mehjabeen, S., Paknejad, N., and Melendez-Vasquez, C.V. (2016). Myelinating glia differentiation is regulated by extracellular matrix elasticity. Sci. Rep. *6*, 33751.

Valko, M., Rhodes, C.J., Moncol, J., Izakovic, M., and Mazur, M. (2006). Free radicals, metals and antioxidants in oxidative stress-induced cancer. Chem. Biol. Interact. *160*, 1–40.

Vande Geest, J.P., Di Martino, E.S., and Vorp, D.A. (2004). An analysis of the complete strain field within Flexercell membranes. J. Biomech. *37*, 1923–1928.

Vezza, T., Rodríguez-Nogales, A., Algieri, F., Utrilla, M., Rodriguez-Cabezas, M., and Galvez, J. (2016). Flavonoids in Inflammatory Bowel Disease: A Review. Nutrients *8*, 211.

Wang, Z., Wu, W., Liu, Y., Wang, T., Chen, X., Zhang, J., Zhou, G., and Chen, R. (2016). Altered Cerebellar White Matter Integrity in Patients with Mild Traumatic Brain Injury in the Acute Stage. PLOS ONE *11*, e0151489.

Witko-Sarsat, V., Friedlander, M., Capeillère-Blandin, C., Nguyen-Khoa, T., Nguyen, A.T., Zingraff, J., Jungers, P., and Descamps-Latscha, B. (1996). Advanced oxidation protein products as a novel marker of oxidative stress in uremia. Kidney Int. *49*, 1304–1313.

Xiong, Y., Mahmood, A., and Chopp, M. (2013). Animal models of traumatic brain injury. Nat. Rev. Neurosci. *14*, 128–142.

Zhang, M., An, C., Gao, Y., Leak, R.K., Chen, J., and Zhang, F. (2013). Emerging roles of Nrf2 and phase II antioxidant enzymes in neuroprotection. Prog. Neurobiol. *100*, 30–47.

Zhou, H., Chen, Q., Kong, D.L., Guo, J., Wang, Q., and Yu, S.Y. (2011). Effect of Resveratrol on Gliotransmitter Levels and p38 Activities in Cultured Astrocytes. Neurochem. Res. *36*, 17–26.

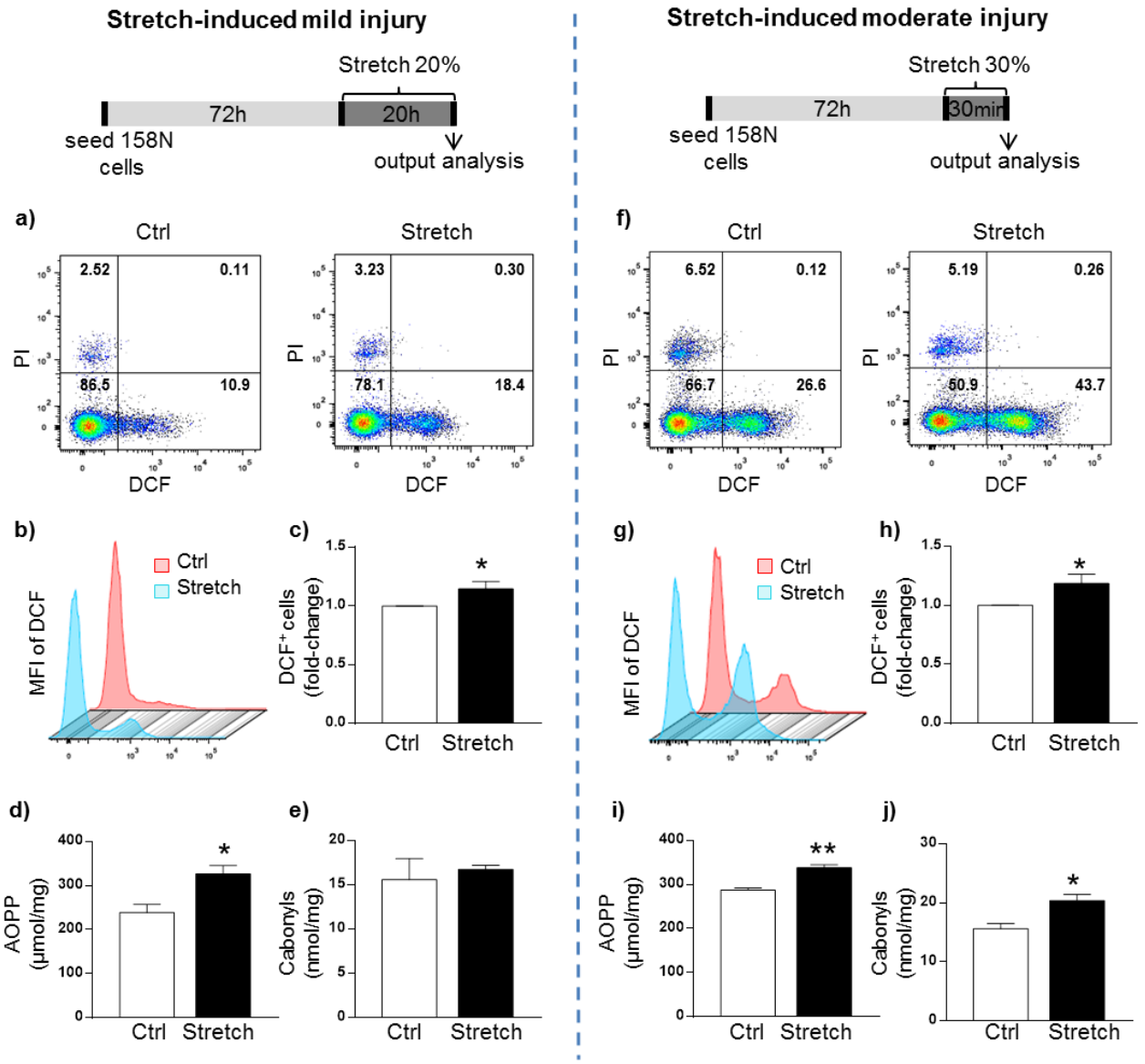

Figure 1: Stretch increased the level of intracellular ROS in 158N cell line in both mild and moderate injury. The intracellular ROS level was detected by DCFH-DA fluorescent probe. Representative pictures of DCF-stained (FITC channel) and PI-stained (PE channel) from control (Ctrl) and stretched (Stretch) cells following mild (a) and moderate (f) injury. Representative picture of the mean fluorescence intensity (MFI) of DCF measured on DCF^+/PI^- cells following mild (b) or moderate (g) injury. Quantitative analysis of the percentage of DCF^+ cells following mild (c) or moderate (h) injury. Results are expressed as the fold change compared to control group. Values are the mean ± SEM of 3 experiments performed in triplicate. AOPP (µmol/l) and carbonyls (nmol/mg) were measured in control (Ctrl) and stretched (Stretch) cells following mild (d , e) or moderate injury (i , j). Results represent the mean ± SEM (n=5). Student's unpaired t-test. *: $p<0.05$; **:$p<0.01$. DCF: 2',7' fluorescent dichlorofluorescein. PI: Propidium Iodide.

Table 1: Effect of stretch on glutathione, enzymes involved in glutathione redox cycle and thiols in 158N cell line after mild and moderate injury

Stretch-induced mild injury			
	Ctrl	**Stretch**	**p value**
GSH (AU)	403.7 ± 9.025	363.3 ± 4.410	0.0159 (*)
GSSH	nd	nd	
GPx (U/mg)	0.392 ± 0.039	0.216 ± 0,024	0.0020 (**)
GRx (U/mg)	0.018 ± 0.005	0.050 ± 0.020	0.1408
Thiols (µmol/mg)	475.9 ± 48.35	452.9 ± 24.53	0.6772
Stretch-induced moderate injury			
GSH (AU)	422.7 ± 21.11	358.7 ± 11.26	0.0555
GSSH	nd	nd	
GPx (U/mg)	0.310 ± 0.021	0.243 ± 0.014	0.0584
GRx (U/mg)	0.013 ± 0.003	0.030 ± 0.006	0.0668
Thiols (µmol/mg)	512.0 ± 13.20	472.0 ± 13.80	0.1043

Glutathione in reduced (GSH) and oxidized (GSSG) state, glutathione peroxidase (GPx), glutathione reductase (GRx) and thiols were measured in control (Ctrl) and stretched (Stretch) cells following mild or moderate injury. Results represent the mean ± SEM (n=9 for mild and n=3 for moderate). Student's unpaired *t*-test. *: $p<0.05$; **: $p<0.01$. nd: not determined.

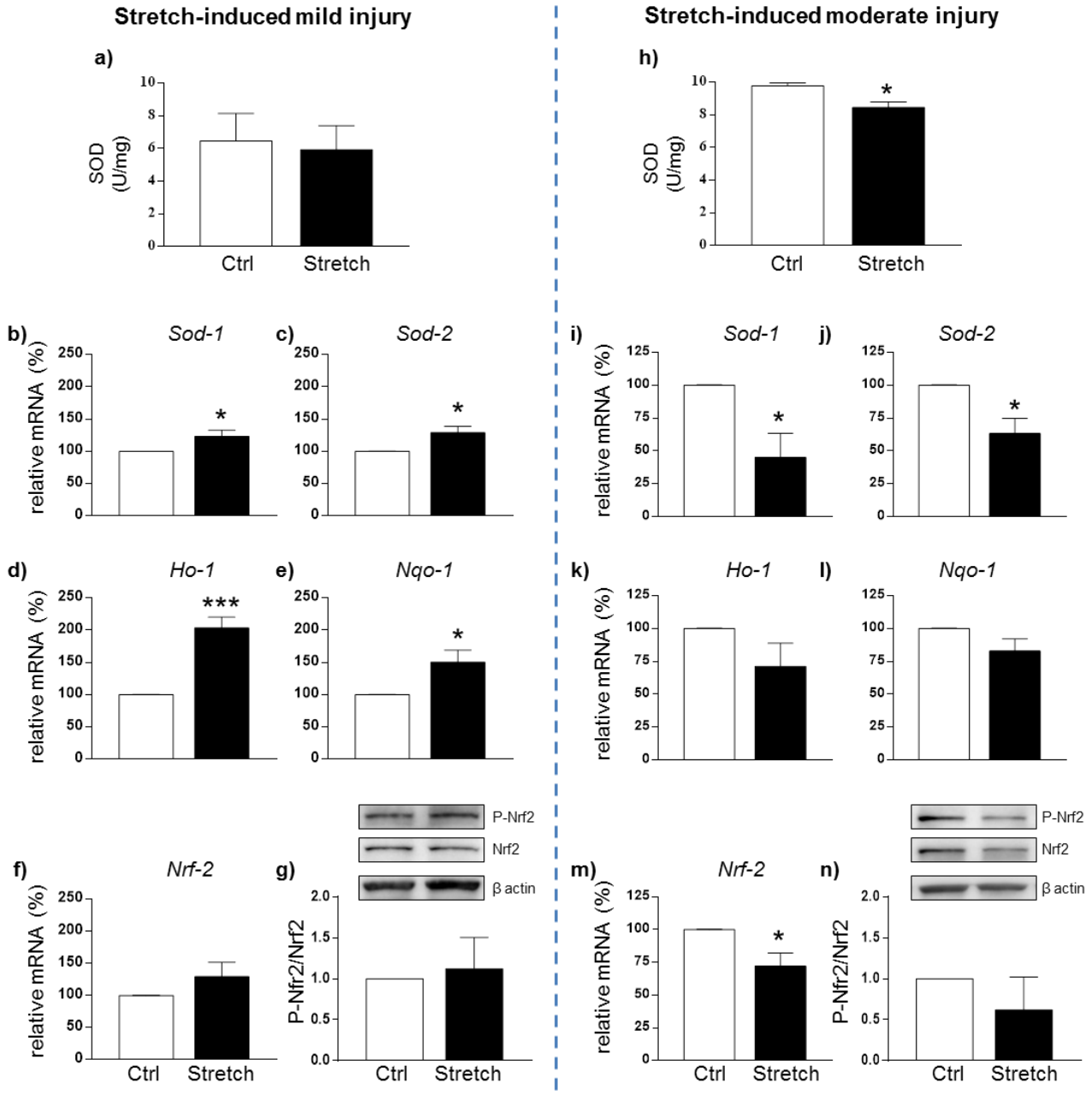

Figure 2: Effect of stretch on different oxidative stress parameters in 158N cell line after mild and moderate injury. SOD was measured in control (Ctrl) and stretched (Stretch) cells following mild (a) or moderate (h) injury. Results represent the mean ± SEM (n=5). RNA was extracted and RT-qPCR was performed in control (Ctrl) and stretched (Stretch) cells following mild and moderate injury for the antioxidant genes *Sod-1* (b , i), *Sod-2* (c , j), *Ho-1*(d , k), *Nqo-1* (e , l), *Nrf-2* (f , m). Proteins were extracted after stretch from control (Ctrl) and stretched (Stretch) cells and western blot was performed for the transcriptional factor Nfr2 following mild (g) or moderate (n) injury. The ratio P-Nrf2 (100 kDa) on total Nrf2 (68 kDa) is presented. Results represent the mean±SEM of 3 independent experiments performed in triplicate. Student's unpaired *t*-test. *: p<0.05; ***: p<0.001.

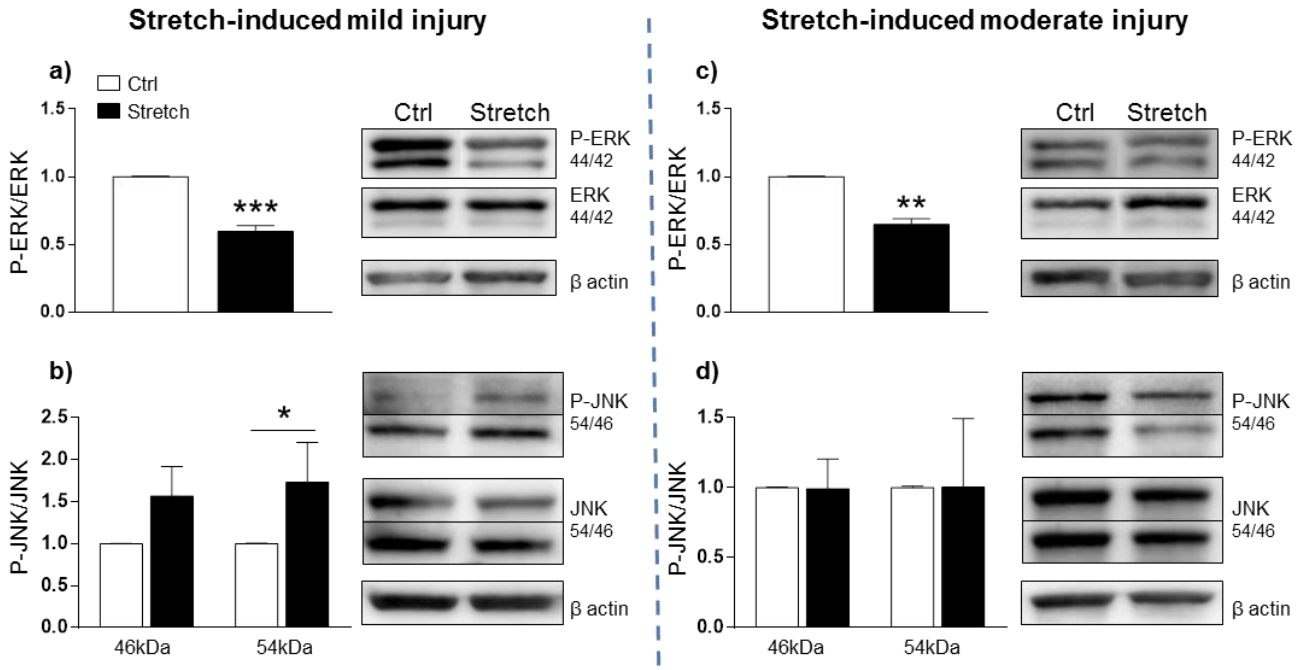

Figure 3: Evaluation of the stretch effect on the amount of the MAP kinases ERK1/2 and JNKs in 158N cell line after mild and moderate injury. Proteins were extracted after stretch from control (Ctrl) and stretched (Stretch) cells and western blot was performed for ERK1/2 (a, c) or JNKs (b, d). β-actin (47kDa) was used as loading control. The ratio P-ERK on total ERK is presented following mild (a) or moderate (c) injury. The ratio P-JNK on total JNK is presented following mild (b) or moderate (d) injury for the isoforms 54 and 46 kDa. Results represent the mean±SEM of three independent experiments. Student's unpaired *t*-test. *: p<0.05; **: p<0.01; ***: p<0.001.

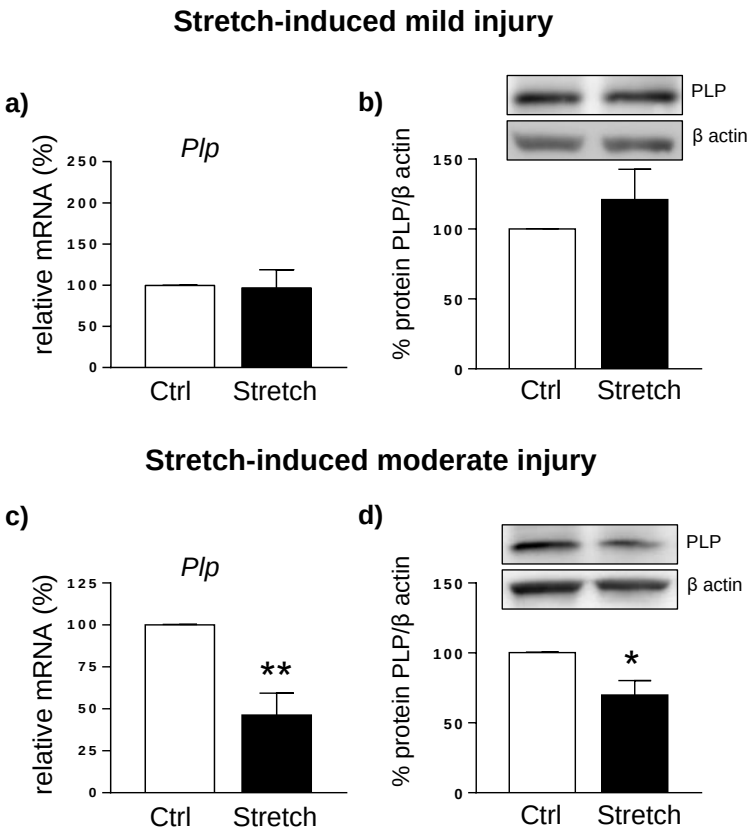

Figure 4: Evaluation of the stretch effect on PLP myelin gene and protein expression in 158N cell line after mild and moderate injury. RNA was extracted and RT-qPCR was performed in control (Ctrl) and stretched (Stretch) cells following mild and moderate injury for the myelin gene *Plp* (a, c). Results represent the mean±SEM of 4-7 independent experiments performed in triplicate. Proteins were extracted after stretch from control (Ctrl) and stretched (Stretch) cells and western blot was performed for the myelin protein PLP (26kDa) following mild (b) or moderate (d) injury. β-actin (47kDa) was used as loading control. Results represent the mean±SEM of three independent experiments. Student's unpaired *t*-test. *: p<0.05; **: p<0.01.

→**Figure 5: Effect of stretch on oligodendrocyte morphology, cell adherence and myelin gene expression in oligodendrocyte-enriched primary culture after mild injury.** (a) Immunostaining of mature oligodendrocytes (MAG in green), their precursors (PDGFR-α in red) and nuclei (Hoechst in blue) was performed in control (Ctrl) and stretched (Stretch) cells following mild injury. Scale bar: 100 µm. (b) Quantitative analysis of the number of Hoechst$^+$ cells per field (0,26 nm^2). (c) Quantitative analysis of the area of MAG$^+$ cells. (d) Quantitative analysis of the area of PDGFR-α$^+$ cells. (e) Quantitative analysis of the percentage of MAG$^+$ and PDGFR-α$^+$ cells. RNA was extracted and RT-qPCR was performed in control (Ctrl) and stretched (Stretch) cells following mild injury for the myelin genes as *Mag* (f), *Plp* (g) and *Cnp* (h). Results represent the mean±SEM of three independent experiments performed in triplicate. Student's unpaired *t*-test. *: p<0.05; ***p < 0.001. DIV: days *in vitro.*

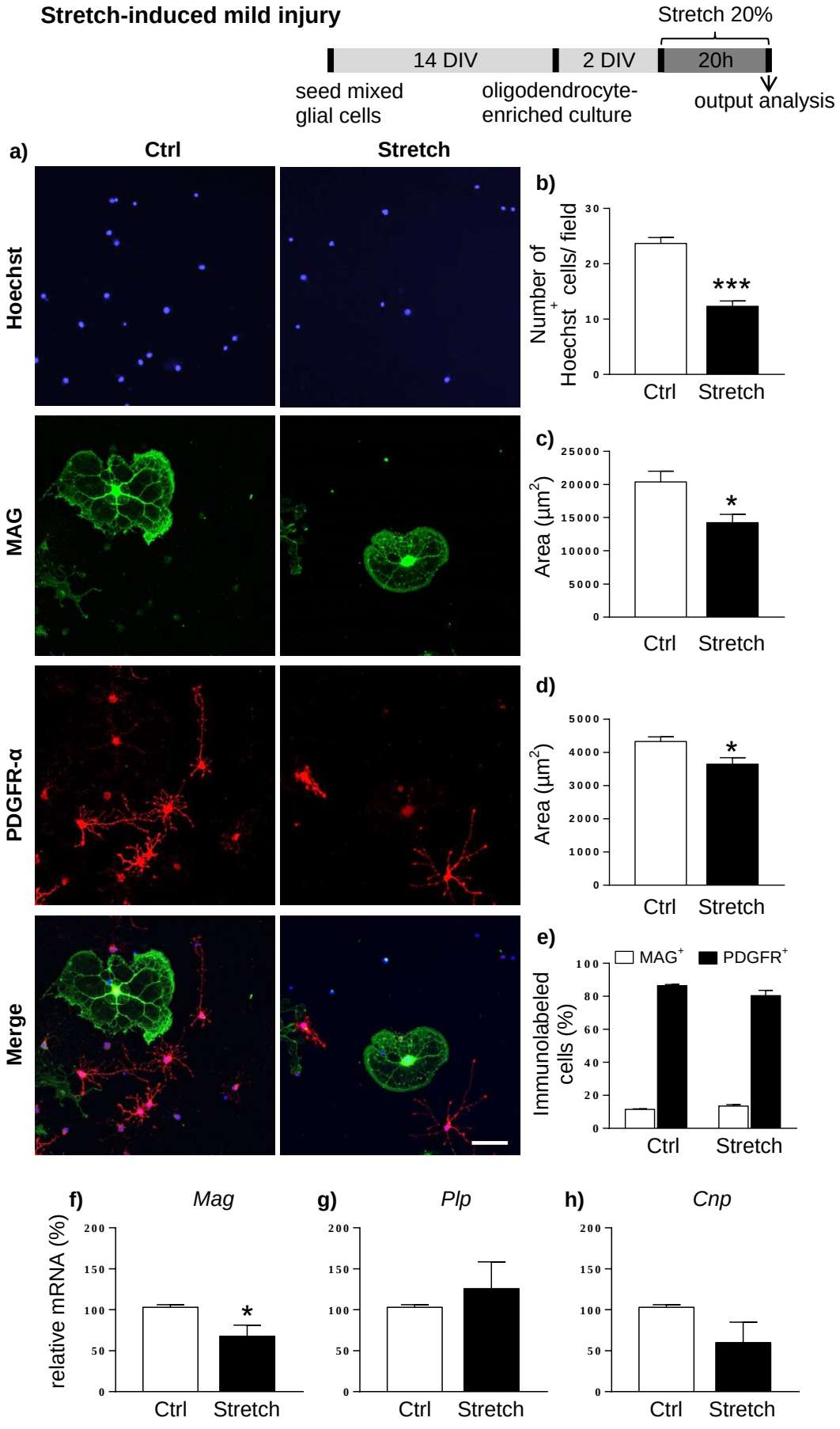
Stretch-induced mild injury
Stretch 20%
14 DIV
2 DIV
20h
seed mixed glial cells
oligodendrocyte-enriched culture
output analysis
a)
Ctrl
Stretch
Hoechst
MAG
PDGFR-α
Merge
b)
Number of Hoechst+ cells/ field
***
Ctrl
Stretch
c)
Area (µm2)
*
d)
e)
MAG+
PDGFR+
Immunolabeled cells (%)
f)
Mag
relative mRNA (%)
g)
Plp
h)
Cnp

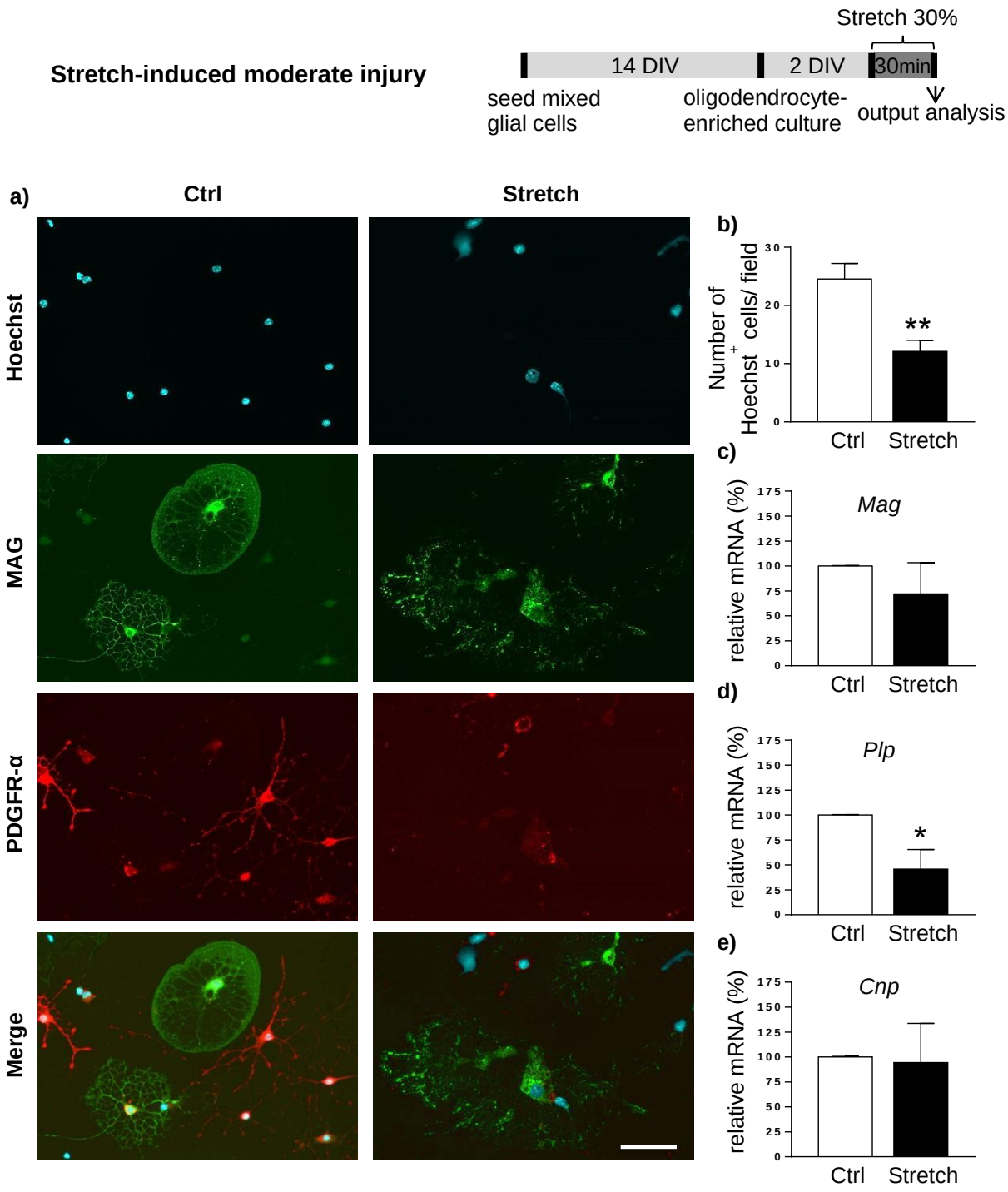

Figure 6: Effect of stretch on oligodendrocyte morphology, cell adherence and myelin gene expression in oligodendrocyte-enriched primary culture after moderate injury. (a) Immunostaining of mature oligodendrocytes (MAG in green), their precursors (PDGFR-α in red) and nuclei (Hoechst in blue) in control (Ctrl) and stretched (Stretch) cells following moderate injury. Scale bar: 100 µm. (b) Quantitative analysis of the number of Hoechst$^+$ cells per field (0,26 nm^2). RNA was extracted and RT-qPCR was performed in control (Ctrl) and stretched (Stretch) cells following moderate injury for the myelin genes as *Mag* (c), *Plp* (d) and *Cnp* (e). Results represent the mean±SEM of three independent experiments performed in triplicate. Student's unpaired *t*-test. *: p<0.05; **p < 0.01. DIV: days *in vitro.*

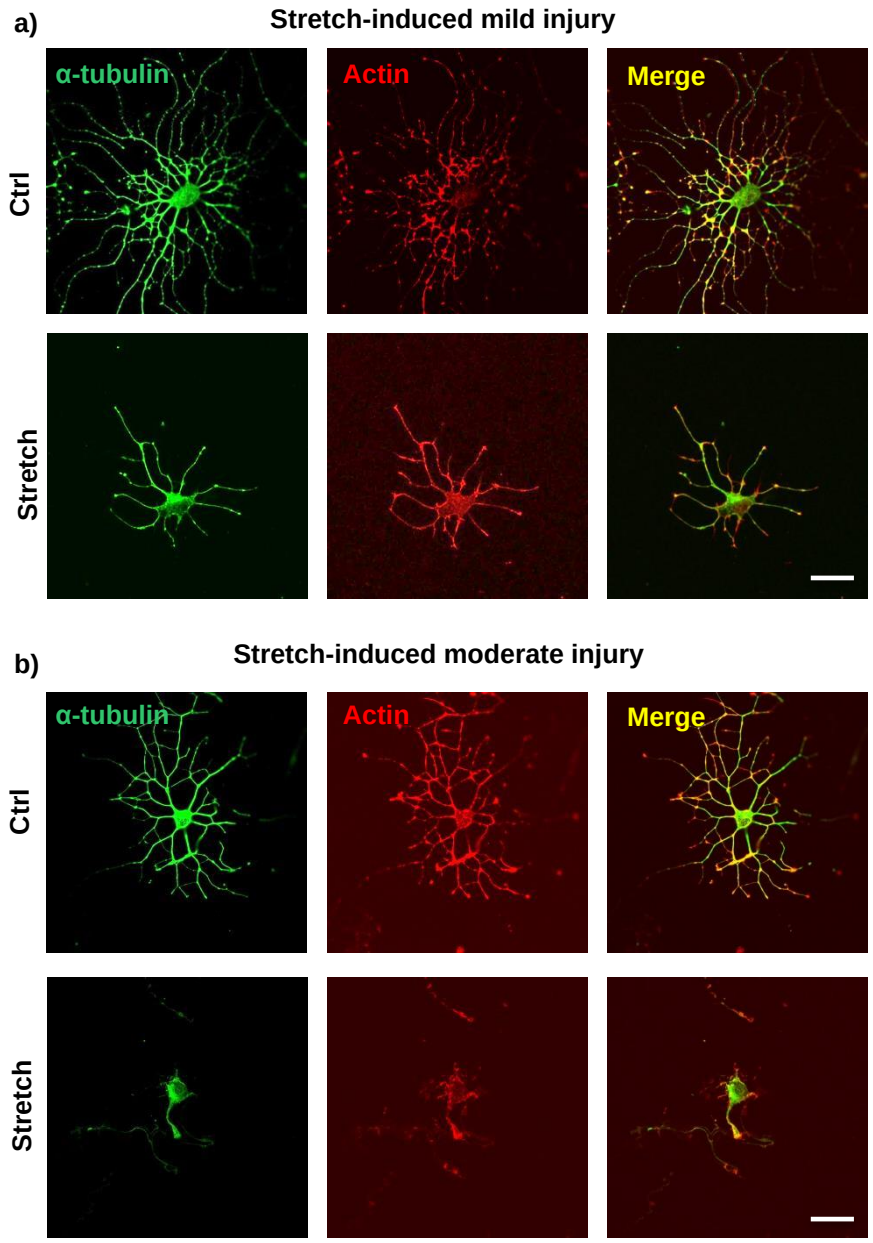

Figure S1: Effect of stretch on the morphology of oligodendrocytes from oligodendrocyte-enriched primary culture after mild and moderate injury. Double immunostaining of α-tubulin (green) and actin (red) in oligodendrocyte-enriched primary culture from control (Ctrl) and stretched (Stretch) cells following mild (a) and moderate (b) injury . Scale bar: 20µm.

Supplementary data to Article 1

Some results, obtained on 158N cell line and oligodendrocyte-enriched primary cell culture, are not included in the article 1, but they will be presented below as complementary data.

3. Cellular and molecular responses of 158N cell line to stretch-induced mild and moderate injury

3.1 Evaluation of the stretch effect on the expression of the pro-oxidant gene Duox-1

Given the increased ROS production and the alterations of the cellular redox status observed following mild and moderate stretch (**Article 1, Fig. 1 and 2**), we decided to investigate on the source of these ROS. As part of pro-oxidant systems, the expression of *Duox-1* gene, member of the NOX/DUOX family of NADPH oxidases, was tested at the mRNA level. These enzymes transfer electrons across the biological membrane and they generate ROS.

After mild injury the expression of *Duox-1* gene was increased by 70% in the stretch condition ($p<0.01$) (**Fig. 41a**), while after moderate injury it was not significantly affected (**Fig. 41b**). The expression of other members of NADPH oxidases family was also tested (*Nox-1, Nox-2, Nox-3, Nox-4)* but they were not detectable in our system by RT-qPCR.

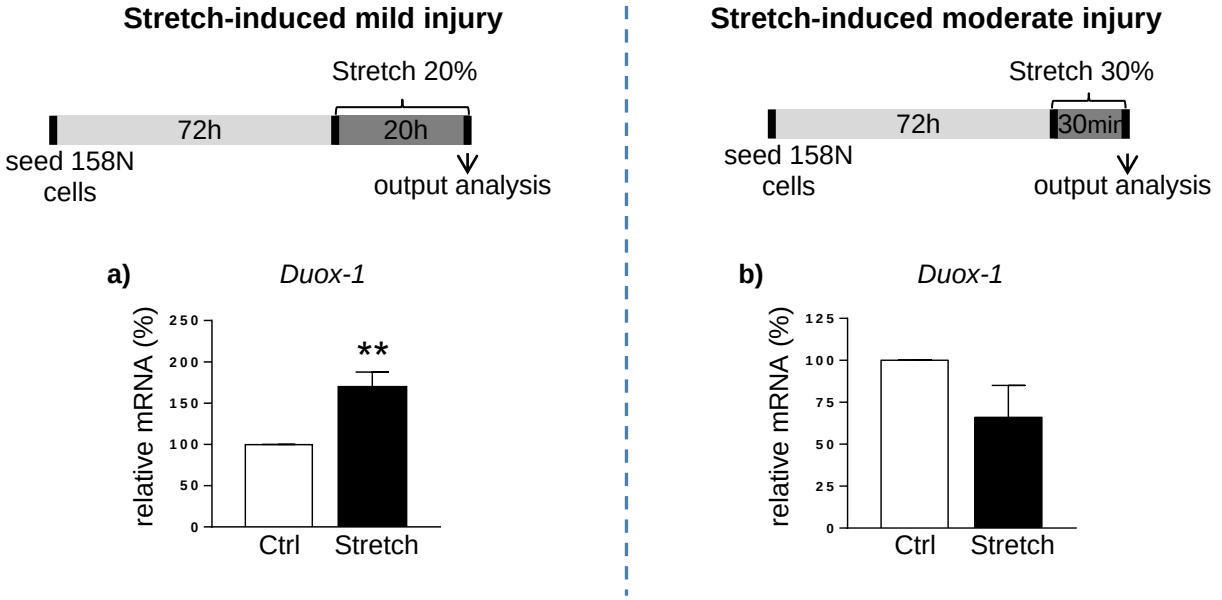

Figure 41: Evaluation of the stretch effect on the expression of the pro-oxidant gene *Duox-1* in 158N cell line at time 0h post-stretch. RNA was extracted and RT-qPCR was performed in control (Ctrl) and stretched (Stretch) cells for the pro-oxidant gene *Duox-1* following mild (a) and moderate (b) injury. Results represent the mean±SEM of 5-8 independent experiments performed in triplicate. Student's unpaired *t*-test. **: $p<0.01$.

3.2 Evaluation of the stretch effect on the expression of the myelin genes Mag and Cnp

In the article 1, the analysis for PLP expression at both mRNA and protein level revealed a marked decrease following moderate injury (**Article 1, Fig.3**). Complementary to these results, the expression of two other myelin genes, *Mag* and *Cnp,* was assessed at mRNA level. The mild injury resulted in an increase in the expression of both genes, *Mag* (+400%, p<0.05) and *Cnp* (+95%, p<0.01), compared to control (**Fig. 42a, b**). The moderate injury, instead, did not significantly affect *Mag* and *Cnp,* even if they showed a tendency to decrease (**Fig. 42c, d**). We were not able to confirm these results by WB, since MAG and CNP proteins are not detectable in 158N cell line in our experimental conditions. Probably the mild injury, lasting for 20h, stimulates the synthesis of new myelin proteins resulting in an increase of *Mag* and *Cnp* expression. The moderate injury instead is more severe and it seems to decrease *Mag* and *Cnp* expression that is in line with PLP results.

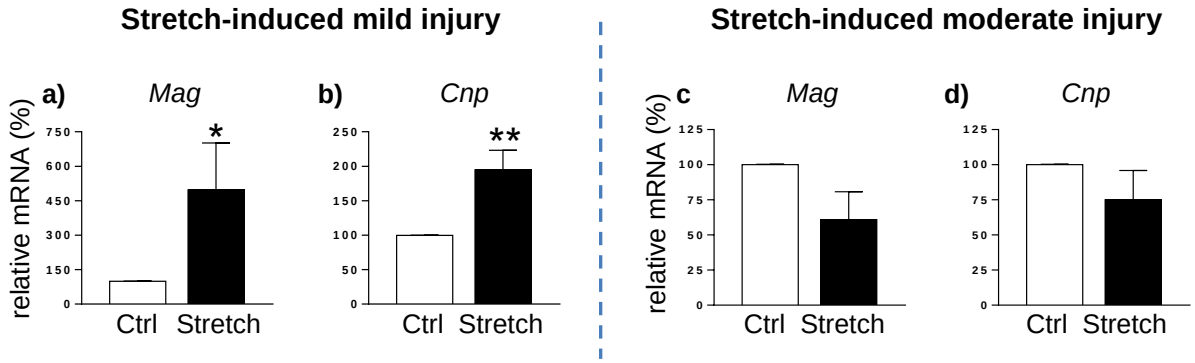

Figure 42: Evaluation of the stretch effect on the expression of the myelin genes *Mag* and *Cnp* in 158N cell line at time 0h post-stretch. RNA was extracted and RT-qPCR was performed in control (Ctrl) and stretched (Stretch) following mild and moderate injury for the myelin genes *Mag* (a,c) and *Cnp* (b,d). Results represent the mean±SEM of 5-8 independent experiments performed in triplicate. Student's unpaired *t*-test. *: p<0.05; **: p<0.01.

3.3 Evaluation of the stretch effect on the myelin protein PLP at 24h post-stretch

The effect of stretch on PLP was assessed immediately after the stretch (time 0h) as reported in the article 1 showing that PLP was decreased following moderate injury only (**Article 1, Fig. 4**). To complete this analysis, the effect of stretch on PLP was also evaluated 24h after the end of the stretch (time 24h) and the protein was still not affected after mild injury (**Fig. 43a**) and was restored to normal level after moderate injury (**Fig. 43b**). This period of time (24h) seems to be enough for this cellular model to restore PLP to normal level.

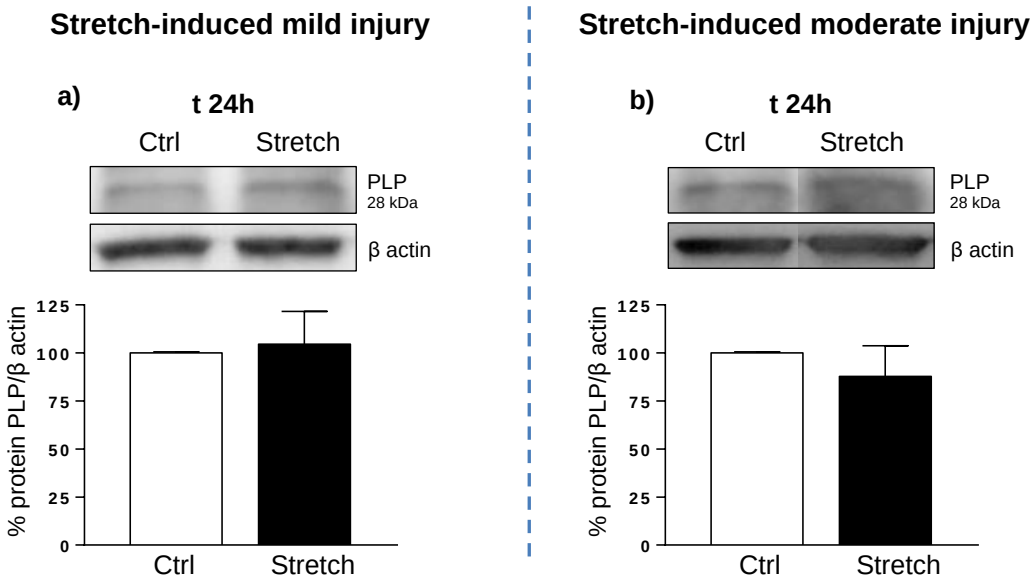

Figure 43: Evaluation of the stretch effect on the myelin protein PLP in 158N cell line at time 24h post-stretch. Proteins were extracted from control (Ctrl) and stretched (Stretch) cells following mild (a) and moderate (b) injury and western blot was performed for the myelin protein PLP. β-actin was used as loading control. Results represent the mean±SEM of three independent experiments. Student's unpaired *t*-test.

3.4 Evaluation of the stretch effect on the expression of the pro-/antioxidant and myelin genes at 24h after stretch-induced mild injury

As reported in the article 1 and in the supplementary data (§ 3.1), the expression of the pro-oxidant gene *Duox-1*, the antioxidant genes *Sod-1, Sod-2, Nrf-2, Ho-1* and *Nqo-1* and the myelin genes *Plp, Mag,* and *Cnp* was assessed immediately after the stretch (time 0h) reporting an alteration in the mRNA levels for both mild and moderate injury (**Article 1, Fig. 2 and 3** and **Fig. 41**).

In order to complete this analysis, the effect of stretch following mild injury was also assessed on the expression of all these genes 24h after the end of the stretch (time 24h). The expression of the pro/antioxidant genes was back to normal level, except for *Ho-1* that was significantly decreased (-20%, $p<0.05$). The myelin genes were also back to normal levels except for *Cnp* that was significantly decreased (-30%, $p<0.001$), results are summarized in the ***Table 11*** (see also **Fig. 44**).

The analysis at time 24h was not performed following the moderate injury, given that the expression of almost all genes analyzed was back to normal after mild injury at late time point 24h.

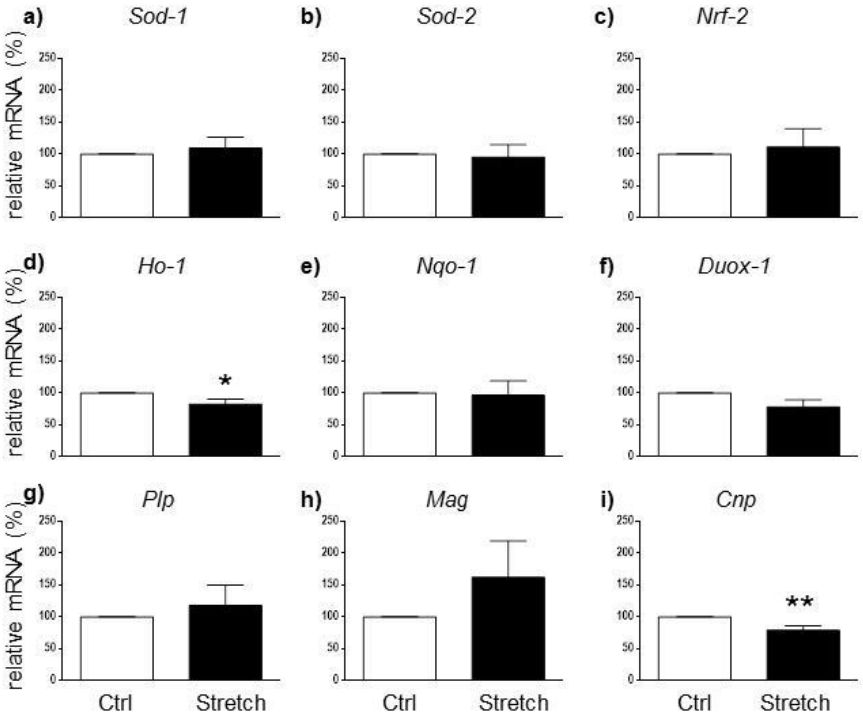

Figure 44: Evaluation of the stretch effect on pro-/antioxidant and myelin gene expression in 158N cell line subjected to stretch-induced mild injury at time 24h post-stretch . RNA was extracted and RT-qPCR was performed in control (Ctrl) and stretched (Stretch) cells for the antioxidant genes *Sod-1, Sod-2, Nrf-2, Ho-1, Nqo-1,* the pro-oxidant gene *Duox-1* and the myelin genes *Plp, Mag* and *Cnp*. Results represent the mean±SEM of 4-6 independent experiments performed in triplicate. Student's unpaired *t*-test. *: p<0.05; **: p<0.01.

Stretch-induced mild injury 24h after stretch *versus* control	
Genes	**158N**
Sod-1	=
Sod-2	=
Nrf-2	=
Ho-1	↓20% (*)
Nqo-1	=
Duox-1	=
Plp	=
Mag	=
Cnp	↓30% (**)

Table 11: Table summarizing the stretch effect on pro-oxidant, antioxidant and myelin gene expression in 158N cells subjected to stretch-induced mild injury at time 24h post-stretch . RNA was extracted and RT-qPCR was performed in control and stretched cells for the antioxidant genes *Sod-1, Sod-2, Nrf-2, Ho-1, Nqo-1,* the pro-oxidant gene *Duox-1* and the myelin genes *Plp, Mag* and *Cnp.* The percentage indicated is the percentage of induction (↑) or inhibition (↓) compared to the control condition. Sign of "=" is reported when no significant differences were observed compared to the control condition. Student's unpaired *t*-test was performed and significant differences are reported in brackets. *: p<0.05; **: p<0.01. See Figure 44 for the corresponding histograms.

4. Cellular and molecular responses of oligodendrocyte-enriched primary cell culture to stretch-induced mild and moderate injury

4.1 Effect of stretch on cytoskeleton

This part of the work on oligodendrocyte-enriched primary cell has been performed with the participation of Giulia Cristinziano, student from the European program Unipharma graduates. A double immunostaining for actin and α-tubulin was performed in order to analyse microfilaments and microtubules respectively, as reported in the article 1 (**Article 1, Fig.S1**), showing that the morphology of oligodendrocytes was deeply affected by stretch, in particular after moderate injury, where the cells appeared really damaged.

Thus, to deeply analyse the effect on cytoskeleton, a double immunostaining for actin and vinculin, which label microfilaments and focal adhesion plaques respectively, was also accomplished. Results confirmed that the oligodendrocytes were damaged following moderate injury, with less or even no branches (**Fig. 45**).

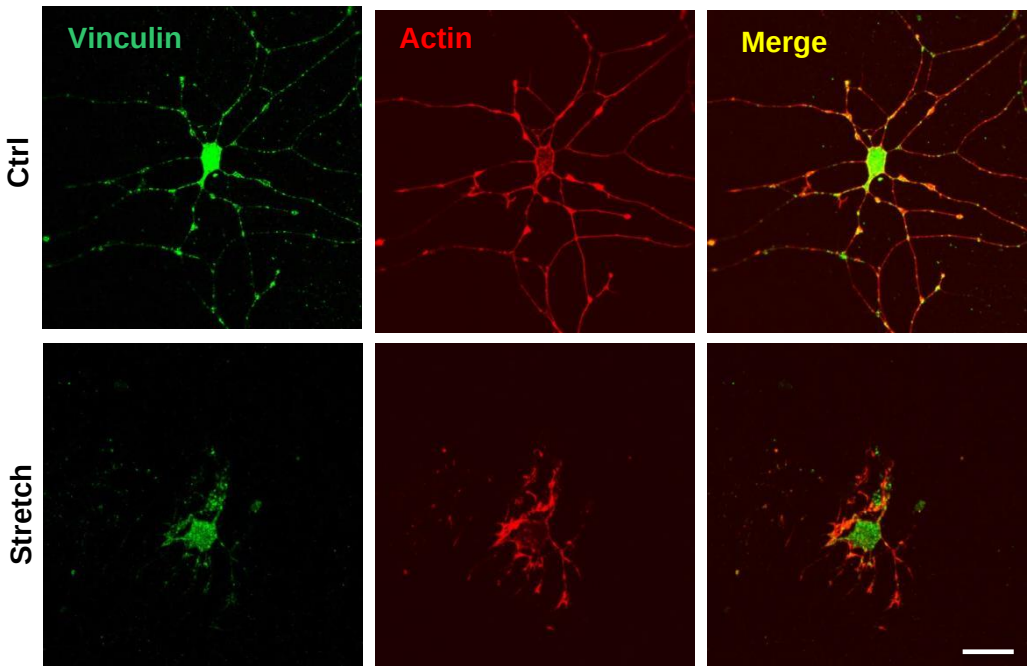

Figure 45: Stretch deeply affects the morphology of primary pure oligodendrocytes after stretch-induced moderate injury at time 0h post-stretch. Double immunostaining of vinculin (green) and actin (red) in oligodendrocyte-enriched primary culture from control (Ctrl) and stretched (Stretch) cells following moderate injury. Scale bar: 20µm.

4.2 Evaluation of stretch-induced mild injury on cellular ramifications in immature oligodendrocytes

Double immunostaining for mature (MAG$^+$) and immature (PDGFR-α$^+$) oligodendrocytes was performed in control and stretched cells following mild injury and less adherent cells were observed in the stretch condition accompanied by a reduced surface for both mature and immature oligodendrocytes (**Article 1, Fig. 5**). Considering the immature oligodendrocytes, PDGFR-α$^+$, a quantification of the number of ramifications was also performed. Cells were divided into three groups on the basis of the number of ramifications: less than 5 (<5), from 5 to 10 (5-10) and more than 10 (>10) ramifications. Results showed no significant differences between the control and the stretch condition, nevertheless there was a tendency to decrease for the intermediate category with 5-10 ramifications (**Fig. 46**). Results are preliminary and need to be confirmed, but in the stretch condition there are fewer cells and the most affected seem to be cells with 5-10 ramifications.

This analysis was not performed following stretch-induced moderate injury because cells are too damaged, with less or even no ramifications.

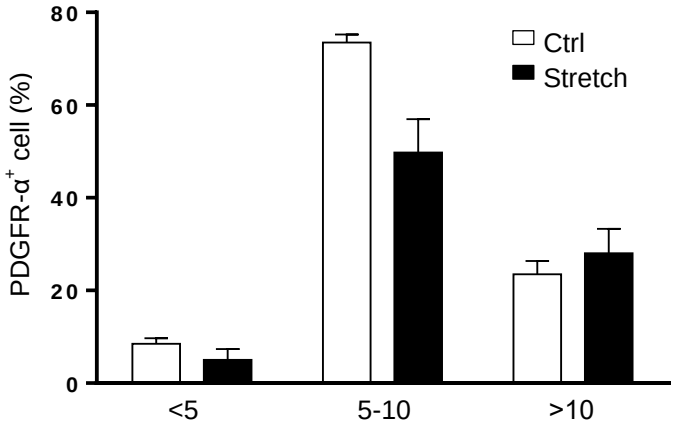

Figure 46: Effect of stretch on the number of ramifications of immature oligodendrocytes (PDGRF-α$^+$ cells) in oligodendrocyte-enriched primary culture after stretch-induced mild injury at time 0h post-stretch. Immunostaining of immature (PDGFR-α$^+$) oligodendrocytes was performed in control (Ctrl) and stretched (Stretch) cells following mild injury. Quantitative analysis of the percentage of PDGFR-α $^+$ cells is reported, cells were divided into three categories of ramifications <5, from 5 to 10, and >10. Results represent the mean±SEM of two experiments, based on the analysis of 15-16 images per condition. One-way ANOVA followed by Bonferroni post-hoc test.

4.3 Evaluation of the stretch effect on cell adherence 24h after stretch

The number of Hoechst$^+$ nuclei is indicative of the number of oligodendrocytes adherent to the silicone membrane, so cell adherence was calculated immediately after the stretch (time 0h) showing a reduction in the number of adherent cells for both mild and moderate injury as reported in the article 1 (**Article 1, Fig. 5 and 6**). The analysis was also performed

24h after the end of the stretch (time 24h) and a decrease in the number of adherent cells was still observed, following both mild (-27%, p<0.05) and moderate injury (-30%, p<0.05) (**Fig. 47**). This suggest that detached cells from the substrate at time 0h are dead, or they undergo cell death in the hours following stretch, since that they do not re-adhere to the silicone membrane.

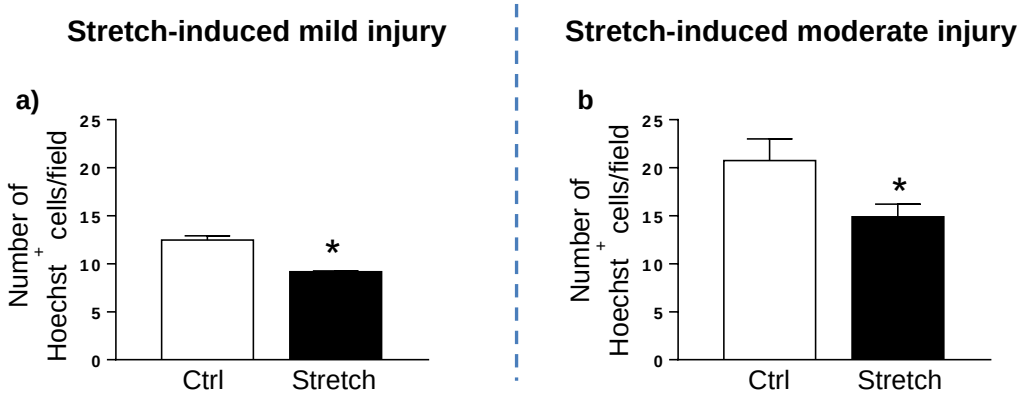

Figure 47: Effect of stretch on oligodendrocyte cell adherence in oligodendrocyte-enriched primary culture after mild and moderate injury at time 24h post-stretch. Quantitative analysis of the number of Hoechst$^+$ nuclei per field (0.26 nm^2) in control (Ctrl) and stretched (Stretch) cells following mild (a) or moderate (b) injury. Results represent the mean±SEM of one (mild) and two (moderate) independent experiments (12 fields analyzed per well, 2 wells per condition). Student's unpaired *t*-test. *: p<0.05.

4.4 Evaluation of the stretch effect on the expression of the antioxidant genes

The expression of the antioxidant genes *Sod-1, Sod-2, Nrf-2, Ho-1* and *Nqo-1* was evaluated in the oligodendrocyte-enriched primary culture after mild and moderate injury. No modifications were observed following mild injury (**Fig. 48**). Following moderate injury, *Sod-2* was reduced by 30% (p<0.0001), *Ho-1* was increased by 35% (p<0.05), while the other genes were not affected (**Fig. 49**). Probably for the mild injury, the stretch is not severe enough to induce an alteration of the antioxidant systems, or the systems are altered but during the 20h of stretch they come back to normal level. The moderate injury is more severe affecting the mitochondrial *Sod-2* and *Ho-1*.

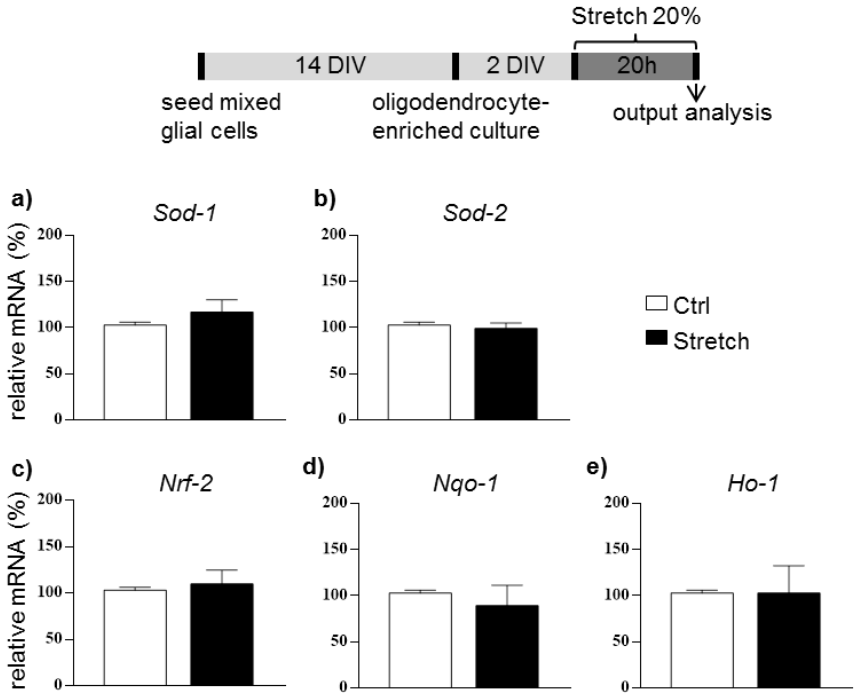

Figure 48: Evaluation of the stretch effect on antioxidant gene expression in oligodendrocyte-enriched primary culture following stretch-induced mild injury at time 0h post-stretch. RNA was extracted and RT-qPCR was performed in control (Ctrl) and stretched (Stretch) cells following mild injury for the antioxidant genes *Sod-1, Sod-2, Nrf-2, Ho-1* and *Nqo-1*. Results represent the mean±SEM of three independent experiments performed in triplicate. Student's unpaired *t*-test. DIV: days *in vitro*.

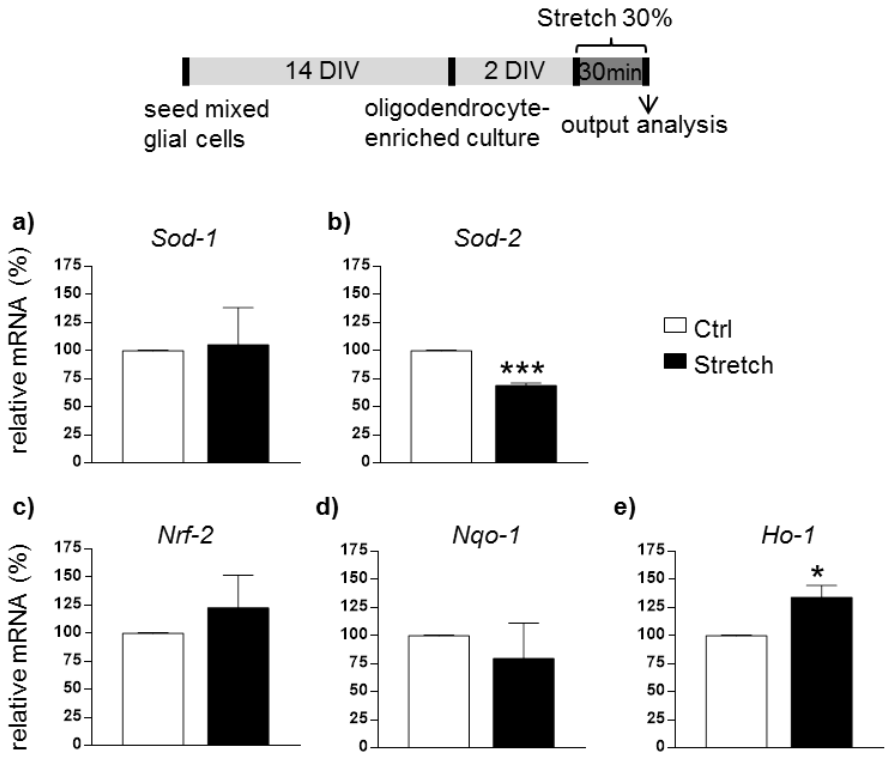

Figure 49: Evaluation of the stretch effect on antioxidant gene expression in oligodendrocyte-enriched primary culture following stretch-induced moderate injury at time 0h post-stretch. RNA was extracted and RT-qPCR was performed in control (Ctrl) and stretched (Stretch) cells following mild injury for the antioxidant genes *Sod-1, Sod-2, Nrf-2, Ho-1* and *Nqo-1*. Results represent the mean±SEM of three independent experiments performed in triplicate. Student's unpaired *t*-test. *: p<0.05; ***p < 0.001. DIV: days *in vitro*.

5. Cellular and molecular responses of mixed glial primary culture to stretch-induced mild injury

Stretch induced-mild injury was also tested on a different cellular model, i.e. the mixed glial primary culture. This culture is composed by a majority of astrocytes growing on a monolayer adherent to the silicone membrane. Oligodendrocytes represent around the 20% of total cells and they grow on the top of astrocytes.

5.1 Stretch did not affect the oligodendrocyte cell adherence within mixed glial culture

In order to analyse the oligodendrocytes in a mixed glial primary culture, $eGFP^+$ cells obtained from PLP-eGFP mice were imaged. The expression of eGFP, under the control of the PLP promoter activity, allowed the visualization of oligodendroglial cells in green under epifluorescent microscope (**Fig. 50a**).

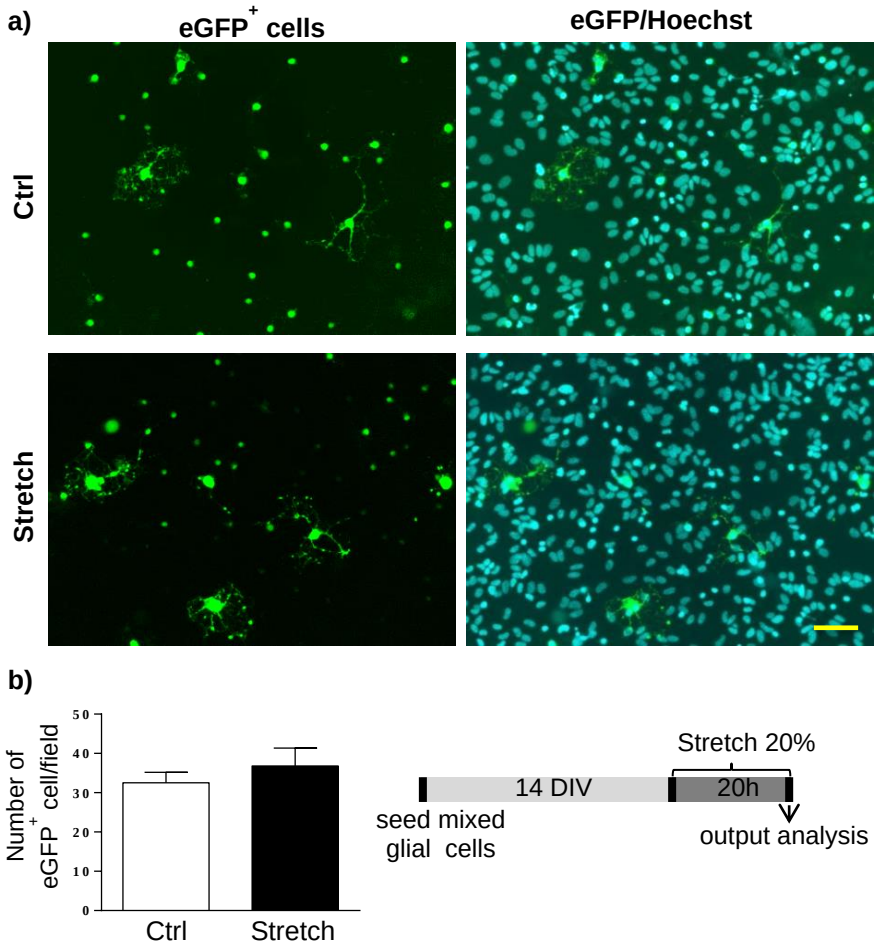

Figure 50: Effect of stretch on oligodendrocyte cell adherence in mixed glial primary culture following stretch-induced mild injury at time 0h post-stretch. Oligodendrocytes were grown on astrocyte layer. Oligodendrocytes from PLP-eGFP mice are visualized in green and Hoechst stained the cell nuclei in blue. (a) Representative images of control (Ctrl) and stretched (Stretch) cells following mild injury. Scale bar: 50µm. (b) Quantitative analysis of the number of $eGFP^+$ cells per field (0.26 nm^2). Results represent the mean±SEM of three independent experiments. Student's unpaired *t*-test.

The cell adherence was calculated immediately after the end of stretch period. The number of Hoechst^{+} nuclei/ eGFP^{+} cells was an indicator of the number of adherent oligodendrocytes and it remained unchanged following stretch (32.5 ± 2.67 cells *versus* 36.8 ± 4.58 cells/field) (**Fig. 50b**).

5.2 Stretch increased the amount of AOPP within mixed glial culture

The oxidant markers, analysed in 158N cell line (**Article 1, Fig.1 and Table 1**), were also analysed in mixed glial culture. Amount of AOPP was significantly increased in stretched cells compared to control group (224.0 ± 5.03 *versus* 250.3 ± 4.63 µmol/mg; $p<0.05$) (**Fig. 51a**). There was also a tendency to increase for carbonyls groups ($p=0.051$) (**Fig. 51c**), while thiols were unchanged after stretch (**Fig. 51b**). There was a tendency to decrease after stretch for SOD activity ($p=0.053$), one of the principal enzymes in the antioxidant defence **(Fig. 51g**). Considering the glutathione redox cycle, it seems not to be affected in this cellular system. In fact, there were no differences between stretch and control groups in the glutathione reductase and glutathione peroxidase activities and in the amount of reduced glutathione (GSH) (**Fig. 51d, 51e, 51f**). These results are in line with the results obtained in 158N cell line, were AOPP and carbonyls where also increased (**Article 1, Fig.1**). In the cell line, the glutathione redox cycle was affected with a decreased in GSH and glutathione peroxidase activity (**Article 1, Table 1**), while in the mixed glial primary culture this was not altered. This is consistent with the fact that in the mixed culture there are astrocytes that are rich in GSH content and have more developed antioxidant defence, so they “protect” the culture from GSH decrease.

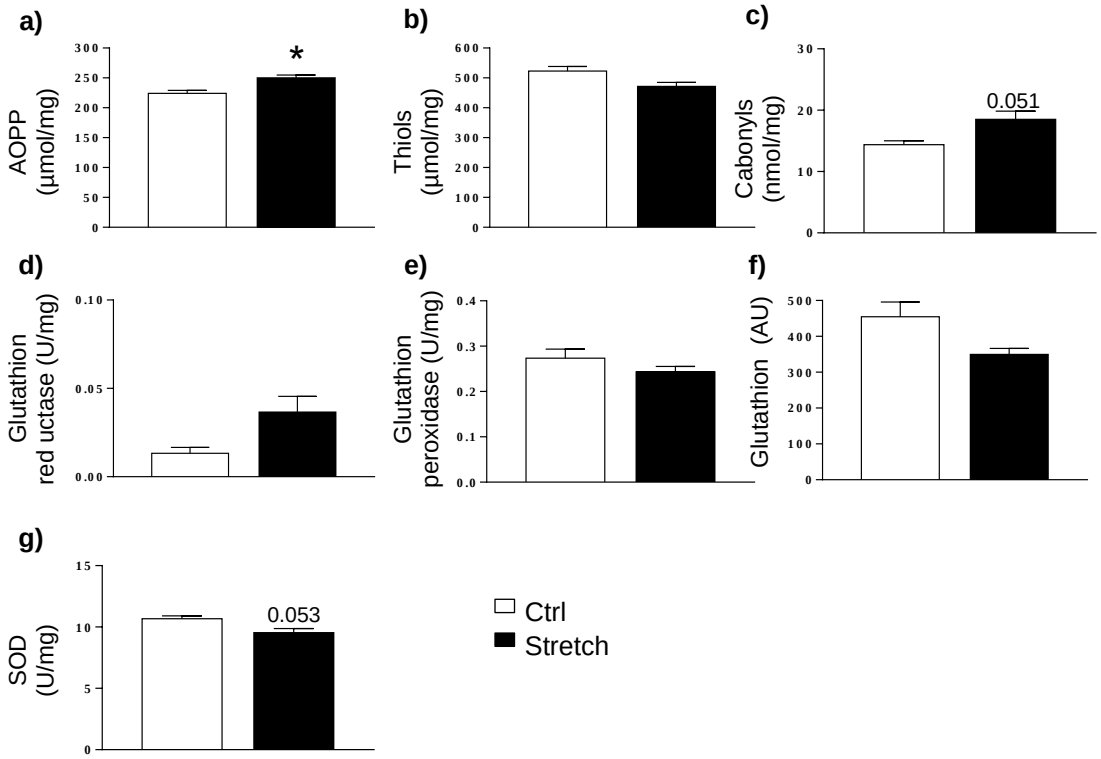

Figure 51: Effect of stretch on different oxidative stress parameters in mixed glial primary culture following stretch-induced mild injury at time 0h post-stretch. (a) AOPP(µmol/l), (b) thiols (µmol/l), (c) carbonyls (nmol/mg), (d) gluthation reductase (U/mg), (e) gluthation peroxidase (U/mg), (f) reduced gluthathion (AU of fluorescence intensity) and (g) SOD (U/mg) were assessed in control (Ctrl) and stretched (Stretch) cells following mild injury. Results represent the mean ± SEM (n=3). Student's unpaired *t*-test. *: p<0.05.

5.3 Stretch decreased the expression of antioxidant and myelin genes within mixed glial culture

Considering the alterations of oxidative stress markers, we decided to investigate the effect of stretch at the mRNA level of different antioxidant genes. We found that *Sod-2* (-30%, p<0.01), *Nqo-1* (-15%, p<0.05), *Ho-1* (-25%, p<0.01) and *Nrf-2* (-40%, p<0.01) were significantly decreased (**Fig. 52b, 52c, 52d, 52e**). Regarding *Sod-1* there was a tendency to decrease but it remained statistically non significant (**Fig. 52a**). The mRNA of the pro-oxidant gene *Duox-1* was not detectable in this cellular system. In parallel, the effect of stretch on the myelin genes *Plp, Mag* and *Cnp* was evaluated and *Plp* (p<0.01) and *Mag* (p<0.01) were significantly decreased after stretch by 60% and 50% respectively (**Fig. 52f, 52g**), with a tendency to decrease for *Cnp* (**Fig. 52h**). For the 158N cell line, an opposite response was reported, with an increase in the antioxidant gene expression and not a decrease (**Article 1, Fig.2**). This can be explained by the presence of astrocytes in the culture. The antioxidant response appeared globally reduced in the mixed glial culture, maybe these cells

during the stretching period of 20h had the time to activate the antioxidant system and then to decrease due to a negative feedback.

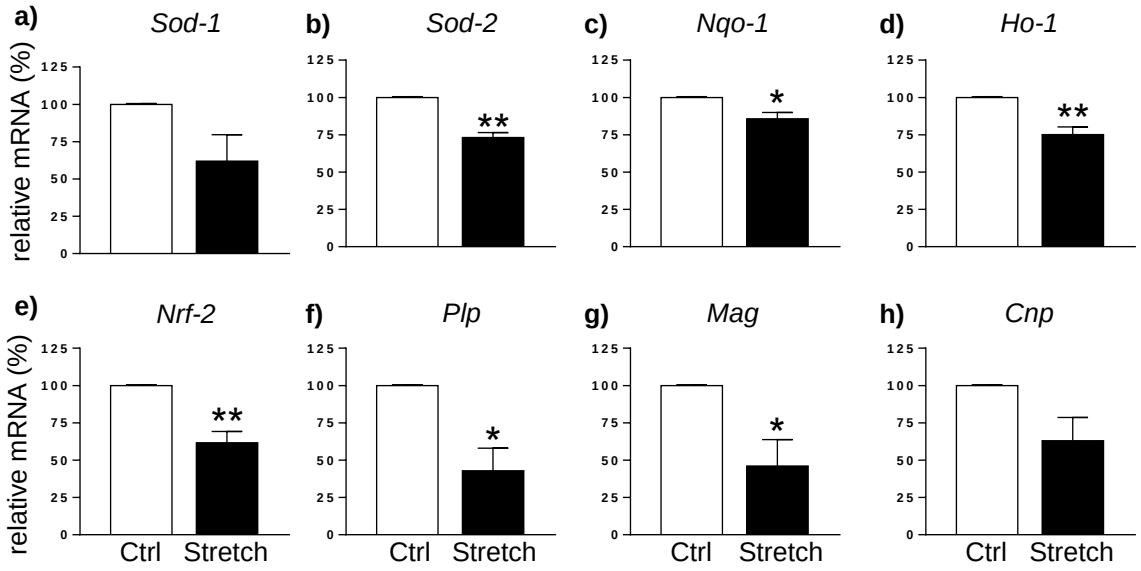

Figure 52: Evaluation of the stretch effect on antioxidant and myelin gene expression in mixed glial primary culture following stretch-induced mild injury at time 0h post-stretch. RNA was extracted and RT-qPCR was performed in control (Ctrl) and stretched (Stretch) cells following mild injury for the antioxidant genes *Sod-1, Sod-2, Nrf-2, Ho-1* and *Nqo-1* and the myelin genes *Plp, Mag* and *Cnp.* Results represent the mean±SEM of three independent experiments performed in triplicate. Student's unpaired *t*-test. *: $p<0.05$; **: $p<0.01$.

6. Development of a model of stretch-induced moderate injury in organotypic cerebellar slices

To deeply analyse the potential effect of stretch-induced injury on demyelination, we decided to move from an *in vitro* model to an *ex vivo* one. The mouse organotypic cerebellar slice culture was chosen for this study because cerebellum is very rich in myelinated fibers. The organotypic culture preserves the 3D architecture of cerebellum maintaining the *in situ* connections between all different cell populations. When I started my PhD in 2013, there were no models available to study stretch-induced injury in cerebellum. Therefore, I had to perform first a successful culture on the silicone membrane of the Bioflex® Plates. However the culture of cerebellar slices on elastomeric sheets constitutes the difficult part of the experiment. In fact in the case of a typical organotypic culture, slices are left on a particular support, a semipermeable membrane, where they are not covered by culture medium allowing them a gas exchange with air. This point is very important for the survival of slices and to reach this goal we had to test different parameters, summarized in the ***Table 12***.

After several attempts, the culture of cerebellar slices was still not successful. Thus we contacted the pioneer of *ex vivo* models of TBI, Pr Barclay Morrison III (Columbia University, New York, USA). He previously described a model of stretch-induced injury in organotypic culture of hippocampal slices (Morrison et al., 2000a, 2000b). Thanks to a mobility grant (IFD, Paris Descartes University), I had the opportunity to do an internship of three months, from June to August 2015, in his laboratory (Neurotrauma and Repair Laboratory at Biomedical Engineering, New York). There, I learned the experimental protocol on hippocampus with their stretching device. After several attempts, I adapted their protocol to cerebellum with our stretching device. This experience allowed me to greatly improve our experimental protocol and finally to obtain a successful organotypic culture on silicone membrane.

Tested parameters	Conditions
Pre-treatment Bioflex® Plates	No treatment **Plasma Cleaner: 2 minutes of cleaning** **Ozone cleaner: 15 minutes of cleaning**
Coating Bioflex® Plates	LN alone (pre-coated plates and home made coating) PLL alone LN/PLL different concentration **LN(80 µg/ml) PLL (320 µg/ml)**
Rocker mouvement	3D **2D**
Inclination angle of rocker tray	7° **14°**
Rocking rate	1 cycle/30s **1 cycle/min**
Humidification	Normal humidification **With humidifier (3 cycles of 10 min a day)**
Medium overnight (before culture)	**Neurobasal medium** Cerebellum medium Cerebellum medium serum free
«Dry» time for slice adherence	From 5 min to 1h30 **15 min**
Medium after slice adherence (1day)	**Neurobasal medium** Cerebellum medium Cerebellum medium serum free
Volume medium /well	From 500µl to 1 ml **800µl**
Percentage serum during stretching	**5%** 25%

Table 12: Table summarizing the different conditions tested during the development of the stretch-induced injury model in organotypic cerebellar slice culture. LN: Laminin, PLL: Poly-L- Lysine. The parameters that have been chosen for the following experiments are highlighted in bold pink.

Pre-treatment Bioflex® Plates

The first attempts of organotypic culture of cerebellar slices were done by performing the culture on coated plates with different proteins. But, even by changing the coating conditions (proteins, concentration), it was impossible to make the slices adherent to the silicone membrane. Once the medium added, they raised up from the membrane and floated in the medium. To solve this problem, the plates were pretreated with an Ozone Cleaner or a Plasma Cleaner. This treatment quickly renders the surface hydrophilic through plasma oxidation. A silicone surface recovers hydrophobic properties with time after plasma

treatment (~1 hour), thus oxidized surfaces should be brought into contact with the coating solution as soon as possible after plasma/ozone treatment in order to achieve strongest bond possible with the adhesion proteins. Thanks to this procedure, the proteins in the coating solution adhere to the membrane and, in turn, this allows a better adhesion of the slices to the silicone membrane.

Coating Bioflex® Plates

Different conditions of coating were tested and the best results were obtained with a combined coating of laminin (LN) and poly-L-lysine (PLL) at high concentration: LN (80 µg/ml) /PLL (320 µg/ml).

Rocking parameters

In order to allow a gas exchange with air, slices had to be kept on a rocker all over the duration of the culture. The slow movement of the rocker makes the slices to be alternatively in contact with the medium and with the air allowing the nourishment and the gas exchange. Three parameters are critical for this system: the type of rocker movement (2D versus 3D), the inclination angle of the rocker tray and the rocking rate. The best results were obtained with a 2D movement, inclination angle of 14° and a speed of 1 cycle per minute.

Humidification

In order to avoid an excessive evaporation of medium, a humidifier was introduced into the incubator. It was turned on during 3 cycles of 10 minutes per day, equally distributed within 24h.

Culture Medium

To allow a better adhesion of slices a particular medium was utilized before and immediately after the culture, different from the medium normally used for organotypic cerebellar slices. This particular medium is a neurobasal medium supplemented with B27, glucose and glutamax that will be referred in this text simply as “neurobasal medium”. After the coating, plates were rinsed but not dried, the neurobasal medium was added in each well the day before the culture. Then, at the moment of the culture, the medium was removed to place the slices on the membrane. Another important parameter is the “dry” time after culture, required for slice adherence. The better results were obtained with 15 minutes, shorter time did not allow an optimal adhesion and longer time exposed the slice to the risk of dry out. Immediately after culture, neurobasal medium was added and, the day after the culture, half of the medium was replaced by classical medium for cerebellum. From this moment all the following medium changes were done with cerebellum medium. Concerning the medium, the

volume was the last parameter to be tested. As reported above, the slices are on a rocker with a particular inclination angle and the volume of the medium should be enough to supply nourishment but not too much to “drown” the slices. The optimal volume was found to be 800µl per well.

Percentage of serum during the experiment

The typical culture medium for cerebellum contains 25% of horse serum. Given that for cells we reduced this percentage by fifth in order to see an effect of stretch, we tried to maintain the same principle and so reduce the percentage of serum from 25% to 5%. Some tests are still ongoing on this parameter. Slices are analysed at 0h, 24h and 72h after the stretch. For the time 0h and 24h post-stretch, the reduced percentage of serum does not present a problem, but for slices analysed at 72h it has to be considered that they are kept in culture 4 days in 5% serum, probably undamaging the tissue.

7. Cellular and molecular responses of mouse organotypic cerebellar slices to stretch-induced moderate injury

The first step was to perform a successful organotypic culture of cerebellar slices on the silicone membrane of the Bioflex® Plates, objective that was reached by working on all parameters described above. After 7 DIV of culture, slices appeared healthy, with preserved neurons and myelin sheaths, as assessed by a double immunostaining for Purkinje cells (marked by CaBP) and myelin sheaths (marked by MAG) (**Fig. 53**). Slices were subjected to a stretch-induced moderate injury and different analyses were performed immediately after the stretch (t 0h), 24h (t 24h) and 72h (t 72h) after the end of the stretch.

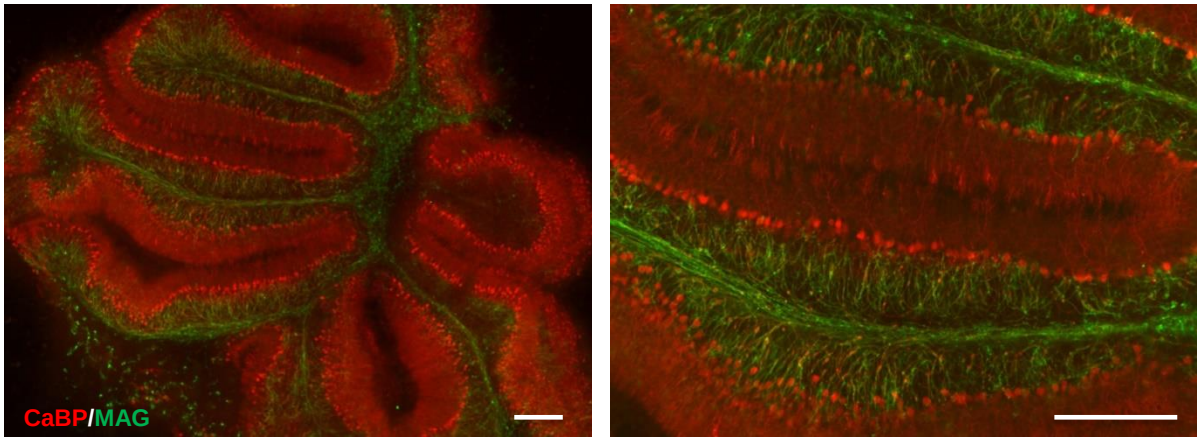

Figure 53: **Double immunostaining of organotypic cerebellar slices for CaBP in red and MAG in green**. Slices were grown on silicone membrane for 7 DIV before performing the immunohistochemistry. Scale bar: 250µm. CaBP: Calbindin protein; MAG: Myelin-associated glycoprotein.

7.1 Effect of stretch on myelin sheaths and neurons

A double immunostaining for Purkinje cells (marked by CaBP) and myelin sheaths (marked by MAG) was performed in control and stretched slices in order to see the effect of stretch. The intensity of staining was assessed for both CaBP and MAG and no differences were observed in stretched slices compared to the control condition at time 0h, 24h and 72h after stretch (**Fig. 54**). These data ruled out a major effect of stretch on cerebellar slices.

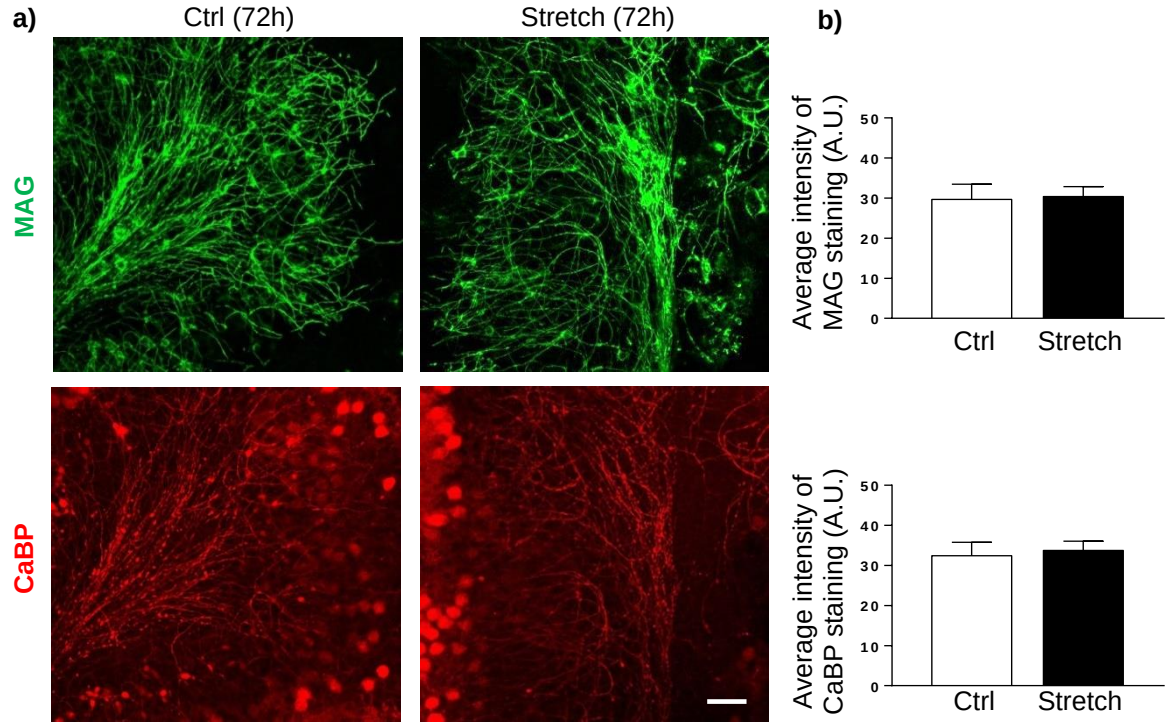

Figure 54: Double immunostaining of organotypic cerebellar slices for CaBP in red and MAG in green after stretch-induced moderate injury. a) Images represent control (Ctrl) and stretched (Stretch) slices analyzed at 72h post-stretch. The same results were also obtained at 0h and 24h post-stretch. Scale bar: 50µm b) Quantitative analysis of MAG and CaBP intensity was performed in control (Ctrl) and stretched (Stretch) slices. Results represent the mean±SEM (n=7-8 from three independent experiments). Student's unpaired *t*-test. CaBP: Calbindin protein; MAG: Myelin-associated glycoprotein.

We analysed the effect of stretch on axonal injury. Accumulation of amyloid precursor protein (APP) is an indicator of axonal injury. Therefore we co-immunolabeled cerebellar slices with APP and SMI-312, a marker of axonal neurofilaments (**Fig. 55a**). The number of APP spheroids was significantly elevated in stretched slices at time 0h after stretch (+ 110%, $p<0.05$) in slices grown in medium containing 5% serum (**Fig. 55b**). The analysis was also performed at 72h after the end of the stretch and number of APP spheroids was also increased in the stretch condition (+ 80%, $p<0.01$) but in this case in slices grown in medium containing 25% of serum (**Fig. 55c**).

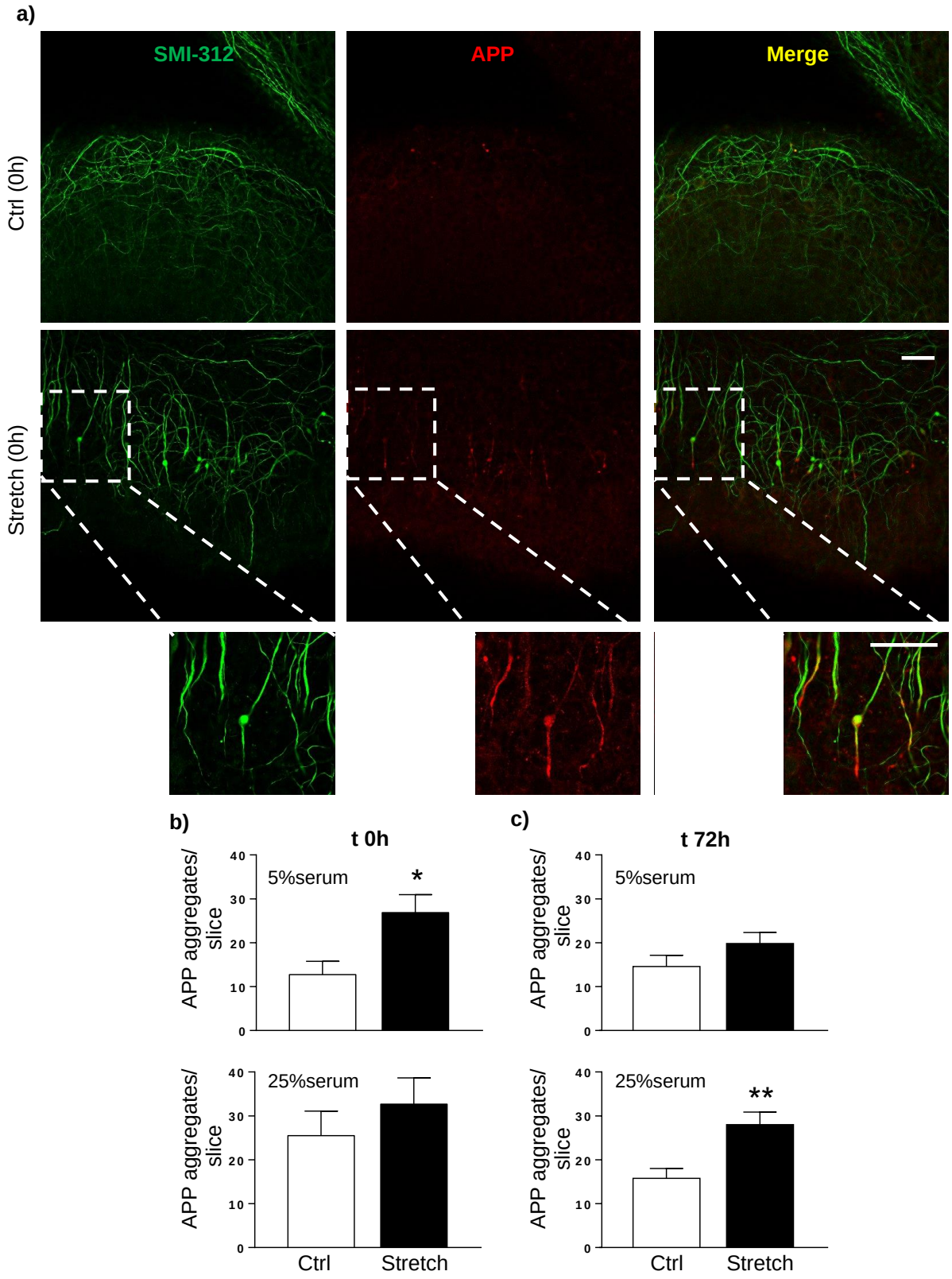

Figure 55: **Double immunostaining of organotypic cerebellar slices for APP in red and SMI-312 in green after stretch-induced moderate injury.** Control (Ctrl) and stretched (Stretch) slices were analysed at time 0h an 72h post-stretch. a) Images represent control (Ctrl) and stretched (Stretch) slices analyzed at 0h post-stretch. Confocal microscopy, scale bar: 50µm. b) Quantitative analysis of the number of APP spheroids per slice following stretch-induced moderate injury in medium containing 5% or 25% serum. Results represent the mean±SEM (n=4-8 slices from two animals per condition). Student's unpaired *t*-test.*: p<0.05. APP: Amyloid precursor protein; SMI-312: Pan-Axonal Neurofilament Marker.

Our results are preliminary but the effect seemed to be more pronounced for slices stretched in medium containing 5% serum at time 0h (in line with our results obtained in 158N cell line, in fact serum can mask the effect of stretch) with no effect at 72h post-stretch. For slices analysed at 72h post-stretch, the accumulation of APP was significant in slices grown in medium containing 25% serum, and not 5%. It is possible that the time course of APP accumulation may be affected by the percentage of serum, the response in slices grown in 25% would be retarded and detectable at 72h and not at 0h. As explained above some tests are still ongoing on the choice of the percentage of serum in the medium at the moment of stretch. This medium is in fact added one day before the culture and it stays till the end of the experiment, meaning that slices analysed at 72h are kept in culture 4 days in 5% serum, we cannot exclude that slices could be undamaged by this relatively prolonged time with reduced serum. Overall, there is either a significant increase or a tendency to increase of the number of APP spheroids and the co-staining with SMI-312 for neurofilament confirm that there is an axonal swelling in line with APP accumulation, sign of altered axonal transport. This demonstrates that slices undergo axonal injury in cerebellar slices submitted to stretch-induced moderate injury.

7.2 Effect of stretch on paranodal junctions

Paranodal junctions are located between the nodes of Ranvier and the juxtaparanodal junctions. The paranodal complex is a structure that connects myelin and the axonal membrane at this region. We investigated the structure of the paranodal junctions at time 0h and 72h after stretch, by labelling the axonal membrane protein Caspr, an integral component of the paranodal complex, and the myelin sheaths *via* MAG. Our preliminary results showed an alteration in Caspr staining that appeared “elongated”, more diffuse in stretched slices compared to control slices (**Fig. 56**) at both 0h and 72h after stretch. This suggests an alteration of the paranodal junctions that starts immediately after stretch and persists for at least 72h.

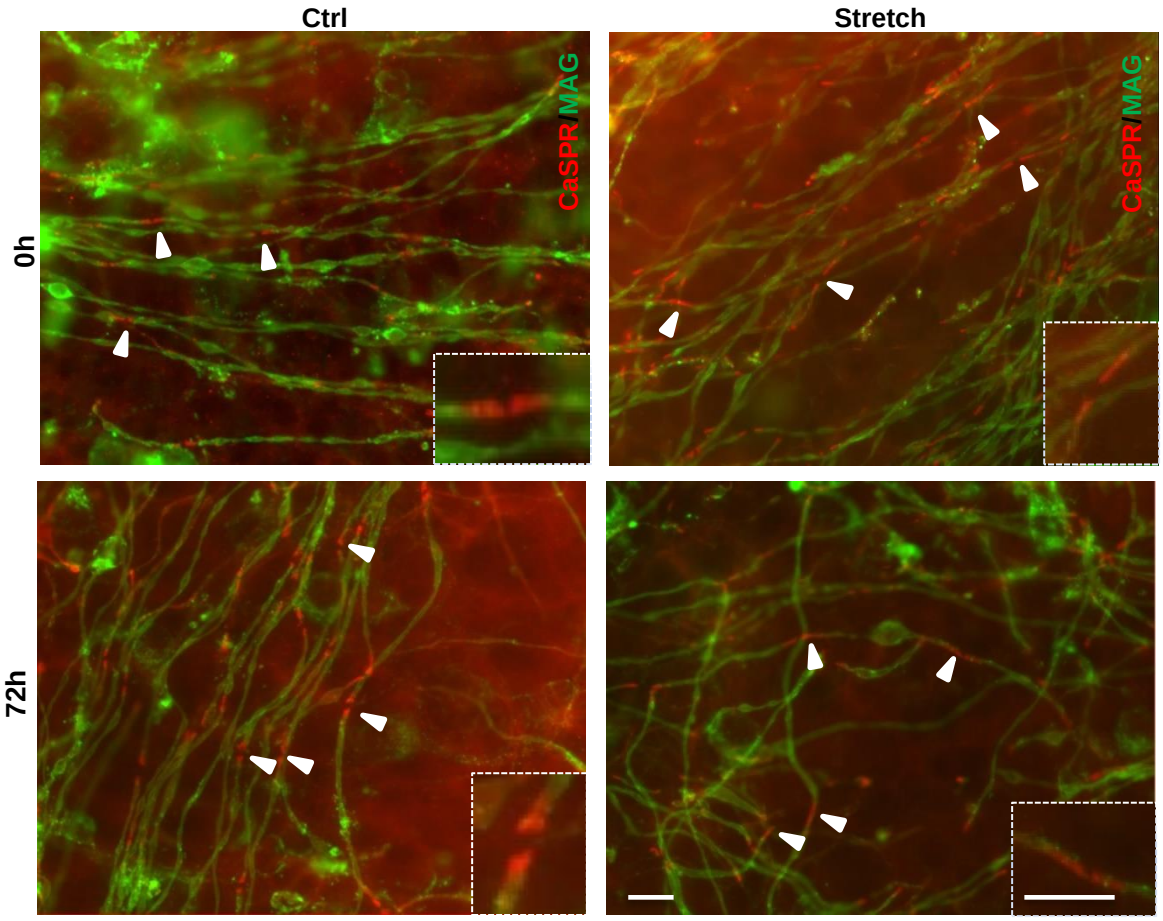

Figure 56: **Double immunostaining of organotypic cerebellar slices for Caspr in red and in green after stretch-induced moderate injury**. Images were obtained from control (Ctrl) and stretched (Stretch) slices at time 0h and 72h post-stretch. Slices were stretched in medium containing 5% (t 0h) or 25% (t 72h) serum. Scale bar: 12.5µm. Caspr: Contactin-associated protein; MAG: Myelin-associated glycoprotein.

7.3 Effect of stretch on different oxidative stress parameters

An increase in oxidative stress markers was observed after stretch injury in 158N cell line and in mixed glial culture. Based on our findings, AOPP, carbonyls groups, thiols, SOD activity and reduced glutathione GSH were also assessed in control and stretched slices at time 0h after stretch. All these parameters seemed not to be affected in cerebellar organotypic slice, since there were no differences between stretch and control groups (**Fig. 57**). It should be interesting to assess these parameters at 24h and 72 after stretch, maybe the tissue has some compensatory systems that protect against oxidative stress at time 0h but it will be compromised at longer time points after stretch.

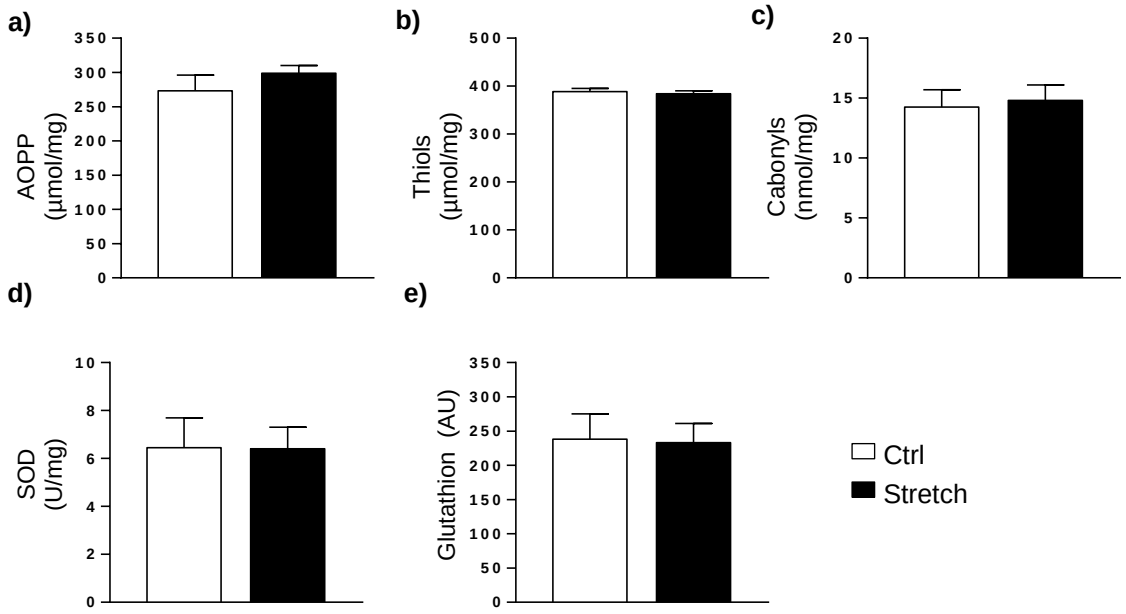

Figure 57: Effect of stretch on different oxidative stress parameters in organotypic cerebellar slices after moderate injury at time 0h post-stretch. (a) AOPP(µmol/l), (b) thiols (µmol/l), (c) carbonyls (nmol/mg), (d) SOD (U/nmg) and (e) reduced gluthathion (AU of fluorescence intensity) were assessed in control (Ctrl) and stretched (Stretch) slices following moderate injury. Results represent the mean ± SEM (n=2). Student's unpaired *t*-test.

7.4 Evaluation of the stretch effect on antioxidant and myelin gene expression

We investigated the effect of stretch in organotypic cerebellar slices subjected to stretch-induced moderate injury at different time points after stretch (0h, 24h and 72h). The mRNA level of different antioxidant and myelin genes was evaluated and no differences were observed between stretch and control groups at time 0h after stretch (**Fig. 58**). Instead at the time 24h after stretch the expression of *Sod-2* (-70%, p<0.001), *Nqo-1* (-60%, p<0.01), *Ho-1* (-60%, p<0.01) was significantly decreased (**Fig. 59b, 59c, 59d**), whereas no effect was obtained on *Sod-1* and *Nrf-2* expression. (**Fig. 59a, 59e**). In parallel, the effect of stretch was evaluated on the myelin genes *Plp, Mag* and *Cnp* showing that *Plp* was significantly decreased (p<0.01) after stretch by 50% (**Fig. 59f**), with a tendency to decrease for *Mag* (**Fig 59g**) and no effect on *Cnp* (**Fig. 59h**). The response of slices was also evaluated at 72h after stretch and no differences were observed between stretch and control groups for both antioxidant and myelin genes (**Fig. 60**).

At time 0h no changes were observed in gene expression in line with no changes in oxidative stress makers, while modifications were observed for both 158N cell line and oligodendrocyte-enriched primary culture following moderate injury. Probably in tissue there are other cells that counteract the detrimental effects of ROS production. Nevertheless at 24h after stretch modifications in the expression of antioxidant and myelin genes were

observed in slices suggesting that in a tissue the response to stretch needs more time to take place. It should be therefore interesting to assess the different oxidative stress markers at 24h, given the alteration in gene expression at this time point.

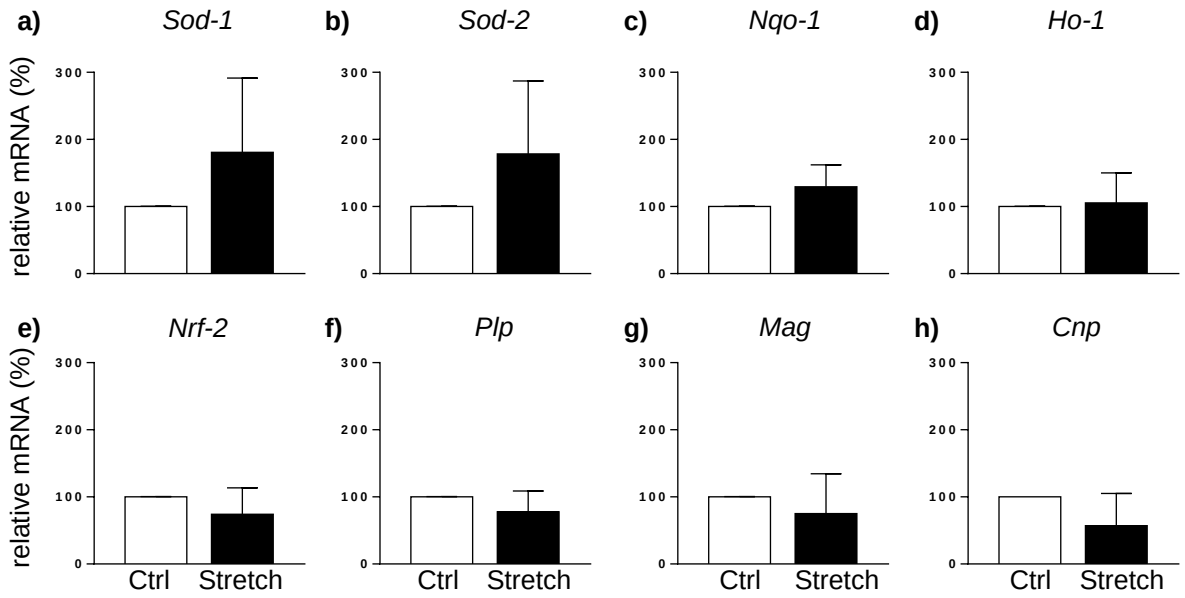

Figure 58: Evaluation of the stretch effect on antioxidant and myelin gene expression in organotypic cerebellar slices subjected to stretch-induced moderate injury at time 0h post-stretch. RNA was extracted and RT-qPCR was performed in control (Ctrl) and stretched (Stretch) slices for the antioxidant genes *Sod-1, Sod-2, Nrf-2, Ho-1* and *Nqo-1* and the myelin genes *Plp, Mag* and *Cnp*. Results represent the mean±SEM of three independent experiments performed in triplicate. Student's unpaired *t*-test.

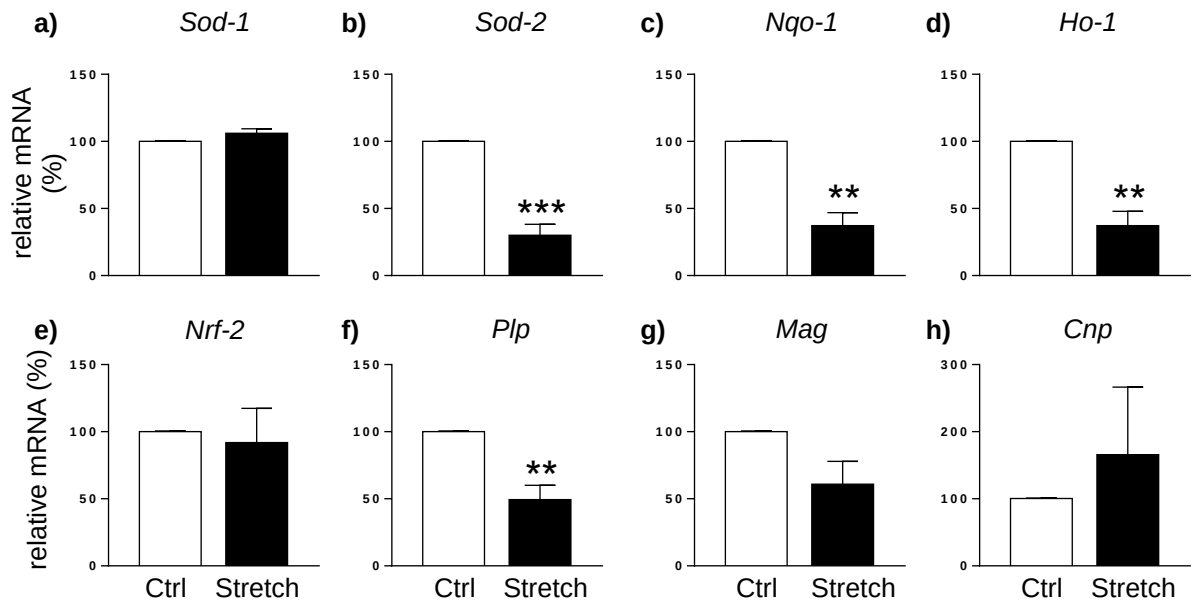

Figure 59: Evaluation of the stretch effect on antioxidant and myelin gene expression in organotypic cerebellar slices subjected to stretch-induced moderate injury at 24h post-stretch. RNA was extracted and RT-qPCR was performed in control (Ctrl) and stretched (Stretch) slices for the antioxidant genes *Sod-1, Sod-2, Nrf-2, Ho-1* and *Nqo-1* and the myelin genes *Plp, Mag* and *Cnp*. Results represent the mean±SEM of three independent experiments performed in triplicate. Student's unpaired *t*-test. **: p<0.01; ***p < 0.001.

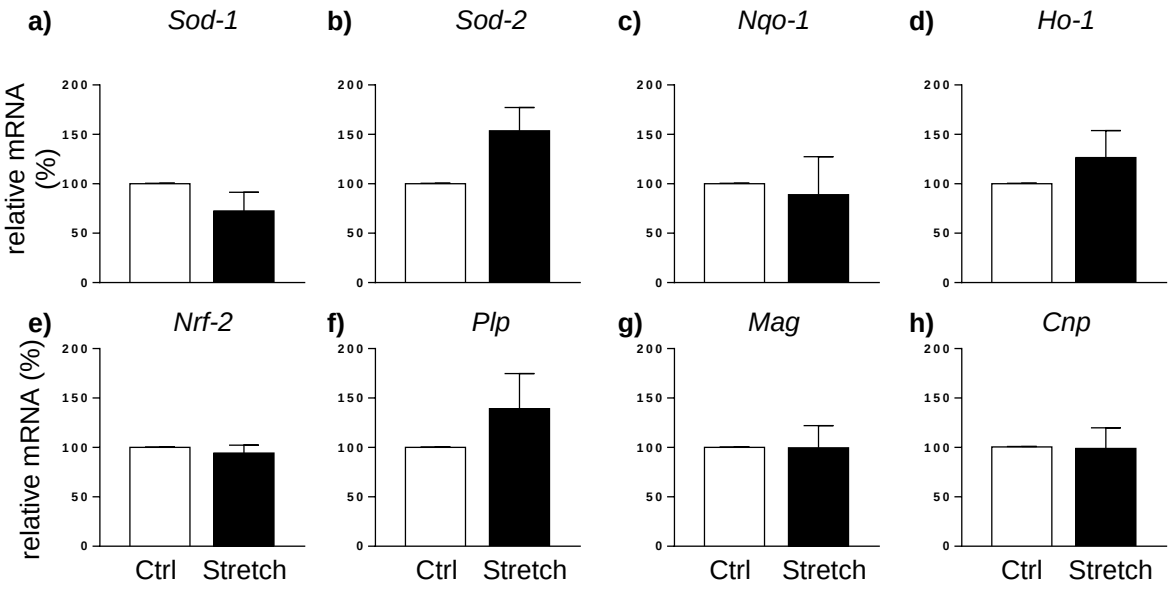

Figure 60: Evaluation of the stretch effect on antioxidant and myelin gene expression in organotypic cerebellar slices subjected to stretch-induced moderate injury at 72h post-stretch. RNA was extracted and RT-qPCR was performed in control (Ctrl) and stretched (Stretch) slices for the antioxidant genes *Sod-1, Sod-2, Nrf-2, Ho-1* and *Nqo-1* and the myelin genes *Plp, Mag* and *Cnp*. Results represent the mean±SEM of three independent experiments performed in triplicate. Student's unpaired *t*-test.

7.5 Effect of stretch on Nrf-2 phosphorylation

The effect of stretch was also evaluated on Nrf-2 activation at time 72h after stretch. No alteration in Nrf-2 phosphorylation was observed in stretched slices compared to the control condition (**Fig. 61**). The pathway Nrf-ARE does not seem to be affected by stretch, at least at 72h after stretch. Nevertheless it should be interesting to evaluate Nfr-2 activation at 24h when the expression of *Nqo-1* and *Ho-1*, genes controlled by Nrf-2, is altered.

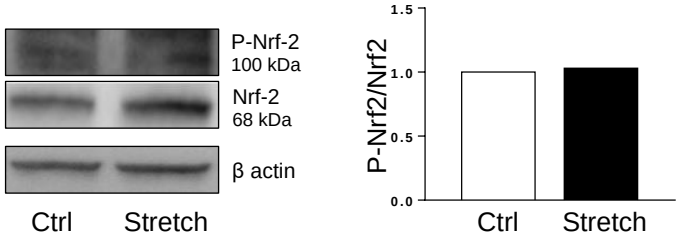

Figure 61: Evaluation of the stretch effect on Nrf-2 phosphorylation in organotypic cerebellar slices at 72h after moderate injury. Proteins were extracted from control (Ctrl) and stretched (Stretch) cells and western blot was performed for the transcriptional factor Nrf-2. The ratio P-Nrf-2 (100 kDa) on total Nrf-2 (68 kDa) is presented. β-actin was used as loading control. Preliminary result represents, for each condition, the mean value of a pool of 10-12 slices from 2 animals.

7.6 Effect of stretch on PLP and MBP

The expression of the two major myelin proteins PLP and MBP was assessed at both mRNA and protein level at time 72h after stretch. No effects were observed for PLP (**Fig. 62a, 62b**), while MBP was increased at mRNA level (+225%, $p<0.01$) but the protein was not affected (**Fig. 62c, 62d**). It should be interesting to evaluate the expression of these proteins also at other time points, especially at 24h, when the expression of *Plp* is decreased at mRNA level. It is possible that the proteins are affected at 24h and then they return to basal level at 72h. It has to be also considered that western blot does not allow to discriminate between intact myelin proteins and myelin debris. In order to have a more precisely information about myelin sheath structure, it would be interesting to perform electron microscopy on cerebellar slices.

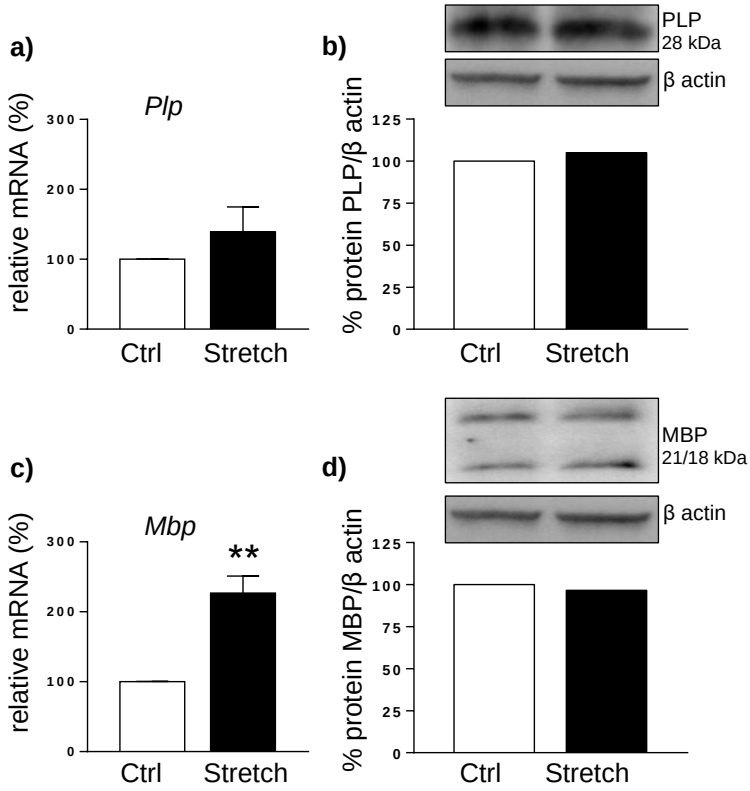

Figure 62: Evaluation of the stretch effect on myelin gene and protein expression in organotypic cerebellar slices at 72h after moderate injury. The response of slices was evaluated at time 72h post-stretch. RNA was extracted and RT-qPCR was performed in control (Ctrl) and stretched (Stretch) slices following moderate injury for the myelin genes *Plp* (a) and *Mbp* (c). Results represent the mean±SEM of three independent experiments performed in triplicate. Student's unpaired *t*-test. **: p<0.01. Proteins were extracted following moderate injury from control (Ctrl) and stretched (Stretch) slices and western blot was performed for the myelin protein PLP (b) and MBP (d). β-actin was used as loading control. Preliminary result represents for each condition, the mean value of a pool of 10-12 slices from 2 animals.

7.7 Effect of stretch on MAPKs pathways

A particularly stretch-responsive pathway involves the mitogen-activated protein kinases (MAPKs), a family of kinases as the extracellular signal-regulated kinase (ERK) and c-Jun NH2- terminal kinase (JNK). This pathway is altered in the 158N cell line subjected to both moderate and mild injury (**Article 1, Fig.4**). Thus, we decided to analyze the effect of stretch-induced moderate injury on ERK1/2 (44 and 42 kDa) and on JNKs (54 and 46 kDa) in cerebellar slices. Preliminary results show that stretch increases the ratio of P-ERK/ERK by 30% (**Fig. 63a**) and the ratio of P-JNK/JNK, in particular for the 46 kDa isoform, by 2.5 fold compared to the control condition (**Fig. 63b**). These results suggest an activation of MAPKs following stretch-induced moderate injury.

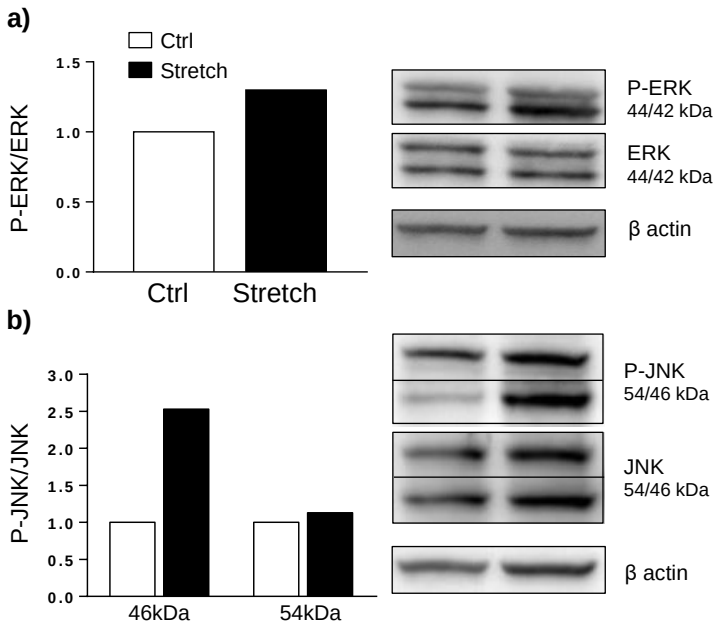

Figure 63: Evaluation of the stretch effect on the expression of the MAP kinases ERK1/2 and JNKs in organotypic cerebellar slices at 72h after moderate injury. The response of slices was evaluated at time 72h post-stretch. Proteins were extracted following moderate injury from control (Ctrl) and stretched (Stretch) slices and western blot was performed for ERK1/2 (a) or JNKs (b), β-actin was used as loading control. The ratio P-ERK on total ERK and the ratio P-JNK on total JNK are presented. Preliminary result represents for each condition the mean value of a pool of 10-12 slices from 2 animals.

SECOND PART

The second part of my PhD project was focused on the evaluation of the potential antioxidant effect of etazolate, a pyrazolopyridine derivate compound, on oligodendrocytes from the 158N cell line following an experimental model of oxidative stress *in vitro*. This compound has been studied in our team for its neuroprotective and anti-inflammatory activities after TBI *in vivo* (Siopi et al., 2013) and for its potential remyelinating effect following demyelination *ex vivo* and *in vitro* (Llufriu-Dabén et al. 2016a,b under revision). Thus, we had first to develop an *in vitro* model of *tert*-butyl hydroperoxide (*t*BHP)-induced oxidative stress using the oligodendrocyte 158N cell line, since *t*BHP is extensively used as oxidative stress-inducing agent to study the effect of free radicals in different cell types.
In order to validate the model, the cell viability and ROS production were evaluated following N-acetylcysteine (NAC) treatment, a known powerful antioxidant. Once the model was validated we tested the potential antioxidant effect of etazolate.

1. Cellular response of 158N cell line to a *t*BHP-induced oxidative stress

This part of the work has been performed with the participation of Francesca Sapone, student from the European program Unipharma graduates.
In order to develop an *in vitro* model of oxidative stress-induced injury, we treated 158N cell line with different doses of *t*BHP (10, 20, 50 and 100 μM) for 2h. As shown in the **Figure 64**, cells were susceptible to *t*BHP at the doses of 20, 50 and 100 μM in a dose-dependent manner, with a significant cytotoxicity observed at the highest dose. Cell viability was in fact reduced by 60% at 100 μM *t*BHP. Therefore the dose of 50 μM was chosen to test the effect of NAC and etazolate on cell viability by a WST-1 assay.

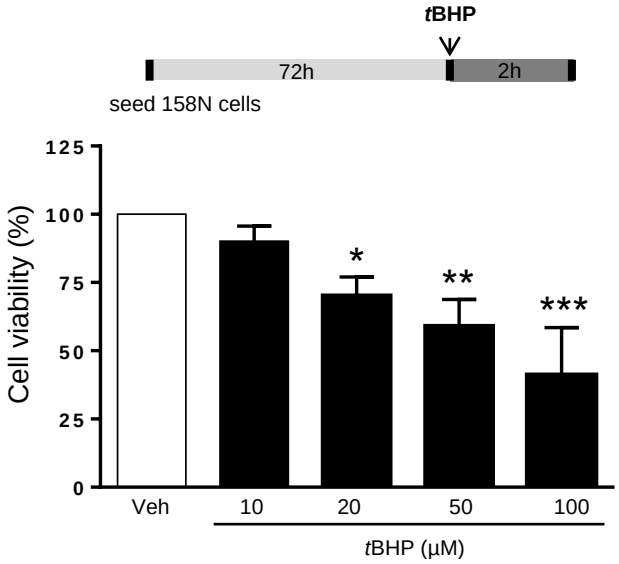

Figure 64: Validation of a model of oxidative stress induced by *t*BHP in 158N cell line. Cells were incubated with different doses of *t*BHP (10, 20, 50 and 100 µM) for 2h. Then medium was removed and cell viability was evaluated by WST-1 assay. Results are expressed as percentage of cell viability compared to that of the control group. Values are the mean ± SEM of three independent experiments. One way ANOVA followed by Bonferroni post-hoc test, *: p<0.05; **: p<0.01; ***: p<0.001.

In order to evaluate more precisely the antioxidant effect of NAC and etazolate, a flow cytometric analysis was also performed to study at the same time the cell viability and ROS production. A double staining with propidium iodide (PI) and the carboxy-dichloro-dihydro-fluorescein diacetate (CM-H2DCFDA) was performed. For this protocol, cells were in suspension and they were treated with *t*BHP at 100 µM for 30 min. In this condition *t*BHP was able to induce a marked ROS production without cell death, probably due to the short incubation period.

2. N-acetylcysteine (NAC) treatment counteracts *t*BHP-induced oxidative stress in 158N cell line

2.1 NAC decreased the cell death induced by tBHP

Cell viability was assessed by WST-1 and a marked decrease in cell viability was observed in *t*BHP group compared to control group (-40%, p<0.01). NAC was able to counteract this effect restoring the cell viability almost to control level (**Fig. 65**).

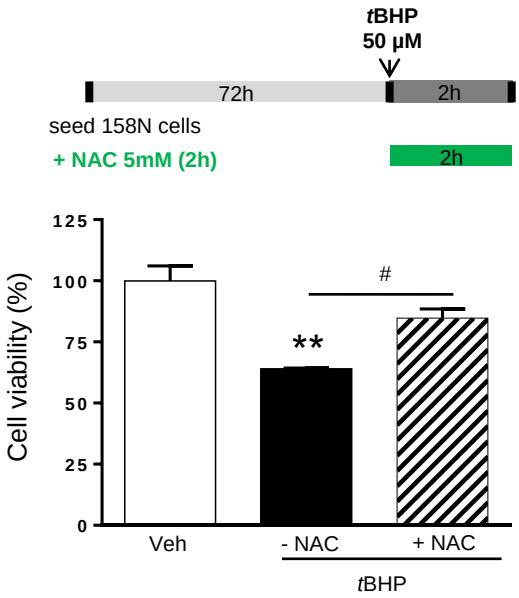

Figure 65: Effect of NAC on cell viability in 158N cell line in a model of oxidative stress induced by *t*BHP 50 µM. NAC 5 mM was incubated at the same time with *t*BHP at 50 µM for 2h. Then medium was removed and cell viability was evaluated by WST-1 assay. NAC 5 mM had a potent antioxidant effect against *t*BHP-induced cell mortality. Results are expressed as percentage of cell viability compared to that of the control group. Values are the mean ± SEM of three independent experiments. One way ANOVA followed by Bonferroni post-hoc test, **: $p<0.01$ compared to control group; # $p<0.05$ compared to *t*BHP group. NAC: N-acetylcysteine; Veh: vehicule.

2.2 NAC decreased the intracellular ROS production induced by tBHP

Cell death and ROS production were also assessed by FACS. Cell death was evaluated by the presence of PI^+ cells. In control, *t*BHP-treated or *t*BHP/NAC-treated cells, a low number of PI^+ cells was present (**Fig. 66d**), excluding *t*BHP-induced cell death in these conditions. The ROS production was evaluated by assessing redox sensitive intracellular conversion of H2DCFDA to DCF. *t*BHP induced a 20-fold increase in the DCF fluorescence compared to control group ($p<0.0001$) and NAC was able to reduce *t*BHP-induced ROS production, by decreasing the DCF fluorescence by 50% compared to *t*BHP condition ($p<0.01$) (**Fig. 66c**).

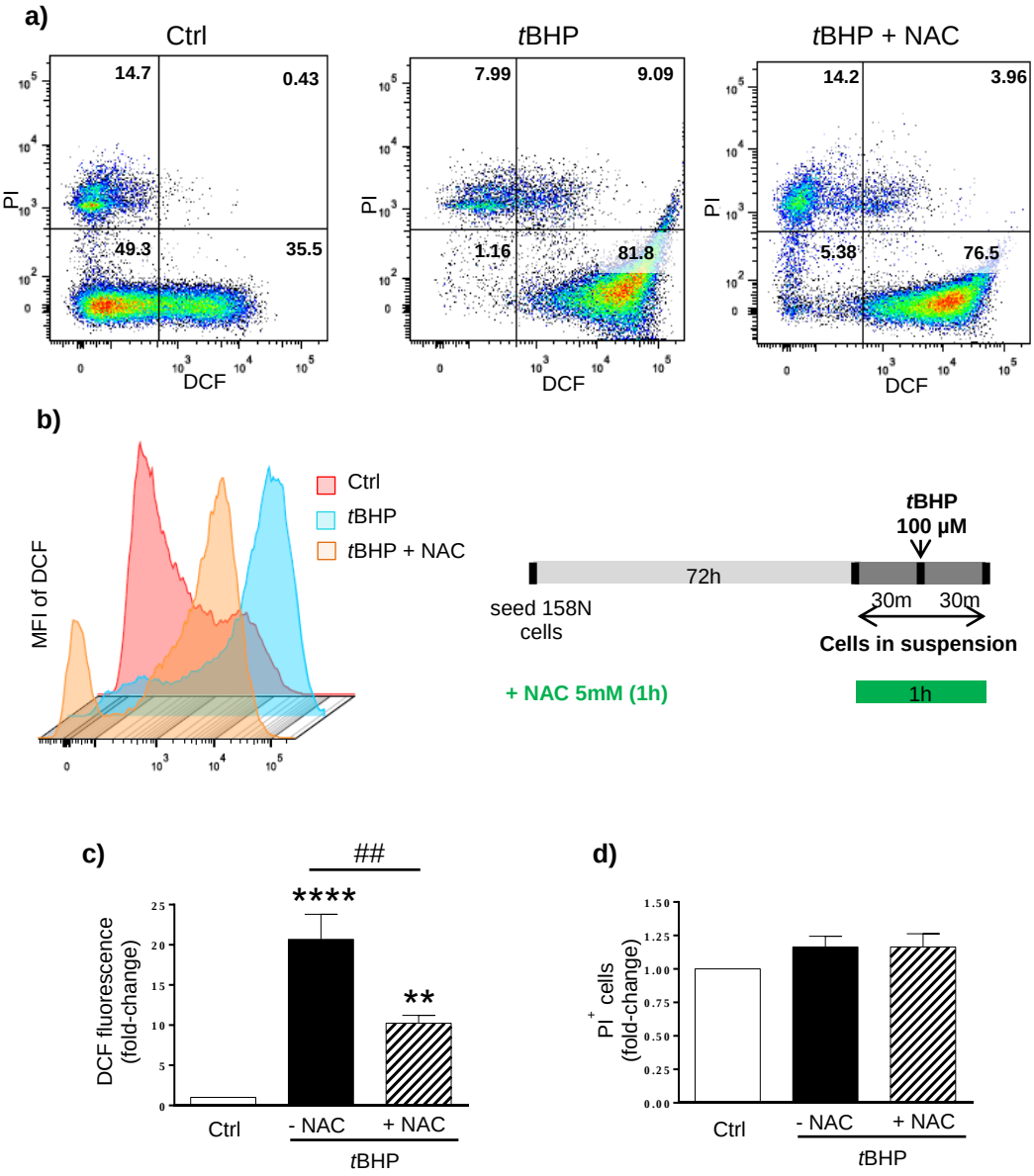

Figure 66: NAC decreased the level of intracellular ROS in 158N cell line in a model of oxidative stress induced by *t*BHP at 100 µM. NAC 5 mM was incubated 1h in cells in suspension and for the last 30 minutes *t*BHP at 100 µM was added. The intracellular ROS level was detected by DCFH-DA fluorescent probe. (a) Representative pictures of DCF-stained (FITC channel) and PI-stained (PE channel) were obtained from control (Ctrl), *t*BHP-treated (*t*BHP) and *t*BHP/NAC-treated (*t*BHP + NAC) cells. (b) Representative picture of the mean fluorescence intensity (MFI) of DCF measured on DCF^+/PI^- cells. (c) Quantitative analysis of the DCF fluorescence expressed as geometric mean. (d) Quantitative analysis of the percentage of PI^+ cells. All results are expressed as fold change compared to control group. Values are the mean ± SEM of 5 experiments. Student's unpaired *t*-test, **: p<0.01; ****: p<0.0001 compared to control group; ## p<0.01 compared to *t*BHP group.

Cell treatment with NAC showed a protective effect in both techniques used, WST-1 assay and FACS, showing that this model is appropriate for studying the potential antioxidant effect of etazolate in 158N cell line.

3. Effect of etazolate treatment on *t*BHP-induced oxidative stress in 158N cell line

3.1 Etazolate did not decrease the cell death induced by tBHP

First we tested a pre-treatment protocol with etazolate. The treatment was started 24 hours before the incubation period (2h) with *t*BHP at 50µM, as proof of concept. Cell viability was assessed by WST-1. As expected *t*BHP induced a decrease in cell viability by 50% compared to control group ($p<0.001$) and etazolate was not able to reduce *t*BHP-induced cell death at none of doses tested in this experiment (0.02, 0.2, 2, 20 and 200 µM) (**Fig. 67b**). Moreover etazolate had no effect by itself on cell viability in control group without *t*BHP (**Fig. 67a**).

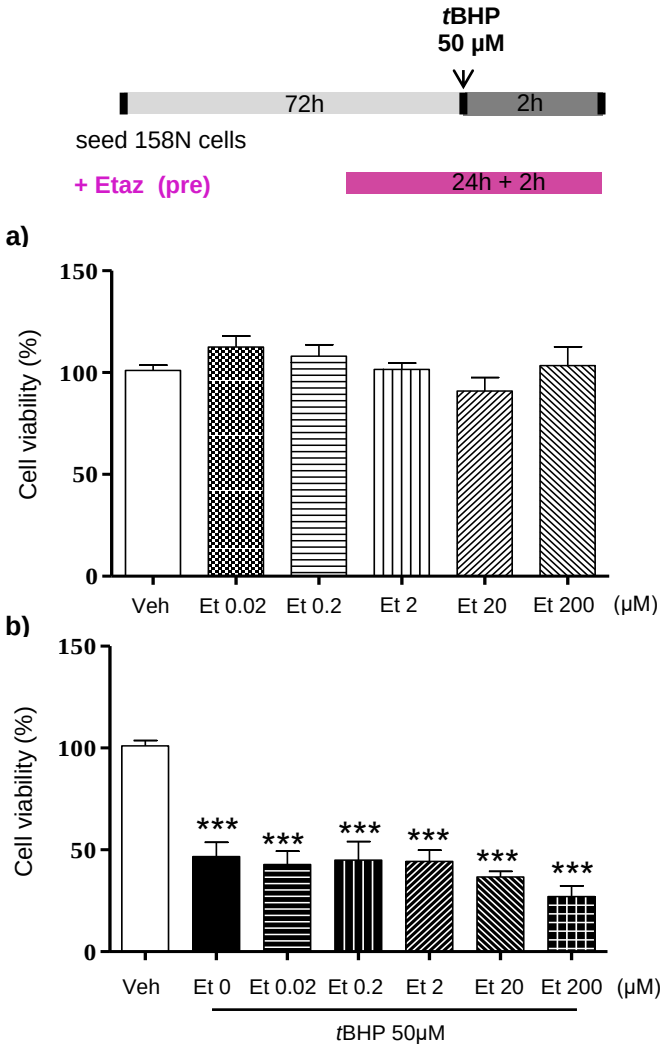

Figure 67: Effect of Etazolate (with pre-treatment protocol) on cell viability in 158N cell line in a model of oxidative stress induced by *t*BHP at 50 µM. Dose-effect study of etazolate was performed from 0.02 to 200 µM without (a) or with (b) *t*BHP. Etazolate or its vehicle (PBS 0.1M, pH 7.4) was added 24h before the addition of *t*BHP, then cells were incubated with *t*BHP at 50 µM for 2h. The medium was removed and cell viability was evaluated by WST-1 assay. Etazolate had no effect either by itself on cell viability (a) or against *t*BHP-induced oxidative stress (b). Results are expressed as percentage of cell viability compared to that of the control group. Values are the mean ± SEM of three independent experiments. One way ANOVA followed by Bonferroni post-hoc test, ***: $p<0.001$. Et: etazolate.

3.2 Etazolate did not decrease the intracellular ROS production induced by tBHP

Cell death and ROS production were also assessed by FACS in order to deeply analyze the potential antioxidant effect of etazolate. The dose of 2µM was chosen, given that etazolate at this dose is able to exert neuroprotective and remyelinating effect (Marcade et al., 2008; Llufriu-Dabén et al. 2016a, under revision). Cell death was assessed by the presence of PI^+ cells. In control, *t*BHP-treated or *t*BHP/Etazolate-treated cells, the number of PI^+ cells was the same (**Fig. 68d**), excluding cell death in all conditions analyzed. Treatment with *t*BHP induced an increase in the DCF fluorescence of 20-fold compared to control group ($p<0.001$) and etazolate was not able to decrease the *t*BHP-induced ROS production either in pre-treatment protocol or without pre-treatment protocol (**Fig. 68c**).

Etazolate by itself did not exert a significant effect on cell viability and ROS production either in pre-treatment protocol or without pre-treatment protocol (**Fig. 69**).

Etazolate does not seem to have a protective effect on cell death and ROS production evaluated by two techniques, WST-1 assay and FACS. It remains to be elucidated whether if the antioxidant effect of etazolate reported *in vivo* (Jindal et al., 2013, 2015) is direct or indirect. In our model, etazolate was tested only on oligodendrocytes. It has also to be considered that *t*BHP induced a very important production of ROS (around 20-fold the basal level) that is not necessarily happened *in vivo.* Maybe the oxidative stress produced by *t*BHP is too severe to be reversed by etazolate. Furthermore, several hypotheses are worth it to be considered. The previously *in vivo* data reported in the literature on the antioxidant activity of etazolate can be due to an indirect effect of this compound *via* its anti-inflammatory effect. It probably exerts its effect *via* membrane receptors (see introduction § 5.1). However we don't have any proves that this compound is capable to cross the lipid membrane in 158N cell line.

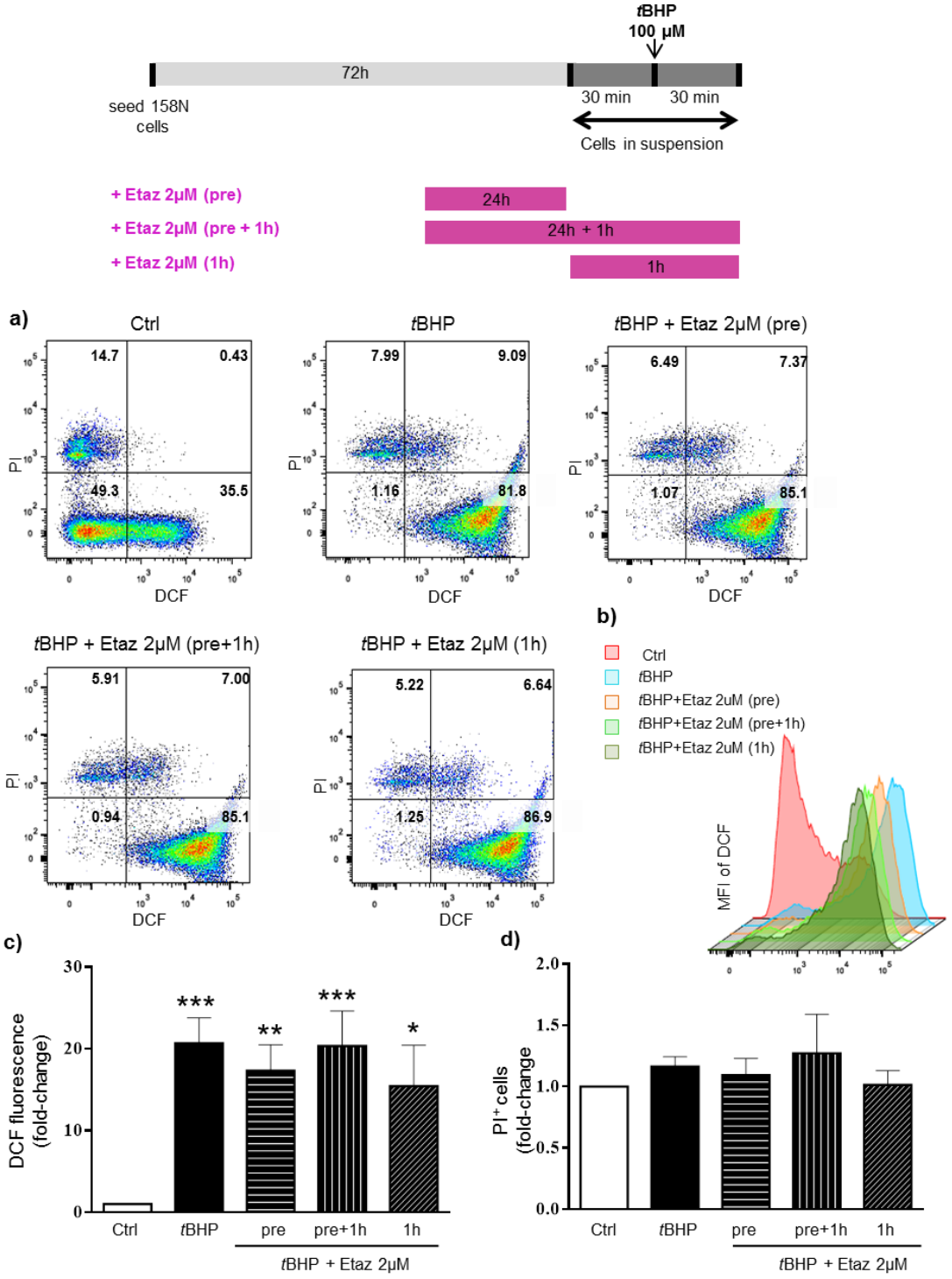

Figure 68: Effect of etazolate on the level of intracellular ROS in 158N cell line in a model of oxidative stress induced by *t*BHP at 100 µM. Etazolate at 2 µM was tested using three different protocols: i) etazolate in pre-treatment was added 24h before the addition of *t*BHP (*t*BHP + Etaz 2µM, pre), ii) etazolate in pre-treatment was added 24h before the addition of *t*BHP and during the 1h *t*BHP incubation (*t*BHP + Etaz 2µM, pre+1h), iii) etazolate was added during the 1h *t*BHP incubation (*t*BHP + Etaz 2µM, 1h). The intracellular ROS level was detected by DCFH-DA fluorescent probe. (a) Representative pictures of DCF-stained (FITC channel) and PI-stained (PE channel) were obtained from control (Ctrl), *t*BHP-treated (*t*BHP) and *t*BHP /Etazolate-treated cells with the three tested protocols. (b) Representative picture of the mean fluorescence intensity (MFI) of DCF measured on DCF^+/PI^-cells. (c) Quantitative analysis of the DCF fluorescence expressed as geometric mean. (d) Quantitative analysis of the percentage of PI^+ cells. Results are expressed as the fold change compared to that of the control group. Values are the mean ± SEM of 5 experiments. Student's unpaired *t*-test. , *: p<0.05; **: p<0.01; ***: p<0.001.

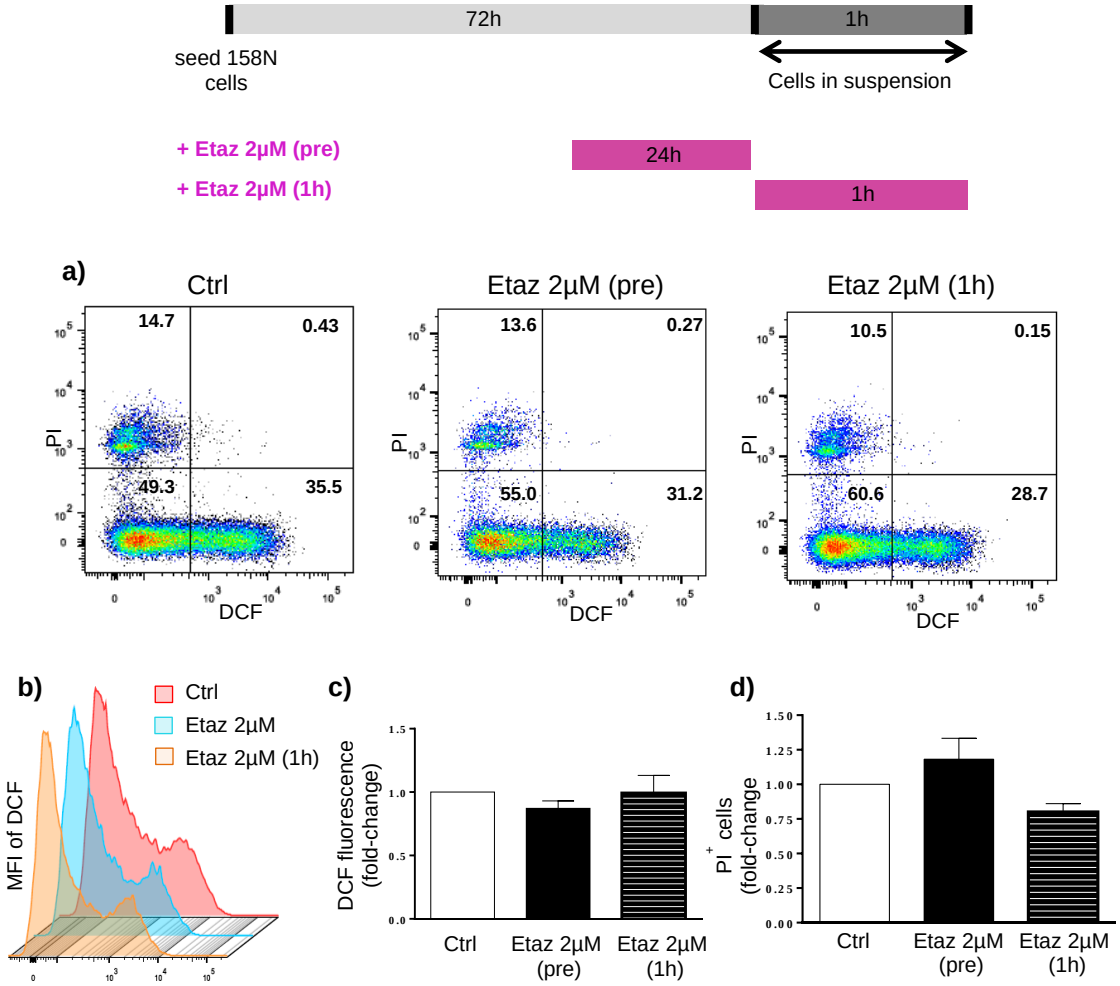

Figure 69: Effect of etazolate on the level of intracellular ROS in 158N cell line without *t*BHP treatment. Etazolate at 2 µM was tested using two different protocols: i) etazolate in pre-treatment was added 24h before the trypsination of cells (Etaz 2µM, pre), ii) etazolate was added on cells in suspension for 1h before the FACS analysis (Etaz 2µM, 1h). The intracellular ROS level was detected by DCFH-DA fluorescent probe. (a) Representative pictures of DCF-stained (FITC channel) and PI-stained (PE channel) were obtained from control (Ctrl) and Etazolate-treated cells with the two tested protocols. (b) Representative picture of the mean fluorescence intensity (MFI) of DCF measured on DCF^+/PI^- cells. (c) Quantitative analysis of the DCF fluorescence expressed as geometric mean. (d) Quantitative analysis of the percentage of PI^+ cells. Results are expressed as the fold change. Results are expressed as the fold change compared to that of the control group. Values are the mean ± SEM of 5 experiments. Student's unpaired *t*-test.

THIRD PART

During my pre-doc training (Unipharma Graduates program), I was also involved in the PhD project of Gemma Llufriu-Dabén, where the aim was to study the remyelinating potential of a neuroprotective compound, etazolate, as an α-secretase activator. I participated in this project by showing that etazolate is able to restore the number of myelinated axons in an *ex vivo* model of lysolecithin-induced demyelination in mouse cerebellar organotypic slices (see **Annexe**, Llufriu-Dabén et al., 2016 under revision) as described below.

Effect of etazolate on myelin sheaths in a model of lysolecithin-induced demyelination *ex vivo*

Etazolate restored the number of myelinated axons following demyelination

As shown in the ***Figure 70*** (or **Fig. 1 Annexe**) lysolecithin did not affect the number of total axons, marked with Calbindin in red, whereas it induced a demyelination. In fact the myelin sheaths, stained with MAG antibody in green, clearly presented a sparse staining, featuring damaged sheaths (**Fig. 70a**).The percentage of myelinated axons was decreased by 50% after lysolecithin treatment. Etazolate was able to restore significantly the percentage of myelinated axons by 25% ($p<0.001$) for the dose of 0.2 µM and by 27% ($p<0.001$) for the dose of 2 µM with no difference between the two doses (**Fig. 70c**). Moreover etazolate had no effect by itself (without lysolecithin) on the percentage of myelinated axons (**Fig. 70b**).

Further work by our group described the therapeutic interest of etazolate in white matter protection and repair by protecting myelin sheaths, enhancing oligodendrocyte differentiation and remyelination process after demyelination *ex vivo*. The beneficial effects of etazolate are blocked by an α-secretase ADAM10 inhibitor suggesting that α-secretase ADAM10 is involved in the remyelinating effect of etazolate (for more details see Llufriu-Dabén et al., 2016 under revision, in Annexe).

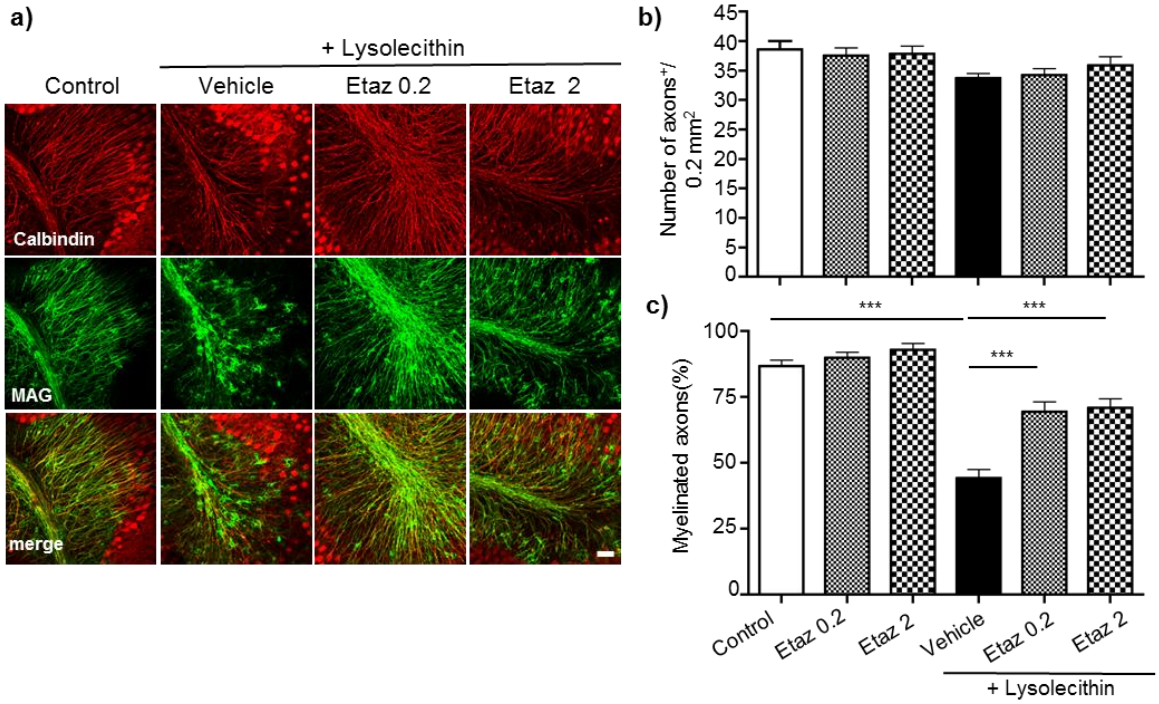

Figure 70: Effect of etazolate on myelin sheaths in a model of lysolecithin-induced demyelination *ex vivo*. Cerebellar organotypic slices were treated at 7 DIV with lysolecithin or its vehicle (methanol:chloroform) for 16h. Then they were treated with etazolate (0.2 or 2 µM) or its vehicle (PBS), for 72h. (a) Double immunostaining for calbindin (Purkinje cells, red) and MAG (myelin sheaths, green) was performed. Scale bar: 50 µm. (b) The number of total axons was not affected by lysolecithin and pharmacological treatments. (c) The percentage of myelinated axons was decreased by lysolecithin treatment, and restored significantly after etazolate treatment. Moreover etazolate had no effect by itself (without lysolecithin) on the percentage of myelinated axons. Results represent the mean±SEM of four independent experiments. One way ANOVA followed by Bonferroni post-hoc test, ***: $p<0.001$.

DISCUSSION

TBI exhibits heterogeneous damage with different impacts on the survival of oligodendrocytes and the myelin integrity (Armstrong et al., 2016). There are increasing clinical and experimental evidences suggesting that demyelination may play an important role in the pathophysiology of TBI showing degeneration of white matter, as loss of myelin and oligodendrocytes that can persist years after a single TBI (Bramlett and Dietrich, 2002; Caprariello et al., 2012; Flygt et al., 2013, 2016; Johnson et al., 2013; Tomaiuolo et al., 2012). All these studies demonstrated that myelin is early affected after TBI, however, the pathophysiological mechanisms underlying this loss of myelin are not yet well known.

The aim of this PhD project was to understand the response of oligodendrocytes and the fate of myelin proteins and myelin sheaths following stretch-induced traumatic injury. The development of *in vitro* and *ex vivo* models of traumatic injury was necessary for the analysis and the comprehension of this response. Since strain is known to be an important component of TBI leading to tissue damage (Ellis et al., 1995), we focused our attention on the development of a stretch-induced injury. Numerous studies were performed on different CNS cell types, but oligodendrocytes have received less attention. Oligodendrocytes are known to be mechanosensitive. To date, some studies attempted to explore the effect of a mechanical stimulation on OPCs and oligodendrocytes (**see introduction, Table 2**) (Arulmoli et al., 2015; Hernandez et al., 2016; Jagielska et al., 2012; Lourenço et al., 2016; Rosenberg et al., 2008; Urbanski et al., 2016). Nevertheless, only one study utilizes stretching as mechanical stimulus (static equibiaxial strain at 10% for 3 to 7 days) in order to differentiate primary neural stem and progenitor cell into neurons, astrocytes or oligodendrocytes (Arulmoli et al., 2015). It is a different context, since they studied the effect of stretch with a low strain on cell differentiation and not the effect of trauma, as stretch with high strain, on oligodendrocytes. Therefore, no study has addressed so far the effects of stretch-induced injury in oligodendrocytes.

The first part of this project was thus focused on the development of *in vitro* models of stretch-induced injury, in particular two different injuries that we defined as “mild” and “moderate”:

- Mild injury: equibiaxial static stretch of 20% strain for 20 hours
- Moderate injury: equibiaxial static stretch of 30% strain for 30 minutes

A strain of 20% and 30% deformation are in the range of stretch relevant to those occurring in humans after rotational acceleration-deceleration injury (Margulies et al., 1990; Meaney et al., 1995). It has been estimated that brain injury occurs at strain between 10% and 65% at strain rates of approximately 10-50 s^{-1} (LaPlaca and Thibault, 1997; Morrison et al., 1998; Morrison III et al., 1998). In our case, we did not want to mimic the rapid initial impact of TBI but the events that intervene secondary in the hours following TBI. That is why we chose a relatively long duration of stretch (30 min or 20h), regarding the cell response obtained to the strain of 20% or 30%.

As a consequence of TBI, the primary injury triggers a secondary complex cascade of metabolic, cellular and molecular alterations such as glutamate excitotoxicity, perturbation of calcium homeostasis, increase in free radical generation, mitochondrial dysfunction, inflammation, apoptosis and diffuse axonal injury (Xiong et al., 2013). The secondary injury occurs within seconds to minutes after the traumatic insult and can last for days, months, or even years.
Among the secondary events triggered following TBI the oxidative stress has a relevant role in the aetiology of progressive neuropathology in TBI (Abdul-Muneer et al., 2015). Free radicals are generated during normal physiological processes in a controlled way without damage for cells and tissue (Mendes Arent et al., 2014). However, under pathological conditions, as TBI, ROS can damage and oxidize macromolecules, such as DNA, proteins, carbohydrates, and lipids (Rodríguez-Rodríguez et al., 2014; Valko et al., 2006). It is noteworthy that the CNS is extremely sensitive to free radical damage, because of its relatively small total antioxidant capacity (Cornelius et al., 2013; Sultana et al., 2013). Besides, oligodendrocytes are particularly sensitive to oxidative stress because of their lipid-rich membranes, the lower glutathione reductase enzyme (GRx) activity, enzyme that reconverts GSSG in GSH, and finally the lower glutathione amount (French et al., 2009; Thorburne and Juurlink, 1996).

Response of oligodendrocytes and myelin to stretch

a) Response of oligodendrocytes to stretch-induced mild and moderate injury

For the evaluation of oligodendrocyte response to stretch-induced injury, three *in vitro* cellular models were chosen as the oligodendrocyte 158N cell line, the mixed glial primary culture and the oligodendrocyte-enriched primary culture. These different models were used

in order to evaluate different aspects of the cellular response, adapting the choice of the model to the biological process studied. In this context, we evaluated the response of oligodendrocytes to a stretch-induced injury based on cellular morphology, cell death, cellular redox status, the stretch effect on myelin genes and proteins and finally the activation of particularly stretch-responsive pathways.

Stretch affects cell adherence and induces cell retraction (mild injury) and severe cellular damage (moderate injury) in oligodendrocytes from oligodendrocyte-enriched primary culture

In order to analyse the effect of stretch on oligodendrocyte morphology, we used the oligodendrocyte-enriched primary culture, a primary culture with more than 95% of oligodendrocytes, excluding astrocytes and microglia. In general, the oligodendrocyte-enriched primary culture is a very delicate culture and after several attempts we were finally able to perform a healthy culture of oligodendrocytes on silicone membrane and thus apply our two models of stretch-induced injury. This cellular system allows a deeper evaluation of cellular morphology that is not possible in the cell line. Cells differentiate through different developmental stages typical of the oligodendrocyte lineage. Precursors are PDGFR-α^+ with more or less branches, while mature oligodendrocytes are MAG^+ and form “myelin-like” membranes according to *in vitro* studies (Baumann and Pham-Dinh, 2001; Jackman et al., 2009; Simons and Nave, 2016). In our experimental conditions, after 2 days in culture, oligodendrocytes are immature at 85% and mature at 15%, and this proportion is not changed following mild injury, suggesting the absence of stretch effect on oligodendrocyte differentiation.

However, when cells are subjected to the mild injury, a significant decrease in cell adherence is observed after stretch. The adherent cells appear smaller and less developed as confirmed by a significant decrease of cell surface in both immature (PDGFR-α^+) and mature (MAG^+) oligodendrocytes following stretch suggesting that the stretch induces cell retraction. Nevertheless, the proportion of mature and immature oligodendrocytes after stretch remains identical meaning that they are equally affected by stretch. When oligodendrocytes are submitted to stretch-induced moderate injury, cells are again less adherent. However, due to a more severe cellular damage after moderate injury, cellular branches appear to be disrupted and it compromises the identification of the real shape of cells as MAG^+ or PDGFR-α^+. Thus, the analysis of cell surface and ramifications become impossible. It is noteworthy that cells that are detached following mild or moderate injury are not able to re-adhere to the membrane, since the number of adherent cells is still reduced 24h after stretch. These findings suggest that detached cells are not alive and they undergo cell death in the hours following stretch.

Cells can respond to a mechanical stretch by increasing or by decreasing their spread area, generally as a function of stretch magnitude and strain frequency, if a dynamic stretch is applied. For example, a cyclic equibiaxial stretch of 10% in aortic endothelial cells decreases cell spreading at 1Hz, but not at 0.01Hz. Cells retract to ~80% of their original area after 5 min and maintained this retracted area throughout the 60 min of experiment (Hsu et al., 2010). Studies also demonstrated that strain can compensate for reduced stiffness. Cui and coworkers showed in fibroblasts that cell spreading, reflected by the total cell area, and stress fiber formation on soft substrates is possible if simultaneous cyclic stretching at low magnitude (1-5%) and low frequency (optimum 0.1 Hz) compensate for the lack of substrate stiffness-induced cell stress. On the other hand, strain at higher magnitude, 15%, reduced the cell area even at low frequency (Cui et al., 2015). In fact, valvular interstitial cells exhibit a rounded morphology on soft static substrate but spread to the same extent as those cultured on stiff substrate upon application of 10% cyclic equibiaxial stretch. Nevertheless cells grown on stiffer substrate are bigger but they reduce their area when the same 10% equibiaxial stretch is applied (Throm Quinlan et al., 2011). In general, the stiffness of substrate and the mechanical force are both important for the cell response and impact on cell morphology. In neurons, neurite growth is also dependent on applied tension. If tension is kept above a resting threshold, axons grow but if tension is released to below the resting tension level, axons retract (Franze et al., 2009; Loverde et al., 2011; Zheng et al., 1991). Taken together, given that the magnitude of strain is relatively elevated in our model, the strain at 20% results in a reduced cell area or cell retraction, while the strain at 30% results in a more severe damage that compromises the analysis of cell morphology.

Both mild and moderate stretch-induced injuries induce ROS production and protein oxidation in oligodendrocytes from 158N cell line

For the study of ROS production we chose as a cellular model, the oligodendrocyte 158N cell line, being more suitable for this kind of study. In fact, it was not possible to perform FACS analysis and biochemical dosages in the oligodendrocyte-enriched primary culture because of cell fragility and low cell density. A stretch-induced mild injury did not induce cell death but caused a significant increase in the production of ROS, resulting in the oxidation of protein (AOPP) and decrease in GSH level, accompanied by a decrease of glutathione peroxidase (GPx), the enzyme that converts H_2O_2 in water using 2GSH. Glutathione is the first line of defence and it is able to efficiently scavenge reactive species. Therefore, the measurement of both reduced glutathione (GSH) and glutathione disulfide (GSSG) is often used as an indicator of the oxidative stress status. A decrease of the ratio GSH/GSSG indicates a shift to an oxidized form of GSH, suggesting the presence of oxidative stress at the cellular or tissue

level (Dalle-Donne et al., 2006; Durackova, 2010; Tunez et al., 2011). In our system, it was not possible to detect GSSG but the dosage of GSH revealed a significant decrease of GSH following stretch-induced injury, indicating an alteration in the glutathione equilibrium.
Mixed glial cells subjected to a mild injury did not show cell death too and they present a similar profile concerning the oxidative stress markers, with an increase of protein oxidations and carbonyls. If compared to the cell line response to stretch, the glutathione system was not altered in mixed glial cells. This could be explained by the presence of astrocytes in the mixed glial cell culture, given that astrocytes are very rich in GSH and they present stronger antioxidant defence that protects the culture against GSH depletion (Juurlink et al., 1996; Ljubisavljevic, 2016; Wilson, 1997). Nevertheless, the antioxidant capacity of astrocytes was not enough to counteract the increase in protein oxidation and carbonyls in our system.

Both mild and moderate stretch-induced injuries induce an alteration of pro- and antioxidant systems in oligodendrocytes

Given the increase in ROS production and the alteration of oxidative stress markers, we decided to investigate more deeply on the cellular oxidative redox status analysing the pro/antioxidant systems in our 158N cells. As one of the principal antioxidant enzyme, we analysed the SOD activity. Mild stretch induced an increase of both *Sod-1* (cytoplasmic isoform) and *Sod-2* (mitochondrial isoform) at mRNA level but it did not result in an alteration of SOD activity. The expression of the transcription factor Nrf-2 was also analysed, since Nrf2/ARE pathway is a major determinant of phase II antioxidant enzyme induction (Espinosa-Diez et al., 2015; Zhang et al., 2013). Upon exposure to ROS, Nrf2 is released from the Keap1-Nrf2 complex and it translocates from the cytoplasm to the nucleus, where it sequentially binds to the antioxidant response element (ARE), a regulatory enhancer region within gene promoters. This binding induces the production of many phase II detoxifying and antioxidant enzymes such as HO-1 and NQO-1, which protect cells against oxidative stress (Jain, 2005; Radjendirane et al., 1998). In 158N cell line, the mild injury did not affect *Nrf-2* expression, nevertheless the expression of the anti-oxidant genes *Ho-1* and *Nqo-1* was increased.
In general after mild injury, cells from 158N cell line presented an activation of the antioxidant system showing that cells are fighting against the oxidative stress, they are able to activate their defence system. Instead cells of the mixed glial primary culture present an opposite profile where the expression of all antioxidant genes was decreased. This difference in the cell response is probably due to the presence of astrocytes. Maybe the antioxidant response was enhanced at the earlier time point and later on, after the 20h of stretching, where cells were analysed, the antioxidant system was downregulated due to a negative feedback.

Considering the pro-oxidant system, in general the principal cellular sources of ROS are the NADPH oxidases and mitochondria. ROS can in fact be generated both enzymatically, e.g. during the NADPH oxidase reaction, and non-enzymatically in the mitochondrial respiratory chain. (Angeloni et al., 2015; Brennan et al., 2009; Dayem et al., 2010; Inoue et al., 2003; Liu et al., 2002). Regarding mitochondria, these organelles are responsible of a continuous production of ROS due to the electron transport chain located in the mitochondrial inner membrane, which is essential for the energy production inside the cell (Inoue et al., 2003; Valko et al., 2006). Stretch is reported to alter the mitochondrial potential in astrocytes and neurons. In particular a rapid stretch corresponding to a mild (31%) and moderate (38%) injury decreases ΔΨm in astrocytes that recover at time 24h after stretch. In neurons ΔΨm drop only after severe injury (54%) and they do not recover (Ahmed et al., 2000). Another study shows that neurons subjected to stretch-induced injury (30% for 1 sec) exhibit a rapid decrease in mitochondrial potential that recovers within hours. If stretch is combined with NMDA administration, neurons are more sensitive and they never recover (Arundine, 2004). In this work we analysed the expression of *Duox-1*, member of the NOX/DUOX family of NADPH oxidases, and it was found to be increased after a mild injury in 158N cell line while it was not detectable in the mixed glial culture and oligodendrocyte-enriched primary culture. We also tried to assess others members of the NADPH oxidases (*Nox-1, Nox-2, Nox-3, Nox-4)* but they were not detectable in our system by RT-qPCR. Our results regarding the pro-oxidant system are preliminary and need to be completed with an analysis of other sources of ROS as mitochondria. However, we can expect that in 158N cell line, the free radicals are produced in part by *Duox-1* after stretch-induced mild injury. The expression of almost all genes (except *Ho-1* and *Cnp*) in the case of 158N cell line and also all genes in the case of mixed glial culture was back to normal level at 24h after the end of the stretch. These suggest that stretch-induced alteration in gene expression was transitory.

Cells from the 158N cell line were also submitted to the moderate injury, at 30% of strain for 30 min. The cell response was compared to that obtained after mild injury, 20% at 20h, and discussed in the article 1. The moderate injury also resulted in an increase of free radicals that attack proteins without cell death, and this attack seems to be more powerful compared to the mild injury.

Interestingly the moderate stretch induced an opposite response to stretch in 158N cell line regarding the antioxidant system. The expression of both *Sod-1* and *Sod-2* was decreased as well as the SOD activity. Moreover the moderate injury resulted in a decrease in the expression of *Nrf-2*, even if it was not confirmed at protein level, and the antioxidant genes *Ho-1* and *Nqo-1* showed a tendency to decrease. Overall, the moderate stretch at 30% induced an opposite response compared to mild stretch. Thirty minutes appeared to be

enough to reduce the antioxidant defence. This confirms that the stretch-induced moderate injury is more severe than the mild injury and cells are not able to properly activate the antioxidant response in order to counteract the oxidative stress. Nrf2 protein has a rapid turnover in basal condition (7-15 min) (McMahon et al., 2004; Nguyen et al., 2003). This maybe explain why in our cell line we found a decrease in the antioxidant response, it is possible that stretch decreases Nrf2 within 30 min and, in turn, the expression of antioxidant genes.

Regarding the expression of the pro-oxidant gene *Duox-1*, it did not seem to be affected after moderate stretch. As already discussed above, our investigations to find out the origin of ROS after mild and moderate injury are preliminary and need to be completed assessing other sources of ROS. However it seems that ROS comes from two different mechanisms in our injury models: activation of pro-oxidant systems for the mild injury as suggested by the activation of *Duox-1* and decrease of the antioxidant defence for the moderate injury. In this case the increase of ROS is not due to an overproduction but to an improper antioxidant defence.

We also assessed the expression of the antioxidant genes in oligodendrocytes from the oligodendrocyte-enriched primary culture. The effect of stretch on these genes does not show any modification after mild injury, while it does alter the expression of *Sod2* (decrease) and *Ho-1* (increase) after moderate injury. The absence of effect after mild injury may be related to the non-activation of antioxidant defence, or more probably related to the long period of stretch (20h). Technically, it is not possible to evaluate the effect of mild stretch at the early time points since the period of stretch is long (20h), so the systems may be altered but during the time of stretch they come back to normal level. In the model of moderate injury, since the strain is more severe and the period of stretch is shorter (30 min), we found an alteration in the expression of some of antioxidant genes, as an increase in *Ho-1*, and a decrease in *Sod2*.

Both mild and moderate stretch-induced injuries affect myelin genes and PLP protein in oligodendrocytes

The main objective of this work was to understand if stretch-induced injury causes oligodendrocyte loss and demyelination. To answer this question we analysed the effect of stretch on the expression of three myelin genes *Plp, Mag* and *Cnp* and the PLP protein when possible. In the cell line, the mild injury did not have any effect on PLP (both mRNA and protein) but it increased the expression of *Mag* and *Cnp.* The mixed glial culture responded

to mild injury by decreasing the expression of the myelin genes. Given that oligodendrocytes represent only the 20% of total cells in this culture, the amount of myelin proteins become insufficient to be assessed by western blot. Overall, oligodendrocytes are affected by stretch-induced mild injury, either in mixed glial culture where they are in minority, or in 158N cell line culture, where the cell population is homogenous and the cell density is at 80% of confluence.

It is noteworthy that 158N cells respond differently to stretch-induced mild or moderate injury. In fact, following the moderate injury, there is a decrease of PLP at both mRNA and protein level. It is surprising that PLP is affected as early as 30 minutes after stretch. However, this effect remains transitory since PLP is back to control values at 24h post-stretch. Overall, the moderate injury seems to be more severe and affects the expression of one of the main myelin proteins. A study reported that nitric oxide (·NO) is able to down-regulate the expression of myelin genes PLP, MBP, MOG and CNP in human primary oligodendrocytes. Exogenous ·NO donors at different incubation time, starting from 3h, are able to suppress the expression of myelin genes with a maximal suppression at 12h (Jana and Pahan, 2013). We should assess the presence of reactive nitrogen species (RNS) in our system, in particular ·NO, in order to have a complete analysis on oxidative and nitrosative stress. It is possible that in our system there are some mechanisms involving ROS/RNS that results in PLP decrease. Malek and collaborators showed that the endothelin-1 (*ET-1*) gene is suppressed after shear stress in endothelial cells. Fluid shear stress is known to modulate ET-1 mRNA, in particular low shear increased its expression, while higher physiological levels of fluid shear induce a transient increase (within 1 h) and then a sustain decrease at times greater than 2h. The suppression of gene expression is magnitude-dependent and it requires intracellular calcium influx, the microtubule network (but not the microfilament network) and, among the mechanosensitive channels, the shear-activated K^+ channel, I_{KS} (Malek et al., 1993, 1999). We can expect that our gene downregulation may be due to a ROS-dependent mechanism or/and to the activation of mechanosensitive channels and calcium influx. Overall our data support that stretch-induced moderate injury results in loss of PLP myelin protein.

The effect of stretch on the expression of myelin genes was also evaluated in the oligodendrocyte-enriched primary culture resulting in a decrease of *Mag* following mild injury and a decrease of *Plp* following moderate injury. In both injury models, the expression of myelin genes is decreased, in line with above data showing an altered morphology of oligodendrocytes.

Both mild and moderate stretch-induced injuries alter MAPK pathways in oligodendrocytes

We also attempted to study the signalling pathways that were responsive to stretch-induced injury in 158N cell line. We focused our research on one of the signalling pathways, known to be stretch-responsive, the mitogen-activated protein kinases (MAPKs), which consist of three principal subgroups, extracellular signal-regulated kinases (ERKs), c-Jun NH2- terminal kinases (JNKs) and p38. JNKs and p38 also known as stress-activated protein kinases (SAPKs). MAPKs regulate different cellular processes as cell survival, proliferation, differentiation, and migration (Pearson et al., 2001), and they are also known to be involved in mechanically induced signalling in various cell types being involved in the signal transduction from the cell membrane to the nucleus. It has been demonstrated that isoforms of JNK, ERK and p38 were phosphorylated in a tension-dependent manner in rat skeletal muscle preparations (Martineau and Gardiner, 2001) and endothelial cells (Hsu et al., 2010; Kaunas et al., 2006; Kito et al., 2000).

MAPK family has indubitably an important role in the transduction of mechanical forces but the activation of different MAPK is strictly dependent on the cell type. ERK is activated in retinal capillary pericytes (Suzuma et al., 2002) and cardiac tissue (Domingos et al., 2002; Takeishi et al., 2001) but not in bladder smooth muscle cells (BSMCs) either following cyclic (Nguyen et al., 2000) or static (Kushida et al., 2001) stretch. Instead, in BSMCs both JNK and p38 are activated within 30 min following stretch (Nguyen et al., 2000). In cardiac fibroblast, the JNK/SAPK pathway is activated in response to a static, equibiaxial stretch, while the p38 SAPK2 pathway is not (MacKenna et al., 1998). In mesangial cells, a 29% cyclic stretch activates the ERK- MAPK and p38 SAPK2 pathways while JNK/SAPK pathway is not activated. The same cyclic stretch at a lesser intensity, 20%, only activates ERK-MAPK and not the other MAP kinases (Ingram et al., 1999).
Finally, mechanical injury activates in CNS glial cells, as astrocytes, ERK (Neary et al., 2003), and p38 (Zhou et al., 2011). The authors reported that ERK activation is dependent on the rate and magnitude of injury when astrocytes are subjected to a rapid, and reversible stretch-induced injury (Neary et al., 2003).

To date, no data on stretch-induced MAPKs pathway activation are reported for oligodendrocytes. Thus we decided to analyse this pathway in the 158N cell line subjected to stretch. Our results showed that ERK is inhibited after both mild and moderate injury, while JNK is activated after mild injury only. A recent study showed that the Ras/Raf/MEK/ERK pathway signalling can be inhibited through the activation of the stress-activated JNK cascade. In fact some components of the ERK pathway, as RasGEF Sos1 and the Rafs, are

phosphorylated on multiple sites in response to JNK activation and the hyperphosphorylation of these sites renders the Rafs and Sos1 unresponsive to upstream signals. This phospho-regulatory circuit is engaged by cancer therapeutics, that activates JNK through mitotic and oxidative stress (Ritt et al., 2016). We cannot exclude a similar pathway regulation in our system, even though ERK is downregulated also after moderate injury, when JNK is not activated. We should extend our study to p38, however, it seems that overall the MAPK pathways are altered by stretch in oligodendrocytes. MAPKs isoforms are preferentially activated by distinctive stimuli, ERK generally is more involved in cell division, migration, and survival, while p38 and JNK are more responsive to cellular and environmental stresses (Hoefen and Berk, 2002; Kyriakis and Avruch, 2012; Owens and Keyse, 2007; Vezza et al., 2016). In our system, given the activation of JNK following stretch, it confirms that mechanical stretch activates the JNK/SAPK pathway known to respond to environmental stresses. However, the activation of JNK in our model seems to be strain-dependent since it is not activated following stretch-induced moderate injury.

Taken together, we developed for the first time two *in vitro* models of stretch-induced injury, mild *versus* moderate injury, to decipher the cellular and molecular response of oligodendrocytes in three different cellular models, 158N cell line, mixed glial culture and oligodendrocyte-enriched primary culture. Our data show that stretch results in ROS production and protein oxidation, alters MAPK signalling pathways, modifies the expression of myelin genes and results in loss of oligodendrocytes with important cellular morphological alteration suggesting that stretch is able to induce demyelination. Therefore, oligodendrocytes should be considered as a potential target to counteract stretch-induced demyelination.

b) Response of cerebellar slices to stretch-induced moderate injury

Stretch induces axonal swelling and APP accumulation in cerebellar slices

To deeply analyse the effect of stretch on myelin and demyelination, we decided to move to an *ex vivo* model of injury. The organotypic cerebellar culture was chosen for this study, since cerebellum is a tissue very rich in myelin (Notterpek et al., 1993). The organotypic culture preserves the 3D architecture of cerebellum maintaining the *in situ* connections between all different cell populations. When I started my PhD, there were no models available to study a stretch-induced injury in cerebellum. The first step was to perform a successful culture of cerebellar slices on the silicone membrane of the Bioflex® Plates. This was made possible through a collaboration with the pioneer of stretch-induced injury model

using organotypic cultures, Pr Barclay Morrison III and his team at the Columbia University (Neurotrauma and Repair Laboratory, Biomedical Engineering Dpt, New York). They work on a model of stretch-induced injury in hippocampal organotypic slices and they are the only specialists for the culture brain slices on silicone membrane. Thanks to a 3-month-mobility grant from *Institut de Formation Doctorale* (Paris Descartes University), I had the opportunity to learn this technique and then I adapted it to our tissue, the cerebellum, and at our stretching device, the Flexcell® Tension System. This experience allowed me to greatly improve our experimental conditions in order to obtain a successful organotypic culture on silicone membrane. Slices are grown for 7 DIV before being subjected to a stretch-induced moderate injury and different analysis are performed at different time points after stretch, 0h, 24h and 72h.

In order to study the effect of stretch, we first analysed if the stretch induces an axonal injury in cerebellar slices. Stretched slices showed an accumulation of amyloid precursor protein (APP), a marker of axonal injury, immediately after stretch (0h) and persisting at least 72h after stretch. The co-staining with SMI-312 (neurofilament marker) confirms that there is an axonal swelling in line with APP accumulation, as sign of altered axonal transport (Tang-Schomer et al., 2012). APP accumulation is recognised as the gold-standard for the identification of axonal pathology (Gentleman et al., 1993; Sherriff et al., 1994), so we can affirm that our slices present an axonal traumatism that is a typical consequence of TBI.

Stretch alters the structure of paranodal junctions in cerebellar slices

We also analyse the effect of stretch on paranodal junctions, located between the nodes of Ranvier and the juxtaparanodal junctions. The paranodal complex is a structure that connects myelin and the axonal membrane and mechanical stretch appears to initially damage axons at the nodes of Ranvier and in the adjacent paranode regions (Maxwell, 1996; Maxwell et al., 1991; Reeves et al., 2012; Sun et al., 2012). The structure of the paranodal junctions was evaluated at time 0h and 72h after stretch, using anti-Caspr to label Caspr, an integral component of the paranodal complex, and anti-MAG to visualize the myelin sheaths. Caspr staining appeared “elongated”, more diffuse in stretched slices than in control slices at both 0h and 72h after stretch. This suggests an alteration of the paranodal junctions that starts immediately after stretch and persists for at least 72h. This is in line with another study where paranodal myelin damage is reported in an *ex vivo* model of stretch-induced injury in guinea pig spinal cord (Sun et al., 2012). It is impossible to discriminate about a primary paranodal demyelination that is inflicted by the mechanical stretching of an axon and that occurs immediately following axonal stretch injury and a secondary demyelination occurred at a later time. A study showed that primary paranodal demyelination

modulates axonal depolarization in a model of axonal injury. The paranode regions, that flank the nodes, contain the voltage-gated potassium channels in high density and the injury-induced paranodal demyelination modulates potassium accumulation and membrane depolarization that, in turn, affect the axonal transition to degradation. They proposed that the extent of paranodal demyelination should be considered as an “injury parameter” that is likely to determine the stability of axonal function in the temporal window of minutes post trauma (Volman and Ng, 2014). Moreover the width of the nodes of Ranvier is crucial for a fast conduction. In fact, in normal myelinated axons the conduction velocity is inversely related to the node width. A study on a mathematical model of myelinated axons showed that even small mechanical retractions of myelin from narrow nodes or slight loosening of paranodal myelin can cause large changes in myelinated nerve conduction velocity (Babbs and Shi, 2013). Taken together, stretch-induced moderate injury in cerebellar slices may affect nerve conduction velocity since stretch results in alteration of paranodal junctions at t0 and t72 post-stretch (preliminary data), suggesting stretch-induced primary and secondary paranodal demyelination.

In line with these observations, we did not however see any modification in the intensity of CaBP and MAG immunolabeling following stretch in cerebellar slices. It may be due to the fact that the demyelination is more focused on paranodal junctions and it may not spread to the whole myelinated fibers of Purkinje cells as labeled by CaBP and MAG. Therefore, complementary analyses by electronic microscopy are necessary to conclude.

Stretch alters the expression of antioxidant and myelin genes at 24h post-stretch in cerebellar slices

The effect of stretch-induced moderate injury was also analysed at the molecular level in cerebellar slices. Unexpectedly, oxidative stress markers as AOPP, carbonyls, thiols and GSH are not affected at time 0h post-stretch. It is possible that the cerebellar tissue has sufficient compensatory systems that protect cells against oxidative stress at time 0h, but maybe not at later time points after stretch. Therefore, it should be interesting to assess all these parameters at 24h and 72 after stretch. In addition, at 24h after stretch, and not at 0h, stretch alters the expression of antioxidant (*Sod, Nqo-1* and *Ho-1)* and myelin genes (*Plp*) suggesting that in cerebellar tissue the response to stretch needs more time to take place. In our experimental conditions, the analyses of myelin proteins by western blot show no modifications of the amount of PLP and MBP at 72h after stretch. It may be possible that the time point analysed was not appropriate for myelin proteins and that stretch alters transiently these proteins at an earlier time point. Indeed, in our cell line model, stretch results in a decrease of PLP immediately after stretch and not at 24h. It has to be also considered that

our antibody used for western blot does not allow to discriminate between proteins within intact myelin and debris.

Stretch activates the MAPK pathways in cerebellar slices

We also attempted to study the effect of stretch-induced moderate injury on MAPKs activation in cerebellar slices. The analysis of MAPKs in cerebellar slices showed an increase in the activity of both ERK1/2 and JNKs, in particular the 46 kDa isoform. This suggests an activation of MAPKs following stretch that is compatible with the role of the MAPKs as points of convergence for various signalling cascades regulating gene expression. Compared to 158N cell line, stretch-induced moderate injury results in ERK inhibition with no effect on JKNs. As discussed earlier, the activation of MAPKs is cell-dependent and in cerebellar slices different subpopulation of cells are present conditioning the final response.

c) Possible mechanisms involved in the response of oligodendrocytes and cerebellar slices to stretch

In general we can hypothesize several mechanisms explaining the biochemical/biophysical responses occurring in damaged cells/slices after the application of tensile strain: i) direct effect on cytoskeleton by the physical forces applied to it and consequent alteration of cell morphology, ii) influx of free calcium which activate proteases causing a widespread proteolysis of different molecules, and iii) increase in ROS production resulting in damage and oxidize macromolecules.

i) Stress fibers are anchored to focal adhesions, which consist of integrins and many other so-called focal adhesion proteins, as vinculin, that serve to physically connect the extracellular matrix to the actin cytoskeleton and to sense mechanical forces (Cramer et al., 1997; Naumanen et al., 2008). Early studies on fibroblasts, arterial smooth muscle cells and endothelial cells showed that cyclic uniaxial strain results in either perpendicular or oblique alignment of the cells and stress fibers relative to the strain axis (Buck, 1980; Dartsch and Betz, 1989; Dartsch et al., 1986), while cyclic equibiaxial stretch results in no cell or stress fiber alignment in endothelial cells (Kaunas et al., 2006; Wang et al., 2001). In our experimental condition, we applied a static equibiaxial stretch, and it doesn't not result in cell alignment as described above in the case of cyclic equibiaxial stretch, suggesting that absence of cell alignment is more related to equibiaxial stretch rather than its frequency as static or cyclic. Overall, static equibiaxial stretch can influence the dynamics of focal adhesion acting on integrins and promoting disorganisation and/or disruption of cytoskeletal

components, resulting in cell retraction or cytoskeletal damage as observed in our mild and moderate injury in oligodendrocyte-enriched primary culture, respectively.

ii) As a consequence of the traumatic impact to the brain, a depolarization of nerve cells take place resulting in uncontrolled and excessive release of excitatory neurotransmitters. This cascade of pathological events is called excitotoxicity and the main responsible is the release of glutamate. Excitotoxic cell death is deeply linked to the downstream calcium influx modulation and dysregulation. In fact, excessive extracellular glutamate initiates a massive influx of Ca^{2+} and Na^{+} into neurons and glial cells (Choi, 1987). Glutamate is able to bind different ionotropic receptors as NMDA receptors, AMPA receptors and the kainate receptors (KARs) and the metabotropic glutamate receptors (mGluRs) over activating the ion channels responsible for Na^{+} and Ca^{2+} influxes (Faden et al., 1989; Park et al., 2008). All these glutamate receptors are expressed in oligodendrocytes (Gudz et al., 2006; Káradóttir et al., 2005; Kolodziejczyk et al., 2010), so it is possible that, following stretch-induced injury, a massive entry of Ca^{2+} is triggered in our cells activating calcium-dependent proteases and resulting in cellular damage. Moreover the NMDA receptor is also a known mechanosensor in the central nervous system, it can “sense” the forces that are applied during a traumatic injury (Kloda et al., 2007; Paoletti and Ascher, 1994; Zhang et al., 1996). NMDA receptor in fact mediates stretch-induced calcium influx leading to neuronal excitotoxicity and it is considered one of the common mediators for the acute and progressive events that occur following TBI (DeRidder et al., 2006; Faden et al., 1989; Geddes-Klein et al., 2006; Singh et al., 2012).

Another way that in fact can provoke a Ca^{2+} influx in response to mechanical stress is *via* specialized mechanosensitive ion channels (MSCs). Ion channels that appeared to be activated by swelling or stretch were first described in 1984 using patch-clump analysis (Guharay and Sachs, 1984). Mechanical forces govern the gating of these channels, the most common type of MSC is the stretch-activated channel (SAC), (Bass et al., 2003; Franco-Obregón and Lansman, 2002; Martinac and Hamill, 2002; Yamaguchi, 2004), but there are also examples of stretch inactivated channels (SICs), that are active at rest and are closed by tension (Chakfe and Bourque, 2001; Franco-Obregón and Lansman, 2002; Martinac and Hamill, 2002; Schumacher et al., 2000). SACs are expressed in glial cell as astrocytes and microglia (Eder et al., 1998; Islas et al., 1993). A study demonstrates that the stretch-activated ion channel Piezo1 directs the lineage choice in human neural stem cells that have the ability to differentiate into neurons, astrocytes, and oligodendrocytes. Mechanical stimulation (induced using a glass pipette positioned on cells) provokes the activation of Piezo1 resulting in Ca^{2+} influx, a known modulator of differentiation, in a substrate-stiffness-dependent manner. Inhibition of this channel activity suppressed

neurogenesis and enhanced astrogenesis. Piezo1 knockdown also reduced the nuclear localization of the mechanoreactive transcriptional coactivator YAP (Pathak et al., 2014). We can hypothesize that these stretch responding channels are also expressed on oligodendrocytes and, as consequence of stretch-induced injury, they result in calcium influx.

Some Transient Receptor Potential (TRP) channels, ion channels located mostly on the plasma membrane, can be considered as mechanosensors, they are non-selective cation channels that serve as cellular sensors for a wide spectrum of physical and chemical stimuli including temperature sensing, chemosensing, nociception, photoreception and mechanoreception (Echeverry et al., 2016; Zheng, 2013).
According to their sequence homology, the TRP family can be divided into six subfamilies: TRPC (canonical), TRPM (melastatin), TRPV (vanilloid), TRPA (ankyrin), TRPP (polycystin), and TRPML (mucolipin). Some TRP family members have been identified in glial cells, as astrocytes and microglia (Echeverry et al., 2016; Shi et al., 2013). Considering oligodendrocytes, it is known that TRPC are expressed, in particular TRPC1 and TRPC3 (Fusco et al., 2004; Paez et al., 2011), and a recent study showed that also TRPA1 and TRPV3 are expressed. In particular TRPA1 is expressed in the cerebellum and oligodendrocytes of rats and mice, while TRPV3 is expressed only in rat (Hamilton et al., 2016). In oligodendrocytes, as controversial to the current ideas, ischemia does not damage myelin and oligodendrocytes by activating Ca^{2+} entry through ionotropic glutamate receptors in their membrane but through the activation of TRPA1 (Hamilton et al., 2016). Thus, ischaemic damage to oligodendrocytes differs fundamentally from that in neurons, where Ca^{2+} is raised by glutamate-gated receptors and only later by TRP channels that are modulated by ROS (Aarts et al., 2003). Another study showed, in rat exposed to infrasound, that the TRPV4 channel expressed in glial cells is able to mediate Ca^{2+} influx and thus, infrasound-induced neuronal injury (Shi et al., 2013). TRP channels can be activated and modulated by ROS, in particular by ·NO and $O_2^{\cdot -}$ (Aarts et al., 2003). In our cellular system, we can hypothesize that ROS activate these TRP channels that, in turn, mediate Ca^{2+} influx and all the consequences at the cellular and molecular levels. High cytosolic Ca^{2+} alters different cellular processes as protein phosphorylation, microtubule polymerisation and protease activation resulting in loss of cell function. Calcium-dependent enzymes can be activated, especially calpain-1 and -2 that are non-lysosomal cysteine proteases (Pike et al., 2000). In oligodendrocyte-enriched primary culture, stretch-induced moderate injury can result in cell damage with loss of oligodendrocyte branches. For 158N cell line, the effect is not obvious morphologically, since cell lines are in general more resistant. Nevertheless, the stretch has a marked effect on the expression of different genes resulting in an overall reduction.

iii) As discussed above, oligodendrocytes are highly sensitive to oxidative stress. In fact, they have physiologically limited antioxidant potential, opposed to the high energy demanded for myelination. If antioxidant systems are not properly regulated, cells are left vulnerable to oxidative and free radical damage (Li et al., 2005). Oxidative stress seems to be a critical player in the pathophysiology of demyelination as reported in different studies (Haider, 2015; Hamilton et al., 2013; Lee et al., 2012; Ljubisavljevic, 2016; Ljubisavljevic and Stojanovic, 2015; di Penta et al., 2013; Shi et al., 2015; Vladimirova et al., 1998).

Oxidative stress may contribute to axonal and myelin damage *via* several mechanisms. Proteins are oxidized in condition of oxidative stress, including the major myelin proteins as MBP and PLP that are altered and, as a consequence, more susceptible to trypsin degradation. Under *in vitro* conditions, myelin, being altered by oxidative stress, is easily subjected to degradation by the effects of extracellular proteases (Chaitanya et al., 2013). In general, proteins modified by oxidation are hydrophobic and more subjected to fragmentation, denaturation and aggregate formation with other oxidatively modified molecules (Park et al., 2006).
Moreover, delamination of myelin sheath makes new amounts of myelin components prone to being damaged by ROS. ROS can also attack lipids, damaging the membranes because of their high lipid content, given that ~70% of oligodendrocyte membranes are composed by lipids (Quarles et al., 2006). In addition, oxidative stress can contribute to an impairment of mitochondrial function due to an accumulation of mutations induced by ROS in mtDNA (Beal, 2005). This leads to an energetic failure and additional production of ROS worsening the situation. Axonal swelling and mitochondria accumulation are observed after TBI and this is consistent with disruption of microtubule by oxidative stress and consequent impairment of axonal transport (Counterman et al., 2006).

A link has also been established between oxidative stress and MAPKs. Several studies have in fact demonstrated that ROS can induce or mediate the activation of the MAPK signalling pathways (see for review Espinosa-Diez et al., 2015; McCubrey et al., 2006; Son et al., 2011). In general increased ROS production leads to the activation of ERKs, JNKs, or p38 MAPK, however the mechanism by which ROS can activate MAPK is not well understood. To give an example, ERK pathway is activated by MAP/ERK Kinase (MEK), which is in turn activated by Raf, a MAP3K. Raf is activated by the Ras-GTPase, whose activation is induced by receptor tyrosine kinases (RTKs) such as the epidermal growth factor (EGF) receptor. Ligand-independent clustering and activation of growth factor receptors in response to ROS have been demonstrated. For example, a study reported that oxidative stress induces EGF

receptor phosphorylation and activation, and H_2O_2 is proposed as critical mediator required for ligand-independent phosphorylation of this receptor in response to oxidative stress (Meves et al., 2001). The MAPK activation by ROS may also be due to the oxidative modification of the intracellular kinases. ASK-1, a member of the MAP3K superfamily for JNK and p38, binds to reduced thioredoxin in non-stressed cells. Following oxidative stress, the thioredoxin becomes oxidized and dissociates from ASK-1, thus leading to the activation of JNK and p38 pathways (Nagai et al., 2007). The activation of MAPK pathways can also induce antioxidant response element-mediated gene expression *via* a Nrf2-dependent mechanism (Yu et al., 2000).

In our system, the molecular mechanism by which oligodendrocytes receive the mechanical stress and convert it into biochemical signals remains to be elucidated. MAPKs should be activated by ROS or also they might be activated by the calcium influx following mechanical stretch.

Study of the antioxidant potential of etazolate *in vitro* and remyelinating properties *ex vivo*

Etazolate does not show an antioxidant effect on oligodendrocytes

The second part of my PhD project was devoted to the evaluation of the antioxidant potential of etazolate, a pyrazolopyridine derivate compound, that previously was showed, in part by our team, to be neuroprotective, anti-inflammatory and antioxidant *in vivo* (Désiré et al., 2013; Drott et al., 2010; Guo et al., 2014; Jindal et al., 2013, 2015; Siopi et al., 2013). In particular Jindal and colleagues demonstrated that etazolate has an antioxidant effect in an *in vivo* model of chronic unpredictable stress depression in mice attenuating the increase of oxidative markers in the brain, in particular it contrasted the lipid peroxidation and the nitrosative level and it normalized the reduced GSH level in brain and the activity of the anti-oxidant enzymes SOD and CAT, that were found to be reduced in depressed animals (Jindal et al., 2013). The same group confirmed this antioxidant effect in a model of olfactory bulbectomy-induced depression in mice where the etazolate contrasted the oxidative and nitrosative stress (Jindal et al., 2015).

In order to evaluate the antioxidant potential of this compound, we first developed an *in vitro* model of oxidative stress induced by *tert*-butyl hydroperoxide (*t*BHP) in the oligodendrocyte 158N cell line by analysing cell viability and ROS production, following its validation by assessing the effects of NAC treatment, a known powerful antioxidant, on our output analysis.

Our results showed that etazolate is not able to exert any protective or antioxidant activity in our model. In fact, etazolate was not able to protect cells against *t*BHP-induced cell death at the doses from 0.02 to 200 µM. It was not also able to reduce ROS production at 2 µM, even though etazolate at this dose is able to exert neuroprotective and remyelinating effect (Marcade et al., 2008; Llufriu-Dabén et al. 2016a, under revision).

The results showing an antioxidant effect of etazolate are obtained *in vivo* (0.5mg/Kg/day and 1mg/Kg/day) (Jindal et al., 2013, 2015) and it remains to be elucidated whether if the antioxidant effect of etazolate is direct or indirect by its anti-inflammatory effect. In our model, etazolate was tested only on oligodendrocytes. The potential antioxidant activity of etazolate has been tested in a model where *t*BHP induces an important production of ROS (20-fold increase). It is possible that ROS production in this model is too high to be reversed by etazolate. Nevertheless, compared to NAC treatment, NAC is able to counteract *t*BHP induced ROS production in our model. Therefore, we can conclude that previously reported beneficial effect of etazolate is not due to its antioxidant activity.

Etazolate contrasts demyelination in cerebellar slices

In addition, I was also involved in the PhD project of Gemma Llufriu-Dabén during my pre-doc training (Unipharma Graduates program), showing that etazolate is able to restore the number of myelinated axons in an *ex vivo* model of lysolecithin-induced demyelination in cerebellar organotypic slices (Llufriu-Dabén et al., 2016a under revision). Later on, in our team, we showed that etazolate has a remyelinating effect in the same model and this work is now continued by another PhD student in our team, Alex Carreté. Etazolate also reduces myelin loss in an *ex vivo* weight-drop model of trauma (Llufriu-Dabén et al., 2016b under revision).

Overall, our data support the protective effect of etazolate on myelin sheaths. So it could be interesting to treat cerebellar slices subjected to stretch with etazolate in order to see if it protects tissue from the stretch-induced traumatic axonal injury and myelin alteration. In addition, etazolate showed good tolerance and a good safety profile in a phase II clinical trial (Vellas et al., 2011), which is an important issue for a potential passage of etazolate in clinic for the treatment of TBI-induced demyelination in head-injured patients.

CONCLUSION AND PERSPECTIVES

The aim of this work was to decipher the response of oligodendrocytes and the fate of myelin proteins and myelin sheaths following traumatic event induced by stretch force. During my PhD, I developed two *in vitro* models, mild and moderate stretch-induced injury, using three cell systems, the 158N cell line, the mixed glial primary culture and the oligodendrocyte-enriched primary culture. In addition, I developed an *ex vivo* model of stretch-induced moderate injury in organotypic cerebellar slice culture.

The stretch-induced mild injury i) decreased the cell adherence and affected the cell morphology with a decrease of surface area in the oligodendrocyte-enriched culture, ii) induced an increase in ROS production, and protein oxidation and an alteration, in the expression of pro- and antioxidant genes in the cell line and in the mixed glial primary culture, ii) induced an inhibition of ERK and an activation of JNK, two proteins belonging to the family of MAP kinases, iii) modified the expression of the myelin genes but it did not modify the expression and the amount of the myelin protein PLP. The stretch-induced moderate injury on cells induced a more pronounced alteration of the cellular redox status with a decrease of PLP amount in the cell line. It also has a stronger effect on the cell morphology with a damage of cell ramifications in the oligodendrocyte-enriched culture. Cerebellar slices were subjected only to stretch-induced moderate injury, showing axonal swelling, APP accumulation, altered paranodal junctions and activation of MAPK pathways.

Oligodendrocytes and myelin response to stretch-induced injury

Regarding the oligodendrocyte response to stretch, we first assess PLP expression at mRNA and protein level in 158N cell line and the stretch-induced moderate injury, but not the mild, was able to reduce the amount of myelin protein PLP. This reduction could be due to different mechanisms. As reported in the discussion, ROS induce protein oxidation that, by consequence, makes the proteins more susceptible to degradation. Another hypothesis is that, PLP as a transmembrane protein, may be directly affected by mechanical stretch. Thus, to verify the involvement of ROS in stretch-induced myelin protein loss, it would be interesting to treat the stretched culture with an antioxidant compound, for example NAC, and to further analyse the cell responses to stretch.

In order to deeply analyse the effect of stretch on oligodendrocytes, we moved to the oligodendrocyte-enriched primary culture, a primary culture with more than 95% of oligodendrocytes. Oligodendrocytes responded to moderate injury by reducing cell adherence (following mild and moderate injury), decreasing cell spreading (mild injury) or resulting in severe cellular damage with loss of branches (moderate injury). Primary oligodendrocytes are more sensitive, as expected, to stretch-induced injury compared to the cell line. Cell death in oligodendrocyte-enriched primary culture has been indirectly evaluated by cell adherence and results suggest that detached cells are dead because they did not re-adhere following 24h after the end of stretch. It would be more relevant to directly evaluate cell death in this system in order to assess if detached cells are really dead. We tried to measure the LDH in the culture medium in order to assess cell death but the signal was too weak, probably too diluted in 3 ml of medium (this volume is necessary for the stretch experience). We have to complete these studies by using other techniques to evaluate cell death by apoptosis or necrosis. A suitable method for the detection of apoptosis is the evaluation by immunocytofluorescence of the active caspase-3 or the fragmented DNA (a feature of apoptotic cells) marked by terminal deoxynucleotidyl transferase dUTP nick-end labelling (TUNEL) assay. Regarding necrosis, the evaluation could be performed based on morphological characteristics typical of necrotic cells, as cytoplasmic swelling, rupture of the plasma membrane, swelling of cytoplasmic organelles (particularly mitochondria), and condensation of nuclear chromatin.

The study on the organotypic cerebellar slices represents the most challenging part of my project due to the difficulties in performing a successful culture of slices on the silicone membrane. Finally the objective was reached and, to best of our knowledge, we are the first to have developed an *ex vivo* model of stretch-induced injury in cerebellar slices. We showed an axonal injury highlighted by APP accumulation, cytoskeleton disruption and alteration of the paranodal region in cerebellar slices subjected to stretch-induced moderate injury. Considering that ours results are preliminary and should be completed, it is important to highlight that our stretch-induced moderate injury resulted in axon and myelin alteration. As discussed above, for a more precise analysis of myelin sheaths it would be interesting to perform electron microscopy on cerebellar slices at different time points after stretch.

Oxidative stress and sources of ROS following stretch-induced injury

Cells from 158N cell line subjected to stretch-induced mild and moderate injury resulted in an oxidative stress as assessed by an increase in oxidized proteins, a decrease in GSH and a marked alteration in antioxidant defence. Our results showed that free radicals are probably produced by *Duox-1* after stretch-induced mild injury. Nevertheless, the question regarding

the source of ROS produced after stretch remains open, since our data are still preliminary. The major sources of ROS are in general coming from the activity of NADPH oxidases and mitochondria. In collaboration with Dr. Assaad Eid (American University of Beirut, Lebanon), we will measure the activity of NADPH oxidases in 158N cell line, by lucigenin-enhanced chemiluminescence, after mild and moderate injury. Regarding mitochondria, the general status of these organelles will be evaluated in our system on 158N cell line using a specific dye, the 3,3'-dihexyloxacarbocyanine iodide, DiOC6(3), to assess a potential alteration in the mitochondrial membrane potential ($\Delta\Psi m$). This will be a first indicator about mitochondria status, if mitochondrial potential is altered, it is possible that part of ROS are produced by mitochondria. Moreover it would be interesting to assess the presence of reactive nitrogen species (RNS) in our system, in particular ·NO, in order to have a complete analysis on oxidative and nitrosative stress. A study in fact reports that nitric oxide is able to down-regulate the expression of myelin genes PLP, MBP, MOG and CNP in human primary oligodendrocytes (Jana and Pahan, 2013).

The response of mixed glial cells submitted to a stretch-induced mild injury was for some points in line with the 158N cell line, as the oxidative stress markers as AOPP are increased after stretch, and for other points contrasting, since the expression of antioxidant genes is inhibited after stretch. This difference in the response is probably due to the presence of astrocytes. Maybe the antioxidant response was enhanced at the earlier time point but when cells were analysed, after the 20h of stretching, it is possible that the antioxidant system was already downregulated due to a negative feedback. It is also interesting to study the effect of stretch (mild and moderate injury) on astrocytes (cell line and primary culture) and on mixed glial culture (moderate injury) in order to analyse the cellular and molecular responses following stretch.

Moreover, it is also interesting to evaluate if ROS are produced in the response to stretch in oligodendrocyte-enriched primary culture. This is a very delicate culture, unfortunately with a limited yield in term of number of cells. Even utilizing a bigger number of animals and cultures, it would not be possible to have a suitable number of cells required for biochemical assays. However, we can address this issue by measuring ROS production with an *in situ* probing of ROS by dihydroethidium (DHE). Alternatively, we can treat cells with NAC in order to verify if the stretch responses are still present or if cells are protect by this antioxidant compound.

Pathways activated by stretch-induced injury

We studied in 158N cell line the potential involvement of MAPK activation following stretch. Both injuries reduced ERK activation, while only the mild injury, and not moderate, was able to activate the JNK pathway. The analysis of MAPKs in cerebellar slices showed an increase in the activity of both ERK1/2 and JNKs, in particular the 46 kDa isoform. In order to have a complete overview of MAPKs pathway in our system, we will evaluate the effect of stretch on p38, another important MAPKs pathway that is responsive to stretch injury in other cell types. Moreover it should be interesting to understand the mechanism that lead to MAPKs alteration. As discussed above, we hypothesize that ROS could be involved in MAPKs activation or also they might be activated by the calcium influx following mechanical stretch. In order to understand the order of events activated by stretch, we can use pharmacological tools to block ROS production (*via* NAC treatment) or to block calcium influx (by Ca^{2+} blocker) and to analyse their effects on MAPK pathways following stretch.

Regarding the effect of stretch in general on signalling pathways, and independently from the model of injury, it would be intriguing to evaluate other pathways activated by stretch. We only evaluated the MAPKs but it could be interesting to evaluate other pathways also known to be responsive to stretch. A study showed that a mechanical stretch is able to induce the activation of JAK/STAT pathway in rat cardiomyocytes (Pan et al., 1999). Mechanical activation of the mTOR/p70S6K signalling pathway has also been reported in muscle cells *in vitro* (Hornberger, 2004; Hornberger and Chien, 2006; Nakai et al., 2015; Sasai et al., 2010).

Physical stimuli are also known to modulate the activity of transcription factors as, yes-associated protein (YAP) and nuclear factor kB (NF-κB) (Mendez and Janmey, 2012).YAP, a crucial member of the Hippo pathway signalling has emerged as a particularly important regulator of the mechano-response. More precisely YAP is known to respond to substrate stiffness (increasing substrate stiffness results in increasing YAP activation) and stretching (stretch in general activates YAP) (Dupont et al., 2011). A study showed that six hours of cyclic uniaxial stretch at 20% increased the nuclear localization of YAP, confirming its activation. Moreover they showed that YAP activation is JNK-dependent through down-regulation of Hippo signalling (Codelia et al., 2014). Studies on NF-κB reported that this transcriptional factor is activated in chondrocytes in response to dynamic compressive strain (Nam et al., 2009) and in osteoblasts following oscillatory, but not continuous, fluid flow (Young et al., 2010). NF-κB is also reported to be activated in pulmonary epithelial cells submitted to 22% equibiaxial stretch (Horie et al., 2016). It is interesting to assess the effect of our models of stretch-induced injuries on these transcriptional factors. In order to have a

complete analysis of all pathways involved in the response to stretch, it would be suitable to perform a proteomic analysis. This global analysis of protein expression will allow us to focus on particular pathways affected by stretch.

Other future perspectives to study the effects of stretch-induced injury

A well-known consequence of stretch is the alteration in calcium homeostasis, generally considered to be one of the initiating factors in transducing a mechanical insult into a cellular response. In general, magnitude of calcium increase is directly related to the applied strain magnitude and rate (Geddes and Cargill, 2001; LaPlaca and Thibault, 1997; Lusardi et al., 2004; Weber et al., 1999). There are no studies on oligodendrocytes and it would be interesting to assess the calcium homeostasis in our models of stretch-induced injury. The most popular calcium indicator is the Fura-2, a fluorescent dye, which binds to free intracellular calcium and allows an accurate measurement of intracellular calcium concentrations. This method is suitable only for live imaging studies. In our condition, we cannot use this probe since we should work on fixed cells or tissue. Therefore, an alternative calcium indicator could be the Alizarin Red S, an anthraquinone derivative, used to identify calcium in tissue sections. Calcium forms an Alizarin Red S-calcium complex in a chelation process, and the end product is birefringent. Another possibility is the von Kossa stain that allows the visualization of deposits of calcium or calcium salts.

As discussed above, Ca^{2+} influx in response to mechanical stress can be stimulated *via* different mechanisms, as the activation of specialized mechanosensitive ion channels. For example some Transient Receptor Potential (TRP) channels, respond to mechanical stretch. TRPA1 has been recently demonstrated to be expressed in the cerebellum and oligodendrocytes of rats and mice (Hamilton et al., 2016). TRPA1 generates ~70% of the ischaemia-evoked Ca^{2+} rise, and TRPA1 blockers reduce ischaemic damage to myelin in cerebellar white matter oligodendrocytes (Hamilton et al., 2016). TRP channels can be activated and modulated by ROS, in particular by ·NO and $O_2^{\cdot -}$ that have been shown to enhance Ca^{2+} uptake and TRPM7 activity in neurons. Conversely, TRPM7 suppression is able to inhibit ROS production, indicating an interdependence (Aarts et al., 2003).
In our cellular system, we can hypothesize that ROS activate these TRP channels that, in turn, mediate Ca^{2+} influx and all the consequences at the cellular and molecular levels. We can use pharmacological tools to block ROS production (*via* NAC treatment) or to block calcium influx (by Ca^{2+} blocker) in order to analyse the link between these two cellular process and eventually the implication of TRPA1 using a TRPA1 blocker (HC-030031).

In our study, we neglected one important aspect of TBI, the inflammation. A complex cascade of inflammatory response is in fact initiated following TBI, with release of cytokines, chemokines and growth factors by different cell types (Wang et al., 2013). It would be interesting to assess in our models, *in vitro* and *ex vivo*, the inflammatory response to stretch. We tried to measure the release of pro-inflammatory cytokines IL-1β and TNF-α in the culture medium by ELISA, but the signal was too weak, probably too diluted in 3 ml of medium, volume necessary for the stretch experience. For the future experience, we can perform RT-qPCR to analyse the effect of stretch on the expression of IL-1β and TNF-α genes. It would be also possible to assess an extended spectrum of pro-inflammatory cytokines by FACS on 158N cell line.

Another possible perspective is the association of stretch with a secondary injury to mimic the *in vivo* context of TBI. For example, it is possible to associate hypoxia with stretch, or stretch could be also associated with an inflammatory stimulus, as IL-1β. Studies reported that stretch can be sub-lethal, as in our case for 158N cell line, but it renders cells more sensitive to a secondary injury. For example stretch (30% for 1 sec) increases the vulnerability of primary neurons to subsequent challenges with L-glutamate or NMDA (Arundine, 2004; Arundine et al., 2003).

An important question is that our study, as the majority in the literature, was conducted on a flat, two-dimensional (2D) substrate, while cells grow physiologically in a complex three-dimensional (3D) environment. The actual knowledge of many biological processes is largely based on studies using cell cultures in 2D system but, over the past years the development of 3D culture knew an incentive and scientists are encouraged to use 3D systems. Some 3D matrixes exist for the Flexcell® Tension System, so it will be technically possible to perform this kind of 3D culture. The 3D culture elicits a more physiological state, with changes in cell geometry and organization that directly impact cell functions. Moreover it’s also important to underline that the dimensionality is strictly linked to the matrix stiffness and traditional 2D cultures are generally performed on glass or plastic which are supraphysiological in terms of stiffness. The matrix used for 3D culture is not necessarily at the physiological range of stiffness, but to date most of the 3D systems offer a matrix with low stiffness. It should be really interesting to adapt our *in vitro* model to a 3D culture, in order to be closer to the physiological state for both the three dimensionality and the stiffness.

Etazolate as promising treatment for TBI treatment

Finally, considering the second part of my project, we analysed the antioxidant potential effect of etazolate. However, the results were not in line with what expected on the basis of the studies reported in the literature *in vivo.* In fact, etazolate did not reduce the ROS production in our condition. Nevertheless it remains a promising treatment for TBI due to its neuroprotective, anti-inflammatory and antioxidant effects *in vivo.*

The *ex vivo* model of demyelination induced by lysolecithin allowed to reveal the remyelinating effects of different pharmacological compounds (Hussain et al., 2011; Meffre et al., 2015a, 2015b; Miron et al., 2010). In this context, we tested the effect of etazolate on myelin sheaths and it showed to be protective, and more precisely it promotes oligodendrocyte differentiation and remyelination (Llufriu-Dabén et al. 2016a, under revision). It would be interesting to complete this study with a more detailed analysis on the proliferation and migration of OPCs. Indeed, in addition to the differentiation of OPCs, the proliferation and migration of OPCs are also essential to the remyelination process. Thus, the study of the effect of etazolate on the proliferation of OPCs could be achieved by the incorporation of bromodeoxyuridine (BrdU) or by the marker Ki67, evaluated by immunofluorescence. The study of the effect of etazolate on migration of OPCs to demyelinated zones would also be crucial. For this study, cerebellar organotypic cultures should be performed in the presence of brain stem slices from PLP-eGFP mice, added after lysolecithin demyelination (Hussain et al., 2011). This system allows the observation of the eventually migration of OPCs-GFP^+ from the brain stem to the demyelinated areas of the cerebellum. In addition, due to the contribution of inflammation to the lysolecithin-induced demyelination (Sheridan and Dev, 2012), it would be interesting to study the anti-inflammatory effects of etazolate with ELISA test or histological study.

It is important to highlight that damage associated with primary brain injury can only be prevented, therefore clinical efforts should be focused on the prevention, recognition and treatment of secondary brain injury. In particular, it is proven that myelin plays an important role in protection of axons following white matter injury, unmyelinated fibers are more susceptible to damage than myelinated ones (Reeves et al., 2012; Staal and Vickers, 2011) and along myelinated fibers, the axon initial segment, which is not myelinated, is the primary site of axotomy.

Recent studies have proposed demyelination as a target to limit the progression of axonal lesions as well as to stimulate axonal regeneration. This therapeutic strategy would promote the recovery of axonal conduction and its functional capacity (Plemel et al., 2014; Shi et al., 2015).

In conclusion, several models of stretch-induced injury were developed for the first time in oligodendrocytes and cerebellar slices suggesting that mechanical stretch can cause loss of oligodendrocytes and demyelination. These findings highlight the importance of developing therapeutic strategies based on oligodendrocyte protection. These models are relevant for studying the pathophysiological events that occur after stretch-induced injury as well as for rapid screening of therapeutic compounds.

REFERENCES

Aarts, M., Iihara, K., Wei, W.-L., Xiong, Z.-G., Arundine, M., Cerwinski, W., MacDonald, J.F., and Tymianski, M. (2003). A key role for TRPM7 channels in anoxic neuronal death. Cell *115*, 863–877.

Abbott, N.J. (2000). Inflammatory mediators and modulation of blood-brain barrier permeability. Cell. Mol. Neurobiol. *20*, 131–147.

Abdel Baki, S.G., Schwab, B., Haber, M., Fenton, A.A., and Bergold, P.J. (2010). Minocycline synergizes with N-acetylcysteine and improves cognition and memory following traumatic brain injury in rats. PloS One *5*, e12490.

Abdul-Muneer, P.M., Chandra, N., and Haorah, J. (2015). Interactions of Oxidative Stress and Neurovascular Inflammation in the Pathogenesis of Traumatic Brain Injury. Mol. Neurobiol. *51*, 966–979.

Accetta, R., Damiano, S., Morano, A., Mondola, P., Paternò, R., Avvedimento, E.V., and Santillo, M. (2016). Reactive Oxygen Species Derived from NOX3 and NOX5 Drive Differentiation of Human Oligodendrocytes. Front. Cell. Neurosci. *10*.

Adams, J.D., Wang, B., Klaidman, L.K., LeBel, C.P., Odunze, I.N., and Shah, D. (1993). New aspects of brain oxidative stress induced by tert-butylhydroperoxide. Free Radic. Biol. Med. *15*, 195–202.

Adams, J.D., Mukherjee, S.K., Klaidman, L.K., Chang, M.L., and Yasharel, R. (1996). Apoptosis and oxidative stress in the aging brain. Ann. N. Y. Acad. Sci. *786*, 135–151.

Adams, J.H., Graham, D.I., Murray, L.S., and Scott, G. (1982). Diffuse axonal injury due to nonmissile head injury in humans: an analysis of 45 cases. Ann. Neurol. *12*, 557–563.

Adams, J.H., Doyle, D., Ford, I., Gennarelli, T.A., Graham, D.I., and McLellan, D.R. (1989). Diffuse axonal injury in head injury: definition, diagnosis and grading. Histopathology *15*, 49–59.

Adly, A. (2010). Oxidative Stress and Disease: An Updated Review. Res. J. Immunol. *3*, 129–145.

Aggarwal, S., Snaidero, N., Pähler, G., Frey, S., Sánchez, P., Zweckstetter, M., Janshoff, A., Schneider, A., Weil, M.-T., Schaap, I.A.T., et al. (2013). Myelin membrane assembly is driven by a phase transition of myelin basic proteins into a cohesive protein meshwork. PLoS Biol. *11*, e1001577.

Ahmed, S.M., Rzigalinski, B.A., Willoughby, K.A., Sitterding, H.A., and Ellis, E.F. (2000). Stretch-induced injury alters mitochondrial membrane potential and cellular ATP in cultured astrocytes and neurons. J. Neurochem. *74*, 1951–1960.

Ahmed, S.M., Weber, J.T., Liang, S., Willoughby, K.A., Sitterding, H.A., Rzigalinski, B.A., and Ellis, E.F. (2002). NMDA receptor activation contributes to a portion of the decreased mitochondrial membrane potential and elevated intracellular free calcium in strain-injured neurons. J. Neurotrauma *19*, 1619–1629.

Aiguo Wu, null, Zhe Ying, null, and Gomez-Pinilla, F. (2010). Vitamin E protects against oxidative damage and learning disability after mild traumatic brain injury in rats. Neurorehabil. Neural Repair *24*, 290–298.

Aitio, M.-L. (2006). N-acetylcysteine -- passe-partout or much ado about nothing? Br. J. Clin. Pharmacol. *61*, 5–15.

Akyol, O., Zoroglu, S.S., Armutcu, F., Sahin, S., and Gurel, A. (2004). Nitric oxide as a physiopathological factor in neuropsychiatric disorders. In Vivo *18*, 377–390.

Alizadeh, A., Dyck, S.M., and Karimi-Abdolrezaee, S. (2015). Myelin damage and repair in pathologic CNS: challenges and prospects. Front. Mol. Neurosci. *8*.

Al-Mehdi, A.-B., Pastukh, V.M., Swiger, B.M., Reed, D.J., Patel, M.R., Bardwell, G.C., Pastukh, V.V., Alexeyev, M.F., and Gillespie, M.N. (2012). Perinuclear mitochondrial clustering creates an oxidant-rich nuclear domain required for hypoxia-induced transcription. Sci. Signal. *5*, ra47.

Ames, B.N. (2001). DNA damage from micronutrient deficiencies is likely to be a major cause of cancer. Mutat. Res. Mol. Mech. Mutagen. *475*, 7–20.

Ames, B.N., Shigenaga, M.K., and Hagen, T.M. (1995). Mitochondrial decay in aging. Biochim. Biophys. Acta *1271*, 165–170.

Amor, S., and Woodroofe, M.N. (2014). Innate and adaptive immune responses in neurodegeneration and repair. Immunology *141*, 287–291.

Amor, S., Puentes, F., Baker, D., and van der Valk, P. (2010). Inflammation in neurodegenerative diseases. Immunology *129*, 154–169.
Andriessen, T.M.J.C., Jacobs, B., and Vos, P.E. (2010). Clinical characteristics and pathophysiological mechanisms of focal and diffuse traumatic brain injury. J. Cell. Mol. Med. *14*, 2381–2392.
Angeloni, C., Prata, C., Vieceli Dalla Sega, F., Piperno, R., and Hrelia, S. (2015). Traumatic Brain Injury and NADPH Oxidase: A Deep Relationship. Oxid. Med. Cell. Longev. *2015*, 1–10.
Ankarcrona, M., Dypbukt, J.M., Bonfoco, E., Zhivotovsky, B., Orrenius, S., Lipton, S.A., and Nicotera, P. (1995). Glutamate-induced neuronal death: a succession of necrosis or apoptosis depending on mitochondrial function. Neuron *15*, 961–973.
Ankur, J., Mahesh, R., and Bhatt, S. (2013). Anxiolytic-like effect of etazolate, a type 4 phosphodiesterase inhibitor in experimental models of anxiety. Indian J. Exp. Biol. *51*, 444–449.
Ansari, M.A., Roberts, K.N., and Scheff, S.W. (2008). Oxidative stress and modification of synaptic proteins in hippocampus after traumatic brain injury. Free Radic. Biol. Med. *45*, 443–452.
Arakawa, M., and Ito, Y. (2007). N-acetylcysteine and neurodegenerative diseases: basic and clinical pharmacology. Cerebellum Lond. Engl. *6*, 308–314.
Arend, C., Brandmann, M., and Dringen, R. (2013). The antiretroviral protease inhibitor ritonavir accelerates glutathione export from cultured primary astrocytes. Neurochem. Res. *38*, 732–741.
Armstrong, R.C., Mierzwa, A.J., Sullivan, G.M., and Sanchez, M.A. (2016a). Myelin and oligodendrocyte lineage cells in white matter pathology and plasticity after traumatic brain injury. Neuropharmacology *110*, 654–659.
Armstrong, R.C., Mierzwa, A.J., Marion, C.M., and Sullivan, G.M. (2016b). White matter involvement after TBI: Clues to axon and myelin repair capacity. Exp. Neurol. *275*, 328–333.
de Arruda Grossklaus, D., Bailão, A.M., Vieira Rezende, T.C., Borges, C.L., de Oliveira, M.A.P., Parente, J.A., and de Almeida Soares, C.M. (2013). Response to oxidative stress in Paracoccidioides yeast cells as determined by proteomic analysis. Microbes Infect. *15*, 347–364.
Arulmoli, J., Pathak, M.M., McDonnell, L.P., Nourse, J.L., Tombola, F., Earthman, J.C., and Flanagan, L.A. (2015). Static stretch affects neural stem cell differentiation in an extracellular matrix-dependent manner. Sci. Rep. *5*, 8499.
Arundine, M. (2004). Vulnerability of Central Neurons to Secondary Insults after In Vitro Mechanical Stretch. J. Neurosci. *24*, 8106–8123.
Arundine, M., Chopra, G.K., Wrong, A., Lei, S., Aarts, M.M., MacDonald, J.F., and Tymianski, M. (2003). Enhanced vulnerability to NMDA toxicity in sublethal traumatic neuronal injury in vitro. J. Neurotrauma *20*, 1377–1395.
Aruoma, O.I., Halliwell, B., Hoey, B.M., and Butler, J. (1989). The antioxidant action of N-acetylcysteine: its reaction with hydrogen peroxide, hydroxyl radical, superoxide, and hypochlorous acid. Free Radic. Biol. Med. *6*, 593–597.
Asano, null (1999). Oxyhemoglobin as the principal cause of cerebral vasospasm: a holistic view of its actions. Crit. Rev. Neurosurg. CR *9*, 303–318.
Ascenzi, P., Bocedi, A., Visca, P., Altruda, F., Tolosano, E., Beringhelli, T., and Fasano, M. (2005). Hemoglobin and heme scavenging. IUBMB Life Int. Union Biochem. Mol. Biol. Life *57*, 749–759.
Ashkenazi, A., and Dixit, V.M. (1998). Death receptors: signaling and modulation. Science *281*, 1305–1308.
Atkins, C.M., Oliva, A.A., Alonso, O.F., Pearse, D.D., Bramlett, H.M., and Dietrich, W.D. (2007). Modulation of the cAMP signaling pathway after traumatic brain injury. Exp. Neurol. *208*, 145–158.
Atkins, C.M., Kang, Y., Furones, C., Truettner, J.S., Alonso, O.F., and Dietrich, W.D. (2012). Postinjury treatment with rolipram increases hemorrhage after traumatic brain injury. J. Neurosci. Res. *90*, 1861–1871.
Atkins, C.M., Cepero, M.L., Kang, Y., Liebl, D.J., and Dietrich, W.D. (2013). Effects of early rolipram treatment on histopathological outcome after controlled cortical impact injury in mice. Neurosci. Lett. *532*, 1–6.
Avery, S.V. (2011). Molecular targets of oxidative stress. Biochem. J. *434*, 201–210.
Ayers, D., Baron, B., and Hunter, T. (2015). miRNA Influences in NRF2 Pathway Interactions within Cancer Models. J. Nucleic Acids *2015*, 143636.
Babbs, C.F., and Shi, R. (2013). Subtle Paranodal Injury Slows Impulse Conduction in a Mathematical Model of Myelinated Axons. PLoS ONE *8*, e67767.
Back, S.A., Gan, X., Li, Y., Rosenberg, P.A., and Volpe, J.J. (1998). Maturation-dependent vulnerability of oligodendrocytes to oxidative stress-induced death caused by glutathione depletion. J. Neurosci. Off. J. Soc. Neurosci. *18*, 6241–6253.

Baer, A.S., Syed, Y.A., Kang, S.U., Mitteregger, D., Vig, R., Ffrench-Constant, C., Franklin, R.J.M., Altmann, F., Lubec, G., and Kotter, M.R. (2009). Myelin-mediated inhibition of oligodendrocyte precursor differentiation can be overcome by pharmacological modulation of Fyn-RhoA and protein kinase C signalling. Brain J. Neurol. *132*, 465–481.

Baker, B.M., and Chen, C.S. (2012). Deconstructing the third dimension - how 3D culture microenvironments alter cellular cues. J. Cell Sci. *125*, 3015–3024.

Bánfi, B., Malgrange, B., Knisz, J., Steger, K., Dubois-Dauphin, M., and Krause, K.-H. (2004). NOX3, a superoxide-generating NADPH oxidase of the inner ear. J. Biol. Chem. *279*, 46065–46072.

Barhoumi, R., Bowen, J.A., Stein, L.S., Echols, J., and Burghardt, R.C. (1993). Concurrent analysis of intracellular glutathione content and gap junctional intercellular communication. Cytometry *14*, 747–756.

Barkhoudarian, G., Hovda, D.A., and Giza, C.C. (2011). The molecular pathophysiology of concussive brain injury. Clin. Sports Med. *30*, 33–48, vii–iii.

Barnes, D.M., White, W.F., and Dichter, M.A. (1983). Etazolate (SQ20009): electrophysiology and effects on [3H]flunitrazepam binding in cultured cortical neurons. J. Neurosci. Off. J. Soc. Neurosci. *3*, 762–772.

Barral, J.-P., and Croibier, A. (2007). Manual Therapy for the Peripheral Nerves (Elsevier Health Sciences).

Barres, B.A., and Raff, M.C. (1994). Control of oligodendrocyte number in the developing rat optic nerve. Neuron *12*, 935–942.

Bass, D.A., Parce, J.W., Dechatelet, L.R., Szejda, P., Seeds, M.C., and Thomas, M. (1983). Flow cytometric studies of oxidative product formation by neutrophils: a graded response to membrane stimulation. J. Immunol. Baltim. Md 1950 *130*, 1910–1917.

Bass, R.B., Locher, K.P., Borths, E., Poon, Y., Strop, P., Lee, A., and Rees, D.C. (2003). The structures of BtuCD and MscS and their implications for transporter and channel function. FEBS Lett. *555*, 111–115.

Baumann, N., and Pham-Dinh, D. (2001). Biology of oligodendrocyte and myelin in the mammalian central nervous system. Physiol. Rev. *81*, 871–927.

Bavarsad Shahripour, R., Harrigan, M.R., and Alexandrov, A.V. (2014). N-acetylcysteine (NAC) in neurological disorders: mechanisms of action and therapeutic opportunities. Brain Behav. *4*, 108–122.

Bazarian, J.J., Zhong, J., Blyth, B., Zhu, T., Kavcic, V., and Peterson, D. (2007). Diffusion tensor imaging detects clinically important axonal damage after mild traumatic brain injury: a pilot study. J. Neurotrauma *24*, 1447–1459.

Beal, M.F. (2005). Mitochondria take center stage in aging and neurodegeneration. Ann. Neurol. *58*, 495–505.

Beauchamp, C., and Fridovich, I. (1971). Superoxide dismutase: improved assays and an assay applicable to acrylamide gels. Anal. Biochem. *44*, 276–287.

Bechler, M.E., Byrne, L., and Ffrench-Constant, C. (2015). CNS Myelin Sheath Lengths Are an Intrinsic Property of Oligodendrocytes. Curr. Biol. CB *25*, 2411–2416.

Bell, B.J., Nauman, E., and Voytik-Harbin, S.L. (2012). Multiscale Strain Analysis of Tissue Equivalents Using a Custom-Designed Biaxial Testing Device. Biophys. J. *102*, 1303–1312.

Bellander, B.M., Singhrao, S.K., Ohlsson, M., Mattsson, P., and Svensson, M. (2001). Complement activation in the human brain after traumatic head injury. J. Neurotrauma *18*, 1295–1311.

Bellomo, G., Palladini, G., and Vairetti, M. (1997). Intranuclear distribution, function and fate of glutathione and glutathione-S-conjugate in living rat hepatocytes studied by fluorescence microscopy. Microsc. Res. Tech. *36*, 243–252.

Bendlin, B.B., Ries, M.L., Lazar, M., Alexander, A.L., Dempsey, R.J., Rowley, H.A., Sherman, J.E., and Johnson, S.C. (2008). Longitudinal changes in patients with traumatic brain injury assessed with diffusion-tensor and volumetric imaging. NeuroImage *42*, 503–514.

Benjamin, M., and Ralphs, J.R. (1998). Fibrocartilage in tendons and ligaments—an adaptation to compressive load. J. Anat. *193*, 481–494.

Bennett, E.R., Reuter-Rice, K., and Laskowitz, D.T. (2016). Genetic Influences in Traumatic Brain Injury. In Translational Research in Traumatic Brain Injury, D. Laskowitz, and G. Grant, eds. (Boca Raton (FL): CRC Press/Taylor and Francis Group), p.

Bercury, K.K., and Macklin, W.B. (2015). Dynamics and Mechanisms of CNS Myelination. Dev. Cell *32*, 447–458.

Berlett, B.S., and Stadtman, E.R. (1997). Protein oxidation in aging, disease, and oxidative stress. J. Biol. Chem. *272*, 20313–20316.

Bernardi, P. (1992). Modulation of the mitochondrial cyclosporin A-sensitive permeability transition pore by the proton electrochemical gradient. Evidence that the pore can be opened by membrane depolarization. J. Biol. Chem. *267*, 8834–8839.

Bertrand, A.T., Ziaei, S., Ehret, C., Duchemin, H., Mamchaoui, K., Bigot, A., Mayer, M., Quijano-Roy, S., Desguerre, I., Laine, J., et al. (2014). Cellular microenvironments reveal defective mechanosensing responses and elevated YAP signaling in LMNA-mutated muscle precursors. J. Cell Sci. *127*, 2873–2884.

Bhatti, F., Mankhey, R.W., Asico, L., Quinn, M.T., Welch, W.J., and Maric, C. (2005). Mechanisms of antioxidant and pro-oxidant effects of alpha-lipoic acid in the diabetic and nondiabetic kidney. Kidney Int. *67*, 1371–1380.

Bielekova, B., Richert, N., Howard, T., Packer, A.N., Blevins, G., Ohayon, J., McFarland, H.F., Stürzebecher, C.-S., and Martin, R. (2009). Treatment with the phosphodiesterase type-4 inhibitor rolipram fails to inhibit blood--brain barrier disruption in multiple sclerosis. Mult. Scler. Houndmills Basingstoke Engl. *15*, 1206–1214.

Biran, V., Verney, C., and Ferriero, D.M. (2012). Perinatal Cerebellar Injury in Human and Animal Models. Neurol. Res. Int. *2012*, 1–9.

Birgbauer, E., Rao, T.S., and Webb, M. (2004). Lysolecithin induces demyelination in vitro in a cerebellar slice culture system. J. Neurosci. Res. *78*, 157–166.

Blakemore, W.F., and Murray, J.A. (1981). Quantitative examination of internodal length of remyelinated nerve fibres in the central nervous system. J. Neurol. Sci. *49*, 273–284.

Blanchoin, L., Pollard, T.D., and Mullins, R.D. (2000). Interactions of ADF/cofilin, Arp2/3 complex, capping protein and profilin in remodeling of branched actin filament networks. Curr. Biol. CB *10*, 1273–1282.

Blasiole, B., Bayr, H., Vagni, V.A., Janesko-Feldman, K., Cheikhi, A., Wisniewski, S.R., Long, J.B., Atkins, J., Kagan, V., and Kochanek, P.M. (2013). Effect of hyperoxia on resuscitation of experimental combined traumatic brain injury and hemorrhagic shock in mice. Anesthesiology *118*, 649–663.

Blasko, I., Beer, R., Bigl, M., Apelt, J., Franz, G., Rudzki, D., Ransmayr, G., Kampfl, A., and Schliebs, R. (2004). Experimental traumatic brain injury in rats stimulates the expression, production and activity of Alzheimer's disease beta-secretase (BACE-1). J. Neural Transm. Vienna Austria 1996 *111*, 523–536.

Blennow, K., Hardy, J., and Zetterberg, H. (2012). The Neuropathology and Neurobiology of Traumatic Brain Injury. Neuron *76*, 886–899.

Bollmann, L., Koser, D.E., Shahapure, R., Gautier, H.O.B., Holzapfel, G.A., Scarcelli, G., Gather, M.C., Ulbricht, E., and Franze, K. (2015). Microglia mechanics: immune activation alters traction forces and durotaxis. Front. Cell. Neurosci. *9*.

Boomkamp, S.D., McGrath, M.A., Houslay, M.D., and Barnett, S.C. (2014). Epac and the high affinity rolipram binding conformer of PDE4 modulate neurite outgrowth and myelination using an in vitro spinal cord injury model. Br. J. Pharmacol. *171*, 2385–2398.

van den Bosch, H., Schutgens, R.B., Wanders, R.J., and Tager, J.M. (1992). Biochemistry of peroxisomes. Annu. Rev. Biochem. *61*, 157–197.

Bottlang, M., Sommers, M.B., Lusardi, T.A., Miesch, J.J., Simon, R.P., and Xiong, Z.-G. (2007). Modeling neural injury in organotypic cultures by application of inertia-driven shear strain. J. Neurotrauma *24*, 1068–1077.

Bouma, G.J., Muizelaar, J.P., Choi, S.C., Newlon, P.G., and Young, H.F. (1991). Cerebral circulation and metabolism after severe traumatic brain injury: the elusive role of ischemia. J. Neurosurg. *75*, 685–693.

Bramlett, H., and Dietrich, D. (2002). Quantitative structural changes in white and gray matter 1 year following traumatic brain injury in rats. Acta Neuropathol. (Berl.) *103*, 607–614.

Brandt, R., and Keston, A.S. (1965). Synthesis of diacetyldichlorofluorescin: a stable reagent for fluorometric analysis. Anal. Biochem. *11*, 6–9.

Braughler, J.M., Duncan, L.A., and Chase, R.L. (1986). The involvement of iron in lipid peroxidation. Importance of ferric to ferrous ratios in initiation. J. Biol. Chem. *261*, 10282–10289.

Braun, P.E., Sandillon, F., Edwards, A., Matthieu, J.M., and Privat, A. (1988). Immunocytochemical localization by electron microscopy of 2'3'-cyclic nucleotide 3'-phosphodiesterase in developing oligodendrocytes of normal and mutant brain. J. Neurosci. *8*, 3057–3066.

Bredesen, D.E. (2008). Programmed cell death mechanisms in neurological disease. Curr. Mol. Med. *8*, 173–186.

Brennan, A.M., Won Suh, S., Joon Won, S., Narasimhan, P., Kauppinen, T.M., Lee, H., Edling, Y., Chan, P.H., and Swanson, R.A. (2009). NADPH oxidase is the primary source of superoxide induced by NMDA receptor activation. Nat. Neurosci. *12*, 857–863.

Bruce, C.C., Zhao, C., and Franklin, R.J.M. (2010). Remyelination - An effective means of neuroprotection. Horm. Behav. *57*, 56–62.

Brunk, U.T., and Terman, A. (2002). The mitochondrial-lysosomal axis theory of aging: Accumulation of damaged mitochondria as a result of imperfect autophagocytosis. Eur. J. Biochem. *269*, 1996–2002.

Buck, R.C. (1980). Reorientation response of cells to repeated stretch and recoil of the substratum. Exp. Cell Res. *127*, 470–474.

Büki, A., Okonkwo, D.O., Wang, K.K., and Povlishock, J.T. (2000). Cytochrome c release and caspase activation in traumatic axonal injury. J. Neurosci. Off. J. Soc. Neurosci. *20*, 2825–2834.

Bullock, R., Zauner, A., Myseros, J.S., Marmarou, A., Woodward, J.J., and Young, H.F. (1995). Evidence for prolonged release of excitatory amino acids in severe human head trauma. Relationship to clinical events. Ann. N. Y. Acad. Sci. *765*, 290–297; discussion 298.

Bullock, R., Zauner, A., Woodward, J.J., Myseros, J., Choi, S.C., Ward, J.D., Marmarou, A., and Young, H.F. (1998). Factors affecting excitatory amino acid release following severe human head injury. J. Neurosurg. *89*, 507–518.

Burger, E.H., and Klein-Nulend, J. (1999). Mechanotransduction in bone--role of the lacuno-canalicular network. FASEB J. Off. Publ. Fed. Am. Soc. Exp. Biol. *13 Suppl*, S101-112.

Burridge, K. (1981). Are stress fibres contractile? Nature *294*, 691–692.

Butt, A.M., Colquhoun, K., and Berry, M. (1994a). Confocal imaging of glial cells in the intact rat optic nerve. Glia *10*, 315–322.

Butt, A.M., Duncan, A., and Berry, M. (1994b). Astrocyte associations with nodes of Ranvier: ultrastructural analysis of HRP-filled astrocytes in the mouse optic nerve. J. Neurocytol. *23*, 486–499.

Calabrese, B., Manzi, S., Pellegrini, M., and Pellegrino, M. (1999). Stretch-activated cation channels of leech neurons: characterization and role in neurite outgrowth. Eur. J. Neurosci. *11*, 2275–2284.

Camins, A., Verdaguer, E., Folch, J., and Pallàs, M. (2006). Involvement of calpain activation in neurodegenerative processes. CNS Drug Rev. *12*, 135–148.

Campbell, J.J., Blain, E.J., Chowdhury, T.T., and Knight, M.M. (2007). Loading alters actin dynamics and up-regulates cofilin gene expression in chondrocytes. Biochem. Biophys. Res. Commun. *361*, 329–334.

Cañas, P.E. (1999). The role of xanthine oxidase and the effects of antioxidants in ischemia reperfusion cell injury. Acta Physiol. Pharmacol. Ther. Latinoam. Órgano Asoc. Latinoam. Cienc. Fisiológicas Asoc. Latinoam. Farmacol. *49*, 13–20.

Cao, G., and Prior, R.L. (1998). Comparison of different analytical methods for assessing total antioxidant capacity of human serum. Clin. Chem. *44*, 1309–1315.

Caprariello, A.V., Mangla, S., Miller, R.H., and Selkirk, S.M. (2012). Apoptosis of oligodendrocytes in the central nervous system results in rapid focal demyelination. Ann. Neurol. *72*, 395–405.

Cargill, R.S., and Thibault, L.E. (1996). Acute alterations in [Ca2+] i in NG108-15 cells subjected to high strain rate deformation and chemical hypoxia: an in vitro model for neural trauma. J. Neurotrauma *13*, 395–407.

Carini, M., Aldini, G., and Facino, R.M. (2004). Mass spectrometry for detection of 4-hydroxy-trans-2-nonenal (HNE) adducts with peptides and proteins. Mass Spectrom. Rev. *23*, 281–305.

Cater, H.L., Sundstrom, L.E., and Morrison, B. (2006). Temporal development of hippocampal cell death is dependent on tissue strain but not strain rate. J. Biomech. *39*, 2810–2818.

Cater, H.L., Gitterman, D., Davis, S.M., Benham, C.D., Morrison, B., and Sundstrom, L.E. (2007). Stretch-induced injury in organotypic hippocampal slice cultures reproduces in vivo post-traumatic neurodegeneration: role of glutamate receptors and voltage-dependent calcium channels. J. Neurochem. *101*, 434–447.

Cavaliere, F., Urra, O., Alberdi, E., and Matute, C. (2012). Oligodendrocyte differentiation from adult multipotent stem cells is modulated by glutamate. Cell Death Dis. *3*, e268.

Cernak, I. (2005). Animal models of head trauma. NeuroRx *2*, 410–422.

Chaitanya, G.V., Omura, S., Sato, F., Martinez, N.E., Minagar, A., Ramanathan, M., Guttman, B.W., Zivadinov, R., Tsunoda, I., and Alexander, J.S. (2013). Inflammation induces neuro-lymphatic protein expression in multiple sclerosis brain neurovasculature. J. Neuroinflammation *10*, 125.

Chakfe, Y., and Bourque, C.W. (2001). Peptidergic Excitation of Supraoptic Nucleus Neurons: Involvement of Stretch-Inactivated Cation Channels. Exp. Neurol. *171*, 210–218.

Chamoun, R., Suki, D., Gopinath, S.P., Goodman, J.C., and Robertson, C. (2010). Role of extracellular glutamate measured by cerebral microdialysis in severe traumatic brain injury. J. Neurosurg. *113*, 564–570.
Chance, B., Sies, H., and Boveris, A. (1979). Hydroperoxide metabolism in mammalian organs. Physiol. Rev. *59*, 527–605.
Chanet, S., and Martin, A.C. (2014). Mechanical Force Sensing in Tissues. In Progress in Molecular Biology and Translational Science, (Elsevier), pp. 317–352.
Charles, A.C., Merrill, J.E., Dirksen, E.R., and Sanderson, M.J. (1991). Intercellular signaling in glial cells: calcium waves and oscillations in response to mechanical stimulation and glutamate. Neuron *6*, 983–992.
Chasin, M., Harris, D.N., Phillips, M.B., and Hess, S.M. (1972). 1-Ethyl-4-(isopropylidenehydrazino)-1H-pyrazolo-(3,4-b)-pyridine-5-carboxylic acid, ethyl ester, hydrochloride (SQ 20009)--a potent new inhibitor of cyclic 3',5'-nucleotide phosphodiesterases. Biochem. Pharmacol. *21*, 2443–2450.
Checler, F. (1995). Processing of the beta-amyloid precursor protein and its regulation in Alzheimer's disease. J. Neurochem. *65*, 1431–1444.
Cheepsunthorn, P., Palmer, C., and Connor, J.R. (1998). Cellular distribution of ferritin subunits in postnatal rat brain. J. Comp. Neurol. *400*, 73–86.
Chen, C.-M., Wu, Y.-R., Cheng, M.-L., Liu, J.-L., Lee, Y.-M., Lee, P.-W., Soong, B.-W., and Chiu, D.T.-Y. (2007). Increased oxidative damage and mitochondrial abnormalities in the peripheral blood of Huntington's disease patients. Biochem. Biophys. Res. Commun. *359*, 335–340.
Chen, G., Shi, J., Hu, Z., and Hang, C. (2008). Inhibitory effect on cerebral inflammatory response following traumatic brain injury in rats: a potential neuroprotective mechanism of N-acetylcysteine. Mediators Inflamm. *2008*, 716458.
Chen, N.X., Geist, D.J., Genetos, D.C., Pavalko, F.M., and Duncan, R.L. (2003). Fluid shear-induced NFκB translocation in osteoblasts is mediated by intracellular calcium release. Bone *33*, 399–410.
Chen, T., Willoughby, K.A., and Ellis, E.F. (2004). Group I metabotropic receptor antagonism blocks depletion of calcium stores and reduces potentiated capacitative calcium entry in strain-injured neurons and astrocytes. J. Neurotrauma *21*, 271–281.
Chen, Y.C., Smith, D.H., and Meaney, D.F. (2009). In-vitro approaches for studying blast-induced traumatic brain injury. J. Neurotrauma *26*, 861–876.
Cheng, G., Kong, R., Zhang, L., and Zhang, J. (2012). Mitochondria in traumatic brain injury and mitochondrial-targeted multipotential therapeutic strategies. Br. J. Pharmacol. *167*, 699–719.
Cheng, Z.-G., Zhang, G.-D., Shi, P.-Q., and Du, B.-S. (2013). Expression and antioxidation of Nrf2/ARE pathway in traumatic brain injury. Asian Pac. J. Trop. Med. *6*, 305–310.
Cherian, L., Hlatky, R., and Robertson, C.S. (2004). Nitric oxide in traumatic brain injury. Brain Pathol. Zurich Switz. *14*, 195–201.
Chevion, M., Berenshtein, E., and Stadtman, E.R. (2000). Human studies related to protein oxidation: protein carbonyl content as a marker of damage. Free Radic. Res. *33 Suppl*, S99-108.
Chhor, V., Le Charpentier, T., Lebon, S., Oré, M.-V., Celador, I.L., Josserand, J., Degos, V., Jacotot, E., Hagberg, H., Sävman, K., et al. (2013). Characterization of phenotype markers and neuronotoxic potential of polarised primary microglia in vitro. Brain. Behav. Immun. *32*, 70–85.
Chiron, S., Tomczak, C., Duperray, A., Lainé, J., Bonne, G., Eder, A., Hansen, A., Eschenhagen, T., Verdier, C., and Coirault, C. (2012). Complex Interactions between Human Myoblasts and the Surrounding 3D Fibrin-Based Matrix. PLoS ONE *7*, e36173.
Cho, H., Shin, J., Shin, C.Y., Lee, S.-Y., and Oh, U. (2002). Mechanosensitive ion channels in cultured sensory neurons of neonatal rats. J. Neurosci. *22*, 1238–1247.
Chodobski, A., Zink, B.J., and Szmydynger-Chodobska, J. (2011). Blood-brain barrier pathophysiology in traumatic brain injury. Transl. Stroke Res. *2*, 492–516.
Choi, D.W. (1987). Ionic dependence of glutamate neurotoxicity. J. Neurosci. Off. J. Soc. Neurosci. *7*, 369–379.
Choi, D.W. (1995). Calcium: still center-stage in hypoxic-ischemic neuronal death. Trends Neurosci. *18*, 58–60.
Choi, B.Y., Jang, B.G., Kim, J.H., Lee, B.E., Sohn, M., Song, H.K., and Suh, S.W. (2012). Prevention of traumatic brain injury-induced neuronal death by inhibition of NADPH oxidase activation. Brain Res. *1481*, 49–58.
Chrast, R., Saher, G., Nave, K.-A., and Verheijen, M.H.G. (2011). Lipid metabolism in myelinating glial cells: lessons from human inherited disorders and mouse models. J. Lipid Res. *52*, 419–434.
Christ, A.F., Franze, K., Gautier, H., Moshayedi, P., Fawcett, J., Franklin, R.J.M., Karadottir, R.T., and Guck, J. (2010). Mechanical difference between white and gray matter in the rat cerebellum measured by scanning force microscopy. J. Biomech. *43*, 2986–2992.

Christman, C.W., Grady, M.S., Walker, S.A., Holloway, K.L., and Povlishock, J.T. (1994). Ultrastructural studies of diffuse axonal injury in humans. J. Neurotrauma *11*, 173–186.
Chrzanowska-Wodnicka, M., and Burridge, K. (1996). Rho-stimulated contractility drives the formation of stress fibers and focal adhesions. J. Cell Biol. *133*, 1403–1415.
Chuckowree, J.A., and Vickers, J.C. (2003). Cytoskeletal and morphological alterations underlying axonal sprouting after localized transection of cortical neuron axons in vitro. J. Neurosci. Off. J. Soc. Neurosci. *23*, 3715–3725.
Chung, R.S., Staal, J.A., McCormack, G.H., Dickson, T.C., Cozens, M.A., Chuckowree, J.A., Quilty, M.C., and Vickers, J.C. (2005). Mild axonal stretch injury in vitro induces a progressive series of neurofilament alterations ultimately leading to delayed axotomy. J. Neurotrauma *22*, 1081–1091.
Church, A.J., and Andrew, R.D. (2005). Spreading depression expands traumatic injury in neocortical brain slices. J. Neurotrauma *22*, 277–290.
Clark, R.S.B., Bayir, H., Chu, C.T., Alber, S.M., Kochanek, P.M., and Watkins, S.C. (2008). Autophagy is increased in mice after traumatic brain injury and is detectable in human brain after trauma and critical illness. Autophagy *4*, 88–90.
Clarner, T., Diederichs, F., Berger, K., Denecke, B., Gan, L., van der Valk, P., Beyer, C., Amor, S., and Kipp, M. (2012). Myelin debris regulates inflammatory responses in an experimental demyelination animal model and multiple sclerosis lesions. Glia *60*, 1468–1480.
Codelia, V.A., Sun, G., and Irvine, K.D. (2014). Regulation of YAP by Mechanical Strain through Jnk and Hippo Signaling. Curr. Biol. CB *24*, 2012–2017.
Collinsworth, A.M., Torgan, C.E., Nagda, S.N., Rajalingam, R.J., Kraus, W.E., and Truskey, G.A. (2000). Orientation and length of mammalian skeletal myocytes in response to a unidirectional stretch. Cell Tissue Res. *302*, 243–251.
Colton, C.A. (2009). Heterogeneity of Microglial Activation in the Innate Immune Response in the Brain. J. Neuroimmune Pharmacol. *4*, 399–418.
Coman, I., Aigrot, M.S., Seilhean, D., Reynolds, R., Girault, J.A., Zalc, B., and Lubetzki, C. (2006). Nodal, paranodal and juxtaparanodal axonal proteins during demyelination and remyelination in multiple sclerosis. Brain J. Neurol. *129*, 3186–3195.
Cooney, S.J., Bermudez-Sabogal, S.L., and Byrnes, K.R. (2013). Cellular and temporal expression of NADPH oxidase (NOX) isotypes after brain injury. J. Neuroinflammation *10*, 1.
Coppi, E., Cellai, L., Maraula, G., Pugliese, A.M., and Pedata, F. (2013). Adenosine A_2A receptors inhibit delayed rectifier potassium currents and cell differentiation in primary purified oligodendrocyte cultures. Neuropharmacology *73*, 301–310.
Coppi, E., Cellai, L., Maraula, G., Dettori, I., Melani, A., Pugliese, A.M., and Pedata, F. (2015). Role of adenosine in oligodendrocyte precursor maturation. Front. Cell. Neurosci. *9*, 155.
Cornelius, C., Crupi, R., Calabrese, V., Graziano, A., Milone, P., Pennisi, G., Radak, Z., Calabrese, E.J., and Cuzzocrea, S. (2013). Traumatic Brain Injury: Oxidative Stress and Neuroprotection. Antioxid. Redox Signal. *19*, 836–853.
Correale, J., and Tenembaum, S.N. (2006). Myelin basic protein and myelin oligodendrocyte glycoprotein T-cell repertoire in childhood and juvenile multiple sclerosis. Mult. Scler. Houndmills Basingstoke Engl. *12*, 412–420.
Corrigan, F., Vink, R., Blumbergs, P.C., Masters, C.L., Cappai, R., and van den Heuvel, C. (2012). sAPPα rescues deficits in amyloid precursor protein knockout mice following focal traumatic brain injury. J. Neurochem. *122*, 208–220.
Counterman, A.E., D'Onofrio, T.G., Andrews, A.M., and Weiss, P.S. (2006). A physical model of axonal damage due to oxidative stress. Proc. Natl. Acad. Sci. U. S. A. *103*, 5262–5266.
Cracowski, J.-L., Durand, T., and Bessard, G. (2002). Isoprostanes as a biomarker of lipid peroxidation in humans: physiology, pharmacology and clinical implications. Trends Pharmacol. Sci. *23*, 360–366.
Cramer, L.P., Siebert, M., and Mitchison, T.J. (1997). Identification of novel graded polarity actin filament bundles in locomoting heart fibroblasts: implications for the generation of motile force. J. Cell Biol. *136*, 1287–1305.
Cui, Y., Hameed, F.M., Yang, B., Lee, K., Pan, C.Q., Park, S., and Sheetz, M. (2015). Cyclic stretching of soft substrates induces spreading and growth. Nat. Commun. *6*, 6333.
Cukierman, E. (2001). Taking Cell-Matrix Adhesions to the Third Dimension. Science *294*, 1708–1712.
Dall'Acqua, P., Johannes, S., Mica, L., Simmen, H.-P., Glaab, R., Fandino, J., Schwendinger, M., Meier, C., Ulbrich, E.J., Müller, A., et al. (2016). Connectomic and Surface-Based Morphometric Correlates of Acute Mild Traumatic Brain Injury. Front. Hum. Neurosci. *10*.
Dalle-Donne, I., Rossi, R., Giustarini, D., Milzani, A., and Colombo, R. (2003). Protein carbonyl groups as biomarkers of oxidative stress. Clin. Chim. Acta *329*, 23–38.

Dalle-Donne, I., Rossi, R., Colombo, R., Giustarini, D., and Milzani, A. (2006). Biomarkers of oxidative damage in human disease. Clin. Chem. *52*, 601–623.
Daly, J.W., Hong, O., Padgett, W.L., Shamim, M.T., Jacobson, K.A., and Ukena, D. (1988). Non-xanthine heterocycles: activity as antagonists of A1- and A2-adenosine receptors. Biochem. Pharmacol. *37*, 655–664.
Damiano, S., Fusco, R., Morano, A., De Mizio, M., Paternò, R., De Rosa, A., Spinelli, R., Amente, S., Frunzio, R., Mondola, P., et al. (2012). Reactive oxygen species regulate the levels of dual oxidase (Duox1-2) in human neuroblastoma cells. PloS One *7*, e34405.
Dartsch, P.C., and Betz, E. (1989). Response of cultured endothelial cells to mechanical stimulation. Basic Res. Cardiol. *84*, 268–281.
Dartsch, P.C., Hämmerle, H., and Betz, E. (1986). Orientation of cultured arterial smooth muscle cells growing on cyclically stretched substrates. Acta Anat. (Basel) *125*, 108–113.
Davidson, L., von Dassow, M., and Zhou, J. (2009). Multi-scale mechanics from molecules to morphogenesis. Int. J. Biochem. Cell Biol. *41*, 2147–2162.
Davies, K.J. (1987). Protein damage and degradation by oxygen radicals. I. general aspects. J. Biol. Chem. *262*, 9895–9901.
Davies, P.F. (1995). Flow-mediated endothelial mechanotransduction. Physiol. Rev. *75*, 519–560.
Davies, M.J., Fu, S., Wang, H., and Dean, R.T. (1999). Stable markers of oxidant damage to proteins and their application in the study of human disease. Free Radic. Biol. Med. *27*, 1151–1163.
Davis, C.A., Zambrano, S., Anumolu, P., Allen, A.C.B., Sonoqui, L., and Moreno, M.R. (2015). Device-based in vitro techniques for mechanical stimulation of vascular cells: a review. J. Biomech. Eng. *137*, 40801.
Dawodu, S.T. (2016). Traumatic Brain Injury (TBI) - Definition and Pathophysiology: Overview, Epidemiology, Primary Injury.
Dayem, A.A., Choi, H.-Y., Kim, J.-H., and Cho, S.-G. (2010). Role of Oxidative Stress in Stem, Cancer, and Cancer Stem Cells. Cancers *2*, 859–884.
De Duve, C., and Wattiaux, R. (1966). Functions of lysosomes. Annu. Rev. Physiol. *28*, 435–492.
Dean, O., Giorlando, F., and Berk, M. (2011). N-acetylcysteine in psychiatry: current therapeutic evidence and potential mechanisms of action. J. Psychiatry Neurosci. JPN *36*, 78–86.
Dehghan, F., Khaksari Hadad, M., Asadikram, G., Najafipour, H., and Shahrokhi, N. (2013). Effect of melatonin on intracranial pressure and brain edema following traumatic brain injury: role of oxidative stresses. Arch. Med. Res. *44*, 251–258.
DeKosky, S.T., Taffe, K.M., Abrahamson, E.E., Dixon, C.E., Kochanek, P.M., and Ikonomovic, M.D. (2004). Time course analysis of hippocampal nerve growth factor and antioxidant enzyme activity following lateral controlled cortical impact brain injury in the rat. J. Neurotrauma *21*, 491–500.
Delpech, J.-C., Madore, C., Nadjar, A., Joffre, C., Wohleb, E.S., and Layé, S. (2015). Microglia in neuronal plasticity: Influence of stress. Neuropharmacology *96*, 19–28.
Del Rio Hortega P. (1922) ¿Son homologables la glía de escasas radiaciones y las células de Schwann ? Bol Soc Esp Biol:10: 25–28.
Dennerll, T.J., Lamoureux, P., Buxbaum, R.E., and Heidemann, S.R. (1989). The cytomechanics of axonal elongation and retraction. J. Cell Biol. *109*, 3073–3083.
DeRidder, M.N., Simon, M.J., Siman, R., Auberson, Y.P., Raghupathi, R., and Meaney, D.F. (2006). Traumatic mechanical injury to the hippocampus in vitro causes regional caspase-3 and calpain activation that is influenced by NMDA receptor subunit composition. Neurobiol. Dis. *22*, 165–176.
Désiré, L., Blondiaux, E., Carrière, J., Haddad, R., Sol, O., Fehlbaum-Beurdeley, P., Einstein, R., Zhou, W., and Pando, M.P. (2013). Blood transcriptomic biomarkers of Alzheimer's disease patients treated with EHT 0202. J. Alzheimers Dis. JAD *34*, 469–483.
DeWitt, D.S., and Prough, D.S. (2009). Blast-induced brain injury and posttraumatic hypotension and hypoxemia. J. Neurotrauma *26*, 877–887.
Dexter, D.T., Holley, A.E., Flitter, W.D., Slater, T.F., Wells, F.R., Daniel, S.E., Lees, A.J., Jenner, P., and Marsden, C.D. (1994). Increased levels of lipid hydroperoxides in the parkinsonian substantia nigra: an HPLC and ESR study. Mov. Disord. Off. J. Mov. Disord. Soc. *9*, 92–97.
Dhawan, V. (2014). Reactive Oxygen and Nitrogen Species: General Considerations. In Studies on Respiratory Disorders, N.K. Ganguly, S.K. Jindal, S. Biswal, P.J. Barnes, and R. Pawankar, eds. (New York, NY: Springer New York), pp. 27–47.
Di, X., Goforth, P.B., Bullock, R., Ellis, E., and Satin, L. (2000). Mechanical injury alters volume activated ion channels in cortical astrocytes. Acta Neurochir. Suppl. *76*, 379–383.
Di Pietro, V., Amorini, A.M., Tavazzi, B., Hovda, D.A., Signoretti, S., Giza, C.C., Lazzarino, G., Vagnozzi, R., Lazzarino, G., and Belli, A. (2013). Potentially neuroprotective gene modulation in an in vitro model of mild traumatic brain injury. Mol. Cell. Biochem. *375*, 185–198.

Diaz-Arrastia, R., Kochanek, P.M., Bergold, P., Kenney, K., Marx, C.E., Grimes, C.J.B., Loh, L.T.C.Y., Adam, L.T.C.G.E., Oskvig, D., Curley, K.C., et al. (2014). Pharmacotherapy of traumatic brain injury: state of the science and the road forward: report of the Department of Defense Neurotrauma Pharmacology Workgroup. J. Neurotrauma *31*, 135–158.

Dizdaroglu, M., Jaruga, P., Birincioglu, M., and Rodriguez, H. (2002). Free radical-induced damage to DNA: mechanisms and measurement. Free Radic. Biol. Med. *32*, 1102–1115.

Dóczi, T. (1993). Volume regulation of the brain tissue--a survey. Acta Neurochir. (Wien) *121*, 1–8.

Dohi, K., Ohtaki, H., Nakamachi, T., Yofu, S., Satoh, K., Miyamoto, K., Song, D., Tsunawaki, S., Shioda, S., and Aruga, T. (2010). Gp91 phox (NOX2) in classically activated microglia exacerbates traumatic brain injury. J. Neuroinflammation *7*, 1.

Domingos, P.P., Fonseca, P.M., Nadruz, W., and Franchini, K.G. (2002). Load-induced focal adhesion kinase activation in the myocardium: role of stretch and contractile activity. Am. J. Physiol. Heart Circ. Physiol. *282*, H556-564.

Downes, N., and Mullins, P. (2013). The Development of Myelin in the Brain of the Juvenile Rat. Toxicol. Pathol. 192623313503518.

Drott, J., Desire, L., Drouin, D., Pando, M., and Haun, F. (2010). Etazolate improves performance in a foraging and homing task in aged rats. Eur. J. Pharmacol. *634*, 95–100.

Du, L., Empey, P.E., Ji, J., Chao, H., Kochanek, P.M., Bayır, H., and Clark, R.S.B. (2016). Probenecid and N-Acetylcysteine Prevent Loss of Intracellular Glutathione and Inhibit Neuronal Death after Mechanical Stretch Injury In Vitro. J. Neurotrauma *33*, 1913–1917.

Dupont, S., Morsut, L., Aragona, M., Enzo, E., Giulitti, S., Cordenonsi, M., Zanconato, F., Le Digabel, J., Forcato, M., Bicciato, S., et al. (2011). Role of YAP/TAZ in mechanotransduction. Nature *474*, 179–183.

Durackova, Z. (2010). Some current insights into oxidative stress. Physiol. Res. *59*, 459.

Eakin, K., Baratz-Goldstein, R., Pick, C.G., Zindel, O., Balaban, C.D., Hoffer, M.E., Lockwood, M., Miller, J., and Hoffer, B.J. (2014). Efficacy of N-Acetyl Cysteine in Traumatic Brain Injury. PLoS ONE *9*.

Eastwood, M., Mudera, V.C., McGrouther, D.A., and Brown, R.A. (1998). Effect of precise mechanical loading on fibroblast populated collagen lattices: morphological changes. Cell Motil. Cytoskeleton *40*, 13–21.

Echeverry, S., Rodriguez, M.J., and Torres, Y.P. (2016). Transient Receptor Potential Channels in Microglia: Roles in Physiology and Disease. Neurotox. Res. *30*, 467–478.

Eder, C., Klee, R., and Heinemann, U. (1998). Involvement of stretch-activated Cl- channels in ramification of murine microglia. J. Neurosci. *18*, 7127–7137.

ElAli, A., Doeppner, T.R., Zechariah, A., and Hermann, D.M. (2011). Increased blood-brain barrier permeability and brain edema after focal cerebral ischemia induced by hyperlipidemia: role of lipid peroxidation and calpain-1/2, matrix metalloproteinase-2/9, and RhoA overactivation. Stroke J. Cereb. Circ. *42*, 3238–3244.

Elkin, B.S., and Morrison III, B. (2007). Region-specific tolerance criteria for the living brain. Stapp Car Crash J. *51*, 127.

Ellis, E.F., McKinney, J.S., Willoughby, K.A., Liang, S., and Povlishock, J.T. (1995). A new model for rapid stretch-induced injury of cells in culture: characterization of the model using astrocytes. J. Neurotrauma *12*, 325–339.

Ellis, E.F., Willoughby, K.A., Sparks, S.A., and Chen, T. (2007). S100B protein is released from rat neonatal neurons, astrocytes, and microglia by *in vitro* trauma and anti-S100 increases trauma-induced delayed neuronal injury and negates the protective effect of exogenous S100B on neurons: Endogenous S100B and brain cell injury. J. Neurochem. *101*, 1463–1470.

Elson, L.M., and Ward, C.C. (1994). Mechanisms and pathophysiology of mild head injury. Semin. Neurol. *14*, 8–18.

Engel, D.C., Slemmer, J.E., Vlug, A.S., Maas, A.I.R., and Weber, J.T. (2005). Combined effects of mechanical and ischemic injury to cortical cells: Secondary ischemia increases damage and decreases effects of neuroprotective agents. Neuropharmacology *49*, 985–995.

Engler, A., Bacakova, L., Newman, C., Hategan, A., Griffin, M., and Discher, D. (2004). Substrate compliance versus ligand density in cell on gel responses. Biophys. J. *86*, 617–628.

Engler, A.J., Sen, S., Sweeney, H.L., and Discher, D.E. (2006). Matrix Elasticity Directs Stem Cell Lineage Specification. Cell *126*, 677–689.

Espinosa-Diez, C., Miguel, V., Mennerich, D., Kietzmann, T., Sánchez-Pérez, P., Cadenas, S., and Lamas, S. (2015). Antioxidant responses and cellular adjustments to oxidative stress. Redox Biol. *6*, 183–197.

Faden, A.I., Demediuk, P., Panter, S.S., and Vink, R. (1989). The role of excitatory amino acids and NMDA receptors in traumatic brain injury. Science *244*, 798–800.
Fancy, S.P.J., Kotter, M.R., Harrington, E.P., Huang, J.K., Zhao, C., Rowitch, D.H., and Franklin, R.J.M. (2010). Overcoming remyelination failure in multiple sclerosis and other myelin disorders. Exp. Neurol. *225*, 18–23.
Faul, M., Xu, L., Wald, M. M. & Coronado, V. G. Traumatic brain injury in the United States: emergency department visits, hospitalizations and deaths 2002–2006. Centers for Disease Control and Prevention, National Center for Injury Prevention and Control [online], http://www.cdc.gov/traumaticbraininjury/tbi_ed.html (2010).
Faust, U., Hampe, N., Rubner, W., Kirchgeßner, N., Safran, S., Hoffmann, B., and Merkel, R. (2011). Cyclic Stress at mHz Frequencies Aligns Fibroblasts in Direction of Zero Strain. PLoS ONE *6*, e28963.
Felts, P.A., Baker, T.A., and Smith, K.J. (1997). Conduction in segmentally demyelinated mammalian central axons. J. Neurosci. Off. J. Soc. Neurosci. *17*, 7267–7277.
Fernandez-Fernandez, S., Almeida, A., and Bolaños, J.P. (2012). Antioxidant and bioenergetic coupling between neurons and astrocytes. Biochem. J. *443*, 3–11.
Ferrándiz, M.L., and Devesa, I. (2008). Inducers of heme oxygenase-1. Curr. Pharm. Des. *14*, 473–486.
Ferreira, A.P.O., Rodrigues, F.S., Della-Pace, I.D., Mota, B.C., Oliveira, S.M., Velho Gewehr, C. de C., Bobinski, F., de Oliveira, C.V., Brum, J.S., Oliveira, M.S., et al. (2013). The effect of NADPH-oxidase inhibitor apocynin on cognitive impairment induced by moderate lateral fluid percussion injury: role of inflammatory and oxidative brain damage. Neurochem. Int. *63*, 583–593.
Feutz, A.C., Bellomi, I., Allinquant, B., Schladenhaufen, Y., and Ghandour, M.S. (1995). Isolation and characterization of defective jimpy oligodendrocytes in culture. J. Neurocytol. *24*, 865–877.
Feutz, A.C., Pham-Dinh, D., Allinquant, B., Miehe, M., and Ghandour, M.S. (2001). An immortalized jimpy oligodendrocyte cell line: defects in cell cycle and cAMP pathway. Glia *34*, 241–252.
Fields, R.D. (2014). Myelin--More than Insulation. Science *344*, 264–266.
Fields, R.D. (2015). A new mechanism of nervous system plasticity: activity-dependent myelination. Nat. Rev. Neurosci. *16*, 756–767.
Filipovic, D., and Sackin, H. (1992). Stretch- and volume-activated channels in isolated proximal tubule cells. Am. J. Physiol. *262*, F857-870.
Filomeni, G., De Zio, D., and Cecconi, F. (2015). Oxidative stress and autophagy: the clash between damage and metabolic needs. Cell Death Differ. *22*, 377–388.
Fineman, I., Hovda, D.A., Smith, M., Yoshino, A., and Becker, D.P. (1993). Concussive brain injury is associated with a prolonged accumulation of calcium: a 45Ca autoradiographic study. Brain Res. *624*, 94–102.
Fleury, C., Mignotte, B., and Vayssière, J.-L. (2002). Mitochondrial reactive oxygen species in cell death signaling. Biochimie *84*, 131–141.
Floyd, C.L., Rzigalinski, B.A., Weber, J.T., Sitterding, H.A., Willoughby, K.A., and Ellis, E.F. (2001). Traumatic injury of cultured astrocytes alters inositol (1,4,5)-trisphosphate-mediated signaling. Glia *33*, 12–23.
Floyd, C.L., Gorin, F.A., and Lyeth, B.G. (2005). Mechanical strain injury increases intracellular sodium and reverses Na+/Ca2+ exchange in cortical astrocytes. Glia *51*, 35–46.
Fluiter, K., Opperhuizen, A.L., Morgan, B.P., Baas, F., and Ramaglia, V. (2014). Inhibition of the membrane attack complex of the complement system reduces secondary neuroaxonal loss and promotes neurologic recovery after traumatic brain injury in mice. J. Immunol. Baltim. Md 1950 *192*, 2339–2348.
Flygt, J., Djupsjö, A., Lenne, F., and Marklund, N. (2013). Myelin loss and oligodendrocyte pathology in white matter tracts following traumatic brain injury in the rat. Eur. J. Neurosci. *38*, 2153–2165.
Flygt, J., Gumucio, A., Ingelsson, M., Skoglund, K., Holm, J., Alafuzoff, I., and Marklund, N. (2016). Human Traumatic Brain Injury Results in Oligodendrocyte Death and Increases the Number of Oligodendrocyte Progenitor Cells. J. Neuropathol. Exp. Neurol. *75*, 503–515.
Förstermann, U., and Sessa, W.C. (2012). Nitric oxide synthases: regulation and function. Eur. Heart J. *33*, 829–837, 837a–837d.
Franco-Obregón, A., and Lansman, J.B. (2002). Changes in mechanosensitive channel gating following mechanical stimulation in skeletal muscle myotubes from the mdx mouse. J. Physiol. *539*, 391–407.
Franklin, R.J.M., and Ffrench-Constant, C. (2008). Remyelination in the CNS: from biology to therapy. Nat. Rev. Neurosci. *9*, 839–855.

Franze, K., Gerdelmann, J., Weick, M., Betz, T., Pawlizak, S., Lakadamyali, M., Bayer, J., Rillich, K., Gögler, M., Lu, Y.-B., et al. (2009). Neurite Branch Retraction Is Caused by a Threshold-Dependent Mechanical Impact. Biophys. J. *97*, 1883–1890.

French, H.M., Reid, M., Mamontov, P., Simmons, R.A., and Grinspan, J.B. (2009). Oxidative stress disrupts oligodendrocyte maturation. J. Neurosci. Res. *87*, 3076–3087.

Fridovich, I. (1997). Superoxide anion radical (O2-.), superoxide dismutases, and related matters. J. Biol. Chem. *272*, 18515–18517.

Fu, J., Wang, Y.-K., Yang, M.T., Desai, R.A., Yu, X., Liu, Z., and Chen, C.S. (2010). Mechanical regulation of cell function with geometrically modulated elastomeric substrates. Nat. Methods *7*, 733–736.

Funfschilling, U., Supplie, L.M., Mahad, D., Boretius, S., Saab, A.S., Edgar, J., Brinkmann, B.G., Kassmann, C.M., Tzvetanova, I.D., Möbius, W., et al. (2012). Glycolytic oligodendrocytes maintain myelin and long-term axonal integrity. Nature *485*, 517–521.

Fusco, F.R., Martorana, A., Giampà, C., March, Z.D., Vacca, F., Tozzi, A., Longone, P., Piccirilli, S., Paolucci, S., Sancesario, G., et al. (2004). Cellular localization of TRPC3 channel in rat brain: preferential distribution to oligodendrocytes. Neurosci. Lett. *365*, 137–142.

Galea, E., Launay, N., Portero-Otin, M., Ruiz, M., Pamplona, R., Aubourg, P., Ferrer, I., and Pujol, A. (2012). Oxidative stress underlying axonal degeneration in adrenoleukodystrophy: A paradigm for multifactorial neurodegenerative diseases? Biochim. Biophys. Acta BBA - Mol. Basis Dis. *1822*, 1475–1488.

Gan, L., and Johnson, J.A. (2014). Oxidative damage and the Nrf2-ARE pathway in neurodegenerative diseases. Biochim. Biophys. Acta BBA - Mol. Basis Dis. *1842*, 1208–1218.

Geddes, D.M., and Cargill, R.S. (2001). An in Vitro Model of Neural Trauma: Device Characterization and Calcium Response to Mechanical Stretch. J. Biomech. Eng. *123*, 247.

Geddes-Klein, D.M., Schiffman, K.B., and Meaney, D.F. (2006). Mechanisms and consequences of neuronal stretch injury in vitro differ with the model of trauma. J. Neurotrauma *23*, 193–204.

Gennarelli, T.A. (1983). Head injury in man and experimental animals: clinical aspects. Acta Neurochir. Suppl. (Wien) *32*, 1–13.

Gennarelli, T.A., Thibault, L.E., Adams, J.H., Graham, D.I., Thompson, C.J., and Marcincin, R.P. (1982). Diffuse axonal injury and traumatic coma in the primate. Ann. Neurol. *12*, 564–574.

Gensert, J.M., and Goldman, J.E. (1997). Endogenous progenitors remyelinate demyelinated axons in the adult CNS. Neuron *19*, 197–203.

Gentleman, S.M., Nash, M.J., Sweeting, C.J., Graham, D.I., and Roberts, G.W. (1993). Beta-amyloid precursor protein (beta APP) as a marker for axonal injury after head injury. Neurosci. Lett. *160*, 139–144.

Gentry, L.R., Godersky, J.C., and Thompson, B. (1988). MR imaging of head trauma: review of the distribution and radiopathologic features of traumatic lesions. AJR Am. J. Roentgenol. *150*, 663–672.

Geoffroy, C.G., and Zheng, B. (2014). Myelin-associated inhibitors in axonal growth after CNS injury. Curr. Opin. Neurobiol. *27*, 31–38.

Gerstmair, A., Fois, G., Innerbichler, S., Dietl, P., and Felder, E. (2009). A device for simultaneous live cell imaging during uni-axial mechanical strain or compression. J. Appl. Physiol. Bethesda Md 1985 *107*, 613–620.

Ghandour, M.S., Feutz, A.-C., Jalabi, W., Taleb, O., Bessert, D., Cypher, M., Carlock, L., and Skoff, R.P. (2002). Trafficking of PLP/DM20 and cAMP signaling in immortalized jimpy oligodendrocytes. Glia *40*, 300–311.

Ghoumari, A.M., Ibanez, C., El-Etr, M., Leclerc, P., Eychenne, B., O'Malley, B.W., Baulieu, E.E., and Schumacher, M. (2003). Progesterone and its metabolites increase myelin basic protein expression in organotypic slice cultures of rat cerebellum. J. Neurochem. *86*, 848–859.

Giannone, G., Dubin-Thaler, B.J., Döbereiner, H.-G., Kieffer, N., Bresnick, A.R., and Sheetz, M.P. (2004). Periodic lamellipodial contractions correlate with rearward actin waves. Cell *116*, 431–443.

Gilgun-Sherki, Y., Rosenbaum, Z., Melamed, E., and Offen, D. (2002). Antioxidant therapy in acute central nervous system injury: current state. Pharmacol. Rev. *54*, 271–284.

Giza, C.C., and Hovda, D.A. (2001). The Neurometabolic Cascade of Concussion. J. Athl. Train. *36*, 228–235.

Gladman, S.J., Ward, R.E., Michael-Titus, A.T., Knight, M.M., and Priestley, J.V. (2010). The effect of mechanical strain or hypoxia on cell death in subpopulations of rat dorsal root ganglion neurons in vitro. Neuroscience *171*, 577–587.

Gladman, S.J., Huang, W., Lim, S.-N., Dyall, S.C., Boddy, S., Kang, J.X., Knight, M.M., Priestley, J.V., and Michael-Titus, A.T. (2012). Improved Outcome after Peripheral Nerve Injury in Mice with Increased Levels of Endogenous Omega-3 Polyunsaturated Fatty Acids. J. Neurosci. *32*, 563–571.

Gledhill, R.F., and McDonald, W.I. (1977). Morphological characteristics of central demyelination and remyelination: a single-fiber study. Ann. Neurol. *1*, 552–560.

Goforth, P.B., Ellis, E.F., and Satin, L.S. (1999). Enhancement of AMPA-mediated current after traumatic injury in cortical neurons. J. Neurosci. *19*, 7367–7374.

Goforth, P.B., Ellis, E.F., and Satin, L.S. (2004). Mechanical injury modulates AMPA receptor kinetics via an NMDA receptor-dependent pathway. J. Neurotrauma *21*, 719–732.

Goldmann, W.H. (2014). Mechanosensation. In Progress in Molecular Biology and Translational Science, (Elsevier), pp. 75–102.

Goldyn, A.M., Rioja, B.A., Spatz, J.P., Ballestrem, C., and Kemkemer, R. (2009). Force-induced cell polarisation is linked to RhoA-driven microtubule-independent focal-adhesion sliding. J. Cell Sci. *122*, 3644–3651.

Goldyn, A.M., Kaiser, P., Spatz, J.P., Ballestrem, C., and Kemkemer, R. (2010). The kinetics of force-induced cell reorganization depend on microtubules and actin. Cytoskeleton *67*, 241–250.

Gomes, A., Fernandes, E., and Lima, J.L.F.C. (2005). Fluorescence probes used for detection of reactive oxygen species. J. Biochem. Biophys. Methods *65*, 45–80.

Gong, B., Vitolo, O.V., Trinchese, F., Liu, S., Shelanski, M., and Arancio, O. (2004). Persistent improvement in synaptic and cognitive functions in an Alzheimer mouse model after rolipram treatment. J. Clin. Invest. *114*, 1624–1634.

Goodman, Y., and Mattson, M.P. (1994). Secreted forms of beta-amyloid precursor protein protect hippocampal neurons against amyloid beta-peptide-induced oxidative injury. Exp. Neurol. *128*, 1–12.

Grady, M.S., McLaughlin, M.R., Christman, C.W., Valadka, A.B., Fligner, C.L., and Povlishock, J.T. (1993). The use of antibodies targeted against the neurofilament subunits for the detection of diffuse axonal injury in humans. J. Neuropathol. Exp. Neurol. *52*, 143–152.

Graham, D.I., Ford, I., Adams, J.H., Doyle, D., Teasdale, G.M., Lawrence, A.E., and McLellan, D.R. (1989). Ischaemic brain damage is still common in fatal non-missile head injury. J. Neurol. Neurosurg. Psychiatry *52*, 346–350.

Gravel, M., Peterson, J., Yong, V.W., Kottis, V., Trapp, B., and Braun, P.E. (1996). Overexpression of 2',3'-cyclic nucleotide 3'-phosphodiesterase in transgenic mice alters oligodendrocyte development and produces aberrant myelination. Mol. Cell. Neurosci. *7*, 453–466.

Green, R.E.A., Colella, B., Maller, J.J., Bayley, M., Glazer, J., and Mikulis, D.J. (2014). Scale and pattern of atrophy in the chronic stages of moderate-severe TBI. Front. Hum. Neurosci. *8*, 67.

Greer, J.M. (2013). Autoimmune T-cell reactivity to myelin proteolipids and glycolipids in multiple sclerosis. Mult. Scler. Int. *2013*, 151427.

Griffith, O.W., and Stuehr, D.J. (1995). Nitric oxide synthases: properties and catalytic mechanism. Annu. Rev. Physiol. *57*, 707–736.

Griffiths, I., Klugmann, M., Anderson, T., Yool, D., Thomson, C., Schwab, M.H., Schneider, A., Zimmermann, F., McCulloch, M., Nadon, N., et al. (1998). Axonal swellings and degeneration in mice lacking the major proteolipid of myelin. Science *280*, 1610–1613.

Grune, T., Reinheckel, T., and Davies, K.J. (1997). Degradation of oxidized proteins in mammalian cells. FASEB J. Off. Publ. Fed. Am. Soc. Exp. Biol. *11*, 526–534.

Gudz, T.I., Komuro, H., and Macklin, W.B. (2006). Glutamate Stimulates Oligodendrocyte Progenitor Migration Mediated via an αv Integrin/Myelin Proteolipid Protein Complex. J. Neurosci. *26*, 2458–2466.

Guerriero, R.M., Giza, C.C., and Rotenberg, A. (2015). Glutamate and GABA imbalance following traumatic brain injury. Curr. Neurol. Neurosci. Rep. *15*, 27.

Guharay, F., and Sachs, F. (1984). Stretch-activated single ion channel currents in tissue-cultured embryonic chick skeletal muscle. J. Physiol. *352*, 685–701.

Gul, M., Kutay, F.Z., Temocin, S., and Hanninen, O. (2000). Cellular and clinical implications of glutathione. Indian J. Exp. Biol. *38*, 625–634.

Gultekin, S.H., and Smith, T.W. (1994). Diffuse axonal injury in craniocerebral trauma. A comparative histologic and immunohistochemical study. Arch. Pathol. Lab. Med. *118*, 168–171.

Günther, M., Davidsson, J., Plantman, S., Norgren, S., Mathiesen, T., and Risling, M. (2015). Neuroprotective effects of N-acetylcysteine amide on experimental focal penetrating brain injury in rats. J. Clin. Neurosci. Off. J. Neurosurg. Soc. Australas. *22*, 1477–1483.

Guo, J., Lin, P., Zhao, X., Zhang, J., Wei, X., Wang, Q., and Wang, C. (2014). Etazolate abrogates the lipopolysaccharide (LPS)-induced downregulation of the cAMP/pCREB/BDNF signaling, neuroinflammatory response and depressive-like behavior in mice. Neuroscience *263*, 1–14.
Gutteridge, J.M. (1995). Lipid peroxidation and antioxidants as biomarkers of tissue damage. Clin. Chem. *41*, 1819–1828.
Haenen, G.R.M.M., and Bast, A. (2014). Glutathione revisited: a better scavenger than previously thought. Front. Pharmacol. *5*.
Haider, L. (2015). Inflammation, Iron, Energy Failure, and Oxidative Stress in the Pathogenesis of Multiple Sclerosis. Oxid. Med. Cell. Longev. *2015*, 725370.
Hall, E.D., and Braughler, J.M. (1993). Free radicals in CNS injury. Res. Publ. - Assoc. Res. Nerv. Ment. Dis. *71*, 81–105.
Hall, E.D., Detloff, M.R., Johnson, K., and Kupina, N.C. (2004). Peroxynitrite-mediated protein nitration and lipid peroxidation in a mouse model of traumatic brain injury. J. Neurotrauma *21*, 9–20.
Halliwell, B. (1992). Reactive oxygen species and the central nervous system. J. Neurochem. *59*, 1609–1623.
Halliwell, B. (1999). Oxygen and nitrogen are pro-carcinogens. Damage to DNA by reactive oxygen, chlorine and nitrogen species: measurement, mechanism and the effects of nutrition. Mutat. Res. *443*, 37–52.
Halliwell, B. (2002). Effect of diet on cancer development: is oxidative DNA damage a biomarker? Free Radic. Biol. Med. *32*, 968–974.
Halliwell, B., and Whiteman, M. (2004). Measuring reactive species and oxidative damage *in vivo* and in cell culture: how should you do it and what do the results mean? Br. J. Pharmacol. *142*, 231–255.
Halliwell, and Gutteridge (1985). Free Radicals in Biology and Medicine.
Hamill, O.P., and Martinac, B. (2001). Molecular basis of mechanotransduction in living cells. Physiol. Rev. *81*, 685–740.
Hamilton, D.W., Maul, T.M., and Vorp, D.A. (2004). Characterization of the Response of Bone Marrow-Derived Progenitor Cells to Cyclic Strain: Implications for Vascular Tissue-Engineering Applications. Tissue Eng. *10*, 361–369.
Hamilton, N.B., Kolodziejczyk, K., Kougioumtzidou, E., and Attwell, D. (2016). Proton-gated Ca2+-permeable TRP channels damage myelin in conditions mimicking ischaemia. Nature *529*, 523–527.
Hamilton, R.T., Bhattacharya, A., Walsh, M.E., Shi, Y., Wei, R., Zhang, Y., Rodriguez, K.A., Buffenstein, R., Chaudhuri, A.R., and Van Remmen, H. (2013). Elevated protein carbonylation, and misfolding in sciatic nerve from db/db and Sod1(-/-) mice: plausible link between oxidative stress and demyelination. PloS One *8*, e65725.
Hånell, A., Greer, J.E., McGinn, M.J., and Povlishock, J.T. (2015). Traumatic brain injury-induced axonal phenotypes react differently to treatment. Acta Neuropathol. (Berl.) *129*, 317–332.
Harauz, G., and Boggs, J.M. (2013). Myelin management by the 18.5-kDa and 21.5-kDa classic myelin basic protein isoforms. J. Neurochem. *125*, 334–361.
Harauz, G., Ladizhansky, V., and Boggs, J.M. (2009). Structural polymorphism and multifunctionality of myelin basic protein. Biochemistry (Mosc.) *48*, 8094–8104.
Harris, C., and Hansen, J.M. (2012). Oxidative Stress, Thiols, and Redox Profiles. In Developmental Toxicology, C. Harris, and J.M. Hansen, eds. (Totowa, NJ: Humana Press), pp. 325–346.
Harrison, F.E., and May, J.M. (2009). Vitamin C function in the brain: vital role of the ascorbate transporter SVCT2. Free Radic. Biol. Med. *46*, 719–730.
Hatic, H., Kane, M.J., Saykally, J.N., and Citron, B.A. (2012). Modulation of transcription factor Nrf2 in an in vitro model of traumatic brain injury. J. Neurotrauma *29*, 1188–1196.
He, Y., Jackman, N.A., Thorn, T.L., Vought, V.E., and Hewett, S.J. (2015). Interleukin-1β protects astrocytes against oxidant-induced injury via an NF-κB-Dependent upregulation of glutathione synthesis: IL-1β Increases GSH and Protects Astrocytes. Glia *63*, 1568–1580.
He, Y.Y., Hsu, C.Y., Ezrin, A.M., and Miller, M.S. (1993). Polyethylene glycol-conjugated superoxide dismutase in focal cerebral ischemia-reperfusion. Am. J. Physiol. *265*, H252-256.
Hemmer, B., Archelos, J.J., and Hartung, H.-P. (2002). New concepts in the immunopathogenesis of multiple sclerosis. Nat. Rev. Neurosci. *3*, 291–301.
Hensley, K., Hall, N., Subramaniam, R., Cole, P., Harris, M., Aksenov, M., Aksenova, M., Gabbita, S.P., Wu, J.F., Carney, J.M., et al. (1995). Brain regional correspondence between Alzheimer's disease histopathology and biomarkers of protein oxidation. J. Neurochem. *65*, 2146–2156.

Hernandez, M., Patzig, J., Mayoral, S.R., Costa, K.D., Chan, J.R., and Casaccia, P. (2016). Mechanostimulation Promotes Nuclear and Epigenetic Changes in Oligodendrocytes. J. Neurosci. *36*, 806–813.

Hernandez-Ontiveros, D.G., Tajiri, N., Acosta, S., Giunta, B., Tan, J., and Borlongan, C.V. (2013). Microglia activation as a biomarker for traumatic brain injury. Front. Neurol. *4*, 30.

Herrera, J.J., Bockhorst, K.H., Kondraganti, S., Stertz, L., DeQuevedo, J.L., and Narayana, P.A. (2016). Acute white matter tract damage following frontal mild traumatic brain injury. J. Neurotrauma.

Herweh, C., Hess, K., Meyding-Lamadé, U., Bartsch, A.J., Stippich, C., Jost, J., Friedmann-Bette, B., Heiland, S., Bendszus, M., and Hähnel, S. (2016). Reduced white matter integrity in amateur boxers. Neuroradiology *58*, 911–920.

Hicdonmez, T., Kanter, M., Tiryaki, M., Parsak, T., and Cobanoglu, S. (2006). Neuroprotective effects of N-acetylcysteine on experimental closed head trauma in rats. Neurochem. Res. *31*, 473–481.

Hildebrand, C., Remahl, S., Persson, H., and Bjartmar, C. (1993). Myelinated nerve fibres in the CNS. Prog. Neurobiol. *40*, 319–384.

Hill, C.S., Coleman, M.P., and Menon, D.K. (2016). Traumatic Axonal Injury: Mechanisms and Translational Opportunities. Trends Neurosci.

Himadri, P., Kumari, S.S., Chitharanjan, M., and Dhananjay, S. (2010). Role of Oxidative Stress and Inflammation in Hypoxia-Induced Cerebral Edema: A Molecular Approach. High Alt. Med. Biol. *11*, 231–244.

Himmelfarb, J., McMonagle, E., and McMenamin, E. (2000). Plasma protein thiol oxidation and carbonyl formation in chronic renal failure. Kidney Int. *58*, 2571–2578.

Hobson, G.M., Huang, Z., Sperle, K., Stabley, D.L., Marks, H.G., and Cambi, F. (2002). A PLP splicing abnormality is associated with an unusual presentation of PMD. Ann. Neurol. *52*, 477–488.

Hoefen, R.J., and Berk, B.C. (2002). The role of MAP kinases in endothelial activation. Vascul. Pharmacol. *38*, 271–273.

Hoffer, M.E., Balaban, C., Slade, M.D., Tsao, J.W., and Hoffer, B. (2013). Amelioration of acute sequelae of blast induced mild traumatic brain injury by N-acetyl cysteine: a double-blind, placebo controlled study. PloS One *8*, e54163.

Hoffman, B.D., Grashoff, C., and Schwartz, M.A. (2011). Dynamic molecular processes mediate cellular mechanotransduction. Nature *475*, 316–323.

Homsi, S., Federico, F., Croci, N., Palmier, B., Plotkine, M., Marchand-Leroux, C., and Jafarian-Tehrani, M. (2009). Minocycline effects on cerebral edema: relations with inflammatory and oxidative stress markers following traumatic brain injury in mice. Brain Res. *1291*, 122–132.

Hong, Y., Yan, W., Chen, S., Sun, C., and Zhang, J. (2010). The role of Nrf2 signaling in the regulation of antioxidants and detoxifying enzymes after traumatic brain injury in rats and mice. Acta Pharmacol. Sin. *31*, 1421–1430.

Horie, S., Ansari, B., Masterson, C., Devaney, J., Scully, M., O'Toole, D., and Laffey, J.G. (2016). Hypercapnic acidosis attenuates pulmonary epithelial stretch-induced injury via inhibition of the canonical NF-κB pathway. Intensive Care Med. Exp. *4*.

Hornberger, T.A. (2004). Intracellular Signaling Specificity in Response to Uniaxial vs. Multiaxial Stretch: Implications for Mechanotransduction. AJP Cell Physiol.

Hornberger, T.A., and Chien, S. (2006). Mechanical stimuli and nutrients regulate rapamycin-sensitive signaling through distinct mechanisms in skeletal muscle. J. Cell. Biochem. *97*, 1207–1216.

Hornberger, T.A., Armstrong, D.D., Koh, T.J., Burkholder, T.J., and Esser, K.A. (2005). Intracellular signaling specificity in response to uniaxial vs. multiaxial stretch: implications for mechanotransduction. Am. J. Physiol. Cell Physiol. *288*, C185-194.

Hosokawa, H., Aiuchi, S., Kambe, T., Hagiwara, Y., and Kubo, T. (2002). Mechanical stretch-induced mitogen-activated protein kinase activation is mediated via angiotensin and endothelin systems in vascular smooth muscle cells. Biol. Pharm. Bull. *25*, 1588–1592.

Hrbac, J., and Kohen, R. (2000). Biological redox activity: Its importance, methods for its quantification and implication for health and disease. Drug Dev. Res. *50*, 516–527.

Hsu, H.-J., Lee, C.-F., and Kaunas, R. (2009). A Dynamic Stochastic Model of Frequency-Dependent Stress Fiber Alignment Induced by Cyclic Stretch. PLoS ONE *4*, e4853.

Hsu, H.-J., Lee, C.-F., Locke, A., Vanderzyl, S.Q., and Kaunas, R. (2010). Stretch-Induced Stress Fiber Remodeling and the Activations of JNK and ERK Depend on Mechanical Strain Rate, but Not FAK. PLoS ONE *5*, e12470.

Hu, M.L. (1994). Measurement of protein thiol groups and glutathione in plasma. Methods Enzymol. *233*, 380–385.

Hughes, E.G., and Appel, B. (2016). The cell biology of CNS myelination. Curr. Opin. Neurobiol. *39*, 93–100.
Hughes, E.G., Kang, S.H., Fukaya, M., and Bergles, D.E. (2013). Oligodendrocyte progenitors balance growth with self-repulsion to achieve homeostasis in the adult brain. Nat. Neurosci. *16*, 668–676.
Hughes, R.H., Silva, V.A., Ahmed, I., Shreiber, D.I., and Morrison, B. (2014). Neuroprotection by genipin against reactive oxygen and reactive nitrogen species-mediated injury in organotypic hippocampal slice cultures. Brain Res. *1543*, 308–314.
Hussain, R., El-Etr, M., Gaci, O., Rakotomamonjy, J., Macklin, W.B., Kumar, N., Sitruk-Ware, R., Schumacher, M., and Ghoumari, A.M. (2011). Progesterone and Nestorone Facilitate Axon Remyelination: A Role for Progesterone Receptors. Endocrinology *152*, 3820–3831.
Ibitoye, R., Kemp, K., Rice, C., Hares, K., Scolding, N., and Wilkins, A. (2016). Oxidative stress-related biomarkers in multiple sclerosis: a review. Biomark. Med. *10*, 889–902.
Ibragic, S., Sofic, E., Suljic, E., Avdagic, N., Bajraktarevic, A., and Tahirovic, I. (2012). Serum nitric oxide concentrations in patients with multiple sclerosis and patients with epilepsy. J. Neural Transm. Vienna Austria 1996 *119*, 7–11.
Ikonomidou, C., and Turski, L. (2002). Why did NMDA receptor antagonists fail clinical trials for stroke and traumatic brain injury? Lancet Neurol. *1*, 383–386.
Ikonomovic, M.D., Uryu, K., Abrahamson, E.E., Ciallella, J.R., Trojanowski, J.Q., Lee, V.M.-Y., Clark, R.S., Marion, D.W., Wisniewski, S.R., and DeKosky, S.T. (2004). Alzheimer's pathology in human temporal cortex surgically excised after severe brain injury. Exp. Neurol. *190*, 192–203.
Imbrosci, B., and Mittmann, T. (2011). Functional consequences of the disturbances in the GABA-mediated inhibition induced by injuries in the cerebral cortex. Neural Plast. *2011*, 614329.
Inci, S., Ozcan, O.E., and Kilinç, K. (1998). Time-level relationship for lipid peroxidation and the protective effect of alpha-tocopherol in experimental mild and severe brain injury. Neurosurgery *43*, 330-335-336.
Inder, T.E., and Huppi, P.S. (2000). In vivo studies of brain development by magnetic resonance techniques. Ment. Retard. Dev. Disabil. Res. Rev. *6*, 59–67.
Ingram, A.J., Ly, H., Thai, K., Kang, M., and Scholey, J.W. (1999). Activation of mesangial cell signaling cascades in response to mechanical strain. Kidney Int. *55*, 476–485.
Inoue, M., Sato, E.F., Nishikawa, M., Park, A.-M., Kira, Y., Imada, I., and Utsumi, K. (2003). Mitochondrial generation of reactive oxygen species and its role in aerobic life. Curr. Med. Chem. *10*, 2495–2505.
Irvine, K.A., and Blakemore, W.F. (2008). Remyelination protects axons from demyelination-associated axon degeneration. Brain J. Neurol. *131*, 1464–1477.
Islas, L., Pasantes-Morales, H., and Sanchez, J.A. (1993). Characterization of stretch-activated ion channels in cultured astrocytes. Glia *8*, 87–96.
Iwata, A., Stys, P.K., Wolf, J.A., Chen, X.-H., Taylor, A.G., Meaney, D.F., and Smith, D.H. (2004). Traumatic axonal injury induces proteolytic cleavage of the voltage-gated sodium channels modulated by tetrodotoxin and protease inhibitors. J. Neurosci. Off. J. Soc. Neurosci. *24*, 4605–4613.
Jackman, N., Ishii, A., and Bansal, R. (2009). Oligodendrocyte development and myelin biogenesis: parsing out the roles of glycosphingolipids. Physiol. Bethesda Md *24*, 290–297.
Jagielska, A., Norman, A.L., Whyte, G., Vliet, K.J.V., Guck, J., and Franklin, R.J.M. (2012). Mechanical Environment Modulates Biological Properties of Oligodendrocyte Progenitor Cells. Stem Cells Dev. *21*, 2905–2914.
Jain, A.K. (2005). Nuclear Import and Export Signals in Control of Nrf2. J. Biol. Chem. *280*, 29158–29168.
Jakovcevski, I., Filipovic, R., Mo, Z., Rakic, S., and Zecevic, N. (2009). Oligodendrocyte development and the onset of myelination in the human fetal brain. Front. Neuroanat. *3*, 5.
Jana, M., and Pahan, K. (2013). Down-regulation of Myelin Gene Expression in Human Oligodendrocytes by Nitric Oxide: Implications for Demyelination in Multiple Sclerosis. J. Clin. Cell. Immunol. *4*.
Jette, N., Coderre, E., Nikolaeva, M.A., Enright, P.D., Iwata, A., Smith, D.H., Jiang, Q., and Stys, P.K. (2006). Spatiotemporal distribution of spectrin breakdown products induced by anoxia in adult rat optic nerve in vitro. J. Cereb. Blood Flow Metab. Off. J. Int. Soc. Cereb. Blood Flow Metab. *26*, 777–786.
Jiang, J.J., Liu, K.J., Jordan, S.J., Swartz, H.M., and Mason, R.P. (1996). Detection of free radical metabolite formation using in vivo EPR spectroscopy: evidence of rat hemoglobin thiyl radical formation following administration of phenylhydrazine. Arch. Biochem. Biophys. *330*, 266–270.

Jin, W., Wang, H., Yan, W., Zhu, L., Hu, Z., Ding, Y., and Tang, K. (2009). Role of Nrf2 in protection against traumatic brain injury in mice. J. Neurotrauma *26*, 131–139.
Jin, X., Ishii, H., Bai, Z., Itokazu, T., and Yamashita, T. (2012). Temporal changes in cell marker expression and cellular infiltration in a controlled cortical impact model in adult male C57BL/6 mice. PloS One *7*, e41892.
Jindal, A., Mahesh, R., Gautam, B., Bhatt, S., and Pandey, D. (2012). Antidepressant-like effect of etazolate, a cyclic nucleotide phosphodiesterase 4 inhibitor--an approach using rodent behavioral antidepressant tests battery. Eur. J. Pharmacol. *689*, 125–131.
Jindal, A., Mahesh, R., and Bhatt, S. (2013a). Etazolate rescues behavioral deficits in chronic unpredictable mild stress model: Modulation of hypothalamic–pituitary–adrenal axis activity and brain-derived neurotrophic factor level. Neurochem. Int. *63*, 465–475.
Jindal, A., Mahesh, R., and Bhatt, S. (2013b). Etazolate, a phosphodiesterase 4 inhibitor reverses chronic unpredictable mild stress-induced depression-like behavior and brain oxidative damage. Pharmacol. Biochem. Behav. *105*, 63–70.
Jindal, A., Mahesh, R., and Bhatt, S. (2015). Etazolate, a phosphodiesterase-4 enzyme inhibitor produces antidepressant-like effects by blocking the behavioral, biochemical, neurobiological deficits and histological abnormalities in hippocampus region caused by olfactory bulbectomy. Psychopharmacology (Berl.) *232*, 623–637.
Johnson, G.B. (2006). The Living World.
Johnson, V.E., Stewart, J.E., Begbie, F.D., Trojanowski, J.Q., Smith, D.H., and Stewart, W. (2013). Inflammation and white matter degeneration persist for years after a single traumatic brain injury. Brain *136*, 28–42.
Johnstone, J.T., Morton, P.D., Jayakumar, A.R., Johnstone, A.L., Gao, H., Bracchi-Ricard, V., Pearse, D.D., Norenberg, M.D., and Bethea, J.R. (2013). Inhibition of NADPH Oxidase Activation in Oligodendrocytes Reduces Cytotoxicity Following Trauma. PLoS ONE *8*, e80975.
Jufri, N.F., Mohamedali, A., Avolio, A., and Baker, M.S. (2015). Mechanical stretch: physiological and pathological implications for human vascular endothelial cells. Vasc. Cell *7*.
Jungbauer, S., Gao, H., Spatz, J.P., and Kemkemer, R. (2008). Two Characteristic Regimes in Frequency-Dependent Dynamic Reorientation of Fibroblasts on Cyclically Stretched Substrates. Biophys. J. *95*, 3470–3478.
Juurlink, B.H. (1997). Response of glial cells to ischemia: roles of reactive oxygen species and glutathione. Neurosci. Biobehav. Rev. *21*, 151–166.
Juurlink, B.H., Schültke, E., and Hertz, L. (1996). Glutathione release and catabolism during energy substrate restriction in astrocytes. Brain Res. *710*, 229–233.
Kabadi, S.V., and Faden, A.I. (2014). Neuroprotective strategies for traumatic brain injury: improving clinical translation. Int. J. Mol. Sci. *15*, 1216–1236.
Kabe, Y., Ando, K., Hirao, S., Yoshida, M., and Handa, H. (2005). Redox regulation of NF-kappaB activation: distinct redox regulation between the cytoplasm and the nucleus. Antioxid. Redox Signal. *7*, 395–403.
Kamata, H., Honda, S.-I., Maeda, S., Chang, L., Hirata, H., and Karin, M. (2005). Reactive oxygen species promote TNFalpha-induced death and sustained JNK activation by inhibiting MAP kinase phosphatases. Cell *120*, 649–661.
Kampfl, A., Posmantur, R., Nixon, R., Grynspan, F., Zhao, X., Liu, S.J., Newcomb, J.K., Clifton, G.L., and Hayes, R.L. (1996). mu-calpain activation and calpain-mediated cytoskeletal proteolysis following traumatic brain injury. J. Neurochem. *67*, 1575–1583.
Kanamori, A., Catrinescu, M.-M., Belisle, J.M., Costantino, S., and Levin, L.A. (2012). Retrograde and Wallerian axonal degeneration occur synchronously after retinal ganglion cell axotomy. Am. J. Pathol. *181*, 62–73.
Kanda, K., Matsuda, T., and Oka, T. (1992). Two-dimensional orientational response of smooth muscle cells to cyclic stretching. ASAIO J. Am. Soc. Artif. Intern. Organs 1992 *38*, M382-385.
Kao, C.-Q., Goforth, P.B., Ellis, E.F., and Satin, L.S. (2004). Potentiation of GABAA currents after mechanical injury of cortical neurons. J. Neurotrauma *21*, 259–270.
Káradóttir, R., Cavelier, P., Bergersen, L.H., and Attwell, D. (2005). NMDA receptors are expressed in oligodendrocytes and activated in ischaemia. Nature *438*, 1162–1166.
Karumbaiah, L., Norman, S.E., Rajan, N.B., Anand, S., Saxena, T., Betancur, M., Patkar, R., and Bellamkonda, R.V. (2012). The upregulation of specific interleukin (IL) receptor antagonists and paradoxical enhancement of neuronal apoptosis due to electrode induced strain and brain micromotion. Biomaterials *33*, 5983–5996.
Kassmann, C.M. (2014). Myelin peroxisomes – Essential organelles for the maintenance of white matter in the nervous system. Biochimie *98*, 111–118.

Kaunas, R., Nguyen, P., Usami, S., and Chien, S. (2005). Cooperative effects of Rho and mechanical stretch on stress fiber organization. Proc. Natl. Acad. Sci. U. S. A. *102*, 15895–15900.
Kaunas, R., Usami, S., and Chien, S. (2006). Regulation of stretch-induced JNK activation by stress fiber orientation. Cell. Signal. *18*, 1924–1931.
Kaverina, I., Krylyshkina, O., Beningo, K., Anderson, K., Wang, Y.-L., and Small, J.V. (2002). Tensile stress stimulates microtubule outgrowth in living cells. J. Cell Sci. *115*, 2283–2291.
Kawahara, K. (1990). A stretch-activated K+ channel in the basolateral membrane of Xenopus kidney proximal tubule cells. Pflüg. Arch. Eur. J. Physiol. *415*, 624–629.
Kay T, Harrington DE, Adams R, Andersen T, Berrol S, Cicerone K, et al. (1993) Definition of mild traumatic brain injury. J Head Trauma Rehabil:8(3):86–87.
Kessaris, N., Fogarty, M., Iannarelli, P., Grist, M., Wegner, M., and Richardson, W.D. (2006). Competing waves of oligodendrocytes in the forebrain and postnatal elimination of an embryonic lineage. Nat. Neurosci. *9*, 173–179.
Khachigian, L.M., Resnick, N., Gimbrone Jr, M.A., and Collins, T. (1995). Nuclear factor-kappa B interacts functionally with the platelet-derived growth factor B-chain shear-stress response element in vascular endothelial cells exposed to fluid shear stress. J. Clin. Invest. *96*, 1169.
Kim, J.J., and Gean, A.D. (2011). Imaging for the diagnosis and management of traumatic brain injury. Neurother. J. Am. Soc. Exp. Neurother. *8*, 39–53.
Kim, S., and Coulombe, P.A. (2007). Intermediate filament scaffolds fulfill mechanical, organizational, and signaling functions in the cytoplasm. Genes Dev. *21*, 1581–1597.
Kim, J., Avants, B., Patel, S., Whyte, J., Coslett, B.H., Pluta, J., Detre, J.A., and Gee, J.C. (2008). Structural consequences of diffuse traumatic brain injury: a large deformation tensor-based morphometry study. NeuroImage *39*, 1014–1026.
Kim, K.Y., Rhim, T., Choi, I., and Kim, S.S. (2001). N-acetylcysteine induces cell cycle arrest in hepatic stellate cells through its reducing activity. J. Biol. Chem. *276*, 40591–40598.
Kinnunen, K.M., Greenwood, R., Powell, J.H., Leech, R., Hawkins, P.C., Bonnelle, V., Patel, M.C., Counsell, S.J., and Sharp, D.J. (2011). White matter damage and cognitive impairment after traumatic brain injury. Brain J. Neurol. *134*, 449–463.
Kirber, M.T., Ordway, R.W., Clapp, L.H., Walsh, J.V., and Singer, J.J. (1992). Both membrane stretch and fatty acids directly activate large conductance Ca(2+)-activated K+ channels in vascular smooth muscle cells. FEBS Lett. *297*, 24–28.
Kito, H., Chen, E.L., Wang, X., Ikeda, M., Azuma, N., Nakajima, N., Gahtan, V., and Sumpio, B.E. (2000). Role of mitogen-activated protein kinases in pulmonary endothelial cells exposed to cyclic strain. J. Appl. Physiol. *89*, 2391–2400.
Kloda, A., Lua, L., Hall, R., Adams, D.J., and Martinac, B. (2007). Liposome reconstitution and modulation of recombinant N-methyl-D-aspartate receptor channels by membrane stretch. Proc. Natl. Acad. Sci. *104*, 1540–1545.
Knebel, A., Rahmsdorf, H.J., Ullrich, A., and Herrlich, P. (1996). Dephosphorylation of receptor tyrosine kinases as target of regulation by radiation, oxidants or alkylating agents. EMBO J. *15*, 5314–5325.
Kochanek, P.M., Dixon, C.E., Shellington, D.K., Shin, S.S., Bayır, H., Jackson, E.K., Kagan, V.E., Yan, H.Q., Swauger, P.V., Parks, S.A., et al. (2013). Screening of biochemical and molecular mechanisms of secondary injury and repair in the brain after experimental blast-induced traumatic brain injury in rats. J. Neurotrauma *30*, 920–937.
Kohen, R. (1999). Skin antioxidants: their role in aging and in oxidative stress--new approaches for their evaluation. Biomed. Pharmacother. Biomed. Pharmacothérapie *53*, 181–192.
Kohen, R., and Gati, I. (2000). Skin low molecular weight antioxidants and their role in aging and in oxidative stress. Toxicology *148*, 149–157.
Kohen, R., and Nyska, A. (2002). Oxidation of Biological Systems: Oxidative Stress Phenomena, Antioxidants, Redox Reactions, and Methods for Their Quantification. Toxicol. Pathol. *30*, 620–650.
Kohen, Moor, and Oron (2004). Measurements of biological reducing power by voltammetric methods. Redox-Genome Interact. Health Dis. *Fuchs and L. Packer (eds.)*, *Marcel Dekker Inc. NY. 13-42*, 13.
Kohler, R., Grundig, A., Brakemeier, S., Rothermund, L., Distler, A., Kreutz, R., and Hoyer, J. (2001a). Regulation of pressure-activated channel in intact vascular endothelium of stroke-prone spontaneously hypertensive rats. Am. J. Hypertens. *14*, 716–721.
Kohler, R., KREUTZ, R., GRUNDIG, A., ROTHERMUND, L., YAGIL, C., YAGIL, Y., PRIES, A.R., and HOYER, J. (2001b). Impaired function of endothelial pressure-activated cation channel in salt-sensitive genetic hypertension. J. Am. Soc. Nephrol. *12*, 1624–1629.

Kolodziejczyk, K., Saab, A.S., Nave, K.-A., and Attwell, D. (2010). Why do oligodendrocyte lineage cells express glutamate receptors? F1000 Biol. Rep. *2*.
Kontos, H.A., and Povlishock, J.T. (1986). Oxygen radicals in brain injury. Cent. Nerv. Syst. Trauma J. Am. Paralys. Assoc. *3*, 257–263.
Kontos, H.A., and Wei, E.P. (1986). Superoxide production in experimental brain injury. J. Neurosurg. *64*, 803–807.
Kotter, M.R., Setzu, A., Sim, F.J., Van Rooijen, N., and Franklin, R.J.M. (2001). Macrophage depletion impairs oligodendrocyte remyelination following lysolecithin-induced demyelination. Glia *35*, 204–212.
Kotter, M.R., Li, W.-W., Zhao, C., and Franklin, R.J.M. (2006). Myelin impairs CNS remyelination by inhibiting oligodendrocyte precursor cell differentiation. J. Neurosci. Off. J. Soc. Neurosci. *26*, 328–332.
Koura, S.S., Doppenberg, E.M., Marmarou, A., Choi, S., Young, H.F., and Bullock, R. (1998). Relationship between excitatory amino acid release and outcome after severe human head injury. Acta Neurochir. Suppl. *71*, 244–246.
Kovacs, W.J., Olivier, L.M., and Krisans, S.K. (2002). Central role of peroxisomes in isoprenoid biosynthesis. Prog. Lipid Res. *41*, 369–391.
Kowaltowski, A.J., Castilho, R.F., and Vercesi, A.E. (1995). Ca(2+)-induced mitochondrial membrane permeabilization: role of coenzyme Q redox state. Am. J. Physiol. *269*, C141-147.
Krajewski, S., Krajewska, M., Ellerby, L.M., Welsh, K., Xie, Z., Deveraux, Q.L., Salvesen, G.S., Bredesen, D.E., Rosenthal, R.E., Fiskum, G., et al. (1999). Release of caspase-9 from mitochondria during neuronal apoptosis and cerebral ischemia. Proc. Natl. Acad. Sci. U. S. A. *96*, 5752–5757.
Krassioukov, A.V., Ackery, A., Schwartz, G., Adamchik, Y., Liu, Y., and Fehlings, M.G. (2002). An in vitro model of neurotrauma in organotypic spinal cord cultures from adult mice. Brain Res. Brain Res. Protoc. *10*, 60–68.
Kristal, B.S., and Dubinsky, J.M. (1997). Mitochondrial permeability transition in the central nervous system: induction by calcium cycling-dependent and -independent pathways. J. Neurochem. *69*, 524–538.
Kruman, I.I., and Mattson, M.P. (1999). Pivotal role of mitochondrial calcium uptake in neural cell apoptosis and necrosis. J. Neurochem. *72*, 529–540.
Kumar, A., and Loane, D.J. (2012). Neuroinflammation after traumatic brain injury: opportunities for therapeutic intervention. Brain. Behav. Immun. *26*, 1191–1201.
Kurland, D., Hong, C., Aarabi, B., Gerzanich, V., and Simard, J.M. (2012). Hemorrhagic Progression of a Contusion after Traumatic Brain Injury: A Review. J. Neurotrauma *29*, 19–31.
Kurpinski, K., Park, J., Thakar, R.G., and Li, S. (2006). Regulation of vascular smooth muscle cells and mesenchymal stem cells by mechanical strain. Mol. Cell. Biomech. MCB *3*, 21–34.
Kushida, N., Kabuyama, Y., Yamaguchi, O., and Homma, Y. (2001). Essential role for extracellular Ca(2+) in JNK activation by mechanical stretch in bladder smooth muscle cells. Am. J. Physiol. Cell Physiol. *281*, C1165-1172.
Kyriakis, J.M., and Avruch, J. (2012). Mammalian MAPK Signal Transduction Pathways Activated by Stress and Inflammation: A 10-Year Update. Physiol. Rev. *92*, 689–737.
Lai, Y., Hickey, R.W., Chen, Y., Bayir, H., Sullivan, M.L., Chu, C.T., Kochanek, P.M., Dixon, C.E., Jenkins, L.W., Graham, S.H., et al. (2008). Autophagy is increased after traumatic brain injury in mice and is partially inhibited by the antioxidant gamma-glutamylcysteinyl ethyl ester. J. Cereb. Blood Flow Metab. Off. J. Int. Soc. Cereb. Blood Flow Metab. *28*, 540–550.
Lamb, R.G., Harper, C.C., McKinney, J.S., Rzigalinski, B.A., and Ellis, E.F. (1997). Alterations in Phosphatidylcholine Metabolism of Stretch-Injured Cultured Rat Astrocytes. J. Neurochem. *68*, 1904–1910.
Lambeth, J.D. (2004). NOX enzymes and the biology of reactive oxygen. Nat. Rev. Immunol. *4*, 181–189.
Lambeth, J.D., and Neish, A.S. (2014). Nox Enzymes and New Thinking on Reactive Oxygen: A Double-Edged Sword Revisited. Annu. Rev. Pathol. Mech. Dis. *9*, 119–145.
Langlois, J.A., and Sattin, R.W. (2005). Traumatic brain injury in the United States: research and programs of the Centers for Disease Control and Prevention (CDC). J. Head Trauma Rehabil. *20*, 187–188.
LaPlaca, M.C., and Thibault, L.E. (1997). Anin vitro traumatic injury model to examine the response of neurons to a hydrodynamically-induced deformation. Ann. Biomed. Eng. *25*, 665–677.

LaPlaca, M.C., Cullen, D.K., McLoughlin, J.J., and Cargill, R.S. (2005). High rate shear strain of three-dimensional neural cell cultures: a new in vitro traumatic brain injury model. J. Biomech. *38*, 1093–1105.

Lappe-Siefke, C., Goebbels, S., Gravel, M., Nicksch, E., Lee, J., Braun, P.E., Griffiths, I.R., and Nave, K.-A. (2003). Disruption of Cnp1 uncouples oligodendroglial functions in axonal support and myelination. Nat. Genet. *33*, 366–374.

Lardinois, O.M. (1995). Reactions of bovine liver catalase with superoxide radicals and hydrogen peroxide. Free Radic. Res. *22*, 251–274.

Lau, A., Arundine, M., Sun, H.-S., Jones, M., and Tymianski, M. (2006). Inhibition of Caspase-Mediated Apoptosis by Peroxynitrite in Traumatic Brain Injury. J. Neurosci. *26*, 11540–11553.

Laule, C., Vavasour, I.M., Kolind, S.H., Li, D.K., Traboulsee, T.L., Moore, G.W., and MacKay, A.L. (2007). Magnetic resonance imaging of myelin. Neurotherapeutics *4*, 460–484.

Lavagnino, M., Gardner, K.L., and Arnoczky, S.P. (2015). High magnitude, in vitro, biaxial, cyclic tensile strain induces actin depolymerization in tendon cells. Muscles Ligaments Tendons J. *5*, 124.

Lawson, L.J., Perry, V.H., Dri, P., and Gordon, S. (1990). Heterogeneity in the distribution and morphology of microglia in the normal adult mouse brain. Neuroscience *39*, 151–170.

Lazo, O., Contreras, M., Yoshida, Y., Singh, A.K., Stanley, W., Weise, M., and Singh, I. (1990). Cellular oxidation of lignoceric acid is regulated by the subcellular localization of lignoceroyl-CoA ligases. J. Lipid Res. *31*, 583–595.

Leccia, E., Batonnet-Pichon, S., Tarze, A., Bailleux, V., Doucet, J., Pelloux, M., Delort, F., Pizon, V., Vicart, P., and Briki, F. (2013). Cyclic stretch reveals a mechanical role for intermediate filaments in a desminopathic cell model. Phys. Biol. *10*, 16001.

Lecuit, T., and Le Goff, L. (2007). Orchestrating size and shape during morphogenesis. Nature *450*, 189–192.

Lee, D.A., Noguchi, T., Frean, S.P., Lees, P., and Bader, D.L. (2000). The influence of mechanical loading on isolated chondrocytes seeded in agarose constructs. Biorheology *37*, 149–161.

Lee, D.-H., Gold, R., and Linker, R.A. (2012a). Mechanisms of Oxidative Damage in Multiple Sclerosis and Neurodegenerative Diseases: Therapeutic Modulation via Fumaric Acid Esters. Int. J. Mol. Sci. *13*, 11783–11803.

Lee, J., Gravel, M., Gao, E., O'Neill, R.C., and Braun, P.E. (2001). Identification of essential residues in 2',3'-cyclic nucleotide 3'-phosphodiesterase. Chemical modification and site-directed mutagenesis to investigate the role of cysteine and histidine residues in enzymatic activity. J. Biol. Chem. *276*, 14804–14813.

Lee, J., Gravel, M., Zhang, R., Thibault, P., and Braun, P.E. (2005). Process outgrowth in oligodendrocytes is mediated by CNP, a novel microtubule assembly myelin protein. J. Cell Biol. *170*, 661–673.

Lee, S., Leach, M.K., Redmond, S.A., Chong, S.Y.C., Mellon, S.H., Tuck, S.J., Feng, Z.-Q., Corey, J.M., and Chan, J.R. (2012b). A culture system to study oligodendrocyte myelination processes using engineered nanofibers. Nat. Methods *9*, 917–922.

Lee, Y., Morrison, B.M., Li, Y., Lengacher, S., Farah, M.H., Hoffman, P.N., Liu, Y., Tsingalia, A., Jin, L., Zhang, P.-W., et al. (2012c). Oligodendroglia metabolically support axons and contribute to neurodegeneration. Nature *487*, 443–448.

Leeb-Lundberg, F., Snowman, A., and Olsen, R.W. (1981). Perturbation of benzodiazepine receptor binding by pyrazolopyridines involves picrotoxinin/barbiturate receptor sites. J. Neurosci. Off. J. Soc. Neurosci. *1*, 471–477.

Ledeen, R. W. Enzymes and receptors of myelin. In R. E. Martenson (ed.), Myelin: biology and chemistry. Boca Raton, FL: CRC Press, 1992, pp. 531–570.

Lei, Q.-Y., Zhang, H., Zhao, B., Zha, Z.-Y., Bai, F., Pei, X.-H., Zhao, S., Xiong, Y., and Guan, K.-L. (2008). TAZ Promotes Cell Proliferation and Epithelial-Mesenchymal Transition and Is Inhibited by the Hippo Pathway. Mol. Cell. Biol. *28*, 2426–2436.

Lesné, S., Ali, C., Gabriel, C., Croci, N., MacKenzie, E.T., Glabe, C.G., Plotkine, M., Marchand-Verrecchia, C., Vivien, D., and Buisson, A. (2005). NMDA receptor activation inhibits alpha-secretase and promotes neuronal amyloid-beta production. J. Neurosci. Off. J. Soc. Neurosci. *25*, 9367–9377.

Levental, I., Georges, P.C., and Janmey, P.A. (2007). Soft biological materials and their impact on cell function. Soft Matter *3*, 299–306.

Levental, K.R., Yu, H., Kass, L., Lakins, J.N., Egeblad, M., Erler, J.T., Fong, S.F.T., Csiszar, K., Giaccia, A., Weninger, W., et al. (2009). Matrix Crosslinking Forces Tumor Progression by Enhancing Integrin Signaling. Cell *139*, 891–906.

Lewén, A., Matz, P., and Chan, P.H. (2000). Free radical pathways in CNS injury. J. Neurotrauma *17*, 871–890.
Li, J., Baud, O., Vartanian, T., Volpe, J.J., and Rosenberg, P.A. (2005). Peroxynitrite generated by inducible nitric oxide synthase and NADPH oxidase mediates microglial toxicity to oligodendrocytes. Proc. Natl. Acad. Sci. U. S. A. *102*, 9936–9941.
Lifshitz, J., Friberg, H., Neumar, R.W., Raghupathi, R., Welsh, F.A., Janmey, P., Saatman, K.E., Wieloch, T., Grady, M.S., and McIntosh, T.K. (2003). Structural and functional damage sustained by mitochondria after traumatic brain injury in the rat: evidence for differentially sensitive populations in the cortex and hippocampus. J. Cereb. Blood Flow Metab. Off. J. Int. Soc. Cereb. Blood Flow Metab. *23*, 219–231.
Lim, S.-N., Gladman, S.J., Dyall, S.C., Patel, U., Virani, N., Kang, J.X., Priestley, J.V., and Michael-Titus, A.T. (2013). Transgenic mice with high endogenous omega-3 fatty acids are protected from spinal cord injury. Neurobiol. Dis. *51*, 104–112.
Lin, S., and Bergles, D.E. (2004). Synaptic signaling between GABAergic interneurons and oligodendrocyte precursor cells in the hippocampus. Nat. Neurosci. *7*, 24–32.
Lipton, S.A., and Rosenberg, P.A. (1994). Excitatory amino acids as a final common pathway for neurologic disorders. N. Engl. J. Med. *330*, 613–622.
Liu, X., Kim, C.N., Yang, J., Jemmerson, R., and Wang, X. (1996). Induction of apoptotic program in cell-free extracts: requirement for dATP and cytochrome c. Cell *86*, 147–157.
Liu, Y., Fiskum, G., and Schubert, D. (2002). Generation of reactive oxygen species by the mitochondrial electron transport chain. J. Neurochem. *80*, 780–787.
Ljubisavljevic, S. (2016). Oxidative Stress and Neurobiology of Demyelination. Mol. Neurobiol. *53*, 744–758.
Ljubisavljevic, S., and Stojanovic, I. (2015). Neuroinflammation and demyelination from the point of nitrosative stress as a new target for neuroprotection. Rev. Neurosci. *26*, 49–73.
Llufriu-Dabén G, Meffre D, Chierto E, Carreté A, Massaad C, Jafarian-Tehrani M (2016a) Etazolate Promotes Oligodendrocyte Differentiation and Remyelination after Demyelination in Organotypic Cerebellar Slice Cultures (under revision).
Llufriu-Dabén G, Meffre D, Camand E, Massaad C, Jafarian-Tehrani M (2016b) The protective effect of etazolate in a novel ex vivo model of trauma-induced white matter injury (under revision).
Lo, C.-M., Wang, H.-B., Dembo, M., and Wang, Y. (2000). Cell movement is guided by the rigidity of the substrate. Biophys. J. *79*, 144–152.
Loane, D.J., and Byrnes, K.R. (2010). Role of microglia in neurotrauma. Neurother. J. Am. Soc. Exp. Neurother. *7*, 366–377.
Loane, D.J., Pocivavsek, A., Moussa, C.E.-H., Thompson, R., Matsuoka, Y., Faden, A.I., Rebeck, G.W., and Burns, M.P. (2009). Amyloid precursor protein secretases as therapeutic targets for traumatic brain injury. Nat. Med. *15*, 377–379.
Loane, D.J., Stoica, B.A., Byrnes, K.R., Jeong, W., and Faden, A.I. (2013). Activation of mGluR5 and inhibition of NADPH oxidase improves functional recovery after traumatic brain injury. J. Neurotrauma *30*, 403–412.
Lomnitski, L., Chapman, S., Hochman, A., Kohen, R., Shohami, E., Chen, Y., Trembovler, V., and Michaelson, D.M. (1999). Antioxidant mechanisms in apolipoprotein E deficient mice prior to and following closed head injury. Biochim. Biophys. Acta *1453*, 359–368.
Lopez, P.H.H. (2014). Role of myelin-associated glycoprotein (siglec-4a) in the nervous system. Adv. Neurobiol. *9*, 245–262.
Loughlin, A.J., Copelman, C.A., Hall, A., Armer, T., Young, B.C., Landon, D.N., and Cuzner, M.L. (1997). Myelination and remyelination of aggregate rat brain cell cultures enriched with macrophages. J. Neurosci. Res. *47*, 384–392.
Lourenço, T., Paes de Faria, J., Bippes, C.A., Maia, J., Lopes-da-Silva, J.A., Relvas, J.B., and Grãos, M. (2016). Modulation of oligodendrocyte differentiation and maturation by combined biochemical and mechanical cues. Sci. Rep. *6*, 21563.
Loverde, J.R., Ozoka, V.C., Aquino, R., Lin, L., and Pfister, B.J. (2011). Live imaging of axon stretch growth in embryonic and adult neurons. J. Neurotrauma *28*, 2389–2403.
Lozano, D., Gonzales-Portillo, G.S., Acosta, S., de la Pena, I., Tajiri, N., Kaneko, Y., and Borlongan, C.V. (2015). Neuroinflammatory responses to traumatic brain injury: etiology, clinical consequences, and therapeutic opportunities. Neuropsychiatr. Dis. Treat. *11*, 97–106.
Lu, X.-Y., Wang, H.-D., Xu, J.-G., Ding, K., and Li, T. (2015). Deletion of Nrf2 Exacerbates Oxidative Stress After Traumatic Brain Injury in Mice. Cell. Mol. Neurobiol. *35*, 713–721.

Lu, Y.-B., Franze, K., Seifert, G., Steinhäuser, C., Kirchhoff, F., Wolburg, H., Guck, J., Janmey, P., Wei, E.-Q., Käs, J., et al. (2006). Viscoelastic properties of individual glial cells and neurons in the CNS. Proc. Natl. Acad. Sci. *103*, 17759–17764.

Luca, L., Rogobete, A.F., and Bedreag, O.H. (2015). Oxidative Stress and Antioxidant Therapy in Critically Ill Polytrauma Patients with Severe Head Injury. J. Crit. Care Med. *1*.

Lusardi, T.A. (2009). Adenosine neuromodulation and traumatic brain injury. Curr. Neuropharmacol. *7*, 228–237.

Lusardi, T.A., Wolf, J.A., Putt, M.E., Smith, D.H., and Meaney, D.F. (2004a). Effect of acute calcium influx after mechanical stretch injury in vitro on the viability of hippocampal neurons. J. Neurotrauma *21*, 61–72.

Lusardi, T.A., Rangan, J., Sun, D., Smith, D.H., and Meaney, D.F. (2004b). A device to study the initiation and propagation of calcium transients in cultured neurons after mechanical stretch. Ann. Biomed. Eng. *32*, 1546–1559.

Maas, A.I.R., Menon, D.K., Steyerberg, E.W., Citerio, G., Lecky, F., Manley, G.T., Hill, S., Legrand, V., Sorgner, A., and CENTER-TBI Participants and Investigators (2015). Collaborative European NeuroTrauma Effectiveness Research in Traumatic Brain Injury (CENTER-TBI): a prospective longitudinal observational study. Neurosurgery *76*, 67–80.

Macco, R., Pelizzoni, I., Consonni, A., Vitali, I., Giacalone, G., Martinelli Boneschi, F., Codazzi, F., Grohovaz, F., and Zacchetti, D. (2013). Astrocytes acquire resistance to iron-dependent oxidative stress upon proinflammatory activation. J. Neuroinflammation *10*, 130.

Maciel, E.N., Vercesi, A.E., and Castilho, R.F. (2001). Oxidative stress in Ca(2+)-induced membrane permeability transition in brain mitochondria. J. Neurochem. *79*, 1237–1245.

MacKenna, D. (2000). Role of mechanical factors in modulating cardiac fibroblast function and extracellular matrix synthesis. Cardiovasc. Res. *46*, 257–263.

MacKenna, D.A., Dolfi, F., Vuori, K., and Ruoslahti, E. (1998). Extracellular signal-regulated kinase and c-Jun NH2-terminal kinase activation by mechanical stretch is integrin-dependent and matrix-specific in rat cardiac fibroblasts. J. Clin. Invest. *101*, 301–310.

Maki, T., Liang, A.C., Miyamoto, N., Lo, E.H., and Arai, K. (2013). Mechanisms of oligodendrocyte regeneration from ventricular-subventricular zone-derived progenitor cells in white matter diseases. Front. Cell. Neurosci. *7*, 275.

Malek, A.M., Greene, A.L., and Izumo, S. (1993). Regulation of endothelin 1 gene by fluid shear stress is transcriptionally mediated and independent of protein kinase C and cAMP. Proc. Natl. Acad. Sci. U. S. A. *90*, 5999–6003.

Malek, A.M., Zhang, J., Jiang, J., Alper, S.L., and Izumo, S. (1999). Endothelin-1 gene suppression by shear stress: pharmacological evaluation of the role of tyrosine kinase, intracellular calcium, cytoskeleton, and mechanosensitive channels. J. Mol. Cell. Cardiol. *31*, 387–399.

Manji, H.K., and Duman, R.S. (2001). Impairments of neuroplasticity and cellular resilience in severe mood disorders: implications for the development of novel therapeutics. Psychopharmacol. Bull. *35*, 5–49.

Marban, E., Yamagishi, T., and Tomaselli, G.F. (1998). Structure and function of voltage-gated sodium channels. J. Physiol. *508*, 647–657.

Marcade, M., Bourdin, J., Loiseau, N., Peillon, H., Rayer, A., Drouin, D., Schweighoffer, F., and Désiré, L. (2008). Etazolate, a neuroprotective drug linking GABA $_A$ receptor pharmacology to amyloid precursor protein processing. J. Neurochem. *106*, 392–404.

Margulies, S.S., Thibault, L.E., and Gennarelli, T.A. (1990). Physical model simulations of brain injury in the primate. J. Biomech. *23*, 823–836.

Marklund, N., Salci, K., Ronquist, G., and Hillered, L. (2006). Energy metabolic changes in the early post-injury period following traumatic brain injury in rats. Neurochem. Res. *31*, 1085–1093.

Marmarou, A., Fatouros, P.P., Barzó, P., Portella, G., Yoshihara, M., Tsuji, O., Yamamoto, T., Laine, F., Signoretti, S., Ward, J.D., et al. (2000). Contribution of edema and cerebral blood volume to traumatic brain swelling in head-injured patients. J. Neurosurg. *93*, 183–193.

Martinac, B., and Hamill, O.P. (2002). Gramicidin A channels switch between stretch activation and stretch inactivation depending on bilayer thickness. Proc. Natl. Acad. Sci. *99*, 4308–4312.

Martinac, B., Buechner, M., Delcour, A.H., Adler, J., and Kung, C. (1987). Pressure-sensitive ion channel in Escherichia coli. Proc. Natl. Acad. Sci. *84*, 2297–2301.

Martineau, L.C., and Gardiner, P.F. (2001). Insight into skeletal muscle mechanotransduction: MAPK activation is quantitatively related to tension. J. Appl. Physiol. *91*, 693–702.

Marzatico, F., Gaetani, P., Cafè, C., Spanu, G., and Rodriguez y Baena, R. (1993). Antioxidant enzymatic activities after experimental subarachnoid hemorrhage in rats. Acta Neurol. Scand. *87*, 62–66.

Matthews, M.A., and Duncan, D. (1971). A quantitative study of morphological changes accompanying the initiation and progress of myelin production in the dorsal funiculus of the rat spinal cord. J. Comp. Neurol. *142*, 1–22.
Mattson, M.P., Cheng, B., Culwell, A.R., Esch, F.S., Lieberburg, I., and Rydel, R.E. (1993). Evidence for excitoprotective and intraneuronal calcium-regulating roles for secreted forms of the beta-amyloid precursor protein. Neuron *10*, 243–254.
Maurice, D.H., Ke, H., Ahmad, F., Wang, Y., Chung, J., and Manganiello, V.C. (2014). Advances in targeting cyclic nucleotide phosphodiesterases. Nat. Rev. Drug Discov. *13*, 290–314.
Maxwell, W.L. (1996). Histopathological changes at central nodes of Ranvier after stretch-injury. Microsc. Res. Tech. *34*, 522–535.
Maxwell, W.L., Watt, C., Pediani, J.D., Graham, D.I., Adams, J.H., and Gennarelli, T.A. (1991). Localisation of calcium ions and calcium-ATPase activity within myelinated nerve fibres of the adult guinea-pig optic nerve. J. Anat. *176*, 71–79.
Mayer, A.R., Ling, J., Mannell, M.V., Gasparovic, C., Phillips, J.P., Doezema, D., Reichard, R., and Yeo, R.A. (2010). A prospective diffusion tensor imaging study in mild traumatic brain injury. Neurology *74*, 643–650.
Mbye, L.H., Singh, I.N., Sullivan, P.G., Springer, J.E., and Hall, E.D. (2008). Attenuation of acute mitochondrial dysfunction after traumatic brain injury in mice by NIM811, a non-immunosuppressive cyclosporin A analog. Exp. Neurol. *209*, 243–253.
McCarter, G.C., Reichling, D.B., and Levine, J.D. (1999). Mechanical transduction by rat dorsal root ganglion neurons in vitro. Neurosci. Lett. *273*, 179–182.
McCord, J.M., and Fridovich, I. (1969). Superoxide dismutase. An enzymic function for erythrocuprein (hemocuprein). J. Biol. Chem. *244*, 6049–6055.
McCubrey, J.A., Lahair, M.M., and Franklin, R.A. (2006). Reactive oxygen species-induced activation of the MAP kinase signaling pathways. Antioxid. Redox Signal. *8*, 1775–1789.
McKenzie, I.A., Ohayon, D., Li, H., Paes de Faria, J., Emery, B., Tohyama, K., and Richardson, W.D. (2014). Motor skill learning requires active central myelination. Science *346*, 318–322.
McKinney, J.S., Willoughby, K.A., Liang, S., and Ellis, E.F. (1996). Stretch-induced injury of cultured neuronal, glial, and endothelial cells. Effect of polyethylene glycol-conjugated superoxide dismutase. Stroke J. Cereb. Circ. *27*, 934–940.
McMahon, M., Thomas, N., Itoh, K., Yamamoto, M., and Hayes, J.D. (2004). Redox-regulated turnover of Nrf2 is determined by at least two separate protein domains, the redox-sensitive Neh2 degron and the redox-insensitive Neh6 degron. J. Biol. Chem. *279*, 31556–31567.
Meaney, D.F., and Smith, D.H. (2015). Cellular biomechanics of central nervous system injury. In Handbook of Clinical Neurology, (Elsevier), pp. 105–114.
Meaney, D.F., Smith, D.H., Shreiber, D.I., Bain, A.C., Miller, R.T., Ross, D.T., and Gennarelli, T.A. (1995). Biomechanical analysis of experimental diffuse axonal injury. J. Neurotrauma *12*, 689–694.
Meffre, D., Massaad, C., and Grenier, J. (2015a). Lithium chloride stimulates PLP and MBP expression in oligodendrocytes via Wnt/β-catenin and Akt/CREB pathways. Neuroscience *284*, 962–971.
Meffre, D., Shackleford, G., Hichor, M., Gorgievski, V., Tzavara, E.T., Trousson, A., Ghoumari, A.M., Deboux, C., Nait Oumesmar, B., Liere, P., et al. (2015b). Liver X receptors alpha and beta promote myelination and remyelination in the cerebellum. Proc. Natl. Acad. Sci. U. S. A. *112*, 7587–7592.
Menconi, M.C., Pellegrini, M., and Pellegrino, M. (2001). Voltage-Induced Activation of Mechanosensitive Cation Channels of Leech Neurons. J. Membr. Biol. *180*, 65–72.
Mendes Arent, A., Souza, L.F. de, Walz, R., and Dafre, A.L. (2014). Perspectives on Molecular Biomarkers of Oxidative Stress and Antioxidant Strategies in Traumatic Brain Injury. BioMed Res. Int. *2014*, 1–18.
Mendez, M.G., and Janmey, P.A. (2012). Transcription factor regulation by mechanical stress. Int. J. Biochem. Cell Biol. *44*, 728–732.
Mendez, D.R., Cherian, L., Moore, N., Arora, T., Liu, P.K., and Robertson, C.S. (2004). Oxidative DNA lesions in a rodent model of traumatic brain injury. J. Trauma *56*, 1235–1240.
Mengler, L., Khmelinskii, A., Diedenhofen, M., Po, C., Staring, M., Lelieveldt, B.P.F., and Hoehn, M. (2014). Brain maturation of the adolescent rat cortex and striatum: changes in volume and myelination. NeuroImage *84*, 35–44.
Menniti, F.S., Faraci, W.S., and Schmidt, C.J. (2006). Phosphodiesterases in the CNS: targets for drug development. Nat. Rev. Drug Discov. *5*, 660–670.

Menon, D.K., Schwab, K., Wright, D.W., Maas, A.I., and Demographics and Clinical Assessment Working Group of the International and Interagency Initiative toward Common Data Elements for Research on Traumatic Brain Injury and Psychological Health (2010). Position statement: definition of traumatic brain injury. Arch. Phys. Med. Rehabil. *91*, 1637–1640.
Meves, A., Stock, S.N., Beyerle, A., Pittelkow, M.R., and Peus, D. (2001). H(2)O(2) mediates oxidative stress-induced epidermal growth factor receptor phosphorylation. Toxicol. Lett. *122*, 205–214.
Meziane, H., Dodart, J.C., Mathis, C., Little, S., Clemens, J., Paul, S.M., and Ungerer, A. (1998). Memory-enhancing effects of secreted forms of the beta-amyloid precursor protein in normal and amnestic mice. Proc. Natl. Acad. Sci. U. S. A. *95*, 12683–12688.
Mierzwa, A.J., Marion, C.M., Sullivan, G.M., McDaniel, D.P., and Armstrong, R.C. (2015). Components of Myelin Damage and Repair in the Progression of White Matter Pathology After Mild Traumatic Brain Injury. J. Neuropathol. Exp. Neurol. *74*, 218.
Mih, J.D., Marinkovic, A., Liu, F., Sharif, A.S., and Tschumperlin, D.J. (2012). Matrix stiffness reverses the effect of actomyosin tension on cell proliferation. J. Cell Sci. *125*, 5974–5983.
Miles, L., Grossman, R.I., Johnson, G., Babb, J.S., Diller, L., and Inglese, M. (2008). Short-term DTI predictors of cognitive dysfunction in mild traumatic brain injury. Brain Inj. *22*, 115–122.
Miller, D.J., Duka, T., Stimpson, C.D., Schapiro, S.J., Baze, W.B., McArthur, M.J., Fobbs, A.J., Sousa, A.M.M., Sestan, N., Wildman, D.E., et al. (2012). Prolonged myelination in human neocortical evolution. Proc. Natl. Acad. Sci. U. S. A. *109*, 16480–16485.
Miller, K., Chinzei, K., Orssengo, G., and Bednarz, P. (2000). Mechanical properties of brain tissue in-vivo: experiment and computer simulation. J. Biomech. *33*, 1369–1376.
Miron, V.E., Ludwin, S.K., Darlington, P.J., Jarjour, A.A., Soliven, B., Kennedy, T.E., and Antel, J.P. (2010). Fingolimod (FTY720) Enhances Remyelination Following Demyelination of Organotypic Cerebellar Slices. Am. J. Pathol. *176*, 2682–2694.
Miyamoto, M., Hashimoto, K., Minagawa, K., Satoh, K., Komatsu, N., Fujimaki, M., Nakashima, H., Yokote, Y., Akahane, K., Guputa, M., et al. (2002). Effect of poly-herbal formula on NO production by LPS-stimulated mouse macrophage-like cells. Anticancer Res. *22*, 3293–3301.
Mokri, B. (2001). The Monro-Kellie hypothesis: applications in CSF volume depletion. Neurology *56*, 1746–1748.
Montuschi, P., Barnes, P.J., and Roberts, L.J. (2004). Isoprostanes: markers and mediators of oxidative stress. FASEB J. Off. Publ. Fed. Am. Soc. Exp. Biol. *18*, 1791–1800.
Moochhala, S.M., Lu, J., Xing, M.C.K., Anuar, F., Ng, K.C., Yang, K.L.S., Whiteman, M., and Atan, S. (2005). Mercaptoethylguanidine inhibition of inducible nitric oxide synthase and cyclooxygenase-2 expressions induced in rats after fluid-percussion brain injury. J. Trauma *59*, 450–457.
Morell, P., and Quarles, R.H. (1999). References.
Moretti, M., Prina-Mello, A., Reid, A.J., Barron, V., and Prendergast, P.J. (2004). Endothelial cell alignment on cyclically-stretched silicone surfaces. J. Mater. Sci. Mater. Med. *15*, 1159–1164.
Morgan, M.J., and Liu, Z. (2011). Crosstalk of reactive oxygen species and NF-κB signaling. Cell Res. *21*, 103–115.
Morita, N., Takada, S., and Okita, K. (2013). Influence of stretch and pressure as mechanical stresses on skeletal muscle. J. Phys. Fit. Sports Med. *2*, 347–350.
Morrison, B., Saatman, K.E., Meaney, D.F., and McIntosh, T.K. (1998). In vitro central nervous system models of mechanically induced trauma: a review. J. Neurotrauma *15*, 911–928.
Morrison, B., Eberwine, J.H., Meaney, D.F., and McIntosh, T.K. (2000a). Traumatic injury induces differential expression of cell death genes in organotypic brain slice cultures determined by complementary DNA array hybridization. Neuroscience *96*, 131–139.
Morrison, B., Meaney, D.F., Margulies, S.S., and McIntosh, T.K. (2000b). Dynamic mechanical stretch of organotypic brain slice cultures induces differential genomic expression: relationship to mechanical parameters. J. Biomech. Eng. *122*, 224–230.
Morrison, B., Cater, H.L., Benham, C.D., and Sundstrom, L.E. (2006). An in vitro model of traumatic brain injury utilising two-dimensional stretch of organotypic hippocampal slice cultures. J. Neurosci. Methods *150*, 192–201.
Morrison, B., Elkin, B.S., Dollé, J.-P., and Yarmush, M.L. (2011). In vitro models of traumatic brain injury. Annu. Rev. Biomed. Eng. *13*, 91–126.
Morrison, B.M., Lee, Y., and Rothstein, J.D. (2013). Oligodendroglia: metabolic supporters of axons. Trends Cell Biol. *23*, 644–651.
Morrison III, B., Meaney, D.F., and McIntosh, T.K. (1998). Mechanical characterization of an in vitro device designed to quantitatively injure living brain tissue. Ann. Biomed. Eng. *26*, 381–390.

Morrison III, B., Cater, H.L., Wang, C.C., Thomas, F.C., and others (2003). A tissue level tolerance criterion for living brain developed with an in vitro model of traumatic mechanical loading. Stapp Car Crash J. *47*, 93.

Moshayedi, P., Ng, G., Kwok, J.C.F., Yeo, G.S.H., Bryant, C.E., Fawcett, J.W., Franze, K., and Guck, J. (2014). The relationship between glial cell mechanosensitivity and foreign body reactions in the central nervous system. Biomaterials *35*, 3919–3925.

Mota, S.I., Costa, R.O., Ferreira, I.L., Santana, I., Caldeira, G.L., Padovano, C., Fonseca, A.C., Baldeiras, I., Cunha, C., Letra, L., et al. (2015). Oxidative stress involving changes in Nrf2 and ER stress in early stages of Alzheimer's disease. Biochim. Biophys. Acta BBA - Mol. Basis Dis. *1852*, 1428–1441.

Mouzon, B., Chaytow, H., Crynen, G., Bachmeier, C., Stewart, J., Mullan, M., Stewart, W., and Crawford, F. (2012). Repetitive Mild Traumatic Brain Injury in a Mouse Model Produces Learning and Memory Deficits Accompanied by Histological Changes. J. Neurotrauma *29*, 2761–2773.

Mukherjee, S.K., and Adams, J.D. (1997). The effects of aging and neurodegeneration on apoptosis-associated DNA fragmentation and the benefits of nicotinamide. Mol. Chem. Neuropathol. Spons. Int. Soc. Neurochem. World Fed. Neurol. Res. Groups Neurochem. Cerebrospinal Fluid *32*, 59–74.

Mukherjee, S.K., Yasharel, R., Klaidman, L.K., Hutchin, T.P., and Adams, J.D. (1995). Apoptosis and DNA fragmentation as induced by tertiary butylhydroperoxide in the brain. Brain Res. Bull. *38*, 595–604.

Mukhin, A.G., Ivanova, S.A., Knoblach, S.M., and Faden, A.I. (1997). New in vitro model of traumatic neuronal injury: evaluation of secondary injury and glutamate receptor-mediated neurotoxicity. J. Neurotrauma *14*, 651–663.

Mukhin, A.G., Ivanova, S.A., Allen, J.W., and Faden, A.I. (1998). Mechanical injury to neuronal/glial cultures in microplates: role of NMDA receptors and pH in secondary neuronal cell death. J. Neurosci. Res. *51*, 748–758.

Murphy, E.J., and Horrocks, L.A. (1993). A model for compression trauma: pressure-induced injury in cell cultures. J. Neurotrauma *10*, 431–444.

Mutai, H., and Heller, S. (2003). Vertebrate and invertebrate TRPV-like mechanoreceptors. Cell Calcium *33*, 471–478.

Myeku, N., Clelland, C.L., Emrani, S., Kukushkin, N.V., Yu, W.H., Goldberg, A.L., and Duff, K.E. (2016). Tau-driven 26S proteasome impairment and cognitive dysfunction can be prevented early in disease by activating cAMP-PKA signaling. Nat. Med. *22*, 46–53.

Myllykoski, M., Raasakka, A., Han, H., and Kursula, P. (2012). Myelin 2',3'-cyclic nucleotide 3'-phosphodiesterase: active-site ligand binding and molecular conformation. PloS One *7*, e32336.

Nagai, H., Noguchi, T., Takeda, K., and Ichijo, H. (2007). Pathophysiological roles of ASK1-MAP kinase signaling pathways. J. Biochem. Mol. Biol. *40*, 1–6.

Nakai, N., Kawano, F., and Nakata, K. (2015). Mechanical stretch activates mammalian target of rapamycin and AMP-activated protein kinase pathways in skeletal muscle cells. Mol. Cell. Biochem. *406*, 285–292.

Nam, J., Aguda, B.D., Rath, B., and Agarwal, S. (2009). Biomechanical Thresholds Regulate Inflammation through the NF-κB Pathway: Experiments and Modeling. PLoS ONE *4*, e5262.

Naumanen, P., Lappalainen, P., and Hotulainen, P. (2008). Mechanisms of actin stress fibre assembly. J. Microsc. *231*, 446–454.

Nave, K.-A. (2010a). Myelination and the trophic support of long axons. Nat. Rev. Neurosci. *11*, 275–283.

Nave, K.-A. (2010b). Myelination and support of axonal integrity by glia. Nature *468*, 244–252.

Nave, K.-A., and Werner, H.B. (2014). Myelination of the nervous system: mechanisms and functions. Annu Rev Cell Dev Biol. *30*, 503–533.

Nave, K.-A., and Trapp, B.D. (2008). Axon-glial signaling and the glial support of axon function. Annu. Rev. Neurosci. *31*, 535–561.

Nazıroğlu, M., Şenol, N., Ghazizadeh, V., and Yürüker, V. (2014). Neuroprotection Induced by N-acetylcysteine and Selenium Against Traumatic Brain Injury-Induced Apoptosis and Calcium Entry in Hippocampus of Rat. Cell. Mol. Neurobiol. *34*, 895–903.

Neary, J.T., and Kang, Y. (2006). P2 purinergic receptors signal to glycogen synthase kinase-3β in astrocytes. J. Neurosci. Res. *84*, 515–524.

Neary, J.T., Kang, Y., Willoughby, K.A., and Ellis, E.F. (2003). Activation of extracellular signal-regulated kinase by stretch-induced injury in astrocytes involves extracellular ATP and P2 purinergic receptors. J. Neurosci. *23*, 2348–2356.

Neary, J.T., Kang, Y., Tran, M., and Feld, J. (2005). Traumatic injury activates protein kinase B/Akt in cultured astrocytes: role of extracellular ATP and P2 purinergic receptors. J. Neurotrauma *22*, 491–500.

Neidlinger-Wilke, C., Wilke, H.J., and Claes, L. (1994). Cyclic stretching of human osteoblasts affects proliferation and metabolism: a new experimental method and its application. J. Orthop. Res. Off. Publ. Orthop. Res. Soc. *12*, 70–78.

Neidlinger-Wilke, C., Grood, E., Claes, L., and Brand, R. (2002). Fibroblast orientation to stretch begins within three hours. J. Orthop. Res. *20*, 953–956.

Nerem, R.M. (1992). Vascular fluid mechanics, the arterial wall, and atherosclerosis. J. Biomech. Eng. *114*, 274–282.

Newell, D.W., Barth, A., Papermaster, V., and Malouf, A.T. (1995). Glutamate and non-glutamate receptor mediated toxicity caused by oxygen and glucose deprivation in organotypic hippocampal cultures. J. Neurosci. *15*, 7702–7711.

Nguyen, H.T., Adam, R.M., Bride, S.H., Park, J.M., Peters, C.A., and Freeman, M.R. (2000). Cyclic stretch activates p38 SAPK2-, ErbB2-, and AT1-dependent signaling in bladder smooth muscle cells. Am. J. Physiol. Cell Physiol. *279*, C1155-1167.

Nguyen, T., Sherratt, P.J., Huang, H.-C., Yang, C.S., and Pickett, C.B. (2003). Increased protein stability as a mechanism that enhances Nrf2-mediated transcriptional activation of the antioxidant response element. Degradation of Nrf2 by the 26 S proteasome. J. Biol. Chem. *278*, 4536–4541.

Nguyen, T., Mehta, N.R., Conant, K., Kim, K.-J., Jones, M., Calabresi, P.A., Melli, G., Hoke, A., Schnaar, R.L., Ming, G.-L., et al. (2009). Axonal protective effects of the myelin-associated glycoprotein. J. Neurosci. Off. J. Soc. Neurosci. *29*, 630–637.

Nicholls, D.G. (1985). A role for the mitochondrion in the protection of cells against calcium overload? Prog. Brain Res. *63*, 97–106.

Nieponice, A., Maul, T.M., Cumer, J.M., Soletti, L., and Vorp, D.A. (2007). Mechanical stimulation induces morphological and phenotypic changes in bone marrow-derived progenitor cells within a three-dimensional fibrin matrix. J. Biomed. Mater. Res. A *81A*, 523–530.

Nilsson, P., Laursen, H., Hillered, L., and Hansen, A.J. (1996). Calcium movements in traumatic brain injury: the role of glutamate receptor-operated ion channels. J. Cereb. Blood Flow Metab. Off. J. Int. Soc. Cereb. Blood Flow Metab. *16*, 262–270.

Norton WT, Cammer W. Isolation and characterization of myelin. In: Myelin, edited by Morell P. New York: Plenum, 1984, p. 147–195.

Notterpek, L.M., Bullock, P.N., Malek-Hedayat, S., Fisher, R., and Rome, L.H. (1993). Myelination in cerebellar slice cultures: development of a system amenable to biochemical analysis. J. Neurosci. Res. *36*, 621–634.

Nunan, J., and Small, D.H. (2000). Regulation of APP cleavage by alpha-, beta- and gamma-secretases. FEBS Lett. *483*, 6–10.

Obermeier, B., Daneman, R., and Ransohoff, R.M. (2013). Development, maintenance and disruption of the blood-brain barrier. Nat. Med. *19*, 1584–1596.

Olszanecki, R., Gebska, A., Kozlovski, V.I., and Gryglewski, R.J. (2002). K ey w ords: flavonoids, nitric oxide synthase, macrophages. J. Physiol. Pharmacol. *53*, 571–584.

Oppenheimer, D.R. (1968). Microscopic lesions in the brain following head injury. J. Neurol. Neurosurg. Psychiatry *31*, 299–306.

Orr, A.W., Helmke, B.P., Blackman, B.R., and Schwartz, M.A. (2006). Mechanisms of Mechanotransduction. Dev. Cell *10*, 11–20.

Ortega, F., Gascón, S., Masserdotti, G., Deshpande, A., Simon, C., Fischer, J., Dimou, L., Chichung Lie, D., Schroeder, T., and Berninger, B. (2013). Oligodendrogliogenic and neurogenic adult subependymal zone neural stem cells constitute distinct lineages and exhibit differential responsiveness to Wnt signalling. Nat. Cell Biol. *15*, 602–613.

Ostergaard, K., Finsen, B., and Zimmer, J. (1995). Organotypic slice cultures of the rat striatum: an immunocytochemical, histochemical and in situ hybridization study of somatostatin, neuropeptide Y, nicotinamide adenine dinucleotide phosphate-diaphorase, and enkephalin. Exp. Brain Res. *103*, 70–84.

Ostrow, L.W., Langan, T.J., and Sachs, F. (2000). Stretch-induced endothelin-1 production by astrocytes. J. Cardiovasc. Pharmacol. *36*, S274–hyhen.

Owens, D.M., and Keyse, S.M. (2007). Differential regulation of MAP kinase signalling by dual-specificity protein phosphatases. Oncogene *26*, 3203–3213.

Owuor, E.D., and Kong, A.-N.T. (2002). Antioxidants and oxidants regulated signal transduction pathways. Biochem. Pharmacol. *64*, 765–770.

Oztürk, E., Demirbilek, S., Köroğlu, A., But, A., Begeç, Z.O., Gülec, M., Akyol, O., and Ersoy, M.O. (2008). Propofol and erythropoietin antioxidant properties in rat brain injured tissue. Prog. Neuropsychopharmacol. Biol. Psychiatry *32*, 81–86.

Pacha, J., Frindt, G., Sackin, H., and Palmer, L.G. (1991). Apical maxi K channels in intercalated cells of CCT. Am. J. Physiol. *261*, F696-705.

Paez, P.M., Fulton, D., Spreuer, V., Handley, V., and Campagnoni, A.T. (2011). Modulation of Canonical Transient Receptor Potential Channel 1 in the Proliferation of Oligodendrocyte Precursor Cells by the Golli Products of the Myelin Basic Protein Gene. J. Neurosci. *31*, 3625–3637.

Paillart, C., Boudier, J.L., Boudier, J.A., Rochat, H., Couraud, F., and Dargent, B. (1996). Activity-induced internalization and rapid degradation of sodium channels in cultured fetal neurons. J. Cell Biol. *134*, 499–509.

Palecek, S.P., Loftus, J.C., Ginsberg, M.H., Lauffenburger, D.A., and Horwitz, A.F. (1997). Integrin-ligand binding properties govern cell migration speed through cell-substratum adhesiveness. Nature *385*, 537–540.

Pamplona, R., Dalfo, E., Ayala, V., Bellmunt, M.J., Prat, J., Ferrer, I., and Portero-Otin, M. (2005). Proteins in Human Brain Cortex Are Modified by Oxidation, Glycoxidation, and Lipoxidation: EFFECTS OF ALZHEIMER DISEASE AND IDENTIFICATION OF LIPOXIDATION TARGETS. J. Biol. Chem. *280*, 21522–21530.

Pan, J., Fukuda, K., Saito, M., Matsuzaki, J., Kodama, H., Sano, M., Takahashi, T., Kato, T., and Ogawa, S. (1999). Mechanical stretch activates the JAK/STAT pathway in rat cardiomyocytes. Circ. Res. *84*, 1127–1136.

Pan, X.-D., Zhu, Y.-G., Lin, N., Zhang, J., Ye, Q.-Y., Huang, H.-P., and Chen, X.-C. (2011). Microglial phagocytosis induced by fibrillar β-amyloid is attenuated by oligomeric β-amyloid: implications for Alzheimer's disease. Mol. Neurodegener. *6*, 45.

Panickar, K.S., Jayakumar, A.R., and Norenberg, M.D. (2002). Differential response of neural cells to trauma-induced free radical production in vitro. Neurochem. Res. *27*, 161–166.

Pantano, C., Reynaert, N.L., van der Vliet, A., and Janssen-Heininger, Y.M.W. (2006). Redox-sensitive kinases of the nuclear factor-kappaB signaling pathway. Antioxid. Redox Signal. *8*, 1791–1806.

Paoletti, P., and Ascher, P. (1994). Mechanosensitivity of NMDA receptors in cultured mouse central neurons. Neuron *13*, 645–655.

Pappius H. M (1974) Fundamental aspects of brain oedema. In: : Handbook of clinical neurology, part I: tumors of the brain and skull, pp pp 167–185. New York: North Holland Publishing Company. (Vinken PJ, Bruyn GW, eds).

Park, B., Lee, S., Kim, E., Cho, K., Riddell, S.R., Cho, S., and Ahn, K. (2006). Redox regulation facilitates optimal peptide selection by MHC class I during antigen processing. Cell *127*, 369–382.

Park, D., Shin, K., Choi, E.-K., Choi, Y., Jang, J.-Y., Kim, J., Jeong, H.-S., Lee, W., Lee, Y.-B., Kim, S.U., et al. (2015). Protective Effects of N-Acetyl-L-Cysteine in Human Oligodendrocyte Progenitor Cells and Restoration of Motor Function in Neonatal Rats with Hypoxic-Ischemic Encephalopathy. Evid.-Based Complement. Altern. Med. ECAM *2015*.

Park, E., Ai, J., and Baker, A.J. (2007). Cerebellar injury: clinical relevance and potential in traumatic brain injury research. In Progress in Brain Research, (Elsevier), pp. 327–338.

Park, E., Bell, J.D., and Baker, A.J. (2008). Traumatic brain injury: can the consequences be stopped? CMAJ Can. Med. Assoc. J. J. Assoc. Medicale Can. *178*, 1163–1170.

Patel, J.B., Malick, J.B., Salama, A.I., and Goldberg, M.E. (1985). Pharmacology of pyrazolopyridines. Pharmacol. Biochem. Behav. *23*, 675–680.

Pathak, M.M., Nourse, J.L., Tran, T., Hwe, J., Arulmoli, J., Le, D.T.T., Bernardis, E., Flanagan, L.A., and Tombola, F. (2014). Stretch-activated ion channel Piezo1 directs lineage choice in human neural stem cells. Proc. Natl. Acad. Sci. U. S. A. *111*, 16148–16153.

Paul, B., and Sbarra, A.J. (1968). The role of the phagocyte in host-parasite interactions. 13. The direct quantitative estimation of H2O2 in phagocytizing cells. Biochim. Biophys. Acta *156*, 168–178.

Pavanato, A., Tuñón, M.J., Sánchez-Campos, S., Marroni, C.A., Llesuy, S., González-Gallego, J., and Marroni, N. (2003). Effects of quercetin on liver damage in rats with carbon tetrachloride-induced cirrhosis. Dig. Dis. Sci. *48*, 824–829.

Pearson, G., Robinson, F., Beers Gibson, T., Xu, B.E., Karandikar, M., Berman, K., and Cobb, M.H. (2001). Mitogen-activated protein (MAP) kinase pathways: regulation and physiological functions. Endocr. Rev. *22*, 153–183.

Pelham, R.J., and Wang, Y. (1997). Cell locomotion and focal adhesions are regulated by substrate flexibility. Proc. Natl. Acad. Sci. *94*, 13661–13665.

Pelicano, H., Xu, R.-H., Du, M., Feng, L., Sasaki, R., Carew, J.S., Hu, Y., Ramdas, L., Hu, L., Keating, M.J., et al. (2006). Mitochondrial respiration defects in cancer cells cause activation of Akt survival pathway through a redox-mediated mechanism. J. Cell Biol. *175*, 913–923.

Penfield W. (1924) Oligodendroglia and its relation to classical neurogha. Brain:47: 430–452

di Penta, A., Moreno, B., Reix, S., Fernandez-Diez, B., Villanueva, M., Errea, O., Escala, N., Vandenbroeck, K., Comella, J.X., and Villoslada, P. (2013). Oxidative Stress and Proinflammatory Cytokines Contribute to Demyelination and Axonal Damage in a Cerebellar Culture Model of Neuroinflammation. PLoS ONE *8*, e54722.

Peterson, B., Stovall, K., Monian, P., Franklin, J.L., and Cummings, B.S. (2008). Alterations in phospholipid and fatty acid lipid profiles in primary neocortical cells during oxidant-induced cell injury. Chem. Biol. Interact. *174*, 163–176.

Petronilho, F., Feier, G., de Souza, B., Guglielmi, C., Constantino, L.S., Walz, R., Quevedo, J., and Dal-Pizzol, F. (2010). Oxidative stress in brain according to traumatic brain injury intensity. J. Surg. Res. *164*, 316–320.

Pfister, B.J., Weihs, T.P., Betenbaugh, M., and Bao, G. (2003). An In Vitro Uniaxial Stretch Model for Axonal Injury. Ann. Biomed. Eng. *31*, 589–598.

Pike, B.R., Zhao, X., Newcomb, J.K., Glenn, C.C., Anderson, D.K., and Hayes, R.L. (2000). Stretch injury causes calpain and caspase-3 activation and necrotic and apoptotic cell death in septo-hippocampal cell cultures. J. Neurotrauma *17*, 283–298.

Plemel, J.R., Keough, M.B., Duncan, G.J., Sparling, J.S., Yong, V.W., Stys, P.K., and Tetzlaff, W. (2014). Remyelination after spinal cord injury: is it a target for repair? Prog. Neurobiol. *117*, 54–72.

Plenz, D., Stewart, C.V., Shew, W., Yang, H., Klaus, A., and Bellay, T. (2011). Multi-electrode Array Recordings of Neuronal Avalanches in Organotypic Cultures. J. Vis. Exp.

Podbielska, M., Banik, N., Kurowska, E., and Hogan, E. (2013). Myelin Recovery in Multiple Sclerosis: The Challenge of Remyelination. Brain Sci. *3*, 1282–1324.

Poli, G., Leonarduzzi, G., Biasi, F., and Chiarpotto, E. (2004). Oxidative stress and cell signalling. Curr. Med. Chem. *11*, 1163–1182.

Potts, M.B., Rola, R., Claus, C.P., Ferriero, D.M., Fike, J.R., and Noble-Haeusslein, L.J. (2009). Glutathione peroxidase overexpression does not rescue impaired neurogenesis in the injured immature brain. J. Neurosci. Res. *87*, 1848–1857.

Poulsen, H.E., Jensen, B.R., Weimann, A., Jensen, S.A., Sørensen, M., and Loft, S. (2000). Antioxidants, DNA damage and gene expression. Free Radic. Res. *33 Suppl*, S33-39.

Powers, J.M., and Moser, H.W. (1998). Peroxisomal disorders: genotype, phenotype, major neuropathologic lesions, and pathogenesis. Brain Pathol. Zurich Switz. *8*, 101–120.

Powers, B.E., Sellers, D.L., Lovelett, E.A., Cheung, W., Aalami, S.P., Zapertov, N., Maris, D.O., and Horner, P.J. (2013). Remyelination reporter reveals prolonged refinement of spontaneously regenerated myelin. Proc. Natl. Acad. Sci. U. S. A. *110*, 4075–4080.

Prior, R.L., and Cao, G. (1999). In vivo total antioxidant capacity: comparison of different analytical methods. Free Radic. Biol. Med. *27*, 1173–1181.

Pryor, W.A. (2006). Free radical biology and medicine: it's a gas, man! AJP Regul. Integr. Comp. Physiol. *291*, R491–R511.

Pudenz, R.H., and Shelden, C.H. (1946). The lucite calvarium; a method for direct observation of the brain; cranial trauma and brain movement. J. Neurosurg. *3*, 487–505.

Pun, P.B.L., Lu, J., and Moochhala, S. (2009). Involvement of ROS in BBB dysfunction. Free Radic. Res. *43*, 348–364.

Purves D, Augustine GJ, Fitzpatrick D, Hall WC, LaMantia AS, McNamara JO, Williams SM, editors. Sunderland (MA): Sinauer Associates; 2001.

Putnam, A.J., Schultz, K., and Mooney, D.J. (2001). Control of microtubule assembly by extracellular matrix and externally applied strain. Am. J. Physiol.-Cell Physiol. *280*, C556–C564.

Quarles, R.H. (2002). Myelin sheaths: glycoproteins involved in their formation, maintenance and degeneration. Cell. Mol. Life Sci. CMLS *59*, 1851–1871.

Quarles, R.H., Macklin, W.B., and Morell, P. (2006). Myelin formation, structure and biochemistry (Elsevier, New York).

Radjendirane, V., Joseph, P., Lee, Y.H., Kimura, S., Klein-Szanto, A.J., Gonzalez, F.J., and Jaiswal, A.K. (1998). Disruption of the DT diaphorase (NQO1) gene in mice leads to increased menadione toxicity. J. Biol. Chem. *273*, 7382–7389.

Raff, M.C., Barres, B.A., Burne, J.F., Coles, H.S., Ishizaki, Y., and Jacobson, M.D. (1993). Programmed cell death and the control of cell survival: lessons from the nervous system. Science *262*, 695–700.

Rahal, A., Kumar, A., Singh, V., Yadav, B., Tiwari, R., Chakraborty, S., and Dhama, K. (2014). Oxidative Stress, Prooxidants, and Antioxidants: The Interplay. BioMed Res. Int. *2014*, 1–19.

Raisz, L.G. (1999). Physiology and pathophysiology of bone remodeling. Clin. Chem. *45*, 1353–1358.

Rangel-Castilla, L., Rangel-Castillo, L., Gopinath, S., and Robertson, C.S. (2008). Management of intracranial hypertension. Neurol. Clin. *26*, 521–541, x.

Reeves, T., Phillips, L., and Povlishock, J. (2005). Myelinated and unmyelinated axons of the corpus callosum differ in vulnerability and functional recovery following traumatic brain injury. Exp. Neurol. *196*, 126–137.

Reeves, T.M., Smith, T.L., Williamson, J.C., and Phillips, L.L. (2012). Unmyelinated axons show selective rostrocaudal pathology in the corpus callosum after traumatic brain injury. J. Neuropathol. Exp. Neurol. *71*, 198–210.

Reinhart-King, C.A. (2008). Chapter 3 Endothelial Cell Adhesion and Migration. In Methods in Enzymology, (Elsevier), pp. 45–64.

Reinhart-King, C.A., Dembo, M., and Hammer, D.A. (2008). Cell-Cell Mechanical Communication through Compliant Substrates. Biophys. J. *95*, 6044–6051.

von Reyn, C.R., Spaethling, J.M., Mesfin, M.N., Ma, M., Neumar, R.W., Smith, D.H., Siman, R., and Meaney, D.F. (2009). Calpain Mediates Proteolysis of the Voltage-Gated Sodium Channel -Subunit. J. Neurosci. *29*, 10350–10356.

von Reyn, C.R., Mott, R.E., Siman, R., Smith, D.H., and Meaney, D.F. (2012). Mechanisms of calpain mediated proteolysis of voltage gated sodium channel α-subunits following in vitro dynamic stretch injury: Mechanisms of calpain mediated NaCh proteolysis. J. Neurochem. *121*, 793–805.

Reznick, A.Z., and Packer, L. (1994). Oxidative damage to proteins: spectrophotometric method for carbonyl assay. Methods Enzymol. *233*, 357–363.

Rice-Evans, and Burdon (1994). Free Radical Damage and its Control, 1st Edition.

Rigg, J.L., Elovic, E.P., and Greenwald, B.D. (2005). A review of the effectiveness of antioxidant therapy to reduce neuronal damage in acute traumatic brain injury. J. Head Trauma Rehabil. *20*, 389–391.

Rink, A., Fung, K.M., Trojanowski, J.Q., Lee, V.M., Neugebauer, E., and McIntosh, T.K. (1995). Evidence of apoptotic cell death after experimental traumatic brain injury in the rat. Am. J. Pathol. *147*, 1575–1583.

Ritt, D.A., Abreu-Blanco, M.T., Bindu, L., Durrant, D.E., Zhou, M., Specht, S.I., Stephen, A.G., Holderfield, M., and Morrison, D.K. (2016). Inhibition of Ras/Raf/MEK/ERK Pathway Signaling by a Stress-Induced Phospho-Regulatory Circuit. Mol. Cell *64*, 875–887.

Rivers, L.E., Young, K.M., Rizzi, M., Jamen, F., Psachoulia, K., Wade, A., Kessaris, N., and Richardson, W.D. (2008). PDGFRA/NG2 glia generate myelinating oligodendrocytes and piriform projection neurons in adult mice. Nat. Neurosci. *11*, 1392–1401.

Roberts, G.W., Gentleman, S.M., Lynch, A., Murray, L., Landon, M., and Graham, D.I. (1994). Beta amyloid protein deposition in the brain after severe head injury: implications for the pathogenesis of Alzheimer's disease. J. Neurol. Neurosurg. Psychiatry *57*, 419–425.

Robertson, C.L., Saraswati, M., and Fiskum, G. (2007). Mitochondrial dysfunction early after traumatic brain injury in immature rats. J. Neurochem. *101*, 1248–1257.

Rodríguez-Rodríguez, A., Egea-Guerrero, J.J., Murillo-Cabezas, F., and Carrillo-Vico, A. (2014). Oxidative stress in traumatic brain injury. Curr. Med. Chem. *21*, 1201–1211.

Roozenbeek, B., Maas, A.I.R., and Menon, D.K. (2013). Changing patterns in the epidemiology of traumatic brain injury. Nat. Rev. Neurol. *9*, 231–236.

Rose, G.M., Hopper, A., De Vivo, M., and Tehim, A. (2005). Phosphodiesterase inhibitors for cognitive enhancement. Curr. Pharm. Des. *11*, 3329–3334.

Rosenberg, S.S., Kelland, E.E., Tokar, E., Asia, R., and Chan, J.R. (2008). The geometric and spatial constraints of the microenvironment induce oligodendrocyte differentiation. Proc. Natl. Acad. Sci. *105*, 14662–14667.

Roth, A.D., and Núñez, M.T. (2016). Oligodendrocytes: Functioning in a Delicate Balance Between High Metabolic Requirements and Oxidative Damage. In Glial Cells in Health and Disease of the CNS, R. von Bernhardi, ed. (Cham: Springer International Publishing), pp. 167–181.

Rothe, G., and Valet, G. (1990). Flow cytometric analysis of respiratory burst activity in phagocytes with hydroethidine and 2',7'-dichlorofluorescin. J. Leukoc. Biol. *47*, 440–448.

Rubattu, S., Pagliaro, B., Pierelli, G., Santolamazza, C., Castro, S., Mennuni, S., and Volpe, M. (2014). Pathogenesis of Target Organ Damage in Hypertension: Role of Mitochondrial Oxidative Stress. Int. J. Mol. Sci. *16*, 823–839.
Rubinek, T., and Levy, R. (1993). Arachidonic acid increases the activity of the assembled NADPH oxidase in cytoplasmic membranes and endosomes. Biochim. Biophys. Acta *1176*, 51–58.
Rutland-Brown, W., Langlois, J.A., Thomas, K.E., and Xi, Y.L. (2006). Incidence of traumatic brain injury in the United States, 2003. J. Head Trauma Rehabil. *21*, 544–548.
Rzigalinski, B.A., Liang, S., McKinney, J.S., Willoughby, K.A., and Ellis, E.F. (1997). Effect of Ca2+ on in vitro astrocyte injury. J. Neurochem. *68*, 289–296.
Rzigalinski, B.A., Weber, J.T., Willoughby, K.A., and Ellis, E.F. (1998). Intracellular free calcium dynamics in stretch-injured astrocytes. J. Neurochem. *70*, 2377–2385.
Saatman, K.E., Bozyczko-Coyne, D., Marcy, V., Siman, R., and McIntosh, T.K. (1996). Prolonged calpain-mediated spectrin breakdown occurs regionally following experimental brain injury in the rat. J. Neuropathol. Exp. Neurol. *55*, 850–860.
Saatman, K.E., Duhaime, A.-C., Bullock, R., Maas, A.I.R., Valadka, A., Manley, G.T., and Workshop Scientific Team and Advisory Panel Members (2008). Classification of traumatic brain injury for targeted therapies. J. Neurotrauma *25*, 719–738.
Saatman, K.E., Creed, J., and Raghupathi, R. (2010). Calpain as a therapeutic target in traumatic brain injury. Neurother. J. Am. Soc. Exp. Neurother. *7*, 31–42.
Sachdeva, S., and Gupta, M. (2013). Adenosine and its receptors as therapeutic targets: An overview. Saudi Pharm. J. SPJ Off. Publ. Saudi Pharm. Soc. *21*, 245–253.
Sackin, H. (1987). Stretch-activated potassium channels in renal proximal tubule. Am. J. Physiol. *253*, F1253-1262.
Sadoshima, J., Jahn, L., Takahashi, T., Kulik, T.J., and Izumo, S. (1992). Molecular characterization of the stretch-induced adaptation of cultured cardiac cells. An in vitro model of load-induced cardiac hypertrophy. J. Biol. Chem. *267*, 10551–10560.
Saez, A., Buguin, A., Silberzan, P., and Ladoux, B. (2005). Is the Mechanical Activity of Epithelial Cells Controlled by Deformations or Forces? Biophys. J. *89*, L52–L54.
Salmeen, A., and Barford, D. (2005). Functions and mechanisms of redox regulation of cysteine-based phosphatases. Antioxid. Redox Signal. *7*, 560–577.
Salzer, J.L., and Zalc, B. (2016). Myelination. Curr. Biol. CB *26*, R971–R975.
Salzer, J.L., Brophy, P.J., and Peles, E. (2008). Molecular domains of myelinated axons in the peripheral nervous system. Glia *56*, 1532–1540.
Samuni, Y., Goldstein, S., Dean, O.M., and Berk, M. (2013). The chemistry and biological activities of N-acetylcysteine. Biochim. Biophys. Acta *1830*, 4117–4129.
Sande, A., and West, C. (2010). Traumatic brain injury: a review of pathophysiology and management. J. Vet. Emerg. Crit. Care *20*, 177–190.
Santulli, P., Chouzenoux, S., Fiorese, M., Marcellin, L., Lemarechal, H., Millischer, A.-E., Batteux, F., Borderie, D., and Chapron, C. (2015). Protein oxidative stress markers in peritoneal fluids of women with deep infiltrating endometriosis are increased. Hum. Reprod. *30*, 49–60.
Sasai, N., Agata, N., Inoue-Miyazu, M., Kawakami, K., Kobayashi, K., Sokabe, M., and Hayakawa, K. (2010). Involvement of PI3K/Akt/TOR pathway in stretch-induced hypertrophy of myotubes. Muscle Nerve *41*, 100–106.
Schafer, F.Q., and Buettner, G.R. (2001). Redox environment of the cell as viewed through the redox state of the glutathione disulfide/glutathione couple. Free Radic. Biol. Med. *30*, 1191–1212.
Schieber, M., and Chandel, N.S. (2014). ROS Function in Redox Signaling and Oxidative Stress. Curr. Biol. *24*, R453–R462.
Schleien, C.L., Eberle, B., Shaffner, D.H., Koehler, R.C., and Traystman, R.J. (1994). Reduced blood-brain barrier permeability after cardiac arrest by conjugated superoxide dismutase and catalase in piglets. Stroke J. Cereb. Circ. *25*, 1830-1834-1835.
Schmidt, O.I., Heyde, C.E., Ertel, W., and Stahel, P.F. (2005). Closed head injury--an inflammatory disease? Brain Res. Brain Res. Rev. *48*, 388–399.
Schnell, L., Fearn, S., Klassen, H., Schwab, M.E., and Perry, V.H. (1999). Acute inflammatory responses to mechanical lesions in the CNS: differences between brain and spinal cord. Eur. J. Neurosci. *11*, 3648–3658.
Schoch, K.M., von Reyn, C.R., Bian, J., Telling, G.C., Meaney, D.F., and Saatman, K.E. (2013). Brain injury-induced proteolysis is reduced in a novel calpastatin-overexpressing transgenic mouse. J. Neurochem. *125*, 909–920.

Schumacher, M.A., Jong, B.E., Frey, S.L., Sudanagunta, S.P., Capra, N.F., and Levine, J.D. (2000). The stretch-inactivated channel, a vanilloid receptor variant, is expressed in small-diameter sensory neurons in the rat. Neurosci. Lett. *287*, 215–218.
Schwank, G., and Basler, K. (2010). Regulation of Organ Growth by Morphogen Gradients. Cold Spring Harb. Perspect. Biol. *2*, a001669–a001669.
Schwarzbold, M.L., Rial, D., De Bem, T., Machado, D.G., Cunha, M.P., dos Santos, A.A., dos Santos, D.B., Figueiredo, C.P., Farina, M., Goldfeder, E.M., et al. (2010). Effects of traumatic brain injury of different severities on emotional, cognitive, and oxidative stress-related parameters in mice. J. Neurotrauma *27*, 1883–1893.
Scorrano, L., Petronilli, V., and Bernardi, P. (1997). On the voltage dependence of the mitochondrial permeability transition pore. A critical appraisal. J. Biol. Chem. *272*, 12295–12299.
Sears, C., and Kaunas, R. (2016). The many ways adherent cells respond to applied stretch. J. Biomech. *49*, 1347–1354.
Semple, B.D., Blomgren, K., Gimlin, K., Ferriero, D.M., and Noble-Haeusslein, L.J. (2013). Brain development in rodents and humans: Identifying benchmarks of maturation and vulnerability to injury across species. Prog. Neurobiol. *0*, 1–16.
Shapiro, H.M. (1972). Redox balance in the body: an approach to quantitation. J. Surg. Res. *13*, 138–152.
Sharp, D.J., and Ham, T.E. (2011). Investigating white matter injury after mild traumatic brain injury. Curr. Opin. Neurol. *24*, 558–563.
Shepard, S.R., Ghajar, J.B., Giannuzzi, R., Kupferman, S., and Hariri, R.J. (1991). Fluid percussion barotrauma chamber: a new in vitro model for traumatic brain injury. J. Surg. Res. *51*, 417–424.
Sheridan, G.K., and Dev, K.K. (2012). S1P1 receptor subtype inhibits demyelination and regulates chemokine release in cerebellar slice cultures. Glia *60*, 382–392.
Sherriff, F.E., Bridges, L.R., and Sivaloganathan, S. (1994). Early detection of axonal injury after human head trauma using immunocytochemistry for beta-amyloid precursor protein. Acta Neuropathol. (Berl.) *87*, 55–62.
Shi, H., Hu, X., Leak, R.K., Shi, Y., An, C., Suenaga, J., Chen, J., and Gao, Y. (2015). Demyelination as a rational therapeutic target for ischemic or traumatic brain injury. Exp. Neurol. *272*, 17–25.
Shi, M., Du, F., Liu, Y., Li, L., Cai, J., Zhang, G.-F., Xu, X.-F., Lin, T., Cheng, H.-R., Liu, X.-D., et al. (2013). Glial cell-expressed mechanosensitive channel TRPV4 mediates infrasound-induced neuronal impairment. Acta Neuropathol. (Berl.) *126*, 725–739.
Shrestha, B.R., Vitolo, O.V., Joshi, P., Lordkipanidze, T., Shelanski, M., and Dunaevsky, A. (2006). Amyloid beta peptide adversely affects spine number and motility in hippocampal neurons. Mol. Cell. Neurosci. *33*, 274–282.
Shyu, K.-G. (2009). Cellular and molecular effects of mechanical stretch on vascular cells and cardiac myocytes. Clin. Sci. *116*, 377–389.
Sidaros, A., Skimminge, A., Liptrot, M.G., Sidaros, K., Engberg, A.W., Herning, M., Paulson, O.B., Jernigan, T.L., and Rostrup, E. (2009). Long-term global and regional brain volume changes following severe traumatic brain injury: a longitudinal study with clinical correlates. NeuroImage *44*, 1–8.
Sieg, F., Wahle, P., and Pape, H.C. (1999). Cellular reactivity to mechanical axonal injury in an organotypic in vitro model of neurotrauma. J. Neurotrauma *16*, 1197–1213.
Signoretti, S., Marmarou, A., Aygok, G.A., Fatouros, P.P., Portella, G., and Bullock, R.M. (2008). Assessment of mitochondrial impairment in traumatic brain injury using high-resolution proton magnetic resonance spectroscopy. J. Neurosurg. *108*, 42–52.
Silva, L.F.A., Hoffmann, M.S., Gerbatin, R. da R., Fiorin, F. da S., Dobrachinski, F., Mota, B.C., Wouters, A.T.B., Pavarini, S.P., Soares, F.A.A., Fighera, M.R., et al. (2013). Treadmill exercise protects against pentylenetetrazol-induced seizures and oxidative stress after traumatic brain injury. J. Neurotrauma *30*, 1278–1287.
Simons, M., and Lyons, D.A. (2013). Axonal selection and myelin sheath generation in the central nervous system. Curr. Opin. Cell Biol. *25*, 512–519.
Simons, M., and Nave, K.-A. (2016). Oligodendrocytes: Myelination and Axonal Support. Cold Spring Harb. Perspect. Biol. *8*, a020479.
Simons, M., Krämer, E.M., Thiele, C., Stoffel, W., and Trotter, J. (2000). Assembly of myelin by association of proteolipid protein with cholesterol- and galactosylceramide-rich membrane domains. J. Cell Biol. *151*, 143–154.
Singh, I., Paintlia, A.S., Khan, M., Stanislaus, R., Paintlia, M.K., Haq, E., Singh, A.K., and Contreras, M.A. (2004). Impaired peroxisomal function in the central nervous system with inflammatory

disease of experimental autoimmune encephalomyelitis animals and protection by lovastatin treatment. Brain Res. *1022*, 1–11.
Singh, I.N., Sullivan, P.G., Deng, Y., Mbye, L.H., and Hall, E.D. (2006). Time course of post-traumatic mitochondrial oxidative damage and dysfunction in a mouse model of focal traumatic brain injury: implications for neuroprotective therapy. J. Cereb. Blood Flow Metab. Off. J. Int. Soc. Cereb. Blood Flow Metab. *26*, 1407–1418.
Singh, P., Doshi, S., Spaethling, J.M., Hockenberry, A.J., Patel, T.P., Geddes-Klein, D.M., Lynch, D.R., and Meaney, D.F. (2012). N-Methyl-D-aspartate Receptor Mechanosensitivity Is Governed by C Terminus of NR2B Subunit. J. Biol. Chem. *287*, 4348–4359.
Siopi, E., Cho, A.H., Homsi, S., Croci, N., Plotkine, M., Marchand-Leroux, C., and Jafarian-Tehrani, M. (2011). Minocycline restores sAPPα levels and reduces the late histopathological consequences of traumatic brain injury in mice. J. Neurotrauma *28*, 2135–2143.
Siopi, E., Llufriu-Dabén, G., Cho, A.H., Vidal-Lletjós, S., Plotkine, M., Marchand-Leroux, C., and Jafarian-Tehrani, M. (2013). Etazolate, an α-secretase activator, reduces neuroinflammation and offers persistent neuroprotection following traumatic brain injury in mice. Neuropharmacology *67*, 183–192.
Slemmer, J.E., Matser, E.J., De Zeeuw, C.I., and Weber, J.T. (2002). Repeated mild injury causes cumulative damage to hippocampal cells. Brain *125*, 2699–2709.
Slemmer, J.E., Weber, J.T., and De Zeeuw, C.I. (2004). Cell death, glial protein alterations and elevated S-100β release in cerebellar cell cultures following mechanically induced trauma. Neurobiol. Dis. *15*, 563–572.
Smith, D.H., and Meaney, D.F. (2000). Axonal damage in traumatic brain injury. The Neuroscientist *6*, 483–495.
Smith, D.H., Wolf, J.A., Lusardi, T.A., Lee, V.M.-Y., and Meaney, D.F. (1999). High tolerance and delayed elastic response of cultured axons to dynamic stretch injury. J. Neurosci. *19*, 4263–4269.
Snaidero, N., Möbius, W., Czopka, T., Hekking, L.H.P., Mathisen, C., Verkleij, D., Goebbels, S., Edgar, J., Merkler, D., Lyons, D.A., et al. (2014). Myelin membrane wrapping of CNS axons by PI(3,4,5)P3-dependent polarized growth at the inner tongue. Cell *156*, 277–290.
Son, Y., Cheong, Y.-K., Kim, N.-H., Chung, H.-T., Kang, D.G., and Pae, H.-O. (2011). Mitogen-Activated Protein Kinases and Reactive Oxygen Species: How Can ROS Activate MAPK Pathways? J. Signal Transduct. *2011*, e792639.
Sorce, S., and Krause, K.-H. (2009). NOX enzymes in the central nervous system: from signaling to disease. Antioxid. Redox Signal. *11*, 2481–2504.
Sorolla, M.A., Reverter-Branchat, G., Tamarit, J., Ferrer, I., Ros, J., and Cabiscol, E. (2008). Proteomic and oxidative stress analysis in human brain samples of Huntington disease. Free Radic. Biol. Med. *45*, 667–678.
Sorolla, M.A., Rodríguez-Colman, M.J., Tamarit, J., Ortega, Z., Lucas, J.J., Ferrer, I., Ros, J., and Cabiscol, E. (2010). Protein oxidation in Huntington disease affects energy production and vitamin B6 metabolism. Free Radic. Biol. Med. *49*, 612–621.
Spain, A., Daumas, S., Lifshitz, J., Rhodes, J., Andrews, P.J.D., Horsburgh, K., and Fowler, J.H. (2010). Mild Fluid Percussion Injury in Mice Produces Evolving Selective Axonal Pathology and Cognitive Deficits Relevant to Human Brain Injury. J. Neurotrauma *27*, 1429–1438.
Staal, J.A., and Vickers, J.C. (2011). Selective Vulnerability of Non-Myelinated Axons to Stretch Injury in an *In Vitro* Co-Culture System. J. Neurotrauma *28*, 841–847.
Stadtman, E.R., Oliver, C.N., Levine, R.L., Fucci, L., and Rivett, A.J. (1988). Implication of protein oxidation in protein turnover, aging, and oxygen toxicity. Basic Life Sci. *49*, 331–339.
Staffa, K., Ondruschka, B., Franke, H., and Dreßler, J. (2012). Cerebellar Gene Expression following Human Traumatic Brain Injury. J. Neurotrauma *29*, 2716–2721.
Steinhubl, S.R. (2008). Why have antioxidants failed in clinical trials? Am. J. Cardiol. *101*, 14D–19D.
Stevens, B., Porta, S., Haak, L.L., Gallo, V., and Fields, R.D. (2002). Adenosine: a neuron-glial transmitter promoting myelination in the CNS in response to action potentials. Neuron *36*, 855–868.
Steyerberg, E.W., Mushkudiani, N., Perel, P., Butcher, I., Lu, J., McHugh, G.S., Murray, G.D., Marmarou, A., Roberts, I., Habbema, J.D.F., et al. (2008). Predicting outcome after traumatic brain injury: development and international validation of prognostic scores based on admission characteristics. PLoS Med. *5*, e165; discussion e165.
Stoica, B.A., and Faden, A.I. (2010). Cell death mechanisms and modulation in traumatic brain injury. Neurother. J. Am. Soc. Exp. Neurother. *7*, 3–12.
Stoppini, L., Buchs, P.A., and Muller, D. (1991). A simple method for organotypic cultures of nervous tissue. J. Neurosci. Methods *37*, 173–182.

Su, X., Wachtel, R.E., and Gebhart, G.F. (2000). Mechanosensitive potassium channels in rat colon sensory neurons. J. Neurophysiol. *84*, 836–843.
Sullivan, G.M., Mierzwa, A.J., Kijpaisalratana, N., Tang, H., Wang, Y., Song, S.-K., Selwyn, R., and Armstrong, R.C. (2013). Oligodendrocyte lineage and subventricular zone response to traumatic axonal injury in the corpus callosum. J. Neuropathol. Exp. Neurol. *72*, 1106–1125.
Sullivan, P.G., Thompson, M.B., and Scheff, S.W. (1999). Cyclosporin A attenuates acute mitochondrial dysfunction following traumatic brain injury. Exp. Neurol. *160*, 226–234.
Sullivan, P.G., Rabchevsky, A.G., Waldmeier, P.C., and Springer, J.E. (2005). Mitochondrial permeability transition in CNS trauma: cause or effect of neuronal cell death? J. Neurosci. Res. *79*, 231–239.
Sultana, R., Perluigi, M., and Allan Butterfield, D. (2013). Lipid peroxidation triggers neurodegeneration: a redox proteomics view into the Alzheimer disease brain. Free Radic. Biol. Med. *62*, 157–169.
Sun, S.-Y. (2010). N-acetylcysteine, reactive oxygen species and beyond. Cancer Biol. Ther. *9*, 109–110.
Sun, W., Fu, Y., Shi, Y., Cheng, J.-X., Cao, P., and Shi, R. (2012a). Paranodal myelin damage after acute stretch in Guinea pig spinal cord. J. Neurotrauma *29*, 611–619.
Sun, X., Liu, Y., Liu, B., Xiao, Z., and Zhang, L. (2012b). Rolipram promotes remyelination possibly via MEK-ERK signal pathway in cuprizone-induced demyelination mouse. Exp. Neurol. *237*, 304–311.
Sunitha, K., Hemshekhar, M., Thushara, R.M., Santhosh, M.S., Yariswamy, M., Kemparaju, K., and Girish, K.S. (2013). N-Acetylcysteine amide: a derivative to fulfill the promises of N-Acetylcysteine. Free Radic. Res. *47*, 357–367.
Supavilai, P., and Karobath, M. (1979). Stimulation of benzodiazepine receptor binding by SQ 20009 is chloride-dependent and picrotoxin-sensitive. Eur. J. Pharmacol. *60*, 111–113.
Suzuma, I., Suzuma, K., Ueki, K., Hata, Y., Feener, E.P., King, G.L., and Aiello, L.P. (2002). Stretch-induced retinal vascular endothelial growth factor expression is mediated by phosphatidylinositol 3-kinase and protein kinase C (PKC)-zeta but not by stretch-induced ERK1/2, Akt, Ras, or classical/novel PKC pathways. J. Biol. Chem. *277*, 1047–1057.
Syed, Y.A., Baer, A., Hofer, M.P., González, G.A., Rundle, J., Myrta, S., Huang, J.K., Zhao, C., Rossner, M.J., Trotter, M.W.B., et al. (2013). Inhibition of phosphodiesterase-4 promotes oligodendrocyte precursor cell differentiation and enhances CNS remyelination. EMBO Mol. Med. *5*, 1918–1934.
Tagliaferri, F., Compagnone, C., Korsic, M., Servadei, F., and Kraus, J. (2006). A systematic review of brain injury epidemiology in Europe. Acta Neurochir. (Wien) *148*, 255–268; discussion 268.
Takahashi, A., and Gotoh, H. (2000). Mechanosensitive whole-cell currents in cultured rat somatosensory neurons. Brain Res. *869*, 225–230.
Takeishi, Y., Huang, Q., Abe, J., Glassman, M., Che, W., Lee, J.D., Kawakatsu, H., Lawrence, E.G., Hoit, B.D., Berk, B.C., et al. (2001). Src and multiple MAP kinase activation in cardiac hypertrophy and congestive heart failure under chronic pressure-overload: comparison with acute mechanical stretch. J. Mol. Cell. Cardiol. *33*, 1637–1648.
Talalay, P., Fahey, J.W., Holtzclaw, W.D., Prestera, T., and Zhang, Y. (1995). Chemoprotection against cancer by phase 2 enzyme induction. Toxicol. Lett. *82–83*, 173–179.
Talsky, A., Pacione, L.R., Shaw, T., Wasserman, L., Lenny, A., Verma, A., Hurwitz, G., Waxman, R., Morgan, A., and Bhalerao, S. (2010). Pharmacological interventions for traumatic brain injury. Br. Columbia Med. J. *53*, 1.
Tang-Schomer, M.D., Patel, A.R., Baas, P.W., and Smith, D.H. (2010). Mechanical breaking of microtubules in axons during dynamic stretch injury underlies delayed elasticity, microtubule disassembly, and axon degeneration. FASEB J. Off. Publ. Fed. Am. Soc. Exp. Biol. *24*, 1401–1410.
Tang-Schomer, M.D., Johnson, V.E., Baas, P.W., Stewart, W., and Smith, D.H. (2012). Partial interruption of axonal transport due to microtubule breakage accounts for the formation of periodic varicosities after traumatic axonal injury. Exp. Neurol. *233*, 364–372.
Tasset, I., Bahamonde, C., Agüera, E., Conde, C., Cruz, A.H., Pérez-Herrera, A., Gascón, F., Giraldo, A.I., Ruiz, M.C., Lillo, R., et al. (2013). Effect of natalizumab on oxidative damage biomarkers in relapsing-remitting multiple sclerosis. Pharmacol. Rep. PR *65*, 624–631.
Tavazzi, B., Batocchi, A.P., Amorini, A.M., Nociti, V., D'Urso, S., Longo, S., Gullotta, S., Picardi, M., and Lazzarino, G. (2011). Serum metabolic profile in multiple sclerosis patients. Mult. Scler. Int. *2011*, 167156.

Teasdale, G., and Jennett, B. (1974). Assessment of coma and impaired consciousness. A practical scale. Lancet Lond. Engl. *2*, 81–84.
Tecoma, E.S., Monyer, H., Goldberg, M.P., and Choi, D.W. (1989). Traumatic neuronal injury in vitro is attenuated by NMDA antagonists. Neuron *2*, 1541–1545.
Thompson, S.-A., Wingrove, P.B., Connelly, L., Whiting, P.J., and Wafford, K.A. (2002). Tracazolate reveals a novel type of allosteric interaction with recombinant gamma-aminobutyric acid(A) receptors. Mol. Pharmacol. *61*, 861–869.
Thorburne, S.K., and Juurlink, B.H. (1996). Low glutathione and high iron govern the susceptibility of oligodendroglial precursors to oxidative stress. J. Neurochem. *67*, 1014–1022.
Thornton, E., Vink, R., Blumbergs, P.C., and Van Den Heuvel, C. (2006). Soluble amyloid precursor protein alpha reduces neuronal injury and improves functional outcome following diffuse traumatic brain injury in rats. Brain Res. *1094*, 38–46.
Throm Quinlan, A.M., Sierad, L.N., Capulli, A.K., Firstenberg, L.E., and Billiar, K.L. (2011). Combining Dynamic Stretch and Tunable Stiffness to Probe Cell Mechanobiology In Vitro. PLoS ONE *6*, e23272.
Ticku, M.K., and Davis, W.C. (1982). Molecular interactions of etazolate with benzodiazepine and picrotoxinin binding sites. J. Neurochem. *38*, 1180–1182.
Tipler (1982). Physics.
Tojkander, S., Gateva, G., and Lappalainen, P. (2012). Actin stress fibers - assembly, dynamics and biological roles. J. Cell Sci. *125*, 1855–1864.
Tomaiuolo, F., Bivona, U., Lerch, J.P., Di Paola, M., Carlesimo, G.A., Ciurli, P., Matteis, M., Cecchetti, L., Forcina, A., Silvestro, D., et al. (2012). Memory and anatomical change in severe non missile traumatic brain injury: ~1 vs. ~8 years follow-up. Brain Res. Bull. *87*, 373–382.
Tondon, A., and Kaunas, R. (2014). The Direction of Stretch-Induced Cell and Stress Fiber Orientation Depends on Collagen Matrix Stress. PLoS ONE *9*, e89592.
Toyama, B.H., Savas, J.N., Park, S.K., Harris, M.S., Ingolia, N.T., Yates, J.R., and Hetzer, M.W. (2013). Identification of long-lived proteins reveals exceptional stability of essential cellular structures. Cell *154*, 971–982.
Trapp, B.D., Nishiyama, A., Cheng, D., and Macklin, W. (1997). Differentiation and death of premyelinating oligodendrocytes in developing rodent brain. J. Cell Biol. *137*, 459–468.
Tripathi, R.B., Rivers, L.E., Young, K.M., Jamen, F., and Richardson, W.D. (2010). NG2 glia generate new oligodendrocytes but few astrocytes in a murine experimental autoimmune encephalomyelitis model of demyelinating disease. J. Neurosci. Off. J. Soc. Neurosci. *30*, 16383–16390.
Trotti, D., Danbolt, N.C., Volterra, A., and others (1998). Glutamate transporters are oxidant-vulnerable: a molecular link between oxidative and excitotoxic neurodegeneration? Trends Pharmacol. Sci. *19*, 328–333.
Truelove, D., Shuaib, A., Ijaz, S., Ishaqzay, R., and Kalra, J. (1994). Neuronal protection with superoxide dismutase in repetitive forebrain ischemia in gerbils. Free Radic. Biol. Med. *17*, 445–450.
Tunez, I., Sánchez-López, F., Agüera, E., Fernández-Bolaños, R., Sánchez, F.M., and Tasset-Cuevas, I. (2011). Important role of oxidative stress biomarkers in Huntington's disease. J. Med. Chem. *54*, 5602–5606.
Uchida, K. (2003a). 4-Hydroxy-2-nonenal: a product and mediator of oxidative stress. Prog. Lipid Res. *42*, 318–343.
Uchida, K. (2003b). Histidine and lysine as targets of oxidative modification. Amino Acids *25*, 249–257.
Unterberg, A.W., Stover, J., Kress, B., and Kiening, K.L. (2004). Edema and brain trauma. Neuroscience *129*, 1021–1029.
Urbanski, M.M., Kingsbury, L., Moussouros, D., Kassim, I., Mehjabeen, S., Paknejad, N., and Melendez-Vasquez, C.V. (2016). Myelinating glia differentiation is regulated by extracellular matrix elasticity. Sci. Rep. *6*, 33751.
Uryu, K., Chen, X.-H., Martinez, D., Browne, K.D., Johnson, V.E., Graham, D.I., Lee, V.M.-Y., Trojanowski, J.Q., and Smith, D.H. (2007). Multiple proteins implicated in neurodegenerative diseases accumulate in axons after brain trauma in humans. Exp. Neurol. *208*, 185–192.
Valencia, A., and Morán, J. (2004). Reactive oxygen species induce different cell death mechanisms in cultured neurons. Free Radic. Biol. Med. *36*, 1112–1125.
Valko, M., Rhodes, C.J., Moncol, J., Izakovic, M., and Mazur, M. (2006). Free radicals, metals and antioxidants in oxidative stress-induced cancer. Chem. Biol. Interact. *160*, 1–40.

Vande Geest, J.P., Di Martino, E.S., and Vorp, D.A. (2004). An analysis of the complete strain field within Flexercell membranes. J. Biomech. *37*, 1923–1928.
Vargas, M.E., and Barres, B.A. (2007). Why is Wallerian degeneration in the CNS so slow? Annu. Rev. Neurosci. *30*, 153–179.
Vellas, B., Sol, O., Snyder, P.J., Ousset, P.-J., Haddad, R., Maurin, M., Lemarié, J.-C., Désiré, L., Pando, M.P., and EHT0202/002 study group (2011). EHT0202 in Alzheimer's disease: a 3-month, randomized, placebo-controlled, double-blind study. Curr. Alzheimer Res. *8*, 203–212.
Venkatesan, C., Chrzaszcz, M., Choi, N., and Wainwright, M.S. (2010). Chronic upregulation of activated microglia immunoreactive for galectin-3/Mac-2 and nerve growth factor following diffuse axonal injury. J. Neuroinflammation *7*, 32.
Verhoeven, N.M., and Jakobs, C. (2001). Human metabolism of phytanic acid and pristanic acid. Prog. Lipid Res. *40*, 453–466.
Verweij, B.H., Muizelaar, J.P., Vinas, F.C., Peterson, P.L., Xiong, Y., and Lee, C.P. (2000). Impaired cerebral mitochondrial function after traumatic brain injury in humans. J. Neurosurg. *93*, 815–820.
Vezza, T., Rodríguez-Nogales, A., Algieri, F., Utrilla, M., Rodriguez-Cabezas, M., and Galvez, J. (2016). Flavonoids in Inflammatory Bowel Disease: A Review. Nutrients *8*, 211.
Vignaud, T., Blanchoin, L., and Théry, M. (2012). Directed cytoskeleton self-organization. Trends Cell Biol. *22*, 671–682.
Villarreal, F.J., and Kim, N.N. (1998). Regulation of myocardial extracellular matrix components by mechanical and chemical growth factors. Cardiovasc. Pathol. *7*, 145–151.
Vincenzi, F., Corciulo, C., Targa, M., Merighi, S., Gessi, S., Casetta, I., Gentile, M., Granieri, E., Borea, P.A., and Varani, K. (2013). Multiple sclerosis lymphocytes upregulate A2A adenosine receptors that are antiinflammatory when stimulated. Eur. J. Immunol. *43*, 2206–2216.
Vladimirova, O., O'Connor, J., Cahill, A., Alder, H., Butunoi, C., and Kalman, B. (1998). Oxidative damage to DNA in plaques of MS brains. Mult. Scler. *4*, 413–418.
Volman, V., and Ng, L.J. (2014). Primary paranode demyelination modulates slowly developing axonal depolarization in a model of axonal injury. J. Comput. Neurosci. *37*, 439–457.
Volpe, J.J. (2000). Overview: normal and abnormal human brain development. Ment. Retard. Dev. Disabil. Res. Rev. *6*, 1–5.
Volpe, J.J., Kinney, H.C., Jensen, F.E., and Rosenberg, P.A. (2011). The developing oligodendrocyte: key cellular target in brain injury in the premature infant. Int. J. Dev. Neurosci. Off. J. Int. Soc. Dev. Neurosci. *29*, 423–440.
Wang, K.K. (2000). Calpain and caspase: can you tell the difference? Trends Neurosci. *23*, 20–26.
Wang, C., Yang, X.-M., Zhuo, Y.-Y., Zhou, H., Lin, H.-B., Cheng, Y.-F., Xu, J.-P., and Zhang, H.-T. (2012). The phosphodiesterase-4 inhibitor rolipram reverses Aβ-induced cognitive impairment and neuroinflammatory and apoptotic responses in rats. Int. J. Neuropsychopharmacol. *15*, 749–766.
Wang, C., Zhang, J., Lu, Y., Lin, P., Pan, T., Zhao, X., Liu, A., Wang, Q., Zhou, W., and Zhang, H.-T. (2014). Antidepressant-like effects of the phosphodiesterase-4 inhibitor etazolate and phosphodiesterase-5 inhibitor sildenafil via cyclic AMP or cyclic GMP signaling in mice. Metab. Brain Dis. *29*, 673–682.
Wang, G., Zhang, J., Hu, X., Zhang, L., Mao, L., Jiang, X., Liou, A.K.-F., Leak, R.K., Gao, Y., and Chen, J. (2013). Microglia/macrophage polarization dynamics in white matter after traumatic brain injury. J. Cereb. Blood Flow Metab. *33*, 1864–1874.
Wang, J.H.-C., Goldschmidt-Clermont, P., Wille, J., and Yin, F.C.-P. (2001). Specificity of endothelial cell reorientation in response to cyclic mechanical stretching. J. Biomech. *34*, 1563–1572.
Wang, N., Tolic-Norrelykke, I.M., Chen, J., Mijailovich, S.M., Butler, J.P., Fredberg, J.J., and Stamenovic, D. (2002). Cell prestress. I. Stiffness and prestress are closely associated in adherent contractile cells. AJP Cell Physiol. *282*, C606–C616.
Wang, P., Myers, J.G., Wu, P., Cheewatrakoolpong, B., Egan, R.W., and Billah, M.M. (1997). Expression, purification, and characterization of human cAMP-specific phosphodiesterase (PDE4) subtypes A, B, C, and D. Biochem. Biophys. Res. Commun. *234*, 320–324.
Wang, Z., Wu, W., Liu, Y., Wang, T., Chen, X., Zhang, J., Zhou, G., and Chen, R. (2016). Altered Cerebellar White Matter Integrity in Patients with Mild Traumatic Brain Injury in the Acute Stage. PLOS ONE *11*, e0151489.
Wardlaw, J.M., Easton, V.J., and Statham, P. (2002). Which CT features help predict outcome after head injury? J. Neurol. Neurosurg. Psychiatry *72*, 188–192.
Weber, J.T., Rzigalinski, B.A., Willoughby, K.A., Moore, S.F., and Ellis, E.F. (1999). Alterations in calcium-mediated signal transduction after traumatic injury of cortical neurons. Cell Calcium *26*, 289–299.

Weber, J.T., Rzigalinski, B.A., and Ellis, E.F. (2001). Traumatic Injury of Cortical Neurons Causes Changes in Intracellular Calcium Stores and Capacitative Calcium Influx. J. Biol. Chem. *276*, 1800–1807.

Whitaker, C.M., Beaumont, E., Wells, M.J., Magnuson, D.S.K., Hetman, M., and Onifer, S.M. (2008). Rolipram attenuates acute oligodendrocyte death in the adult rat ventrolateral funiculus following contusive cervical spinal cord injury. Neurosci. Lett. *438*, 200–204.

WHO Model List of Essential Medicines. World Health Organization. April 2015. Amended November 2015

Williams, M., and Risley, E.A. (1979). Enhancement of the binding of 3H-diazepam to rat brain membranes in vitro by SQ 20009, A novel anxiolytic, gamma-aminobutyric acid (GABA) and muscimol. Life Sci. *24*, 833–841.

Wilson, J.X. (1997). Antioxidant defense of the brain: a role for astrocytes. Can. J. Physiol. Pharmacol. *75*, 1149–1163.

Witko-Sarsat, V., Friedlander, M., Capeillère-Blandin, C., Nguyen-Khoa, T., Nguyen, A.T., Zingraff, J., Jungers, P., and Descamps-Latscha, B. (1996). Advanced oxidation protein products as a novel marker of oxidative stress in uremia. Kidney Int. *49*, 1304–1313.

Witko-Sarsat, V., Friedlander, M., Nguyen Khoa, T., Capeillère-Blandin, C., Nguyen, A.T., Canteloup, S., Dayer, J.M., Jungers, P., Drüeke, T., and Descamps-Latscha, B. (1998). Advanced oxidation protein products as novel mediators of inflammation and monocyte activation in chronic renal failure. J. Immunol. Baltim. Md 1950 *161*, 2524–2532.

Wolf, J.A., Stys, P.K., Lusardi, T., Meaney, D., and Smith, D.H. (2001). Traumatic axonal injury induces calcium influx modulated by tetrodotoxin-sensitive sodium channels. J. Neurosci. *21*, 1923–1930.

Wong, J., Hoe, N.W., Zhiwei, F., and Ng, I. (2005). Apoptosis and traumatic brain injury. Neurocrit. Care *3*, 177–182.

Wu, C., and Sun, D. (2015). GABA receptors in brain development, function, and injury. Metab. Brain Dis. *30*, 367–379.

Xiao, L., Ohayon, D., McKenzie, I.A., Sinclair-Wilson, A., Wright, J.L., Fudge, A.D., Emery, B., Li, H., and Richardson, W.D. (2016). Rapid production of new oligodendrocytes is required in the earliest stages of motor-skill learning. Nat. Neurosci. *19*, 1210–1217.

Xiong, Y., Gu, Q., Peterson, P.L., Muizelaar, J.P., and Lee, C.P. (1997). Mitochondrial dysfunction and calcium perturbation induced by traumatic brain injury. J. Neurotrauma *14*, 23–34.

Xiong, Y., Peterson, P.L., and Lee, C.P. (1999). Effect of N-acetylcysteine on mitochondrial function following traumatic brain injury in rats. J. Neurotrauma *16*, 1067–1082.

Xiong, Y., Mahmood, A., and Chopp, M. (2013). Animal models of traumatic brain injury. Nat. Rev. Neurosci. *14*, 128–142.

Xiong, Z.-G., Zhu, X.-M., Chu, X.-P., Minami, M., Hey, J., Wei, W.-L., MacDonald, J.F., Wemmie, J.A., Price, M.P., Welsh, M.J., et al. (2004). Neuroprotection in ischemia: blocking calcium-permeable acid-sensing ion channels. Cell *118*, 687–698.

Xu, X.-Y., Guo, Chung, Yan, Y.-X., Guo, Y., Li, R.-X., Song, M., and Zhang, X.-Z. (2012). Differential effects of mechanical strain on osteoclastogenesis and osteoclast-related gene expression in RAW264.7 cells. Mol. Med. Rep.

Yakovlev, A.G., and Faden, A.I. (2001). Caspase-dependent apoptotic pathways in CNS injury. Mol. Neurobiol. *24*, 131–144.

Yamaguchi, O. (2004). Response of bladder smooth muscle cells to obstruction: signal transduction and the role of mechanosensors. Urology *63*, 11–16.

Yamashima, T. (2004). Ca2+-dependent proteases in ischemic neuronal death: a conserved “calpain-cathepsin cascade” from nematodes to primates. Cell Calcium *36*, 285–293.

Yamashima, T., Tonchev, A.B., Tsukada, T., Saido, T.C., Imajoh-Ohmi, S., Momoi, T., and Kominami, E. (2003). Sustained calpain activation associated with lysosomal rupture executes necrosis of the postischemic CA1 neurons in primates. Hippocampus *13*, 791–800.

Yamazaki, T., Komuro, I., Kudoh, S., Zou, Y., Shiojima, I., Mizuno, T., Takano, H., Hiroi, Y., Ueki, K., and Tobe, K. (1995). Mechanical stress activates protein kinase cascade of phosphorylation in neonatal rat cardiac myocytes. J. Clin. Invest. *96*, 438–446.

Yang, J., Weimer, R.M., Kallop, D., Olsen, O., Wu, Z., Renier, N., Uryu, K., and Tessier-Lavigne, M. (2013). Regulation of axon degeneration after injury and in development by the endogenous calpain inhibitor calpastatin. Neuron *80*, 1175–1189.

Yeung, M.S.Y., Zdunek, S., Bergmann, O., Bernard, S., Salehpour, M., Alkass, K., Perl, S., Tisdale, J., Possnert, G., Brundin, L., et al. (2014). Dynamics of oligodendrocyte generation and myelination in the human brain. Cell *159*, 766–774.

Yeung, T., Georges, P.C., Flanagan, L.A., Marg, B., Ortiz, M., Funaki, M., Zahir, N., Ming, W., Weaver, V., and Janmey, P.A. (2005). Effects of substrate stiffness on cell morphology, cytoskeletal structure, and adhesion. Cell Motil. Cytoskeleton *60*, 24–34.

Yi, J.-H., and Hazell, A.S. (2005). N-acetylcysteine attenuates early induction of heme oxygenase-1 following traumatic brain injury. Brain Res. *1033*, 13–19.

Yokoyama, H., Yano, R., Aoki, E., Kato, H., and Araki, T. (2008). Comparative pharmacological study of free radical scavenger, nitric oxide synthase inhibitor, nitric oxide synthase activator and cyclooxygenase inhibitor against MPTP neurotoxicity in mice. Metab. Brain Dis. *23*, 335–349.

Yoritaka, A., Hattori, N., Uchida, K., Tanaka, M., Stadtman, E.R., and Mizuno, Y. (1996). Immunohistochemical detection of 4-hydroxynonenal protein adducts in Parkinson disease. Proc. Natl. Acad. Sci. U. S. A. *93*, 2696–2701.

Yoshida, T., and Kikuchi, G. (1974). Sequence of the reaction of heme catabolism catalyzed by the microsomal heme oxygenase system. FEBS Lett. *48*, 256–261.

Young, K.M., Psachoulia, K., Tripathi, R.B., Dunn, S.-J., Cossell, L., Attwell, D., Tohyama, K., and Richardson, W.D. (2013). Oligodendrocyte dynamics in the healthy adult CNS: evidence for myelin remodeling. Neuron *77*, 873–885.

Young, S.R.L., Gerard-O'Riley, R., Harrington, M., and Pavalko, F.M. (2010). Activation of NF-κB by fluid shear stress, but not TNF-α, requires focal adhesion kinase in osteoblasts. Bone *47*, 74–82.

Yu, C., Friday, B.B., Lai, J.-P., McCollum, A., Atadja, P., Roberts, L.R., and Adjei, A.A. (2007). Abrogation of MAPK and Akt signaling by AEE788 synergistically potentiates histone deacetylase inhibitor-induced apoptosis through reactive oxygen species generation. Clin. Cancer Res. Off. J. Am. Assoc. Cancer Res. *13*, 1140–1148.

Yu, R., Chen, C., Mo, Y.-Y., Hebbar, V., Owuor, E.D., Tan, T.-H., and Kong, A.-N.T. (2000). Activation of Mitogen-activated Protein Kinase Pathways Induces Antioxidant Response Element-mediated Gene Expression via a Nrf2-dependent Mechanism. J. Biol. Chem. *275*, 39907–39913.

Yuen, T.J., Silbereis, J.C., Griveau, A., Chang, S.M., Daneman, R., Fancy, S.P.J., Zahed, H., Maltepe, E., and Rowitch, D.H. (2014). Oligodendrocyte-encoded HIF function couples postnatal myelination and white matter angiogenesis. Cell *158*, 383–396.

Zafarullah, M., Li, W.Q., Sylvester, J., and Ahmad, M. (2003). Molecular mechanisms of N-acetylcysteine actions. Cell. Mol. Life Sci. CMLS *60*, 6–20.

Zahn, J.T., Louban, I., Jungbauer, S., Bissinger, M., Kaufmann, D., Kemkemer, R., and Spatz, J.P. (2011). Age-Dependent Changes in Microscale Stiffness and Mechanoresponses of Cells. Small *7*, 1480–1487.

Zaleska, M.M., and Floyd, R.A. (1985). Regional lipid peroxidation in rat brain in vitro: possible role of endogenous iron. Neurochem. Res. *10*, 397–410.

Zambonin, J.L., Zhao, C., Ohno, N., Campbell, G.R., Engeham, S., Ziabreva, I., Schwarz, N., Lee, S.E., Frischer, J.M., Turnbull, D.M., et al. (2011). Increased mitochondrial content in remyelinated axons: implications for multiple sclerosis. Brain J. Neurol. *134*, 1901–1913.

Zeis, T., Graumann, U., Reynolds, R., and Schaeren-Wiemers, N. (2008). Normal-appearing white matter in multiple sclerosis is in a subtle balance between inflammation and neuroprotection. Brain J. Neurol. *131*, 288–303.

Zemel, A., Rehfeldt, F., Brown, A.E.X., Discher, D.E., and Safran, S.A. (2010). Optimal matrix rigidity for stress-fibre polarization in stem cells. Nat. Phys. *6*, 468–473.

Zhang, K., and Sejnowski, T.J. (2000). A universal scaling law between gray matter and white matter of cerebral cortex. Proc. Natl. Acad. Sci. U. S. A. *97*, 5621–5626.

Zhang, L., Rzigalinski, B.A., Ellis, E.F., and Satin, L.S. (1996). Reduction of voltage-dependent Mg2+ blockade of NMDA current in mechanically injured neurons. Science *274*, 1921–1923.

Zhang, M., An, C., Gao, Y., Leak, R.K., Chen, J., and Zhang, F. (2013). Emerging roles of Nrf2 and phase II antioxidant enzymes in neuroprotection. Prog. Neurobiol. *100*, 30–47.

Zhang, Q.-G., Laird, M.D., Han, D., Nguyen, K., Scott, E., Dong, Y., Dhandapani, K.M., and Brann, D.W. (2012). Critical Role of NADPH Oxidase in Neuronal Oxidative Damage and Microglia Activation following Traumatic Brain Injury. PLoS ONE *7*, e34504.

Zhang, Y., Taveggia, C., Melendez-Vasquez, C., Einheber, S., Raine, C.S., Salzer, J.L., Brosnan, C.F., and John, G.R. (2006). Interleukin-11 potentiates oligodendrocyte survival and maturation, and myelin formation. J. Neurosci. Off. J. Soc. Neurosci. *26*, 12174–12185.

Zhao, X., Sun, G., Zhang, J., Strong, R., Dash, P.K., Kan, Y.W., Grotta, J.C., and Aronowski, J. (2007). Transcription factor Nrf2 protects the brain from damage produced by intracerebral hemorrhage. Stroke J. Cereb. Circ. *38*, 3280–3286.

Zheng, J. (2013). Molecular Mechanism of TRP Channels. Compr. Physiol. *3*, 221–242.

Zheng, J., Lamoureux, P., Santiago, V., Dennerll, T., Buxbaum, R.E., and Heidemann, S.R. (1991). Tensile regulation of axonal elongation and initiation. J. Neurosci. Off. J. Soc. Neurosci. *11*, 1117–1125.

Zhou, H., Chen, Q., Kong, D.L., Guo, J., Wang, Q., and Yu, S.Y. (2011). Effect of Resveratrol on Gliotransmitter Levels and p38 Activities in Cultured Astrocytes. Neurochem. Res. *36*, 17–26.

Zhu, H., and Li, Y. (2012). NAD(P)H: quinone oxidoreductase 1 and its potential protective role in cardiovascular diseases and related conditions. Cardiovasc. Toxicol. *12*, 39–45.

Zhu, X., Hill, R.A., Dietrich, D., Komitova, M., Suzuki, R., and Nishiyama, A. (2011). Age-dependent fate and lineage restriction of single NG2 cells. Dev. Camb. Engl. *138*, 745–753.

Zipfel, G.J., Babcock, D.J., Lee, J.M., and Choi, D.W. (2000). Neuronal apoptosis after CNS injury: the roles of glutamate and calcium. J. Neurotrauma *17*, 857–869.

(2005). Mechanosensitivity in Cells and Tissues (Moscow: Academia).

ANNEXE

Etazolate Promotes Oligodendrocyte Differentiation and Remyelination after Demyelination in Organotypic Cerebellar Slice Cultures

Gemma Llufriu-Dabén, Delphine Meffre, Elena Chierto, Alex Carreté, Charbel Massaad, Mehrnaz Jafarian-Tehrani*

INSERM UMR-S 1124, Université Paris Descartes, Sorbonne Paris Cité, Faculté des Sciences Fondamentales et Biomédicales, 45 rue des Saints-Pères, 75006 Paris, France.

Highlights

- Etazolate protects myelin sheaths following lysolecithin-induced demyelination
- Etazolate enhances remyelination in demyelinated cerebellar slices
- Etazolate promotes oligodendrocyte differentiation after demyelination *ex vivo*
- Etazolate stimulates morphological maturation of oligodendrocyte *in vitro*
- Benefical effects of etazolate are blocked by the ADAM10 inhibitor GI254023X

Abstract

Remyelination is an endogenous regenerative process responsible of myelin repair after a demyelinating insult in the central nervous system. It is mediated by oligodendrocyte precursor cells (OPCs) differentiation into mature myelinating oligodendrocytes. However, the efficacy of remyelination is limited in demyelinating disorders, leading to a progressive axonal loss and irreversible functional impairments, for which no efficient therapy is available nowadays. The aim of this study was to evaluate the potential therapeutic activity of etazolate, a pyrazolopyridine derivative with neuroprotective α-secretase activity, on myelinated axons, oligodendrocyte differentiation and remyelination following lysolecithin-induced demyelination in organotypic cerebellar slice cultures. Etazolate treatment (0.2 or 2 µM) was able i) to protect MAG^+/$Calbindin^+$ axons from demyelination, ii) to increase the number of mature oligodendrocyte $CC1^+$ cells and iii) to promote the reappearance of the paired $Caspr^+$ at the nodes of Ranvier. It is noteworthy that etazolate was also able to increase the percentage of myelinated axons with short internodes under 20 µm, as an indicator of remyelination. Besides, etazolate treatment stimulated oligodendrocyte morphological maturation, characterized by an increase of multi-branched GFP^+ cells, in primary mixed glial cultures from PLP-eGFP mice. Etazolate failed to promote its beneficial effects in the presence of GI254023X, a specific ADAM10 (α-secretase) inhibitor, suggesting that ADAM10 is involved in the mechanism of action of etazolate. Our results provide a strong evidence for etazolate therapy as a protective and remyelinating strategy and support further testing of etazolate in models of demyelination *in vivo*.

Keywords: etazolate; remyelination; oligodendrocyte differentiation; ADAM10; lysolecithin; demyelination

Abbreviations: OPCs: oligodendrocyte precursor cells; GFP: green fluorescent protein; MS: multiple sclerosis.

Corresponding author:
Prof. Mehrnaz Jafarian-Tehrani, INSERM UMR-S 1124, Paris Descartes University, Sorbonne Paris Cité, Faculté des Sciences Fondamentales et Biomédicales, 45 rue des Saints-Pères, 75006 Paris, FRANCE.
Phone: + 33 1 70 64 99 76, mehrnaz.jafarian@parisdescartes

1. Introduction

Demyelination in the central nervous system (CNS) is characterized by myelin sheath loss and oligodendrocyte cell death. It contributes to progressive axonal injury leading to neurological disability as observed in demyelinating diseases as multiple sclerosis (MS) (Compston and Coles, 2008; Trapp and Nave, 2008) or in acute CNS injuries as traumatic brain injury (TBI) (Armstrong et al., 2015a, 2015b). At the opposite, remyelination is an endogenous regenerative process occurring in response to demyelination, essential for restoration of saltatory conduction and subsequent prevention of further axonal damage (Franklin and Ffrench-Constant, 2008; Franklin and Goldman, 2015).

However, remyelination is limited or inadequate in demyelinating diseases leading to progressive axonal loss and irreversible neurological dysfunction in long-term (Dutta and Trapp, 2011). Oligodendrocyte precursor cells (OPCs), the main source of mature myelinating cells in the adult brain, are not considered as a limited factor for remyelination since they are abundant within demyelinated regions (Chang et al., 2002). In fact, the main cause of failure in remyelination has been suggested to be the inability of OPCs to differentiate into mature myelinating oligodendrocytes (Fancy et al., 2010; Franklin, 2002). Therefore, therapeutic strategies promoting OPCs differentiation, myelin sheath protection and remyelination may contribute to a better axonal preservation and long-term functional recovery (Franklin, 2015; Kremer et al., 2015). It is noteworthy that pharmacological therapies enhancing remyelination in demyelinating diseases as MS are still missing nowadays (Gajofatto and Benedetti, 2015).

Therefore, the purpose of this study was to investigate the protective and potential remyelinating effect of a pharmacological compound, etazolate, following demyelination. Etazolate, a pyrazolopyridine derivative, is able i) to enhance the α-secretase processing of β amyloid precursor protein (βAPP) to sAPPα, an endogenous neurotrophic and neuroprotective protein (Chasseigneaux and Allinquant, 2012), and ii) to promote neuroprotection against Aβ peptide neurotoxicity *in vitro* (Marcade et al., 2008). We have also shown that etazolate promotes a neuroprotective effect in a mouse model of acute CNS injury as TBI (Siopi et al., 2013). However, the potential therapeutic interest of etazolate in myelin sheath protection and remyelination remains unknown.

It is noteworthy that etazolate acts on multiple targets. In addition to α-secretase activation (Marcade et al., 2008), etazolate is an agonist of adenosine receptor (Daly et al., 1988), an inhibitor of PDE_4 (Chasin et al., 1972), and a modulator of $GABA_A$ (Thompson et al., 2002). The two latter pharmacological effects promote potential benefits on remyelination after experimental demyelination (Ghoumari et al., 2003; Gilani et al., 2014; Sun et al., 2012; Syed et al., 2013).

Among different targets of etazolate, our interest has been focused on α-secretases. Enzymes with α-secretase activity include different members of ADAM (A Disintegrin And Metalloproteinase) family as ADAM9, ADAM10 and ADAM17 (Allinson et al., 2003). Within the brain, ADAM10 is the most relevant since it leads to a constitutive and regulated α-secretase cleavage of βAPP under physiological conditions (Kuhn et al., 2010; Prox et al., 2013). The expression of ADAM10 is widespread in the brain (Kärkkäinen et al., 2000), including oligodendrocytes (Lin et al., 2008) and neural progenitor cells (NPCs) (Klingener et al., 2014). However, the role of ADAM10 in CNS re/myelination has not yet been fully elucidated. Recently, one report has described the involvement of ADAM10 in the migration of NPCs towards demyelinating regions to promote repair of injured brain (Klingener et al., 2014), suggesting the role of ADAM10 in brain repair. Therefore, we hypothesized that etazolate, as an α-secretase activator, acts on ADAM10 to promote remyelination.

In this context, our study aimed to investigate the protective and remyelinating effect of etazolate after demyelination *ex vivo*. We used the model of lysolecithin-induced demyelination in murine organoytpic cellebellar slice cultures, a very well known model to study the de/re-myelination processes (Birgbauer et al., 2004; Zhang et al., 2011). In parallel, we have also investigated the effect of etazolate on oligodendrocyte morphological maturation using the primary mixed glial culture from PLP-eGFP mice. In addition, we used as a pharmacological tool, the specific ADAM10 inhibitor GI254023X (Jangouk et al., 2009; Ludwig et al., 2005), to address the mechanism of action of etazolate. Our results showed that etazolate has a protective effect on myelin sheaths, and enhances oligodendrocyte differentiation and remyelination following lysolecithin-induced

demyelination. In addition, our data suggest that etazolate acts on ADAM10 to promote its beneficial effects.

2. Materials and Methods

2.1. Animals

For the organotypic culture of cerebellar slices and primary mixed glial cultures, we used either C57BL/6 mouse pups (Janvier, Le Genet St Isle, France), or transgenic PLP-eGFP mice (generated by Dr. W.B. Macklin, Cleveland Clinic Foundation, Ohio, USA). The latter overexpress the enhanced green fluorescent protein (eGFP) in the oligodendrocyte lineage under the control of the proteolipid protein (PLP) promoter. Animals were housed in a controlled temperature environment (22 ± 2°C), under a 12h light/dark cycle. Animal care and experiments were approved by the Paris Descartes University Animal Ethics Committee (CEEA34.MJT.075.12), respecting the French regulations and the European Communities Council Directive on the protection of animals used for scientific purposes (September 2010/63/UE).

2.2. Organotypic culture of cerebellar slices

Organotypic cerebellar slices were obtained from C57BL/6 mouse pups aged from 8 to 10 post-natal days (P8-P10), as previously described (Meffre et al., 2015a, 2015b). Brains were removed and placed in cold-PBS supplemented with 5 mg/mL D-glucose (Sigma-Aldrich). After removing the meninges, the cerebellum was dissected and 350 μm-thick parasagittal slices were cut using a tissue chopper (McIlwain Tissue Chopper, UK). Isolated slices were transferred onto membranes of 30 mm Millipore culture inserts with 0.4 μm pore size (Millipore, Bedford, MA). The inserts were placed in 6-well tissue culture plates with 1 mL of medium containing 50% basal medium with Earle's salts (Invitrogen, Gaithersburg, MD), 2.5% Hank's balanced salt solution (Life Technologies, Grand Island, NY), 25% heat-inactivated horse serum (Life Technologies), glutaMAX® 1% (Life Technologies), 5 mg/mL D-glucose (Sigma-Aldrich) and penicillin (0.1 U/mL)-streptomycin (0.1 µg/mL). Slices were maintained at 35°C in an atmosphere of humidified 5% CO_2 and the medium was changed every 3-4 days.

2.3. Model of lysolecithin-induced demyelination in organotypic cerebellar slice cultures

At 7 DIV (days *in vitro*), slices were treated with lysolecithin (0.5 mg/mL) (PubChem CID: 24798682; Sigma-Aldrich) or its vehicle (0.5% methanol:chloroform, 1:1) for 16h, as previously described (Birgbauer et al., 2004; Meffre et al., 2015a, 2015b). The slices were then treated either by vehicle (PBS 0.1M and DMSO 0.025% mixture), etazolate (PubChem CID: 3277; Tocris Bioscience) at the neuroprotective concentrations of 0.2 or 2 µM (Marcade et al., 2008), etazolate (2 µM) plus GI254023X (PubChem CID: 9952396; Tocris Bioscience) at 2 µM, as a selective ADAM10 inhibitor (Jangouk et al., 2009). After 72h of treatment, cerebellar slices were fixed with 4% paraformaldehyde solution (PFA) for subsequent immunolabelling.

2.4. Primary mixed glial culture

Newborn (P1-P3) PLP-eGFP mouse pups were decapitated and the hemispheres were collected in cold-PBS containing 5 mg/mL glucose. After removing meninges, the hemispheres were mechanically dissociated into DMEM (Invitrogen, France) and the solution obtained was filtered (100 µm, BD Biosciences) and seeded into 12-well plates containing one glass cover-slide per well (Ø 14 mm, Knittel Glass, Germany), previously coated by 20 µg/mL of poly-L-lysine (Sigma, St Louis, Missouri, USA). Cells were incubated at 37°C in an atmosphere of humidified 5% CO_2, in a medium containing 10% Fetal Bovine Serum (Invitrogen, France), L-glutamine 2 mM, sodium pyruvate 1 mM, fungizone 0.5 µg/mL, penicillin (0.1 U/mL)/streptomycin (0.1 µg/mL) diluted in DMEM. Medium was changed at 5 DIV and then every 2 days. Cells were treated at 7 DIV, either by vehicles (PBS and DMSO 0.025% mixture), etazolate at 2 µM, GI254023X at 2 µM, or a combination of both compounds. After 72h of treatment, cells were fixed with 4% PFA for subsequent immunolabelling.

2.5. Immunocyto-immunohistochemistry

All simples were washed with PBS and then blocked with L-lysine (0.1M) in a PBS solution containing triton-X (0.25%), gelatin (0.2%) and sodium azide (0.1%) (PBS-GTA) for 1h. Before blocking, fixed primary cells were first permeabilized with PBS-GTA for 10 min. The

samples were then incubated with primary antibodies overnight for organotypic slices or during 2h for primary cells, in a PBS-GTA medium buffer: mouse anti-MAG (1/1000; MAB1567, Millipore) for myelin sheaths; rabbit anti-Calbindin (1/10 000; CB38a, Swant) for Purkinje cells; rabbit anti-Caspr (1/1000; ab34151, Abcam) for paranodal junctions; rabbit anti-PDGFRα (1/500; sc-338, Santa Cruz) for OPCs; mouse anti-CC1 (1/200; OP80, Calbiochem) for mature oligodendrocytes, and rabbit anti-Ki67 (1/100; RB-1510-P1ABX, Thermo Scientific) for cell proliferation. Then, samples were incubated with secondary antibodies during 2h or 1h for the *ex vivo* and *in vitro* samples, respectively: goat anti-mouse coupled to Alexa-488 (1/1000; A21121, Invitrogen) and goat anti-rabbit coupled to Cy3 (1/500 *ex vivo* or 1/200 *in vitro*; 111-165-003, Jackson Immuno Research Laboratories, Inc.). The samples were mounted with Fluoromount (Southern Biotech, Birmingham, USA) or with Permafluor mounting medium (Thermo Scientific).

2.6. Immunocyto-immunohistochemistry analysis

Images from *ex vivo* samples were acquired using a confocal microscope LSM 510 (Carl Zeiss Inc., Germany) with a 20x objective (Plan-Neofluar 20x/0.5) or a 40x objective (Plan-Neofluar 40x/1.3 OilDic). Confocal configurations were adapted for 488 and 543 nm excitations corresponding to Alexa-488 and Cy3 fluorochromes, respectively. Images were then processed with LSM Image Browser (version 4.2).

The percentage of myelinated axons in cerebellar slices was determined using ImageJ software (1.46r, NIH, USA). The number of MAG^+ fibers was counted over the $Calbindin^+$ fibers crossing an imaginary line, localized in a region of interest around the apical ends of cerebellar lobules, from 3 different images acquired per stain and per slice, as previously described (Hussain et al., 2013; Meffre et al., 2015a, 2015b). Caspr staining was quantified in 4 to 6 different regions per slice. The results were expressed as the number of paired $Caspr^+$ representing paranodal junctions, adjacent to the nodes of Ranvier. Furthermore, we measured the length of the internodes by tracing myelin sheaths stained by MAG marker from one paranodal junction to the next one, using ImageJ (1.46r, NIH, USA). Results are expressed as the percentage of internodes under or above 20 µm, over the total internodes per region (0.05 mm^2). The quantification of oligodendrocyte cell bodies as $CC1^+$ or $PDGFR\alpha^+$ was performed in 3 different regions per slice, corresponding to the apical ends of cerebellar lobules.

The GFP-fluorescence from PLP-eGFP cells was captured with an Olympus BX51 microscope equipped with a QImaging Retiga camera (2000R). Images were obtained using a 20x lens (20x/NA 0.3; Zeiss EC-Plan-NEOFLUO) and digitalized using specialized software (Image-Pro Plus, version 6.0, Media Cybernetics). The morphology of GFP^+ cells, highlighting oligodendroglial cells, was determined on the basis of different ramified category as defined by simple- (1-2 processes) or multi-branched (> 3 processes) (Blanchard et al., 2013; Meffre et al., 2015a, 2015b). Results are expressed as the percentage of GFP^+ cells from one category over total GFP^+ cells per field (0.26 mm^2). To determine cell proliferation, GFP^+ and $Ki67^+$ cells were also quantified using ImageJ software (1.46r, NIH, USA). All quantifications have been performed by blind analysis.

2.7. Statistical analysis

Data were expressed as mean ± standard error of the mean (s.e.m). The data were analyzed using GraphPad Prism statistical software (Prism v4, GraphPad, La Jolla, CA). One-way ANOVA followed by Bonferroni's multiple comparison post-test was used. Differences with a *P* value under 0.05 were considered to be statistically different.

3. Results

3.1. Etazolate protects myelin sheaths from lysolecithin-induced demyelination *ex vivo*

Treatment with lysolecithin was able to induce demyelination in cerebellar slices, characterized by a disorganized MAG-staining (**Fig. 1A**) and a marked decrease by 42% in the percentage of myelinated axons ($P<0.001$) (**Fig. 1B**). Etazolate at 0.2 µM and 2 µM was able to counteract the myelin sheath loss (**Fig. 1A**), increasing the percentage of myelinated axons by 25% and 27%, respectively, compared to vehicle-treated demyelinated slices ($P<0.001$) (**Fig. 1B**). In addition, etazolate did not affect the myelin staining in non-demyelinated slices, since the percentage of myelinated axons was not changed compared to control slices (**Fig. 1B**). Finally, the number of Purkinje axons ($Calbindin^+$) was

not affected by lysolecithin or etazolate compared to vehicle-treated slices (**Fig. 1A, 1C**).
In order to decipher the mechanism of action of etazolate, we targeted ADAM10 by a selective pharmacological inhibitor, GI254023X. When GI254023X was added together with etazolate at 2 µM, the protective effect of etazolate was not anymore significant (**Fig. 2A, 2B**). Alone, GI254023X did not have any deleterious or beneficial effect on myelin sheaths (**Fig. 2A, 2B**). In non-demyelinated slices, the pharmacological compounds did not also modify the percentage of myelinated axons, consistent with the absence of effect on myelin maintenance (**Fig. 2B**). Moreover, the number of Purkinje axons (Calbindin$^+$) was not affected by any treatment in demyelinated slices compared to control slices (**Fig. 2C**).

3.2. Etazolate induces remyelination after lysolecithin-induced demyelination *ex vivo*: role of ADAM10

It is well known that remyelination induces changes in myelin architecture as i) re-aggregation of Caspr proteins highlighting the paranodal junctions, adjacent to the nodes of Ranvier, and ii) reduction in the length of remyelinated internodes (Podbielska et al., 2013). Therefore, the potential remyelinating effect of etazolate was investigated by labeling Caspr clusters, and MAG to highlight paranodal junctions and remyelinated internodes. Lysolecithin-induced demyelination led to a diffused Caspr staining with no more aggregation of paired-Caspr$^+$ 72h following demyelination (**Fig. 3A**). Therefore, the number of these clusters was decreased in vehicle-treated demyelinated slices (P<0.001) (**Fig. 3B**). In contrast, etazolate treatment at 2 µM led to a reappearance of Caspr staining and thus an increase in the number of paired-Caspr$^+$ (P<0.001) (32.65 ± 3.45 for control; 1.54 ± 0.46 for lysolecithin + vehicle; 21.13 ± 2.7 for lysolecithin + etazolate) (**Fig. 3A, 3B**). When GI254023X was added together with etazolate, the number of paired-Caspr$^+$ decreased significantly compared to etazolate-treated demyelinated slices (P<0.001) (7.03 ± 1.80 for lysolecithin + etazolate + GI254023X) (**Fig. 3A, 3B**), counteracting the effect of etazolate treatment. However, GI254023X alone did not modify the number of paired-Caspr$^+$ in demyelinated slices compared to vehicle-treated demyelinated slices (3.09 ± 0.93 lysolecithin + GI254023X) (**Fig. 3A, 3B**).
In addition, the reappearance of Caspr staining following etazolate treatment was accompanied by MAG$^+$ internode staining. Demyelinated slices treated with etazolate exhibited a high frequency of short internodes under 20 µm (P<0.001) (36% for control, 79% for lysolecithin + etazolate). Consequently, we observed a reduction in the frequency of large internodes over 20 µm in etazolate-treated demyelinated slices (P<0.001) (64% for control, 21% for lysolecithin + etazolate) (**Fig. 3A, 3C**).

3.3. Etazolate promotes oligodendrocyte differentiation and morphological maturation *ex vivo* and *in vitro*: role of ADAM10

To better understand how etazolate acts at the cellular level, we studied the oligodendrocyte differentiation by immunolabelling of OPCs (PDGFRα$^+$) and mature oligodendrocytes (CC1$^+$) in cerebellar slices. Treatment with lysolecithin only tended to decrease the number of both PDGFRα$^+$ cells (**Fig. 4A, 4B**) and CC1$^+$ cells (**Fig. 4A, 4C**) at 72h post-demyelination. In contrast, etazolate at 2 µM significantly increased the number of CC1$^+$ cells by 32%, compared to vehicle-treated demyelinated slices (P<0.01) (**Fig. 4A, 4C**), with a trend towards an increase in the number of PDGFRα$^+$ (**Fig. 4A, 4B**). However, when GI254023X was added together with etazolate, the number of CC1$^+$ cells was significantly reduced by 26% compared to etazolate-treated demyelinated slices (P<0.01) (**Fig. 4A, 4C**). Treatment with GI254023X alone did not exert a significant effect on the number of CC1$^+$ and PDGFRα$^+$ cells, compared to vehicle-treated demyelinated slices (**Fig. 4A, 4B, 4C**). In addition, neither etazolate nor GI254023X changed the number of PDGFRα$^+$ and CC1$^+$ cells in non-demyelinated slices (data not shown).
Furthermore, we analyzed the effect of etazolate on morphological modifications of oligodendrocytes using primary mixed glial cell culture obtained from PLP-eGFP mice. Indeed, it has been shown that cell differentiation is accompanied by morphological changes of oligodendrocytes, particularly with the development of multiple processes emerging from the cell body (Baumann and Pham-Dinh, 2001). Treatment with etazolate (2 µM, for 72h) reduced by 20% the percentage of GFP$^+$-oligodendrocytes with simple processes (**Fig. 5A, 5B**), and concomitantly stimulated by 20% the percentage of multi-branched GFP$^+$-oligodendrocytes compared to vehicle-treated

cultures (P<0.01) (**Fig. 5A, 5C**). Treatment with GI254023X abolished the effect of etazolate on simple-branched cells and on multi-branched cells, compared to etazolate-treated cultures (P<0.01) (**Fig. 5A, 5B**), suggesting that the effect of etazolate is ADAM10-dependent. GI254023X alone did not significantly alter the percentage of neither simple-branched nor multi-branched GFP^+-oligodendrocytes compared to vehicle-treated cultures (**Fig. 5A, 5B**). In parallel the effect of etazolate on cell proliferation (Ki67 staining) has also been investigated. All the pharmacological compounds, alone or in combination, did not modify the percentage of $Ki67^+$-GFP^+-oligodendrocytes (**Fig. 5C**).

4. Discussion

Chronically demyelinated axons are more vulnerable to the irreversible degeneration leading to axonal loss (Dutta and Trapp, 2011). Therefore, recent therapeutic strategies aimed to enhance the endogenous remyelination, in order to restore the axonal function, and to limit their loss (Franklin, 2015; Kremer et al., 2015). Our present study brought new evidence for etazolate therapy as protective of myelin sheaths with remyelinating capacity in in the context of CNS demyelination *ex vivo* in organoytpic cerebellar slice cultures.

The organotypic culture of cerebellar slices presents several advantages. It mimics the *in vivo* state of the cerebellar tissue, and maintains the architectural connexions, allowing an easy and fast access to the tissue, particularly useful to study myelin sheaths (Notterpek et al., 1993). Therefore, treatment of cerebellar slices with lysolecithin allows the study of demyelination and the screening of pharmacological compounds with potential remyelinating effect (Zhang et al., 2011). Consistent with previous studies, lysolecithin-induced demyelination in organotypic cerebellar slice cultures led to a loss of myelin staining (MAG) and a reduction of the percentage of myelinated axons 72h following demyelination (Meffre et al., 2015a, 2015b). Treatment with etazolate at 0.2 and 2 µM, immediately after lysolecithin removal, preserves myelin sheath immunostaining leading to an increase of the myelinated axon percentage, highlighting the protective effect of etazolate on myelin sheaths. In addition, the protective effect of etazolate has been also observed after a 72h delayed treatment with etazolate highlighted by an increase in the percentage of myelinated axon (**Fig. S1A**).

This current work also emphasizes the remyelinating capacity of etazolate, highlighted by the appearance of short myelin internodes, and re-aggregation of paired-$Caspr^+$ at 72h post-demyelination. The same results have been also observed when treatment with etazolate was delayed by 72h following lysolecithin removal (**Fig. S1B**), confirming the remyelinating capacity of etazolate. It has been shown that in demyelinated lesions, paranodal proteins as Caspr are diffusely distributed along the axons, and they do not present anymore a paired-aggregate distribution (Podbielska et al., 2013). However, in the case of remyelination, marked changes are observed in myelin architecture as a reduction of the myelin internode length, and the re-aggregation of paired $Caspr^+$ (Podbielska et al., 2013).

It is well established that the prerequisites for remyelination are OPCs recruitment and subsequent differentiation into myelinating oligodendrocytes (Franklin and Ffrench-Constant, 2008). Therefore, we studied whether etazolate affects OPCs differentiation, and provide evidence that etazolate treatment enhances i) oligodendrocyte differentiation *ex vivo* by an increase in the number of mature $CC1^+$ oligodendrocytes and ii) morphological maturation of oligodendrocytes *in vitro* by an increase of multi-branched cells.

In order to decipher the mechanism of action of etazolate, we focused our study on one of its targets, α-secretases (Marcade et al., 2008; Siopi et al., 2013), and particularly ADAM10 (Kärkkäinen et al., 2000). Interestingly, the protective effect of etazolate on myelin sheaths and its remyelinating effect were attenuated or even blocked in the presence of the specific ADAM10 inhibitor GI254023X. Our data suggest that ADAM10 is involved in the beneficial effects of etazolate on oligodendrocyte differentiation/maturation and on remyelination. Although the role of ADAM10 in CNS remyelination is not well understood, a recent work showed that ADAM10 activity is required for NPCs migration from the subventricular zone (SVZ) into demyelinated lesions and thereby promotes repair following demyelination (Klingener et al., 2014). However, the role of ADAM10 in oligodendrocyte differentiation and remyelination requires further investigation. Besides, we cannot exclude the involvement of other α-secretases as ADAM17 in the beneficial effects exerted by etazolate. In fact,

a recent study proposed the modulation of ADAM17 as a therapeutic strategy for demyelinating disorders by promoting oligodendrocyte regeneration and myelin repair *in vivo* (Palazuelos et al., 2015). Besides, α-secretases ADAM10 and ADAM17 are both able to cleave a variety of substrates including βAPP and N-cadherin (Edwards et al., 2008) and the cleaved products may mediate the remyelinating effect of etazolate.
In addition, other benefits of etazolate have been also reported as anti-inflammatory (Guo et al., 2014; Siopi et al., 2013), pro-cognitive (Drott et al., 2010), antidepressant and anxiolytic (Ankur et al., 2013; Jindal et al., 2012). Since etazolate acts on multiple targets as an inhibitor of PDE4 and a modulator of $GABA_A$ receptor (Chasin et al., 1972; Thompson et al., 2002), known to be the modulators of myelination (Sun et al., 2012; Syed et al., 2013), it can not be ruled out that these targets may be also involved in the remyelinating effect of etazolate.

5. Conclusion

Taken together, we described the therapeutic interest of etazolate in white matter protection and repair by protecting myelin sheaths, enhancing oligodendrocyte differentiation and remyelination process after demyelination *ex vivo*. In addition, our work also suggests that the α-secretase ADAM10 is involved in etazolate-induced myelin repair. Overall, etazolate is a promising candidate drug for the treatment of demyelination in MS or acute CNS injuries as TBI, since this compound presents a good tolerability and safety profile in humans (Vellas et al., 2011). However, further studies are required to investigate the remyelinating effect of etazolate after demyelination *in vivo*.

Conflict of interest disclosure statement

No potential conflicts of interest were disclosed.

Acknowledgments

We acknowledge the non-profit organization "*Fondation des Gueules Cassées*" (grants to GLD and MJT), Paris Descartes University and INSERM (*Institut National de la Santé Et de la Recherche* Médicale) for financially supporting this work, and Dr Abdel M. Ghoumari (INSERM UMR 788, Paris) for providing transgenic PLP-eGFP mice.

References

Allinson, T.M.J., Parkin, E.T., Turner, A.J., Hooper, N.M., 2003. ADAMs family members as amyloid precursor protein alpha-secretases. J. Neurosci. Res. 74, 342–352. doi:10.1002/jnr.10737

Ankur, J., Mahesh, R., Bhatt, S., 2013. Anxiolytic-like effect of etazolate, a type 4 phosphodiesterase inhibitor in experimental models of anxiety. Indian J. Exp. Biol. 51, 444–449.

Armstrong, R.C., Mierzwa, A.J., Marion, C.M., Sullivan, G.M., 2015a. White matter involvement after TBI: Clues to axon and myelin repair capacity. Exp. Neurol. 275, 328-333. doi:10.1016/j.expneurol.2015.02.011

Armstrong, R.C., Mierzwa, A.J., Sullivan, G.M., Sanchez, M.A., 2015b. Myelin and Oligodendrocyte Lineage Cells in White Matter Pathology and Plasticity after Traumatic Brain Injury. Neuropharmacology. doi:10.1016/j.neuropharm.2015.04.029

Baumann, N., Pham-Dinh, D., 2001. Biology of oligodendrocyte and myelin in the mammalian central nervous system. Physiol. Rev. 81, 871–927.

Birgbauer, E., Rao, T.S., Webb, M., 2004. Lysolecithin induces demyelination in vitro in a cerebellar slice culture system. J. Neurosci. Res. 78, 157–166. doi:10.1002/jnr.20248

Blanchard, B., Heurtaux, T., Garcia, C., Moll, N.M., Caillava, C., Grandbarbe, L., Klosptein, A., Kerninon, C., Frah, M., Coowar, D., Baron-Van Evercooren, A., Morga, E., Heuschling, P., Nait Oumesmar, B., 2013. Tocopherol derivative TFA-12 promotes myelin repair in experimental models of multiple sclerosis. J. Neurosci. Off. J. Soc. Neurosci. 33, 11633–11642. doi:10.1523/JNEUROSCI.0774-13.2013

Chang, A., Tourtellotte, W.W., Rudick, R., Trapp, B.D., 2002. Premyelinating oligodendrocytes in chronic lesions of multiple sclerosis. N. Engl. J. Med. 346, 165–173. doi:10.1056/NEJMoa010994

Chasin, M., Harris, D.N., Phillips, M.B., Hess, S.M., 1972. 1-Ethyl-4-(isopropylidenehydrazino)-1H-pyrazolo-(3,4-b)-pyridine-5-carboxylic acid, ethyl ester, hydrochloride (SQ 20009)--a potent new inhibitor of cyclic 3',5'-nucleotide phosphodiesterases. Biochem. Pharmacol. 21, 2443–2450.

Chasseigneaux, S., Allinquant, B., 2012. Functions of Aβ, sAPPα and sAPPβ : similarities and differences. J. Neurochem. 120 Suppl 1, 99–108. doi:10.1111/j.1471-4159.2011.07584.x

Compston, A., Coles, A., 2008. Multiple sclerosis. The Lancet 372, 1502–1517. doi:10.1016/S0140-6736(08)61620-7

Daly, J.W., Hong, O., Padgett, W.L., Shamim, M.T., Jacobson, K.A., Ukena, D., 1988. Non-xanthine heterocycles: activity as antagonists of A1- and A2-adenosine receptors. Biochem. Pharmacol. 37, 655–664.

Drott, J., Desire, L., Drouin, D., Pando, M., Haun, F., 2010. Etazolate improves performance in a foraging and homing task in aged rats. Eur. J. Pharmacol. 634, 95–100. doi:10.1016/j.ejphar.2010.02.036

Dutta, R., Trapp, B.D., 2011. Mechanisms of neuronal dysfunction and degeneration in multiple sclerosis. Prog. Neurobiol. 93, 1–12. doi:10.1016/j.pneurobio.2010.09.005

Edwards, D.R., Handsley, M.M., Pennington, C.J., 2008. The ADAM metalloproteinases. Mol. Aspects Med. 29, 258–289. doi:10.1016/j.mam.2008.08.001

Fancy, S.P.J., Kotter, M.R., Harrington, E.P., Huang, J.K., Zhao, C., Rowitch, D.H., Franklin, R.J.M., 2010. Overcoming remyelination failure in multiple sclerosis and other myelin disorders. Exp. Neurol. 225, 18–23. doi:10.1016/j.expneurol.2009.12.020

Franklin, R.J.M., 2015. Regenerative Medicines for Remyelination: From Aspiration to Reality. Cell Stem Cell 16, 576–577. doi:10.1016/j.stem.2015.05.010

Franklin, R.J.M., 2002. Why does remyelination fail in multiple sclerosis? Nat. Rev. Neurosci. 3, 705–714. doi:10.1038/nrn917

Franklin, R.J.M., Ffrench-Constant, C., 2008. Remyelination in the CNS: from biology to therapy. Nat. Rev. Neurosci. 9, 839–855. doi:10.1038/nrn2480

Franklin, R.J.M., Goldman, S.A., 2015. Glia Disease and Repair-Remyelination. Cold Spring Harb. Perspect. Biol. 7. doi:10.1101/cshperspect.a020594

Gajofatto, A., Benedetti, M.D., 2015. Treatment strategies for multiple sclerosis: When to start, when to change, when to stop? World J. Clin. Cases 3, 545–555. doi:10.12998/wjcc.v3.i7.545

Ghoumari, A.M., Ibanez, C., El-Etr, M., Leclerc, P., Eychenne, B., O'Malley, B.W., Baulieu, E.E., Schumacher, M., 2003. Progesterone and its metabolites increase myelin basic protein expression in organotypic slice cultures of rat cerebellum. J. Neurochem. 86, 848–859.

Gilani, A.A., Dash, R.P., Jivrajani, M.N., Thakur, S.K., Nivsarkar, M., Gilani, A.A., Dash, R.P., Jivrajani, M.N., Thakur, S.K., Nivsarkar, M., 2014. Evaluation of GABAergic Transmission Modulation as a Novel Functional Target for Management of Multiple Sclerosis: Exploring Inhibitory Effect of GABA on Glutamate-Mediated Excitotoxicity. Adv. Pharmacol. Sci. Adv. Pharmacol. Sci. 2014, 2014, e632376. doi:10.1155/2014/632376, 10.1155/2014/632376

Guo, J., Lin, P., Zhao, X., Zhang, J., Wei, X., Wang, Q., Wang, C., 2014. Etazolate abrogates the lipopolysaccharide (LPS)-induced downregulation of the cAMP/pCREB/BDNF signaling, neuroinflammatory response and depressive-like behavior in mice. Neuroscience 263, 1–14. doi:10.1016/j.neuroscience.2014.01.008

Hussain, R., Ghoumari, A.M., Bielecki, B., Steibel, J., Boehm, N., Liere, P., Macklin, W.B., Kumar, N., Habert, R., Mhaouty-Kodja, S., Tronche, F., Sitruk-Ware, R., Schumacher, M., Ghandour, M.S., 2013. The neural androgen receptor: a therapeutic target for myelin repair in chronic demyelination. Brain J. Neurol. 136, 132–146. doi:10.1093/brain/aws284

Jangouk, P., Dehmel, T., Meyer Zu Hörste, G., Ludwig, A., Lehmann, H.C., Kieseier, B.C., 2009. Involvement of ADAM10 in axonal outgrowth and myelination of the peripheral nerve. Glia 57, 1765–1774. doi:10.1002/glia.20889

Jindal, A., Mahesh, R., Gautam, B., Bhatt, S., Pandey, D., 2012. Antidepressant-like effect of etazolate, a cyclic nucleotide phosphodiesterase 4 inhibitor--an approach using rodent behavioral antidepressant tests battery. Eur. J. Pharmacol. 689, 125–131. doi:10.1016/j.ejphar.2012.05.051

Kärkkäinen, I., Rybnikova, E., Pelto-Huikko, M., Huovila, A.P., 2000. Metalloprotease-disintegrin (ADAM) genes are widely and differentially expressed in the adult CNS. Mol. Cell. Neurosci. 15, 547–560. doi:10.1006/mcne.2000.0848

Klingener, M., Chavali, M., Singh, J., McMillan, N., Coomes, A., Dempsey, P.J., Chen, E.I., Aguirre, A., 2014. N-cadherin promotes recruitment and migration of neural progenitor cells from the SVZ neural stem cell niche into demyelinated lesions. J. Neurosci. Off. J. Soc. Neurosci. 34, 9590–9606. doi:10.1523/JNEUROSCI.3699-13.2014

Kremer, D., Küry, P., Dutta, R., 2015. Promoting remyelination in multiple sclerosis: current drugs and future prospects. Mult. Scler. Houndmills Basingstoke Engl. 21, 541–549. doi:10.1177/1352458514566419

Kuhn, P.-H., Wang, H., Dislich, B., Colombo, A., Zeitschel, U., Ellwart, J.W., Kremmer, E., Rossner, S., Lichtenthaler, S.F., 2010. ADAM10 is the physiologically relevant, constitutive alpha-secretase of the amyloid precursor protein in primary neurons. EMBO J. 29, 3020–3032. doi:10.1038/emboj.2010.167

Lin, J., Luo, J., Redies, C., 2008. Differential expression of five members of the ADAM family in the developing chicken brain. Neuroscience 157, 360–375.

doi:10.1016/j.neuroscience.2008.08.053

Ludwig, A., Hundhausen, C., Lambert, M.H., Broadway, N., Andrews, R.C., Bickett, D.M., Leesnitzer, M.A., Becherer, J.D., 2005. Metalloproteinase inhibitors for the disintegrin-like metalloproteinases ADAM10 and ADAM17 that differentially block constitutive and phorbol ester-inducible shedding of cell surface molecules. Comb. Chem. High Throughput Screen. 8, 161–171.

Marcade, M., Bourdin, J., Loiseau, N., Peillon, H., Rayer, A., Drouin, D., Schweighoffer, F., Désiré, L., 2008. Etazolate, a neuroprotective drug linking GABA(A) receptor pharmacology to amyloid precursor protein processing. J. Neurochem. 106, 392–404. doi:10.1111/j.1471-4159.2008.05396.x

Meffre, D., Massaad, C., Grenier, J., 2015a. Lithium chloride stimulates PLP and MBP expression in oligodendrocytes via Wnt/β-catenin and Akt/CREB pathways. Neuroscience 284, 962–971. doi:10.1016/j.neuroscience.2014.10.064

Meffre, D., Shackleford, G., Hichor, M., Gorgievski, V., Tzavara, E.T., Trousson, A., Ghoumari, A.M., Deboux, C., Nait Oumesmar, B., Liere, P., Schumacher, M., Baulieu, E.-E., Charbonnier, F., Grenier, J., Massaad, C., 2015b. Liver X receptors alpha and beta promote myelination and remyelination in the cerebellum. Proc. Natl. Acad. Sci. U. S. A. 112, 7587–7592. doi:10.1073/pnas.1424951112

Notterpek, L.M., Bullock, P.N., Malek-Hedayat, S., Fisher, R., Rome, L.H., 1993. Myelination in cerebellar slice cultures: development of a system amenable to biochemical analysis. J. Neurosci. Res. 36, 621–634. doi:10.1002/jnr.490360603

Palazuelos, J., Klingener, M., Raines, E.W., Crawford, H.C., Aguirre, A., 2015. Oligodendrocyte Regeneration and CNS Remyelination Require TACE/ADAM17. J. Neurosci. Off. J. Soc. Neurosci. 35, 12241–12247. doi:10.1523/JNEUROSCI.3937-14.2015

Podbielska, M., Banik, N.L., Kurowska, E., Hogan, E.L., 2013. Myelin recovery in multiple sclerosis: the challenge of remyelination. Brain Sci. 3, 1282–1324. doi:10.3390/brainsci3031282

Prox, J., Bernreuther, C., Altmeppen, H., Grendel, J., Glatzel, M., D'Hooge, R., Stroobants, S., Ahmed, T., Balschun, D., Willem, M., Lammich, S., Isbrandt, D., Schweizer, M., Horré, K., De Strooper, B., Saftig, P., 2013. Postnatal disruption of the disintegrin/metalloproteinase ADAM10 in brain causes epileptic seizures, learning deficits, altered spine morphology, and defective synaptic functions. J. Neurosci. Off. J. Soc. Neurosci. 33, 12915–12928, 12928a. doi:10.1523/JNEUROSCI.5910-12.2013

Siopi, E., Llufriu-Dabén, G., Cho, A.H., Vidal-Lletjós, S., Plotkine, M., Marchand-Leroux, C., Jafarian-Tehrani, M., 2013. Etazolate, an α-secretase activator, reduces neuroinflammation and offers persistent neuroprotection following traumatic brain injury in mice. Neuropharmacology 67, 183–192. doi:10.1016/j.neuropharm.2012.11.009

Sun, X., Liu, Y., Liu, B., Xiao, Z., Zhang, L., 2012. Rolipram promotes remyelination possibly via MEK-ERK signal pathway in cuprizone-induced demyelination mouse. Exp. Neurol. 237, 304–311. doi:10.1016/j.expneurol.2012.07.011

Syed, Y.A., Baer, A., Hofer, M.P., González, G.A., Rundle, J., Myrta, S., Huang, J.K., Zhao, C., Rossner, M.J., Trotter, M.W.B., Lubec, G., Franklin, R.J.M., Kotter, M.R., 2013. Inhibition of phosphodiesterase-4 promotes oligodendrocyte precursor cell differentiation and enhances CNS remyelination. EMBO Mol. Med. 5, 1918–1934. doi:10.1002/emmm.201303123

Thompson, S.-A., Wingrove, P.B., Connelly, L., Whiting, P.J., Wafford, K.A., 2002. Tracazolate reveals a novel type of allosteric interaction with recombinant gamma-aminobutyric acid(A) receptors. Mol. Pharmacol. 61, 861–869.

Trapp, B.D., Nave, K.-A., 2008. Multiple sclerosis: an immune or neurodegenerative disorder? Annu. Rev. Neurosci. 31, 247–269. doi:10.1146/annurev.neuro.30.051606.094313

Vellas, B., Sol, O., Snyder, P.J., Ousset, P.-J., Haddad, R., Maurin, M., Lemarié, J.-C., Désiré, L., Pando, M.P., EHT0202/002 study group, 2011. EHT0202 in Alzheimer's disease: a 3-month, randomized, placebo-controlled, double-blind study. Curr. Alzheimer Res. 8, 203–212.

Zhang, H., Jarjour, A.A., Boyd, A., Williams, A., 2011. Central nervous system remyelination in culture--a tool for multiple sclerosis research. Exp. Neurol. 230, 138–148. doi:10.1016/j.expneurol.2011.04.009

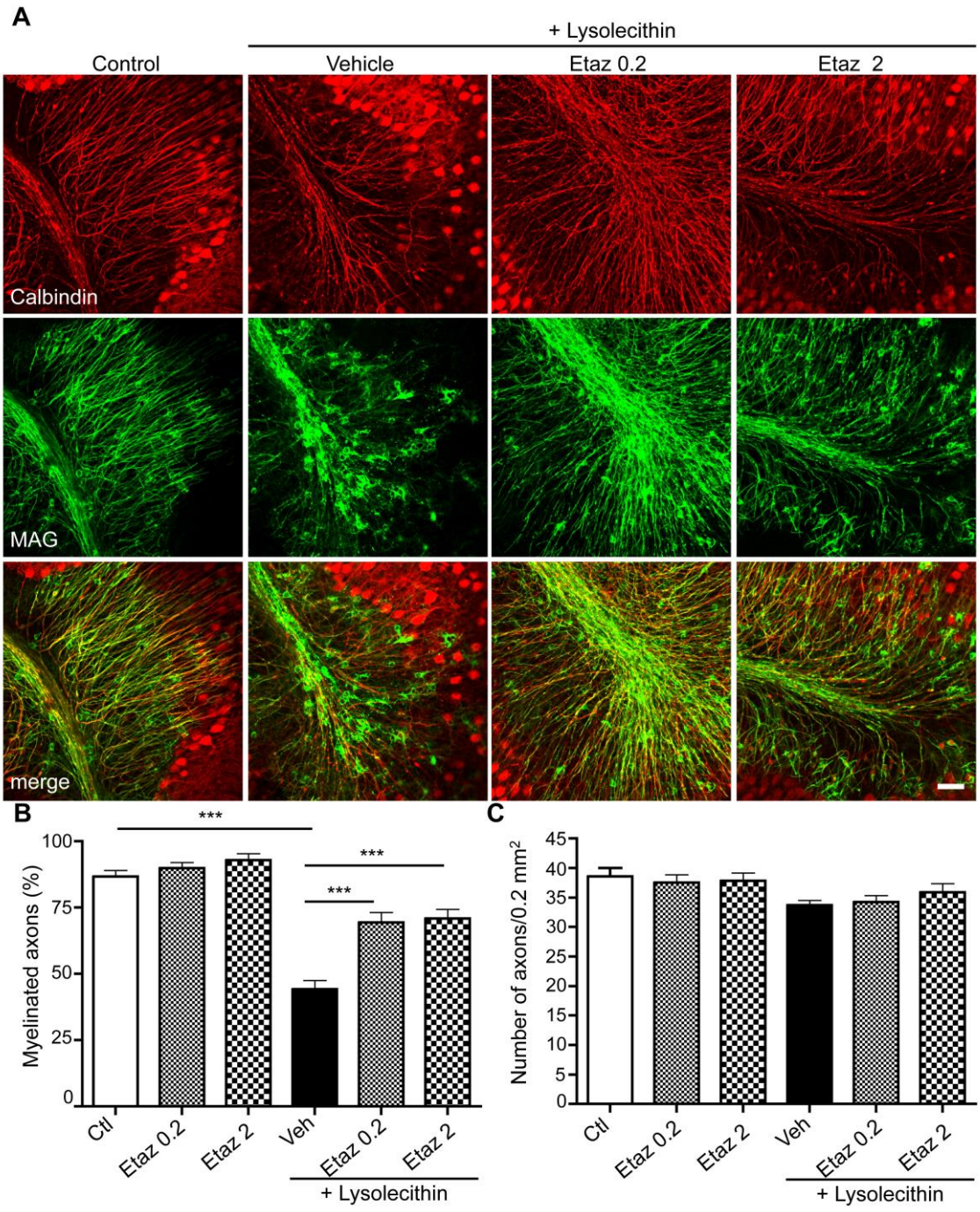

Fig. 1. Dose-response study of etazolate on myelin sheath protection after lysolecithin-induced demyelination. (**A)** Confocal images of double immunostaining for calbindin (Purkinje cells, red) and MAG (myelin sheaths, green). Scale bar: 50 µm. (**B**) Effect of lysolecithin and etazolate at 0.2 and 2 µM on the percentage of myelinated axons. (**C**) Effect of pharmacological compounds on the total number of axons in control and demyelinated slices. Results are expressed as mean ± s.e.m of 3 different regions (0.2 mm^2) quantified per stain and per slice, from 24 slices per condition obtained from 4 independent experiments. ****P*<0.001 (One-way ANOVA following Bonferroni's post-test). Ctl: control slices; Veh: vehicle (PBS); Etaz 0.2: etazolate 0.2 µM; Etaz 2: etazolate 2 µM; MAG: myelin associated glycoprotein; Calbindin: calcium-binding protein.

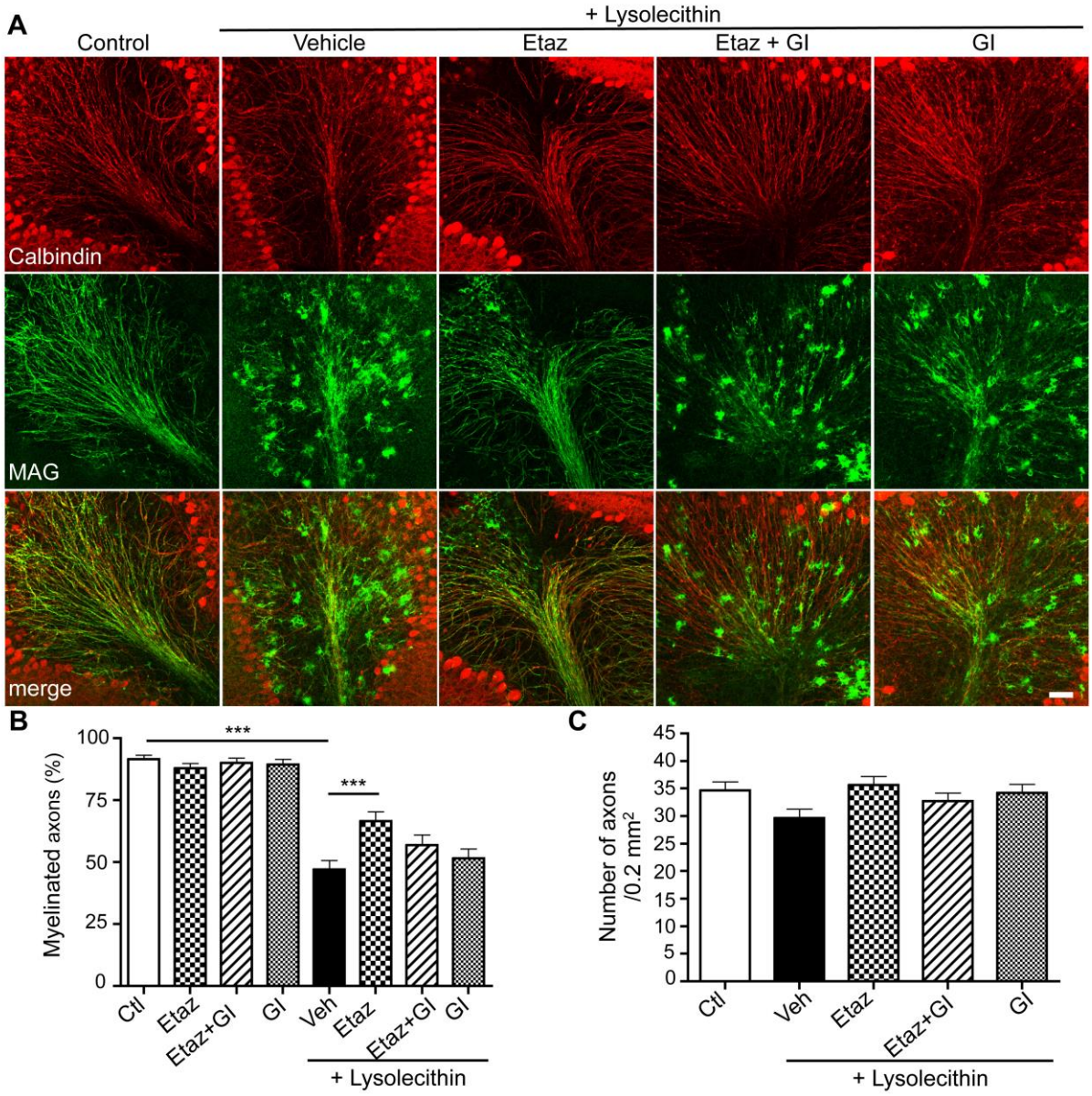

Fig. 2. The protective effect of etazolate on myelin sheaths from lysolecithin-induced demyelination: role of ADAM10. (**A**) Confocal images of double immunostaining for calbindin (Purkinje cells, red) and MAG (myelin sheaths, green). Scale bar: 50 µm. (**B**) Effect of pharmacological compounds on the percentage of myelinated axons in control (without lysolecithin) and demyelinated slices. (**C**) The histogram shows the effect of pharmacological compounds on the total number of axons in demyelinated slices. Results are expressed as mean ± s.e.m of 3 different regions (0.2 mm^2) quantified per stain per slice, from 18 slices per condition obtained from 3 independent experiments. ****P*<0.001 (One-way ANOVA following Bonferroni's post-test). Ctl: control slices; Veh: vehicle (PBS+DMSO); Etaz: etazolate 2 µM; GI: GI254023X 2 µM; MAG: myelin associated glycoprotein; Calbindin: calcium-binding protein.

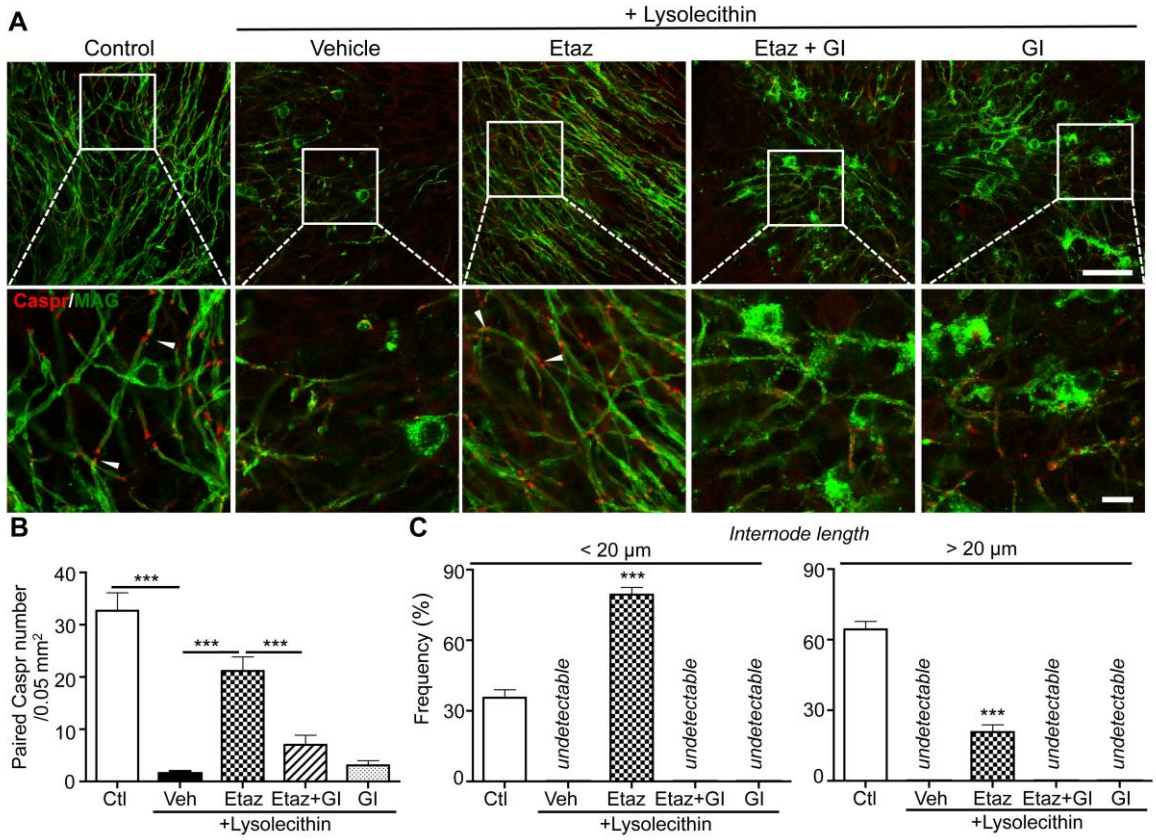

Fig. 3. Etazolate enhances remyelination after lysolecithin-induced demyelination: role of ADAM10. (**A**) Confocal images of double immunostaining for Caspr (paranodal junctions, red) and MAG (myelin internodes, green). Scale bar: 50 µm. A 3X magnification of paired-Caspr$^+$ pointed by close arrowheads and internodes are shown in the second row of images. Scale bar: 10 µm. (**B**) Effect of pharmacological compounds on the number of paired-Caspr$^+$. (**C**) Effect of pharmacological compounds on the frequency of short internodes (<20 µm) and long internodes (>20 µm). Results are expressed as mean ± s.e.m of 4 to 6 different regions (0.05 mm^2) quantified per slice, from 12 slices per condition obtained from 2 independent experiments. ***P<0.001 (One-way ANOVA following Bonferroni's post-test). Ctl: control slices; Veh: vehicle (PBS+DMSO); Etaz: etazolate 2 µM; GI: GI254023X 2 µM; Caspr: contactin-associated protein; MAG: myelin associated protein.

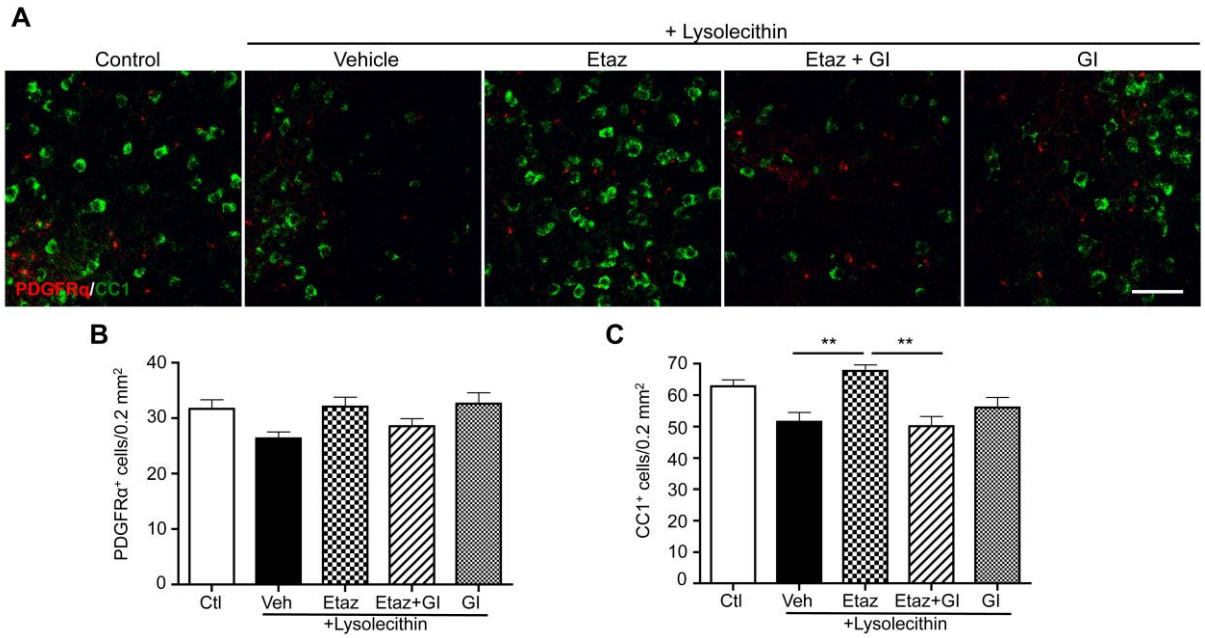

Fig. 4. Etazolate promotes oligodendrocyte differentiation after lysolecithin-induced demyelination: role of ADAM10. (**A**) Confocal images of double immunostaining for PDGFRα (OPCs, red) and CC1 (mature oligodendrocytes, green). Scale bar: 50 µm. (**B**) Quantification of the number of PDGFRα$^+$ cells and (**C**) the number of CC1$^+$ cells. Results are expressed as mean ± s.e.m of three different regions (0.2 mm^2) quantified per stain per slice, from 18 slices per condition obtained from 3 independent experiments. ***P*<0.01 (One-way ANOVA following Bonferroni's post-test). Veh: vehicle (PBS+DMSO); Etaz: etazolate 2 µM; GI: GI254023X 2 µM.

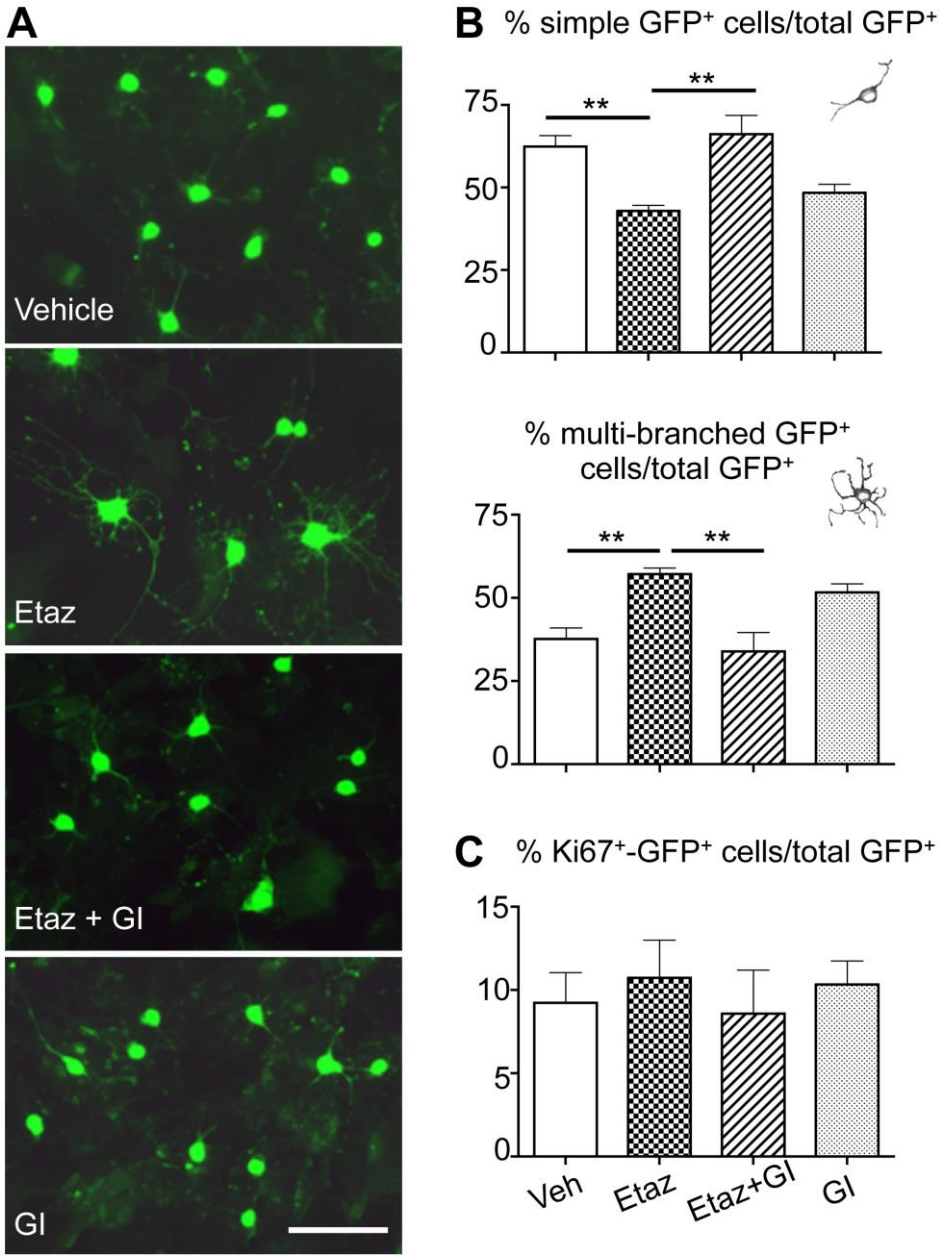

Fig. 5. Etazolate promotes oligodendrocyte morphological maturation *in vitro*: role of ADAM10. (**A**) Images of primary mixed glial cell cultures obtained from PLP-eGFP mice were grown in culture for 7 DIV and then treated with pharmacological compounds for 72h. Scale bar: 50 µm. (**B**) Quantifications of the percentages of simple-branched and multi-branched GFP^+-oligodendrocytes. (**D**) Quantification of the effect of pharmacological treatments on the percentage of $Ki67^+$-GFP^+-oligodendrocytes. Results are expressed as mean ± s.e.m of 6 different regions (0.26 mm^2) quantified per sample, from 3 to 5 samples per condition, obtained from 2 independent experiments. ***P*<0.01 (One-way ANOVA following Bonferroni's post-test). Veh: Vehicle (PBS+DMSO); Etaz: etazolate 2 µM; GI: GI254023X 2 µM.

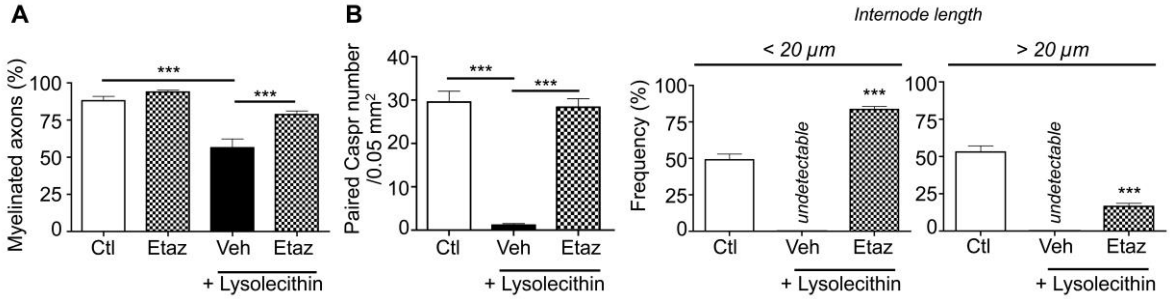

Supplementary material

Fig. S1. Effects of a delayed treatment with etazolate after lysolecithin-induced demyelination. Etazolate at 2 µM was added to cerebellar slices at 72h post-demyelination *ex vivo* and maintained for 48h. (**A**) Quantification of the effect of etazolate on myelin sheath protection highlighted by the percentage of myelinated axons. (**B**) Quantification of the effect of etazolate on the number of paired Caspr^{+} and the frequency of short (<20 µm) and long myelin internodes (>20 µm). Results are expressed as mean ± s.e.m of 4 to 6 different regions (0.05 mm^{2}) quantified per slice, from 6 slices per condition. ***P<0.001 (One-way ANOVA following Bonferroni's post-test). Ctl: control slices; Veh: vehicle (PBS); Etaz: etazolate 2 µM.

ABSTRACT

Traumatic brain injury (TBI) is caused by rapid deformation, stretching and tearing of the brain tissue. Among the mechanical forces, strain is known to be an important component of TBI. Understanding how the mechanical forces and mechanostimulation lead to tissue damage remains a considerable challenge. TBI initiates a cascade of secondary pathophysiological events, as excitotoxicity, inflammation and oxidative stress. Experimental evidences suggest that demyelination may play an important role in the pathophysiology of TBI. Our hypothesis was that stretch-induced traumatic injury may initiate demyelination. The aim of my PhD thesis was to develop innovative models of stretch-induced injury in oligodendrocytes and in organotypic cerebellar slices, rich in myelinated fibers, in order to decipher the pathophysiological mechanisms, such as oxidative stress, initiated following stretch. I developed several models of stretch-induced injury using i) the mouse oligodendrocyte 158N cell line, ii) the mixed glial primary culture, iii) the oligodendrocyte-enriched primary culture and finally, iv) the organotypic culture of cerebellar slices in mice. Cells or slices were subjected to an equibiaxial static stretch using Flexcell® Tension system device in order to reproduce two models of stretch-induced injury: “mild” (20% strain) *versus* “moderate” (30% strain) injury. Our results showed that the “mild” stretch i) decreased the cell adherence and affected the cell morphology with a decrease of surface area in both mature and immature oligodendrocytes in the oligodendrocyte-enriched culture, ii) induced an increase in reactive oxygen species (ROS) production, protein oxydation (AOPP), and an alteration in the expression of pro- (*Duox-1*) and anti-oxidant genes (*Sod-1, Sod-2, Ho-1, Nqo-1, Nrf-2*) in the cell line and in the mixed glial primary culture, iii) modified the expression of the myelin genes (*Plp, Mag, Cnp*) in all studied models. The “moderate” stretch on cells induced a more pronounced alteration of the cellular redox status and a stronger effect on the cell morphology with a damage of cell ramifications in the oligodendrocyte-enriched culture. Cerebellar slices, subjected to a “moderate” stretch, showed an accumulation of amyloid precursor protein (APP), a marker of axonal injury, and an alteration of paranodal junctions morphology which appeared elongated. An alteration in the expression of pro- /anti-oxidant and myelin genes was also observed. Therefore, stretch-induced injury in cerebellar slices led to axonal and myelin injury, similar to what observed following TBI *in vivo*. In conclusion, several models of stretch-induced injury were developed for the first time in oligodendrocytes and cerebellar slices showing that mechanical stretch initiates loss of oligodendrocytes and demyelination. These findings highlight the importance of developing therapeutic strategies based on oligodendrocyte protection. These models are relevant for studying the pathophysiological events that occur after stretch-induced injury as well as for rapid screening of therapeutic compounds.

Keywords: oligodendrocytes; traumatic brain injury; mechanostimulation; stretch-induced injury; demyelination; oxidative stress; organotypic culture of cerebellar slices; oligodendrocyte-enriched primary culture; 158N oligodendrocytes cell line